University of Glasgow

Ritchie, Neil Douglas (2016) *The role of IL-17 and IL-22 in the immune response to infection and colonisation with S. pneumoniae.* PhD thesis.

https://theses.gla.ac.uk/7095/

Copyright and moral rights for this work are retained by the author

A copy can be downloaded for personal non-commercial research or study, without prior permission or charge

This work cannot be reproduced or quoted extensively from without first obtaining permission from the author

The content must not be changed in any way or sold commercially in any format or medium without the formal permission of the author

When referring to this work, full bibliographic details including the author, title, awarding institution and date of the thesis must be given

Enlighten: Theses
https://theses.gla.ac.uk/
research-enlighten@glasgow.ac.uk

The role of IL-17 and IL-22 in the immune response to infection and colonisation with *S. pneumoniae*

DR NEIL DOUGLAS RITCHIE

MB ChB, BSc(Med Sci), MRCPSG

A thesis submitted to the College of Medical, Veterinary and Life Sciences, University of Glasgow, in fulfilment of the requirements for the degree of Doctor of Philosophy

Institute of Infection, Immunity and Inflammation
University of Glasgow
120 University Place
Glasgow G12 8TA

February 2016

Dedication

For my father, Andrew. He was always a model of support and encouragement but couldn't see me reach the end of my University study.

> *Σὺ δὲ παρηκολούθησάς μου τῇ διδασκαλίᾳ, τῇ ἀγωγῇ, τῇ προθέσει, τῇ πίστει, τῇ μακροθυμίᾳ, τῇ ἀγάπῃ, τῇ ὑπομονῇ, τοῖς διωγμοῖς, τοῖς παθήμασιν*

For you have followed me closely: the teaching, the way of life, the purpose, the faith, the patience, the love, the steadfastness, the persecution, the sufferings. Paul writing shortly before his death (my own translation).

I declare that, except where explicit reference is made to the contribution of others, that this dissertation is the result of my own work and has not been submitted for any other degree at the University of Glasgow or any other institution.

Signature

Neil Douglas Ritchie

Abstract

Introduction: *Streptococcus pneumoniae* is an important cause of morbidity and mortality worldwide and a leading cause of pneumonia, bacteraemia and meningitis. Nasal colonisation is a vital prerequisite to disease. Memory T cells and the cytokine IL-17 has been reported to be required for the control of murine nasal colonisation and humans have pneumococcus specific memory T cells but the role of IL-17 in invasive pneumococcal disease remains poorly understood.

Methods: Human pneumococcus specific T cells from peripheral blood using a co-culture model. Young and old adults as well as patients with invasive pneumococcal disease were included. A mouse model of colonisation and disease was used to assess the role of IL-17 and the related cytokine IL-22 in naïve mice using transgenic mice deficient in IL-17 and IL-22 signalling. Data from this model was supplemented with next generation sequencing to investigate the microbiome and prokaryotic transcriptome during colonisation and infection respectively.

Results: Pneumococcal specific memory T cells were identified in human peripheral blood samples and some of these expressed IL-17, IL-22 and interferon-γ following clonal stimulation. IL-17 expressing T cells arose from the $CCR6^{+}$ subset of T cells. The memory T cell responses of young and old adults were compared. Young adults had greater T cell proliferative in response to pneumococci than old adults and also less expressed more IL-17, IL-22 and interferon-γ.

Two principal models of pneumococcal disease were investigated in animal models. TIGR4 is a highly invasive strain which causes bacteraemia while SRL1 causes severe pneumonia and empyema. RNA-Seq was used to identify differential gene expression in infection relative to growth in broth. Peak IL-17 and IL-22 are production occurs within hours of induction of infection and the likely source of IL-17 was identified as γδ lymphocytes. When $IL\text{-}17RA^{-/-}$ mice were infected either strain they demonstrated decreased neutrophil recruitment to blood and lung. TIGR4 infected $IL\text{-}17RA^{-/-}$ mice had decreased survival

whereas SRL1 infected IL-17RA$^{-/-}$ mice had increased survival. TIGR4 is significantly more susceptible to neutrophil phagocytosis than SRL1 *in vitro* and experiments with mice depleted of neutrophils suggested that neutrophils were important in the survival difference demonstrated between strains. Subsequent studies with a further pneumonic strain (serotype 6B) also demonstrated increased survival in IL-17RA$^{-/-}$ mice. IL-17 was important in the control of nasal colonisation with both TIGR4 and SRL1. The nasal microbiome of IL-17RA$^{-/-}$ mice was significantly less diverse than that of wild type mice with the microbiome dominated by a small number of bacterial species. IL-22$^{-/-}$ mice had impaired resolution of inflammation and increased collagen deposition in lungs following treatment of pneumonia compared to wild type.

Conclusions: IL-17 is an important component of the immune response to pneumococcal disease although it can be either beneficial or harmful depending on the pneumococcal strain and site of infection. Further work will expand on the role of this cytokine in colonisation and disease.

Table of Contents

List of Figures 12

List of Tables 18

Acknowledgements 19

Abbreviations 20

1. Introduction 24

1-1 Streptococcus pneumoniae 24

1-1.1 Microbiology 24

1-1.2 Colonisation and infection 26

1-1.3 Virulence factors 32

1-1.4 Role of serotype in disease 37

1-2 Immune response to pneumococcal infection 42

1-2.1 Innate immunity 42

1-2.2 Humoral immunity 52

1-2.3 Cellular immunity 56

1-3 Interleukin-17 and interleukin-22 57

1-3.1 Background 57

1-3.2 IL-17 58

1-3.3 IL-22 61

1-3.4 IL-17 and IL-22 in health and disease 62

1-3.5 IL-17 and IL-22 in pneumococcal disease 64

1-4 Vaccination 66

1-4.1 History of pneumococcal vaccination 66

1-4.2 Capsular polysaccharide vaccine 67

1-4.3 Conjugate vaccine 68

1-4.4 Next generation vaccines 69

1-5 Summary, hypothesis and aims 70

1-5.1 IL-17 and IL-22 in pneumococcal disease 70

1-5.2 Hypotheses 70

1-5.3 Aims 71

2. Materials and Methods 82

2-1 Introduction 82
2-2 General Microbiology 82
2-2.1 Bacterial strains used 82
2-2.2 Cultivation of bacterial strains and colony counting 82
2-2.3 Identification of strains as pneumococci 83
2-2.4 Establishing serotype 83
2-2.5 Multilocus sequence typing 84
2-2.6 Electron Microscopy 84
2-2.7 Capsular thickness by dextran exclusion 85
2-2.8 Haemolysis assay 86
2-3 Human Co-culture Methods 86
2-3.1 Selection of healthy volunteers and patients with pneumococcal disease 86
2-3.2 Preparation of bacterial inoculum 87
2-3.3 Preparation of heat killed *Candida albicans* 87
2-3.4 Isolation of PBMCs and human serum 87
2-3.5 Isolation of monocytes and memory $CD4^+$ lymphocytes 88
2-3.6 Co-culture of monocytes and lymphocytes 88
2-3.7 Flow cytometry 90
2-3.8 Sorting of cells by CCR6 status 90
2-3.9 ELISA 90
2-3.10 Data analysis 90
2-3.11 Ethics statement 91
2-4 Animal models 91
2-4.1 Source, care and maintenance of animals 91
2-4.2 Clinical monitoring of infected animals 91
2-4.3 Confirmation of knockout phenotype of genetically modified mice 92
2-4.4 Generation of pneumococcal standard innocula 92
2-4.5 Innoculation of substances 93
2-4.6 Collection of samples 94
2-4.7 Organ homogenates 96
2-4.8 Myeloperoxidase and collagen assays 96
2-4.9 Wet/Dry ratio 97
2-4.10 Histopathology 97

2-4.11 Immunohistochemistry 100
2-4.12 Flow cytometry 101
2-4.13 In vivo Brefeldin A studies 102
2-4.14 Quantitative rt-PCR 102
2-4.15 Respiratory Tract Microbiome 103
2-4.16 Infection model RNA extraction and RNA-Seq 104
2-4.17 In vitro neutrophil studies 105
2-4.18 Studies with fluorescent bacteria 106
2-4.19 Neutrophil extracellular trap detection 107

3. Human T cell Responses to pneumococci 119

3-1 Introduction 119
3-2 Method Development 120
3-2.1 Development of co-culture model 120
3-2.2 Isolation of $CD14^+$ monocytes and $CD4^+$ memory T cells 120
3-2.3 $CD4^+$ memory T cell proliferation and cytokine secretion is dependent on monocytes 121
3-2.4 Gating strategy 121
3-3 Memory T cell responses in healthy young adult volunteers 121
3-3.1 Proliferative responses 121
3-3.2 Chemokine receptor staining 122
3-3.3 Secreted cytokines 123
3-3.4 Intra-cellular cytokine staining 123
3-3.5 Intracellular staining of CCR6 sorted cells 124
3-3.6 CD161 surface staining 124
3-3.7 Pooled analysis of intra-cellular cytokine staining 125
3-4 Memory T cell responses in healthy older adult volunteers 126
3-4.1 Proliferative responses 126
3-4.2 Secreted cytokines 126
3-4.3 Intra-cellular cytokines 127
3-5 Patients with IPD 128
3-5.1 Recruitment 128
3-5.2 Results 128
3-6 Discussion 129

4. Development of models of pneumococcal infection 151

4-1 Introduction 151
4-2 Characterisation of pneumococci 152
4-2.1 Identification of pneumococci and colony morphology 152
4-2.2 Serotyping 152
4-2.3 Capsule size 153
4-2.4 Electron microscopy 153
4-2.5 Haemolysis assay 154
4-2.6 Determination of MLST 154
4-3 Development of methods 154
4-3.1 Administration of substances via i.n. route 154
4-3.2 Development of neutrophil immunohistochemistry 155
4-4 Model of TIGR4 infection 156
4-4.1 General characteristics 156
4-4.2 Histopathological findings 157
4-5 Model of SRL1 infection 158
4-5.1 Selection of SRL1 as candidate bacterium 158
4-5.2 Dose titration 159
4-5.3 Time course experiment 160
4-6 Summary comparison of TIGR4 and SRL1 161
4-7 Cellular sources of IL-17 and IL-22 162
4-7.1 Clonal stimulation of cells in lung 162
4-7.2 In-vivo brefeldin A model 164
4-7.3 Depletion of gamma delta cells with monoclonal antibody 165
4-8 Discussion 165

5. The role of IL-17 and IL-22 in Invasive Pneumococcal Disease 204

5-1 Introduction 204
5-2 Confirmation of status of knockout animals 205
5-3 High dose TIGR4 infection in knockout animals 205
5-4 Low dose TIGR4 infection in knockout animals 206
5-5 Validation of flow cytometric method for quantifying neutrophils 207
5-6 TIGR4 infection in knockout animals (time point) 208
5-7 SRL1 infection in knockout animals 210

5-8 SRL1 infection in knockout animals (time point) 211
5-9 Bacteriology of SRL1 survivors 212
5-10 Summary of TIGR4 and SRL1 in knockout animals 212
5-11 Neutrophil mediated pneumococcal phagocytosis and killing 213
5-12 Neutrophil extracellular traps 213
5-13 Neutrophil depletion 214
5-14 Neutrophil depletion in TIGR4 infected mice 215
5-15 Neutrophil depletion in SRL1 infected mice 216
5-16 Summary of neutrophil studies 216
5-17 Characterisation of other pneumococcal strains 217
5-18 SRL2 in knockout animals 218
5-19 Discussion 220

6. The Role of IL-17 in Nasal Colonisation 271

6-1 Introduction 271
6-2 Nasal Colonisation studies 272
6-2.1 Establishment of nasal colonization model 272
6-2.2 Nasal colonization in IL-17RA$^{-/-}$ mice – TIGR4 272
6-2.3 Nasal colonization in IL-17RA$^{-/-}$ mice – SRL1 273
6-2.4 Nasal colonisation in IL-17RA$^{-/-}$ mice – time course 273
6-2.5 Presence of non-*S. pneumoniae* species in nasal wash 273
6-3 Nasal Microbiome 274
6-3.1 16S RNA Sequencing 274
6-3.2 Wild Type Microbiome 275
6-3.3 IL-17RA$^{-/-}$ Microbiome – Upper Respiratory Tract 276
6-3.4 IL-17RA$^{-/-}$ Microbiome – Lower Respiratory Tract 277
6-3.5 Respiratory tract microbiome following colonisation with SRL1 278
6-4 Discussion 282

7. RNA-Seq to Quantify Bacterial Gene Expression during SRL1 Infection 314

7-1 Introduction 314
7-2 SRL1 genome sequencing 315
7-3 SRL1 *In vivo* infection RNA-Seq 316
7-3.1 Infection with SRL1 316

7-3.2 Extraction and sequencing of RNA from infection model 316
7-3.3 Gene expression analysis 317
7-3.4 Upregulated region 1: ΦSpn_OXC prophage 317
7-3.5 Upregulated region 2: purine metabolism and *VanZ* 318
7-3.6 Upregulated region 3: *Blp* bacteriocin locus 318
7-3.7 Upregulated region 4: Pneumococcal surface adhesin A 319
7-4 Discussion 319

8. The role of IL-22 in recovery following pneumococcal pneumonia 331

8-1 Introduction 331
8-2 Recovery following pneumococcal pneumonia 332
8-3 Histopathology of recovering lung tissue 333
8-4 Collagen composition of recovering lung tissue 333
8-4.1 Histological assessment 333
8-4.2 Chemical assessment 334
8-5 Discussion 334

9. General Discussion 341

9-1 Key findings 341
9-2 Therapeutic implications and limitations 343
9-3 Future directions 345

References 350

List of Figures

1-1. Dynamics of pneumococcal colonisation in young children and the association with symptomatic disease. 72

1-2. Radiological and pathological features of pneumococcal pneumonia. 73

1-3. The variation in pneumococcal carriage and disease with age. 74

1-4. Structure of selected pneumococcal capsular polysaccharides and associated genetic loci. 75

1-5. Relationship between carriage acquisitions, invasive pneumococcal disease incidence and mortality. 76

1-6. Major pattern recognition receptors involved in innate sensing of *S. pneumoniae*. 77

1-7. IL-17 signaling and effects on target cells. 78

2-1. Algorithm for identification of pneumococci. 108

2-2. Method of image analysis used in measuring bacterial dextran exclusion. 109

2-3. Human antibodies. 110

2-4. Mouse antibodies. 111

3-1. Isolation of cells for co-culture. 133

3-2. Proliferation of memory T lymphocytes in response to pneumococcal stimulation is antigen presenting cell dependent. 134

3-3. Gating strategy used in analysis of lymphocyte/monocyte co-cultures. ... 135

3-4. Proliferation of memory $CD4^+$ cells in response to stimulation with pneumococci or *Candida albicans*. 136

3-5. Characterisation of chemokine receptor profile of proliferating and non-proliferating cells following stimulation with TIGR4 or HKCA. 137

3-6. Cytokine concentrations in co-culture supernatants. 138

3-7. Intracellular staining for cytokines following stimulation with PMA and ionomycin in the presence of Brefeldin A. 139

3-8. Pneumococcal responsive IL-17A and IL-22 producing CD4+ memory T cells are contained in the CCR6+ cells. 140

3-9. Lymphocytes proliferating in response to TIGR4 but not HKCA stimulation are enriched for CD161hi cells and are the principal IL-17A producing cells. 141

3-10. Proliferation of cytokine positive cells in co-cultures. 142

3-11. Combined cytokine expression of proliferating cells in co-cultures from young adults. 143

3-12. Total CD4+ proliferative responses among young and old adults. 144

3-13. Cytokine concentrations in co-culture supernatants. 145

3-14. Proliferation of cytokine positive cells in co-cultures. 146
3-15. Combined cytokine expression of proliferating cells in co-cultures from young and old adults. 147
3-16. T cell responses are similar between patients with recent IPD and healthy controls. 148

4-1. Appearance of Streptococcus pneumoniae isolates. 172
4-2. Molecular serotyping of streptococcus pneumoniae isolates. 173
4-3. Assessment of capsular area by fluorescent dextran exclusion. 174
4-4. Transmission electron microscopy of pneumococcal isolates. 175
4-5. Quantification of haemolytic activity of pneumococcal clones. 176
4-6. Deduction of multi-locus sequence type (MLST) of study bacteria. 177
4-7. Intra-nasal innoculation. 178
4-8. Use of anti-Ly6G antibody (clone 1A8) for immunohistochemistry in zinc fixed lung tissue. 179
4-9. Course of infection with TIGR4: weight loss and clinical score. 180
4-10. Course of infection with TIGR4: bacterial burden. 181
4-11. Course of infection with TIGR4: myeloperoxidase activity and BALF cytokine concentration. 182
4-12. Course of infection with TIGR4: histology. 183
4-13. Course of infection with TIGR4: immunohistochemistry and gram stain. . 184
4-14. Dose titration using SRL1: weight loss and clinical score. 185
4-15. Dose titration using SRL1: bacterial burden. 186
4-16. Dose titration using SRL1: gross pathology. 187
4-17. Dose titration using SRL1: histopathology. 188
4-18. Dose titration using SRL1: gram stain. 189
4-19. Course of infection with SRL1: weight loss and clinical score. 190
4-20. Course of infection with SRL1: bacterial burden. 191
4-21. Course of infection with SRL1: myeloperoxidase activity and BALF cytokine concentration. 192
4-22. Course of infection with SRL1: histopathology of lung parenchyma. 193
4-23. Course of infection with SRL1: histopathology of pleura. 194
4-24. Course of infection with SRL1: immunohistochemistry. 195
4-25. Comparison of TIGR4 and SRL1. 196
4-26. Cellular sources: gating strategy. 197
4-27. Cellular sources: cell populations. 198
4-28. Cellular sources: intracellular staining. 199

4-29. Cellular sources: summary of intracellular staining. 200
4-30. In-vivo Brefeldin A assay: gating strategy 201
4-31. In-vivo Brefeldin A assay: intracellular staining. 202
4-32. Gamma-delta depletion. ..... 203\

5-1. Confirmation of knockout animals. 226
5-2. Administration of high dose TIGR4 in knockout animals. 227
5-3. Administration of high dose TIGR4 in knockout animals. 228
5-4. Administration of low-dose TIGR4 in knockout animals. 229
5-5. Administration of low-dose TIGR4 in knockout animals. 230
5-6. Pooled analysis from two experiments involving low dose TIGR4 infection in knock-out animals. 231
5-7. Neutrophil identification by flow cytometry 232
5-8. Neutrophils in TIGR4 infection. 233
5-9. Bacterial density in TIGR4 infection. 234
5-10. Other measures of inflammation during TIGR4 infection 235
5-11. Comparison of IL17RA$^{-/-}$ and wild type mice in TIGR4 infection. 236
5-12. Comparison of IL17RA-/- and wild type mice in TIGR4 infection 237
5-13. Gene expression of IL-17 target genes in TIGR4 infection. 238
5-14. Comparison of IL17RA$^{-/-}$, IL22$^{-/-}$ and WT mice in SRL1 infection 239
5-15. Comparison of IL17RA-/-, IL22-/- and WT mice in SRL1 infection. 240
5-16. Comparison of IL17RA$^{-/-}$, IL22$^{-/-}$ and WT mice in SRL1 infection 241
5-17. Comparison of IL17RA$^{-/-}$ and wild type mice in SRL1 infection. 242
5-18. Comparison of IL17RA$^{-/-}$ and wild type mice in SRL1 infection. 243
5-19. Comparison of IL17RA$^{-/-}$ and wild type mice in SRL1 infection. 244
5-20. Comparison of IL17RA$^{-/-}$ and wild type mice in SRL1 infection. 245
5-21. Comparison of IL17RA$^{-/-}$ and wild type mice in SRL1 infection. 246
5-22. Gene expression of IL-17 target genes in SRL1 infection. 247
5-23. Persistant lower respiratory tract bacteria in IL17RA$^{-/-}$ mice following infection with 10^6 cfu SRL1. 248
5-24. Comparison of TIGR4 and SRL1 in neutrophil phagocytosis and killing assay. 249
5-25. Comparison of TIGR4 and SRL1 phagocytosis using flow cytometry. 250
5-26. Comparison of TIGR4 and SRL1 phagocytosis using fluorescence microscopy. 251
5-27. Detection of NET formation in neutrophils following stimulation with Streptococcus pneumoniae. 252

5-28. High resolution confocal images of Streptococcus pneumoniae caught in neutrophil extracellular traps (NET). 253

5-29. Summary statistics from comparison of NET formation after stimulation with SRL1 or TIGR4. 254

5-30. Depletion of neutrophils with antibodu 1A8. 255

5-31. Peripheral blood neutrophils are effectively depleted by the monoclonal antibody 1A8 24 hours after intra-peritoneal injection. 256

5-32. Neutrophil depletion in TIGR4 infection. 257

5-33. Weight loss and clinical score in animals infected with TIGR4 after depletion of neutrophils with anti-Ly6G antibody. 258

5-34. Peripheral blood neutrophil percentage and pneumococcal bacteraemia during the first 48 hours of TIGR4 infection following treatment with anti-Ly6G antibody or isotype control. 259

5-35. Depletion of neutrophils with monoclonal antibody 1A8 improves survival following infection with SRL1. 260

5-36. Weight loss and clinical score in animals infected with SRL1 after depletion of neutrophils with anti-Ly6G antibody. 261

5-37. Depletion of neutrophils with monoclonal antibody 1A8 results in depletion of neutrophils for at least 48 hours after the induction of infection with 10^6 SRL1. 262

5-38. Course of infection caused by SRL2-5 in wild type mice. 263

5-39. Bacteriology from mice infected 48 hours previously with various innocula of SRL2-5. 264

5-40. Histology from animals infected with 10^7 cfu/mouse SRL2-5 48 hours before. 265

5-41. Outcome after intranasal infection with 10^7 cfu SRL4 in IL17RA$^{-/-}$ and wild type animals. 266

5-42. Outcome after intranasal infection with 10^7 cfu SRL4 in IL17RA$^{-/-}$ and wild type animals. 267

5-43. Peripheral blood neutrophil percentages in wild type and IL-17RA$^{-/-}$ mice 24 hours after infection with SRL2. 268

5-44. Persistant presence of SRL4 in the lower airways of survivors one week after infection occurs only in IL-17RA$^{-/-}$ animals. 269

6-1. Establishment of nasal colonisation in wild type mice with SRL1 and TIGR4. 288

6-2. The role of IL-17 in TIGR4 nasal colonisation. 289

6-3. The role of IL-17 in TIGR4 nasal colonisation. 290

6-4. The role of IL-17 in SRL1 nasal colonisation: survival and weight change. 291

6-5. The role of IL-17 in SRL1 nasal colonisation: nasal wash. 292

6-6. The role of IL-17 in SRL1 nasal colonisation: time series. 293

6-7. Amplification of V_1-V_2 region of bacterial 16S gene from respiratory tract samples. 294

6-8. Assessment of sequencing depth. 295

6-9. Comparison between nasal wash and BALF in untreated wild type animals. 296

6-10. OTU level analysis of respiratory tract microbiome. 297

6-11. Differences among bacterial families in the respiratory tract. 298

6-12. Multiple testing of differences between bacterial species at the phylum level between upper and lower respiratory tract samples from wild type mice. 299

6-13. Comparison of diversity among upper respiratory tract samples of wild type and IL-17RA$^{-/-}$ mice. 300

6-14. Role of IL-17 in determining phyla distribution in the upper airways. 301

6-15. OTU level analysis of upper respiratory tract samples. 302

6-16. Multiple testing of differences between bacterial species at the family level between upper respiratory tract samples from wild type and IL-17RA$^{-/-}$ mice. 303

6-17. Comparison of diversity among lower respiratory tract samples of wild type and IL-17RA$^{-/-}$ mice. 304

6-18. Multiple testing of differences between bacterial species at the phylum level between upper respiratory tract samples from wild type mice and IL-17RA$^{-/-}$ mice. 305

6-19. OTU level analysis of lower respiratory tract microbiome. Taxa relative abundance among wild type and IL-17RA$^{-/-}$ mice. 306

6-20. Multiple testing of differences between bacterial species at the family level between lower respiratory tract samples from wild type and IL-17RA$^{-/-}$ mice. 307

6-21. Dispersion of all respiratory tract samples by Bray distance. 308

6-22. Identification of streptococci within respiratory tract microbiome. 309

6-23. Change in alpha diversity over time. 310

6-24. Distribution of individual OTUs in upper respiratory tract following SRL1 exposure. 311

6-25. Distribution of individual OTUs in lower respiratory tract following exposure to SRL1. 312

6-26. Association between OTU2 (Streptococcus including SRL1) and OTU1 (Ochrobactrum). 313

7-1. Sequencing of the SRL1 genome aligned against the OXC141 reference genome. 323

7-2. Course of SRL1 infection. 324

7-3. Isolation of RNA from in vivo samples. 325

7-4. Outcome of read mapping against OXC141 reference genome. 326
7-5. Mapping of reads against reference genome.....327
7-6. Correlation between normalised gene expression in broth and pleura. 328

8-1. Course of SRL1 infection interrupted with antibiotic therapy. 337
8-2. Histological changes in animals recovering from pneumococcal pneumonia. 338
8-3. Summary of histological scoring in SRL1 infection treated with antibiotics. 339
8-4. Collagen composition of lungs during recovery from pneumococcal pneumonia.....340

9-1. Absence of positive correlation between attack rates of donor and recipient seortypes in naturally occurring serotype switches.....349

List of Tables

1-1. Summary of studies investigating the role of IL-17 and/or IL-22 in pneumococcal disease in humans or animal models. 81

2-1. Serotyping primers. 113
2-2. MLST primers. 114
2-3. Scoring system for the monitoring of animals infected with pneumococcal strains. 115
2-4. Animals found dead while on ASPA procedure during study. 116
2-5. Scoring system for assessing pulmonary inflammatory change on histological sections of mouse lung. 117
2-6. V_1-V_2 16S RNA sequencing primers with Golay barcode. 118

3-1. List of healthy volunteers recruited to the study. 149
3-2. List of patients with IPD recruited to the study. 150

5-1. Sex balancing of groups in experiments involving male and female mice. 270

7-1. Upregulation of coding regions during infection in SRL1. 329
7-2. Downregulation of coding regions during infection in SRL1. 330

Acknowledgements

There are a great many people that I need to thank for their assistance in helping to make this thesis a reality. Firstly, I would like to thank my supervisors. Professor Tom Evans encouraged me to do research for years before I started working in his group and his support throughout every stage of the process that led to this piece of work was invaluable. I am very grateful. Although my second supervisor, Professor Tim Mitchell left Glasgow at the same time as my project started, his assistance particularly in the early days of setting up the animal model and working with the pneumococcus was invaluable. My faculty assessors, Andy Roe and Robb Nibbs also provided help and advice freely. The other members of the Evans group over the last five years (Cecilia Lindestam, Alex Macpherson, Hannah Bayes, Sharon Irvine, Ihsan Ullah, Majid Jabir and Ruth Mccartney) have all contributed to helping me with words of support and practical help - the 6am starts were particularly appreciated.

There have been a large number of other researchers who have also provided me with help and advice. I would like to thank Ryan Ritchie, Eleanor Anderson and Andrea Mitchell who all assisted me with the practical aspects of animal modelling. Giles Edwards provided pneumococcal strains from the reference laboratory. Jim Reilly and Shauna Kerr taught me how to be a passible histologist and given my previous complete failure to learn anything so fiddly proficiently this was a considerable achievement. Margaret Mullen provided technical support and specimen processing expertise for electron microscopy. Chris Quince, Asha Rani and Umer Ijaz provided invaluable help with conducting and interpreting microbiome studies while the staff at the Centre for Genomic Research at the University of Liverpool, particularly John Kenny, helped with the challenging process of generating samples of high quality RNA from empyema fluid. With regard to the clinical research study reported here I would like to acknowledge the assistance of Alisdair MacConnachie and Mary Brown who kindly allowed me to approach patients attending their clinics. Aleks Marek and Andrew Seaton helped me to identify patients with pneumococcal bacteraemia for the study. I would particularly like to thank the patients who contributed to this study; without their help it would not have been possible to perform this research.

Abbreviations

1%AA	1% acid alcohol
ABC	Adenosine triphosphate binding cassette
Act1	NFκB activator 1
aliA	ami-like ABC transporter
AOM	Acute otitis media
ASC	Apoptosis-associated speck-like protein containing a CARD
ASPA	Animals (Scientific Proceedures) Act
ATP	Adenosine triphosphate
BAL	Broncho-alveolar lavage
BHI	Brain heart infusion
Blp	Bacteriocin-like peptide
BSA	Bovine serum albumin
CbpA	Choline binding protein A
CCL	Chemokine ligand
CCR	C-C chemokine receptor
CD	Complex of differentiation
CDC	Centres for Disease Control
CGR	Centre for Genomic Research, University of Liverpool
cps	Capsular polysaccharide
CSF	Cerebrospinal fluid
CTLA	Cytotoxic T lymphocyte antigen
CXCL	Chemokine (C-X-C motif) ligand
DAB	3,3'-diaminobenzidine
dexB	Glucan 1,6-alpha-glucosidase

EDTA	Ethylenediaminetetraacetic acid
ELISA	Enzyme linked immunosorbant assay
FACS	Fluorescence-activated cell sorting
FCS	Foetal calf serum
FDR	False discovery rate
G-CSF	Granulocyte colony stimulting factor
GATA	GATA motif binding transcription factor
GlpD	Glyceraldehyde 3-phosphate dehydrogenase
GlpF	Glycerol uptake facilitator
GM-CSF	Granulocyte-monocyte colony stimulating factor
H&E	Haematoxylin and eosin
HBSS	Hank’s balanced salt solution
HIV	Human immunodeficiency virus
HKCA	Heat killed *Candida albicans*
HTAB	Hexadecyltrimethylammonium bromide
IBW	Initial body weight
i.n.	Intra-nasal
IFN	Interferon
IL	Interleukin
ILC	Innate lymphoid cells
IMDM	Isocove's modified Dulbecco's medium
iNKT	Invariant natural killer T cells
IPD	Invasive pneumococcal disease
LOD	Limit of detection
LytA	Autolysin A

MACS	Magnetic-activated cell sorting
MAPK	Mitogen activated protein kinase
MHC	Major histocompatibility complex
MLST	Multilocus sequence typing
MOI	Multiplicity of infection
MPO	Myeloperoxidase
MyD88	Myeloid differentiation primary response gene 88
NBF	Neutral buffered formalin
NET	Neutrophil extracellular trap
NF-κB	Nuclear factor-κB
NGS	Next generation sequencing
NLR	Nod-like receptor
NLRP3	Nod-like receptor family, pyrin domain containing 3
NMDS	Non-metric multidimensional scaling
Nod-2	Nucleotide-binding oligomerization domain-containing protein 2
OD	Optical density
OR	Odds ratio
OTU	Operational taxonomic unit
PAMP	Pathogen associated molecular pattern
PBMC	Peripheral blood mononuclear cells
PBS	Phosphate buffered saline
PCR	Polymerase chain reaction
PCV	Pneumococcal conjugate vaccine
PhtD	Pneumococcal histidine triad protein D
Ply	Pneumolysin

PMA	Phorbol 12-myristate 13-acetate
PMEN	Pneumococcal molecular epidemiology network
PRR	Pattern recognition receptor
PsaA	Pneumococcal surface adhesin A
PspA	Pneumococcal surface protein A
PspC	Pneumococcal surface protein C
qRT-PCR	Quantitative RT-PCR
ROR-gt	RAR-related orphan receptor gamma
RPMI	Roswell Park Memorial Institute
SHLMPRL	Scottish Haemophilus, Legionella, Meningococcus and Pneumococcus Reference Laboratory
STAT	Signal transducer and activation of transcription
STWS	Scott's tap water substitute
TBP	TATA-binding protein
TCR	T cell receptor
TCS	Two component signal transduction system
Th	T helper
TLR	Toll-like receptor
TNF	Tumour necrosis factor
TRAF6	Tumor necrosis factor receptor-associated factor 6
URTI	Upper respiratory tract infection
WCV	Whole cell vaccine
xid	x-linked immune deficiency
ZTF	Zinc-Tris fixative

1. INTRODUCTION

1-1 Streptococcus pneumoniae

1-1.1 Microbiology

Streptococcus pneumoniae (the pneumococcus) is an alpha haemolytic gram-positive coccus which is a common cause of human disease. It has an important place in the history of medicine and is one of the longest studied of human pathogens.

The pneumococcus was discovered independently by Sternberg in the United States[1] and Pasteur in Europe[2] after experiments involving the injection of human saliva into rabbits which subsequently developed sepsis and died. A gram-positive coccus was isolated from the blood of the animals and as its propensity to cause pulmonary disease became clear it was named *Diplococcus pneumoniae* in reference to the typical appearance of the organism on microscopy where it occurs in pairs. Until 1974, the pneumococcus was regarded as part of a separate genus from the streptococci (which are usually seen occurring in chains on microscopy). However, it was increasingly recognised that pneumococci shared many of the characteristics of streptococci, including the formation of chains in liquid culture, and the organism was renamed *S. pneumoniae*[3].

Pneumococci can be identified as gram-positive cocci which are catalase negative and can be dissolved in bile salts[4]. Pneumococci are sensitive to the antibiotic Optochin and this is useful in distinguishing them from other streptococci associated with the oral and nasal cavity such as *Streptococcus viridans*. Pneumococci usually require rich media for cultivation and grow well on agar plates supplemented with blood. Growing on blood agar, the colonies

are alpha haemolytic due to the presence of the pneumococcal haemolysin — pneumolysin — and usually have a characteristic “draughtsman” appearance due to the autolysis of bacteria at the centre of the colony. Pneumococci grow best at 37˚C in an atmosphere supplemented with CO_2 but many also grow well in room air. A minority of pneumococci are mucoid in appearance; a feature that is thought to represent a high degree of encapsulation.

It was recognised early in the history of pneumococcal science that pneumococci vary widely in their characteristics and virulence. Shortly after being among the first to describe the pneumococcus, Sternberg wrote:

> *"How it happens that the [pneumococcus] in one man's mouth possesses just the proper degree of vital activity to kill a rabbit in two days, while that from another man's mouth kills in four days and that from another does not kill at all, is a most interesting question and one worthy of the attention of future investigations."* [1]

It has since been recognised that pneumococci are a highly diverse bacterial species. Early researchers used serotyping of bacterial isolates as the primary means of classification and more than 90 pneumococcal serotypes are now known[5]. Pulsed field gel electrophoresis (PGFE) was subsequently used to classify strains[6] and it became clear that pneumococci are able to undergo capsular switch events so that closely related clones can express different polysaccharide capsules[7]. More recently, multi-locus sequence typing (MLST) based on the sequence of short segments of housekeeping genes has been used [8]. This has allowed rapid identification of related pneumococci and ready comparison with strains in other reference laboratories around the world. The pneumococcus has a core genome consisting of 70% of its total genes with the remainder widely variable between clones[9]. Accessory regions often contain putative virulence factors and this variation demonstrates the redundancy in pneumococcal virulence and creates formidable challenge for those seeking to understand how pneumococci cause disease[10].

There is also evidence that pneumococci are evolving in response to human intervention [11]. Penicillin non-susceptible *S. pneumoniae* (PNSSP) appeared

within a few years of the widespread introduction of antibiotics[12] and are now common throughout much of the world – although not the United Kingdom (UK)[13]. More recently, evidence has emerged of pneumococci responding to vaccine induced selection pressure by undergoing capsular switch events so that highly virulent lineages such as the penicillin resistant PMEN1 clonal complex could evade conjugate vaccine[14].

1-1.2 Colonisation and infection

1-1.2.1 Nasal colonisation

All episodes of pneumococcal infection are thought to begin with an episode of asymptomatic nasal colonisation[15]. Pneumococci are well adapted to successfully colonise the upper respiratory tract and episodes of nasal colonisation are essentially ubiquitous throughout all periods of life. However, nasal colonisation is much more common in young children and tends to be longer in duration[16,17]. Prevalence of nasal colonisation increases again with advancing age once patients reach middle age at least in some populations[18] although colonisation in hospitalised elderly people is uncommon[19]. Nasal colonisation, at least in developed countries, demonstrates seasonality with increased incidence of colonisation during the winter months[20]. There is a widely reported association of carriage with coryzal illness and it may be that the pneumococcus is able to take advantage of upper respiratory tract viral infection to facilitate the establishment of carriage and person-to-person spread[21].

Pneumococci within the nose are found in one of two phases. Transparent pneumococci express relatively modest amounts of polysaccharide capsule while opaque phase pneumococci have a thick capsule[21]. Pneumococci have been observed to switch phase spontaneously[22]. Transparent phase pneumococci most readily establish experimental nasal colonisation in animals and are readily recovered from colonised animals by gentle nasal washing[23]. In contrast, opaque phase organisms are usually recovered from normally sterile sites during symptomatic disease and are more virulent than transparent phase organisms in animal models of invasive disease[24]. Opaque phase organisms have also been shown to be more closely associated with the nasal mucosa during colonisation so that they are more readily detected in dissected nasal tissue than in nasal

washes suggesting that expression of capsule is important in deep attachment and invasion[25].

Duration of colonisation is variable but some in some cases can last for many months. However, when symptomatic infection does occur it usually follows shortly after acquisition of carriage[15] (figure 1-1). The factors affecting the outcome of a colonisation event are not well understood. Factors specific to the pneumococcus will be discussed later in sections 1.3-4. Host factors include intercurrent viral infection, age, comorbidity and alcohol dependence[26].

1-1.2.2 Otitis media

Acute otitis media (AOM) is the most common form of symptomatic pneumococcal infection in children and pneumococci are the most commonly identified bacterial cause. It results from the entry of the bacteria into the middle ear. Purulent material builds up in this space and rising pressure causes pain and can lead to local damage such as perforation of the tympanic membrane and hearing loss.

AOM is very common in childhood and is often recurrent[27]. An elegant study demonstrated that viral upper respiratory tract infection (URTI) in the presence of nasal colonisation with one of the bacterial causes of AOM is the aetiology of this infection[28]. It is hypothesised that viral URTI leads to Eustachian tube dysfunction and failure of mucocilliary clearance which creates conditions facilitating the proliferation of bacteria (including *S. pneumoniae*) within the middle ear[29]. Development of AOM has been shown to correlate with the number of bacterial species colonising the nose[30] and the bacterial burden as determined by qRT-PCR[31].

As infants mature into older children and adults, the combination of reduced incidence of nasal colonisation and anatomical changes to the Eustachian tube that encourage drainage make AOM uncommon and if it occurs in adults it is often related to an underlying medical condition.

1-1.2.3 Pneumonia

In order to cause pulmonary infection, the pneumococcus must enter the lower respiratory tract and overwhelm initial pulmonary defences. Even healthy humans aspirate small quantities of nasal contents, including colonising bacteria, during sleep[32]. High colonisation density or disruption of the normal mucocilliary clearance could then lead to the development of pneumonia (figure 1-2).

Pneumococcal pneumonia in otherwise healthy individuals is usually confined to a single lobe – probably representing the initial focus where pulmonary defences were overwhelmed[33]. In contrast, those at the extremes of age or with significant underlying co-morbidity often develop a more diffuse bronchopneumonia, characterised by the presence of patchy areas of consolidation distributed throughout the lungs. Bacterial pneumonia is characterised by acute inflammation of the lung parenchyma. It is traditionally divided into four pathological stages:

1. Congestion: the alveoli become filled with proteinaceous fluid and the lung has a characteristic dense, red appearance on gross pathology. This stage lasts for around one day.

2. Red hepatisation: the affected lung becomes densely infiltrated with inflammatory cells, particularly neutrophils. There is also extensive extravasation of red blood cells. By this stage, the lung loses its aeration and its gross appearance is similar to that of liver. This stage lasts for around one week.

3. Grey hepatisation: as the inflammation matures, the inflammatory cells have undergone apoptosis and the red cells have been broken down. The lung changes colour from red to grey during this stage but remains densely infiltrated. This stage typically lasts for a few days.

4. Resolution: the underlying lung architecture typically remains intact during an episode of bacterial pneumonia and so, as the exudate and

cellular infiltrate are removed, the lung usually recovers completely from the acute insult after a period of a few weeks.

Pneumonia causes serious disease because it may lead to respiratory failure but also because the high density of bacteria within the consolidated lung can lead to dissemination to distant body sites.

1-1.2.4 Bacteraemia

The presence of bacteraemia is the hallmark of invasive pneumococcal disease (IPD), defined as the isolation of pneumococci from a normally sterile body site which is taken to exclude the lower respiratory tract and middle ear[34]. Since the route of entry to other body sites is believed to be via haematogenous spread, when pneumococci are isolated from these sites bacteraemia can be assumed. The incidence of IPD in the young follows a similar age related distribution to nasal colonisation but the rise in older adults is more pronounced than any observed increase in carriage[35] (figure 1-3). IPD is uncommon in young adults except in the presence of risk factors such as chronic respiratory disease[36], diabetes[37] or heart disease[38]. Cigarette smoking has also been implicated as an important risk factor for IPD[39]. Historically, the most important risk factor for IPD measured in terms of individual risk was asplenia (including functional asplenia)[40]. Immunoglobulin deficiencies are major risk factors for IPD and in the last years of the 20th century human immunodeficiency virus (HIV) infection emerged as an important risk factor in young adults[41]. Even patients with HIV but a normal $CD4^+$ count are at substantially increased risk of IPD[42]. A large population based study in England and Wales found that 7.8% of those diagnosed with IPD aged between 15 and 44 years were HIV positive (almost a third of these were undiagnosed at the time)[43].

Prior to the introduction of effective vaccination for infants, 4% of children presenting to outpatient departments with undifferentiated fever and no signs of severe illness were found to have pneumococcal bacteraemia[14] and only around 2% of such children go on to develop meningitis or another serious complication[44]. This finding is in contrast to the finding of unexpected *Neisseria meningitidis* bacteraemia, which was associated with subsequent development

of meningitis in 50% of cases in the same study. Recent studies suggest that occult pneumococcal bacteraemia has become much less common since the introduction of pneumococcal conjugate vaccine (PCV)[45]. The practice of culturing the blood of children presenting with fever but are to be discharged from the emergency department or from primary care is now being discouraged in North America[46]. In Europe, blood cultures have never been widely performed in this population and potential for ascertainment bias must be considered when evaluating studies of pneumococcal bacteraemia in children.

In adults, occult pneumococcal bacteraemia is rare[47] and the presence of pneumococci in the blood is an indicator of severe disease. Prior to the development of antibiotics and serum therapy, fewer than one in five adults survived an episode of pneumococcal bacteraemia[48]. The situation has dramatically improved over the last 60 years since the introduction of penicillin therapy but the 30-day mortality following IPD in Scotland remains 13% increasing to 25% in those over the age of 75[49].

1-1.2.5 Meningitis

In developed countries, the pneumococcus is the most common cause of bacterial meningitis in adults and is the second most common cause in children after *N. meningitidis*[50,51]. With the recent decline in the incidence of meningococcal meningitis following the introduction of an effective vaccine against all types other than sergroup B, pneumococcal disease is now the most common bacterial cause of meningitis overall in the UK and USA[50,51].

Meningitis occurs when bacteria cross the blood brain barrier and are able to multiply within the cerebro-spinal fluid (CSF). It is thought that the critical event is likely to be bacterial entry into the CSF since the central nervous system is an immunoprivileged site and bacteria will be free to replicate within it for some time without restraint. In the absence of trauma, haematogenous spread has been assumed to be the route by which the pneumococcus gains access to the CSF in most instances as evidenced by the subsequent development of meningitis in some children with bacteraemia[44] and the well recognised association of meningitis with endovascular infection[52,53]. However,

some animal studies have demonstrated penetration of organisms from the nasal cavity into the olfactory bulb in animal models[25,54] and it may be that some cases occur by direct spread without the occurrence of preceding bacteraemia.

Pneumococcal meningitis is an extremely destructive disease. Tissue destruction has multifaceted causes. It is partly due to bacterial factors such as the action of toxins[55], induction of tissue hypoxia and hypoglycorrhachia[56]. However, host factors such as blockage of CSF flow leading to raised intracranial pressure and the exuberant immune response are also responsible for much of the tissue damage[57]. This has prompted the use of corticosteroids for their anti-inflammatory action in pneumococcal meningitis with evidence of decreased mortality and long-term neurological sequelae such as deafness[58].

1-1.2.6 Empyema thoracis

Para-pneumonic effusion is common in humans with pneumococcal pneumonia[59,60]. Usually the pleural fluid is sterile and it is thought to result from inflammatory changes in the visceral pleura overlying the affected lung. Such uncomplicated parapneumonic effusion usually responds well to systemic antibiotic therapy for the underlying pneumonia and the pleural fluid is resorbed over several weeks. Complicated para-pneumonic effusion occurs when the pleural fluid becomes infected because of direct or haematogenous spread of bacteria from the lungs. Left untreated, infected pleural fluid will become purulent and may become loculated. Treatment for complicated pleural effusion and empyema is drainage or surgical excision of pleural fluid in combination with antibiotic treatment. However, in contrast to consolidated lung which usually undergoes complete resolution of the inflammation, empyema frequently results in scarring and persistant pleural abnormality[61].

1-1.2.7 Other clinical presentations

Pneumococcal conjunctivitis is a relatively common clinical finding especially in children[62]. Culprit pneumococci are usually untypable which implies lack of capsular polysaccharide and therefore these organisms are extremely unlikely to cause IPD.

Other clinical presentations of pneumococcal disease are unusual but include endocarditis (which is usually destructive)[63], primary pneumococcal peritonitis[64] and septic arthritis[65].

1-1.3 Virulence factors

1-1.3.1 Capsular polysaccharide

As discussed above, pneumococci isolated from normally sterile body sites almost ubiquitously express capsular polysaccharide emphasising its importance as a critical virulence factor. There is tremendous variation in pneumococcal capsular polysaccharide with over 90 serotypes currently known[5]. Most capsular polysaccharides are relatively complex structures with many different sugars in branching arrangements and are covalently anchored onto the cell wall peptidoglycan[66]. However, the serotype 3 capsule is much simpler, consisting of just two repeating carbohydrates (figure 1-4). Serotypes 3, along with serotype 37, also lacks the genes necessary for Wzx/Wzy-dependent capsule formation which generates polysaccharide covalently joined to the cell wall peptidoglycan[67]. Instead, serotype 3 expresses a membrane bound polysaccharide synthase and the polysaccharide remains non-covalently associated with the enzyme complex[68].

Genes required for the expression of capsular polysaccharide are found within the *cps* locus of the pneumococcal chromosome. This is a 10-25 kb locus flanked by the genes *dexB* and *aliA*[69]. The consistent structure of the *cps* locus and flanking regions allows genetic exchange of the entire locus between pneumococci resulting in mutants of a different serotype. Such capsular switch mutants occur relatively frequently[11,70] and may be a mechanism by which pneumococci evolve under vaccine pressure[71].

Capsule appears to play multiple roles in determining the virulence of the organism. Capsule inhibits opsonophagocytosis by a number of different mechanisms. These include: prevention of the binding of complement to the cell surface[72], shielding of cell surface antigens[73], inhibition of the interaction of bound antibody and complement to their receptors[74,75], protection from

mucociliary clearance[76] and protection of pneumococci from neutrophil extracellular traps (NET)[77].

As discussed above, pneumococci exist in one of two states – opaque and transparent. Transition from one phase to the other is possible in both directions[78] and occurs relatively frequently in liquid culture (with a reported frequency of 10^{-3} to 10^{-6})[22]. Electron microscopy of phase switched pneumococci reveals distinct cellular structures. Opaque pneumococci have thick capsular polysaccharide but thin cell wall whereas transparent pneumococci have thin capsular polysaccharide but a thick cell wall structure[22]. Transparent pneumococci demonstrated increased adhesion to respiratory epithelial cells through a process thought to be mediated by binding of phosphorylcholine to human surface adhesins and the platelet-activating factor receptor[79]. Phase switching has been associated with the presence of the genes *GlpD* and GlpF, which are similar to glycerol metabolism genes[80]. These genes were not absolutely required for phase switching however and the molecular mechanism leading to phase switching remains unclear, although a genetic modification seems the likely method. It has been observed that pneumococci down-regulate capsule expression when in close association with respiratory epithelial cells within an hour of infection suggesting that such phase variation is likely to be induced by environmental stimuli[81]. Hypoxia is likely be one such stimulus to capsule production[82] and this may allow the pneumococcus to sense penetration to deeper sites where capsule mediated protection from complement and phagocytes is more important. Recent work emphasising the importance to pneumococcal virulence of a promoter capable of dynamically altering capsular gene expression demonstrates the importance of phase variation in the survival of pneumococci[83].

1-1.3.2 Pneumolysin

Pneumolysin (Ply) is a cholesterol dependent cytolysin produced by virtually all clinical pneumococcal strains. It is structurally related to similar toxins produced by other gram positive pathogenic bacteria such as *Streptococcus pyogenes*, *Clostridium perfringens* and *Listeria monocytogenes*[84]. Ply is a pore-forming toxin that has several well-defined actions of which the most prominent are

cytolysis and complement activation. Cytolysis occurs when Ply becomes associated with the cell membrane and assembles into a multi-unit membrane attack complex generating a pore in the cell membrane[85]. Pore formation can cause cell death directly or can stimulate apoptosis at sub-lytic concentrations[86]. Ply mediated complement activation is thought to be due to interaction with C1q and the Fc portion of immunoglobulin leading to the activation of the classical pathway[87]. In compartments in which the availability of complement is a limiting factor in the host response, this Ply mediated consumption of complement may protect pneumococci from complement attachment.

Ply is an important mechanism of interaction between the immune system and the pneumococcus. Ply causes inflammasome activation via mechanisms that have been variously described as Toll-like receptor (TLR)-4 dependent[86,88] and independent[89]. Since the inflammasome is a major mediator of acute inflammation through stimulation of IL-1ß release from cells, Ply leads to substantial activation of the immune response[90]. Indeed, infusion of Ply into the lungs of a mouse is sufficient to cause inflammatory changes very similar to acute pneumococcal pneumonia[91].

Ply is unique amongst the cholesterol dependent cytolysins in that it lacks a N-terminal secretion signal sequence[92] and it used to be thought that Ply was released from the bacterial cell only on lysis[93]. However, recent work suggests that Ply is transported outside intact pneumococci and displayed on the surface[94]. The mechanism and relative contribution of these mechanisms remains unclear.

This complex dynamic in which Ply stimulates the immune response and also facilitates immune evasion results in a multifaceted contribution of Ply to *in vivo* virulence. Ply null mutants were significantly attenuated following intra-nasal inoculation[95]. Ply null mutants administered by intra-venous injection caused persistent moderate level bacteraemia that could be present for several weeks in contrast to the exponential expansion and rapid death in wild type infection[96]. Targeted point mutation of the pneumolysin gene to ablate the cytolytic activity, complement activating activity, or both together demonstrated that both roles are important in microbial pathogenesis (at least in the serotype 2

organism tested)[97]. Interestingly, pneumococci expressing Ply with a combination of mutations ablating both actions of pneumolysin were still significantly more virulent than a Ply knockout strain, implying a further, as yet unrecognised, role for the toxin in virulence. However, pneumococci expressing attenuated Ply variants had an early survival advantage in mouse lung compared to wild type organisms[98]. Despite this survival advantage, pulmonary inflammation as detected by histology in mice infected with mutant Ply (either cytolysis or complement activation inactive) was significantly reduced. Therefore while pneumolysin in clearly a critical virulence factor in pneumococcal disease, its potent immune activating functions result in more rapid recruitment of immune cells (particularly polymorphs) and inflammation which may be detrimental to the persistence of the organism.

Some naturally occurring Ply alleles have been observed that lack cytolytic activity[99]. These alleles have been observed in pneumococci that, as will be discussed later, are associated with invasive disease but rarely with colonisation[100] and such alleles were not found in a collection of strains collected from asymptomatically colonised children[101].

The role of pneumolysin in nasal colonisation is less clear. Several studies have shown that deletion of the Ply gene leads to prolonged pneumococcal carriage in mice[102-104]. In contrast, one study found decreased bacterial numbers early in colonisation in a Ply deficient mutant[105] while another found rapid clearance of a similarly constructed Ply^- strain[106]. It is surprising that a virulence factor expressed by almost all clinical isolates is not clearly associated with survival in the organism's primary niche. While strain related differences may be important, this suggests that there is a further function of Ply that remains to be elucidated or that mouse models are not adequately replicating this aspect of the human system.

1-1.3.3 Pneumococcal surface protein A

S. pneumoniae has a number of proteins which bind to phosphorylcholine on the cell wall. One of these, pneumococcal surface protein A (PspA) is able to inhibit the binding of complement[107] and apolactoferrin[81] to the pneumococcal surface.

The contribution of PspA to virulence has been conflicting and may be serotype dependent[72].

1-1.3.4 Pneumococcal surface protein C

Pneumococcal surface protein C (PspC) is a further choline binding protein expressed by the majority of pneumococcal isolates. Like PspA, PspC appears to have two distinct functions that aid virulence. PspC is a factor H binding protein. Since factor H is an endogenous inhibitor of complement activation, association of pneumococci with factor H inhibits the activation of complement associated with the pneumococcal cell[108]. PspC also binds to the IgA receptor on the surface of respiratory epithelial cells[109]. This function aids adhesion of pneumococci to respiratory epithelium and may aid invasion.

1-1.3.5 Pneumococcal surface adhesin A

Pneumococcal surface adhesin A (PsaA) is the lipoprotein component of an ATP-binding cassette with important functions in manganese transport[110]. This basic function has confounded investigation of the significance of PsaA as an adhesin[111]. However, it does appear that PsaA also has an important role in pneumococcal virulence as a promoter of adhesion.

1-1.3.6 IgA1 Protease

Most IgA present within the nasal cavity is IgA1. Many prevalent nasal colonising bacteria produce IgA proteases including the pneumococcus. The pneumococcal IgA1 protease cleaves human IgA but does not have activity against mouse IgA[112], which may be a significant deficiency of mouse models of nasal colonisation. Cleavage of IgA1 by pneumococcal protease protects pneumococci from the opsonic effect of IgA[113] and also promotes pneumococcal adherence[114]. IgA1 protease expressing organisms are resistant to the passive immunising effect of anti-pneumococcal human IgA1 in a mouse model[115].

1-1.3.7 Autolysin A

Autolysin A (LytA) is the pneumococcal virulence factor that is responsible for the characteristic central colony lysis of the pneumococcus[116]. LytA mutants

have reduced virulence in animal models[117]. It is thought that the importance of LytA is related to the autolysis mediated release of other virulence factors such pneumolysin and cell wall components[118].

1-1.4 Role of serotype in disease

1-1.4.1 Clinical associations of serotype with disease

As discussed in the previous section, pneumococci have enormous diversity in the capsular polysaccharide and more than 90 different serotypes can be distinguished by immunophenotyping and genetic studies[67]. It has long been recognised that there are differences in the epidemiological characteristics of pneumococcal serotypes. In the early 20th century only serotypes 1-3 (at the time referred to as types I-III) were immunologically defined and other encapsulated pneumococci were placed in type IV. It was recognised that serotypes 1 and 2 were overrepresented in blood culture isolates compared to their prevalence in nasal colonisation studies[119]. As more serotypes were defined, it was possible to more accurately define the clinical characteristics of infection and Robert Austrian was able to demonstrate that serotype 3 was a associated with a higher mortality than other serotypes despite being less likely to be isolated from blood than other common serotypes such as 1 and 2[120].

In the modern era, several large studies have examined the clinical outcome of patients with invasive pneumococcal disease. The largest of these is a Danish study which was able to report the outcome of every patient with IPD in Denmark over a ten year period[121]. Compared to the serotype 1, which was the reference serotype and had the lowest associated 30-day mortality, nine serotypes had odds ratio for mortality greater than three. This was despite adjustment for several confounders including age, comorbidity and site of infection. The most common serotypes in this high mortality group were serotypes 3 and 19F. In contrast, common serotypes with an odds ratio for mortality below two include 4, 5 and 7F. A subsequent meta-analysis of similar studies replicated these findings and demonstrated that the relative mortality associated with pneumococcal serotypes was stable in different times and geographical locations[122]. A recent analysis of Scottish outcome data produced similar trends – although the smaller sample size limited the study power[49].

Disease complications have also been compared between serotypes although, since complications are rarely reported to reference laboratories, the sample size of these studies is generally less with concomitant loss of power. Some specific associations have been consistently reported. Several studies have found serotype 3 to be associated with an increased risk of presentation with septic shock[123,124] and necrotising pneumonia[125]. In contrast, non-pulmonary foci of disease have often been associated with the lower mortality serotypes such as serotype 1, 5 or 7F.

It should be noted that since these studies are based on a case definition that includes isolation of pneumococci from blood or CSF, they are not applicable to pneumonia or other non-invasive forms of disease. However, the study by Austrian also performed culture and typing of pneumococci from sputum and demonstrated a higher mortality in infections caused by serotype 3 compared to serotype 1[48]. More recently, a further Danish study compared bacteraemic and non-bacteraemic pneumococcal pneumonia in which the infecting serotype was known[126]. The study was too small to estimate mortality from individual serotypes but the study compared severity at presentation in patients with 1, 5 and 7F with all the others. In bacteraemic pneumonia, these serotypes were associated with greater severity in keeping with previous IPD studies. However in non-bacteraemic pneumonia the converse was observed with serotypes 1, 5 and 7F causing more severe disease. Most disease caused by serotypes 1, 5 and 7F was bacteraemic (63/77, 82%) whereas only a minority of disease caused by the other serotypes was bacteraemic (129/387, 33%). This suggests that the high odds ratio for mortality associated with the other serotypes in IPD studies may be due to ascertainment bias and that rather than causing more severe disease, these serotypes only enter the blood during more severe disease. This is in contrast to serotypes 1, 5 and 7F which are likely to enter the blood even in non-severe disease. The increasing availability of molecular diagnostics for pneumococcal infection is likely to clarify our understanding of this area since they allow identification of the infecting serotype in non-bacteraemic pneumonia with much higher sensitivity.

Empyema is an unusual disease complication since it is associated with both high mortality serotypes, such as serotype 3 and 19A, as well as low mortality

serotypes, such as 1 and 7F. It is attractive to hypothesise that this may be due to different routes of entry of the bacteria into the pleural space. Since serotypes associated with high mortality are more likely to cause necrotising infections, they may translocate directly across damaged lung into the pleura whereas those with lower associated mortality may arrive by invasive spread by infiltrating blood or lymphatic vessels. This is supported by the finding that only the high mortality serotypes have been associated with the development of bronchopleural fistula complicating empyema in children[127,128]. Among cases in which the pneumococcal serotype was known in the McKee study[128], 11/11 (100%) empyemata complicated by broncho-pleural fistula were caused by high mortality serotypes whereas 8/9 (89%) of those not resulting in bronchopleural fistula were caused by serotypes 1 or 7F.

There has also been extensive work done on the role of serotype in nasal colonisation. As mentioned above, although serotype 1 is a relatively common cause of IPD throughout the world, it is relatively rarely found in nasal colonisation except in close contacts of those with serotype 1 pulmonary disease or during epidemics of serotype 1 disease[129]. In contrast, there are some serotypes which are commonly found in studies of nasal colonisation but are rare in invasive disease such as serotypes 11A and 35F[130,131]. Nasal colonisation studies also frequently identify unencapsulated pneumococci (often called non-typable since they do not react with pneumococcal typing serum)[132]. While unencapsulated pneumococci do not directly contribute to disease, recent evidence demonstrates their central role in recombination events that generate genetic diversity among colonising organisms[133].

It can be inferred that the difference between serotypes in terms of the ratio between colonisation prevalence and IPD incidence reflects an increased attack rate among serotypes overrepresented in IPD. Therefore, serotypes rare in colonisation but common in IPD such as serotypes 1, 5 and 7F are considered highly invasive while those found only rarely in IPD are relatively non-invasive. There is a spectrum of invasiveness with the majority of serotypes lying between the two extremes (figure 1-5). Invasiveness tends to inversely correlate with severity of disease, so highly invasive serotypes usually have a low OR for mortality. Highly invasive serotypes are also more likely to cause invasive

infection in young, otherwise healthy adults, whereas less invasive serotypes dominate in the elderly[134]. This is irrespective of whether the pneumonia is bacteraemic or not[126].

1-1.4.2 Historical and geographical variation

There have been a large number of studies conducted over the last 100 years which investigated serotype diversity among pneumococci. However, there is a relative paucity of data allowing direct comparison of serotype variation over time. Inverarity and Diggle[135] identified three historical datasets from Glasgow, Edinburgh and Boston which all show a dramatic fall in the relative frequency of serotype 1 IPD in the mid-twentieth century from 35-60% to less than 10%. A large systematic study in Denmark demonstrated similar findings with highly invasive serotypes tending to become less common with a steep fall after the second world war[136]. However, temporal variation in these serotypes is clear with peaks in serotype incidence occurring every few years. For example, in 1952, serotype 1 accounted for more than 25% of IPD but the following year no serotype 1 isolates were identified.

The high frequency of invasive serotypes that was common historically is still found in other parts of the world – most notably sub-Saharan Africa. Highly invasive serotypes dominate IPD in this part of the world, including meningitis (which is an unusual manifestation of highly invasive serotype IPD in Europe and North America). Annual variations in disease incidence are also much more pronounced with marked epidemics of disease, most notably of serotype 1 IPD. Such epidemics have been observed elsewhere, for example in Papua New Guinea.

1-1.4.3 Molecular mechanisms for serotype differences

The consistent finding that serotypes differ in their clinical and epidemiological characteristics leads to consideration of the molecular mechanisms involved in determining whether a pneumococcal serotype will be likely to cause IPD. There are marked differences between serotypes in a number of capsular characteristics including capsular thickness, charge and complement binding

characteristics. However, apart from a few specific characteristics the implications of these differences for virulence are poorly understood.

There are some specific molecular mechanisms for individual serotype differences that have clearly defined. The zwitterionic structure of the serotype 1 capsular polysaccharide allows presentation on MHC-II molecules and the development of a T-cell dependent immune response. This contributes to the accumulation of IL-17 secreting T-cells in mouse models but it is not clear if this is a major determinant of the unusual epidemiological and clinical characteristics of serotype 1 discussed above. Serotype 3 capsular polysaccharide is not covalently bound to the cell wall and this results in shedding of type 3 capsular polysaccharide into the extracellular space. There is some evidence that this can neutralise serotype 3 anti-capsular antibodies and inhibit opsonisation both *in vitro* and *in vivo*. This would fit with the finding of reduced efficacy of the serotype 3 component of the 13 valent conjugate vaccine but whether the two are causally related remains uncertain. Finally, serotype 14 contains a N-acetyl-glucosamine residue as part of its repeating structure[137] and this may define the susceptibility of patients with mutations in the mannose binding lectin pathway of complement activation[138].

Other studies have sought to correlate the spectrum of invasiveness with molecular characteristics of the capsular polysaccharide. For example, capsular thickness correlates well with both resistance to opsonophagocytosis and serotype prevalence in nasal colonisation. For example, the highly invasive serotypes (1, 4, 5 and 7F) are rarely found in nasal colonisation and have relatively low capsular thickness while serotypes 6B and 19F have among the thickest capsules and highest colonisation prevalence[139]. The same research group has also investigated the association of capsular charge with colonisation prevalence finding that capsular polysaccharides with low ζ potential were associated with rapid neutrophil mediated killing and low carriage prevalence[140]. Another study found that high PspC dependent factor H binding and low complement binding correlated with serotype invasiveness[141].

In summary, there is evidence that molecular characteristics of the capsular polysaccharide correlate with some of the epidemiological characteristics of *S.*

pneumoniae serotypes. However, much uncertainty remains about how these serotype related differences impact on infection *in vivo*.

1-2 Immune response to pneumococcal infection

1-2.1 Innate immunity

It has already been observed that the pneumococcus expresses a toxin (pneumolysin) that has potent activity to both stimulate and disrupt the innate immune response. In addition, there are many other points of interaction between the innate immune system and the pneumococcus that have an important role in determining the outcome of host-pathogen interactions. The components of the innate immune response involved in protection against pneumococcal disease include mucosal barriers, the soluble anti-bacterial systems such as complement, professional phagocytes such as macrophages and neutrophils, and atypical lymphocytes such as γδ cells. Natural antibodies produced by innate B-cells will be addressed in the later section on humoral immunity.

1-2.1.1 Barrier Protection

The barrier defences contribute substantially to the control of pathogens in the respiratory tract. Barrier protection includes nasal filtering of inhaled air and mucocilliary clearance. The respiratory epithelial barrier also secretes a range of antimicrobial peptides.

The pneumococcus has been shown to reduce the rate of mucocilliary clearance by pneumolysin dependent[142] and independent mechanism[143]. Furthermore influenza virus infection, which predisposes to IPD in mice and humans, has a significant adverse effect on ciliary function[144]. Mice with ciliary dysfunction had inability to clear pneumococci from the lower respiratory tract and increased pulmonary inflammation[145].

The role of antimicrobial peptides has proved more challenging to determine. A large number of antimicrobial peptides are secreted within the lung including the ß-defensins and cathelicidins. B-defensins are strongly upregulated by

pneumococcal infection in cultured human epithelial cells in a manner at least partially dependent on pneumolysin[146,147] and at least some are active against pneumococci[148]. However, a mouse deficient in beta-defensin 1 showed no increased susceptibility to pulmonary pneumococcal infection[149].

1-2.1.2 Complement

The complement system represents a group of heat-labile proteins capable of enhancing the opsonisation and phagocytosis of pneumococci in the presence of antibody dramatically[150]. Complement can be activated in three principal ways: interaction with antigen-antibody complexes (the classical pathway), interaction with microbial sugars (the lectin pathway) and interaction with microbial polysaccharides (the alternate pathway). All three mechanisms of activation result in the same common process involving the cleaving of C3. C3b binds to the microbial surface and serves as an opsonin as well as initiating the membrane attack complex (terminal complement) which promotes lysis of bacteria.

The importance of complement in pneumococcal defence has been demonstrated repeatedly through studies of humans with complement deficiencies and more recently knockout mice. Patients with defects in the classical pathway and C3 function have a markedly increased risk of IPD with little or no evidence of increased susceptibility to infection among patients with defects of the alternative and lectin pathways or terminal complement[151]. A study involving several knockout mice demonstrated concordant findings with mice deficient in classical pathway proteins found to be highly susceptible to IPD whereas the effect in mice deficient in proteins involving other pathways was small[152].

As already discussed in the section on pneumococcal virulence factors, several of the important pneumococcal virulence factors interact with complement. Notably, PspA, PspC and pneumococcal histidine triad protein D (PhtD) all inhibit complemement binding or degrade complement[153]. Pneumolysin, an exotoxin, is thought to deplete complement by inducing activation away from the pneumococcal surface[87].

1-2.1.3 Innate immune recognition of pneumococci

A considerable number of molecular mechanisms have evolved to allow the recognition of pathogens by the cells of the innate immune system. Highly conserved components of bacteria and viruses may represent a general sign of infection and those that are recognised by the innate immune system are termed pathogen associated molecular patterns (PAMPs). Sensors involved in the detection of PAMPs by the innate immune system are termed pattern recognition receptors (PRRs). These receptors are usually expressed by professional phagocytes such as macrophages and dendritic cells. The most important of the PRRs are the TLRs and Nod-like receptors (NLRs). The principal PRRs relevant to pneumococcal disease and their ligands are summarised in figure 1-6.

While several TLRs have been implicated in immune detection of pneumococci, most attention has focused on the cell surface receptors TLR-2 and TLR-4 along with TLR-9, which is usually located within endosomes. TLR-2 has been reported to recognise lipoteichoic acid[154], a component of the gram-positive cell wall, however this conclusion has been challenged. More recent work using bacteria deficient in lipoproteins suggests a significant role for these components in the activation of TLR-2 in *S. aureus*[155] and *S. pneumoniae*[156]. TLR-9 recognises non-methylated CpG dinucleotides that are common in bacteria but rare in eukaryotic cells[157]. TLR-4 has been reported to recognise Ply[88], although this finding has also been challenged[89]. Studies of Ply are particularly complex because of the wide range of biological effects of the protein. Taken together, these studies emphasise the difficulty of reliably determining the bacterial components involved in activating the innate immune system since such studies are dependent on obtaining entirely pure bacterial components for study and ensuring they act only on the target receptor. Once activated, TLRs interact with cytoplasmic adaptor molecules to initiate inflammation. In the case of TLRs 2, 4 and 9 signalling is dependent on the adaptor myeloid differentiation primary response gene 88 (MyD88) which initiates a signalling cascade resulting in the activation and nuclear translocation of the transcription factor nuclear factor-κB (NF-κB)[158,159].

NF-κB initiates a program of altered gene expression which promotes the development of inflammation. Among the important effects is the upregulation of pro-inflammatory cytokines such as tumour necrosis factor (TNF), interleukin-6 (IL-6) and pro-IL-1ß. NF-κB also induces production of other PRRs such as the inflammasomes that are required for the secretion of mature IL-1ß[160].

Other PRRs that signal through NF-κB include the nucleotide-binding oligomerization domain-containing protein 2 (Nod-2)[161], which senses murmayl dipeptide, a component of cell wall peptidoglycan within the cytosol having been released from phagosomes[162,163]. CD14 is also able to detect pneumococcal cell wall components[164].

Absence of TLRs in IPD has been explored in mouse models of pneumococcal disease. In general, knockout of the individual TLRs has been associated with a relatively mild phenotype: TLR-2$^{-/-}$ mice died more rapidly after induction of experimental pneumococcal meningitis but no significant difference in outcome was noted in pulmonary infection with virulent organisms[165] (there was some increased susceptibility when Ply^{-} bacteria were used); TLR-4$^{-/-}$ mice were more susceptible to pulmonary infection[88] and TLR-9$^{-/-}$ mice had increased pulmonary bacterial load in a pneumonia model although in this study TLR-4$^{-/-}$ mice were not more susceptible[166]. In contrast to the heterogenous results for individual TLRs, MyD88$^{-/-}$ mice have very marked impairment of cytokine release following pulmonary infection[167] and survival[168] and humans with MyD88 deficiency and other related signalling deficiencies are highly susceptible to IPD[169].

Further important sensing and signalling systems for inflammation with the innate immune system are the inflammasomes. These complex multi-protein structures are up-regulated by NF-κB and are finely tuned to sense cellular stress and a variety of danger signals[160]. The most commonly studied inflammasome in pneumococcal disease is the nod-like receptor family, pyrin domain containing 3 (NLRP3) inflammasome. This inflammasome consists of the NLRP3 protein, an adapter protein ASC (Apoptosis-associated speck-like protein containing a CARD) and pro-caspase-1, which is cleaved by ASC when the inflammasome is activated and assembled[170]. Activation cannot occur without an initial activation of NF-κB to induce production of inflammasome components. However, the mechanism by

which the NLRP3 inflammasome subsequently becomes activated remains incompletely understood. The stimuli for NLRP3 activation are varied and include organic and inorganic material. It has been proposed that disruption of membrane integrity and subsequent potassium loss is the key factor which determines NLRP3 activation[171] and the finding that Ply effectively activates NLRP3 would be consistent with this and pneumococci expressing pneumolysin variants associated with a lack of haemolytic activity failed to illicit IL-1ß release from peripheral blood mononuclear cells (PBMCs)[90]. NLRP3$^{-/-}$ mice show increased susceptibility to pneumococcal pneumonia[89,90].

1-2.1.4 Resident phagocytes

Resident phagocytes represent an important first line of defence against pneumococcal infection. The principal mucosal surfaces protected from pneumococcal invasion by resident macrophages are the upper and lower airways. The principal lower airway macrophage is the alveolar macrophage which is well characterised experimentally. Much less is known about the function of macrophages in the nasal cavity. However, evidence suggests a central role of macrophages in clearance of pneumococci from upper and lower respiratory tract.

In studies of nasal colonisation, macrophage influx is crucial to the control of bacterial numbers and subsequent clearance of the bacteria and depends on Nod-2 signalling[161]. Depletion of nasal macrophages using clodronate liposomes increased colonisation density[172].

In the lower airways, alveolar macrophages are able to phagocytose and clear a low dose inoculation of pneumococci from the lungs without significant recruitment of neutrophils whereas higher doses of pneumococci cannot be cleared by local phagocytes and significant infiltration of neutrophils occurs[173]. During infection caused by higher innocula, the role of alveolar macrophages in bacterial clearance are reduced[174], presumably due to saturation, but they exert other roles in directing the inflammatory response, possibly by removing apoptotic neutrophils[154].

Macrophages kill bacteria through a number of mechanisms including enzymatic attack, production of nitric oxide and production of reactive oxygen species. The enzyme lysozyme is secreted into phagosomes by macrophages and is capable of lysing pneumococci. Mice deficient in lysozyme were more susceptible to infection in a model of otitis media[175] and had impaired recruitment of macrophages to the mucosa in a model of nasal colonisation[161] implying an important role for lysozyme in pneumococcal killing and innate immune recognition. Generation of reactive oxygen species appear to have a limited role in alveolar macrophage killing pneumococci[176,177] possibly due to pneumococci being well adapted to withstand oxidative stress[178]. The ability to generate nitric oxide is important in pneumococcal defence within the lung[177,179] although, in keeping with the role of NO in septic shock, deficiency in inducible nitric oxide synthase was beneficial in systemic infection[179]. Alveolar macrophage apoptosis also contributes to pneumococcal killing *in vivo* once macrophage killing by other methods becomes saturated[173].

1-2.1.5 Neutrophils

Neutrophils represent a double-edged sword in bacterial infection. Neutrophils are capable of rapid recruitment in large numbers to sites of infection and possess an extensive armamentarium for killing infecting bacteria. However, neutrophils are also capable of causing considerable tissue damage and may contribute to disease without promoting survival in some models of infection. In non-infectious models of murine acute lung injury – pulmonary haemorrhage and endotoxinaemia – neutropenia reduced lung oedema and expression of pro-inflammatory cytokines[180].

During bacterial infection inflammatory mediators are released by epithelial cells and innate immune cells which promote maturation of neutrophils in bone marrow and release into the circulation, neutrophil chemotaxis and neutrophil activation. The large number of factors with overlapping functions involved in neutrophil recruitment lead to considerable redundancy. The key mediator in neutrophil homeostasis is granulocyte colony stimulating factor (G-CSF). G-CSF promotes the proliferation of granulocyte precursors within the bone marrow and increases the egress of neutrophils from the bone marrow into the

circulation. Mice lacking G-CSF[181] or its receptor[182] have resting neutropenia and an impaired neutrophilic response to infection. However, other factors are clearly important in stimulation of neutrophil production and release both at rest and during infection since such mice had blunted rather than absent responses. During acute inflammation, other mediators such as granulocyte-monocyte colony stimulating factor (GM-CSF) and IL-6 have an important role in granulopoesis and mobilisation and mice lacking all three mediators are profoundly neutropenic with death due to overwhelming infection occurring within early life[183]. However, G-CSF does not cause neutrophil chemotaxis to the site of inflammation[184].

Neutrophil chemoattraction involves a complex process in which neutrophils become associated with vascular endothelium, transmigrate out of the blood vessel and into the interstitium before migrating to the site of inflammation[185]. Each of these processes is influenced by a wide range of soluble and membrane bound factors. Early in the inflammatory cascade vascular endothelium is stimulated by signals from PRRs or pro-inflammatory cytokines such as IL-1β to upregulate a range of selectins, chemokines and cell adhesion molecules that are required to allow neutrophils to initially roll along the blood vessel wall and ultimately come to rest on it. Neutrophils then leave the blood vessel via either para-cellular or trans-cellular routes.

Once neutrophils arrive at the site of infection, they are believed to kill bacteria through at least three distinct processes. Phagocytosis, principally of opsonised bacteria, results in bacterial killing through mechanisms similar to those of macrophages except that neutrophils also produce hypochlorous acid through the action of myeloperoxidase. Neutrophils also degranulate, releasing anti-microbial proteins such as defensins, cathepsins and lysozyme as well as myeloperoxidase into the extracellular space causing direct bacterial toxicity. Finally, neutrophil extracellular traps (NETs) can be formed by extrusion of neutrophil DNA and nuclear proteins complexed with granule proteins[186]. Bacteria become trapped in the NETs and may be killed directly or phagocytosed.

Neutrophil mediated lung injury occurs when neutrophils enter the alveolar space and are activated. Features of acute lung injury include interstitial and alveolar oedema, damage to the pneumocytes, vascular endothelial dysfunction and surfactant deficiency[187]. Each of these contributes to impaired alveolar function and subsequent respiratory failure. It is clear that acute lung injury is a multifactorial disorder and while depletion of neutrophils is protective in some models it is ineffective in others. This is also reflected in studies involving the manipulation of neutrophils and neutrophil proteins in pneumococcal disease. Pneumolysin promotes acute lung injury characterised by influx of neutrophils and vascular permeability. In this model, depletion of systemic or pulmonary neutrophils did not reduce pneumolysin induced pulmonary oedema[188]. Use of pharmacological neutrophil elastase inhibitors has been associated with decreased lung injury and improved survival in pneumococcal pneumonia in mice and hamsters[189-191] but a neutrophil elastase knockout mouse was more susceptible to pneumococcal pneumonia[192]. The depletion of neutrophils has also produced mixed results. Investigators using mice depleted of neutrophils by injection of anti-neutrophil monoclonal antibodies have found no impact [193], increased susceptibility[192,194] and decreased susceptibility[195] to pulmonary infection. An early study of neutrophil depletion demonstrated increased bacterial burden but delayed (although not reduced) mortality in mice depleted of neutrophils following high dose pulmonary challenge[196]. Within the nasal cavity, fewer studies have examined the effect of neutrophil depletion but no difference in colonisation density early in colonisation was detected in two studies[194,197]. The variation in impact of neutrophil depletion demonstrates the fine balance between inflammatory bacterial clearance and tissue damage in pneumococcal disease and also underlines the heterogeneity of the animal models involved.

1-2.1.6 Atypical lymphocytes

Lymphocytes are traditionally regarded as the mediators of acquired immunity. However, there are a growing number of lymphocytes involved in co-ordinating the innate immune response including at mucosal sites which have attracted attention in models of pneumococcal disease. Lymphocytes active in the innate

immune response include gamma delta cells, natural killer T cells and innate lymphoid cells.

Gamma delta cells are lymphocytes which display the γδ T cell receptor (TCR) on their surface in contrast to the more common αß TCR present on helper and cytotoxic T cells. Gamma delta lymphocytes differ in function from conventional alpha beta T cells in a number of important respects. They express a much more limited repertoire of TCRs than alpha beta T cells[198] and the mechanisms of antigen recognition (while not fully defined) are different; most importantly that gamma delta T cells are able to recognise antigen without the need for processing and display on major histocompatibility complex molecules[199]. Gamma delta T cells are also enriched in epithelial surfaces including the lung[200]. Gamma delta T cells may be activated by binding of the TCR or alternatively that may be activated by cytokines alone without the need for TCR binding[201]. This allows gamma delta T cells to be active early in the course of an inflammatory response without the delay required for chemotaxis and antigen processing, display and recognition inherent in the mechanics of the alpha beta T cell response. Gamma delta cells are capable of expressing most T cell associated cytokines including interferon (IFN)-γ, IL-4, IL-10, IL-17 and IL-22 and the cytokines produced depend on the ontogeny of the lymphocyte[202] and the nature of the inflammatory situation at the time of activation[203]. In addition to their role in the immune response to bacterial infection, gamma delta cells have also been implicated in viral and tumour immunosurveillance and autoinflammatory disease such as multiple sclerosis[204]. In the context of bacterial pneumonia, gamma delta T cells have a well-established role. Effective immune responses to bacteria as diverse as *Mycobacterium tuberculosis*[205], *Staphylococcus aureus*[206], *Listeria monocytogenes*[207] and *Klebsiella pneumoniae*[208] are dependent on gamma delta T cells. An important feature of these studies is the impaired production of pro-inflammatory cytokines such as IL-6, IL-17 and GM-CSF early in the course of infection.

Natural killer T cells are a subset of lymphocytes involved in the recognition of lipids and glycolipids. They were named because of their ability to stimulate natural killer cell function and the presence of natural killer cell surface markers but they are now known to have a much larger repertoire of actions.

The most common group of NKT cells features a single TCR rearrangement and these cells are therefore called invariant natural killer T cells (iNKT). iNKT cells recognise glycolipid antigens presented by the MHC-like molecule CD1d[209] and, in a similar manner to gamma delta T cells, can be activated either by TCR binding or stimulation by cytokines and release cytokines including IFN-γ, IL-17 and IL-4[210]. iNKT cells recognise a number of microbial components including diacylglycerol-containing glycolipids which are present in gram-positive bacteria including *S. pneumoniae*[211]. iNKT cells have been implicated in protective immune responses to a diverse range of bacterial pathogens including pulmonary infection with *Chlamydophila pneumonia*[212], *Pseudomonas aeruginosa*[213] and *Mycobacterium tuberculosis*[214]. Similarly to experiments with gamma delta deficient mice, animals lacking iNKT cells tended to have impairments in early cytokine production.

Innate lymphoid cells (ILC) are a recently defined group of cells that form a number of different cellular lineages linked by the lack of several of the usual lymphocyte surface markers such as CD3 and the TCR. The group includes natural killer cells, which have a long established role in tumour surveillance and viral immunity, but also includes several more recently identified cell types. Given that all ILCs lack the TCR, they are incapable of becoming activated in the manner of conventional T lymphocytes and therefore rely on cytokine signals to activate[215]. ILCs are classified according to their transcription factor and cytokine secretion profile[216]: type 1 produce IFN-γ, type 2 produce cytokines associated with Th2 responses such as IL-5 and IL-13, and type 3 produce cytokines associated with Th17 responses such as IL-17 and IL-22. Given that ILCs have only been recently described, evidence for their role in pulmonary infection is limited. Two recent studies found a role for ILCs in pulmonary defence against *Pseudomonas aeruginosa*[217] and *Klebsiella pneumoniae*[218].

There are several studies investigating the role of innate lymphocytes in pneumococcal infection. Gamma delta T cells accumulate in the lung rapidly following pneumococcal infection[219]. TCR-Vγ4 deficient mice failed to adequately recruit neutrophils to the lung and had increased mortality following induction of pneumococcal pneumonia[220] and negative regulation of gamma delta T cells by type I interferons associated with influenza infection was

associated with increased susceptibility to secondary pneumococcal pneumonia[221]. Gamma delta T cells may also have a role in the resolution of pneumococcal pneumonia[222]. iNKT cells were also found to be critical in host defence against pneumococcal pneumonia[223] and pretreatment of mice with a agonist of the iNKT cell TCR was protective[224]. A recent study found that Type 3 ILCs were the dominant source of IL-22 in lung following pneumococcal infection[225].

Lymphocytes with the ability to produce pro-inflammatory cytokines innately within the first few hours of infection are critical to the early immune response to bacterial infection. However, it remains unclear the extent to which each group of innate cells contributes to the immune response and the degree of redundancy involved. For example, TCR δ knockout mice developed alpha beta T cells with a gamma delta like phenotype[226] suggesting a plasticity not evident in the knockout models outlined above.

1-2.2 Humoral immunity

The production of antibody has been regarded as a critical step in the protection against IPD. Antibodies directed against pneumococcal components promote opsonphagocytosis. The most widely studied immune response to *S. pneumoniae* is anti-capsular antibodies which are directed against the capsular polysaccharide and are therefore serotype specific. In contrast, antibodies directed against pneumococcal surface proteins are serotype independent and therefore could offer broadly protective immunity. Antibodies also develop to the pneumococcal exotoxin pneumolysin, which is present in almost all invasive isolates and is an important virulence factor. Finally, there is a growing understanding of the role of natural antibodies, which are produced by innate B cells, and have opsonophagocytic activity against pneumococcal antigens.

1-2.2.1 Anti-capsular antibody

That convalescent sera from patients with pneumococcal disease has the ability to agglutinate pneumococci of the same type only has been known since the late 19th century and was shown to be directed against the polysaccharide capsule in the 1920s [227]. Prior to the discovery of penicillin, serum therapy was an effective

treatment for IPD [120] and vaccines that elicit production of anti-capsular antibodies with purified polysaccharides remain the principal strategy of adult pneumococcal vaccination[228]. Infants benefit from placental transfer of maternal antibody but after birth the antibody levels fall[229].

Anti-capsular antibodies are produced by B cells following stimulation with pneumococcal capsular polysaccharide in a T-cell independent manner[230]. T-cell independent antibodies are produced rapidly following stimulation because B-cells can proliferate independent of the need for $CD4^+$ help. However, antibodies generated in this manner undergo limited affinity maturation, have a restricted ability to undergo class switching (usually limited to IgM and IgG2 [IgG3 in mice])[231] and are unable to produce robust memory responses [232]. Furthermore, infant T cell independent antibody responses are very poor and so infants develop relatively poor anti-capsular antibody levels in serum[233]. However, most healthy adults have high levels of anti-capsular antibody without the need for vaccination[234]. The mechanism of T-cell independent antibody generation remains unclear. It was suggested that interactions involving CD1 were responsible for inducing B-cells to secrete antibody without T-cell help[235], however it has subsequently been demonstrated that CD1 deficient mice have normal anti-capsular antibody production[236]. A further complication is that while anti-capsular antibody production is formally T-cell independent, T cells influence the intensity of the response as demonstrated in athymic mice[237] and HIV infected humans[238]. One exception is serotype 1 capsule which is a zwitterionic polysaccharide capable of being processed and presented by antigen presenting cells on MHC[239]. This means that serotype 1 capsule can drive T-cell dependent immune responses *in vitro* and *in vivo* although the extent that this feature contributes to the clinical and epidemiological differences associated with this serotype remains unclear[240].

The presence of anti-pneumococcal capsular antibody is thought to correlate well with protection against IPD and the age related incidence of IPD among infants and children shows a clear inverse correlation with mean antibody concentration for each age group[241]. Mice can be protected from IPD and colonisation by passive transfer of anti-capsular antibodies raised by natural infection or vaccination[242].

Despite the evidence of protection against IPD afforded by anti-capsular antibodies, it is not clear whether naturally acquired immunity to pneumococcal colonisation and disease is dependent on the development of anti-capsular antibodies. The incidence of IPD declines uniformly for all serotypes regardless of relative colonisation prevalence suggesting that a serotype independent process is responsible for this decline[243]. This same pattern is seen in colonisation prevalence[244]. Anti-capsular antibody concentrations do not rise above the protective level in many children before 3 years of age[245] but yet the incidence of IPD is already in steep decline before this. In a mouse model of nasal colonisation, vaccination with whole cell vaccine (WCV) from encapsulated and unencapsulated strains was equivalent[246]. Therefore, research has focused on other mechanisms of protective immunity that could be exploited to prevent and treat disease.

1-2.2.2 Anti-pneumococcal protein antibodies

Pneumococcal colonisation and infection also produce antibodies directed against many of the pneumococcal surface proteins described earlier in this chapter. Antibodies to pneumococcal proteins have to potential to be broadly protective since they offer serotype independent activity. However, as discussed earlier, pneumococcal capsule protects the bacterium from effective opsonophagocytosis by inhibiting antibody/complement interactions and while anti-pneumococcal protein antibodies are protective in mouse models the antibody levels required to provide protection are significantly higher than for anti-capsular antibodies[247]. Furthermore, there is significant diversity in surface protein epitopes which allows pneumococci to evade antibody binding[248]. In spite of this, experimental vaccines based on combinations of pneumococcal antigens have been successful in inducing protection against IPD[247]. In a model of experimental human carriage the presence of anti-PspA antibody at baseline was associated with failure of the inoculum to successfully colonise the nasopharynx and the appearance of this antibody was associated with clearance of colonisation[249]. However, these studies do not demonstrate that these anti-surface protein antibodies are the causative factor in clearance or protection and mouse models suggest that colonisation is cleared independently of antibody[250,251]. Observational studies addressing correlation between future

colonisation and anti-surface protein antibody levels have been mixed[252-254]. Therefore, the role of these antibodies in naturally acquired immunity in humans remains uncertain.

Pneumolysin antibodies do not contribute to opsonophagocytosis since pneumolysin is an exotoxin. However, antibodies against pneumolysin are protective in mouse models of pneumococcal disease[255,256] and act by neutralisation of the toxin[257]. Maternal serum pneumolysin antibody concentrations but not surface protein antibodies negatively correlate with neonatal pneumococcal colonisation[258,259] and children with nasopharyngeal colonisation have lower anti-pneumolysin serum and saliva concentrations that non-colonised children[260]. However, such studies are hampered by the same uncertainty regarding causation as surface protein antibodies and the role of pneumolysin antibodies in human protective immunity remains uncertain.

1-2.2.3 Natural antibodies

The antibody responses outlined above have been assumed to require prior exposure to antigen to induce immunity, whether T cell independent anti-capsular antibodies or T cell dependent anti-pneumococcal protein antibodies. However, there are also B cells capable of producing antibody without previous contact with the antigen. These antibodies are known as “natural” and are usually IgM antibodies with relatively low affinity for antigen but an ability to bind a wide range of different antigens[261]. The antibodies are usually expressed from germ line sequence and tend to be expressed by the B1a subset of B lymphocytes. Natural antibody binds capsular polysaccharide and other pneumococcal surface components such as phosphocholine[262]. A natural antibody against phsophocholine found in normal mouse serum induced passive protection against IPD in antibody deficient mouse[23] and mice deficient in B1a cells were lacking natural antibody but able to respond normally to vaccination were more susceptible to pneumococcal infection[263]. Natural antibodies are also present in humans and are believed to also be produced by B1 cells, however the role of natural antibodies in innate protection against pneumococcal disease in humans remains largely unexplored[264].

1-2.2.4 Humoral immunity: overview

Acquired immunity to pneumococcal disease is important in the prevention of IPD. Anti-capsular antibodies develop in childhood and have been convincingly demonstrated to be involved in protection against IPD. However, young children do not develop anti-capsular antibody until after the incidence of IPD has fallen significantly. Anti-protein antibodies offer protection in animal models but the quality of this protection is poor and there is evidence that anti-protein antibody may correlate with rather than cause immunity. Therefore alternative mechanisms of naturally acquired immunity have been sought to explain this protection.

1-2.3 Cellular immunity

That acquired immunity to pneumococcal nasal colonisation can occur independently of antibody mediated protection has been established by several different investigators and methods. Although clearance of nasal colonisation was temporally associated with development of anti-pneumococcal serum antibodies, mice with x-linked immune deficiency (*xid*), which have impaired polysaccharide antibodies, and *μMT* mice, which lack mature B cells, did not have impaired clearance of nasal colonisation[250]. The immunising effect of nasal colonisation, which speeds clearance on subsequent rechallenge, is also independent of B cell function but is eliminated by depletion of $CD4^+$ cells with neutralising antibodies[172,251]. Similar results were obtained with heat inactivated WCV using *nu*$^{-/-}$ mice, which are deficient in T cells, MHC Class-II deficient mice[246] and using adoptive transfer of $CD4^+$ cells into $Rag^{-/-}$ mice[265]. The findings were also replicated using a combination of pneumococcal proteins as a mucosal vaccine[266].

It should be noted that the immunising effect of colonisation or mucosal vaccination assessed in the above studies was expressed in decreased colonisation duration and the antibody independent protection in models of systemic sepsis was not assessed. Mucosally administered vaccines can protect against IPD in the murine model, for example vaccination by administration of live attenuated pneumococci followed by i.n. challenge to induce systemic sepsis[267] or vaccination with a trivalent conjugate vaccine followed by similar

i.n. challenge[268]. However, in the study by Roche *et al*[267] the systemic protection was abrogated in *μMT* mice and MHC Class-II$^{-/-}$ mice suggesting antibody dependence.

In humans, T cell responses to whole pneumococci and recombinant pneumococcal proteins can be detected in peripheral blood, tonsillar material and bronchial washings although the extent to which these cells are contributing to protective immunity remains to be determined. As already discussed, patients with HIV, which principally induces a CD4$^+$ cell immunosuppression, are highly vulnerable to invasive and non-invasive pneumococcal disease even at peripheral CD4$^+$ cell counts usually thought to confer relatively mild immunosuppression[42].

In conclusion, while antibody mediated immunity is required for systemic protection against the pneumococcus, antibodies are dispensible for clearance of nasopharyngeal colonisation (at least within the murine system) and it is CD4$^+$ mediated immunity that is critical for adequate clearance. Evidence is accumulating that mucosal immune responses to pneumococci depend critically on the action of lymphocytes secreting IL-17. The role of general function of IL-17 and its associated cytokine IL-22 will be addressed in the next sections.

1-3 Interleukin-17 and interleukin-22

1-3.1 Background

IL-17 was first described in 1993 as cytotoxic T lymphocyte antigen (CTLA)-8 and homologous genes identified in mice, rats and humans[269]. Six IL-17 family cytokines were identified: IL17A-F[270]. Since the major cytokine from this group remains IL-17A, the remainder of this manuscript refers to IL-17A as IL-17 unless this would result in ambiguity. Other IL-17 family cytokines are always referred to by their full name although other IL-17 family cytokines with the exception of IL-17F have very different biological functions and are not discussed further. Early work on IL-17 identified the principal source of the cytokine as memory CD4$^+$ lymphocytes[271]. IL-17 was found to be pro-inflammatory, inducing a wide range of inflammatory cytokines in target cells. The discovery that CD4$^+$ cells secreting IL-17 were usually negative for the cardinal cytokines defining the T helper (Th)1 and Th2 subsets of CD4$^+$ lymphocytes and that they were negative

for the signature transcription factors of these lineages led to the designation these cells as a new helper T cell subset: Th17 cells[272,273]. However, Th17 cells are not the only important cellular sources of IL-17 – subsets of lymphocytes able to respond innately are able to rapidly secrete IL-17 after activation[205].

IL-22 was first described in 2000 as a cytokine within the IL-10 family of cytokines[274]. In many respects it is similar to IL-17; *inter alia* it is secreted principally by $CD4^+$ memory T cells[275] although also produced by innate lymphocytes[202], it acts principally on epithelial cells and has many similar cellular effects[276]. However, IL-22 is a less potent inducer of many pro-inflammatory cyotkines than IL-17 and in some contexts may have a role in the regulation of inflammatory responses.

1-3.2 IL-17

1-3.2.1 Structure and signaling

IL-17A and IL-17F are adjacent genes and share more than 50% sequence homology[270]. They are secreted as dimers and both homodimers and IL-17A/F heterodimers exist and are biologically active although the heterodimer is considerably less potent than the homodimers[277]. IL-17A and IL-17F signalling is through a dimeric receptor containing IL-17RA and IL-17RC[278]; both receptors are required for IL-17A and IL-17F signalling although mice lacking IL-17RA are also deficient in signalling from other IL-17 family cytokines. Once IL-17A binds its receptor, it signals through NFκB activator 1 (Act1)[279] and tumor necrosis factor receptor-associated factor (TRAF6) [280] to activate a number of important inflammation control pathways including the NF-κB and mitogen activated protein kinase (MAPK) pathways.

1-3.2.2 Target cells and effects

IL-17RA is widely expressed on both haematopoietic and non-haematopoietic cells. However, IL-17RC is more limited in its expression, being found on largely non-haematopoietic cells. Since both receptor proteins are required for IL-17 signalling it is the distribution of IL-17RC that defines the cells that are capable of responding to IL-17.

IL-17RC is expressed strongly on the surface epithelial cells within most organs including the lung[281]. Therefore, within the lung the principal target of IL-17 is the epithelium. Stimulation of epithelial cells with IL-17 induces a number of responses summarised in figure 1-7. Cells stimulated with IL-17 produce pro-inflammatory cytokines and chemokines which lead to the recruitment of neutrophils and macrophages to the site[282]. Neutrophil growth factors such as G-CSF, GM-CSF and IL-6 encourage the maturation of neutrophils in the bone marrow and their release into the circulation[283] while chemokines recruit neutrophils to the site of inflammation. Unfortunately human chemokines frequently do not have direct homologues in mice. Key IL-17 dependent chemokines include IL-8 in humans[284], and the functional homologues chemokine (C-X-C motif) ligand (CXC)L1 and CXCL2 in rodents[282]. Epithelial cells also respond to IL-17 stimulation by releasing products such as ß-defensins, cathepsins and calprotectin which are capable of direct anti-microbial action[285]. Following IL-17 stimulation, matrix metalloproteinases are also released, which degrade structural material such as collagen[286]. Taken together, these cellular products act to alter the environment of the lung to inhibit the growth of micro-organisms by attracting large numbers of neutrophils and upregulating innate anti-microbial defence products. Neutrophils exposed to cell culture supernatant from endothelial cells treated with IL-17 developed increased motility and became activated[282]. IL-17 administered intra-nasally to rats resulted in brisk recruitment of neutrophils to the alveolar space within 4 hours, a process that was dependent on the release of CXCL2[282]. Blockade of IL-17 with neutralising antibody reduced production of IL-6 and CXCL2 and significantly reduced neutrophil recruitment following stimulation with endotoxin[287]. Therefore, IL-17 is of major importance in the recruitment of neutrophils to the alveolar space.

1-3.2.3 Th17 cells

The first cells identified to produce IL-17 were $CD4^+$ T cells and these were thought to be the principal source of IL-17[271]. It was recognised that cells positive for IL-17 were usually negative for IFN-γ and IL-4, the signature cytokines of Th1 and Th2 cells respectively. Furthermore, IFN-γ and IL-4 both negatively regulated the development of IL-17 secreting memory T cells[272]. These cells did not express the transcription factors associated with Th1 and Th2

cells – T box expressed in T-cells (T-bet) and GATA motif binding transcription factor (GATA)-3 respectively. A novel transcription factor, RAR-related orphan receptor gamma (ROR)-γt was identified which, together with signal transducer and activation of transcription (STAT)-3, was required for development of IL-17 producing memory T-cells[288]. Given the emergence of these cells as a subset quite distinct from previously defined T cell subsets they were named Th17[272,273]. Along with IL-17A, Th17 cells often co-secreted the related cytokines IL-17F, IL-21 and IL-22.

The conditions required for the development of Th17 cells proved challenging to elicit. It was initially reported that IL-23 only was sufficient to permit the generation of Th17 cells[289]. However, it subsequently became clear that, while IL-23 was important in maintaining Th17 cells and inhibiting differentiation of other Th subsets, a combination of the cytokines IL-1ß, IL-6 and TGF-ß was required for differentiation of Th17 cells[290]. However, in practice the limiting step for Th17 development is availability of IL-23 and mice deficient in IL-23p19 are deficient in Th17 cells[289]. Th17 cells express C-C chemokine receptor (CCR)6[291]. The ligand for CCR6 is CCL20, which is principally found in mucosal areas including lung and is upregulated in inflammation[292,293]. In keeping with this, mice deficienct in CCR6 had significantly reduced Th17 cells in mucosal tissues such as intestine and lung[294].

1-3.2.4 Other IL-17 producing cells

Since the initial reports that IL-17 was produced only by memory $CD4^+$ cells there has been a steadily growing list of cells found to produce IL-17 including several innate lymphocytes. These include gamma delta T cells[205], iNKT cells[276], type 3 ILCs[295]. Neutrophils[296] and macrophages[297] have also been reported to produce IL-17.

Since these other cells are members of the innate immune system, they are capable of producing IL-17 rapidly in response to stimulation. While gamma delta cells express a TCR, it appears to be dispensible in activation of IL-17 producing gamma delta T cells and instead and combination of cytokine and TLR stimulation is reported to be sufficient – with IL-1ß and IL-23 in combination

with stimulation of TLR-2 capable of inducing IL-17 secretion in vitro and mice deficient in these cytokines/signals having significantly impaired gamma delta IL-17 secretion[298]. Other innate lymphocytes are capable of activation by cytokine stimulation alone and therefore innate lymphocytes are capable of producing IL-17 rapidly after the onset of inflammation.

1-3.3 IL-22

1-3.3.1 Structure and signaling

IL-22 is a member of the IL-10 family of cytokines and shares structural similarities with them[274]. It is a monomeric cytokine which binds to a receptor consisting of the ubiquitously expressed IL-10R2 complexed with IL-22R1. IL-22R1 expression is much more limited than IL-10R2 and as such it is this receptor subunit that defines the cells that can respond to IL-22[299]. Once IL-22 binds to its receptor complex it signals through Janus kinase (JAK)-1 and tyrosine kinase (TYK)-2 to activate STAT-3 and to a lesser extent STATs -1 and -5. IL-22 binding also activates p38MAPK[274,300].

1-3.3.2 Target cells and effects

Like IL-17, the principal target cells of IL-22 are stromal and epithelial cells and these cells constitutively express IL-22RA1. IL-22RA1 expression was not detected in haematopoietic cells which suggests that IL-22 does not have an action on cells of the immune system[299]. There is some evidence that macrophages can respond to IL-22 in the context of *in vitro* infection with *Mycobacterium tuberculosis* but the significance of this remains largely unexplored[301].

Once stimulated with IL-22, epithelial cells produce a range of factors similar to those produced by cells stimulated with IL-17. These include anti-microbial products such as ß-defensins and pro-inflammatory cytokines[302]. However, IL-22 is significantly less pro-inflammatory that IL-17 although it does synergise with other pro-inflammatory cytokines[303]. For example, in the bleomycin model of acute lung inflammation IL-22 is harmful in wild type animals but protective in IL-17 receptor knock out mice suggesting that the pro- and anti-inflammatory

properties of IL-22 are modulated by the presence of other pro-inflammatory cytokines[304]. IL-22 also has a role in wound healing[305] and promotes proliferation among epithelial cells[306].

1-3.3.3 IL-22 producing cells

IL-22 was initially reported to be a Th1 cytokine although Th17 cells were subsequently revealed to be the major subset producing IL-22. Th22 cells producing IL-22 in the absence of IL-17 and IFN-γ have also been reported[307]. It is likely that there are significant differences between mouse and human IL-22 secretion with Th22 cells more common in the human system[308]. In the murine system, IL-22 is strongly correlated with ROR γ t expression[309] whereas this is not the case in humans[310]. In addition most of the cells capable of producing IL-17 have also been observed producing IL-22 including gamma delta cells[311], iNKT cells[312], ILCs[313], neutrophils[306] and macrophages[314]. IL-22 secretion is also highly dependent on the aryl-hydrocarbon receptor which is able to detect toxic products associated with tissue damage in inflammation[315].

1-3.4 IL-17 and IL-22 in health and disease

IL-17 and its associated cytokines have been associated with the development of autoimmune disease including experimental autoimmune encephalomyelitis (a model of multiple sclerosis)[316], inflammatory arthritides including rheumatoid arthritis[317], inflammatory bowel diseases[318] and psoriasis[319]. Monoclonal antibodies targeting IL-17 or the IL-17 receptor have now entered clinical trials for all of the above conditions[320].

Within the lung, IL-17 and IL-22 have been implicated in the pathophysiology of asthma[321] and pulmonary fibrosis[322]. However, the remainder of this section will focus on the importance of IL-17 and IL-22 in immune responses to infection. As inflammatory cytokines active at mucosal sites and involved in the generation of anti-microbial factors and neutrophil recruitment it is reasonable to expect a role for the cytokines in infection by extra-cellular microbes at mucosal sites such as lung and gastrointestinal tract. This is indeed the case, IL-17 is a critical cytokine in defence against pulmonary infection with diverse organisms such as *Klebsiella pneumoniae*[323], *Pseudomonas aeruginosa*[324], *Mycobacterium BCG*[325],

Bacillus arthracis[326] *and Mycoplasma pneumoniae*[327]. IL-17 deficient mice are also more susceptible to oral infection with *Candida albicans*[328] and periodontal disease caused by *Porphyromonas gingivalis* [329]. Gastrointestinal infection with *Citrobacter rodentium*[290,330] and *Salmonella enterica*[331] are also associated with poor outcome in mice deficient in IL-17. IL-17 was required for cutaneous defence against *Staphylococcus aureus*[332,333]. A feature common to almost all models of infection in IL-17 deficient mice is an impairment in neutrophil recruitment to sites of infection and failed bacterial clearance. However, in some models of bacterial infection, there is evidence that IL-17 can be harmful. Following intra-abdominal challenge with *Bacteroides fragilis*, animals deficient in IL-17 did not form intra-abdominal abscesses but were still able to clear bacteria[334]. Similarly, in a model of caecal ligation and puncture, IL-17 was detrimental with increased pro-inflammatory cytokines, bacteraemia and mortality in IL-17 competent animals[335]. Within the stomach, IL-17 increased inflammation and impaired clearance of *Helicobacter pylori*[336]. IL-17 signaling was not required for clearance of influenza A from the lung but mediated acute lung injury[337]. IL-17RA knockout mice had reduced weight loss, reduced neutrophil infiltration and reduced histological inflammation. Recently, a study found that polarizing the immune response towards an IL-17 immune response by the use of mucosal adjuvants before infection with influenza was deleterious with increased lung inflammation[338].

IL-22 is also required for the optimal immune response against infection in a number of different models. IL-22 was required for host defense against *Klebsiella pneumoniae*[339]*, Salmonella enterica* [340] and *Citrobacter rodentium*[341]. In pulmonary infection caused by *K. Pneumoniae,* IL-22 was more important than IL-17 in host defence although IL-17 and IL-22 were synergistic in promoting liberation of pro-inflammatory cytokines[339]. IL-22 has also been implicated in wound healing and tissue repair in the context of infection. For example, chronic *Bacillis subtilis* lung exposure also leads to fibrosis in mice and this is exacerbated by IL-22 deficiency[342]. IL-22 is important in maintaining the integrity of the intestinal mucosa and is an important protective factor in IBD[343].

In humans, IL-17 is found in increased concentrations in sepsis and is associated with an increase in IL-17 producing cells[344]. There are a number of disorders

known to lead to impaired IL-17 and IL-22 mediated immunity. For example, patients with loss of function mutations in STAT-3 have Hyper-IgE syndrome and lack Th17 cells[345]. These patients develop muco-cutaneous candidiasis, recurrent staphylococcal skin infections and recurrent pneumonias leading to bronchiectasis. Acquired IL-17 and IL-22 deficiency due to endogenous production of neutralizing antibodies occurs in the syndrome of autoimmune polyendocrinopathy with chronic mucocutaneous candidiasis[346]. Genetic polymorphisms in the IL-17 gene have been associated with susceptibility to gram positive sepsis[347] and pulmonary tuberculosis[348]. IL-22 polymorphisms have been associated with treatment response in hepatitis C infection[349].

1-3.5 IL-17 and IL-22 in pneumococcal disease

Given the role of IL-17 and IL-22 in mucosal bacterial immunity, it is likely that these cytokines have a role in pneumococcal disease. A significant number of studies have now been published investigating the role of IL-17 in pneumococcal disease. However, the role of IL-22 remains largely unexplored. The studies in mice and humans exploring the role of IL-17 and IL-22 are outlined in table 1-1.

Several studies have addressed the role of IL-17 and IL-22 in the innate immune response to pneumococcal disease. Three studies have implicated IL-23 deficiency – either genetic or acquired – in a blunted early IL-17 response from innate cells and impaired survival. IL-23p19$^{-/-}$ mice have reduced neutrophil influx early in the course of pneumococcal infection and increased dissemination of a serotype 1 strain [350]. Functional IL-23 deficiency induced by type 1 interferons[221] and opiates[351] produced a similar phenotype in serotype 3 disease. In these two models of acquired IL-23 deficiency, gamma delta T cells were identified as the principal source of IL-17. Two studies have addressed the role of other innate lymphocytes other than gamma delta cells. These studies involved the use of pre-treatment protective agents to augment cytokine release. iNKT cells were implicated in one study only after pre-treatment with a glycolipid [224] while ILCs were stimulated with bacterial flagellin to produce IL-22 in another [225]. In this study, ILCs were implicated as a principal source of IL-17 and IL-22. Both pre-treatments were successful in attenuating the infection caused by challenge with a serotype 1 pneumococcus. Therefore, it seems that

IL-17 and IL-22 are produced by innate lymphocytes in response to pneumococcal infection and have a role in host defense in this context.

The role of IL-17 but not IL-22 has been explored in the context of acquired immunity. Several studies have demonstrated that colonisation with pneumococci or nasal vaccination has an immunising effect that shortens the duration of subsequent pneumococcal colonisation. Such an effect is dependent on $CD4^+$ cells, IL-17 and independent of antibody[352]. It can be transmitted to $Rag^{-/-}$ mice by adoptive transfer of memory $CD4^+$ cells[265]. Generation of a Th17 response was found to be dependent on TLR2 signalling[172]. The immunising event can be live wild type[265], attenuated[353],[354] or killed pneumococci[265] and Th17 mediated immunity to further colonisation can be achieved. In humans, experiments on cord blood, tonsils and adult peripheral blood mononuclear cells (PBMC) demonstrate that pneumococcal specific Th17 cells exist[352] and experimental nasal colonisation has demonstrated that mucosal exposure to pneumococci induces Th17 cells in lung and peripheral blood[355]. Bangladeshi children, who are likely to have greater exposure to pneumococci than Swedish children, had higher Th17 responses than their Swedish counterparts[356].

There have now been several studies investigating the pneumococcal components that illicit an IL-17 response when administered mucosally. Cell wall polysaccharide illicits IL-17 mediated immunity dependent on its zwitterionic structure and sensitive to protein conjugation while several approaches involving fusion of pneumococcal surface proteins, pneumolysin toxoids and/or cell wall polysaccharide can also be immunising[266,268,352]. In one study, similar pneumococcal antigens that mouse Th17 cells recognised were also recognised by human Th17 cells suggesting similar vaccines might be effective in both species[357]. It should be noted that currently available evidence strongly supports the role of Th17 in protection against nasal colonisation but the evidence of a role in invasive disease is limited. A single study shows an early difference in lung bacterial density following vaccination with a recombinant pneumococcal protein (DnaJ) fused with pneumolysin toxoid[358]. However, generation of antibody in this study was also IL-17 dependent, which is an atypical finding, and the significance of this study in understanding the role of Th17 in protection against invasive disease remains uncertain. Two studies have examined the role

of the protective effect of colonisation on subsequent disease with contrasting results. In one study, Th17 cells were generated by nasal colonisation but the subsequent protection against invasive disease was not $CD4^+$ but antibody dependent[359]. In the other study, prior nasal colonisation was associated with improved control of bacterial numbers in mice. This effect was neutrophil and IL-17 dependent[360]. Taken together, these studies suggest that IL-17 expression is unlikely to be important in bacteraemia but that it may be an important factor in localised pulmonary infection in the absence of severe disease.

In conclusion, Th17 responses to pneumococci exist in mice and humans and can be generated by experimental colonisation and (at least in mice) by immunisation with pneumococcal components. Th17 cells shorten murine nasal colonisation but their role in invasive disease is questionable. In the context of innate immunity, IL-17 and IL-22 have been implicated in innate immunity but largely by association with other cytokines or cells – principally IL-23. Therefore, the role of IL-17 in systemic infection and particularly innate immunity remains largely unexplored.

1-4 Vaccination

1-4.1 History of pneumococcal vaccination

Pneumococcal vaccination began in the early 20th century in South Africa where the incidence of lobar pneumonia among miners was high enough to threaten the profitability of the mines. Wright and then Lister investigated using inactivated whole cell vaccines to achieve protection and while Lister demonstrated the immunogenicity of comparatively large innocula they were unable to conclusively demonstrate vaccine efficacy [361].

The first demonstrably effective vaccine was in World War II US air force recruits when a tetravalent vaccine consisting of purified capsular polysaccharide was used to prevent pneumonia[362]. However, the development of penicillin limited the uptake of vaccines and it was not until the 1970s that Robert Austrian demonstrated the effectiveness of a 14 valent pneumococcal polysaccharide vaccine (PPV) in preventing pneumonia and bacteraemia in South African gold miners [363].

Unfortunately, for reasons discussed in section 3.3 PPV was not immunogenic in infants. This prompted the development of PCV which elicit a T-cell dependent antibody response by conjugating capsular polysaccharide to a protein antigen. Such vaccines are highly immunogenic in infants and as such have been effective in reducing the incidence of pneumococcal disease in this age group.

1-4.2 Capsular polysaccharide vaccine

As described above, PPV is effective in protecting young adults [228] but ineffective in young children[233]. The currently used PPV is a polyvalent vaccine containing 23 of the most common pneumococcal serotypes. It is currently recommended for use in adults with risk factors for pneumococcal disease including chronic disease and for all those aged over 65 years[364]. However, the effectiveness of PPV in this age group has been recently questioned[365]. Older adults have a significant blunting to the antibody response to PPV and the antibody response wanes significantly over 2 years post-vaccination[366] – much shorter than the recommended 10 year dosing interval. Epidemiological evidence suggests that there is likely a small beneficial effect of vaccination which persists for only 1-2 years post vaccination[367]. Furthermore there is concern that, since PPV does not induce the differentiation of memory B-cells, administration of the vaccine may lead to immunological fatigue and hyporesponsiveness[368] with vaccine failure and even a paradoxical increase in risk particularly with repeated dosing. Elderly patients previously exposed to PPV have a poorer antibody response when subsequently exposed to PCV than those not previously exposed to PPV[369]. A randomised controlled trial of PPV in immunosuppressed African patients with HIV found a paradoxical increase in IPD[370] although the cause of the increase was not clear and PPV remains the recommended vaccine for HIV positive individuals in the UK. Therefore, while PPV is effective in preventing IPD and pneumonia in young otherwise healthy adults at high risk of pneumococcal disease because of epidemiological reasons – i.e. army recruits or during outbreaks- young healthy adults in general are not considered a priority for vaccination because of their very low disease incidence. In contrast, among groups who are targeted for vaccination PPV is either ineffective (infants) or of borderline efficacy (older adults and at risk groups). It is clear that superior vaccines were required to meet this need.

1-4.3 Conjugate vaccine

Pneumococcal conjugate vaccines were developed in order to improve immunogenicity. In order to achieve this, pneumococcal capsular polysaccharides were conjugated to a protein carrier (an H. influenza surface protein, tetanus toxoid and diphtheria toxoid are used in the currently licensed formulations)[371]. The result is a polyvalent vaccine capable of inducing strong antibody responses in individuals of all ages[369,372]. Clinical trials demonstrated the efficacy of PCV in the prevention of IPD in young children and PCV-7 was licensed based on these data[245]. PCVs are now used in the routine childhood immunisation programme of most high income countries and many low income countries[373]. The effect of routine use of PCV on the serotypes covered has been dramatic with near elimination of those serotypes not only from vaccinated individuals but also from unvaccinated adults who are protected through herd immunity[374]. This reinforces the importance of young children as reservoirs of pneumococci for the whole population. The initial pneumococcal conjugate vaccine was heptavalent and, while it was highly effective with regard to the vaccinated serotypes, it did not lead to a reduction in the overall prevalence of pneumococcal nasal colonization among young children[375]. Therefore, other pneumococcal serotypes expanded to replace the vaccine serotypes and this was reflected in an increase in the incidence of IPD caused by non-vaccine serotypes[374]. There was also some evidence of capsular switch events allowing virulent clones to evade vaccine. The emergence of antibiotic resistant serotype 19A in North America is probably the best documented example of the so-called serotype replacement[376,377].

In response to serotype replacement, conjugate vaccines with higher valency were developed. PCV-13 is now included in the UK childhood vaccination schedule and has proved similarly effective to PCV-7 against vaccine serotypes (with the possible exception of serotype 3) [378]. It had been hoped that the increased valency would exhaust the highly virulent serotypes and prevent significant further serotype replacement but there is early evidence of further serotype replacement in the UK around four years after the introduction of PCV-13[379]. Overall, PCVs have reduced IPD among infants by around 75% but the reduction in adults due to herd immunity has been much more modest (around

10-15%)[378]. PCV-13 is highly immunogenic in adults and is effective in the reduction of pneumococcal pneumonia[380]. However, the role of routine PCV administration to adult populations where childhood vaccination rates are high is unclear since vaccine serotypes are becoming uncommon in this population.

PCVs are complex, multicomponent vaccines which are expensive to produce. This has limited the uptake of PCV in developing economies. Adding additional serotypes to PCV will only increase cost and it is not clear how many more serotypes could be added without sacrificing vaccine efficacy. Therefore, not withstanding the substantial effect on IPD incidence in young children there is a need to develop simpler vaccines with serotype independent coverage if further gains against pneumococcal disease are to be achieved.

1-4.4 Next generation vaccines

Serotype independent vaccines have been a goal for vaccine developers for some time. There are several different strategies with the aim of inducing serotype independent protection. In animal models, vaccines based on recombinant pneumococcal proteins and toxoids[266], cell wall (not capsular) polysaccharide[352], vectors carrying pneumococcal DNA[381], inactivated pneumococcal cells[246] and live attenuated pneumococci[382] have all been found to offer serotype independent protection to shorten nasal colonisation and in some cases against IPD. As has already been discussed, many of these vaccines have been found to rely on $CD4^+$ cells and IL-17 but not antibody (although none of the published reports demonstrating protection against IPD has thus far been found to be antibody independent).

Some next-generation vaccines have entered phase 1 trials although none have been investigated for efficacy. What is clear though is that there is a current interest in exploiting serotype independent factors to promote antibody and Th17 mediated immunity to pneumococcal disease. Therefore, increasing the understanding of the role of IL-17 in pneumococcal disease is an important research goal.

1-5 Summary, hypothesis and aims

1-5.1 IL-17 and IL-22 in pneumococcal disease

In this literature review I have outlined the importance of pneumococcal disease to global health and the urgent need for effective vaccination to prevent morbidity and mortality. While current vaccines are effective, they have a number of deficiencies and so improvements – particularly in terms of increased serotype coverage and cost – would be welcome. There are important differences between pneumococcal serotypes which impact on virulence and clinical disease but the molecular mechanisms underlying these differences and particularly the host-pathogen interactions at play remain poorly understood.

The last ten years have seen the emergence of IL-17 and IL-22 as key players within the immune response to mucosal infection. These cytokines have key roles in the maintenance of mucosal integrity, production of anti-microbial factors and the recruitment of phagocytes such as macrophages and particularly neutrophils to the site of inflammation. The role of IL-17 is now well established in models of acquired immunity to nasal colonisation but the role of IL-17 and IL-22 in invasive pneumococcal disease remains poorly understood. IL-17 has also been identified as a maladaptive factor in certain models of inflammatory and infectious disease and evidence suggests that pneumococcal disease often straddles the boundary between successful inflammatory responses clearing bacteria and over-exuberant inflammation causing tissue destruction and poor outcome. Therefore, the role of highly pro-inflammatory cytokines in this system remains unclear.

1-5.2 Hypotheses

I hypothesised that IL-17 and IL-22 are important cytokines in the immune response against pneumococcal disease and that there might be important serotype and strain related differences which define this role in invasive disease. Specifically, I hypothesised that differences in IL-17 and IL-22 mediated immunity might explain the increased risk of IPD among the elderly and that there might be important differences between young and old adults in this regard. We also hypothesised that these cytokines would also be important in a

murine model of pneumococcal disease and that pneumococcal strain and site of infection might define the role of these cytokines.

1-5.3 Aims

Human work

- To identify pneumococcal specific T cell responses in healthy volunteers particularly focusing on IL-17 and IL-22.
- To compare these pneumococcal specific T cell responses with those in elderly volunteers and patients with recent invasive pneumococcal disease

Animal modelling

- To establish a murine model of invasive pneumococcal disease
- To explore the role of IL-17 and IL-22 using mice deficient in signalling involving these cytokines
- To explore the importance of pneumococcal strain in influencing the role of these cytokines

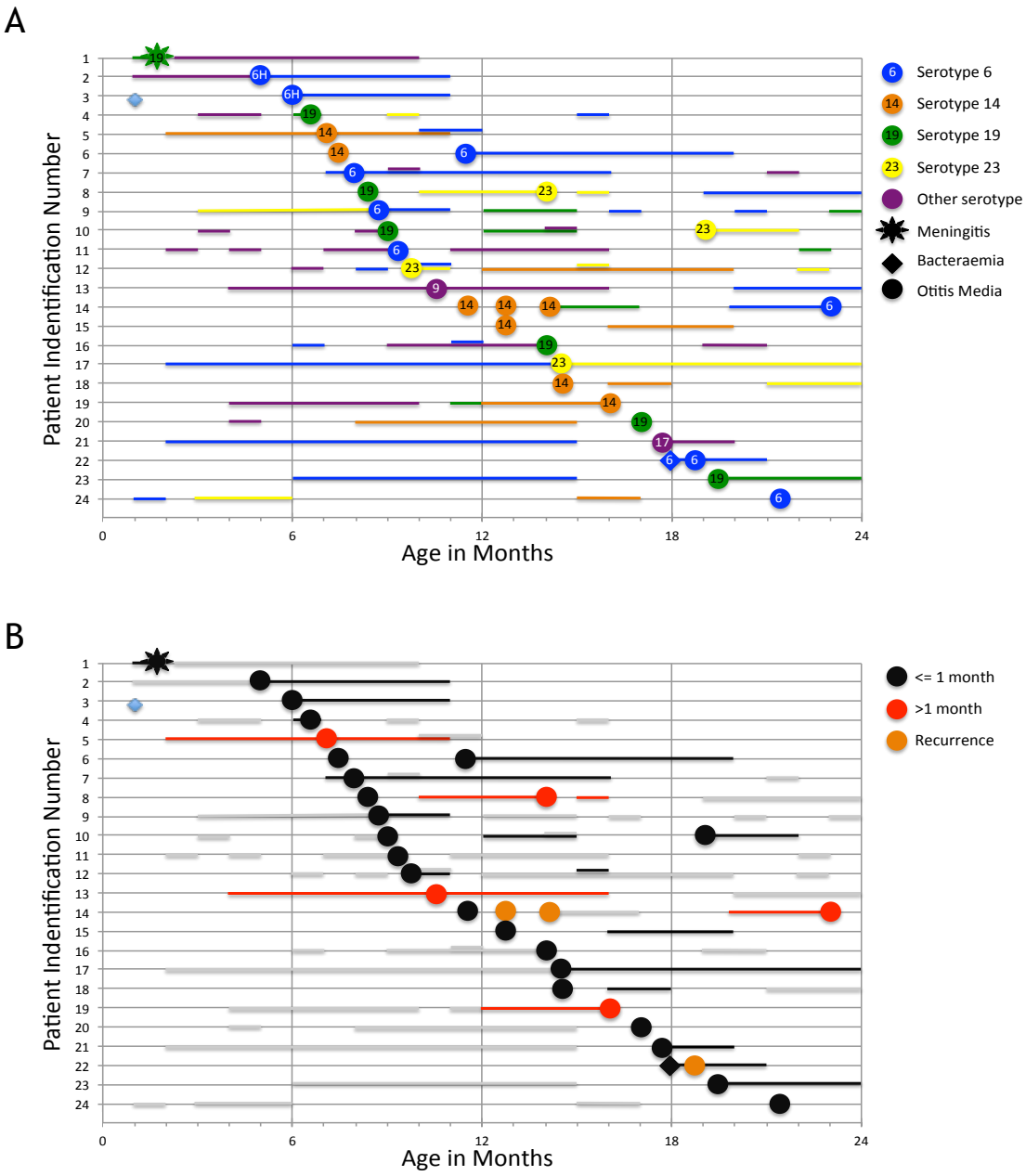

Figure 1-1. Dynamics of pneumococcal colonisation in young children and the association with symptomatic disease.

Colonisation with pneumococci is represented by horizontal lines and the onset of symptomatic infection is shown by solid shapes. Colours represent the serotype involved (A) and the duration of colonisation (B) prior to the onset of symptomatic disease caused by the same serotype. The letter H after some serotype numbers denotes co-infection with *Haemophilus* influenzae. Figure adapted from Gray et al (1980) with the permission of the publisher.

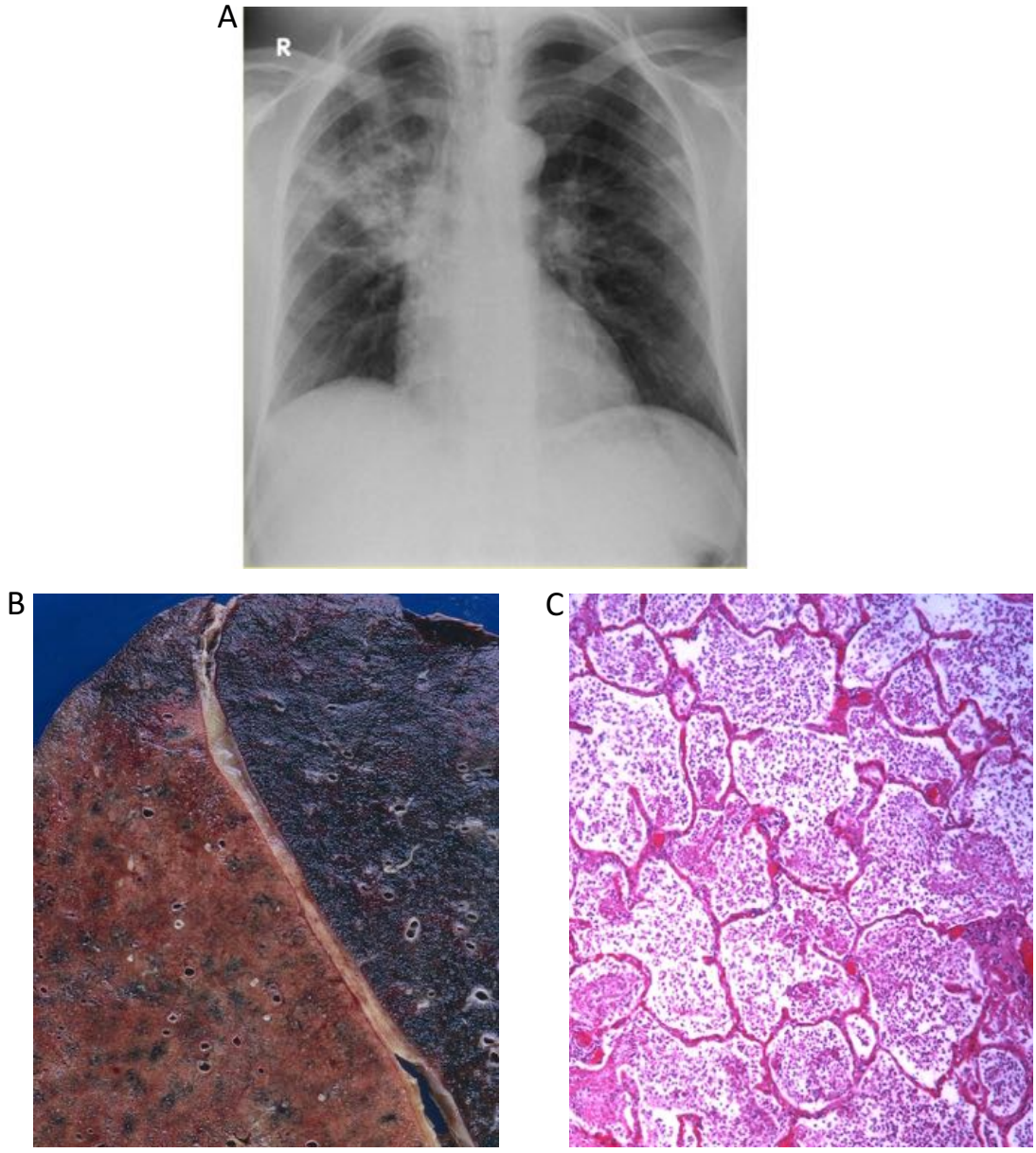

Figure 1-2. Radiological and pathological features of pneumococcal pneumonia.

A. Right upper lobe pneumococcal pneumonia (image reproduced from Loebinger MR, Wilson R. Pneumonia. Medicine. 2012 Jun;40(6):329–34 with permission of the publisher) B. Gross pathology of lobar pneumonia with consolidation at red hepatisation stage. C. H&E stained section of human lung during red hepatisation stage of pneumococcal pneumonia. B & C courtesy of Dr Yen Rosen.

A

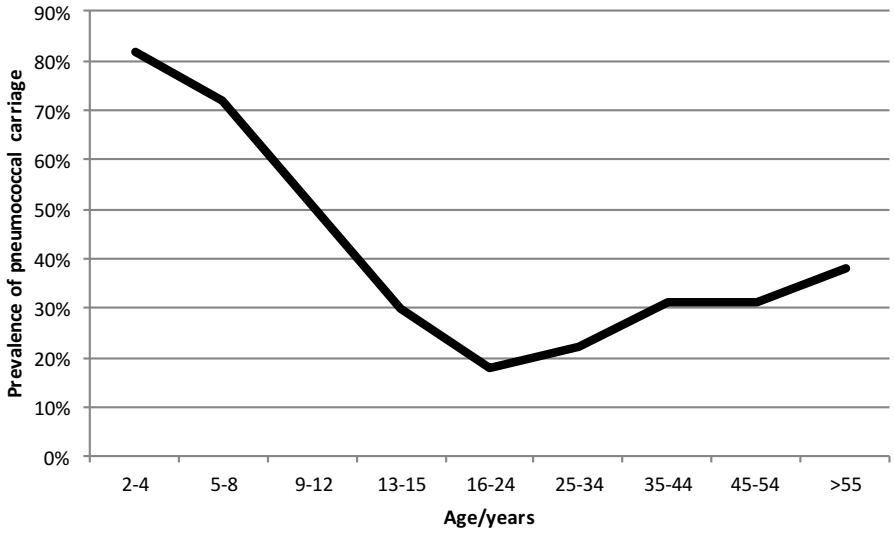

B

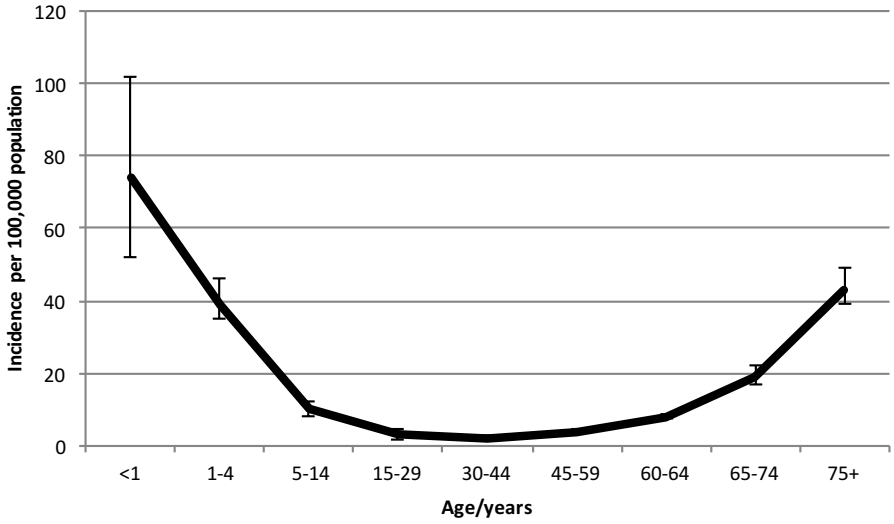

Figure 1-3. The variation in pneumococcal carriage and disease with age. Prevalence of pneumococcal carriage (A) and incidence of invasive pneumococcal disease (B) decrease with age throughout childhood and then rise with age in adulthood. A is adapted from MacKenzie et al (2010). B is adapted from data published by Public Health England (http://www.hpa.org.uk/Topics/InfectiousDiseases/InfectionsAZ/Pneumococcal/EpidemiologicalDataPneumococcal/BackgroundEpidemiologyPneumococcal/IPDTables/pneumoNumberLabConfirmedIPDAgeSpecific/, accessed May 2014).

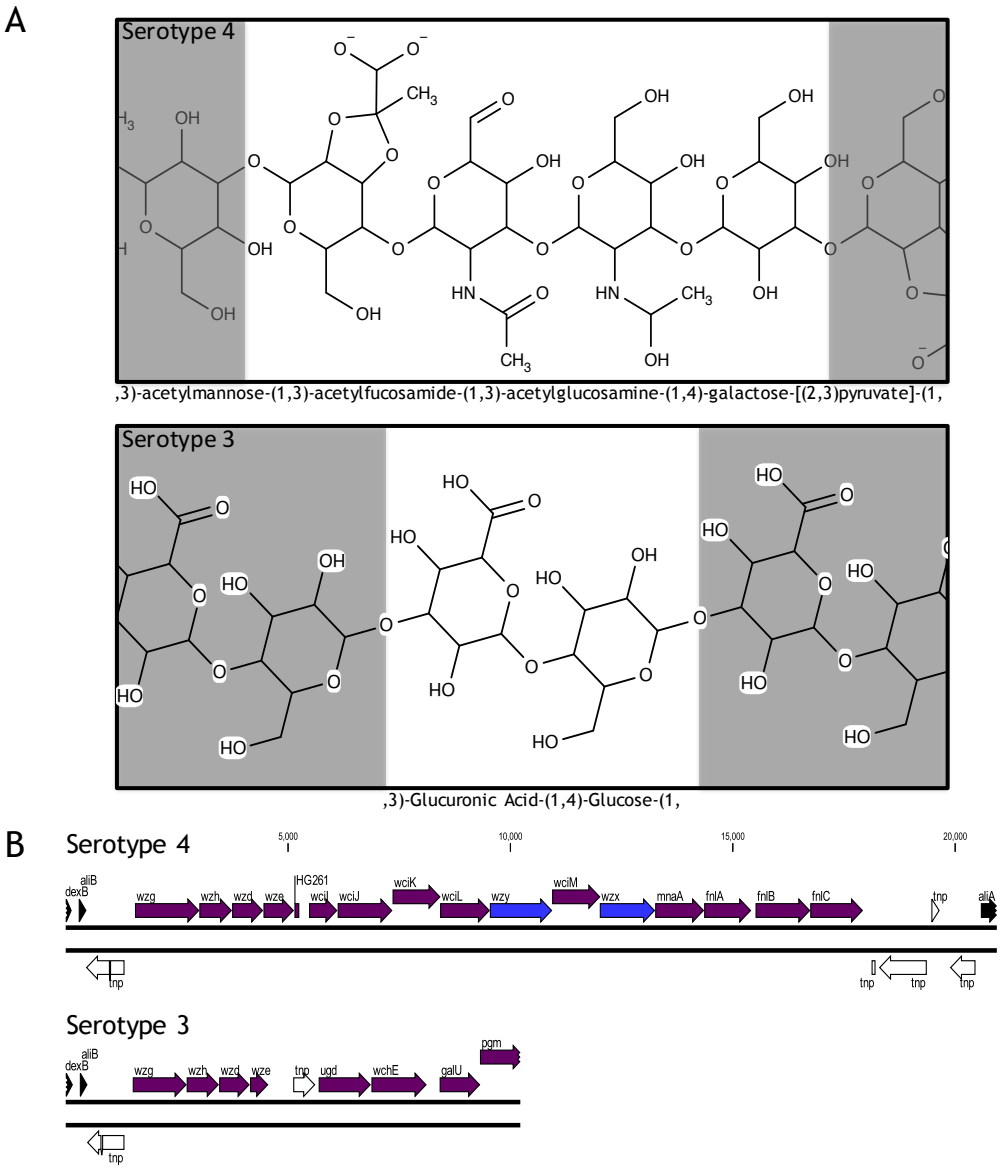

Figure 1-4. Structure of selected pneumococcal capsular polysaccharides and associated genetic loci.

A. Carbohydrate. Most, like the serotype 4 capsule consist of 3-7 carbohydrates – often with additional side chains and branches. In contrast, the serotype 3 capsule consists of only two repeating simple carbohydrates. B. cps locus. Serotype 4 is typical of pneumococcal capsular loci with a several carbohydrate modification enzymes as well as the Wzx/Wzy genes (blue). In contrast, serotype 3 is lacking the Wzx/Wzy genes and has a much shorter capsular locus with fewer carbohydrate modifiying enzymes. cps loci were analysed in CLC Genomics 7.0 using sequences deposited in Genbank by Bentley et al (2006).

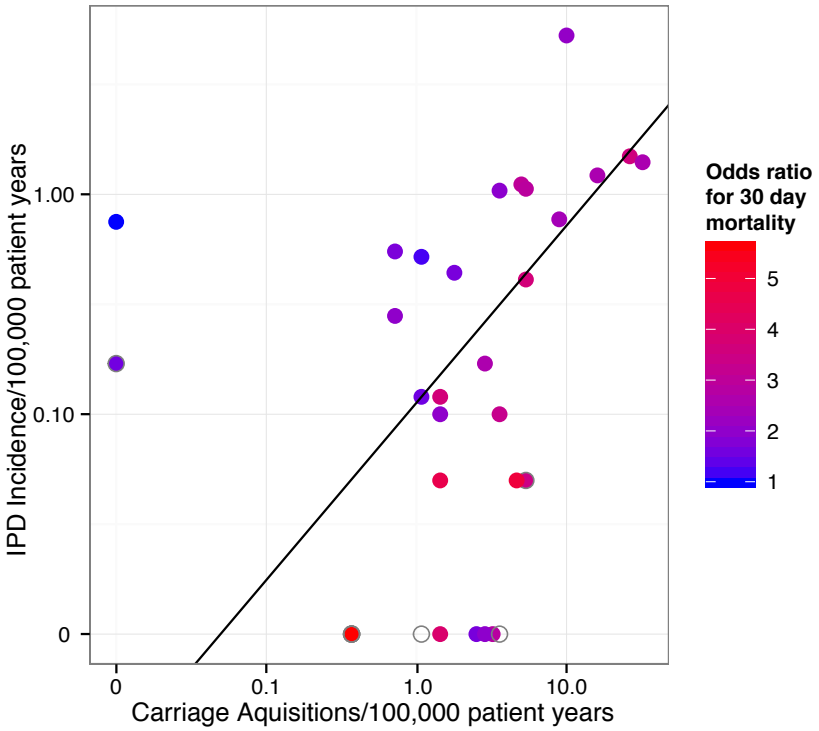

Figure 1-5. Relationship between carriage acquisitions, invasive pneumococcal disease incidence and mortality.

Each point represents one serotype. Colour indicates adjusted odds ratio for mortality compared to serotype 1. Line represents the ratio of carriage to IPD of the median serotype (6B). Open circles represent serotypes isolated too infrequently to allow calculation of mortality OR. Highly invasive serotypes lie above the line. Note that serotypes with high associated mortality tend to lie below the line. Data adapted from Sleeman (2006) and Harboe (2009).

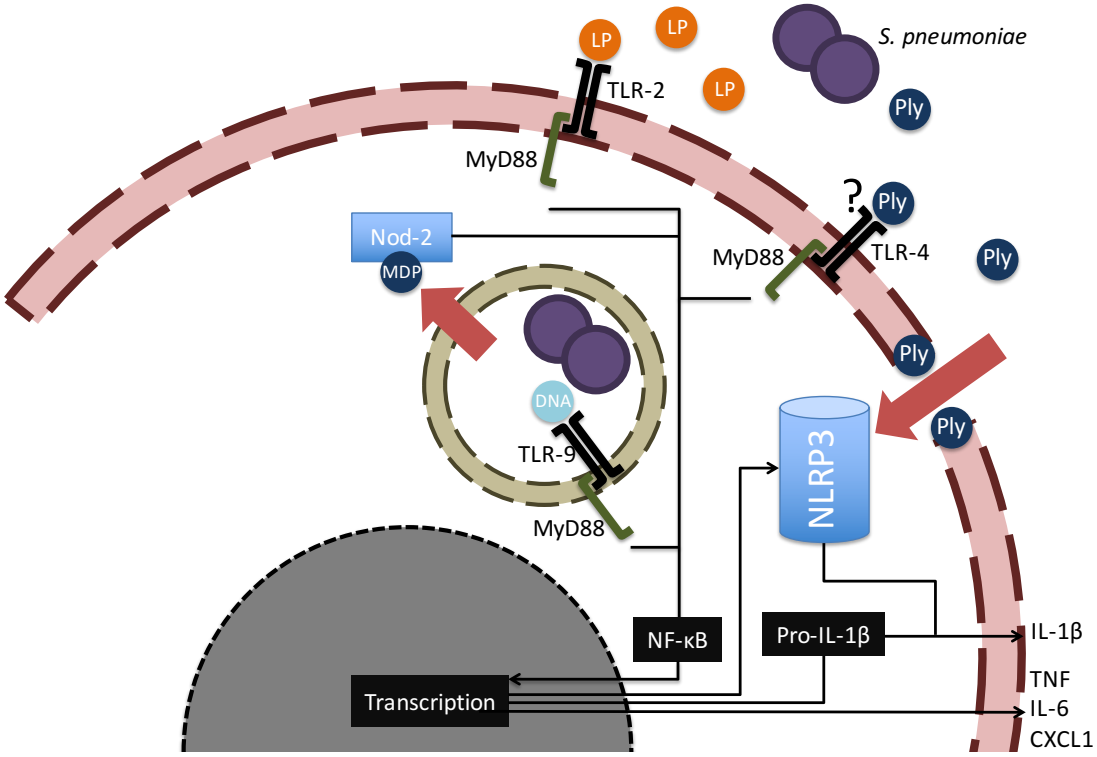

Figure 1-6. Major pattern recognition receptors involved in innate sensing of *S. pneumoniae*.

The binding of ligands to TLRs results in activation of the effector molecule MyD88 which initiates a signalling pathway resulting in the activation of NF-κB. Stimulation of NOD-2 by bacterial peptidoglycan also results in NF-κB activation by a MyD88 independent pathway. This transcription factor initiates the production of pro-inflammatory mediators such as cytokines and chemokines. IL-1ß is produced in an inactive pro form and must be activated by an inflammasome such as NLRP3 prior to secretion. Activation of NLRP3 is dependent on a number of factors including potassium eflux dependent on the pore-forming activity of pneumolysin. ? The role of Ply as a TLR-4 ligand is controversial. TLR: Toll-like receptor; MyD88: myeloid differentiation primary response 88; LP: lipopeptide; Ply: pneumolysin; MDP: muramyl dipeptide; Nod-2: Nucleotide-binding oligomerization domain-containing protein 2; NLRP3: nod-like receptor family, pyrin domain containing 3

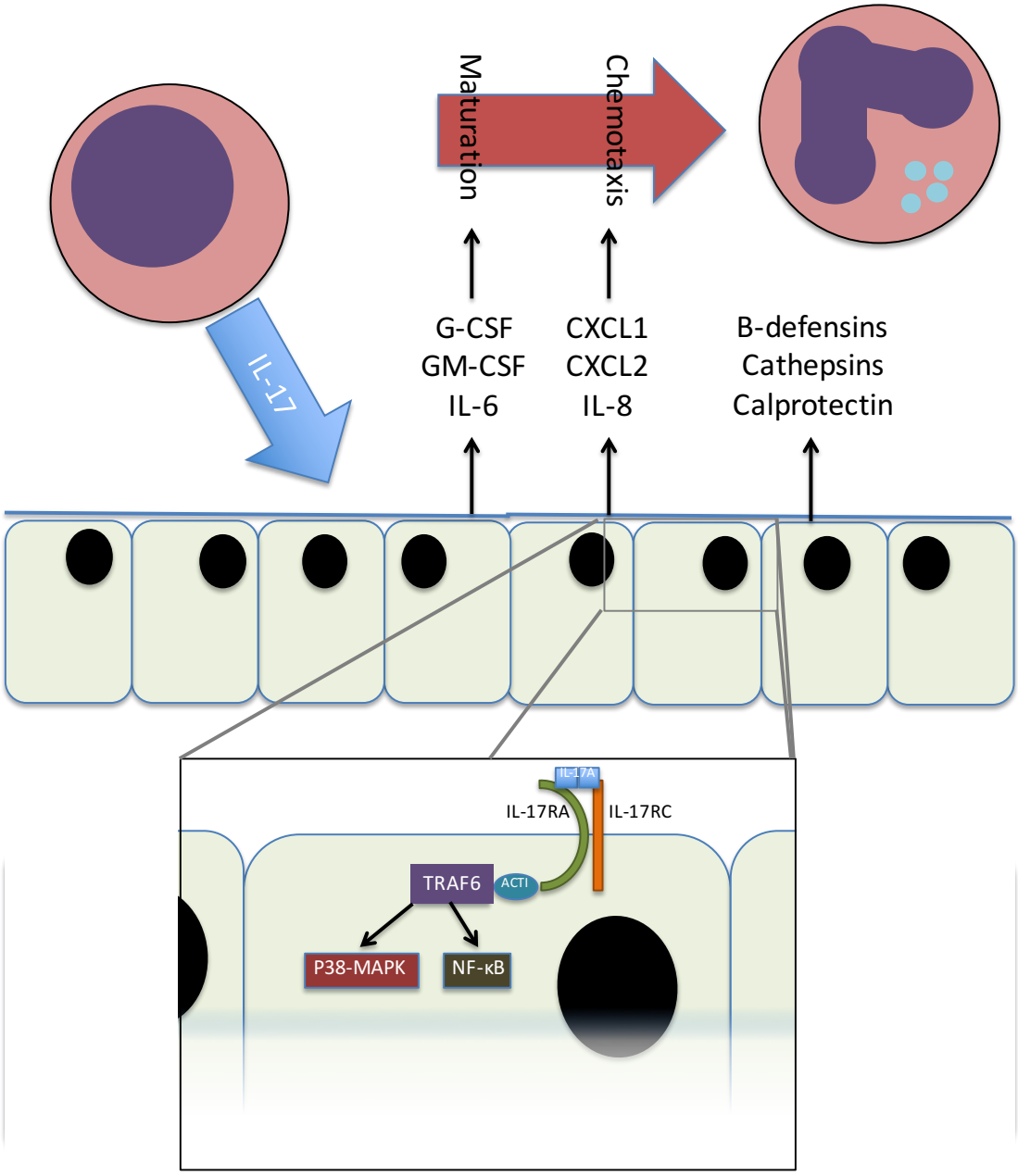

Figure 1-7. IL-17 signaling and effects on target cells.

Principal cellular products are shown with intracellular signaling shown in the inset. G-CSF: Granulocyte colony stimulating factor; GM-CSF: Granulocyte-monocyte colony stimulating factor; TRAF6: TNF receptor associated protein; p38-MAPK: mitogen-activated protein kinase; NF-κB: nuclear factor-κB; ACT1: NF-κB activator 1.

		Reference	Design	Role of IL-17/IL-22
Mouse	Innate	Ma, 2010	Murine model of opiate abuse with chronic exposure to morphine	Chronic opiate exposure inhibits IL-23 release from macrophages blunting IL-17 release and impairs host defense.
		Ivanov, 2012	iNKTs activated with glycolipid prior to *S. pneumoniae* challenge	Glycolipid stimulation augmented early IL-17 release through $CD103^+$ dendritic cells.
		Li, 2012	Murine influenza infection with subsequent *S. pneumoniae* challenge	Influenza infection induces type I interferons which inhibit IL-17 release from γδ cells and impair innate immune response.
		Kim, 2013	Pneumococcal challenge in $IL\text{-}23^{-/-}$ mice	IL-23 deficiency impairs innate IL-17 secretion and is associated with impaired neutrophil recruitment and survival.
		Ivanov, 2013	Murine influenza infection with subsequent *S. pneumoniae* challenge	IL-22 required for bacterial control and secreted by a range of innate lymphocytes within the lung including γδ T cells and ILCs
	Adaptive	Malley, 2006	Pneumococcal cell wall polysaccharide with cholera toxin given intra-nasally	Subsequent shortening of colonisation dependent on $CD4^+$ T cells and IL-17A but not antibody.
		Basset, 2007	Vaccine consisting of mucosally administered PspC, PsaA and pneumolysin toxoid.	Subsequent shortening of colonisation dependent on $CD4^+$ T cells but not antibody. Strong splenic Th17 responses to vaccine observed.
		Lu, 2008	Nasal inoculation of whole killed or live pneumococci	Subsequent shortening of colonisation can be induced in $Rag^{-/-}$ mice by adoptive transfer of $CD4^+$ cells and is IL-17 dependent.
		Yu, 2009	Mucosal or systemic vaccination with trivalent fusion complex of PsaA, pneumolysoid and cell wall polysaccharide.	Vaccine elicits strong Th17 responses and protects against colonisation and systemic infection but dependency not assessed.
		Ferreira, 2009	Mucosally administered vaccine consisting of recombinant PspA5.	Subsequent protection against invasive challenge correlated with Th17 response but dependency not assessed.
		Zhang, 2009	Natural course of nasal colonisation with S. pneumoniae in naïve and previously colonised mice	Clearance of primary colonisation and accelerated clearance of subsequent colonisation is dependent on TLR2 signaling and Th17 cells.

Mouse	Adapt	Groneck, 2009	Intra-peritoneal administration of serotype 1 capsular polysaccharide to induce abscess formation	Serotype 1 capsular polysaccharide induces accumulation of Th1 and Th17 cells
		Lu, 2009	Cell wall polysaccharide adminiatered nasally with or without conjugation.	Subsequent shortening of colonisation is dependent on functional IL-17 signaling. Protein conjugation ineffective.
		Fernandes, 2010	Splenectomised mice exposed to systemic infection with pneumococci.	Splenectomised mice had increased susceptibility to pneumococci associated with decreased IL-17 and antibody
		Richards, 2010	Nasal colonisation with wild type and pneumolysin deficient pneumococci	Colonisation with wild type and attenuated pneumococci protects against subsequent nasal and systemic challenge. Protection is likely dependent on both antibody and Th17.
		Cohen, 2011	Nasal colonisation followed by experimental pneumoniae	Prior colonisation generated Th17 cells but antibody rather than $CD4^+$ cells was required for protection against invasive disease
		Moffitt, 2011	An expression library was used to identify pneumococcal antigens recognised by Th17 cells derived from animals previously colonised	Th17 antigens were distinct from Th1 antigens. Vaccine developed from candidate Th17 antigens. Subsequent vaccine protected against colonisation in a manner that was dependent on $CD4^+$ cells and IL-17.
		Marques, 2012	Nasal challenge with low dose serotype 1 S. pneumoniae	Protective immunity against subsequent lethal challenge is induced. Antibody and Th17 immune responses present.
		Liu, 2014	Mucosal vaccination with recombinant DnaJ-pneumolysin toxoid fusion protein	Salivary IgA production and protective immunity against subsequent challenge is dependent on IL-17.
		Wilson, 2015	Nasal colonisation followed by experimental pneumonia	Prior colonisation protected against pneumonia in an IL-17 and neutrophil dependent manner

Human	Adapt	Lu, 2008	Stimulation of cord blood, tonsillar cells or adult peripheral blood	Tonsillar cells and adult peripheral blood but not cord blood secrete IL-17 in response to pneumococcal stimulation
		Chen, 2010	IL-17 SNP analysis in asthmatic patients and controls	IL-17 genotype is associated with lower respiratory tract bacterial colonisation (inc. *S. pneumoniae*) in asthmatics
		Moffitt, 2011	Stimulation of human PBMCs with antigens identified in murine screen	Antigens identified as Th17 antigens in mice also stimulate the release of IL-17 from human PBMCs.
		Oliver, 2011	Co-culture model of human moocytes and T cells stimulated with live or heat inactivated pneumococci	Pneumococci induce IFN-γ and IL-17 secretion from human T-cells. IL-17 secretion is dependent on TLR-2 signalling only when stimulated with dead pneumococci.
		Glennie, 2011	T-cell responses of asymptomatic HIV patients in Malawi.	HIV patients have dysregulated immune responses with relative preservation of Th17 responses
		Wright, 2012	Experimental nasal challenge	Antibody responses but not Th17 responses were augmented
		Lundgren, 2012	PBMCs from adults and children from Sweden and Bangladesh stimulated with pneumococci	IL-17 was secreted by PBMCs from all four groups. Adults and children from Bangladesh had the greatest secreted IL-17. Children from Sweden had the lowest.
		Wright, 2013	Experimental nasal colonisation	Colonisation causes expansion of pneumococcal specific Th17 cells in the lung and peripheral blood

Table 1-1. Summary of studies investigating the role of IL-17 and/or IL-22 in pneumococcal disease in humans or animal models.

Studies of particular interest are highlighted in black.

2. MATERIALS AND METHODS

2-1 Introduction

Throughout this chapter, all materials were sourced from Sigma Aldrich unless otherwise specified. Manufacturers' instructions were generally followed and deviations are indicated in the text.

2-2 General Microbiology

2-2.1 Bacterial strains used

TIGR4 (Serotype 4) was obtained from Prof Tim Mitchell (University of Birmingham). Strains SRL1-5 (Serotypes 3, 6B, 7F, 14, 19F respectively) were obtained from Dr Giles Edwards at the Scottish Haemophilus, Legionella, Meningococcus and Pneumococcus Reference Laboratory (SHLMPRL).

2-2.2 Cultivation of bacterial strains and colony counting

Bacteria were grown on blood agar plates (blood agar base supplemented with 5% defibrinated horse blood). Bacteria grown in liquid culture were maintained in brain heart infusion (BHI) without agitation. Where appropriate, filter paper disks impregnated with Optochin (ethylhydrocupreine) were placed on plates. Pneumococci were grown at 37˚C either under air or 5% CO_2. Air was used where it was desirable to have reduced colony size, usually when colony counting was being undertaken on the mucoid strain SRL1.

Colony counting was conducted by performing serial tenfold dilutions of pneumococcal suspensions in phosphate buffered saline (PBS). 10 µl drops of each dilution were placed on the surface of a blood agar plate in triplicate and

allowed to dry into the plate at room temperature. Plates were then incubated overnight and the colonies counted the following morning.

2-2.3 Identification of strains as pneumococci

Pneumococci were identified as alpha-haemolytic, catalase negative, gram-positive cocci sensitive to Optochin and soluble in bile salts. The algorithm used to identify presumptive pneumococci is shown in
figure 2-1. The catalase testing was performed by placing a colony of pneumococci from an overnight plate on a glass slide and adding 500 µl of 3% H_2O_2 and observing for bubbling. Gram staining was performed using a gram stain kit (BD Bioscience) according to the manufacturer's instructions. To perform Optochin sensitivity testing, bacteria were spread over a blood agar plate and an Optochin disk was placed on the plate before incubating under 5% CO_2 overnight. The following day, a zone of clearance greater than 14 mm indicated sensitivity. Bile salt solubility was assessed by making a dense suspension of bacteria in PBS before mixing 1:1 with 2% sodium deoxycholate and incubating at 37˚C for 30 minutes. Clearing of the suspension indicated a positive test.

2-2.4 Establishing serotype

Pneumococci were typed using the multiplex polymerase chain reaction (PCR) designed by the Centres for Disease Control (CDC). DNA was extracted from pneumococci using a DNeasy Blood and Tissue Kit (Qiagen) according to the manufacturer's instructions using the protocol for gram positive bacteria. PCR was carried out using Qiagen Multiplex PCR mastermix according to the protocol from the CDC (http://www.cdc.gov/ncidod/biotech/strep/pcr.htm, accessed June 2012). Primers used in this analysis are shown in table 2-1. After an initial incubation at 95˚C for 15 minutes to activate the DNA polymerase, 35 cycles were performed consisting of denaturation at 95˚C for 30 seconds, annealing at 54˚C for 90 seconds and extension at 72˚C for 60 seconds. A terminal extension step of 10 minutes was included. Final mixtures were run on a 2% agarose gel at 100V for 2 hours. Each reaction mixture generated a 160bp control band amplified from the CSPA gene common to all typeable pneumococci demonstrating a viable reaction while a band larger than 160bp was measured against a DNA ladder to identify the serotype from the CDC's scheme.

To confirm the serotype 6B strain, the PCR band was extracted using a Qiaquick gel extraction kit (Qiagen) and subjected to Sanger sequencing using the 6A/B forward primer to confirm the presence of the *wciP* substitution defining serotype 6B.

2-2.5 Multilocus sequence typing

DNA was extracted from pneumococci using a DNeasy Blood and Tissue Kit (Qiagen) according to the manufacturer's instructions using the protocol for gram positive bacteria. Seven PCR reactions were set up for each isolate using the primers shown in table 2-2 using Qiagen Taq polymerase. After an initial incubation at 95˚C for 3 minutes to activate the DNA polymerase, 30 cycles were performed consisting of denaturation at 95˚C for 30 seconds, annealing at 50˚C for 60 seconds and extension at 72˚C for 60 seconds. A terminal extension step of 10 minutes was included. Final mixtures were run on a 1.5% agarose gel at 100V for 1 hour to confirm the presence of a single band and cleaned up using a Qiaquick PCR purification kit. Fragments were sequenced using the same primer pairs used for PCR and processed using the multilocus sequence typing (MLST) database (http://spneumoniae.mlst.net/misc/info.asp#dbase) to obtain the sequence type.

2-2.6 Electron Microscopy

Electron microscopy wash buffer was prepared as follows: cacodylate buffer supplemented with 0.075% ruthenium red. Fixation buffer was similar in composition to wash buffer except that it was further supplemented with 2% formaldehyde and 2.5% glutaraldehyde.

*S. pneumonia*e strains were grown to mid-log phase (optical density (OD) = 0.6). Pneumococci were then washed once by centrifugation at 3000g and resuspension in PBS. Fixation was then undertaken with fixation buffer supplemented with 0.075M lysine-acetate for 20 minutes on ice. The samples were then further incubated for 3 hours on ice in fixation buffer without the lysine-acetate, washed with wash buffer and then subjected to further fixation with 1% osmium in wash buffer. Samples were then washed three times with wash buffer.

Further processing was conducted in the electron microscopy department at Glasgow University by the department staff. Samples were dehydrated on ice through serial alcohols before infiltration with LRWhite acrylic resin mixed with decreasing concentrations of alcohol for three changes and then placed in gelatin capsules filled with pure resin. Samples were then polymerised for 48 hours at 60˚C before ultrathin sections were cut using a diamond knife and counterstained using 4% aqueous uranyl acetate for 5 minutes. Samples were then examined by transmission electron microscopy.

At least 10 bacteria were assessed from each pneumococcal strain by delineating the bacterial perimeter and capsule perimeter using ImageJ. Capsular area was expressed as the percentage of the bacterial area measured.

2-2.7 Capsular thickness by dextran exclusion

Bacteria were grown to mid-log phase (OD = 0.6) in 10ml of BHI and washed three times by centrifugation at 3000g for 10 minutes and resuspending in PBS. The final resuspension was in 1ml of PBS. 10µl of bacterial suspension was then mixed with 2µl of anionic 3,000 MW dextran conjugated to Alexa Fluor 488 (Life Technologies) on a glass slide and a cover slip firmly applied. Bacteria were imaged by confocal microscopy (Zeiss LSM 510) using the x100 lens. Images were taken using the confocal detector on an appropriate filter set and via the transmitted light detector to allow counting of bacteria in a chain.

Images were corrected with Photoshop (Adobe Systems) analysed by using ImageJ 1.47v (US National Institutes of Health). The background illumination was normalised by applying a division layer with a 50 pixel Gaussian blur over the uncorrected image. A mask was generated over the zones of exclusion using the automated thresholding tool in ImageJ and particle analysis performed to determine the size of each masked area in μm^2. This area was then divided by the number of bacteria present in it on the matched transmitted light view to generate the area of dextran excluded per cell. At least 200 areas of dextran exclusion were assessed per strain. The image analysis process is demonstrated in figure 2-2.

2-2.8 Haemolysis assay

Bacteria were grown to mid-long phase (OD = 0.6) before washing three times by centrifugation at 3000g for 10 minutes and resuspending in PBS. Bacteria were then sonicated on ice using a Soniprep 150 (MSE, UK) for 8 rounds of 30 seconds followed by a 30 second gap. Lysates were then cleared by centrifugation at 18,000g for 10 minutes and activated with 10mM dithiothreitol (Sigma) at room temperature for 20 minutes. Lysates were then serially diluted in a 1:1 ratio with PBS with 10mM dithiothreitol across a 96 well plate to generate dilutions from 1 to 1:2048 with a final volume of 50µl. 50µl of a 1.8% washed horse erythrocyte solution was then added and gently mixed before incubation at 37˚C for 1 hour. A standard curve was generated by making a lysed horse blood suspension with distilled water and diluting this with PBS. At the end of the incubation step, plates were centrifuged at 400g for 5 minutes to clear intact red blood cells and the supernatant carefully aspirated to avoid carrying over intact red cells. Supernatants were read using a Sunrise ELISA plate reader measuring absorbance at 405nm. A dose response curve was generated and the EC50 calculated. Haemolysis units were defined as the reciprocal of the dilution at which 50% of red blood cells were lysed. Since the EC50 was mathematically calculated, this value could lie between measured dilutions.

2-3 Human Co-culture Methods

2-3.1 Selection of healthy volunteers and patients with pneumococcal disease

Healthy volunteers aged between 18 and 35 years were recruited from a hospital pre-travel clinic prior to the administration of any travel related vaccines. Subjects aged 65 years and older were recruited from hospital surgical clinics when they attended with diagnoses unrelated to immune/inflammatory disorders. Subjects had to be healthy and without intercurrent infections. Patients with pneumococcal infection were identified in collaboration with the local microbiology laboratory. Patients were eligible for inclusion if they had identification of culture confirmed *S. pneumoniae* in a normally sterile body fluid. Subjects were excluded if they had been diagnosed with any inflammatory, malignant or immunosuppressive condition. Subjects were also

excluded if they had a diagnosis of any chronic respiratory condition including asthma.

Participants gave written, informed consent to be included and gave blood at the time of recruitment.

2-3.2 Preparation of bacterial inoculum

Frozen stock of TIGR4 was prepared by intra-peritoneal passage through MF1 mice as described in section 1.9. Colony counts were conducted on at least three stock vials to ensure consistent bacterial density.

Pneumococci were thawed to room temperature and then washed three times in PBS by centrifugation at 3000g for 10 minutes before resuspending the pellet by gentle agitation. On the final wash the pneumococci were resuspended in antibiotic free media.

2-3.3 Preparation of heat killed *Candida albicans*

Candida albicans was obtained courtesy of Dr Donald Inverarity (Dept of Microbiology, Monklands Hospital) having been isolated from the respiratory secretions of a patient on the intensive care unit. The candida was grown on Sabouraud agar and a single colony was inoculated into Sabouraud dextrose broth. Candida was grown to mid-log phase and then colony counts were performed by serial dilution and plating onto Sabouraud agar. Cells were washed three times in PBS by centrifugation at 600g for 10 minutes before resuspending in 1ml of PBS by gentle agitation. Cells were then inactivated by heating in a water bath to 56˚C for 30 minutes. Inactivation was confirmed by plating 100µl onto Sabouraud agar. The following day, the inactivated candida was diluted to achieve a concentration of 10^9 cfu/ml. Stocks of heat killed *Candida albicans* (HKCA) were refreshed on a monthly basis.

2-3.4 Isolation of PBMCs and human serum

Phlebotomy was performed according to standard methods using sealed vacuum tubes. Blood for PBMCs was placed into lithium heparin tubes and blood for

serum used a gel separator tube (both BD Biosciences). Tubes were stored at room temperature until blood used (always within 3 hours).

To extract PBMCs, anti-coagulated blood was mixed 1:3 with Hank's balanced salt solution (HBSS) and 30ml per tube carefully layered onto 15ml of Ficoll Paque Plus (GE Healthcare) before centrifugation with gentle start and the brakes off at 400g for 40 minutes at room temperature. The buffy coat was then carefully aspirated from each tube and washed twice with 45ml of HBSS for 10 minutes at 400g and then a final wash at 200g to deplete any contaminating platelets before resuspending into magnetic- activated cell sorting (MACS) buffer (PBS supplemented with 2 mmol/l ethylenediaminetetraacetic acid (EDTA) and 0.5% bovine serum albumin (BSA)).

Gel separator tubes were left for at least 1 hour at room temperature to allow complete coagulation to take place before centrifugation at 1300g for 10 minutes. Serum was then inactivated by immersion in a water bath at 56°C for 30 minutes.

2-3.5 Isolation of monocytes and memory $CD4^+$ lymphocytes

PMBCs were counted and $CD14^+$ monocytes were separated using human CD14 MicroBeads (Miltenyi Biotec) and LS MACS columns according to the manufacturer's instructions. The run through from the MACS positive selection was then immediately used to carry out negative selection of memory $CD4^+$ lymphocytes using the Memory $CD4^+$ T cell isolation kit (Miltenyi Biotec) according to the manufacturer's instructions except that the input cell number was taken to be the cell number prior to depletion of $CD14^+$ cells.

Where appropriate, sorted cells were labelled with anti-CD14 or anti-CD4 and anti-CD45RO antibodies and purity was assessed using Flow Cytometry.

2-3.6 Co-culture of monocytes and lymphocytes

Prior to co-culture, memory $CD4^+$ cells were stained using 10mM eFluor 450 proliferation dye (eBiosciences) according to the manufacturer's instructions except that excess dye was bound by suspending cells in 20% human serum and

cells were washed in 5% human serum. Stained memory $CD4^+$ cells were then co-cultured with monocytes in a 10:1 ratio in antibiotic free co-culture media at a density of 10^6 lymphocytes/ml. Isocove's modified Dulbecco's medium (IMDM) was chosen as the base media for this step because of reported superiority for the culturing of Th17 cells [383].

Co-cultures were conducted in triplicate by incubating 2 x 10^5 lymphocytes with 2 x 10^4 monocytes in 200 µl per well in round bottom 96 well plates. Co-cultures were stimulated with bacteria or HKCA as appropriate and after 30 minutes penicillin/streptomycin solution (Invitrogen) was added to the co-culture to a final concentration of 1%. Co-cultures were supplemented with 100 µl of media on day 4 and incubated for a total of 7 days.

On the seventh day, culture medium was carefully aspirated off the plate and frozen at -20˚C until analysis. Cells were recovered with media containing anti-CD4 antibody for 30 minutes before media was gently exchanged for media containing phorbol 12-myristate 13-acetate (PMA) (50 ng/ml), ionomycin (1 µg/ml) and Brefeldin A (5 µg/ml). Cells were then incubated for 6 hours at 37˚C.

Cells were washed three times at 400g for 5 minutes and resuspended in serum free buffer. Cells were stained with eFluor 506 fixable viability dye (eBioscience) according to the manufacturer's instructions and washed three times at 400g for 5 minutes. Cells were then fixed by resuspending in 4% paraformaldehyde for 20 minutes at 4˚C. After three further washes at 400g for 5 minutes cells were stored overnight at 4˚C suspended in fluorescence-activated cell sorting (FACS) buffer (PBS supplemented with 2mmol/l EDTA, 10% foetal calf serum (FCS) and 0.09g/l sodium azide). The next day, cells were washed at 400g for 5 minutes and resuspended in Cell Permeabilization solution (Biolegend) for 20 minutes at 4˚C. Cells were then washed and stained in Cell Permeabilization solution with antibodies against a selection of cytokines (usually IL-17A, IL-22, IFN-γ and either IL-17F or IL-4). Finally, cells were washed three times at 400g for 5 minutes and resuspended in FACS buffer.

2-3.7 Flow cytometry

Flow cytometry was conducted using a Beckman Coulter CyAnADP or BD LSR II. After doublet exclusion and dead cell exclusion, cells were gated on $CD4^+$ cells and proliferating cells expressing each cytokine were enumerated as a percentage of total $CD4^+$ cells. Figure 2-3 contains a table outlining the antibodies used in these experiments and, where appropriate, isotype controls.

2-3.8 Sorting of cells by CCR6 status

Proliferation dye stained memory T lymphocytes were prepared as outlined in section 2.4. Cells were then stained with anti-CCR6 antibody and sorted based on CCR6 status using a BD FACS Aria cell sorter using azide free FACS buffer. Sort purity was determined by running a small number of the sorted cells back through the flow cytometer. After sorting, $CCR6^-$ and $CCR6^+$ cells were co-cultured with monocytes as described in section 2-3.6.

2-3.9 ELISA

ELISA was conducted using IL-17A, IL-22 or IFN-γ Ready-SET-GO! kits (eBioscience) in triplicate according to the manufacturer's instructions except that only 95 µl of supernatant or control per well was used and analysis was carried out sequentially decanting supernatants from one plate to another to allow all analysis to be conducted using the available supernatant volume. Where required, supernatant was diluted to obtain values in the valid range.

2-3.10 Data analysis

Flow cytometry data was analysed using FlowJo version 8 for Mac OS X. Analysis of the pooled flow cytometry data was conducted in part using SPICE 5.3 (National Institute of Allergy and Infectious Diseases, https://exon.niaid.nih.gov/spice/). Statistical analysis was conducted using Prism 6 (GraphPad Software). Groups were compared using a one-way ANOVA and Mann-Whitney test for non-parametric data.

2-3.11 Ethics statement

The study was approved by the local regional ethics committee and NHS research and development department. It was conducted in accordance with principals of Good Clinical Practice at all times.

2-4 Animal models

2-4.1 Source, care and maintenance of animals

MF1 and C57Bl/6 mice were obtained from Harlan laboratories (Oxfordshire, UK). C57Bl/6 mice to be bred in house were obtained from Prof Rob Nibbs (University of Glasgow). IL-17RA$^{-/-}$ mice were obtained from Prof Tim Mitchell (University of Glasgow) and IL-22$^{-/-}$ mice were obtained from Dr Wenjun Ouyang (Genentech, CA). Both genetically modified mice were on a C57Bl/6 background.

Animals were maintained in specific pathogen free conditions at the Joint Research Facility at the University of Glasgow. IL-17RA$^{-/-}$ mice bred poorly and this required the use of both male and female mice in most experiment. At all times, mice were selected to be age and sex matched and were used between 6 and 12 weeks of age except where noted in the text.

Mice were culled either by manual dislocation of the cervical vertebrae or inhalation of an increasing concentration of CO_2. All techniques involving animals were performed in accordance with Home Office guidance and in compliance with the legal framework.

2-4.2 Clinical monitoring of infected animals

Clinical monitoring of infected animals was conducted using the scoring system outlined in table 2-3. This scoring system had two principal aims: to allow the recording of clinical illness in infected animals and to prevent unnecessary suffering through detecting animals becoming severely unwell. Animals were scored at least twice per day except in the terminal stages of experiments when animals had been seen to recover.

Table 2-4 is a table showing all animals found dead while on an ASPA licence procedure during the study.

2-4.3 Confirmation of knockout phenotype of genetically modified mice

IL-17RA$^{-/-}$ status of mice was confirmed by gently homogenising spleens by mechanical disruption and passing through a 40µm cell strainer. Splenocytes from WT and IL-17RA$^{-/-}$ mice were stained with an antibody specific for IL-17RA or isotype control to confirm the absence of IL-17RA staining from IL-17RA$^{-/-}$ animals.

Ear-lobe punch biopsies were taken from IL-22$^{-/-}$ and wild type mice and DNA extracted using the Qiagen DNeasy blood and tissue kit according to the manufacturer's instructions. PCR was then conducted using following primers: p-1 (5'- CTC AGA CCT CTA CAG ACA ATC ATC-3') and p-2 (5'- CAG CTG GCG GCC AAA GTC CC-3') were used to amplify the wild type gene product (194bp) while p-1 and p-3 (5'- GAT ACA GGT GCA GCT AAG CGA G-3') were used to amplify IL-22-/- gene product (374bp). All three primers were added to the reaction mixture to exclude heterozygotes (which would produce two products). PCR was conducted using Hot Start Green Master Mix (Promega). PCR was performed as follows: 95˚C for 3 minutes to activate the DNA polymerase, 30 cycles were performed consisting of denaturation at 95˚C for 30 seconds, annealing at 58˚C for 60 seconds and extension at 72˚C for 60 seconds. A final extension step of 10 minutes was employed. Final reaction mixtures were run on a 2% agarose gel at 200V for 2 hours and visualised using SYBR Safe (Life Technologies).

2-4.4 Generation of pneumococcal standard innocula

Pneumococci were grown to mid-log phase in BHI and then pelleted by centrifugation at 3000g for 10 minutes. Bacteria were resuspended into BHI supplemented with 25% glycerol and frozen at -80˚C until use. Stocks were thawed, washed three times with PBS and colony counting conducted on at least three vials to ensure consistent bacterial density.

A suspension of 1 x 10^5 cfu/ml of bacteria was prepared from the above stocks and 100 µl was injected intraperitoneally into a 6-week-old MF1 mouse. Mice

were monitored closely for signs of disease and after 18 hours mice were anaesthetised by inhalation of isofluorane and blood obtained by cardiac puncture. Blood was added to 45ml of BHI and incubated at 37˚C in a water bath overnight. The next morning, 1 ml of BHI was added to a new container with 50ml of BHI supplemented with 20% heat inactivated foetal calf serum and grown to mid-log phase. At this point the culture was aliquotted into 1 ml cryovials and stored at -80˚C until use. Colony counting was performed on at least three thawed vials to ensure even bacterial density.

For some strains of pneumococci as noted in the text, broncho-alveolar lavage (BAL) fluid obtained from intra-nasally infected C57Bl/6 mice was used to seed the BHI rather than blood but the remainder of the generation of the standard inoculum was conducted using the same method.

2-4.5 Innoculation of substances

2-4.5.1 Intra-nasal innoculation of mice under general anaesthesia

Mice were anaesthetised by inhalation of 3-4L/min isofluorane with 2L/min supplemental oxygen. Depth of anaesthesia was judged by observing respiratory rate and intra-nasal inoculation given as soon as the breathing slowed. Animals were processed in a maximum group size of three to attempt to give uniform anaesthesia.

Mice were inoculated with 25µl of appropriate substance on each nostril and allowed to fully aspirate the first inoculation before the second was given. Animals were placed on their backs between and after innoculations to facilitate aspiration. Animals were observed closely until fully recovered from effects of anaesthesia. To assess the consistency of the method, animals were inoculated with 0.4% Trypan blue and culled 2 hours later.

2-4.5.2 Intra-nasal innoculation of mice without anaesthesia

For nasal colonisation studies, a 50ml Falcon tube was prepared by cutting off the tip of the bevelled base of the tube. Mice were encouraged to enter the tube so that their nose emerged from the tip of the tube. 10µl of bacterial suspension or other appropriate substance was then inoculated onto the nares

and the animal gently held in position until the liquid had entered the nose.

2-4.5.3 Intra-peritoneal injection

Mice were gently restrained by grasping the scruff and injected with up to 1ml into the right lower quadrant of the abdomen.

2-4.5.4 Administration of antibiotics

In experiments involving antibiotic treatment, ceftriaxone (Roche Pharmaceuticals) was administered by intraperitoneal injection at a dose of 50μg/g. Antibiotics were administered once animals began to show clinical signs of infection and the treatment was repeated 36 hours later. No adverse effects of antibiotic administration were observed at any time.

2-4.6 Collection of samples

2-4.6.1 Blood

Blood was obtained from live animals by tail vein bleeding. Animals were warmed to 37˚C in a hot box before restraint and puncture of the superficial vessels of the tail with a stylet and aspirated with a pipette. Alternatively where the animal had been culled, blood was obtained by severing the great vessels in the abdomen and aspirating blood. To prevent clotting prior to processing, blood was added in a 1:10 ratio to PBS containing 15 USP units of heparin per ml.

To obtain larger volumes of blood, cardiac puncture was performed by anaesthetising mice by inhalation of isofluorane. Blood was then aspirated from the heart by piercing the thoracic wall at the left sternal edge and slowly aspirating blood. Once aspiration was complete, mice were culled by manual dislocation of cervical vertebrae.

Where appropriate, blood films were prepared and air-dried before fixation and staining with a Rapid Romanowsky stain (Thermo Scientific).

2-4.6.2 Bronchoalveolar lavage

Taking care to avoid puncturing the cervical vessels, the anterior neck was dissected down to expose the trachea and a small nick made in the anterior portion of the trachea to allow the insertion of a 1ml fine tip pastette containing 1ml of ice cold PBS. PBS was carefully lavaged three times with collection back into the pastette.

2-4.6.3 Pleural lavage

The anterior chest wall was dissected to expose the ribs. The abdomen was opened and the diaphragm exposed by carefully withdrawing the liver. The thoracic cavity was then infused through an exposed intercostal space with 5ml of ice cold PBS. The mouse was gently shaken to mix the fluid and it was then aspirated via a transdiaphargmatic approach.

2-4.6.4 Peritoneal lavage

The anterior abdominal wall was dissected to expose the anterior abdominal wall and 5ml of ice cold PBS was injected into the right lower quadrant. The animal was gently shaken to mix the fluid and then fluid was aspirated from the left side of the abdominal wall.

2-4.6.5 Nasal lavage

The trachea was exposed and incised in the manner described above. The trachea was cannulated with an extended tip fine pipette in retrograde direction and the tip advanced until mild resistance was felt. 1ml of ice cold PBS was then slowly infused through the nose and collected by allowing it to drip from the tip of the nose into a 2ml centrifuge tube.

2-4.6.6 Solid organs

In some experiments both lungs were taken for histology, In this case the lungs were gently inflated with fixative before removing the lungs and placing them in 7ml of fixative.

In other experiments the right lung was divided into lobes and placed into containers appropriate for the assay to be performed. The left main bronchus was then cannulated and the left lung gently inflated with fixative prior to removal and placing into 4ml of fixative.

2-4.7 Organ homogenates

2-4.7.1 Lungs

After removal from the animal, lungs were placed into 2 ml IMDM media supplemented with 1% FBS, 50 µg/ml DNAse and 0.65 units/ml liberase TM (Roche, CH). Samples were then shaken vigorously for 1 hour at 37˚C. The samples were gently mashed through a 40 µm cell strainer and washed three times by centrifugation for 5 minutes at 400g and resuspended in PBS. Red blood cells were then lysed by resuspending in 5ml red cell lysis buffer for 10 minutes at room temperature before the addition of 45ml ice cold PBS. Cells were then washed on a further three occasions with PBS before proceeding to preparation for flow cytometry.

2-4.7.2 Spleen

After removal from the mouse, spleen was stored in IMDM supplemented with 5% FBS until processed. Spleen was gently disrupted with forceps to release the cells. Cells were then washed and processed as described above for lungs.

2-4.8 Myeloperoxidase and collagen assays

In early experiments, lungs were weighed and the myeloperoxidase activity calculated by measuring the units per gram of lung tissue. However, once SRL1 was used and the marked difference in lung composition in inflamed lung was recognised, it was decided that for later experiments the total MPO activity per lobe of lung should be calculated as this would be more representative.

After removal from the animal, lungs were placed in a buffer containing 50 mMol KH_2PO_4 with 0.5% hexadecyltrimethylammonium bromide (HTAB) in ddH_2O. Lungs were then homogenised using a mechanical tissue grinder and sonicated on ice using a Soniprep 150 (MSE, UK) for 8 rounds of 30 seconds followed by a 30

second gap. Lysates were then cleared by centrifugation at 18,000g for 10 minutes. 14µl of each lysate was then placed into wells of an ELISA plate in triplicate. Immediately before analysis, 200µl of a buffer containing 10 mMol KH_2PO_4 with 0.05% HTAB and 0.006% H_2O_2 in ddH_2O supplemented with 168µg/ml O-dianisidine was added to each well of the ELISA plate and the plate analysed immediately.

7 measurements over 210 seconds of absorbance at 540nm were taken and a regression line plotted for each well. The slope of the line was normalised to give the rate of change in absorbance per minute per lobe of lung.

Collagen assays were conducted using the Total Collagen Assay (Quickzyme Biosciences) according to the manufacturer's instructions using a lung dilution factor of 50.

2-4.9 Wet/Dry ratio

A single lobe of lung was blotted on tissue paper to remove surface fluid and carefully weighed. The lung was then placed in an oven at 60˚C for 48 hours and the dessicated lung weighed again. Results were presented as a ratio of the wet to dry weight of the lung.

2-4.10 Histopathology

2-4.10.1 Chemicals and solutions

All components are from Sigma Aldrich unless otherwise stated

Zinc-Tris fixative (ZTF)

- 0.05% Calcium Acetate, 0.5% Zinc Acetate, 0.5% Zinc Chloride in a 0.1M Tris buffer adjusted to pH 7.4

1% Acid Alcohol (1%AA)

- 1% HCl in 70% ethanol

Scott's Tap Water Substitute (STWS)

- 0.2% sodium hydrogen carbonate with 2% magnesium sulphate in distilled water

Picro-sirius Red Solution

- 1% Sirius red F3B (Direct Red 80) in saturated aqueous solution of picric acid

Acidified Water

- 0.5% acetic acid in distilled water

Tartrazine solution

- 0.25% tartrazine and 0.25% acetic acid in distilled water

2-4.10.2 Fixation and processing

Tissue was fixed in 10% neutral buffered formalin (NBF) or zinc-tris fixative (ZTF). Formalin fixed tissue was stored in NBF for 48 hours and transferred to 70% ethanol. Zinc fixed tissue was stored in ZTF for 48 hours and then washed under running tap water for 30 minutes. Tissue was then transferred into 70% ethanol. Processing of samples was identical from this point on regardless of the fixation method.

Tissue was processed in a Shandon Citadel 1000 tissue processor (Fisher Scientific) by dehydration through serial alcohols, cleared in two changes in xylene and embedded in paraffin.

Sections were cut on a Hacker-Bright 5040 microtome (Fisher Scientific), placed on Colorfrost charged slides (Fisher Scientific) and dried overnight. The next day, sections were heated to 55˚C in an oven for 10 minutes before being deparaffinised in two changes of xylene for 5 minutes each and rehydrated in two changes each of 100%, 90% and 70% ethanol for 3 minutes before being rinsed in PBS.

2-4.10.3 Haematoxylin and Eosin

Sections were stained with Mayer's haematoxylin (Leica Microsystems) for 5 minutes before differentiation with 1%AA. Bluing was performed with 10 dips in STWS before staining with 1% aqueous Eosin (Leica Microsystems). Sections were dehydrated in serial alcohols before two changes of xylene for 5 minutes each. Slides were coverslipped using DPX mountant (VWR).

Lung inflammation was assessed by blinded examination of sections using the scoring system outlined in Table 2-5.

2-4.10.4 Picrosirius red staining

Hydrated sections were postfixed in Bouin's solution overnight and then rinsed thoroughly in tap water. Sections were then placed in Picro-sirius Red solution for one hour at room temperature before being washed in two changes of acidified water. Slides were then dehydrated rapidly in three changes of 100% ethanol before clearing in xylene and mounting with DPX mountant.

2-4.10.5 Tissue gram staining

Standard gram staining solutions were obtained from BD Biosciences. Hydrated sections were covered with 5 drops of crystal violet solution and 1 drop of 5% sodium bicarbonate solution for 1 minute and rinsed with distilled water. Sections were then covered with Gram's iodine solution for 5 minutes and differentiated with absolute acetone by repeatedly changing the acetone until no more crystal violet bleeds from the sections. Sections were then rinsed in ddH_2O and covered with sarfarin O solution for 1 minute. Sections were rinsed in ddH_2O and then dipped in tartrazine solution for 10 seconds. Sections were rinsed in ddH_2O and then rapidly dehydrated in three changes of alcohol for around 10 seconds per change. Sections were cleared in two changes of xylene for 1 minute per change and mounted with DPX mountant.

2-4.11 Immunohistochemistry

2-4.11.1 Chemicals and solutions

Methyl Green Solution

- 1.36g sodium acetate in 100ml distilled water adjusted to pH 4.2 with acetic acid. Acetate buffer then supplemented with 0.5g methyl green

Incubation Solution

- 5% normal goat serum, 10mg/ml BSA, 0.02% sodium azide in PBS

Blocking/Permeabilisation Solution

- Incubation solution with the addition of 0.3% Triton-X 100

2-4.11.2 Immunohistochemistry

After hydration, where appropriate to the imaging method, endogenous peroxidase was blocked by immersion in a 3% H2O2 in PBS for 30 minutes and endogenous biotin blocked using an Avidin/Biotin blocking kit (Vector Laboratories) according to the manufacturer's instructions. Sections were then incubated at room temperature for 1 hour with blocking/permeabilisation solution and then subsequent washes and incubations were carried out using incubation solution unless otherwise specified. Washes were performed by changing the solution over the section five times leaving 5 minutes between changes.

Sections were incubated overnight at 4˚C with primary antibody or matched isotype controls. The following day, sections were washed before incubation for 1 hour at room temperature with the appropriate secondary antibody and subsequently washed again.

For immunohistochemistry, sections were then incubated for 30 minutes at room temperature with avidin/biotinylated peroxidase complex (VECTASTAIN ABC, Vector Laboratories) and washed. Sections were then incubated at room temperature with 3,3'-diaminobenzidine (DAB, Vector Laboratories) until adequate colour change occurred. Sections were rinsed in water before nuclei

were stained for 5 minutes with methyl green solution and rinsed in distilled water. Sections were then dehydrated rapidly through serial alcohols, cleared in two changes of xylene for 5 minutes each and coverslipped as before.

For immunofluorescence microscopy, where appropriate, sections were incubated with an appropriate fluorophore/streptavidin conjugate for 30 minutes at room temperature and washes. Finally, sections were incubated with 100nM Sytox Green or Sytox Orange (Invitrogen) in PBS for 30 minutes at room temperature and washed. Sections were mounted in Fluoromount-G (eBioscience) and coverslipped.

2-4.12 Flow cytometry

2-4.12.1 Flow cytometers

Flow cytometry was performed on FACSCalibur, LSR II, Aria II (all BD) or CyAN ADP (Beckman Coulter) flow cytometers as appropriate to the experiment.

2-4.12.2 Neutrophil detection

Blood and BALF were washed three times by centrifugation at 400g for 5 minutes and resuspension in PBS before lysis of red blood cells with red cell lysis buffer at room temperature for 10 minutes before resuspending in FACS buffer. Cells were stained with anti-Gr-1 antibody (clone RB6-8C5, Biolegend) conjugated to PE diluted 1:1000 with FACS buffer for 30 minutes at 37˚C. For some experiments, CountBright absolute counting beads (Life Technologies) were added prior to the first wash to enable absolute counting of neutrophils.

Neutrophils were gated based on Gr-1^{+}Side scatter^{hi}.

2-4.12.3 Solid organ homogenates

Lung homogenates were prepared as in section 2-4.7.1. In some experiments lung homogenates were resuspended in IMDM supplemented with 5% FBS, 1% penicillin/streptomycin solution and supplemented with PMA (50 ng/ml), ionomycin (1 μg/ml) and Brefeldin A (5 μg/ml) for 6 hours before preparation for flow cytometry. Alternatively, cells were prepared directly for flow cytometry.

Cells were washed three times by centrifugation at 400g for 5 minutes and respension in PBS without the addition of serum. Cells were then stained with fixable viability dye (FVD) 506 or FVD 750 (both eBioscience) according to the manufactuer's instructions. Cells were then washed as before but resuspended in FACS buffer. Cells were then stained for cell surface markers as shown in figure 2-4 for 30 minutes at 4˚C. Cells were then washed three times as before and resuspended in FACS buffer before fixing with 4% paraformaldehyde in PBS (VWR) at 4˚C for 20 minutes. Cells were washed three times as before and resuspended in FACS buffer. At this stage cells were optionally kept at in the dark at 4˚C overnight. Cells were then washed as before and resuspended in permeabilisation buffer (Biolegend). After a further incubation at 4˚C for 20 minutes the cells were stained with antibodies against intracellular cytokines for 30 minutes at 4˚C. Finally cells were washed three times as before and resuspended in FACS buffer for flow cytometry.

2-4.13 In vivo Brefeldin A studies

Animals were infected as previously described. Brefeldin A powder (Sigma) was dissolved in DMSO to a concentration of 20mg/ml. Immediately prior to use, Brefeldin A stock solution was diluted to a concentration of 500µg/ml in PBS pre-warmed to 37˚C.

6 hours prior to the time of planned cull the mice were administered an intraperitoneal injection of 250 µg of Brefeldin A. No adverse effects of Brefeldin A administration were observed at any time.

2-4.14 Quantitative rt-PCR

Immediately after dissection, lungs were placed in RNA later solution (Life Technologies) and frozen at -80˚C until use. After gentle thawing, lungs were transferred into a 2ml centrifuge tube with a 5mm steel bearing (Qiagen) and 1ml Trizol (Life Technologies). Samples were loaded into a TissueLyser LT (Qiagen) and pulsed at 50 Hz for 5 minutes. RNA was then extracted from the lung homogenate using a PureLink RNA Mini Kit (Life Technologies) and first strand cDNA generated using s SuperScript First-Strand Synthesis System (Life Technologies) using oligoDT primers according to the manufacturer's instructions.

PCR was then conducted using Fast SYBR Master Mix (Life Technologies) according to the manufacturer's instructions using the following primers: TBP forward CCCCACAACTCTTCCATTCT, reverse GCAGGAGTGATAGGGGTCAT; ß-defensin 4 forward TCTCTTCACATTTCTCCTGGTG, reverse TGGATTGTTGATAATTTGGGTAAA; S100A8 forward TGCGATGGTGATAAAAGTGG, reverse GGCCAGAAGCTCTGCTACTC; MIP-1α forward CGTTCCTCAACCCCCATC, reverse TGTCAGTTCATGACTTTGTCATCAT. Gene expression was compared to that of the housekeeping gene TATA-binding protein (TBP) and expressed as relative gene expression according to the ΔΔCT method.

2-4.15 Respiratory Tract Microbiome

Genomic DNA was extracted from nasal washes and BALF using a Qiagen DNeasy Blood and Tissue Mini Kit according to the manufacturer's instructions using the suggested modification to enhance lysis of gram-positive organisms and eluted into 100 µl. After extraction the V_1-V_2 region of the 16S RNA was amplified using NEB Next High Fidelity 2x PCR Master Mix (New England Biolabs) using 10 µl of genomic DNA and 12.5 pmol of the high performance liquid chromatography barcoded primers shown in Table 2-6 (Eurofins Genomics). PCR was conducted using an initial denaturation period of 30 seconds at 98˚C followed by 25 cycles consisting of denaturation for 10 seconds at 98˚C, annealing for 30 seconds at 58˚C, and extension for 30 seconds at 72˚C before a final extension for 1 minute at 72˚C.

Presence of a single PCR product at the expected band size of 440 bp was confirmed by 1.8% agarose gel electrophoresis before purification of the PCR product using a Qiagen PCR purification kit according to the manufacturer's instructions. PCR products were roughly quantified by comparing the band intensity and then roughly equal quantities of products were mixed together and a final confirmation of band size by gel electrophoresis was performed.

Sequencing was performed by the Centre for Genomic Research (CGR), University of Liverpool. Paired end (2x250bp) sequencing of pooled amplicon sample on the Illumina MiSeq platform was conducted using higher levels of Phix to increase diversity. Sequences were demultiplexed by the CGR.

Sequences were processed using the AMPLICONprocessing pipeline[384]. Briefly, sequences were trimmed and forward and reverse reads were overlapped using PANDASEQ[385]. Sequences were then dereplicated and chimeric sequences removed using UCHIME[386]. Operational taxonomic units (OTUs) were then generated using UPARSE[387] and taxonomic assignments were generated using RDP Classifier[388].

Analysis was conducted using the R packages vegan[389], phyloseq[390] and visualised using ggplot2[391].

2-4.16 Infection model RNA extraction and RNA-Seq

Wild type mice were infected with SRL1 and culled at 48 hours as previously described. BALF and pleural aspirate were obtained from each animal and placed immediately into 5ml Trizol with 1ml 0.1mm Zirconia beads before mechanically lysing the material by vortexing tubes for 10 minutes. 1,330 µl of chloroform was added to the mixture and mixed by vigorous manual shaking for 15 seconds before incubation at room temperature for 10 minutes. Samples were then separated by centrifugation at 4,500 rpm for 15 minutes at 4˚C. The aqueous phase was then extracted by pipette. RNA was then purified using the Zymo RNA Clean and Concentrator kit (Zymo Research, CA) according to the manufacturer's instructions.

RNA was further processed at the CGR, Liverpool. Samples were further purified using Agencourt RNAClean XP beads (Beckman Coulter) and ribosomal RNA depleted using the Ribo-Zero rRNA Removal Kit (Illumina, CA) before library preparation, multiplexing and sequencing on the Illumina Hi-Seq platform.

Reads were de-multiplexed and analysed using CLC Genomics Workbench 7 (Qiagen). Reads were aligned against the ST180 reference genome (OXC141, GenBank ID 50733) [392] and differential gene expression calculated using the default settings in CLC with statistical analysis using EDGE-R [393]. A false discovery rate adjusted (FDR) P value <0.05 was taken to imply a significant difference in gene expression.

2-4.17 In vitro neutrophil studies

2-4.17.1 Isolation of murine neutrophils

9% casein suspension was made by slowly adding casein powder to distilled water over a period of several hours while heating to around 55˚C with continuous stirring.

Mice were administered two 1ml i.p. injections of 9% casein solution at an interval of 21 hours. 3 hours after the second injection, the mice were killed by inhalation of CO_2. The parietal peritoneal surface was exposed and cleaned. 6ml of PBS with 0.02% EDTA at room temperature was injected through the peritoneal wall with care to ensure the abdominal contents were not traumatised. The abdominal cavity was then agitated gently before the fluid was carefully aspirated and cooled to 4˚C on ice. Cells were then washed in PBS and resuspended in 4 ml 52% Percoll.

15ml centrifuge tubes were prepared with 4ml of 64% Percoll layered onto 4ml 72% Percoll. The peritoneal lavage cells resuspended in 52% Percoll were then carefully layered onto the Percoll gradient. The gradient was then centrifuged at 600g with low acceleration and the brakes off for 30 minutes at 4˚C. Cells from the top layer (consisting of a mixture of macrophages, lymphocytes with neutrophils) were discarded and cells from the second (more poorly defined layer) were aspirated carefully into a centrifuge tube and washed with PBS. Neutrophils were then counted and resuspended in media for use in further experiments. Optionally, cytospin preparations of isolated cells were prepared and stained with a Hema 3 modified Wright-Giemsa stain (Fisher Scientific).

2-4.17.2 Isolation of human neutrophils

Blood was drawn into lithium heparin tubes before layering 5ml over 5ml of Lymphocyte Poly (Cedarlane Labs). Density separation was performed by centrifugation at 500g for 35 minutes at room temperature with low acceleration and the brakes off. After aspirating the upper layers containing plasma and mononuclear cells the remaining layers containing neutrophils and isolation solution were washed in HBSS and red cells lysed using lysis buffer and washed

twice in HBSS. Neutrophils were then resuspended in media and used for downstream applications.

2-4.17.3 Phagocytosis and killing studies

Bacteria were grown to mid-log and then washed before resuspending in PBS with 10% mouse serum. Bacteria were then incubated at 37˚ while being mixed end over end on a rotary shaker for 30 minutes to allow binding of complement. Neutrophils were suspended at a concentration of 5 x 10^6/ml in PBS. Neutrophils were then mixed with bacteria at to achieve a multiplicity of infection (MOI) of 2 and placed on the rotary shaker at 37˚C. As a control, bacteria were mixed with an equivalent volume of PBS without neutrophils and similarly incubated. At intervals, 500µl of mixture was aspirated and added to 1.5ml of ice cold PBS to inhibit further phagocytosis. Samples were centrifuged at 100g to pellet neutrophils but leave extracellular bacteria in supernatant. Supernatants were collected and neutrophils washed twice more in 2ml of ice cold PBS. In total 6ml of supernatant was collected from each sample. Pellets were then lysed using 0.05% saponin in PBS for 5 minutes. Bacteria in supernatant and lysate were enumerated by serial dilution and colony counting.

After correction for the dilution of samples during the process of washing and lysis, the rate of killing was calculated by performing the following transformation:

$$-\ln\left(\frac{Intracellular\ bacteria + Extracellular\ bacteria}{Bacteria\ in\ \ control\ sample}\right)$$

Linear regression was then performed with the slope of the line representing the rate of killing.

2-4.18 Studies with fluorescent bacteria

Bacteria were prepared as above except that prior to resuspension in PBS with mouse serum the bacteria were resuspended in a solution of 10µM eFluor Proliferation Dye 450 (eBioscience) in PBS and incubated at 37˚C for 10 minutes. Bacteria were then washed with PBS and resuspended in PBS with 10% mouse

serum. Neutrophils were suspended in PBS and then mixed with bacteria in mouse serum as described above. As a control, mixtures were incubated in the present of 5μM Cytochalasin D (Sigma) or at 4˚C throughout to inhibit phagocytosis. At intervals, 200μl of mixture were aspirated and washed with ice-cold FACS buffer before storage on ice until the conclusion of the experiment. Cells were then analysed by flow cytometry.

Alternatively, neutrophils and fluorescent bacteria were prepared as for flow cytometry. However, once 200μl of mixture was aspirated it was stored unwashed on ice until the conclusion of the experiment. Neutrophils were pelleted by centrifugation and fixed by resuspension in 4% paraformaldehyde for 15 minutes at 4˚C. Cells were then washed in PBS and resuspended in PBS with 500nM SYTOX Green (Invitrogen) for 10 minutes. Cells were again washed in PBS and spun onto glass microscope slides by cytocentrifugation at 450rpm for 6 minutes. Slides were air dried in the dark overnight and coverslipped with Fluoromount-G (eBioscience). Cells were imaged with confocal microscopy.

2-4.19 Neutrophil extracellular trap detection

Human neutrophils were seeded in (Roswell Park Memorial Institute) RPMI 1640 medium supplemented with 2% heat inactivated human serum onto sterile, round glass coverslips placed in 24 well tissue culture plates. Neutrophils were infected with bacterial strains stained with eFluor 450 as previously described or activated with 1μg/ml PMA as a positive control and incubated at 37˚C under 5% CO_2 for 4 hours.

Neutrophils were fixed in 4% paraformaldehyde in PBS for 60 minutes before being removed from tissue culture plates with curved forceps and washed three times by inversion onto a drop of PBS on a parafilm sheet. Neutrophils were then permeabilised, blocked and stained with anti-neutrophil elastase and SYTOX Orange as described above before coverslipping and mounting with Fluoromount-G and imaging with confocal microscopy.

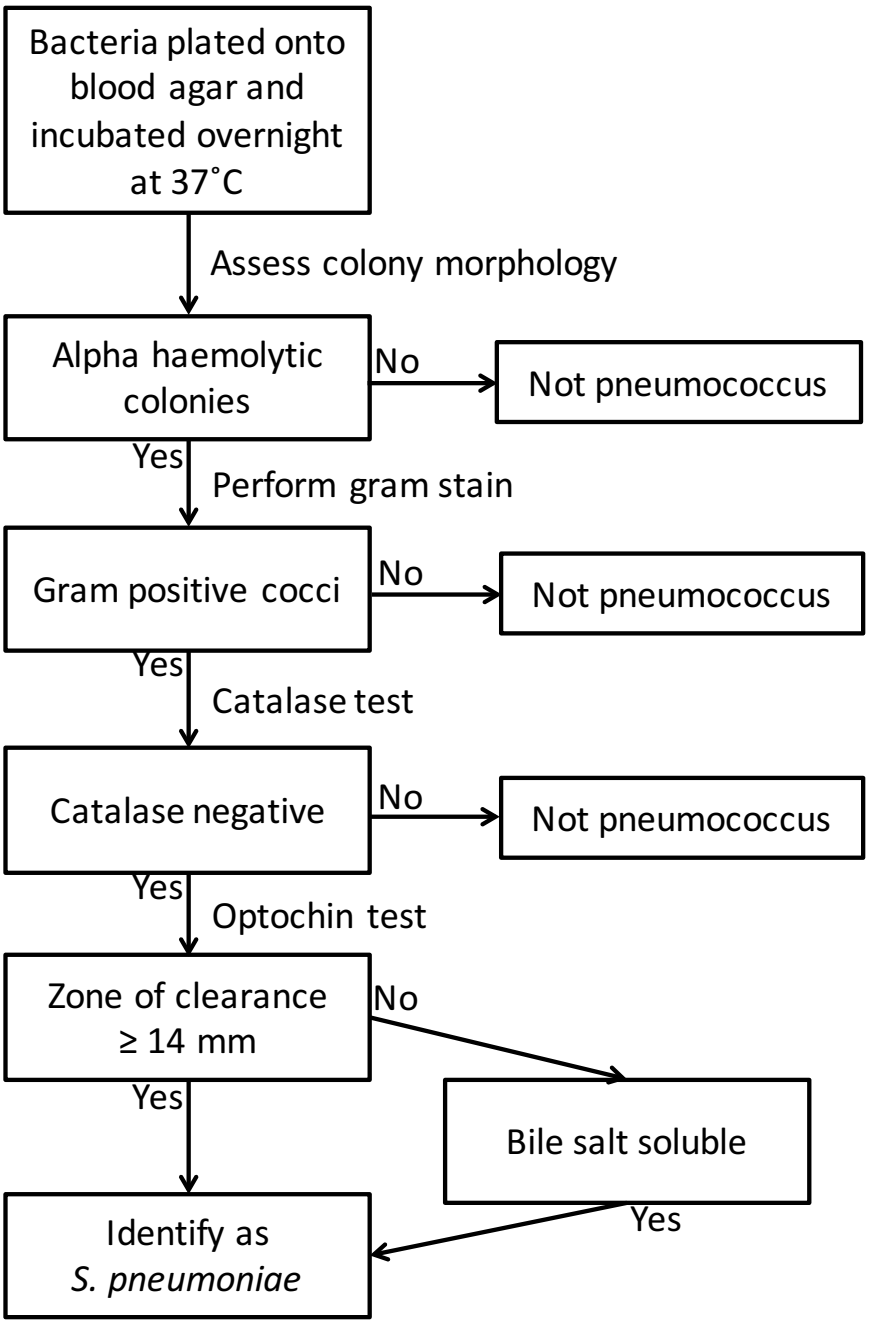

Figure 2-1. Algorithm for identification of pneumococci.

Used when initially characterising bacteria or in the presence of doubt about bacteria identification. Adapted from the CDC meningitis laboratory algorithm. See main text for description of the individual tests involved.

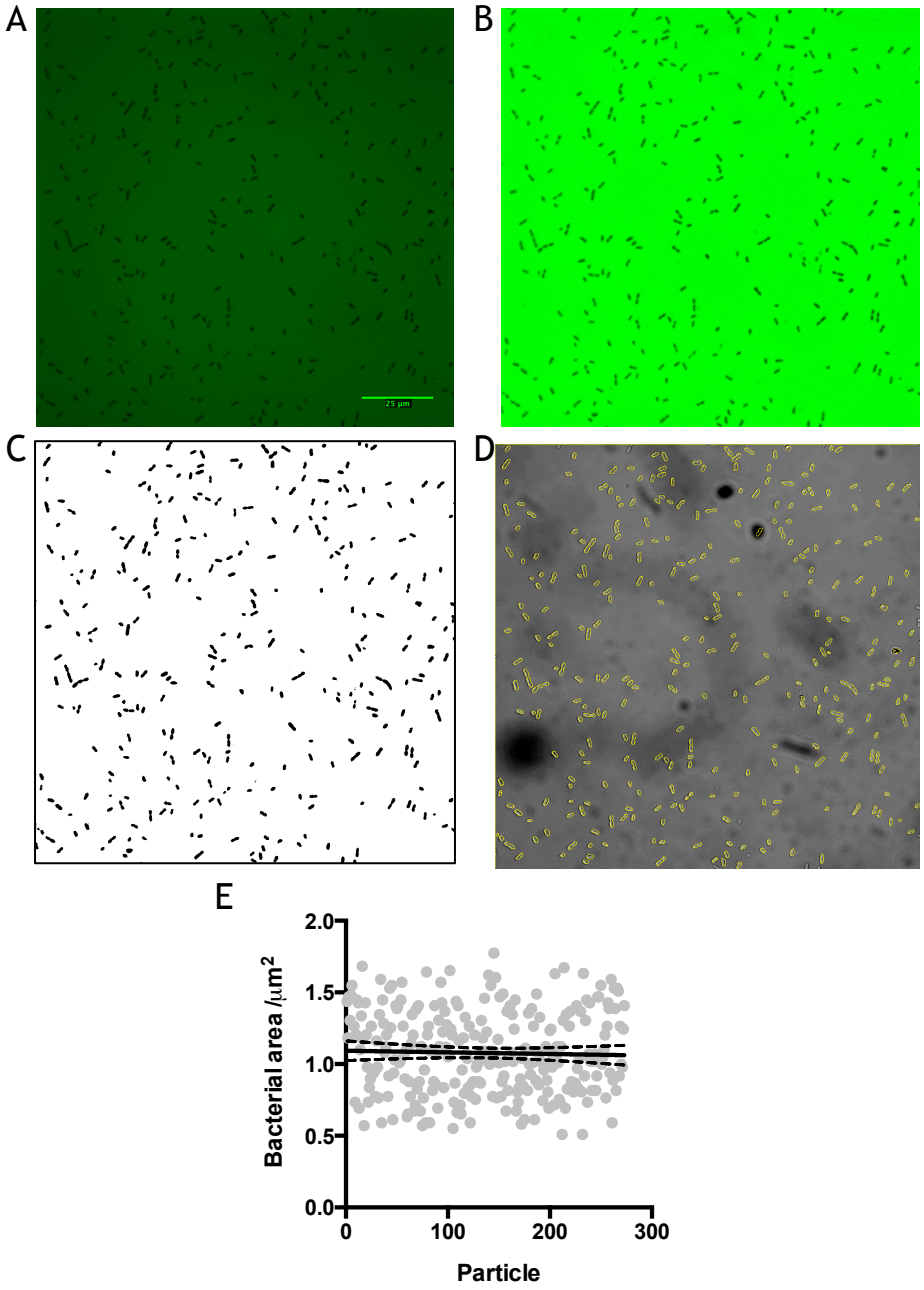

Figure 2-2. Method of image analysis used in measuring bacterial dextran exclusion.

A. Initial confocal image captured using x63 lens. B. Image after adjustment to ensure even intensity of background fluorescence. C. Image after application of thresholding tool to isolate particles. D. Particles were identified and the area of each particle was measured before particle masks were overlayed onto the transmitted light image to allow enumeration of bacteria per mask. E. Bacterial particles related to position on the image to indicate effect of background normalisation of stability of bacterial size across image.

Target	Clone	Fluorophore	Isotype	Isotype Ctrl	Source	Conc
CD4	RPA-T4	PE or PE-Cy7	IgG1 Kappa	Below	eBioscience	1:200
CD45 RO	UCHL1	APC	IgG2a Kappa	Below	eBioscience	1:200
IL-17A	64DEC17	Alexa Fluor 488	IgG1 Kappa	Below	eBioscience	1:200
IFNg	4S.B3	PerCP-Cy5.5	IgG1 Kappa	Below	eBioscience	1:500
IL-22	22URTI	eFluor 660	IgG1 Kappa	Below	eBioscience	1:200
CD14	61D3	APC	IgG2B	Figure 1	eBioscience	1:200
CCR7	GO43H7	Alexa Fluor 488	IgG2a Kappa	Figure 5	BD Pharminogen	1:200
CCR10	FAB3478P	PE	Rat IgG2a	Figure 5	R&D Systems	1:200
CCR6	R6H1	PE or PerCP-Cy5.5	IgG1 Kappa	Figure 5	eBIoscience	1:200
CCR4	1G1	PE-Cy7	IgG1 Kappa	Figure 5	BD Pharminogen	1:200
IL-4	8D4-8	PE	IgG1 Kappa	Below	eBioscience	1:200
IL-17F	SHLR17	PE	IgG1 Kappa	Below	eBioscience	1:200
CD161	DX12	APC	IgG2B	Below	BD Pharminogen	1:200
C3	Polyclonal	FITC	Rabbit IgG	Ch 4, Fig 7	Abcam	1:50

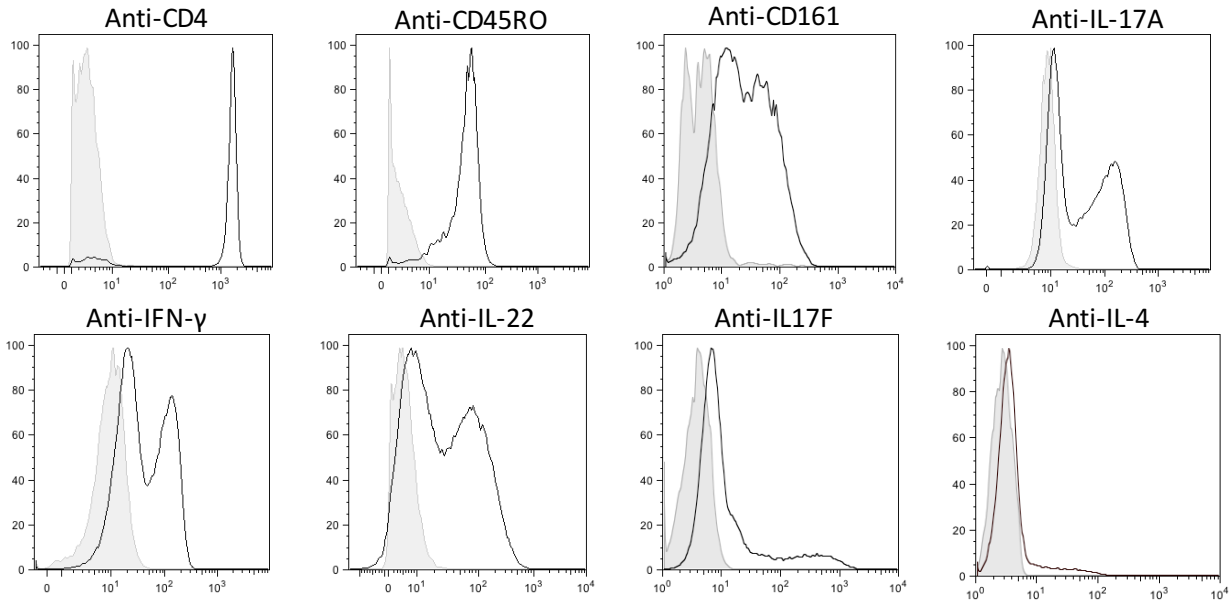

Figure 2-3. Human antibodies.

Table showing antibodies with human targets used in this thesis with isotype control antibodies not pictured in figures elsewhere. Antibodies are derived from mouse unless otherwise stated. Black line represents fluorescence with specific antibody and grey tint is the isotype control antibody.

Target	Clone	Fluorophore	Isotype	Isotype Ctrl	Source	Conc
Gr-1	RB6-8C5	PE or eFluor605NC	IgG2b Kappa	Ch 5, Fig 7	eBioscience	1:1000
IL-17A	TC11-18H10.1	PE	IgG1 Kappa	Ch 4, Fig 28	eBioscience	1:200
B220	RA3-6B2	PE-Cy7	IgG2a Kappa	Below	Biolegend	1:200
CD3	17A2	PE-Cy7	IgG2b Kappa	Below	Biolegend	1:200
CD4	RM4-5	PerCP-Cy5.5 or eFluor605NC	IgG2a Kappa	Below	eBioscience	1:200
GDTCR	UC7-13D5	Alexa Fluor 488	Hamster IgG	Below	Biolegend	1:200
IL-17RA	PAJ-17R	PE	IgG2a Kappa	Ch 5, Fig 1	eBioscience	1:200
Elastase	Polyclonal	None, Alexa fluor 488 2˚	Rabbit IgG	Below	Abcam	1:100
Gr-1	1A8	N/A	IgG2a Kappa	N/A	Bio X Cell	N/A
GDTCR	UC7-13D5	N/A	Hamster IgG	N/A	eBioscience	N/A

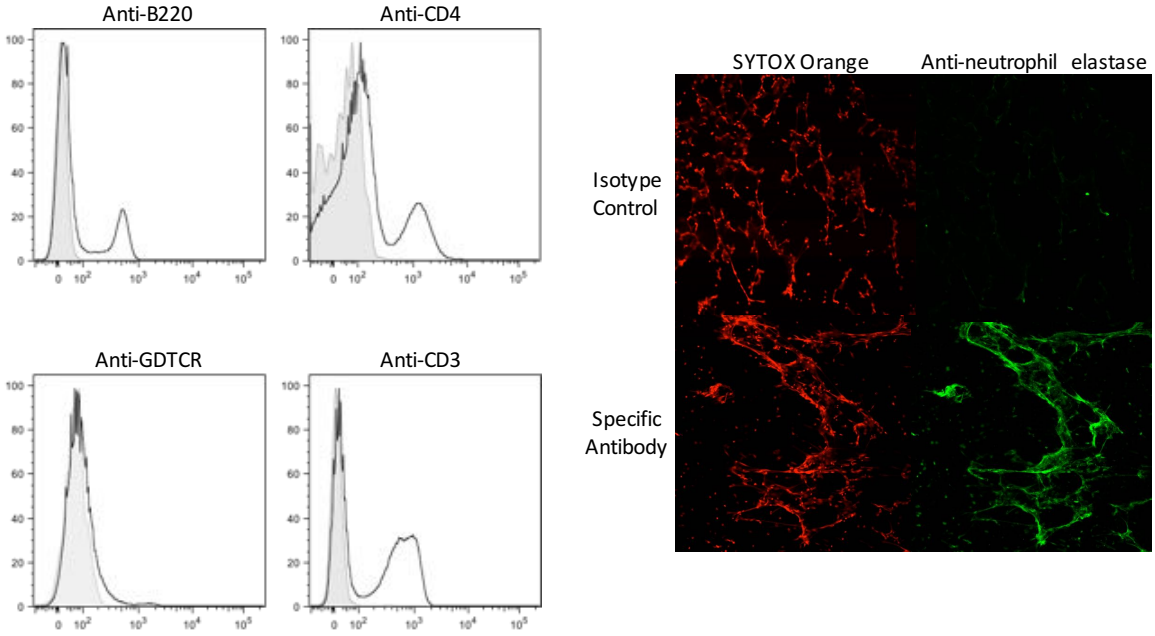

Figure 2-4. Mouse antibodies.

Table showing antibodies used in this thesis with isotype control antibodies not pictured in figures elsewhere shown below. Antibodies are derived from rat unless otherwise stated. Black line represents fluorescence with specific antibody and grey tint is the isotype control antibody. Monoclonal antibody RB6-8C5 was used in flow cytometry while 1A8 was used in immunohistochemistry and depletion experiments.

Name	Sequence
1f	CTC TAT AGA ATG GAG TAT ATA AAC TAT GGT TA
1r	CCA AAG AAA ATA CTA ACA TTA TCA CAA TAT TGG C
2f	TAT CCC AGT TCA ATA TTT CTC CAC TAC ACC
2r	ACA CAA AAT ATA GGC AGA GAG AGA CTA CT
3f	ATG GTG TGA TTT CTC CTA GAT TGG AAA GTA G
3r	CTT CTC CAA TTG CTT ACC AAG TGC AAT AAC G
4f	CTG TTA CTT GTT CTG GAC TCT CGA TAA TTG G
4r	GCC CAC TCC TGT TAA AAT CCT ACC CGC ATT G
5f	ATA CCT ACA CAA CTT CTG ATT ATG CCT TTG TG
5r	GCT CGA TAA ACA TAA TCA ATA TTT GAA AAA GTA TG
6ABDCf	AAT TTG TAT TTT ATT CAT GCC TAT ATC TGG
6ABCDR	TTA GCG GAG ATA ATT TAA AAT GAT GAC TA
6CDf	CAT TTT AGT GAA GTT GGC GGT GGA GTT
6CDr	AGC TTC GAA GCC CAT ACT CTT CAA TTA
7BC/40f	CTA TCT CAG TCA TCT ATT GTT AAA GTT TAC GAC GGG A
7BC/40r	GAA CAT AGA TGT TGA GAC ATC TTT TGT AAT TTC
7FAf	TCC AAA CTA TTA CAG TGG GAA TTA CGG
7FAr	ATA GGA ATT GAG ATT GCC AAA GCG AC
8f	GAA GAA ACG AAA CTG TCA GAG CAT TTA CAT
8r	CTA TAG ATA CTA GTA GAG CTG TTC TAG TCT
9NLf	GAA CTG AAT AAG TCA GAT TTA ATC AGC
9NLr	ACC AAG ATC TGA CGG GCT AAT CAA T
9VAf	GGGTTCAAAGTCAGACAGTGAATCTTAA
9VAr	CCATGAATGAAATCAACATTGTCAGTAGC
10Af	GGT GTA GAT TTA CCA TTA GTG TCG GCA GAC
10Ar	GAA TTT CTT CTT TAA GAT TCG GAT ATT TCT C
10FC/33Cf	GGA GTT TAT CGG TAG TGC TCA TTT TAG CA
10FC/33Cr	CTA ACA AAT TCG CAA CAC GAG GCA ACA
11ADf	GGA CAT GTT CAG GTG ATT TCC CAA TAT AGT G
11ADr	GAT TAT GAG TGT AAT TTA TTC CAA CTT CTC CC
12FAB/44/46f	GCA ACA AAC GGC GTG AAA GTA GTT G
12FAB/44/46r	CAA GAT GAA TAT CAC TAC CAA TAA CAA AAC
13f	TAC TAA GGT AAT CTC TGG AAA TCG AAA GG
13r	CTCATGCATTTTATTAACCGCTTTTTGTTC
14f	GAA ATG TTA CTT GGC GCA GGT GTC AGA ATT
14r	GCC AAT ACT TCT TAG TCT CTC AGA TGA AT
15AFf	ATT AGT ACA GCT GCT GGA ATA TCT CTT C
15AFr	GAT CTA GTG AAC GTA CTA TTC CAA AC
15BCf	TTG GAA TTT TTT AAT TAG TGG CTT ACC TA
15BCr	CAT CCG CTT ATT AAT TGA AGT AAT CTG AAC C
16Ff	GAA TTT TTC AGG CGT GGG TGT TAA AAG
16Fr	CAG CAT ATA GCA CCG CTA AGC AAA TA
17Ff	TTC GTG ATG ATA ATT CCA ATG ATC AAA CAA GAG
17Fr	GAT GTA ACA AAT TTG TAG CGA CTA AGG TCT GC

Name	Sequence
18CFBAf	CTT AAT AGC TCT CAT TAT TCT TTT TTT AAG CC
18CFBAr	TTA TCT GTA AAC CAT ATC AGC ATC TGA AAC
19Af	GAG AGA TTC ATA ATC TTG CAC TTA GCC A
19Ar	CAT AAT AGC TAC AAA TGA CTC ATC GCC
19Ff	GTT AAG ATT GCT GAT CGA TTA ATT GAT ATC C
19Fr	GTA ATA TGT CTT TAG GGC GTT TAT GGC GAT AG
19Fvarf	GAC AAT TCT GGT TGA CTT GTT GAT TTT G
19Fvarr	CTA CCA AAT ACC TCA CCA GCT TCC
20f	GAG CAA GAG TTT TTC ACC TGA CAG CGA GAA G
20r	CTA AAT TCC TGT AAT TTA GCT AAA ACT CTT ATC
21f	CTA TGG TTA TTT CAA CTC AAT CGT CAC C
21r	GGC AAA CTC AGA CAT AGT ATA GCA TAG
22FAf	GAG TAT AGC CAG ATT ATG GCA GTT TTA TTG TC
22FAr	CTC CAG CAC TTG CGC TGG AAA CAA CAG ACA AC
23Af	TAT TCT AGC AAG TGA CGA AGA TGC G
23Ar	CCA ACA TGC TTA AAA ACG CTG CTT TAC
23Bf	CCACAATTAGCGCTATATTCATTCAATCG
23Br	GTC CAC GCT GAA TAA AAT GAA GCT CCG
23Ff	GTA ACA GTT GCT GTA GAG GGA ATT GGC TTT TC
23Fr	CAC AAC ACC TAA CAC TCG ATG GCT ATA TGA TTC
24FABf	GCT CCC TGC TAT TGT AAT CTT TAA AGA G
24FABr	GTG TCT TTT ATT GAC TTT ATC ATA GGT CGG
31f	GGA AGT TTT CAA GGA TAT GAT AGT GGT GGT GC
31r	CCG AAT AAT ATA TTC AAT ATA TTC CTA CTC
33FA/37f	GAA GGC AAT CAA TGT GAT TGT GTC GCG
33FA/37r	CTT CAA AAT GAA GAT TAT AGT ACC CTT CTA C
34f	GCT TTT GTA AGA GGA GAT TAT TTT CAC CCA AC
34r	CAA TCC GAC TAA GTC TTC AGT AAA AAA CTT TAC
35AC/42f	ATT ACG ACT CCT TAT GTG ACG CGC ATA
35AC42r	CCA ATC CCA AGA TAT ATG CAA CTA GGT T
35Bf	GAT AAG TCT GTT GTG GAG ACT TAA AAA GAA TG
35Br	CTT TCC AGA TAA TTA CAG GTA TTC CTG AAG CAA G
35F/47Ff	GAA CAT AGT CGC TAT TGT ATT TTA TTT AAA GCA A
35F/47Fr	GAC TAG GAG CAT TAT TCC TAG AGC GAG TAA ACC
38/25FAf	CGT TCT TTT ATC TCA CTG TAT AGT ATC TTT ATG
38/25FAr	ATG TTT GAA TTA AAG CTA ACG TAA CAA TCC
39f	TCA TTG TAT TAA CCC TAT GCT TTA TTG GTG
39r	GAG TAT CTC CAT TGT ATT GAA ATC TAC CAA
cpsAf	GCA GTA CAG CAG TTT GTT GGA CTG ACC
cpsAr	GAA TAT TTT CAT TAT CAG TCC CAG TC

Table 2-1. Serotyping primers.

Primers used for serotyping of pneumococcal isolates using PCR multiplex reactions as described by the CDC.

Name	Sequence
aroE up	GCC TTT GAG GCG ACA GC
aroE dn	TGC AGT TCA (G/A)AA ACA T(A/T)T TCT AA
gdh up	ATG GAC AAA CCA GC(G/A/T/C) AG(C/T) TT
gdh dn	GCT TGA GGT CCC AT(G/A) CT(G/A/T/C) CC
gki up	GGC ATT GGA ATG GGA TCA CC
gki dn	TCT CCC GCA GCT GAC AC
recP up	GCC AAC TCA GGT CAT CCA GG
recP dn	TGC AAC CGT AGC ATT GTA AC
spi up	TTA TTC CTC CTG ATT CTG TC
spi dn	GTG ATT GGC CAG AAG CGG AA
xpt up	TTA TTA GAA GAG CGC ATC CT
xpt dn	AGA TCT GCC TCC TTA AAT AC
ddl up	TGC (C/T)CA AGT TCC TTA TGT GG
ddl dn	CAC TGG GT(G/A) AAA CC(A/T) GGC AT

Table 2-2. MLST primers.

Primers used for amplification and sequencing of isolates for multilocus sequence typing

Score Category	0	1	2
Coat	Normal*	Starey – limited to upper back/head	Starey – more extensive than required to score 1
Movement	Normal	Mildly reduced – spontaneous movement continues	Markedly reduced – limited or absent spontaneous movement
Posture	Normal	Crouched posture at rest but extends body when moving	Crouched posture without extension on movement
Moribundity	Absent	Present – animal unable to walk, unable to remain upright following a gentle push or any other condition requiring termination to prevent suffering	

Table 2-3. Scoring system for the monitoring of animals infected with pneumococcal strains.

To calculate clinical score, add score in each domain together to obtain total score. Moribund animals are assigned a score of 7 regardless of the scores in the other domains. * minor distruption of the coat sheen may be normal in some males and does not mandate a score > 0.

Mice found dead	Information
IL-22$^{-/-}$ animal during mortality study.	Failed to recover from anaesthetic following intranasal innoculation of bacteria – this was the only procedure related fatality in this study
Animal placed on ASPA procedure but found dead prior to experiment commencing	Injured in cage structure – became trapped between the cage lid and side wall.
Wild type animal in nasal colonisation study	Unclear cause of death, found dead in cage– no previous weight loss or clinical score despite twice daily monitoring. Culture of BAL and blood revealed mixed flora but no pneumococci.

Table 2-4. Animals found dead while on ASPA procedure during study. Animals found dead during ASPA procedures are shown excluding animals maintained under the terms of the animal licence purely for breeding.

Score Category	0	1	2	3
Peribronchial	Normal	Mild, patchy	Dense in places, <50% of visualised airways	Dense in places, >50% visualised airways
Alveolar	Normal	Mild, patchy infiltrate	Moderate, dense areas of infiltrate	Severe, extensive, dense consolidation
Pleural	Normal	Abnormal pleural surface	Presence of frank pus within pleural space	N/A

Table 2-5. Scoring system for assessing pulmonary inflammatory change on histological sections of mouse lung.

To calculate clinical score, add score in each domain together to obtain total score.

Forward Primer	AATGATACGGCGACCACCGAGATCTACAC TATGGTAATT CC AGMGTTYGATYMTGGCTCAG				
Reverse Primer	CAAGCAGAAGACGGCATACGAGAT XXXXXXXXXXXX AGTCAGTCAG AA GCTGCCTCCCGTAGGAGT				
Primer	Barcode	Primer	Barcode	Primer	Barcode
338rcbc1	ACGAGACTGATT	338rcbc33	CAACTCCCGTGA	338rcbc65	ACTTCCAACTTC
338rcbc2	GCTGTACGGATT	338rcbc34	TTGCGTTAGCAG	338rcbc66	CTCACCTAGGAA
338rcbc3	ATCACCAGGTGT	338rcbc35	TACGAGCCCTAA	338rcbc67	GTGTTGTCGTGC
338rcbc4	TGGTCAACGATA	338rcbc36	CACTACGCTAGA	338rcbc68	CCACAGATCGAT
338rcbc5	ATCGCACAGTAA	338rcbc37	TGCAGTCCTCGA	338rcbc69	TATCGACACAAG
338rcbc6	GTCGTGTAGCCT	338rcbc38	ACCATAGCTCCG	338rcbc70	GATTCCGGCTCA
338rcbc7	AGCGGAGGTTAG	338rcbc39	TCGACATCTCTT	338rcbc71	CGTAATTGCCGC
338rcbc8	ATCCTTTGGTTC	338rcbc40	GAACACTTTGGA	338rcbc72	GGTGACTAGTTC
338rcbc9	TACAGCGCATAC	338rcbc41	GAGCCATCTGTA	338rcbc73	ATGGGTTCCGTC
338rcbc10	ACCGGTATGTAC	338rcbc42	TTGGGTACACGT	338rcbc74	TAGGCATGCTTG
338rcbc11	AATTGTGTCGGA	338rcbc43	AAGGCGCTCCTT	338rcbc75	AACTAGTTCAGG
338rcbc12	TGCATACACTGG	338rcbc44	TAATACGGATCG	338rcbc76	ATTCTGCCGAAG
338rcbc13	AGTCGAACGAGG	338rcbc45	TCGGAATTAGAC	338rcbc77	AGCATGTCCCGT
338rcbc14	ACCAGTGACTCA	338rcbc46	TGTGAATTCGGA	338rcbc78	GTACGATATGAC
338rcbc15	GAATACCAAGTC	338rcbc47	CATTCGTGGCGT	338rcbc79	GTGGTGGTTTCC
338rcbc16	GTAGATCGTGTA	338rcbc48	TACTACGTGGCC	338rcbc80	TAGTATGCGCAA
338rcbc17	TAACGTGTGTGC	338rcbc49	GGCCAGTTCCTA	338rcbc81	TGCGCTGAATGT
338rcbc18	CATTATGGCGTG	338rcbc50	GATGTTCGCTAG	338rcbc82	ATGGCTGTCAGT
338rcbc19	CCAATACGCCTG	338rcbc51	CTATCTCCTGTC	338rcbc83	GTTCTCTTCTCG
338rcbc20	GATCTGCGATCC	338rcbc52	ACTCACAGGAAT	338rcbc84	CGTAAGATGCCT
338rcbc21	CAGCTCATCAGC	338rcbc53	ATGATGAGCCTC	338rcbc85	GCGTTCTAGCTG
338rcbc22	CAAACAACAGCT	338rcbc54	GTCGACAGAGGA	338rcbc86	GTTGTTCTGGGA
338rcbc23	GCAACACCATCC	338rcbc55	TGTCGCAAATAG	338rcbc87	GGACTTCCAGCT
338rcbc24	GCGATATATCGC	338rcbc56	CATCCCTCTACT	338rcbc88	CTCACAACCGTG
338rcbc25	CGAGCAATCCTA	338rcbc57	TATACCGCTGCG	338rcbc89	CTGCTATTCCTC
338rcbc26	AGTCGTGCACAT	338rcbc58	AGTTGAGGCATT	338rcbc90	ATGTCACCGCTG
338rcbc27	GTATCTGCGCGT	338rcbc59	ACAATAGACACC	338rcbc91	TGTAACGCCGAT
338rcbc28	CGAGGGAAAGTC	338rcbc60	CGGTCAATTGAC	338rcbc92	AGCAGAACATCT
338rcbc29	CAAATTCGGGAT	338rcbc61	GTGGAGTCTCAT	338rcbc93	TGGAGTAGGTGG
338rcbc30	AGATTGACCAAC	338rcbc62	GCTCGAAGATTC	338rcbc94	TTGGCTCTATTC
338rcbc31	AGTTACGAGCTA	338rcbc63	AGGCTTACGTGT	338rcbc95	GATCCCACGTAC
338rcbc32	GCATATGCACTG	338rcbc64	TCTCTACCACTC	338rcbc96	TACCGCTTCTTC

Table 2-6. V_1-V_2 16S RNA sequencing primers with Golay barcode.
Primers used for 16S amplification in microbiome analysis. Top two rows represent full forward and reverse primer. Subsequent rows contain barcodes associated with specific reverse primers. Primer regions are colour coded as follows: green, Illumina adapter; orange, barcode on reverse primer only; blue, primer pad; red, primer linker; black, specific primer sequence.

3. HUMAN T CELL RESPONSES TO PNEUMOCOCCI

3-1 Introduction

As discussed in the introduction to this thesis, cellular immunity has been implicated in the immune response to pneumococcal disease in murine models, especially models of nasal colonisation. However, the memory T cell response to pneumococcal disease in human remains poorly understood. It has been known for several years that PBMCs secrete a variety of cytokines in response to pneumococcal stimulation including IFN-γ and IL-17[394]. IL-17 secretion from PBMCs was dependent on the presence of $CD4^+$ lymphocytes and pneumolysin specific T cells capable of secreting IL-17 were found in human tonsils[395]. Evidence suggests that the ability to secrete IL-17 from PBMCs is an acquired immune response since it is not found in PBMCs isolated from cord blood[265] and PBMCs from Swedish adults secreted more IL-17 in response to pneumococcal stimulation than children[356]. Bacterial infection is known to increase numbers of circulating innate cells capable of secreting IL-17[203]. However, the dynamics of a pneumococcal T cell response remain poorly understood with limited understanding of how these responses change through adult life and in response to infection.

It is challenging to characterise pneumococcal specific T cells. Stimulation of unfractionated PBMCs does not allow characterisation of the individual cells involved whereas using clonal stimulation to enable intra-cellular cytokine staining is not specific for pneumococcal responses. I sought to identify pneumococcal specific T cells and the cytokines secreted by these cells by identifying T cells proliferating in response to pneumococcal stimulus during a

co-culture model with monocytes as antigen presenting cells and using clonal stimulation to characterise the cytokine profile of responding T cells.

I hypothesised that young, healthy adults would have robust pneumococcal T cell responses and sought to characterise these. Having demonstrated that young healthy adults have T cell responses, including Th17 responses, I then sought to characterise how these responses change in an aging population and following disease. Since Th17 responses have been strongly implicated in immunity to *Candida albicans* infection, I used heat killed *Candida albicans* as a positive control to elicit a Th17 response.

3-2 Method Development

3-2.1 Development of co-culture model

Initial experiments were based on the co-culture model developed in my laboratory group by Hannah Bayes[396] to study cellular immune responses to *Pseudomonas aeruginosa*. This model involved differentiating monocytes into dendritic cells for 1 week, stimulating the dendritic cells and then co-culturing them with memory T cells the following day. However, this method required the use of two separate collections of blood one week apart. It quickly became clear that, since I planned to obtain blood from patients with IPD who would often be hospitalised for less than one week, a single step protocol allowing just one phlebotomy session was desirable. Therefore, the co-culture model was adapted to use monocytes immediately after isolation and to stimulate the co-culture after the addition of lymphocytes.

3-2.2 Isolation of $CD14^+$ monocytes and $CD4^+$ memory T cells

$CD14^+$ monocytes and $CD4^+CD45RO^+$ T lymphocytes were obtained by magnetic bead separation. Purity of isolated cell populations was confirmed by flow cytometry and was ~ 95% (figure 3-1).

3-2.3 $CD4^+$ memory T cell proliferation and cytokine secretion is dependent on monocytes

Memory T cells in co-culture were stained with eFluor 450 proliferation dye and underwent flow cytometry seven days after stimulation with pneumococci or HKCA. Supernatants were also taken for cytokine analysis. Stimulation with pneumococci and HKCA induced proliferation of $CD4^+$ memory T cells only in cultures containing monocytes (figure 3-2).

3-2.4 Gating strategy

Flow cytometry data were analysed according to the strategy outlined in figure 3-3. After doublet exclusion and exclusion of dead cells, $CD4^-$ cells were excluded. Proliferating cells were identified based on the dilution of proliferation dye intensity. Because in many experiments the percentage of proliferating cells was relatively low (<1%) the proliferation dye histogram could not consistently be used to fit a model and so the percentage of cells proliferating in the original culture could not be estimated. Therefore, proliferating cells are expressed as the percentage of the total number of $CD4^+$ cells with proliferation dye dilution in the culture. Cells stained intracellularly for cytokines were then identified as shown in figure 3-3. Isotype controls for the antibodies used are shown in the materials and methods at figure 2-3.

3-3 Memory T cell responses in healthy young adult volunteers

3-3.1 Proliferative responses

12 young healthy volunteers were recruited to the study and gave blood (mean age 25.4, range 18-34). Details of the patients recruited is shown in table 3-1. Live pneumococci (TIGR4, MOI 10) and HKCA (MOI 4) both induced proliferation of memory T-cells in co-cultures after seven days (figure 3-4). Very little proliferation was observed in unstimulated cultures (median percentage proliferating 0.4%). HKCA was a significantly more potent mitotic stimulus on T-lymphocytes than pneumococci (Median percentage of cells proliferating: TIGR4 5.2%, HKCA 39%; $P < 0.001$) but 11/12 (93%) of young healthy volunteers had detectable memory T-cell proliferation in response to pneumococci. One subject

(4) had no detectable proliferative response to stimulation with pneumococci (proliferation in TIGR4 culture corrected for proliferation in unstimulated culture: 0.03%) also had a lower than typical response to HKCA (4.4% after correction for background proliferation which was 9% lower than any other young (or elderly) volunteer. It may be that this reflects a technical issue with this sample or an undetected immunoparesis (for example caused by intercurrent viral illness) in this volunteer. There was no evidence of a broader correlation between responses to TIGR4 and HKCA (Spearman's $\rho = 0.28$, $P = 0.36$, figure 3-4C). There was also no evidence of a gender difference in responses (median TIGR4 proliferation: male 3.41%, female 3.57%, $P = 1.00$, figure 3-4D).

3-3.2 Chemokine receptor staining

To explore the chemokine receptor profile of lymphocytes following stimulation with TIGR4 and HKCA, after seven days co-cultures were stained for chemokine receptors without further stimulation. Chemokine receptors are important for trafficking of lymphocytes into target tissues. T cells trafficking through mucosal sites have been associated with particular chemokine receptor profiles. CCR7 is associated with T cells homing to lymph nodes and $CCR7^{+}$ lymphocytes are associated with a 'central memory' phenotype whereas the absence of CCR7 is associated with an 'effector memory' phenotype homing to non-lymphoid tissues[397]. CCR4 has been associated with skin[398] and lung homing[399]. Th17 cells have been reported to be $CCR6^{+}CCR10^{-}$[400]. Therefore, these chemokine receptors were selected for further study.

The principle difference between proliferating and non-proliferating cells was in CCR7 expression. Proliferating cells were predominantly CCR7 positive while most non-proliferating cells were CCR7 negative. Other chemokines receptors were broadly similar between proliferating and non-proliferating cells although proliferating cells in HKCA stimulated cultures only tended to more strongly express CCR6 and CCR4 than non-proliferating cells. As discussed above, the absence of CCR7 on proliferating T cells suggests an effector function.

3-3.3 Secreted cytokines

Co-culture supernatants from healthy volunteers were also analysed for secreted cytokines by ELISA (figure 3-6). In unstimulated cultures, supernatant had levels of IL-17A, IL-22 or IFN-γ below or near to the limit of detection (IL-17A: 1/12 detectable; IL-22: 0/12 detectable; IFN-γ: 1/12). Most cultures stimulated with pneumococci or HKCA had detectable levels of the assayed cytokines in contrast to unstimulated cultures, which were unlikely to have detectable levels ($P \leq 0.001$ for all cytokines). HKCA was a more potent stimulus to cytokine release than pneumococci for all three cytokines although this did not reach statistical significance for IFN-γ (IL-17A: 22.5pg and 378.3pg ($P = 0.002$); IL-22: 10.7pg and 508.4pg ($P = 0.002$); IFN-γ: 466.9 and 1489.0 ($P = 0.14$)). Subject 4 (who had an undetectable pneumococcal proliferative response and poor proliferation to HKCA) had undetectable cytokine secretion in pneumococcal cultures and relative poverty of secretion in HKCA stimulated cultures.

3-3.4 Intra-cellular cytokine staining

After stimulation with PMA/ionomycin and Brefeldin A, lymphocytes from all patients were stained for IL-17A, IL-22 and IFN-γ while some co-cultures were stained for IL-17F or IL-4. For all the cytokines tested, some proliferating lymphocytes stained positive. Some proliferating lymphocytes fell into conventional T helper subsets – Th1, Th17, Th22. However, there were many T-lymphocytes with cytokine profiles such as triple positive cells (IFN-γ^+ IL-17A$^+$ IL-22$^+$) and combinations of IFN-γ with either IL-17A or IL-22 that do not fit the conventional T helper subsets (figure 3-7A**).** Only some of the samples were stained for IL-17F and IL-4. IL-17F was only occasionally found on IL-17A negative T lymphocytes and was strongly correlated with IL-17A positivity (figure 3-7B and C). In contrast to the other cytokines, which were expressed on a higher proportion of proliferating than non-proliferating cells, few of the proliferating lymphocytes were positive for IL-4 despite easily detectable non-proliferating IL-4$^+$ lymphocytes suggesting that the Th-2 response to TIGR4 among healthy adults was limited (figure 3-7D and E).

3-3.5 Intracellular staining of CCR6 sorted cells

Th17 cells are reported to be $CCR6^+$ and so I sought to determine if pneumococcal IL-17 and IL-22 T cell responses originated from $CCR6^+$ T cells. As has been demonstrated previously[401], CCR6 is lost from the cell surface when stimulated with PMA and ionomycin and this loss cannot be overcome by staining with antibody prior to poly-clonal stimulation (data not shown). Therefore, I sorted T-lymphocytes based on CCR6 staining and co-cultured $CCR6^+$ and $CCR6^-$ cells as previously. Sorting cells using this method was complicated by the relatively low expression of CCR6 which made it difficult to clearly discriminate $CCR6^+$ and $CCR6^-$ cells (figure 3-8A). Further, there was a modest reduction in the fluorescence intensity of the $CCR6^+$ cells post-sort which made assessing sort purity for $CCR6^+$ cells difficult.

Since only small numbers of $CCR6^+$ cells were obtained by sorting, only pneumococcal responses were assessed by this method. Proliferation in response to pneumococcal stimulation occurred in both $CCR6^+$ and $CCR6^-$ cultures (figure 3-8B). IFN-γ^+ cells were found in both cultures but IL-17^+ and IL-22^+ cells were rare in $CCR6^-$ cultures (figure 3-8C). This experiment suggests that pneumococcal responsive IL-17A and IL-22 producing T cells are derived from the $CCR6^+$ population.

3-3.6 CD161 surface staining

CD161 has also been associated with expression on the surface of Th17 cells although its function is uncertain and it is found only in humans[402]. I evaluated whether CD161 was present on the surface of IL-17 secreting proliferating T-lymphocytes. Lymphocytes proliferating in co-culture after stimulation with TIGR4 had higher surface expression of CD161 than non-proliferating lymphocytes and IL-17A staining was found in the $CD161^{hi}$ cells (figure 3-9). In contrast, lymphocytes proliferating in response to HKCA did not have as high surface expression of CD161 and IL-17A expression did not preferentially arise from $CD161^{hi}$ cells.

3-3.7 Pooled analysis of intra-cellular cytokine staining

Two analyses of pooled intracellular cytokine data were performed. Firstly, the frequency of proliferating, memory $CD4^+$ cells found to produce a cytokine following PMA/ionomycin stimulation was expressed as a total of all $CD4^+$ cells in the culture. This allowed the raw frequency of such cells to be analysed. Because this analysis was presented on a logarithmic scale, an arbitrary minimum of 0.05% was selected as the minimum percentage of cytokine positive cells that could be detected. Secondly, cells were classified according to the production of combinations of cytokines (i.e. IFN-γ positive, IL-17A negative, IL-22 negative cells) and each of the possible combinations expressed as a proportion of the proliferating $CD4^+$ cells in the culture.

In the first analysis, the data for individual cytokines mirrors the data for overall proliferation (figure 3-10). As would be expected from the very limited proliferation in unstimulated cultures, very few proliferating cytokine positive cells were found. Among stimulated co-cultures, HKCA stimulation induced substantially more cytokine positive proliferating cells than TIGR4 for each of the three cytokines tested (IL-17A: 14.75 and 0.63 ($P = 0.001$); IL-22: 15.25 and 0.52 ($P < 0.001$); IFN-γ: 16.55 and 2.47 ($P = 0.01$)).

In the second analysis, proliferating cells were classified according to the combination of positive cytokines using SPICE (NIH). There was evidence of a significant difference in the distribution of cytokine combinations between TIGR4 and HKCA stimulated co-cultures (figure 3-11, Monte Carlo analysis of distribution $P = 0.0038$). Amongst co-cultures stimulated with TIGR4, the largest group of proliferating T-cells were those producing IFN-γ only (conventional Th1 cells) which made up more than 50% of the cells. In contrast, amongst cultures stimulated with HKCA the proportion of Th1 cells was considerably smaller (less than 25% of cells). The majority of cells in this context secreted a combination one of the signature cytokines of Th17 cells (IL-17A or IL-22); roughly half of these also secreted IFN-γ and were therefore not easily classifiable into a canonical T helper subset.

3-4 Memory T cell responses in healthy older adult volunteers

In order to compare memory T-cell responses in older adults with those in the younger population I sought to recruit volunteer subjects aged over 65. To try to ensure that volunteers were representative of a healthy, older adult population I approached adults attending urology hospital clinics with conditions thought unlikely to affect mucosal immunity.

3-4.1 Proliferative responses

14 patients were recruited. However, the final four patients all had significant proliferation in the unstimulated culture and were therefore excluded. These four patients were the last four patients recruited. It is likely that this resulted from contamination of one of the solutions used. Therefore, 10 patients were available for analysis (table 3-1)

Proliferative responses among $CD4^+$ memory T-cells were compared between young and old adults (figure 3-12). The overall pattern of the proliferative response between TIGR4 and HKCA stimulated co-cultures was similar. However, compared to those <35 years of age, volunteers aged >65 had lower proliferative responses to TIGR4 (median proliferating cells 5.22% and 1.60%, P = 0.02) but similar responses to HKCA (39.05% and 33.55%, P = 0.28).

3-4.2 Secreted cytokines

Many of the TIGR4 stimulated co-culture supernatants from older adults had undetectable concentrations of tested cytokines. Since this resulted in a large number of tied values when comparing young and old adults, two methods of analysis were used and are presented here. Conservative analysis of the data used a contingency table and Fisher's exact test while the second less conservative analysis used a Mann-Whitney test corrected for multiple tied values. In the data that follows, the P values for these two analyses are designated P_F (Fisher's) and P_M (Mann-Whitney).

Following stimulation with TIGR4, co-cultures with cells taken from older adults tended to lower concentrations of all three tested cytokines than those from young adults although only IFN-γ reached statistical significance (median concentration IL-17A: 7.58 pg/ml and 22.51 pg/ml (P_M = 0.23, P_F = 0.06), IL-22: <limit of detection (LOD) and 10.71 pg/ml (P_M = 0.23, P_F = 0.07), IFN-γ: <LOD and 466.90 pg/ml (P_M = 0.05, P_F = 0.07), figure 3-13). In contrast, following stimulation with HKCA co-cultures from older adults tended to produce more cytokines than those from young adults. However, apart from IL-17A which just reached statistical significance the differences were not statistically significant(IL-17A: 767.3 pg/ml and 387.3 pg/ml (P_M = 0.05), IL-22: 1009 pg/ml and 508.4 pg/ml (P_M = 0.23), IFN-γ: 2561 pg/ml and 1489 pg/ml (P_M = 0.57)).

3-4.3 Intra-cellular cytokines

Intra-cellular cytokines were again analysed according to the two methods outlined in 3-3.4. Mirroring the findings in total proliferation, the percentage of cytokine producing, proliferating cells was significantly reduced in co-cultures from older adults compared to young adults for IL-17A and IFN-γ, although statistical significance was not reached for IL-22 (median percentage of $CD4^+$ lymphocytes proliferating, IL-17A: 0.23% and 0.62% (P = 0.03), IL-22: 0.17% and 0.52% (P = 0.052), IFN-γ: 0.34% and 2.47% (P = 0.02), figure 3-14). In contrast, there was no significant difference in proliferation between young and old adult co-cultures stimulated with HKCA (IL-17A: 14.8% and 7.07% (P = 0.57), IL-22: 15.25% and 8.17% (P = 0.34), IFN-γ: 16.55% and 8.00% (P = 0.45)).

When the distribution of cells producing combinations of cytokines was analysed (figure 3-15), there was no significant difference between age groups in the distribution of cytokine producing cells between TIGR4 stimulated cultures (P = 0.30) with a very similar distribution of cytokine combinations. There was a significant difference in distribution for HKCA stimulated cultures (P = 0.02) with more conventional Th1 cells and fewer cells secreting IL-17A or IL-22 in combination with IFN-γ in the older adults.

3-5 Patients with IPD

3-5.1 Recruitment

I aimed to recruit 12 young and 12 older patients with recent IPD to compare T cell responses with healthy adults. To achieve this, I collaborated with the local microbiology laboratory to identify patients with *S. pneumoniae* isolated from their blood or cerebrospinal fluid. Patients were approached once clinically stable and no longer septic but within one week of the detection of their IPD.

However, despite recruiting patients for over a year, recruitment proved slow. 56 patients were screened for eligibility but the majority were ineligible because of co-morbidities (malignancies, inflammatory conditions or significant cognitive impairment) or the severity of their illness making it inappropriate to approach them for consent. 12 patients were approached to give consent. Three patients declined to take part in the study and nine patients gave consent. Unfortunately, one of the co-cultures became infected during the experiment and was excluded. Therefore the results from eight patients were included in the study (5 older adults, 3 young adults). The characteristics of the patients included are shown in table 3-2.

3-5.2 Results

The limited numbers of patients recruited to the study made detailed analysis difficult. However, there was no evidence of a significant difference in total proliferation, cytokine positive proliferating cells or supernatant cytokines in either the >65 or <35 age groups (figure 3-16). In the young adult group, the three patients recruited were insufficient to draw any conclusions regarding the relative magnitude of memory T cell responses. The five patients recruited to the older adult IPD group had a very weak trend towards lower proliferation than the healthy controls ($P = 0.35$). However, the existing data make it extremely unlikely that older adults with recent IPD have expanded T cell responses.

3-6 Discussion

In this chapter I have characterised the pneumococcal memory $CD4^+$ T cell responses in the peripheral blood of adults – both healthy and recently infected. I was able to demonstrate that pneumococcal T cell responses in this co-culture model were dependent on monocytes as an antigen-presenting cell and that significant proliferation did not occur in the absence of stimulation. My principal goal was to characterise Th17 responses, but in fact it was Th1 responses that were most prominently seen in this model. In both typical young and old adults, more than 50% of T cells proliferating in response to pneumococcal stimulus produced IFN-γ in the absence of IL-17 or IL-22 and many of those that produced IL-17 or IL-22 also produced IFN-γ. This was in contrast to the responses produced by *Candida albicans*, in which IL-17 and IL-22 producing cells (either with or without IFN-γ co-production) were much more prominent. The presence of large numbers of IL-17 and/or IL-22 producing cells that also produced IFN-γ does not fit into the canonical view of Th1 and Th17 cells as mutually exclusive. However, Th1/17 cells are well described in a number of disease states and some evidence suggests that they may develop from Th17 cells under the influence of certain pro-inflammatory cytokines such as IL-1β and IL-12[403]. There is also some evidence that Th17 cells may develop a Th1 phenotype over time in the context of both infection[404] and autoinflammation[405]. The IL-17A and IL-22 secreting cells identified in my study were otherwise typical of those described in the literature in that they arose out of the $CCR6^+$ group of lymphocytes[291] and expressed CD161 on their surface[402]. There was a difference between proliferating cells stimulated with HKCA and pneumococcus in chemokine receptor profile since (while both expressed similar levels of CCR7 and CCR10) HKCA stimulated cells were more likely to be $CCR6^+$ and tended to be $CCR4^{hi}$ but those stimulated by pneumococci were $CCR4^{int}$. This is in keeping with previous phenotypic characterisation of lymphocytes homing to specific organs which found lung and tonsil lymphocytes to be $CCR4^{int}$ but those homing to skin and external mucosal sites to be $CCR4^{hi}$[406].

When I examined a subset of the patients for Th2 responses, these were not a prominent component of the proliferative response to pneumococcal stimulation. This is perhaps surprising since the principal immune response to

pneumococci is thought to be humoral and antibody responses are unquestionably vital for protection against IPD. While anti-capsular antibodies are T cell independent and the conjugate vaccine naïve population studied here would not be expected to have T cell responses to capsule, anti-pneumococcal surface protein and pneumolysin antibodies are detectable in the majority of adult humans[407]. It is possible that the large amounts of IFN-γ present in the co-cultures in this model inhibit the proliferation of Th2 cells[408] and therefore the contribution of IL-4 producing T cells to the pneumococcal response may be underestimated by this model.

It is well known that older adults are at substantially increased risk of IPD compared to young adults in whom the disease is relatively uncommon. Therefore, I compared the T cell responses between apparently healthy older adults and younger people. There was evidence of significantly reduced proliferative responses to pneumococci from the memory T cells of older adults compared to younger adults. While there was a small reduction in the responses to HKCA, this effect was small and did not reach statistical significance. Secretion of cytokines into the culture supernatant showed similar results. Therefore, this model suggests that elderly patients may have an organism specific reduction in T cell responses to pneumococcus. There was no significant difference in the cytokine profile of proliferating T cells between the two groups and therefore it was the quantity and not quality of the response which was reduced in the older group. The reason for this reduction is not clear. It may be that older adults are less commonly exposed to pneumococci than younger adults. As discussed in the introduction, the frequency of nasal colonisation in older adults is poorly described but was uncommon in the frail elderly[19]. Since people are likely to be exposed to *Candida albicans* throughout their lives, this may explain the difference between these two responses in older adults although it may simply be a higher longevity among Candidal responses.

One limitation of this method is the inability to standardise the APC stimulation given to T-cells. Therefore, the lymphocyte proliferation is dependent on the quality of monocyte interaction they receive as well as the inherent characteristics of the lymphocytes themselves. Standardising APCs in these experiments because of the need for HLA matched monocytes to avoid non-

specific T-cell activation. Generating standardised HLA matched heterologous APCs for stimulation, for example by using exclusively young adult monocytes exclusively, would have been extremely resource intensive and was not possible within the limits of this study. It might be expected that APC function decreases with age although evidence from mouse and human experiments do not support this and demonstrate paradoxically increased stimulation of lymphocytes by APCs from the healthy elderly[409-411]. The concern the APC function may influence the results is controlled for by the HKCA positive control. HKCA was chosen as it has been shown to stimulate APC dependent Th17 responses[412], including within our research group[396]. These responses are partially mediated by interaction with dectin-1 and TLR-2[413]. HKCA has been used in similar co-culture experiments[414,415]. Since no correlation was observed between TIGR4 and HKCA responses and HKCA responses were similar between young and old adults, differences in monocyte quality as an explanation for the reduced TIGR4 responses seen in elderly humans are unlikely.

Unfortunately, recruitment to the study of patients with IPD was more difficult than anticipated. However, based on the available data it is unlikely that there is a large difference between healthy volunteers and patients with IPD in terms of T-cell responses. This is in contrast to a study of experimental human colonisation which showed an increase in T cell responses among healthy adults. However, the dynamics of the immune response to sepsis and localised nasal disease are likely to be different and the responses measured are not directly comparable. The degree to which T cell responses contribute to protection against IPD in mouse models is not clear and therefore this may not be the optimal disease state to investigate.

In conclusion, the co-culture model used in this study demonstrates the presence of pneumococcal responsive memory $CD4^+$ cells which have a predominantly Th1 cytokine expression profile but IL-17 and IL-22 secreting lymphocytes are also present. Responses in older adults are reduced relative to those in young adults but despite small numbers there was no evidence of a difference in patients with recent IPD. Since older adults are at increased risk of IPD and are targeted for pneumococcal vaccine it may be that augmenting this immune response could improve protection. Current next generation vaccines often target Th17

immunity but it may be that other T cell subsets are relevant to the immune response as well.

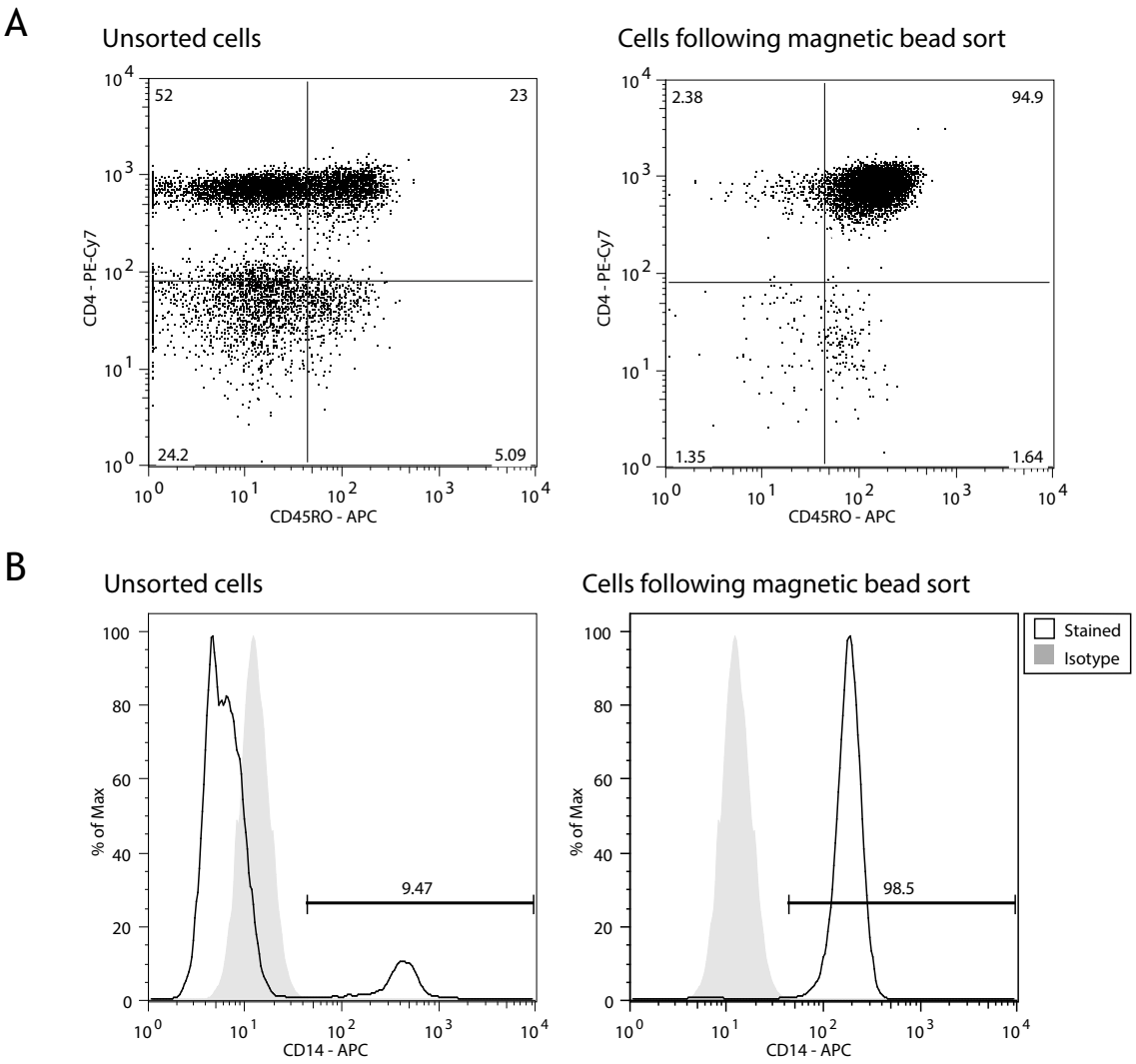

Figure 3-1. Isolation of cells for co-culture.

Human PBMCs were sorted by magnetic bead separation to isolate (A) $CD4^+CD45RO^+$ memory T lymphocytes and (B) $CD14^+$ monocytes. Cell populations from pre- and post- sort were stained for (A) CD4 and CD45RO and (B) CD14. Flow cytometry was conducted to assess purity.

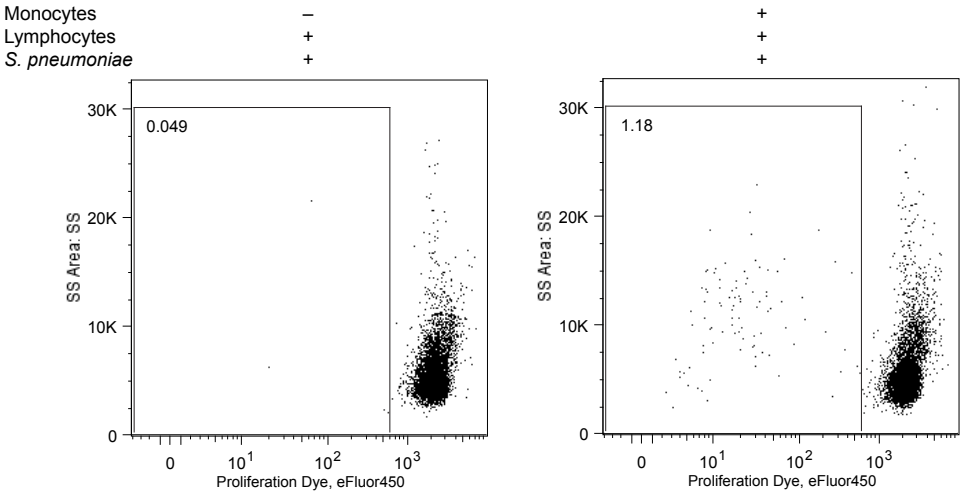

Figure 3-2. Proliferation of memory T lymphocytes in response to pneumococcal stimulation is antigen presenting cell dependent.
Human memory T-lymphocytes stained with proliferation dye were stimulated with *S. pneumoniae* (TIGR4, MOI 10) in the presence or absence of monocytes in co-culture. After seven days, lymphocytes were analysed by flow cytometry and gated on live, CD4+ cells. Proliferation in the culture was dependent on the presence of monocytes. Representative of two independent experiments.

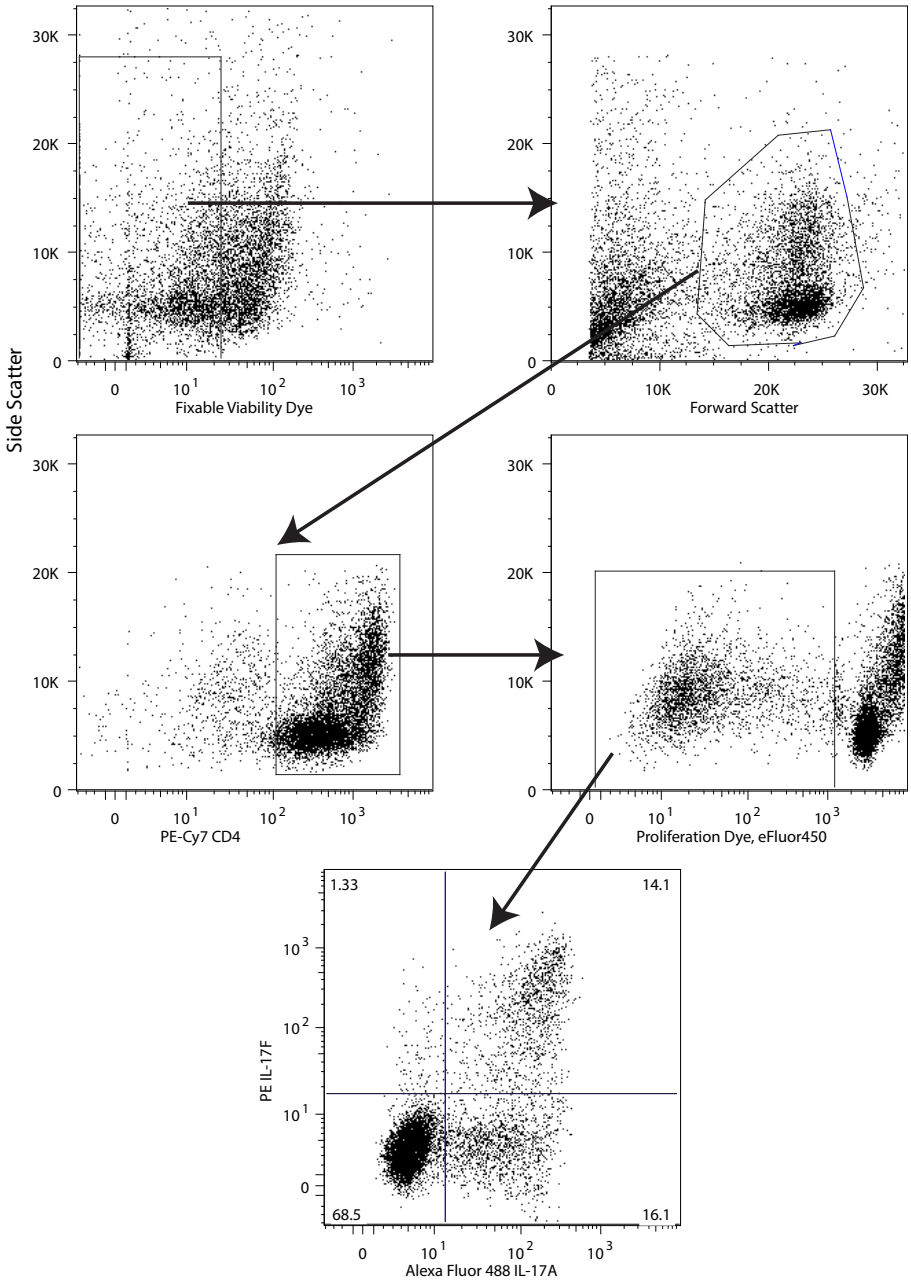

Figure 3-3. Gating strategy used in analysis of lymphocyte/monocyte co-cultures.

After doublet exclusion, dead cells were excluded and a mononuclear gate used. $CD4^+$ cells were then selected and proliferating cells selected based on dilution of proliferation dye. Cells were then analysed for intracellular cytokine staining.

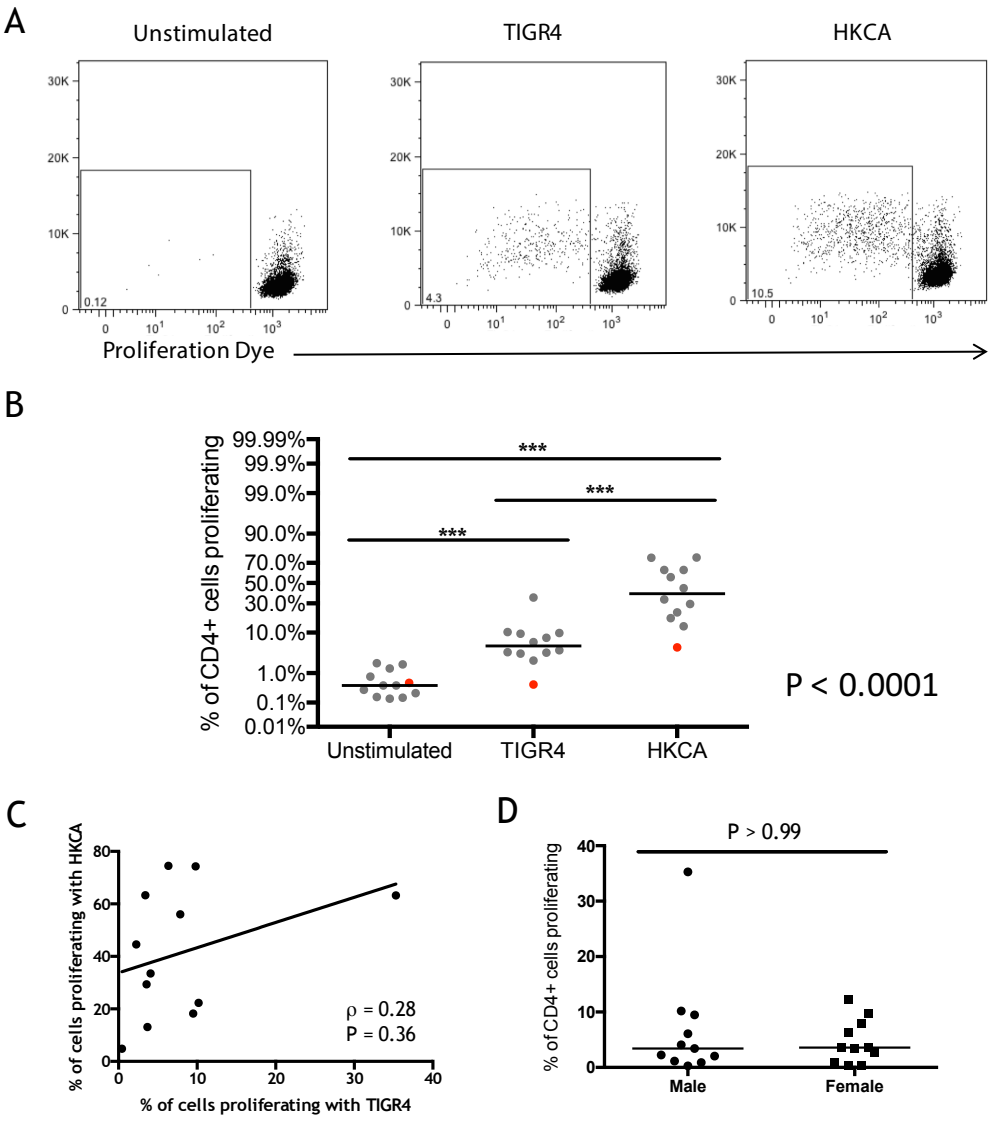

Figure 3-4. Proliferation of memory CD4$^+$ cells in response to stimulation with pneumococci or *Candida albicans* among young healthy volunteers.
Co-cultures were stimulated with TIGR4 (MOI 10), HKCA (MOI 4) or left unstimulated. After seven days in culture, proliferation was measured by detecting dilution of proliferation dye by flow cytometry. A. Representative plots of proliferation of CD4$^+$ cells in co-cultures. B. Summary plots from all young healthy volunteers. Line represents median value. P value represents a Kruskal-Wallis test. *** denotes P < 0.001. The data highlighted in red are that derived from the volunteer with undetected T-cell proliferation following pneumococcal stimulation (see text). C. Scatterplot of proliferative responses to TIGR4 and HKCA. Line represents Spearman best fit curve with Spearman's ρ and P value for correlation shown. D. Healthy volunteer responses shown according to volunteer gender. P value represents Mann-Whitney test.

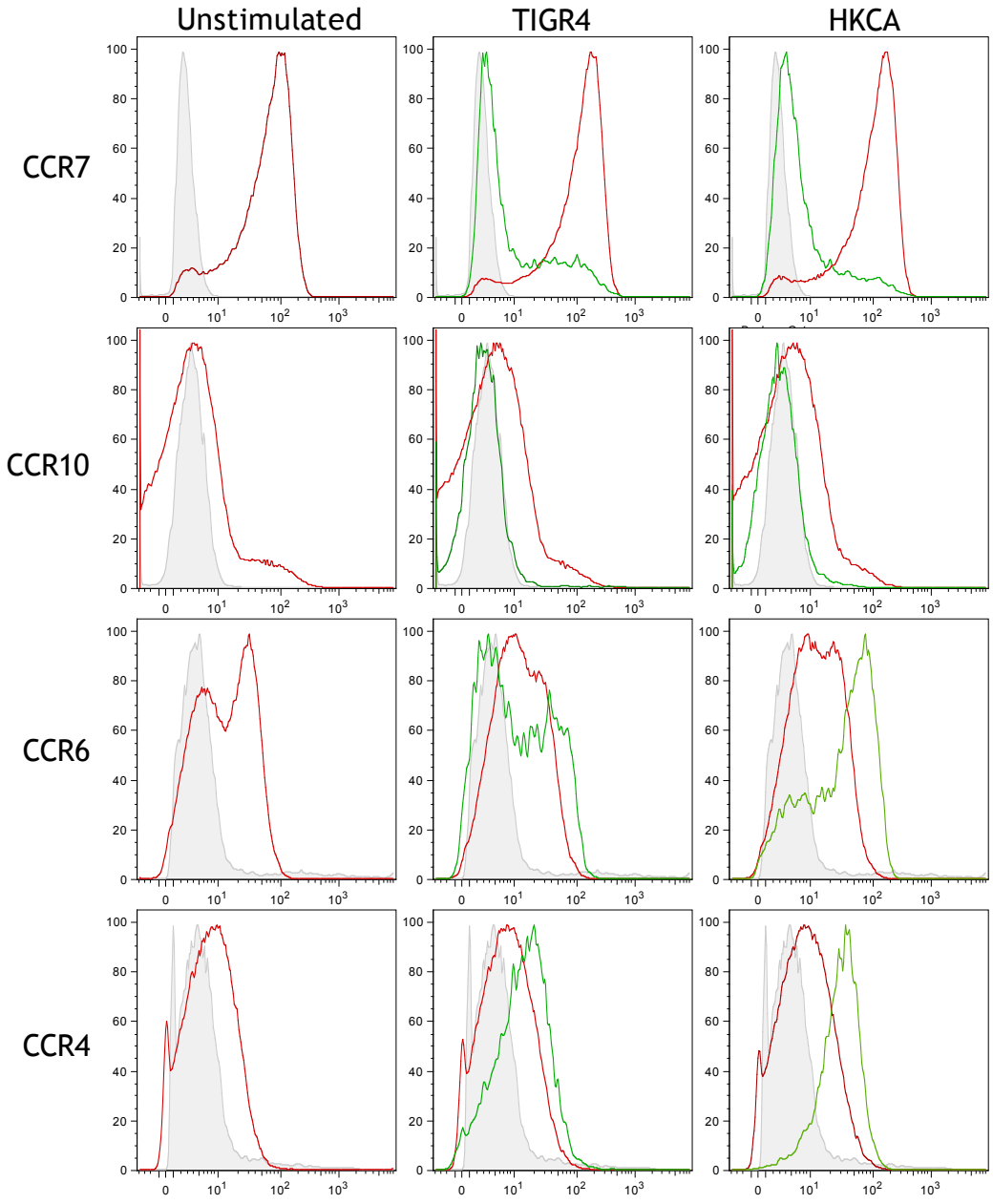

Figure 3-5. Characterisation of chemokine receptor profile of proliferating and non-proliferating cells following stimulation with TIGR4 or HKCA.
Co-cultures were stimulated as shown. After seven days, cells were stained for chemokine receptors without polyclonal stimulation or intracellular staining and gated on live $CD4^+$ cells. Proliferating and non-proliferating cells were then selected and staining for chemokine receptors for each group shown. Non-proliferating cells are shown in red, proliferating cells in green and the isotype control in grey. Unstimulated lymphocytes had very few proliferating cells and these cells were not analysed. Representative of 2 independent experiments.

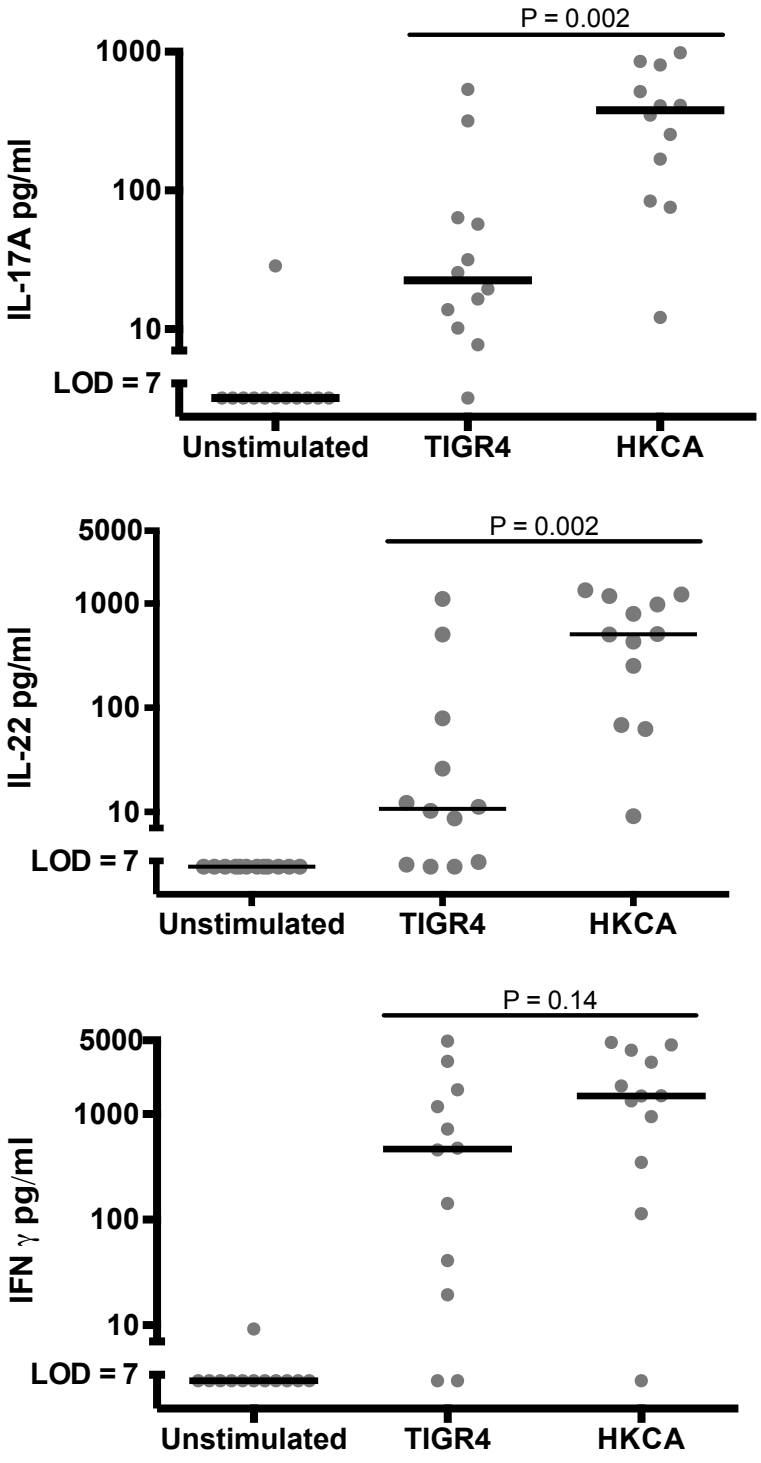

Figure 3-6. Cytokine concentrations in co-culture supernatants.
Supernatants were aspirated from triplicate co-cultures and analysed by ELISA. Horizontal lines represent group median values. P value represents Mann-Whitney test. LOD, limit of detection.

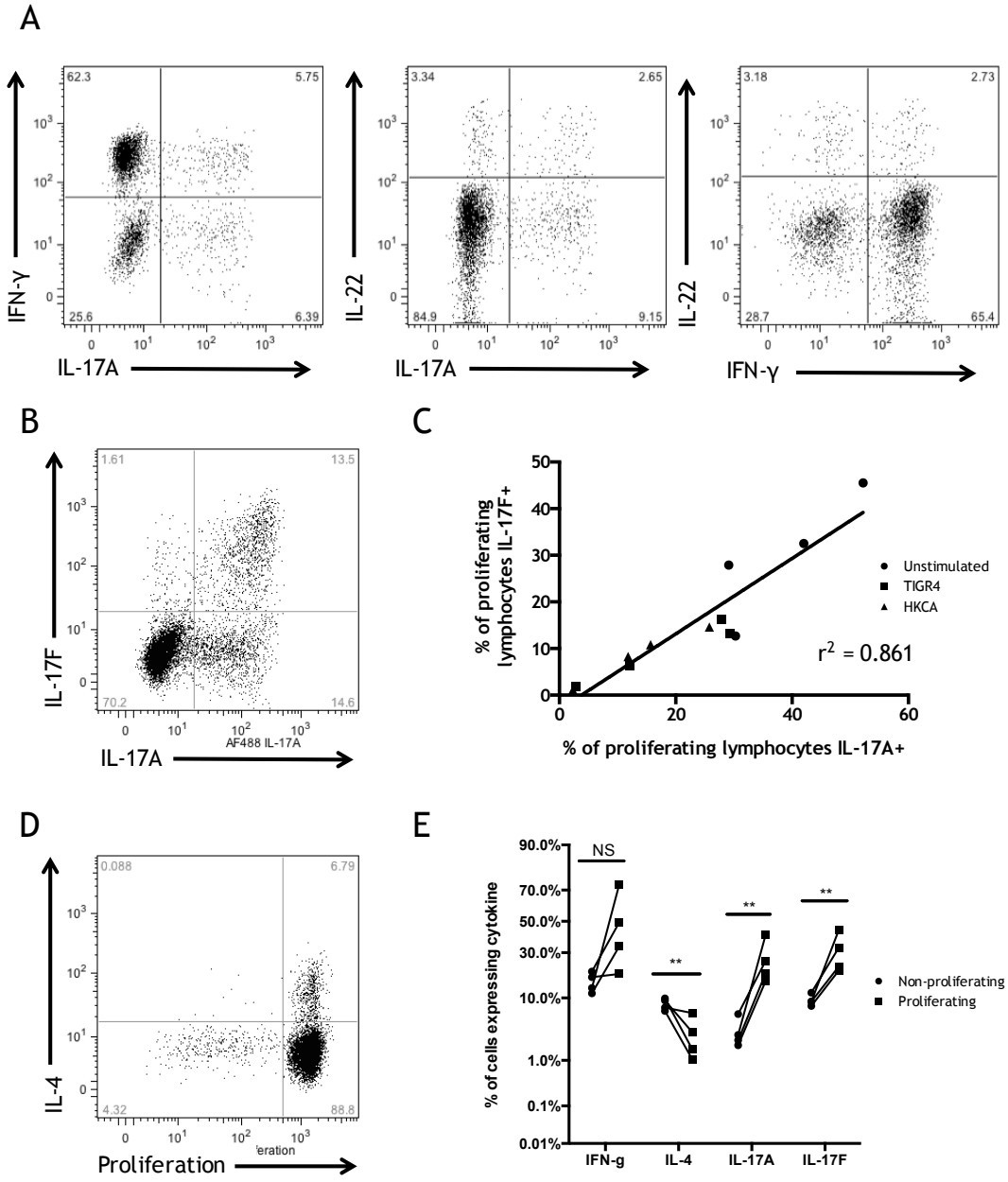

Figure 3-7. Intracellular staining for cytokines following stimulation with PMA and ionomycin in the presence of Brefeldin A.

A. Representative dot plots of intra-cellular staining of proliferating CD4+ cells with IL-17A, IL-22 and IFN-gamma after stimulation with TIGR4. B. Representative staining of proliferating lymphocytes with IL-17A and IL-17F. IL-17F is mostly produced by IL-17A producing cells and (C) IL-17F positive cells are strongly correlated with IL-17F. D. Representative dot plot of IL-4 staining of CD4+ lymphocytes with proliferation dye fluorescence. E. Cytokine staining of proliferating and non-proliferating cells. ** denotes $P < 0.01$.

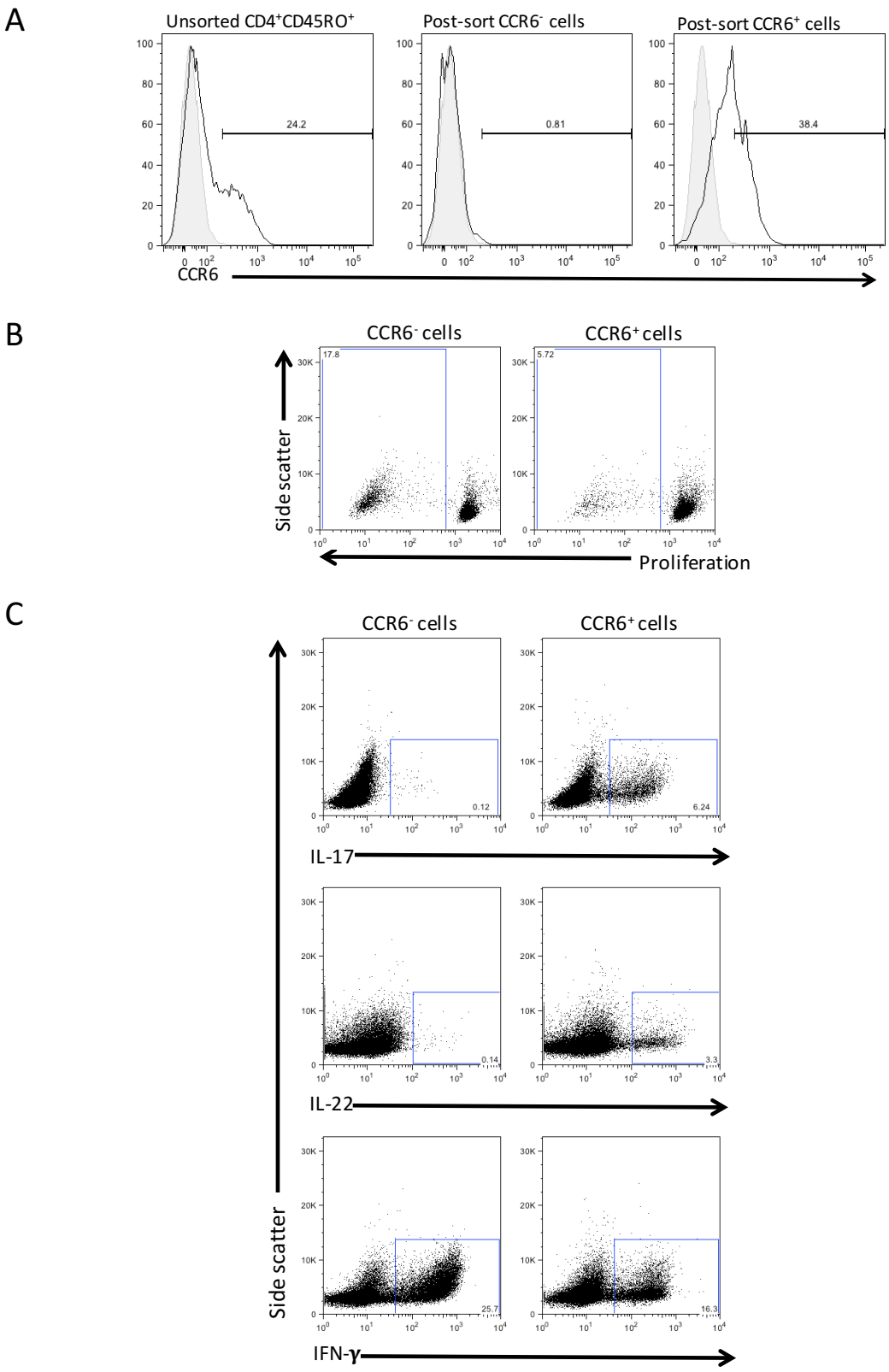

Figure 3-8. Pneumococcal responsive IL-17A and IL-22 producing CD4+ memory T cells are contained in the CCR6+ cells.

Full legend is shown on the next page under figure 9.

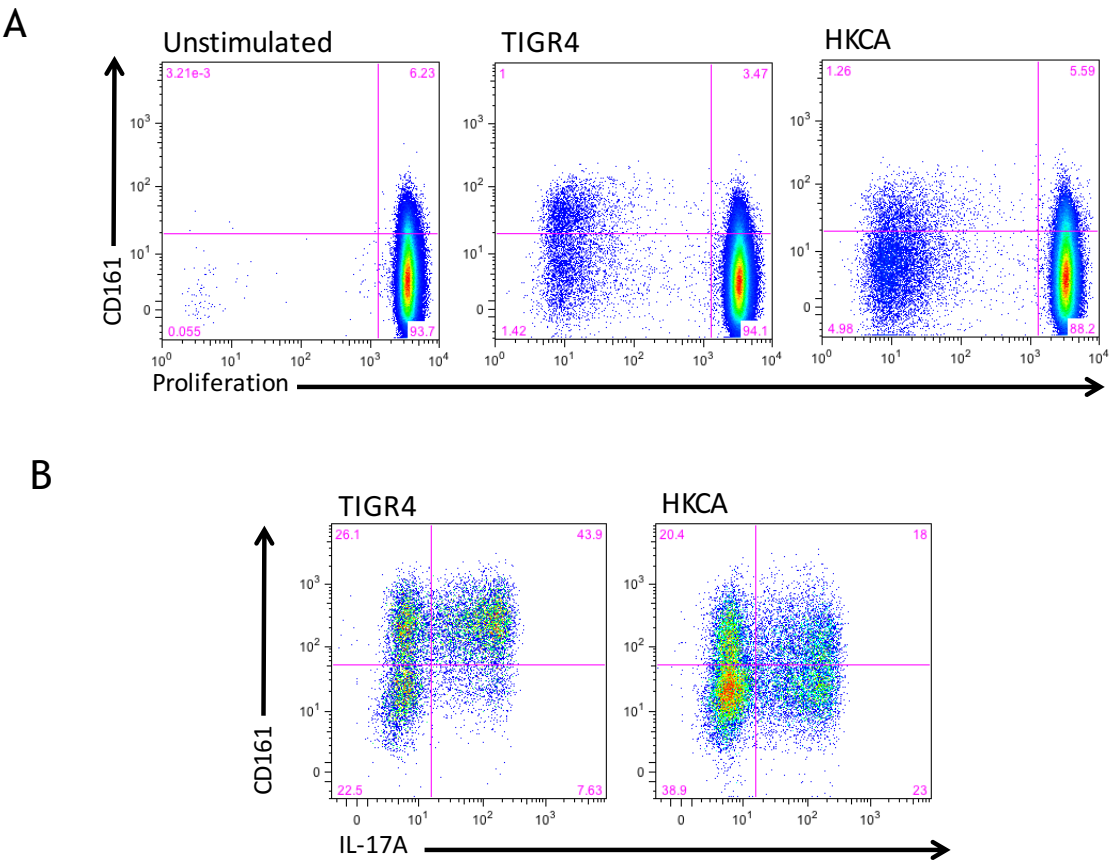

Figure 3-9. Lymphocytes proliferating in response to TIGR4 but not HKCA stimulation are enriched for CD161hi cells and are the principal IL-17A producing cells.

Co-cultures of proliferation dye stained lymphocytes and monocytes were stimulated with TIGR4 or HKCA and after seven days clonally stimulated with PMA and inomycin in the presence of Brefeldin A. Cells were stained for CD161 and IL-17A. A. CD161 staining plotted against proliferation dye. B. CD161 staining plotted against IL-17A staining. Representative of two independent experiments

---

figure 3-8. Pneumococcal responsive IL-17A and IL-22 producing CD4+ memory T cells are contained in the CCR6+ cells.

Proliferation dye stained lymphocytes were stained and sorted based on CCR6 staining (A). Cells were then mixed with monocytes and stimulated with TIGR4 before co-culture for seven days. Cells were then clonally stimulated with PMA and inomycin in the presence of Brefeldin A. B. Proliferation of T cells occurred in co-cultures containing both CCR6- and CCR6+ cells. C. IL-17$^+$ and IL-22$^+$ cells were rare in CCR6$^+$ cultures but IFN-γ$^+$ cells were found in both cultures.

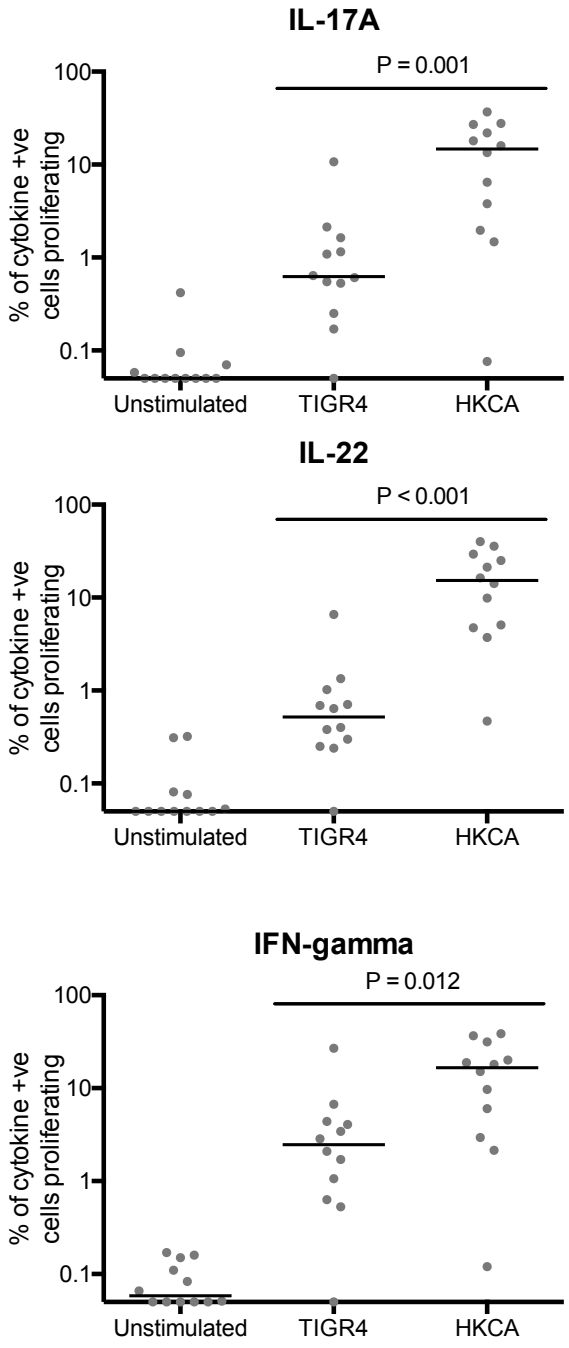

Figure 3-10. Cytokine positive cells in co-cultures.

After stimulation with PMA/ionomycin in the presence of Brefeldin A, cells were stained for intra-cellular cytokines. Proliferating cells were identified by dilution of proliferation dye and the cells positive for each cytokine are expressed as a percentage of the total number of CD4+ cells in the culture. Horizontal lines represent group median values. P value represents Mann-Whitney test.

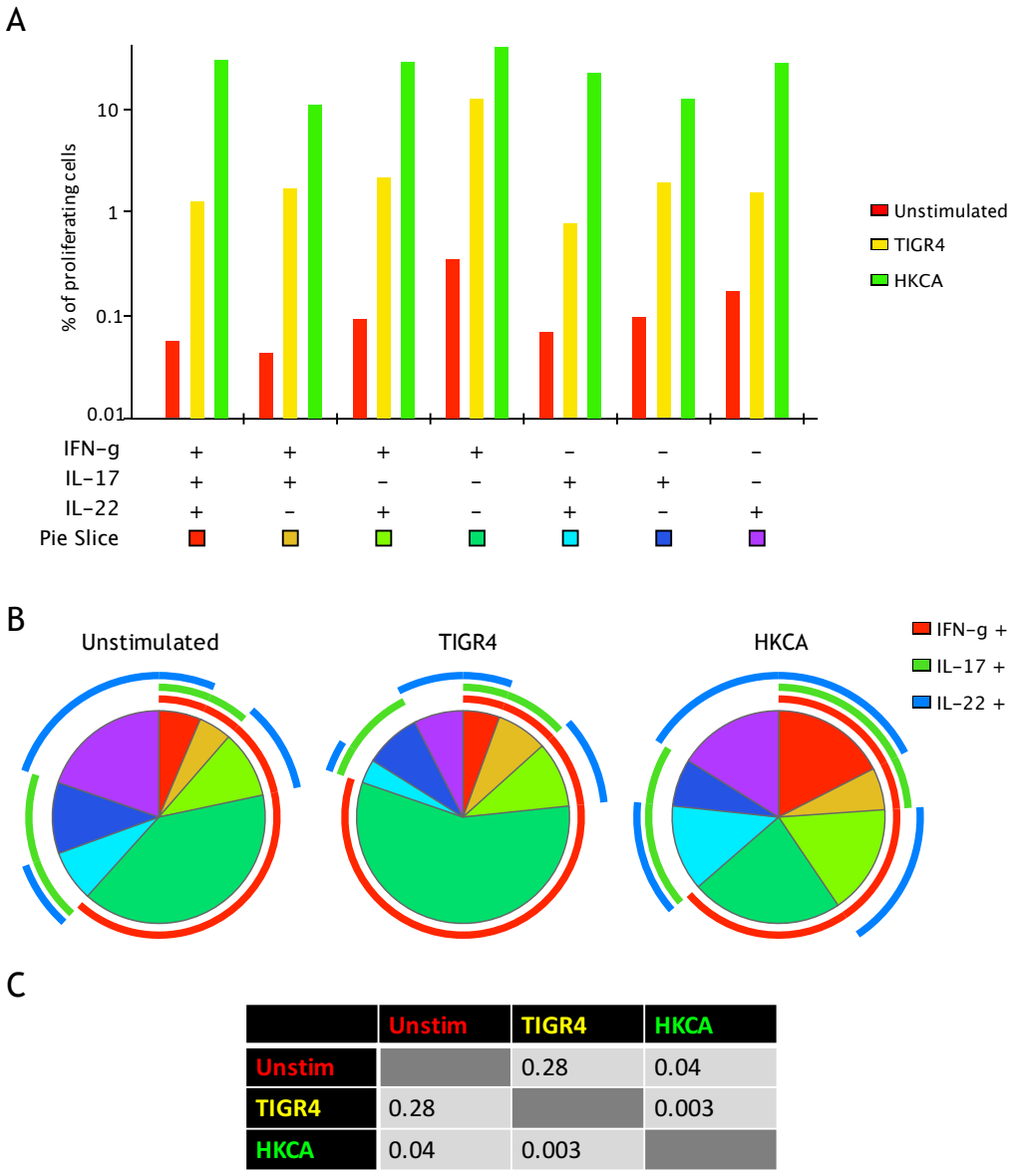

C

	Unstim	TIGR4	HKCA
Unstim		0.28	0.04
TIGR4	0.28		0.003
HKCA	0.04	0.003	

Figure 3-11. Combined cytokine expression of proliferating cells in co-cultures from young adults.

A. Relative frequency of proliferating cytokine producing cells classified according to combined cytokine positivity. B. Pie charts showing the relative contribution of different cytokine combinations to the proliferative T-cell response to stimulation. Pie slices are coloured according to the sceme in the bar chart above. Coloured arcs represent production of the cytokine shown in the legend. C. Comparison of distributions between stimulated co-cultures. P value represents Monte Carlo analysis of distribution statistic with 10,000 permutations.

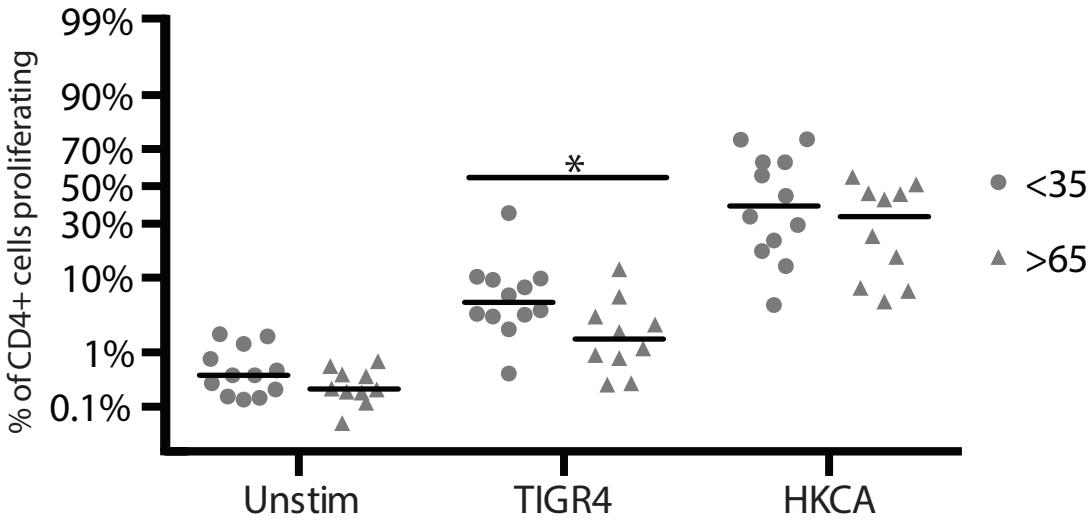

Figure 3-12. Total CD4+ proliferative responses among young and old adults. Cells plotted are all proliferating CD4+ T-cells in the culture. Horizontal lines represent the group median and P values represent a Mann Whitney test.

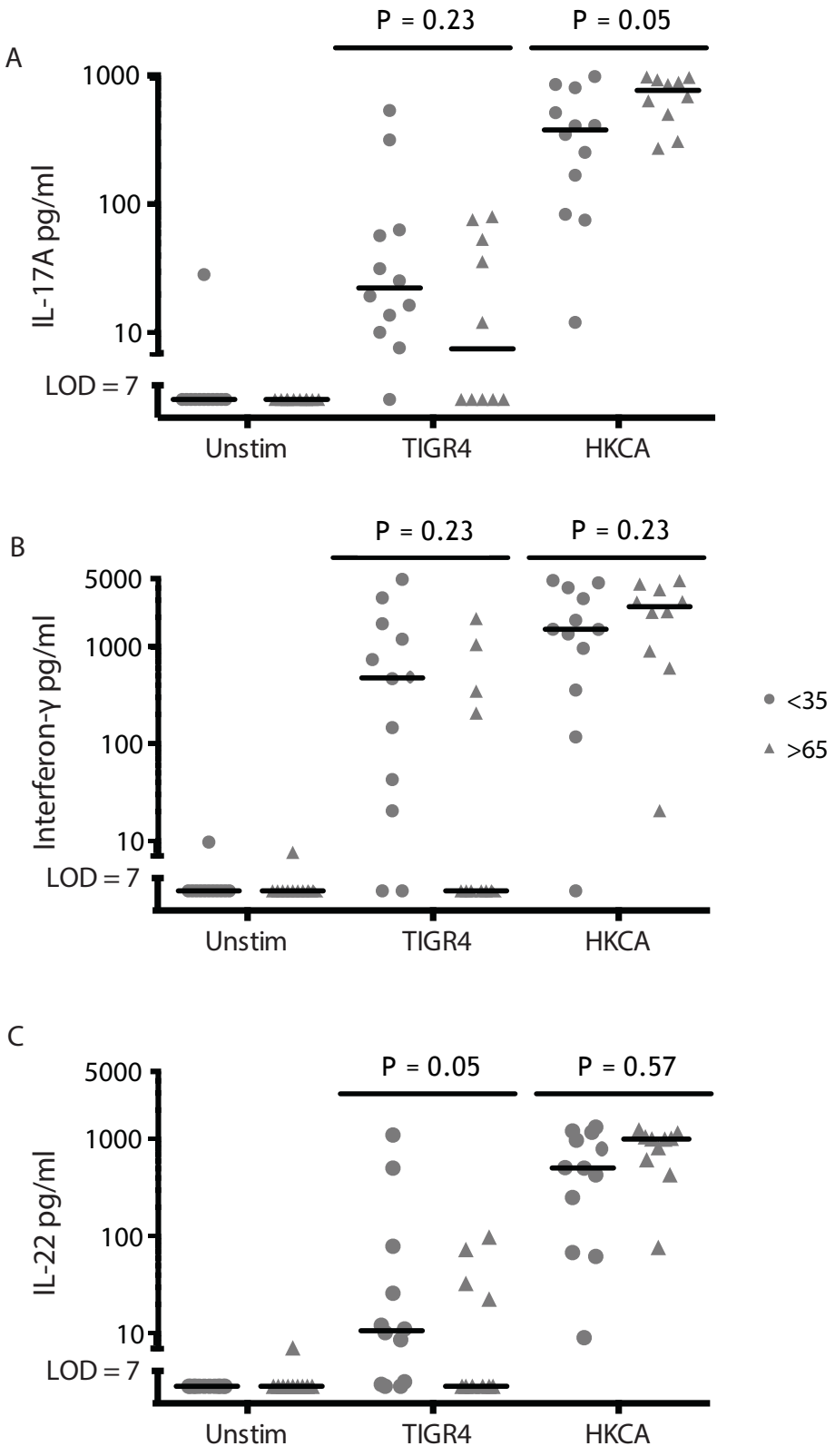

Figure 3-13. Cytokine concentrations in co-culture supernatants.
Supernatants were aspirated from triplicate co-cultures and analysed by ELISA. Horizontal lines represent group median values. P value Mann-Whitney test.

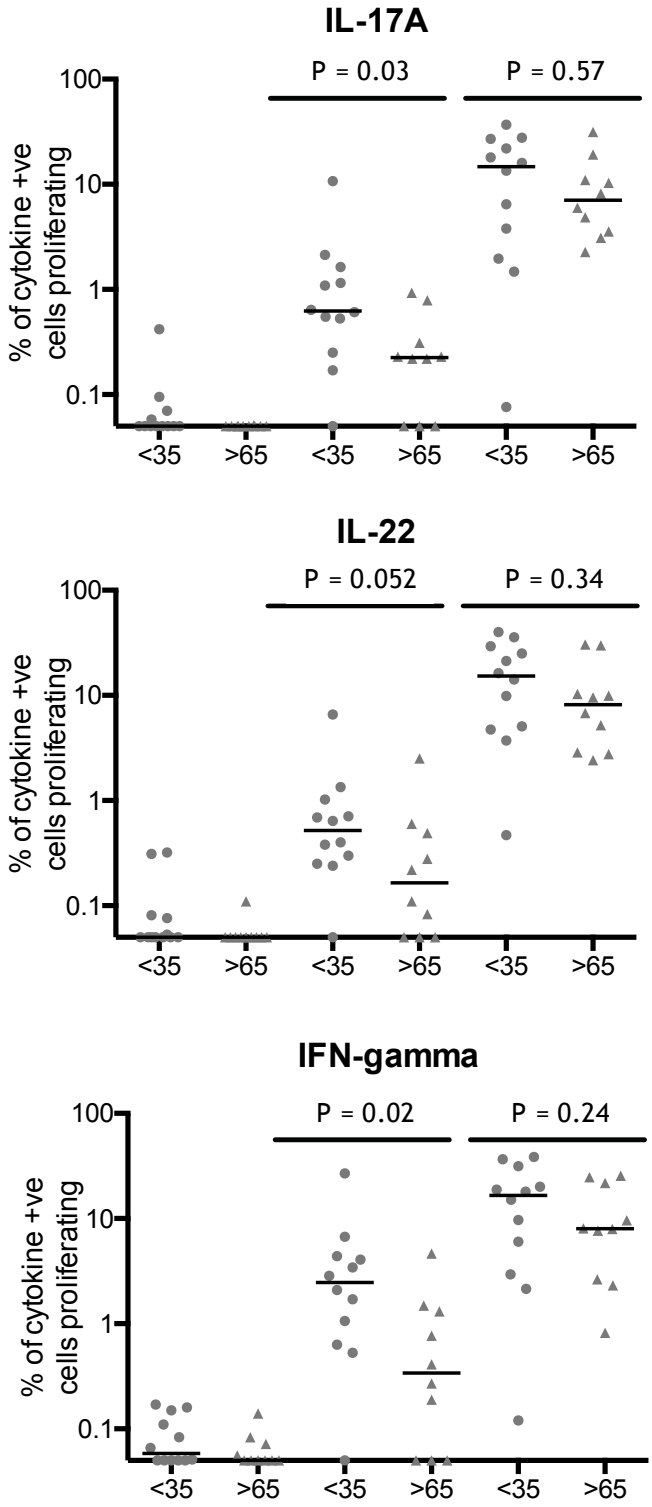

Figure 3-14. Proliferation of cytokine positive cells in co-cultures.
After stimulation with PMA/ionomycin in the presence of Brefeldin A, cells were stained for intra-cellular cytokines. Proliferating cells were identified by dilution of proliferation dye and the cells positive for each cytokine are expressed as a percentage of the total number of CD4+ cells in the culture. Horizontal lines represent group median values. P value represents Mann-Whitney test.

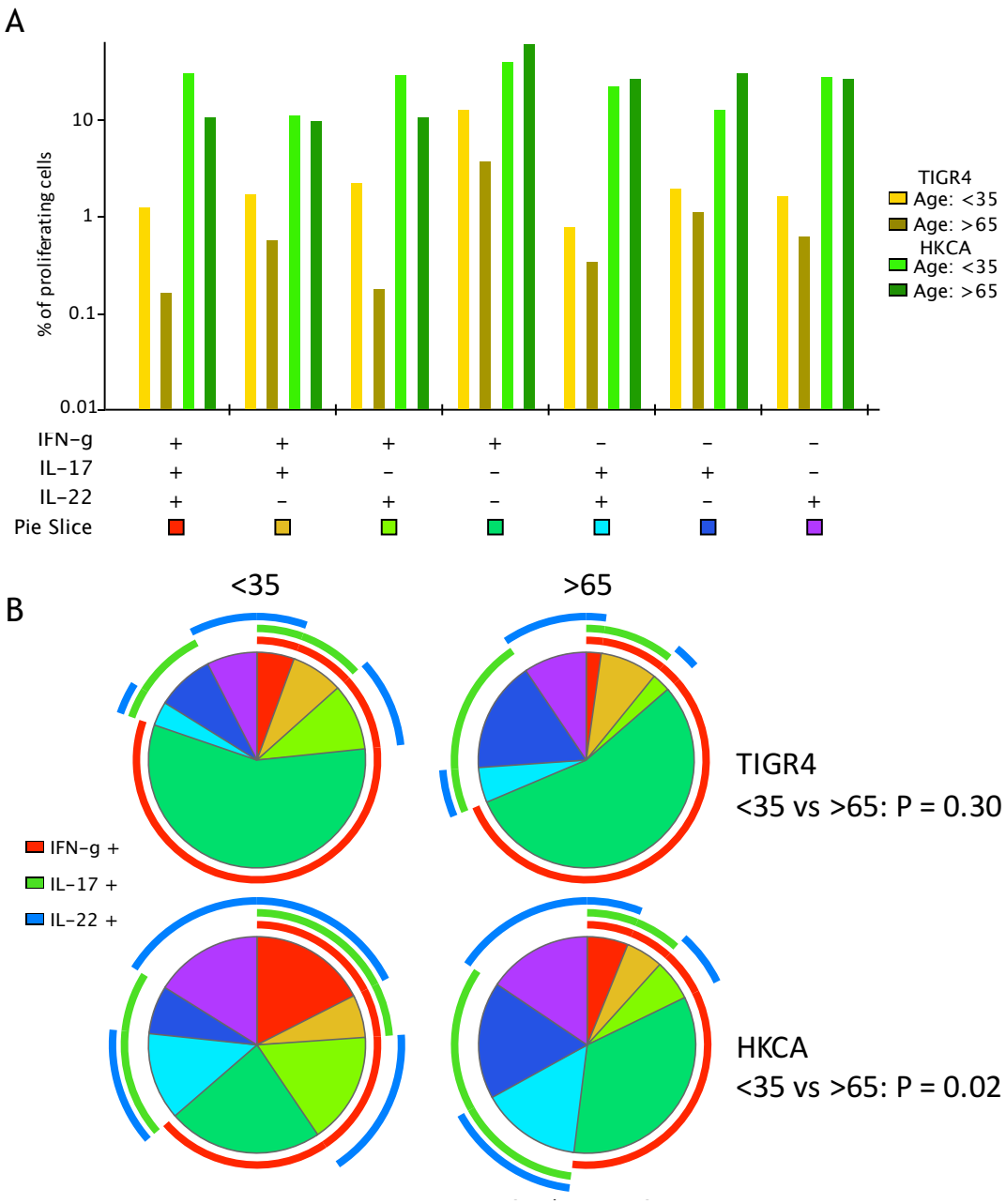

Figure 3-15. Combined cytokine expression of proliferating cells in co-cultures from young and old adults.

A. Relative frequency of proliferating cytokine producing cells classified according to combined cytokine positivity. B. Pie charts showing the relative contribution of different cytokine combinations to the proliferative T-cell response to stimulation. Pie slices are coloured according to the sceme in the bar chart above. Coloured arcs represent production of the cytokine shown in the legend. P value represents Monte Carlo analysis of distribution statistic with 10,000 permutations.

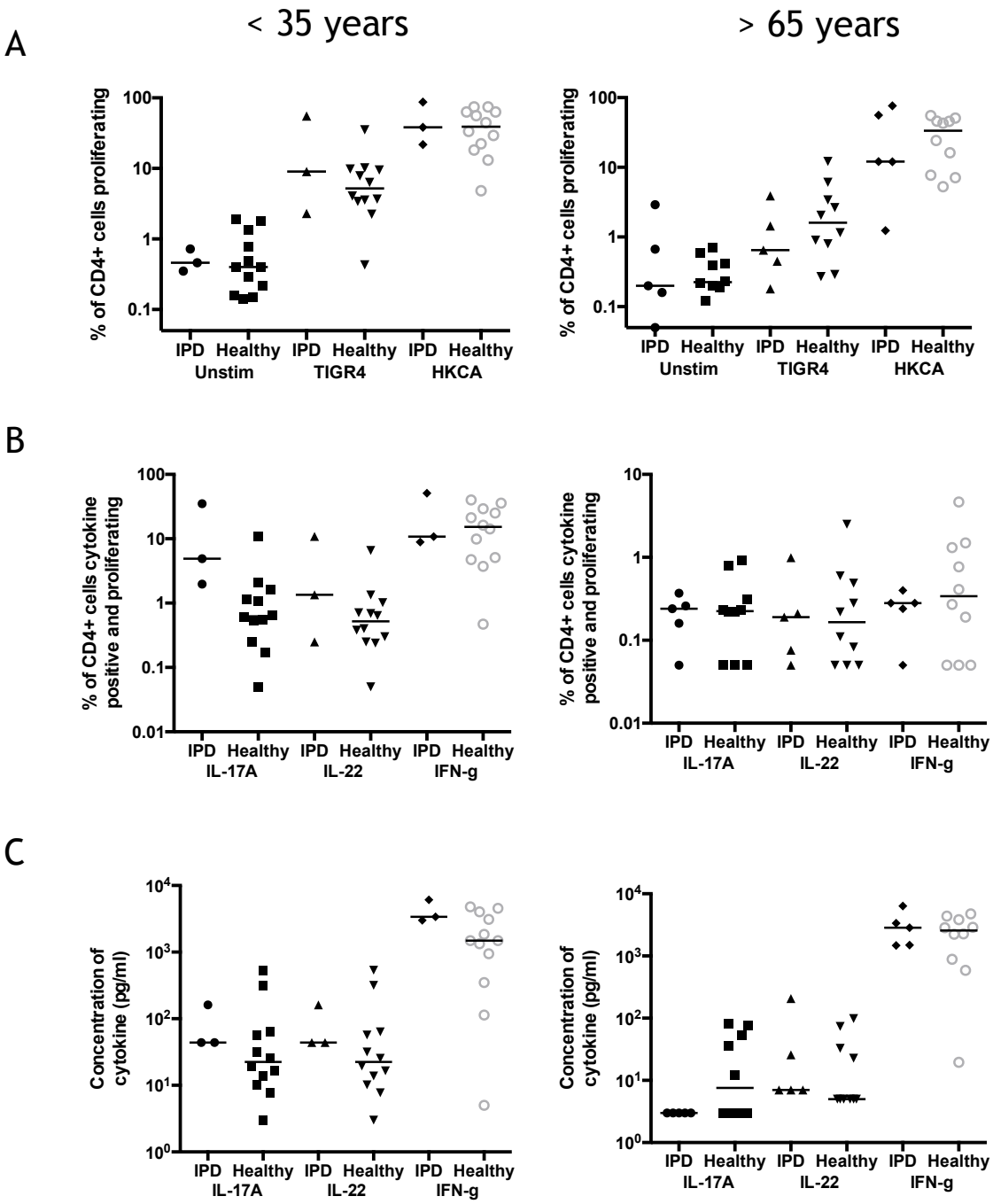

Figure 3-16. T cell responses are similar between patients with recent IPD and healthy controls.

Co-cultures were set up as previously described and total proliferation recorded by flow cytometry at seven days. (A) Total proliferation, (B) proliferation of $CD4^+$ cells producing IL-17, IL-22 and IFN-γ and (C) secretion of cytokines into cell culture supernatant after TIGR4 stimulation were compared between patients with recent IPD and healthy controls. There were no significant differences between groups for any of the assays conducted.

Volunteer	Age	Sex	Clinical Syndrome
1	28	F	Healthy Volunteer
2	30	M	Healthy Volunteer
3	27	M	Healthy Volunteer
4	18	M	Healthy Volunteer
5	22	M	Healthy Volunteer
6	34	F	Healthy Volunteer
7	25	F	Healthy Volunteer
8	32	F	Healthy Volunteer
9	21	F	Healthy Volunteer
10	19	F	Healthy Volunteer
11	26	M	Healthy Volunteer
12	23	F	Healthy Volunteer
13	74	M	Healthy Volunteer
14	72	M	Healthy Volunteer
15	81	F	Healthy Volunteer
16	79	F	Healthy Volunteer
17	73	M	Healthy Volunteer
18	65	M	Healthy Volunteer
19	88	M	Healthy Volunteer
20	86	M	Healthy Volunteer
21	75	F	Healthy Volunteer
22	84	F	Healthy Volunteer

Group	Age	%M	Clinical Details
<35	25.4	42	Recruited from pre-travel clinic
>65	77.7	60	Recruited from urology clinic

Table 3-1. List of healthy volunteers recruited to the study.

Summary statistics are shown in the table below: age is a mean, %M represents the % of the population which was male.

Patient	Age	Sex	Clinical Syndrome
1	75	M	Pneumonia
2	36	F	Meningitis
3	79	F	Pneumonia
4	81	M	Septic Arthritis
5	72	F	Pneumonia
6	71	M	Pneumonia
7	26	F	Meningitis
8	32	M	Meningitis

Table 3-2. List of patients with IPD recruited to the study.

4. DEVELOPMENT OF MODELS OF PNEUMOCOCCAL INFECTION

4-1 Introduction

S. pneumoniae is an important cause of human disease, however (apart from serotype 3 infection in horses caused by clones lacking typical virulence factors [416]) it is not known to cause natural disease in non-human mammals. However, the pneumococcus is a virulent organism in mammals and there is a long history of animal models of pneumococcal disease. The pneumococcus was discovered in the 1880s after mice died of overwhelming infection following the intra-peritoneal injection of saliva. Currently, there is a wide range of animal models of pneumococcal disease. Most models involve rodents: particularly mice and rats. However, other small mammals used include rabbits, gerbils, chinchillas and guinea pigs. Animal models have been used to investigate nasal colonisation, pneumonia, sepsis, meningitis and otitis as well as models that seek to explore more theoretical aspects of pathophysiology. The most commonly used method of pneumococcal infection involves delivery of pneumococci to anaesthetised mice via the intra-nasal route. This has the advantage that it is quick and easy to carry out but has the disadvantage that some of the bacteria delivered to the mouse fail to reach the lower respiratory tract. Intra-tracheal administration and inhalation of aerosolised bacteria are alternatives but both have significant costs in terms of complexity and resources.

Intra-nasal administration of pneumococci classically cause a bronchial pneumonia due to large scale aspiration of pneumococci which is in contrast to

the typical course of pneumococcal infection in humans, which tends to cause lobar pneumonia. Around 20 years ago, a technique of intra-nasal inoculation of pneumococci obtained by intra-peritoneal passage was developed. This model generally leads to early dissemination of pneumococci and the mice succumb to sepsis rather than respiratory failure.

I sought to develop a model of pneumococcal infection and to explore the role of IL-17 and IL-22 in this context. I initially planned to attempt this using a single strain of pneumococcus but for reasons described below I subsequently developed models of pneumococcal disease involving several strains of bacteria.

4-2 Characterisation of pneumococci

Prior to exposing mice to pneumococcal infection, I sought to characterise the bacterial characteristics with a range of chemical and molecular tests. By doing this I sought to define the characteristics of the organisms available in terms of their production of capsular polysaccharide, production of pneumolysin, serotype and clonal type.

4-2.1 Identification of pneumococci and colony morphology

All isolates were identified as pneumococci based on their colony morphology (alpha-haemolytic, optochin resistant), gram stain appearance (gram positive cocci), catalase negative and bile salt soluble. Strain SRL1 had a markedly different morphology when grown on blood agar than the other pneumococcal strains; it was mucoid in appearance rather than the classic punctate draughtsman colonies of the other pneumococcal isolates (figure 4-1).

4-2.2 Serotyping

The serotyping of isolates was confirmed using the multiplex PCR scheme devised by the CDC (figure 4-2A). TIGR4 is widely known to belong to serotype 4 and this was confirmed by the molecular method. The serotypes of the other isolates had been previously determined by Quellung reaction at the NHS reference laboratory and were confirmed by PCR. SRL1 was confirmed to belong to serotype 3 while SRL3, SRL4 and SRL5 were confirmed to belong to serotypes

7F, 14 and 19F respectively. SRL2 was determined to belong to serogroup 6 by PCR and the absence of *wciN$_{B}$* demonstrated that the isolate did not belong to serotypes 6C or 6D. The PCR product was sent for Sanger sequencing and this demonstrated the presence of asparagine at residue 196 in the *wciP* gene confirming that SRL2 belongs to serotype 6B (figure 4-2B).

4-2.3 Capsule size

Capsule size was measured by dextran exclusion (figure 4-3). SRL1 and 2 were seen to have large capsule size with SRL3 and 4 the smallest. TIGR4 and SRL5 had intermediate capsule sizes. Since a large number of masked areas were used to calculate the size of the dextran excluded area, the analysis had high statistical power and there were statistically significant differences between all of the serotypes at the $P<0.001$ level for all comparisons except those between SRL3 and SRL4 and between TIGR4 and SRL5, which were both non-significant. Analysis of the size of the SRL1 capsule was complicated by the unusual appearance of this organism on microscopy. Rather than the sharp dextran exclusion seen with the other organisms, SRL1 had a more gradual edge to the area of exclusion. In order to reduce bias, the automatic thresholding function in ImageJ was used rather than manual selection of the edge of the area but it is acknowledged that there is some subjectivity in selecting the edge of the SRL1 capsule using this method.

4-2.4 Electron microscopy

Transmission electron microscopy of fixed mid-log cultures of the pneumococcal strains was conducted. Representative images of pneumococcal strains are shown in figure 4-4A. As with dextran exclusion imaging of the capsule, imaging of the capsule of SRL1 was difficult. When SRL1 was first processed and imaged by TEM the capsule of SRL1 was found to have detached completely (data not shown). When preparation was repeated with particular attention to speed of fixation, the capsule remained attached to around half of bacteria. Only bacteria with capsule attached were used to calculate capsular size. Capsular detachment was not a prominent feature of the other bacterial strains. The serotype 3 capsule expressed by SRL1 had a different appearance to the other capsules with increased density on imaging compared to the other bacteria.

When capsular size was quantified, the results were correlated with those from dextran exclusion with SRL1 and 2 having the largest capsule, SRL 3 and 4 the smallest and TIGR4 and SRL5 intermediate (figure 4-4B).

4-2.5 Haemolysis assay

Assessment of the haemolytic activity of lysates of pneumococci was conducted (figure 4-5). The haemolytic activity of all isolates except SRL3 was similar with all achieving 50% lysis of red blood cells even at dilutions exceeding 1:256. However, SRL3 had significantly lower haemolytic activity compared to the other isolates (figure 4-5C, $P < 0.001$).

4-2.6 Determination of MLST

Sequences of strain housekeeping alleles were obtained and MLST was obtained from the MLST database (figure 4-6). As expected, analysis confirmed that the MLST of TIGR4 was 205 and SRL1 was 180. The MLST of the other strains is shown in figure 4-6B.

4-3 Development of methods

4-3.1 Administration of substances via i.n. route

To assess the technique of intra-nasal administration, mice were inoculated with 25 µl per nostril of 0.4% trypan blue under a light general anaesthetic and culled after 2 hours. Gross examination of the internal organs revealed penetration of trypan blue into the lungs of all animals.

The gross appearance of representative mice is shown in figure 4-7. Blue dye tended to appear most strongly in the posterior portion of the upper lobes of the lungs. This is typical of aspiration pneumonitides which occur in the dependent portion of the lungs of affected animals – mice were placed on their backs after inhaling the trypan blue and therefore the observed area would be the dependent region at this time. Outside the dependent region, the distribution of trypan blue was patchy and could often be seen following the path of the major bronchi.

As expected, there was clear trypan blue staining within the upper airways of mice. The stomachs of mice were also dissected and variable amounts of trypan blue staining were also present within stomach. This is also to be expected, since some material is likely to remain within the upper airways of mice at the conclusion of the general anaesthesia and may be swallowed.

4-3.2 Development of neutrophil immunohistochemistry

I wished to accurately visualise neutrophils in the lungs of infected animals. I therefore sought to develop an immunohistochemical assay to stain neutrophils. The neutrophil surface marker used elsewhere in this study was Gr-1 and I therefore sought to use this marker to detect neutrophil infiltration in lungs.

Because of the need to prevent bacterial aerosolisation during the cutting of frozen sections, it was important that tissue was fixed prior to sectioning to inactivate infecting bacteria. However, the Gr-1 staining antibodies 1A8 and RB6-8C5 are reported not to bind in formalin fixed sections. This was confirmed using paraffin embedded formalin fixed sections using several antigen retrieval techniques: proteinase K, high and low pH solutions and heat induced antigen retrieval. None of the methods of antigen retrieval gave any specific staining at concentrations of antibody up to 50 µg/ml (data not shown). Furthermore, RB6-8C5 is not entirely specific for neutrophils as it binds not only to the Gr-1 marker (Ly-6G) but also to the closely related Ly-6C, which is expressed on subpopulations of monocytes and lymphocytes[417]. Therefore, 1A8 is the more specific antibody. Therefore, I sought to find a method to use this antibody on fixed tissue.

Zinc salt solutions are reported to give adequate fixation of tissues including the ability to dehydrate and clear tissue for embedding in paraffin but give superior antigen protection to aldehyde fixatives[418]. I investigated using zinc salt fixative to fix lung tissue for 48 hours followed by paraffin embedding and immunohistochemistry without antigen retrieval. This method was successful in generating specific staining in lungs at low concentrations of 1A8 down to 1:10,000 (50ng/ml). Representative staining of infected and control lungs is shown in figure 4-8. Some background staining of inflamed tissues was seen at

higher concentrations of antibody which was not seen on isotype sections and may therefore have been due to the presence of neutrophil fragments in inflamed tissue. While a multilobed nucleus is visible in many of the stained cells on high power magnification, cells in infected lungs were tightly packed and it was not possible to see the nuclear morphology of all stained cells (figure 4-8C).

Even after quenching of endogenous peroxidases with H_2O_2 there was still some peroxidase activity present in red blood cells but these were easily distinguished from neutrophils on the basis of size and lack of nuclei.

4-4 Model of TIGR4 infection

The first pneumococcal clone investigated in this project was TIGR4. This bacterium was delivered to mice at a dose of 5×10^6 based on previous experience of Professor Mitchell with this bacterium. After infection, mice were monitored for up to 48 hours and culled at intervals during the experiment to establish a time course of infection.

4-4.1 General characteristics

The change in weight and clinical score of mice infected with TIGR4 are shown in figure 4-9. Animals were always infected at 9am and the diurnal variation in weight of healthy animals which tend to lose weight during the day and gain weight overnight explains the fall in weight seen in the control group in figure 4-9A. Infected animals lost weight steadily throughout the experiment so that some animals approached the weight loss limit of 20% by 48 hours. Animals started to become clinically unwell at 36 hours after infection and were severely unwell by 48 hours post infection.

The bacterial burden in infected mice is shown in figure 4-10 and demonstrates a highly invasive bacterial pathogen. Bacterial burden in BALF peaked at 6 hours post infection before declining thereafter. The peak burden in lung homogenate was at 12 hours and this then declined later in the experiment. In contrast, bacteria entered the blood within 6 hours of infection and bacterial density steadily increased throughout the experiment. Bacteria were also detectable within the pleura in some animals as early as six hours and were readily

detectable within 12 hours. Bacteria expanded steadily within the pleura reaching densities up to 10^8 cfu/ml. It should be noted that pleural samples were washes involving injection of 5ml implying that the pleura of such animals contained bacteria in extremely high density, possibly reaching the densities reached in late-log phase liquid cultures of pneumococci (around 10^9 cfu/ml).

Lung myeloperoxidase (MPO) activity correlates with infiltration of neutrophils into mouse lung. MPO activity was measured in samples of lung from infected animals (figure 4-11A). MPO activity mirrored bacterial density within lungs in that it rose over the first 12 hours of the experiment and then declined through the remainder of the time course. It must be noted that lungs sampled for MPO activity had been subjected to broncho-alveolar lavage and this is likely to have removed large numbers of neutrophils from affected lungs and is therefore likely to have underestimated MPO activity.

IL-17A and IL-22 concentrations in BALF determined by ELISA are shown in figure 4-11B. IL-17A and IL-22 concentration were detectable at 6 hours and both peaked at 12 hours post infection before declining over the remainder of the experiment.

4-4.2 Histopathological findings

Representative histopathology from mice infected with TIGR4 is shown in figure 4-12. As early as 6 hours following infection, there was evidence of infiltration of inflammatory cells into the peribronchial region. This inflammatory infiltrate became more prominent at 12 and 24 hours with evidence of alveolar neutrophils in the areas adjacent to the peribronchial inflammation. By 48 hours, the inflammatory change had tended to become well defined with bands of inflammation running alongside bronchi but regression of the alveolar infiltrate.

The pleural surface of infected animals was also abnormal (figure 4-12B). In contrast to the sharp, thin pleural surface seen in uninfected animals, by 24 hours there was thickening of the pleural surface and by 48 hours post infection

the pleural surface was markedly thickened with subpleural alveolar inflammatory infiltrate.

Neutrophil immunohistochemistry comfirmed the impression from H&E staining with patchy peribronchial infiltration of neutrophils at 12 hours becoming more intense by 12 hours (figure 4-13A). As with the H&E staining, the infiltration was rarely dense and remained largely confined to the peribronchial region even in severely unwell animals.

Gram staining of the lung tissue confirmed the paucibacterial nature of the lung disease with the vast majority of high power fields lacking a single bacterium (figure 4-13B). Bacteria were only seen occasionally, requiring many fields to be inspected.

4-5 Model of SRL1 infection

4-5.1 Selection of SRL1 as candidate bacterium

As demonstrated above, TIGR4 is a highly invasive pneumococcal isolate with the ability to cause severe sepsis following administration into the lower respiratory tract even without the presence of severe pulmonary disease. Indeed the pulmonary inflammation produced in TIGR4 infection is relatively modest and the vast majority of the alveolar spaces appear normal microscopically.

IL-17 is principally active at mucosal sites and I hypothesised that IL-17 is therefore unlikely to play a significant role in the course of highly invasive disease. Therefore, we sought a pneumococcal isolate that would be likely to produce a more localised pulmonary infection. Given the association of serotype 3 with severe, necrotising pneumonias (discussed more fully in the introduction to this thesis) I decided to investigate a serotype 3 strain and characterise the course of infection with this organism. The most commonly identified serotype 3 strain in human infection belongs to ST180 clonal complex and this complex has recently been subjected to genomic analysis. I therefore obtained a ST180 serotype 3 organism and decided to investigate its virulence in the same mouse model used to investigate TIGR4. Given that I was seeking to generate a pathogen successful at causing pulmonary infection, the organism was passaged

through the lung of mice rather than through intra-peritoneal passage with mice being infected and the bacterium isolated from BALF 24 hours later.

4-5.2 Dose titration

To establish the optimum dose for SRL1 infection a dose titration was performed. Details of this experiment are shown in figure 4-14. Mice were infected with 10^5 – 10^7 cfu/mouse and monitored for 48 hours. Mice infected with 10^7 bacteria developed severe clinical illness by 48 hours and lost a significant amount of weight. In contrast, mice infected with 10^5 and 10^6 bacteria lost little weight and developed only mild clinical illness characterised only by some loss of coat sheen.

Bacteriology data from this experiment is presented in figure 4-15. All animals had detectable bacteria in BALF at 48 hours although those infected with 10^5 cfu/mouse had much lower bacterial densities than the animals infected with larger innocula. The 10^5 cfu/mouse group had no detectable bacteria in pleura and blood whereas mice in the 10^6 and 10^7 groups had bacteria detectable at high level in pleura and at somewhat lower density in blood. While animals infected with 10^7 cfu/mouse were significantly more unwell in terms of weight loss and clinical score they did not have increased bacteria burden at the sites sampled. However, it should be understood that colony counting of SRL1 is challenging due to the mucoid nature of the organism and, while increased experience allowed more accurate colony counting as further experiments were conducted, the possibility of a difference in these experiments cannot be excluded.

Pathological studies of mice infected with SRL1 were conducted. Gross images of lungs from infected mice are shown in figure 4-16. Mice infected with 10^5 cfu of SRL1 had an essentially normal appearance of the lungs at 48 hours. However, there were gross abnormalities of the lungs of mice with higher innocula. Lungs from mice infected with 10^6 cfu had areas of dark coloured focal consolidation usually limited to a single lobe. Finally, mice receiving 10^7 cfu had extensive discolouration of the lung surface with consolidation affecting more than 50% of the lung surface. H&E staining revealed dense alveolar infiltrate which increased

in maximal severity with increasing dose of bacteria (figure 4-17). In the most severely affected mice there were large areas of confluent inflammatory change often involving entire lobes of lung. In such inflamed areas, the alveoli were packed with inflammatory cells arranged in sheets with some areas of focal necrosis. Gram staining of the affected lung revealed the presence of large numbers of gram positive cocci (figure 4-18).

My aim in developing this model was to assess the impact of IL-17 and IL-22 deficiency on the course of infection. Since it was hypothesised that lack of IL-17 and IL-22 would adversely impact on outcome, the 10^6 cfu/mouse dose was selected for further study since this caused an illness of moderate severity in wild type animals leaving open the possibility of more severe infection in knockouts.

4-5.3 Time course experiment

The progression of SRL1 infection was further characterised in time course experiments. Mice were infected with 10^6 cfu/mouse of SRL1 and then culled at intervals over the next 48 hours. The clinical progression of this infection was, in fact, similar to the course of infection in 10^7 mice in the original dose finding experiment. Weight loss and clinical score data is shown in figure 4-19. After 48 hours mice were severely unwell and approaching the 20% weight loss limit.

Bacteriology data are shown in figure 4-20. Bacterial burden in BAL increased steadily throughout the experiment reaching high level at 48 hours. However, there was no evidence of early invasion with blood and pleura sterile in all animals in both time course experiments at 24 hours. However, at 48 hours there was evidence of high levels of bacterial burden in pleura and penetration into blood in most animals.

Myeloperoxidae assay of infected lungs revealed evidence of steady accumulation of neutrophils in the lungs prior over the first 24 hours of infection with a levelling off of MPO activity at 48 hours (figure 4-21A).

IL-17A and IL-22 BAL concentrations measured by ELISA are shown in figure 4-21B. There was little detectable cytokine at 6 and 12 hours before

concentrations of both cytokines peaked at 24 hours and fell markedly by 48 hours.

The progression of SRL1 pneumonia over 48 hours is shown in figure 4-22. At 6 hours, early infiltration of inflammatory cells in a peribronchial distribution similar to that observed in TIGR4 infection is seen. At 12 hours this inflammation has progressed in a largely peri-bronchial pattern. At 24 hours there is dense alveolar infiltrate with neutrophils filling the alveolar spaces within large areas of lung but still clearly centred on a bronchovascular bundle. However by 48 hours there is clear development of a lobar pneumonia with the dense infiltration of non-aerated lung and some evidence of focal necrosis.

The extent of pleural disease is demonstrated in H&E staining of an infected mouse at 48 hours in figure 4-23. The pleural space contains a large amount of purulent material with many neutrophils (figure 4-23A). The lung surface is coated with cells and purulent material (figure 4-23B). The lungs of severely infected animals often contained areas of dense subpleural inflammation with an impression of breaches in the lung surface (figure 4-23C).

Immunohistochemical staining of lungs for neutrophils is shown in figure 4-24. At 6 hours post infection only a very few neutrophils were visible but there was steady progression in the density of the neutrophil staining through the 48 hours of the experiment.

4-6 Summary comparison of TIGR4 and SRL1

As has been demonstrated above, TIGR4 and SRL1 induce very different infectious phenotypes with TIGR4 rapidly invading into the blood and causing a septic illness with relatively modest pulmonary inflammation but SRL1 remaining within the lungs and reaching high bacterial density within the lung before entering the blood at a late stage once the animal is already severely unwell.

The marked difference in the localisation and severity of pulmonary inflammation is shown in figure 4-25. Lungs from mice culled with significant weight loss and a high clinical score after infection with TIGR4, such as the one

shown in figure 27B, had modest peribronchial and perivascular inflammatory change and limited mild alveolar infiltrate. Moderate pleural thickening was also seen in some animals. In contrast, lungs from similarly unwell mice infected with SRL1, such as that shown in figure 4-25C had extensive alveolar infiltrate with large areas of dense consolidation and often had empyema.

Both TIGR4 and SRL1 stimulated the release of IL-17 and IL-22 early in the course of infection; infection with both serotypes resulted in a peak in cytokine concentration 12-24 hours post infection with a decline in IL-17 and IL-22 concentration in the later stages of infection. This pattern of IL-17 and IL-22 secretion suggested an innate source of the cytokines since Th17 cells would be expected to accumulate at the site of infection later than 12-24 hours post infection in naïve mice.

4-7 Cellular sources of IL-17 and IL-22

4-7.1 Clonal stimulation of cells in lung

I initially sought to characterise the cells in the lung capable of producing IL-17 in response to a clonal stimulation. Lung homogenates from mice infected with TIGR4 and SRL1 were stimulated *in vitro* with PMA and ionomycin to produce broad activation of immune cells. This stimulation was conducted in the presence of Brefeldin A to inhibit the secretion of cytokines and therefore cause accumulation of cytokines within the cells that could subsequently be stained with antibodies after fixation and permeabilisation.

I hypothesised that the secretion of IL-17 and IL-22 was likely to come from one of the known sources of such cytokines such as Th17 cells or γδ lymphocytes. The percentage of candidate IL-17 producing cells was measured by flow cytometry in uninfected and infected lung homogenates. The gating strategy used is shown in figure 4-26. It was not possible to calculate the absolute number of cells due to losses in the process of homogenisation and variation in the volume of lung sampled. After exclusion of dead cells, neutrophils were identified as Gr-1^{+}, side scatter^{hi} cells. Other cells were identified and quantified after the exclusion of neutrophils, since the expected rise in neutrophils following infection would obscure changes the other populations.

The cell populations found in lungs of mice infected with SRL1 and TIGR4 are shown in figure 4-27. As expected, there was a substantial increase in neutrophils in infected lungs compared to uninfected lungs ($P < 0.01$ for both TIGR4 and SRL1). After exclusion of neutrophils, there was a modest increase in the percentage of γδ lymphocytes and $CD3^+CD4^-\gamma\delta TCR^-$ cells 48 hours post infection. There was a corresponding decrease in the percentage of $B220^+$ cells (significant only in SRL1 infected lungs) while the percentage of other cell fractions was not significantly different although there was a non-significant trend towards a decreased percentage of $CD3^+CD4^+$ lymphocytes ($P = 0.12$).

Unfortunately, despite using two different monoclonal antibodies, no consistent intracellular IL-22 staining could be obtained on flow cytometry. Therefore the remainder of this section addresses the cellular sources of IL-17 for which specific staining could be obtained (figure 4-26B). In the resting lung, typically less than 1% of cells expressed IL-17 and this increased marginally in lungs 48 hours post infection (figure 4-26C).

Representative staining of the cell types examined is shown in figure 4-28 and summary plots are shown in figure 4-29. Only rare neutrophils and $B220^+$ cells stained positive for IL-17 and the percentage of these cells producing IL-17 was close to that of the fluorescence minus one (FMO) isotype control. Therefore, it was concluded that these cells did not produce significant IL-17 in this context. Other cell types produced detectable amounts of IL-17 with around 1-2% of $CD3^+CD4^+$ cells, $CD3^+CD4^-\ \gamma\delta TCR^-$ and $CD3^-B220^-$ cells staining positive for IL-17. $CD3^+\ \gamma\delta TCR^+$ cells represented a small proportion of lung cells but many of them were $IL\text{-}17^+$ (typically 25-30%). Therefore, the increase in IL-17 producing cells in the non-neutrophil gate in infected mice was largely due to a fall in $B220^+$ cells, which produce little IL-17 and a rise in the percentage of other cell types (notably γδ lymphocytes) which were more likely to produce IL-17. The design of this experiment does not permit the quantification of total cells and so it is not known whether there was a true rise in IL-17 producing cells or a fall in IL-17 negative cells.

4-7.2 In-vivo brefeldin A model

The use of a pharmacological stimulation of cells from lung homogenate was useful to clarify the cells in the lung capable of producing IL-17 but the detection of IL-17 in a cell following pharmacological stimulation does not provide evidence that the cell has been producing IL-17 *in vivo* since the clonal stimulation activates all cells including those that were not activated within the lung. Therefore, I decided to explore methods of defining the cells producing IL-17 *in vivo*.

The first method I employed involved the use of Brefeldin A *in vivo* to trap cytokines within cells during the course of the model and then detect it with flow cytometry. This would have the advantage of confirming that the cells were producing IL-17 within the animal and not simply in response to clonal stimulation. However, this method has the disadvantage that much smaller quantities of cytokine being expressed by fewer cells will be detected with intracellular staining. I was therefore careful to ensure that IL-17 expression was robustly detected through the use of fluorescence minus one controls in all samples. Because the number of IL-17 expressing cells was small, it was necessary to combine the lungs of animals involved in the experiments and therefore the results are presented as representative staining of pooled lung homogenate.

Mice were culled 6 hours after the intra peritoneal administration of 250 μg of Brefeldin A. I initially attempted to detect intracellular IL-17 using this method at 48 hours post-infection. However, no IL-17 was detected (data not shown). This initial experiment was performed because I had hypothesised that Th17 cells were an important source of IL-17. In retrospect, there was little IL-17 detectable in BALF supernatant at this time point and therefore it was always unlikely that significant intra-cellular IL-17 would be detected. I therefore performed further experiments at the much earlier time point of 6 hours. TIGR4 and Brefeldin A were administered simultaneously. This experiment was performed three times using TIGR4, on one occasion there was no convincing IL-17 expression. However, on the other two occasions IL-17 was detected in small amounts within γδ lymphocytes (figure 4-30 and figure 4-31). No IL-17 was

detected above the FMO control background within other cells examined in any experiment. I therefore concluded that early production of IL-17 within this model was likely to be originating predominantly in γδ lymphocytes.

4-7.3 Depletion of gamma delta cells with monoclonal antibody

To further explore and confirm the role of γδ lymphocytes in the early release of IL-17 following infection with TIGR4 I used a monoclonal antibody previously shown to deplete γδ lymphocytes. The Armenian hamster monoclonal antibody UC7-13D5 or matched isotype control was given by interperitoneal injection to wild type mice at a dose of 100 μg per mouse. 24 hours later, mice were infected with 10^6 cfu/mouse TIGR4 and the animals culled after 6 hours before cytokine concentrations in BALF were measured (figure 4-32). Concentrations of IL-22 in BALF were consistently low in this experiment and no valid comparison could be made between animals treated with antibody and isotype control. However, for IL-17 there was a significant reduction in IL-17 concentration in animals administered the neutralising antibody.

4-8 Discussion

In this chapter, I have characterised a small collection of pneumococcal strains and demonstrated the marked differences between different strains of pneumococci in an animal model of aspiration following intra-nasal administration of bacteria.

Several strains of pneumococcus were characterised by molecular and *in vitro* testing. This has identified the pneumococci as belonging to common serotypes all found in the UK childhood (PCV-13) and adult (PPV-23) vaccines. The capsular thickness of strains was performed by two methods and confirmed that serotype 3 is associated with a thick capsular polysaccharide with the other serotypes studied having smaller capsules of varying thickness. That the serotype 3 capsule is atypical is well known but this was emphasised by the appearance of the capsule under imaging by dextran exclusion and electron microscopy. The haemolytic activity (a surrogate for pneumolysin activity) of SRL3 (serotype 7F) was a significant outlier consistent with this strain carrying a non-haemolytic pneumolysin originally associated with serotype 1 but subsequently found in

other highly invasive serotypes including serotype 7F. Therefore, this collection of pneumococci represents a varied group that I went on to study further in more detail.

The strain initially used in animal modelling, TIGR4, has been widely used in laboratory investigation of pneumococcal disease and was the first pneumococcus to be sequenced[419]. TIGR4 was initially isolated from a young man with IPD in Norway and is known to be highly virulent following peritoneal challenge with an LD50 of around 4 cfu/mouse[420]. Following intra-nasal administration, TIGR4 is known to enter the blood and cause a high level bacteraemia with relatively modest bacterial numbers in lungs[421]. In this study, I found that bacterial numbers were often extremely low in the lung parenchyma and BALF of mice with severe systemic sepsis. To the best of my knowledge, this has not been noted before with most investigators finding bacteria present within the lungs during TIGR4 infection (for example Orihuela *et al*[422]). In my study, great care was taken to wash lungs and blood was flushed out of the vasculature prior to homogenisation and it may be that this contributed to the low bacterial numbers seen in the lungs at later time points in this model. There are also marked strain related differences between mice in models of pneumococcal disease and this is also likely to contribute to heterogeneity in observations between researchers[423]. The histological changes associated with TIGR4 infection are also relatively mild and this contributes to the impression of an organism that transits through the lungs to cause a septic illness. In the vast majority of cases, mice that would succumb to TIGR4 infection had detectable bacteraemia at 24 hours post infection and only one mouse in the study was observed to have bacteraemia and then survive a mortality study (the mouse had a single colony only of pneumococcus on the blood culture plate; it is impossible to exclude the possibility that this was a contaminant).

In marked contrast was SRL1. I selected a serotype 3 organism because I sought to find a pneumococcus that would cause localised pulmonary infection and I further selected for this phenotype by passaging it *in vivo* through mouse lung rather than peritoneum to blood. As anticipated, this organism produced a severe localised pneumonia with invasion only late in the course of disease. SRL1 is a clinical strain obtained from the blood of an elderly patient in Scotland and

since it was obtained for this study it has not been investigated in animal models previously. However, serotype 3 strains are widely used in animal models. Most cause prominent pulmonary disease with a variable degree of invasion. A66.1 and WU2 are commonly used serotype 3 strains in laboratory investigation. Both are reported to cause early bacteraemia [422] and belong to an unrelated clonal type to SRL1 (ST378, 0/7 allele matches to SRL1) [424,425]. The ST180 complex to which SRL1 belongs has been studied in a metagenomic study and in several animal models. In the metagenomic study, the ST180 complex was found to be remarkably homogenous with little evidence of recombination despite evidence that the clonal complex has existed for many years[392]. We obtained the whole genome sequence for SRL1 as part of the transcriptomic analysis outlined in chapter 8 of this thesis. This sequence was assembled against the OXC141 genome used as the reference genome in the Croucher study and there was little evidence of variation in the sequences which is in keeping with the general observation of the study (SHLMPRL was a collaborator in the Croucher study and so SRL1 may in fact have been included in the strain collection for this study). Several animal models have investigated the virulence of ST180 serotype 3 S. pneumoniae isolates. One study identified two ST180 isolates (clinical isolates from children with otitis media) and compared them with other serotype 3 isolates including WU2 [425]. All the serotype 3 isolates had similar virulence in this study but survival time was the only reported outcome measure in a disease model. In another study from the same laboratory group, significant differences were found between different ST180 strains depending on original site of isolation: ear isolates caused mucosal colonisation but not bacteraemia whereas blood isolates effectively entered the blood but were less successful at mucosal sites [426]. The differences did not appear to be due to differences in capsule expression.

Another observation regarding the two strains used in this chapter was the tendency for both to cause pleural infection with high bacterial density. Since pleural lavage involves introducing several ml of additional volume into the pleural space, the bacterial density required to produce a final concentration of 10^7 – 10^9 cfu/ml must be significantly higher. The pleural infection generated by the two strains was quite different phenotypically. TIGR4 was detectable in the pleural space within 6 hours of infection but despite a duration of pleural

infection greater than 36 hours the pleural histology showed only moderate evidence of inflammatory change. SRL1 was detectable in the pleura only in the late stages of infection but, despite the shorter duration of pleural infection, the pleural inflammatory change was severe with the lungs and other thoracic contents coated in thick pus. In section 1.4.1 of the introduction to this thesis, I hypothesised that while both high and low invasive potential serotypes have been associated with empyema there may be different pathophysiology in terms of mechanism of entry into the pleura. Given the early pleural entry of TIGR4 it seems likely that it enters the pleura by active invasion: possibly through haematogenous spread or crossing the parietal pleura. One previous study demonstrated that the highly invasive serotype 2 organism D39 could cause pleural infection and was able to migrate directly across lung mesothelial cell membranes[427]. The late entry of SRL1 and the finding of necrotic areas of lung which may involve the pleura in severely infected animals supports the hypothesis that the entry of SRL1 into the lung is due to disruption of the lung surface and parenchyma leading to spilling of the bacteria into the pleural space through fistulation. These differences are interesting future targets for research since there are little published data on the pathophysiology of empyema and these strain related differences may have implications for the management of complicated pleural effusion in humans.

The final experiments outlined in this chapter focused on identifying the cellular sources of IL-17 in murine lung during pneumococcal infection. Unfortunately, I was unable to obtain reliable IL-22 intracellular staining in mouse cells and this prevented me from exploring the source of this cytokine. Both cytokines were detectable early in the course of infection and peaked within 24 hours of infection in infection with both pneumococcal strains. I had initially set out to look for Th17 cells in the lungs of these animals but the early secretion of IL-17 in these naïve animals suggested an innate source. A wide range of cells are reported to produce IL-17 innately including innate lymphocytes, lymphoid cells and neutrophils. I initially used pharmacological stimulation of lung cells to identify the cells within the mouse lung capable of producing IL-17. In these experiments several cell types with intra-cellular IL-17 staining were found including γδ lymphocytes, $CD4^+$ lymphocytes (probably Th17 cells), $CD3^+CD4^-$ cells and $CD3^-B220^-$ cells. These cells have all been reported to produce IL-17 in

the mouse lung before. However, the ability to produce a cytokine following pharmacological simulation does not imply that the cytokine is produced by the cell *in vivo*. This is reinforced by the finding that, while IL-17 was undetectable in resting BALF, the percentage of cells with intracellular IL-17 staining was only increased by a relatively small amount after 48 hours of infection. The percentage of gamma delta cells within the lung at 48 hours post infection increased and this has been noted before [220]. The same study also demonstrated that gamma delta deficiency impairs early recruitment of neutrophils to lung – which would be consistent with these cells being a significant source of IL-17.

I went on to explore the cellular sources of IL-17 in the lung by more direct methods. The *in vivo* brefeldin assay was developed by researchers investigating early IFN-γ responses to viral infections [428] but has proved versatile in facilitating the detection of cells producing a wide range of cytokines including IL-17 from γδ lymphocytes [429] and innate lymphoid cells [430]. The initial description of the method involved intra-venous injection of brefeldin A but intra-peritoneal injection has also been reported to be effective both for cells within the peritoneum[430] and outside it[431]. Using this assay, IL-17 was found within γδ lymphocytes only with other cell types not stained. The finding was not entirely consistent with only two out of three experiments demonstrating the intracellular IL-17 staining. A disadvantage of the *in vivo* brefeldin A technique is that the intensity of fluorescent staining and the frequency of positive cells is lower than with *ex vivo* stimulation. This makes it more difficult to accurately analyse the flow cytometry data but this was carefully controlled with isotype and fluorescence minus one controls. I also reinforced the conclusions of the *in vivo* Brefeldin A assay by using a monoclonal antibody known to deplete γδ lymphocytes. Treatment with this antibody significantly reduced IL-17 concentration in BALF.

A further limitation of these studies is inherent to the generation of organ homogenates. Lungs were perfused with PBS prior to harvesting in order to minimise the number of blood leukocytes found in the homogenate. However, methods using *in vivo* labelling of blood leukocytes have demonstrated that the majority of leukocytes in a lung homogenate are actually marginated rather than interstitial[432]. Furthermore, since absolute cell numbers were not quantified, it

is not possible to distinguish between a genuine increase in cell numbers and an apparent increase caused by loss of other cells from the homogenate. There is ample evidence from BALF and histology that neutrophils are increased in infected lungs but the change in other leukocytes observed was modest and demonstrated only by one method. These results must be interpreted in the light of this.

There was a significant difference in the concentration of IL-17 found in BALF between mice after infection in the early studies (peaking at 370 pg/ml) and in the gamma delta depletion (median 18 pg/ml). The key difference between these experiments was the dose of bacteria used, since the early studies used 5 x 10^6 cfu/mouse compared to 1 x 10^6 cfu/mouse. This reduced inoculum was associated with significantly less lung inflammation and mortality in wild type animals (although they were never directly compared). It is possible that other cells begin to produce IL-17 with higher innocula but the abrogation of detectable IL-17 following administration of the anti-gamma delta TCR antibody suggests that they are the dominant source in low dose infection. The depletion of gamma delta cells was carried out only once and the quality of the depletion was not assessed by flow cytometry. It is therefore important that this experiment is repeated to ensure consistency of this observation.

Several studies have explored the cellular sources of IL-17 in pneumococcal disease. Vaccination studies have found Th17 cells responsive to vaccine components but such cells are detected by *ex vivo* stimulation[433]. In naïve mice, γδ lymphocytes have been implicated in IL-17 secretion by infection of knockout mice[351] and quantitative rt-PCR for IL-17 from sorted cells in wild type mice[221]. TCR $V\gamma4^{-/-}$ mice have impaired neutrophil recruitment early in infection which is also consistent with these cells being the major source of IL-17 in this context[220]. iNKT cells have also been implicated in early IL-17 release in a model of pneumococcal infection, although this study augmented this effect with pharmacological stimulation and the significance of this source in natural infection is not clear[224]. Therefore, this study reinforces the conclusions of other work suggesting that γδ lymphocytes are the principal source of IL-17 in early pneumococcal pulmonary disease.

It is assumed throughout that the mice used in this study are *S. pneumoniae* naïve. This is despite the animals being handled by staff likely to have intermittent nasal colonisation with *S. pneumoniae*. Animals exposed to *S. pneumoniae* in the course of experiments were always housed in a separate accommodation of the animal facility to other mice. In the studies of nasal colonisation outlined later in this thesis, no colony of *S. pneumoniae* was ever identified in the nasal wash of any mouse not intentionally exposed to the organism and *cpsA* could not be detected in nasal wash of unexposed mice (see figure 6-22). Furthermore, murine adaptive immune responses to *S. pneumoniae* have generally not been found in vaccine studies[268,354,434].

This chapter has set the scene for further study of the role of IL-17 and IL-22 in pneumococcal disease. In the next chapter, I examine the infectious models developed in this chapter using animals genetically modified to have defects in IL-17 and IL-22 signalling to clarify the importance of these cytokines in disease.

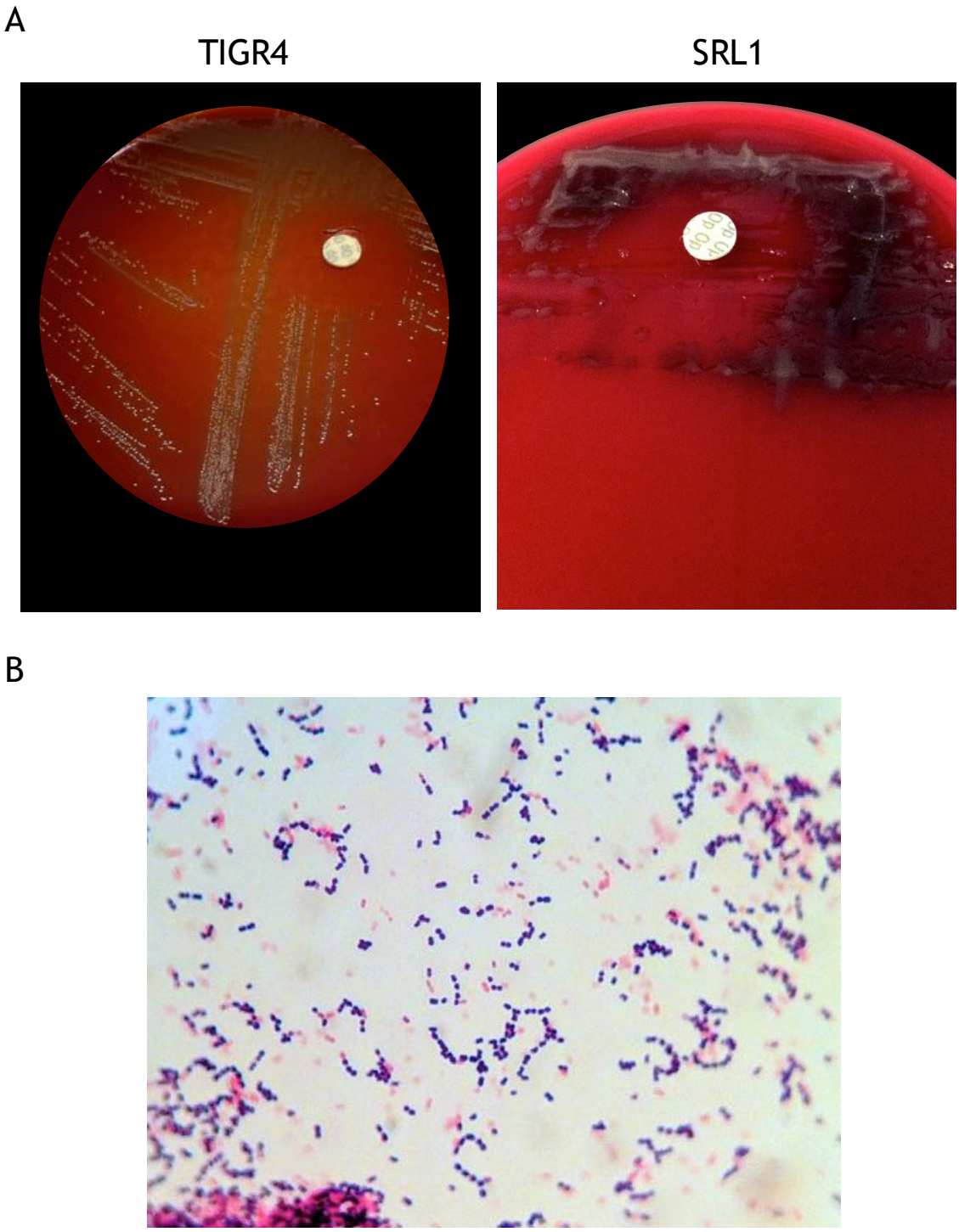

Figure 4-1. Appearance of S. pneumoniae isolates.

A. Macroscopic appearance of principal pneumococcal isolates on 5% horse blood agar plates with Optochin impregnated paper disk. Pneumococcal isolates other than SRL1 could not be distinguished from TIGR4 morphologically B. Microscopic appearance of TIGR4 isolated from blood of MF1 mouse cultured in BHI and visualised with Gram's stain.

A

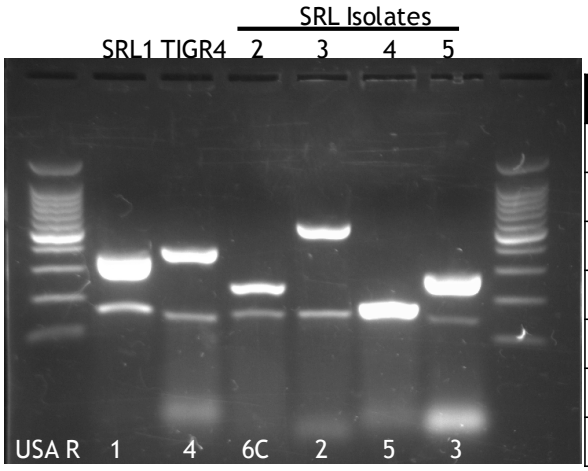

Lane	Band	Type
SRL1	371 bp	3
TIGR4	430 bp	4
SRL2	250 bp	6A/B*
SRL3	599 bp	7F
SRL4	180 bp	14
SRL5	304 bp	19F
All	160 bp	N/A¶

B

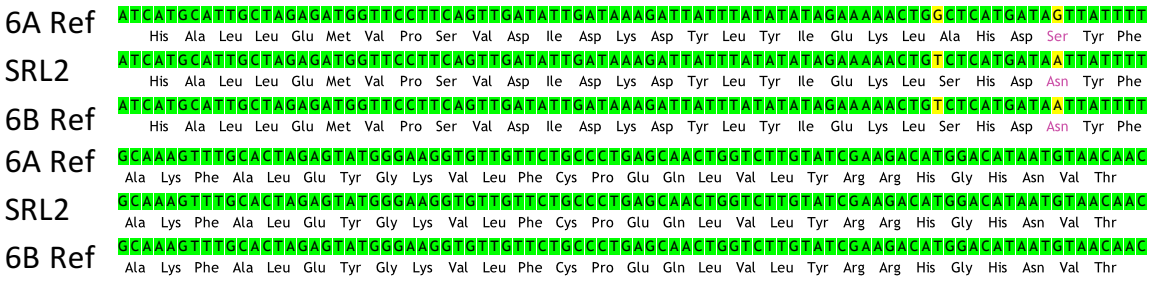

Figure 4-2. Molecular serotyping of S. pneumoniae isolates.

A. DNA from strains was subjected to multiplex PCR to distinguish between 40 different serotypes/serogroups. For ease of presentation, the reaction resulting in the serotyping band from each isolate was re-run in a single gel. The reaction number from the CDC USA multiplex scheme is shown at the bottom of the gel. Band sizes and serotypes associated with these bands are shown in the table. * 6AB cannot be distinguished based on PCR alone, the 250bp band confirms a serogroup 6 isolate while the absence of a band at 727bp implies that the isolate is 6A/B and not 6C/D. ¶ the 160 bp band in each lane is a positive control band amplified from the CPS A gene common to all typeable pneumococci. B. Sequence of the fragment obtained from the SRL2 serotyping PCR aligned against the reference sequences of serotypes 6A and 6B (Bentley et al, 2006). Variant nucleotides are shown in yellow and wciP codon 196 is shown in lilac. The presence of asparagine at this codon implies expression of serotype 6B capsular polysaccharide.

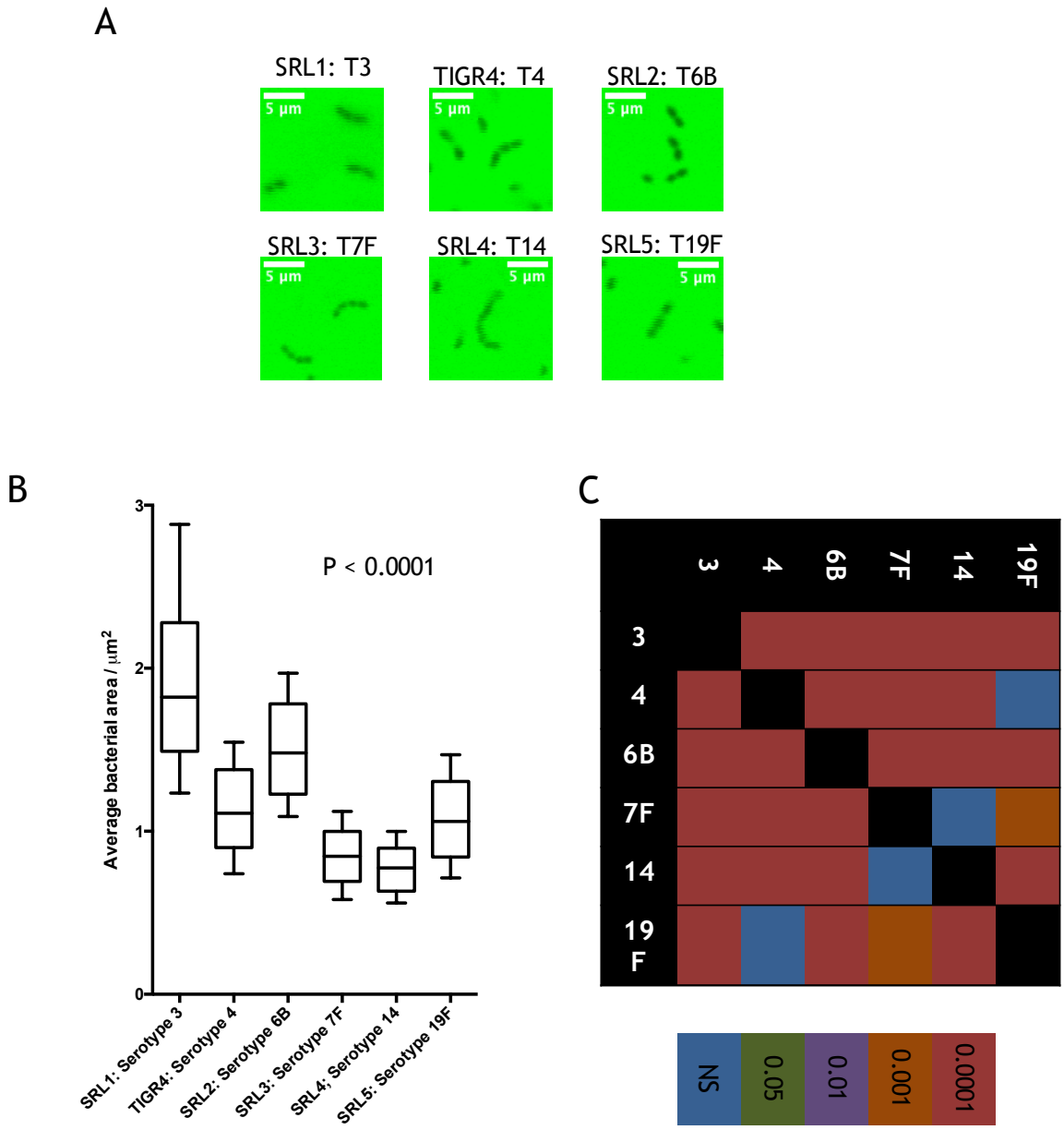

Figure 4-3. Assessment of capsular area by fluorescent dextran exclusion. Mid-log phase bacteria were washed with PBS and resuspended in an Alexa Fluor 488 dextran solution before imaging with confocal microscopy. Images were corrected according to the method outlined in section 2-2.13. A. Representative appearances of each strain. B. At least 200 particles per strain were analysed to produce summary statistics. P value represents one-way ANOVA. C. Significance tests comparing bacterial strains using Tukey's method. Significance levels are colour coded according to the legend shown beneath the table. Representative of two independent experiments.

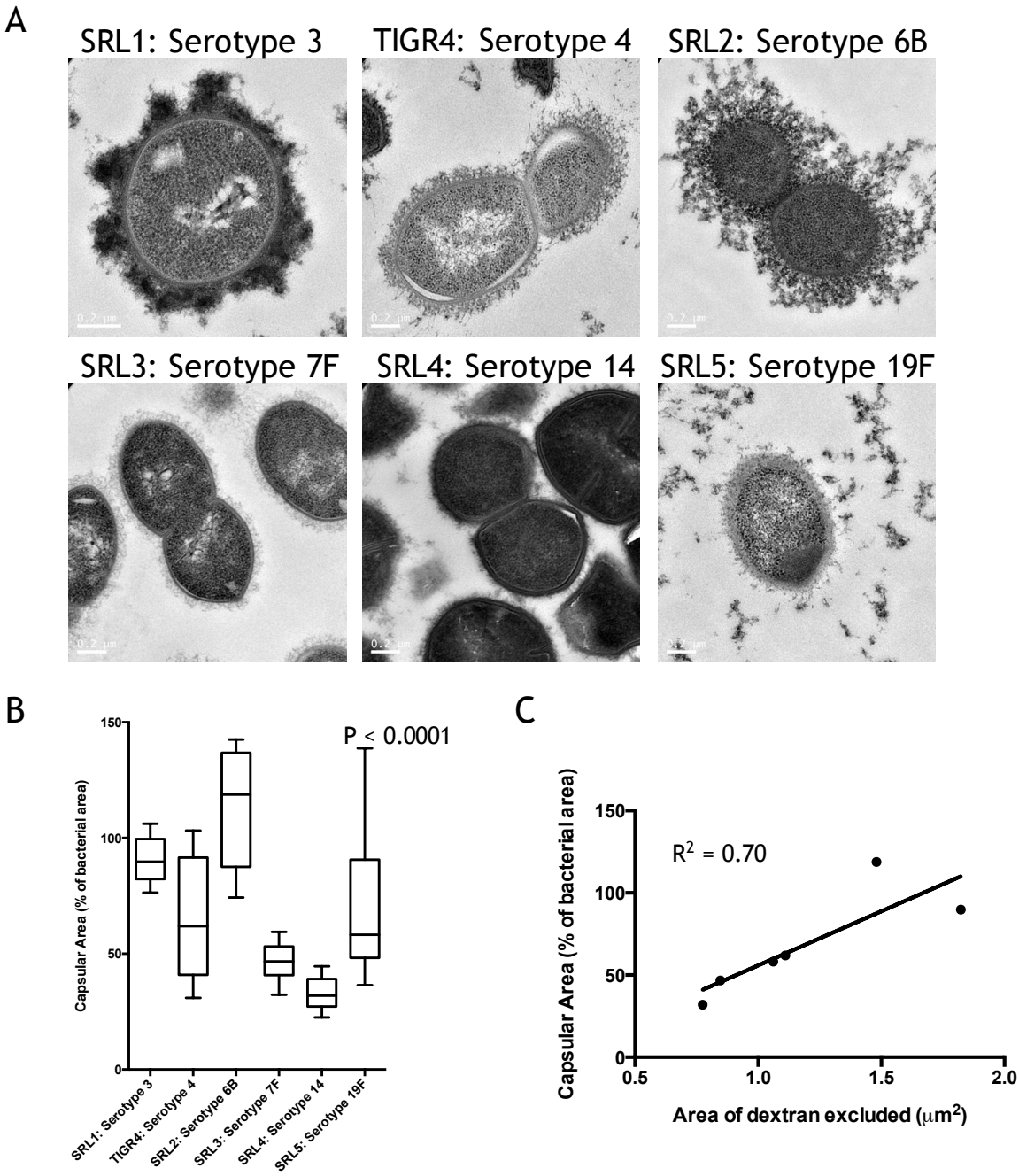

Figure 4-4. Transmission electron microscopy of pneumococcal isolates. Bacteria were fixed using lysine, ruthenium red fixation procedure. A. Respresentative images for each strain of bacteria. B. Capsular area presented as a percentage of bacterial area. P value represents one-way ANOVA. C. Correlation between capsular area and dextran exclusion area for bacterial strains. * SRL1 bacteria often lost the capsular polysaccharide during fixation. Bacteria with intact capsule were selected for capsular area measurement.

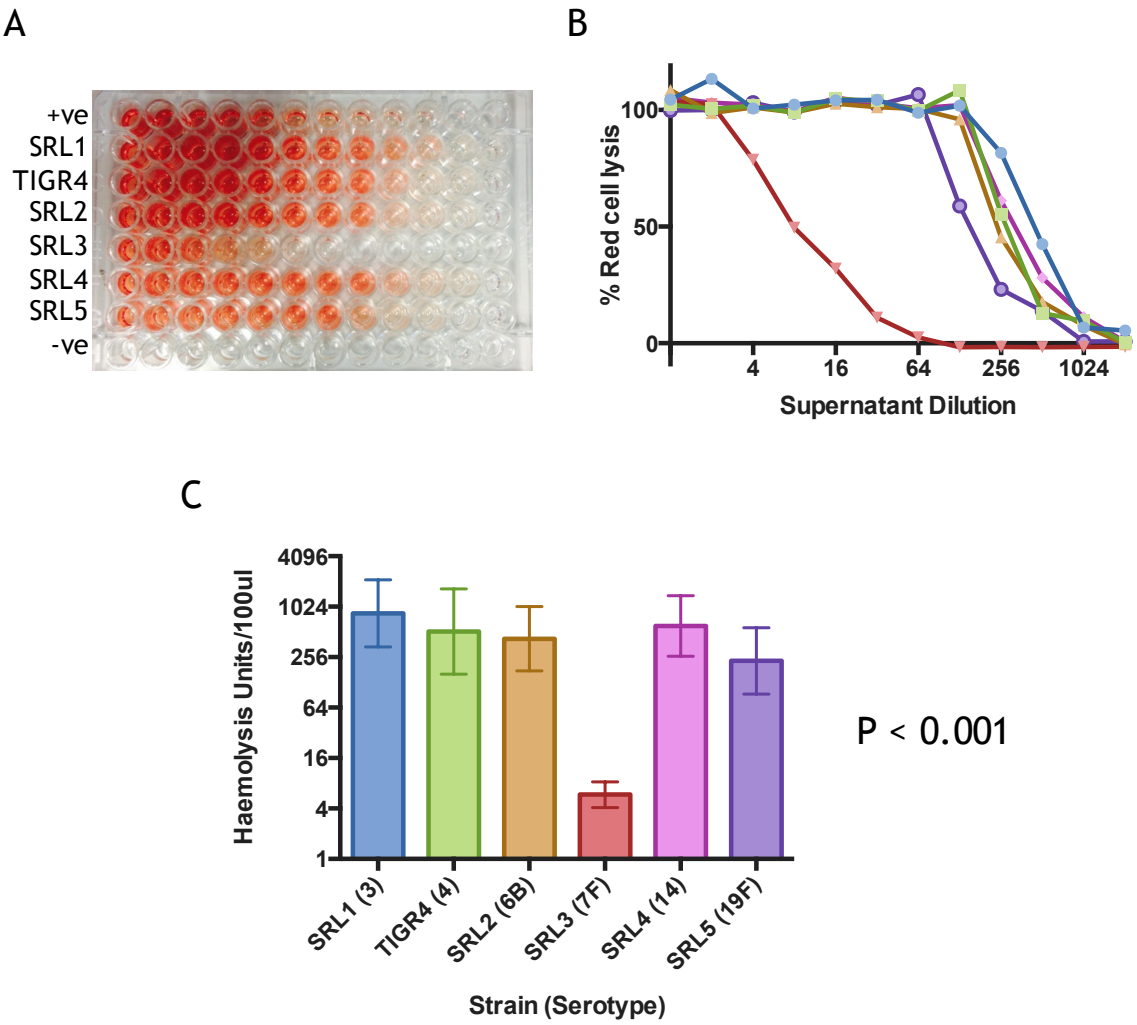

Figure 4-5. Quantification of haemolytic activity of pneumococcal clones. Bacteria were grown to mid-log phase (OD = 0.6) before lysis was induced by sonication, cleared by centrifugation and pneumolysin activated for 20 minutes with 10mM DTT. A. Lysis of 1.8% horse red cell solution was then quantified after 1 hour of incubation at 37˚C. B. dose response curves were plotted and non-linear regression performed to establish the EC50 (C). Colour scheme for the dose response curve matches that of the chart in C. Barchart shows point estimate ± 95% confidence interval for EC50. Representative of two independent experiments. P value represents two-way ANOVA.

A

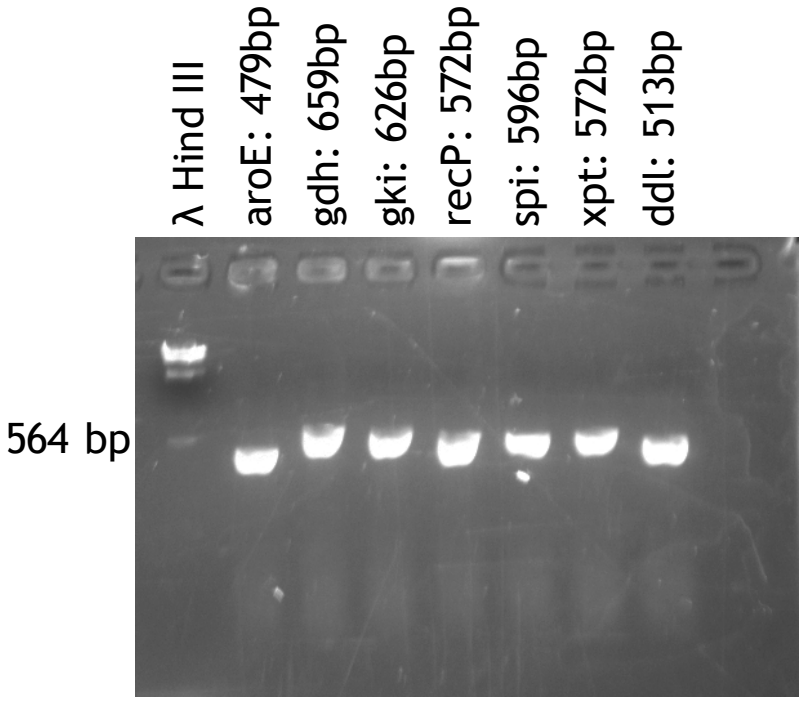

B

	Allele							
Strain	**aroE**	**gdh**	**gki**	**recP**	**Spi**	**Xpt**	**ddl**	**MLST**
TIGR4	10	5	4	5	13	10	18	205
SRL1	7	15	2	10	6	1	22	180
SRL2	7	5	8	5	10	6	14	138
SRL3	8	9	2	1	6	1	17	191
SRL4	7	5	1	8	14	11	14	124
SRL5	18	9	4	18	15	1	14	422

Figure 4-6. Deduction of multi-locus sequence type (MLST) of study bacteria. A. Representative electrophoresis gel showing PCR product of housekeeping gene products. B. Alleles identified through sequencing of PCR products and corresponding MLST.

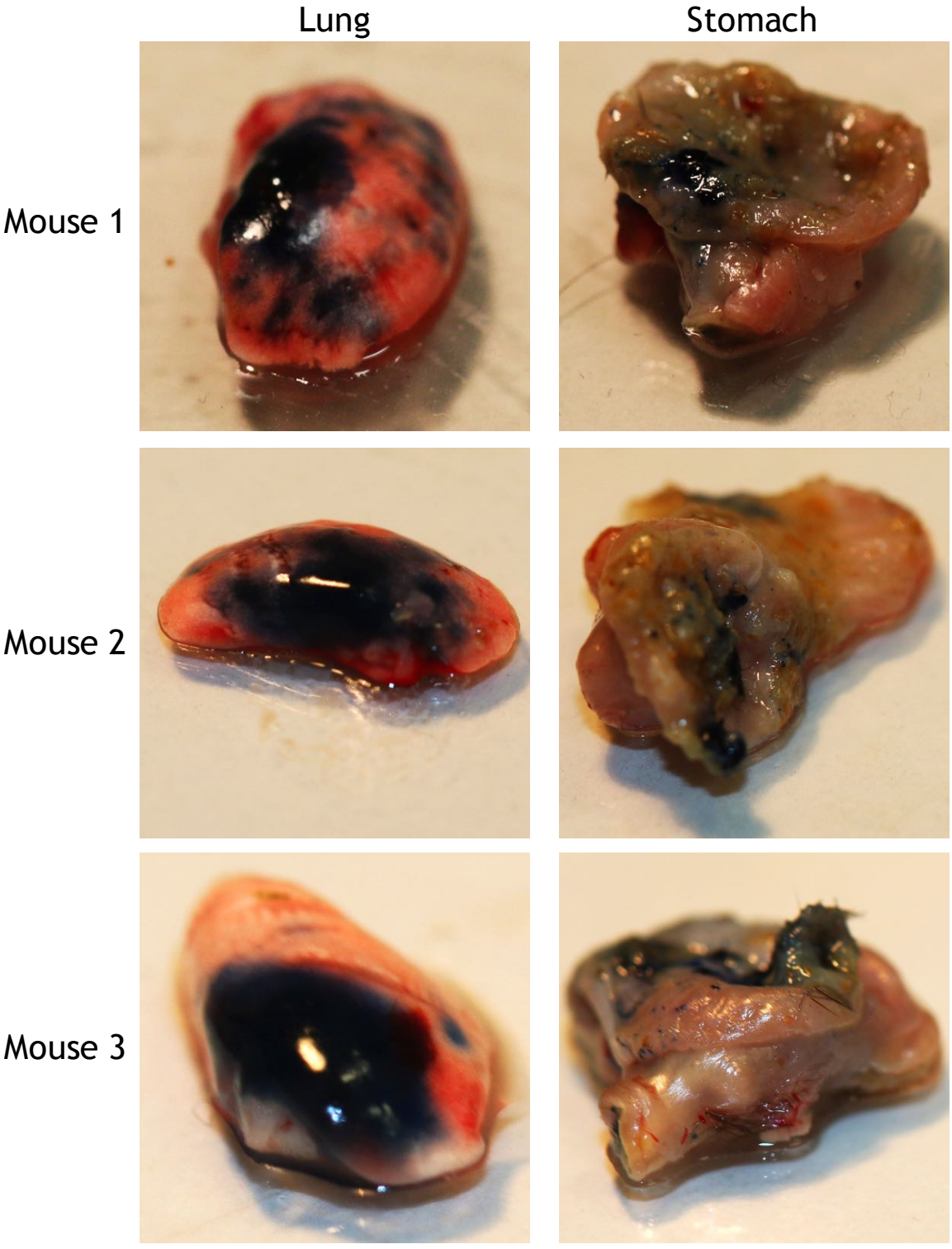

Figure 4-7. Intra-nasal innoculation.

Representative macroscopic appearance of lungs and stomachs from mice inoculated 2 hours before with 50 µl (25 µl per nostril) of 0.4% trypan blue under light gaseous anaesthesia induced with isofluorance. Lungs were dissected whole out of the thorax while the stomach was incised to reveal internal structure.

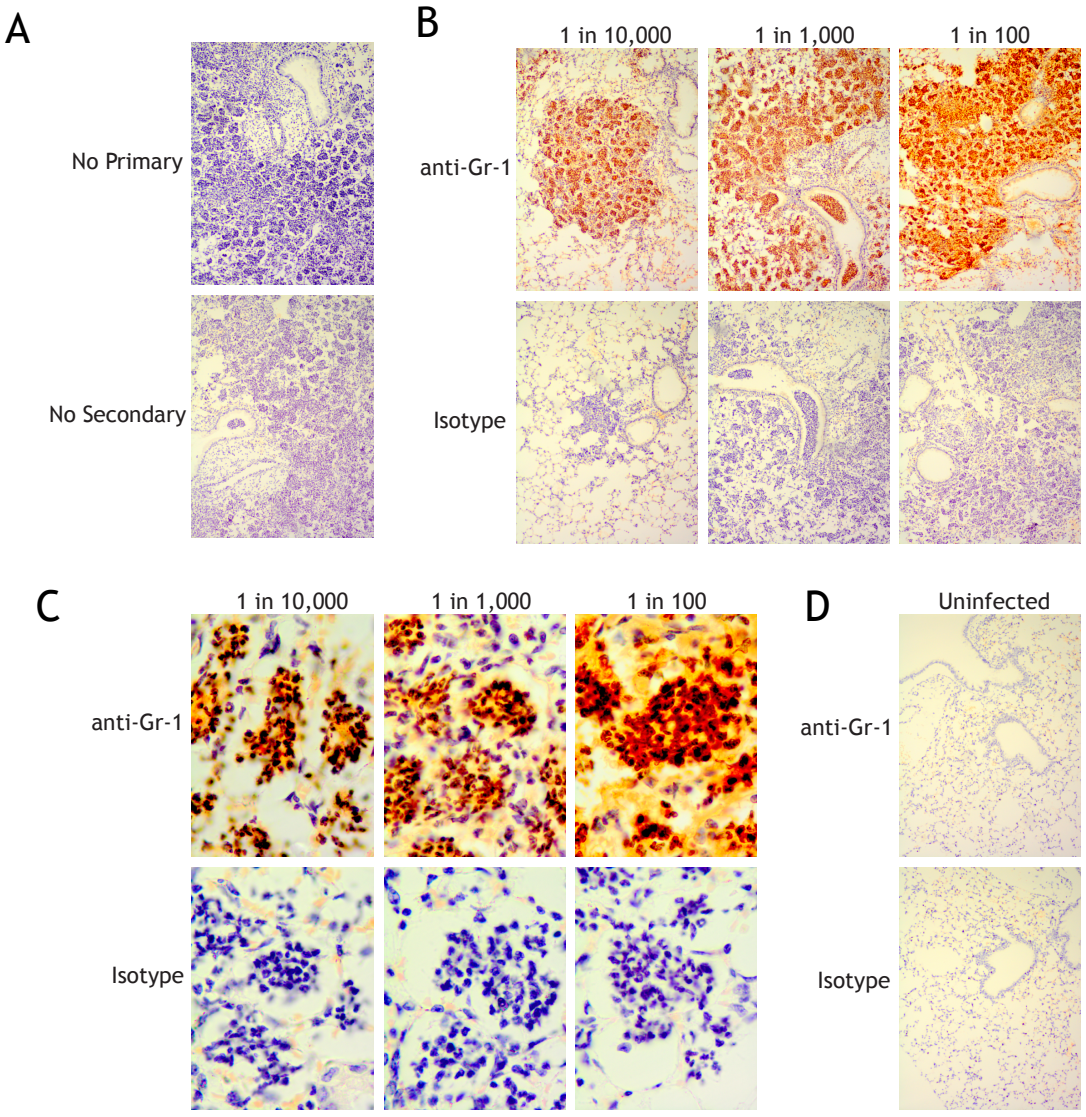

Figure 4-8. Use of anti-Ly-6G antibody (clone 1A8) for immunohistochemistry in zinc fixed lung tissue.

Lungs taken from animals infected with SRL1 for 48 hours or uninfected controls were fixed in zinc salt solution for 48 hours before processing and embedding in paraffin. Sections were prepared as described in section 2-4.10.2. Tissue sections were then incubated overnight at 4˚C with anti-Ly6G antibody or isotype control before incubation with secondary antibody, avidin biotin complex and developing with DAB. Nuclear counterstaining was performed with haematoxylin. A. No staining was observed if the primary or secondary antibodies were excluded. B and C. Staining intensity and specificity using tenfold serial dilutions of primary antibody visualised at original magnification of x10 (B) and x100 (C). D. Absence of anti-Ly6G staining in uninfected lung stained with 1:1000.

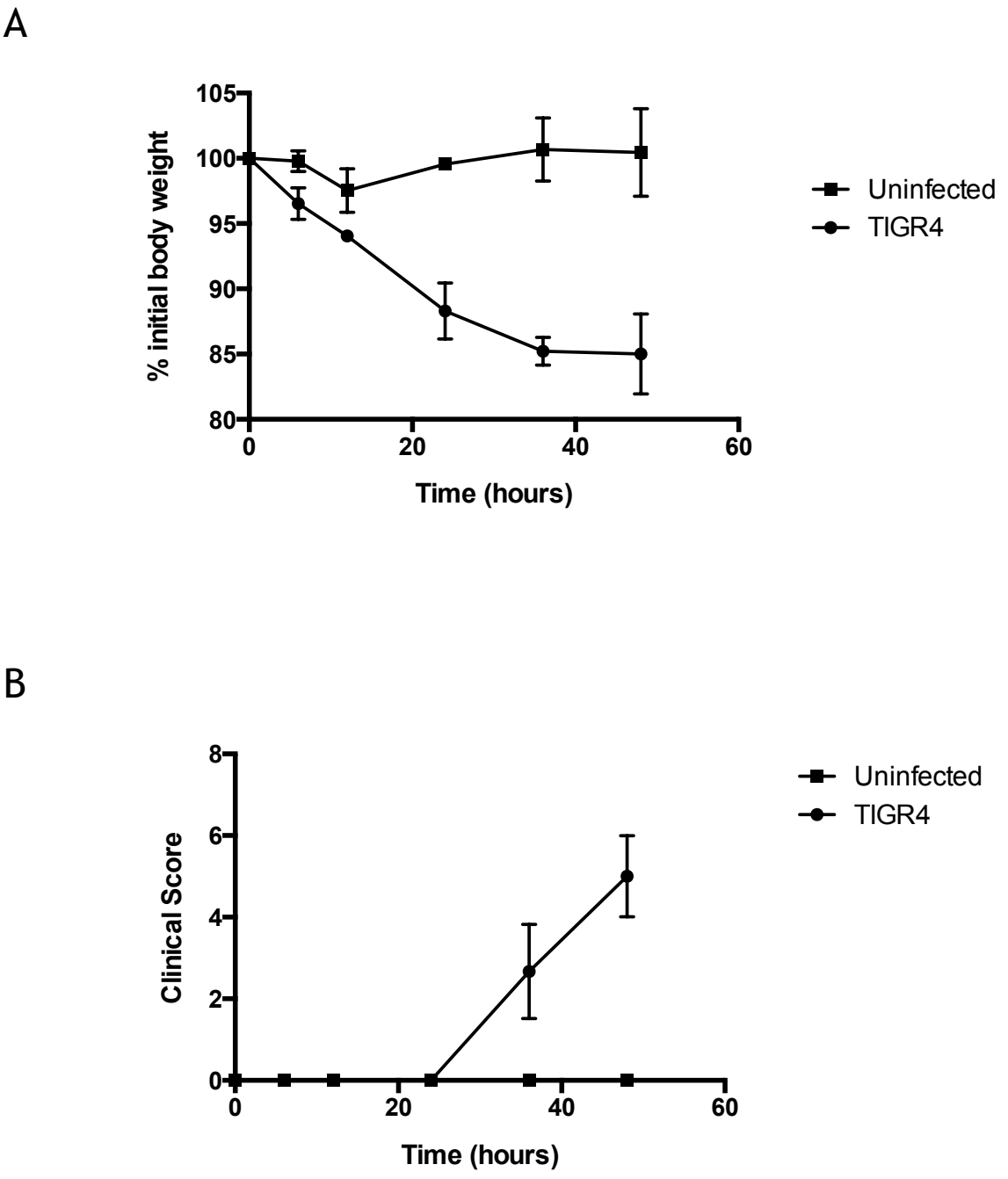

Figure 4-9. Course of infection with TIGR4: weight loss and clinical score. Mice were infected with 5 x 10^6 cfu/mouse of TIGR4 and monitored for 48 hours. Change in body weight (A) and clinical score (B) during experiment are shown. Data are presented as mean ± SEM (n = 3 females per group, representative of 2 independent experiments).

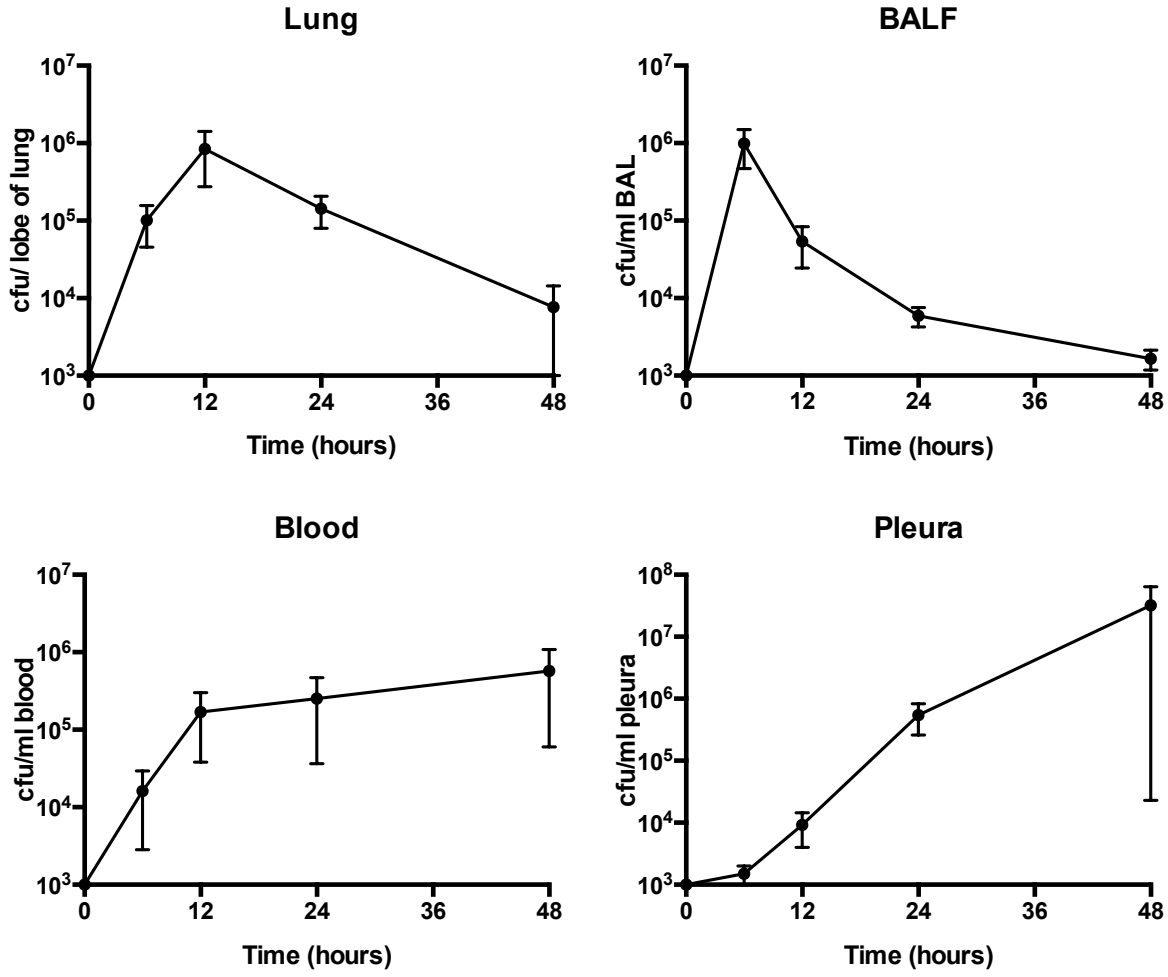

Figure 4-10. Course of infection with TIGR4: bacterial burden.
Bacterial burden following infection with 5 x 10^6 TIGR4. Animals were culled at pre-determined time points after infection and fluid (blood, BALF and pleural wash) or a lobe of lung collected and homogenised. Bacterial burden is shown as cfu/ml except for lung which is total cfu in the lobe collected. Data are presented as mean ± SEM (n = 3 females per group, representative of 2 independent experiments).

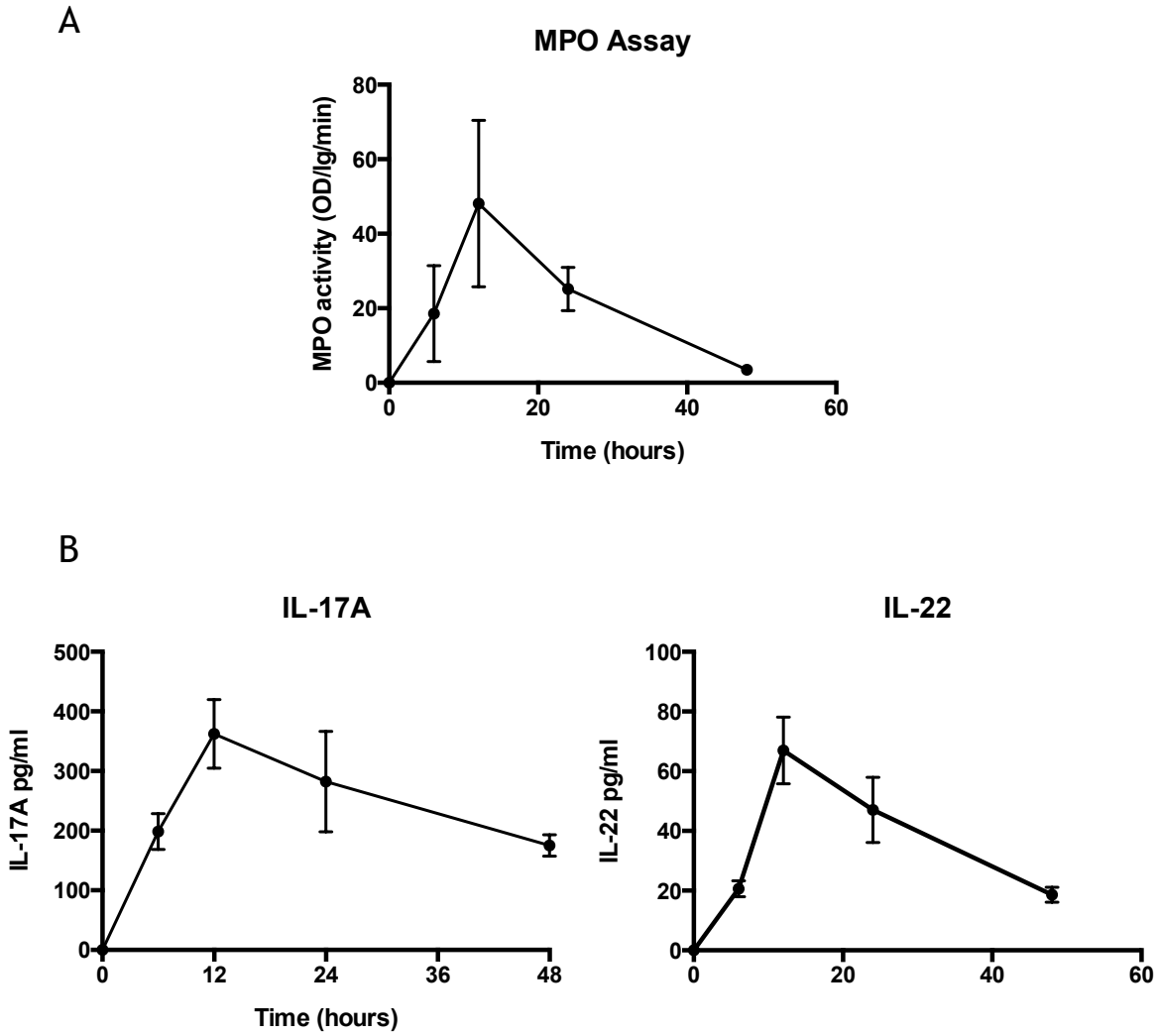

Figure 4-11. Course of infection with TIGR4: myeloperoxidase activity and BALF cytokine concentration.

Mice were infected with 5 x 10^6 cfu/mouse of TIGR4 and culled at pre-determined time points. A. A lobe of lung was taken for determination of myeloperoxidase activity and (B) BALF taken and supernatant used to determine cytokine concentration. Data are presented as mean ± SEM (n = 3 females per group, representative of 2 independent experiments).

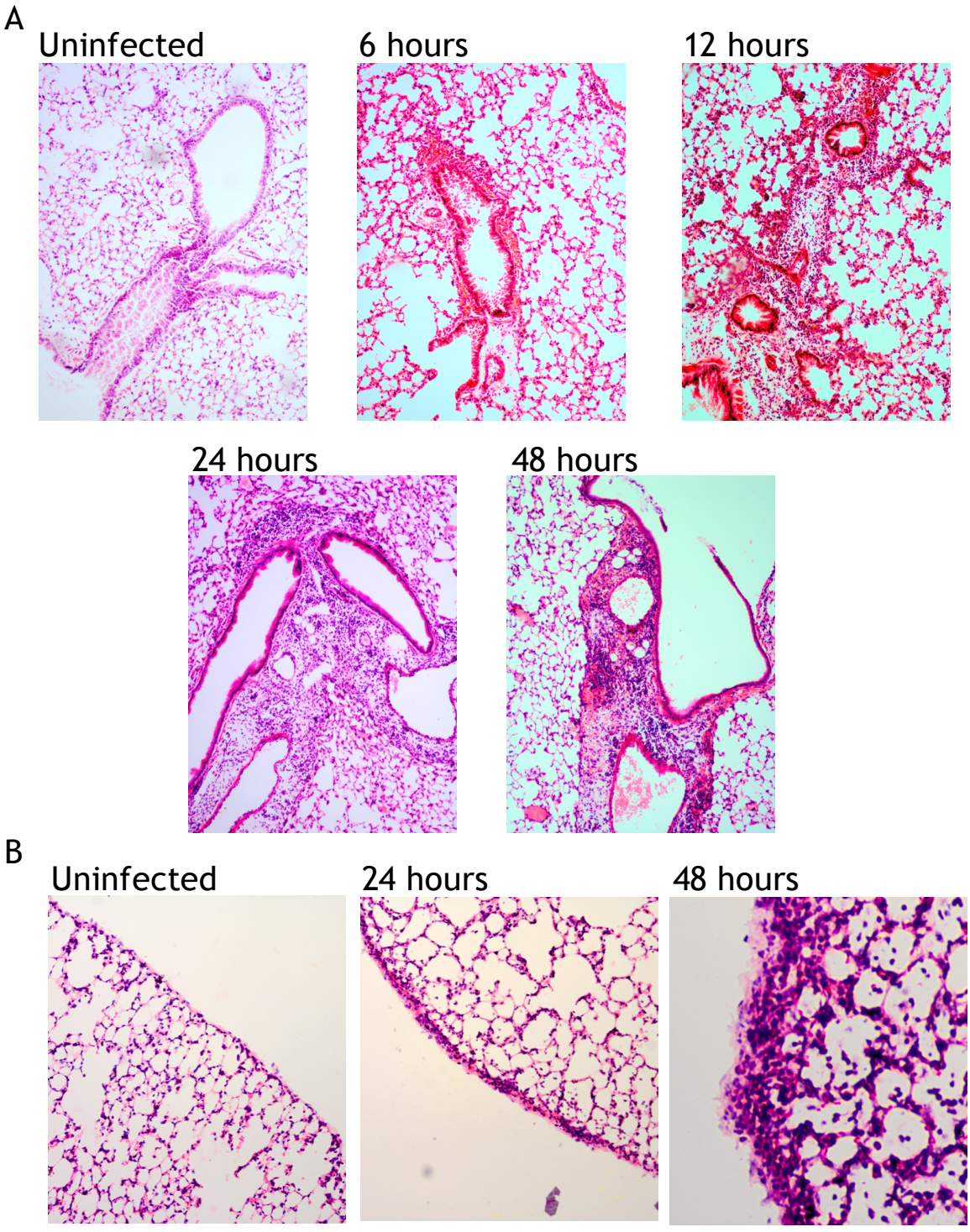

Figure 4-12. Course of infection with TIGR4: histology.

H&E staining of lung from animals infected with 5 x 10^6 cfu/mouse TIGR4. Representative sections of (A) lung prenchyma (original magnification x4) and (B) pleural surface (original mangification x10).

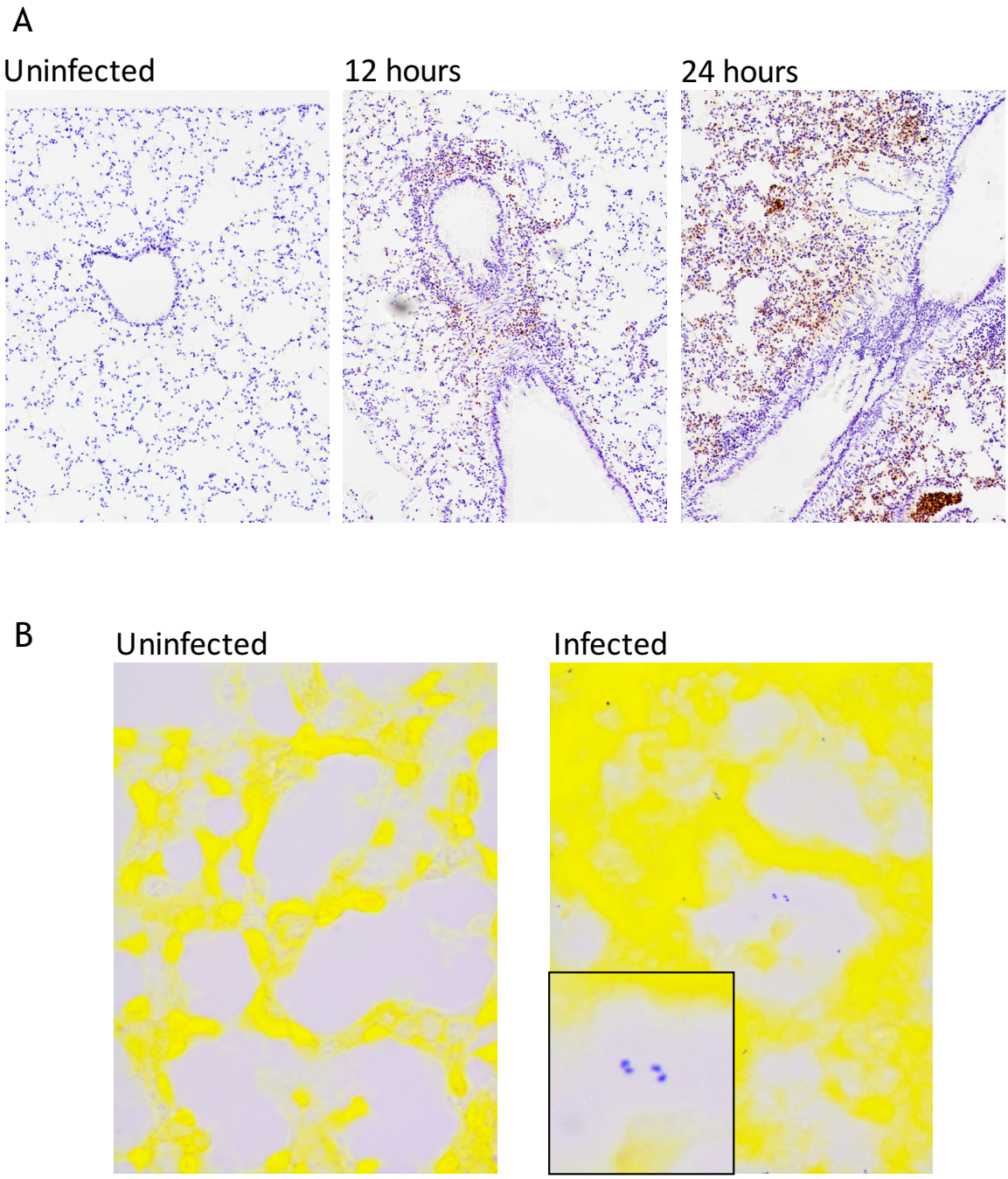

Figure 4-13. Course of infection with TIGR4: immunohistochemistry and gram stain.

Mice were infected with 5 x 106 cfu/mouse TIGR4. A. Lungs were incubated overnight at 4˚C with 500 ng/ml anti-Ly6G antibody before further incubation with goat anti-rat secondary, avidin biotin complex with HRP and DAB. B. Bacteria in infected lungs were visualised with Gram's stain and visualised at x100 under oil immersion.

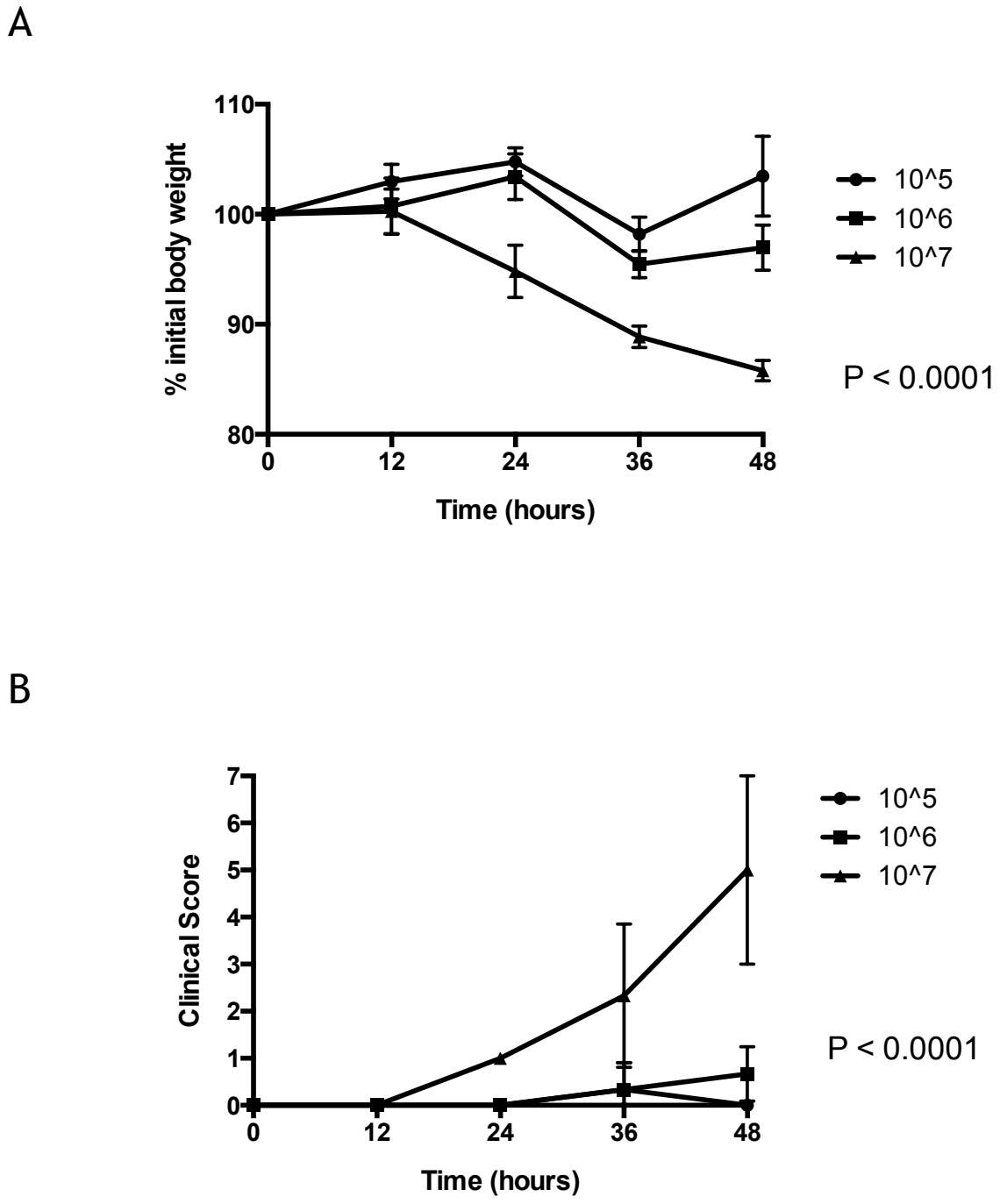

Figure 4-14. Dose titration using SRL1: weight loss and clinical score.
Mice were infected intra-nasally with increasing doses of SRL1 and monitored for 48 hours. Change in body weight (A) and clinical score (B) over course of experiment. P values represent 2-way ANOVA corrected for multiple measurements. Data are presented as mean ± SEM (n = 3 females per group).

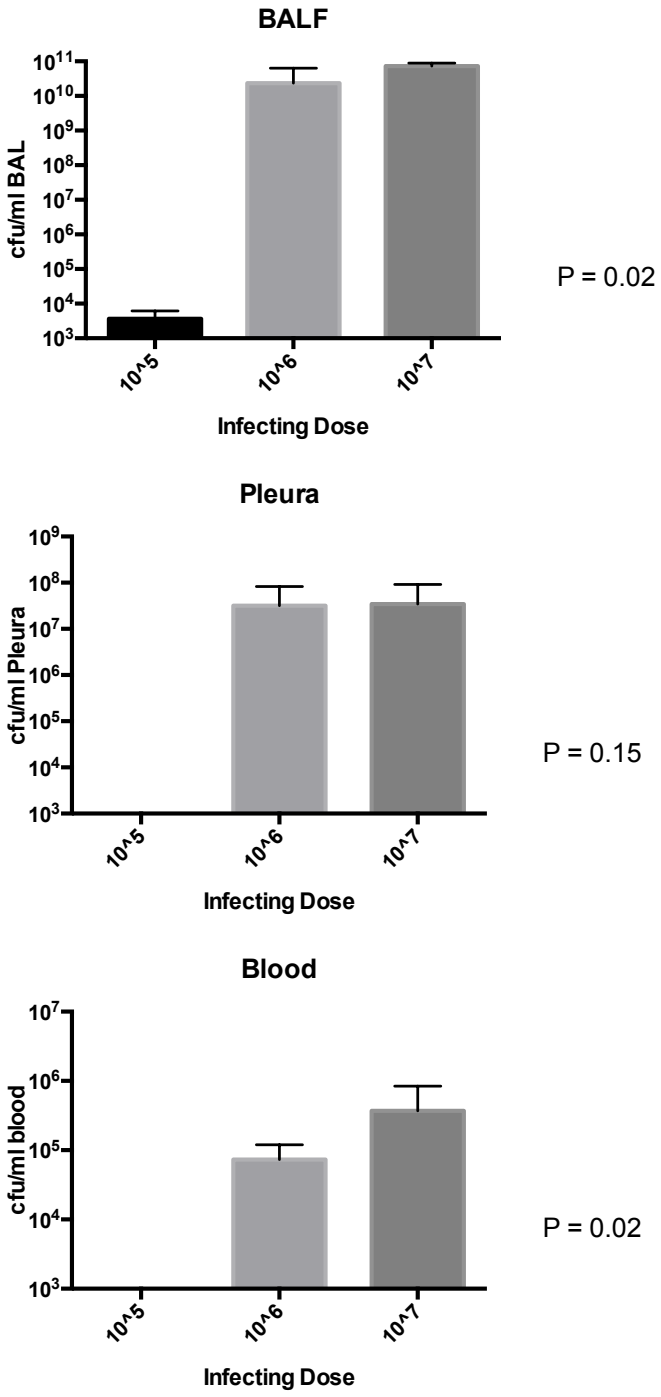

Figure 4-15. Dose titration using SRL1: bacterial burden.

Bacterial burden in BALF, pleura and blood 48 hours intra-nasal infection with increasing doses of SRL1. Limit of detection was 10^3 cfu/ml. Data are presented as mean ± SEM (n = 3 females per group). P values represent Kruskal-Wallis test.

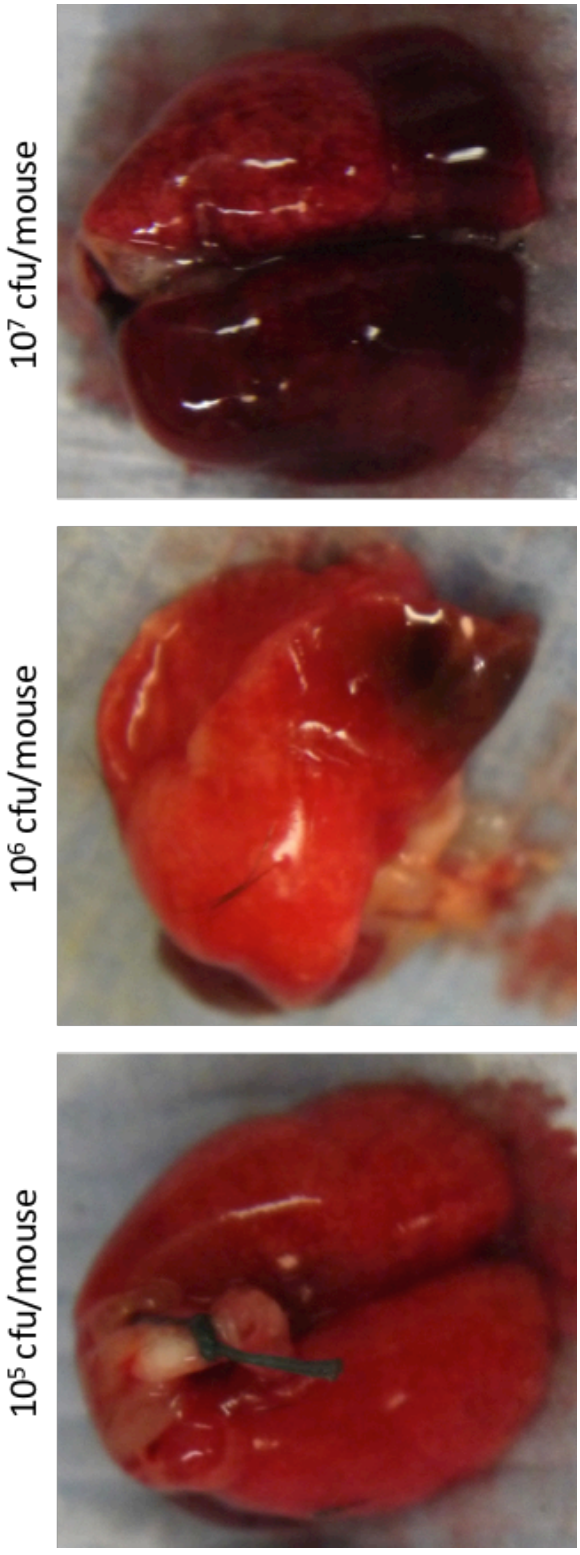

Figure 4-16. Dose titration using SRL1: gross pathology.
Gross dissection images of lungs from animals infected 48 hours previously with increasing doses of SRL1. Lungs were gently infused with PBS to obtain BALF and then infused with fixative before trachea was occluded with a stitch.

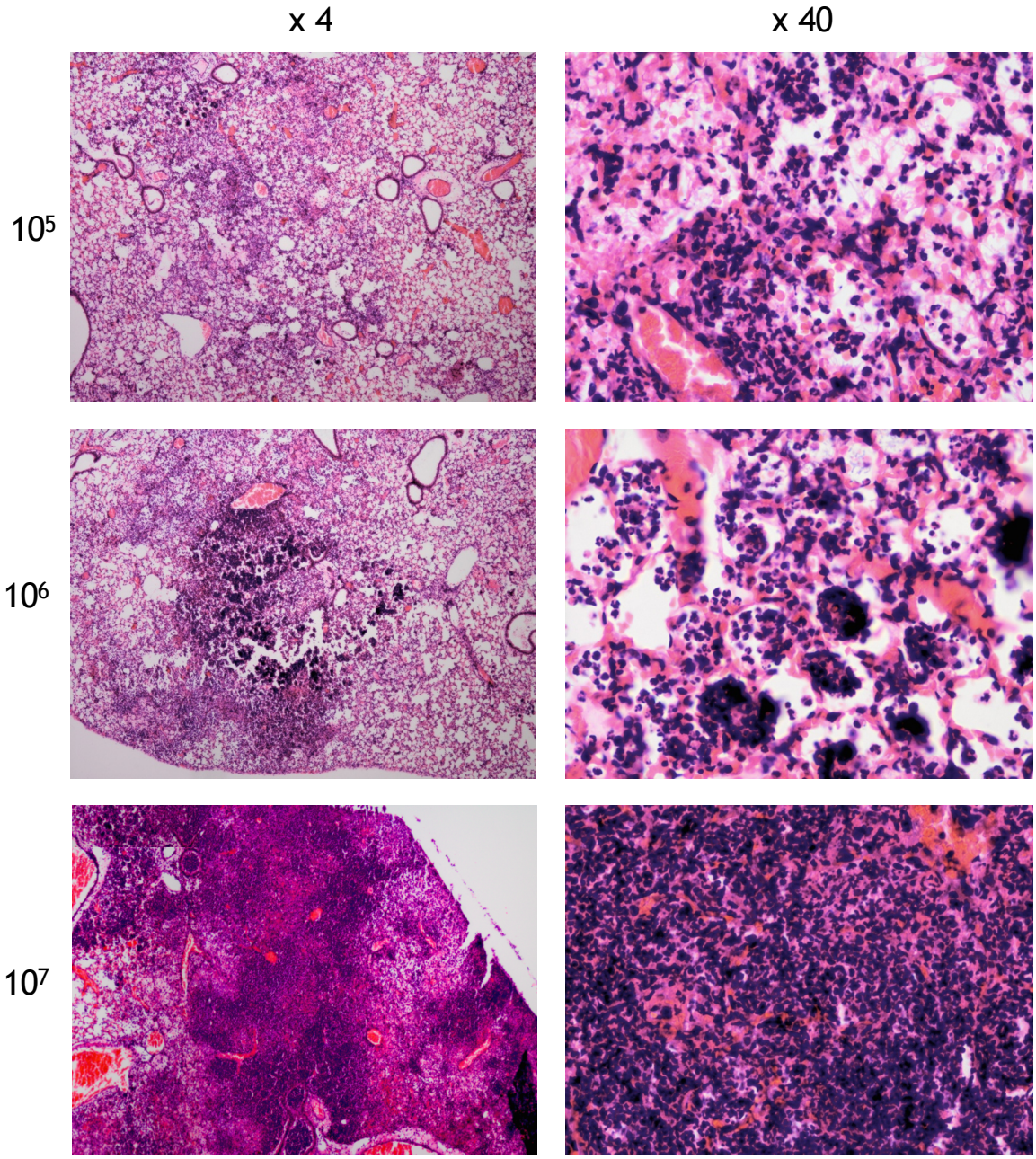

Figure 4-17. Dose titration using SRL1: histopathology.
Histological sections of lung from mice infected 48 hours before with increasing doses of SRL1 and stained with H&E. Representative areas of inflammation from each dose are shown at x 4 and x 40 original magnification.

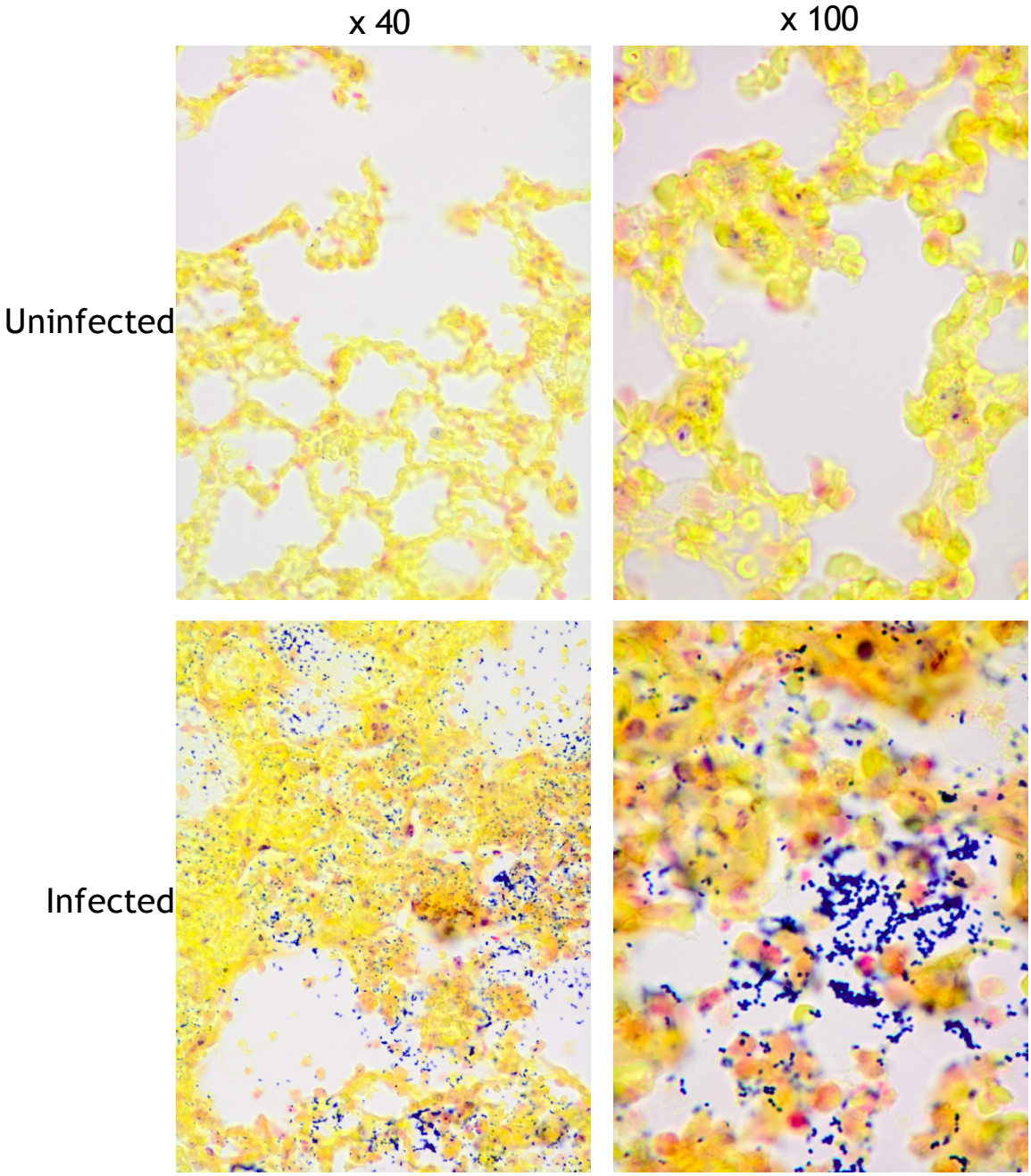

Figure 4-18. Dose titration using SRL1: gram stain.
Histological sections of lung from mice infected 48 hours before with 10^6 cfu/mouse of SRL1. Bacteria were visualised with Gram's stain and representative areas of inflammation from each dose are shown at x 40 and x 100 original magnification.

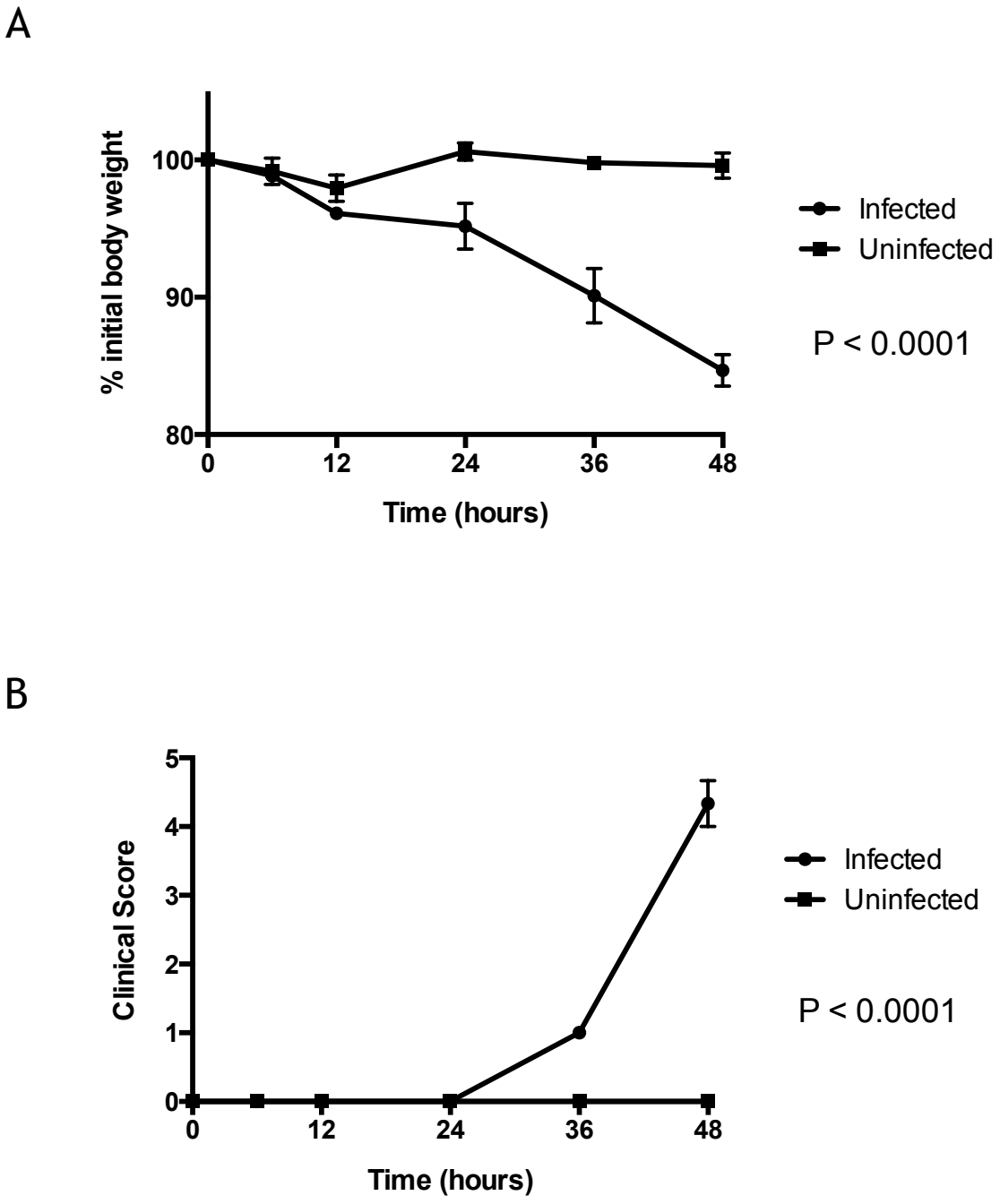

Figure 4-19. Course of infection with SRL1: weight loss and clinical score. Mice were infected with 10^6 cfu/mouse of SRL1 and monitored for 48 hours. Change in body weight (A) and clinical score (B) during experiment are shown. Data are presented as mean ± SEM (n = 3 females per group, representative of 2 independent experiments).

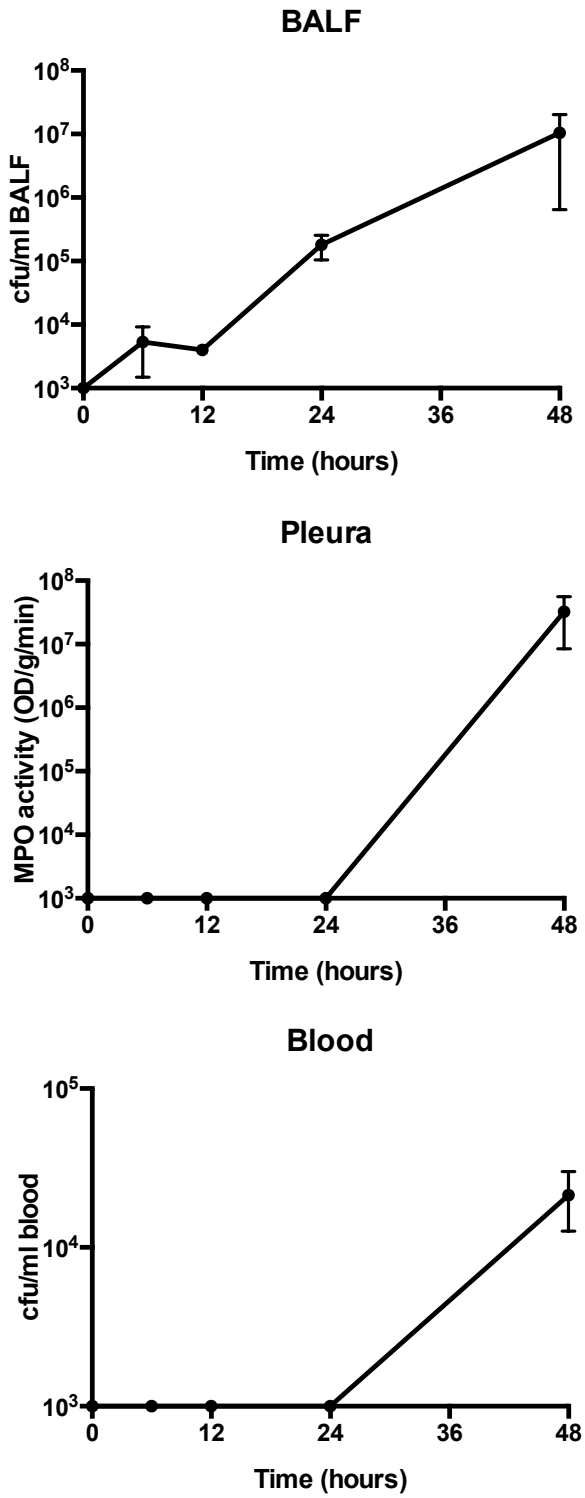

Figure 4-20. Course of infection with SRL1: bacterial burden.
Bacterial burden following infection with 10^6 SRL1. Animals were culled at pre-determined time points after infection and fluid (blood, BALF and pleural wash) cultured for pneumococci. Bacterial burden is shown as cfu/ml. Data are presented as mean ± SEM (n = 3 females per group, representative of 2 independent experiments).

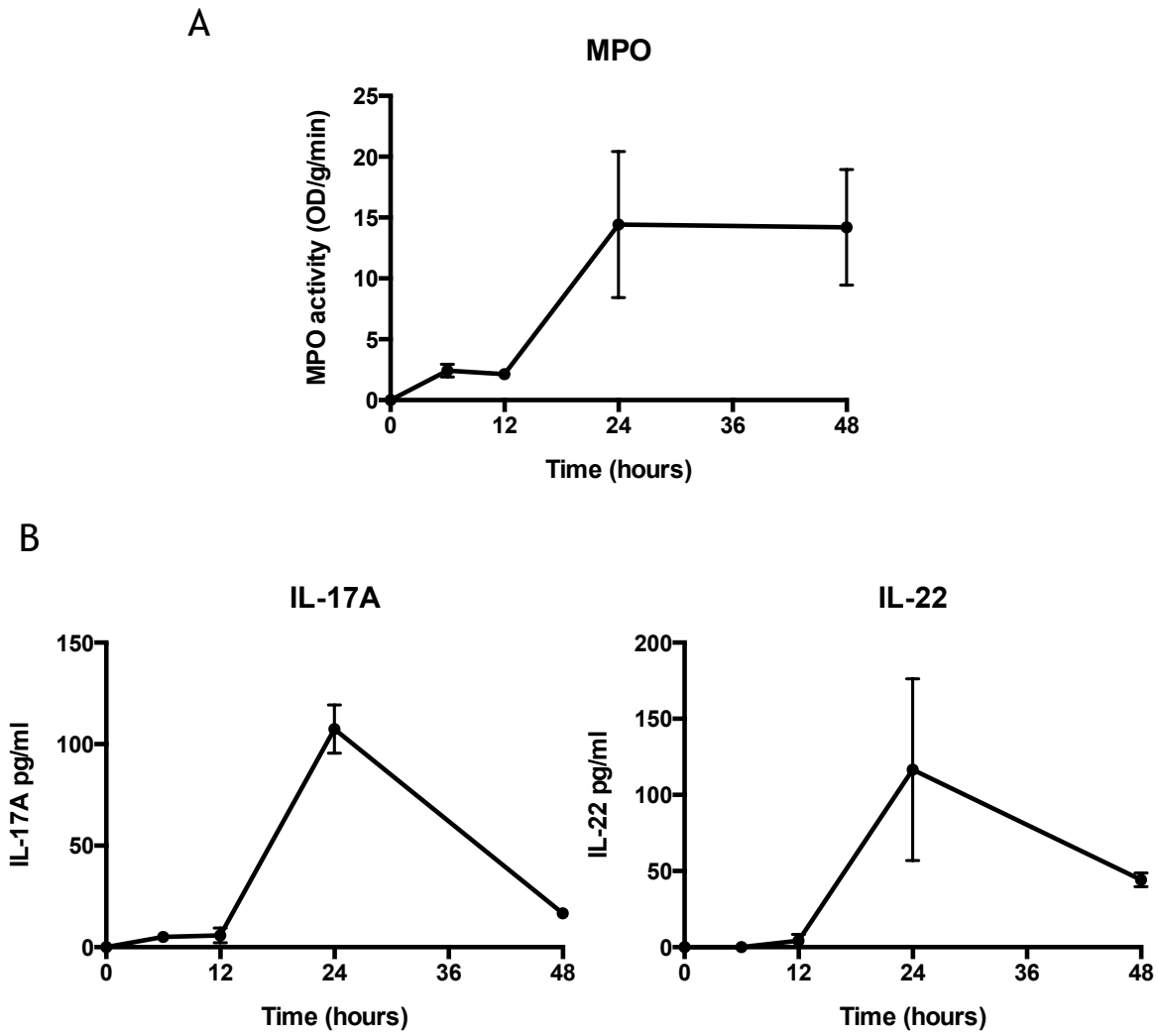

Figure 4-21. Course of infection with SRL1: myeloperoxidase activity and BALF cytokine concentration.

Mice were infected with 10^6 cfu/mouse of SRL1 and culled at pre-determined time points. A lobe of lung was taken for determination of myeloperoxidase activity (A) and BALF collected and supernatant used to determine cytokine concentration (B). Data are presented as mean ± SEM (n = 3 females per group, representative of 2 independent experiments).

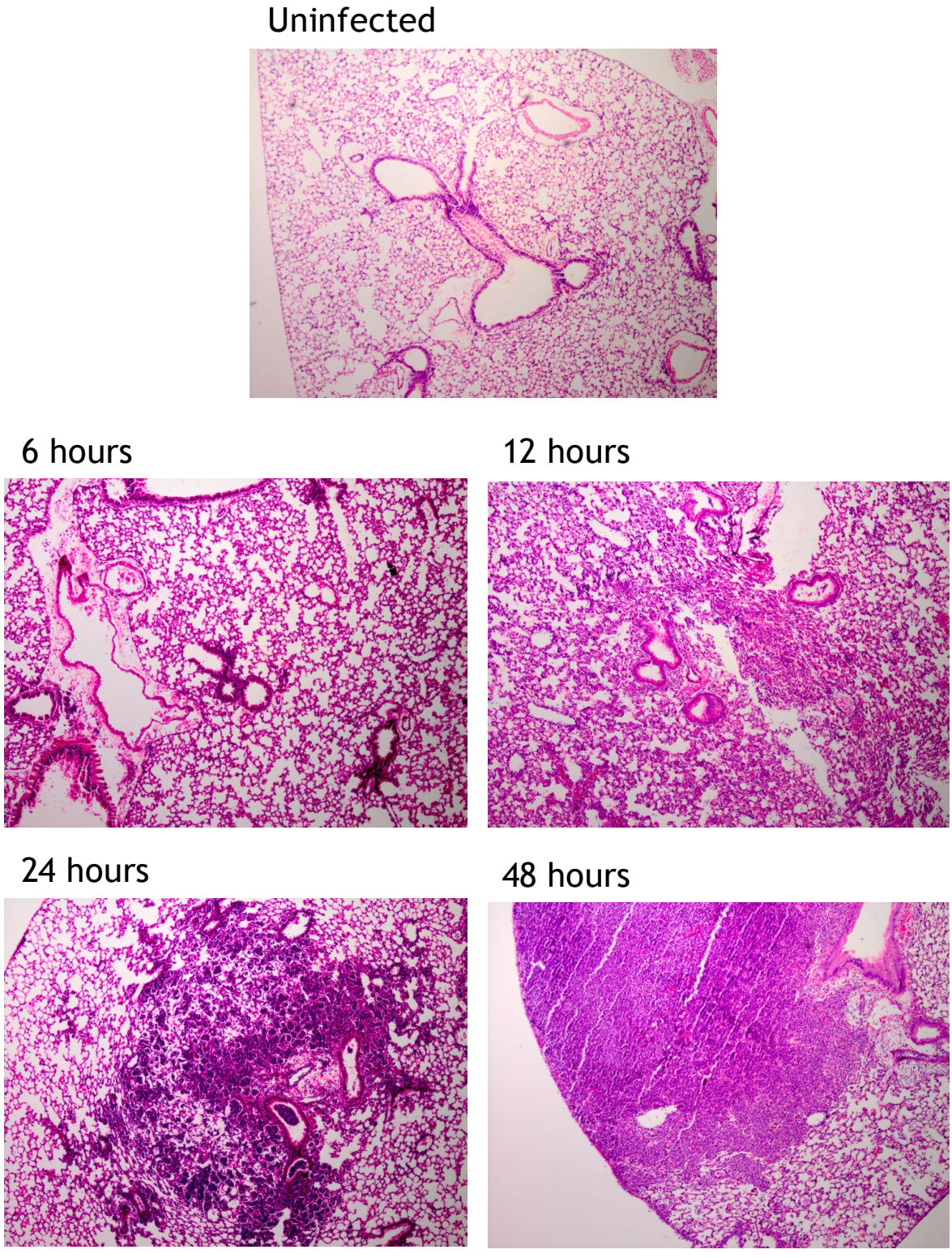

Figure 4-22. Course of infection with SRL1: histopathology of lung parenchyma.

H&E staining of lung from animals infected with 10^6 cfu/mouse SRL1. Representative sections of lung prenchyma (original magnification x4).

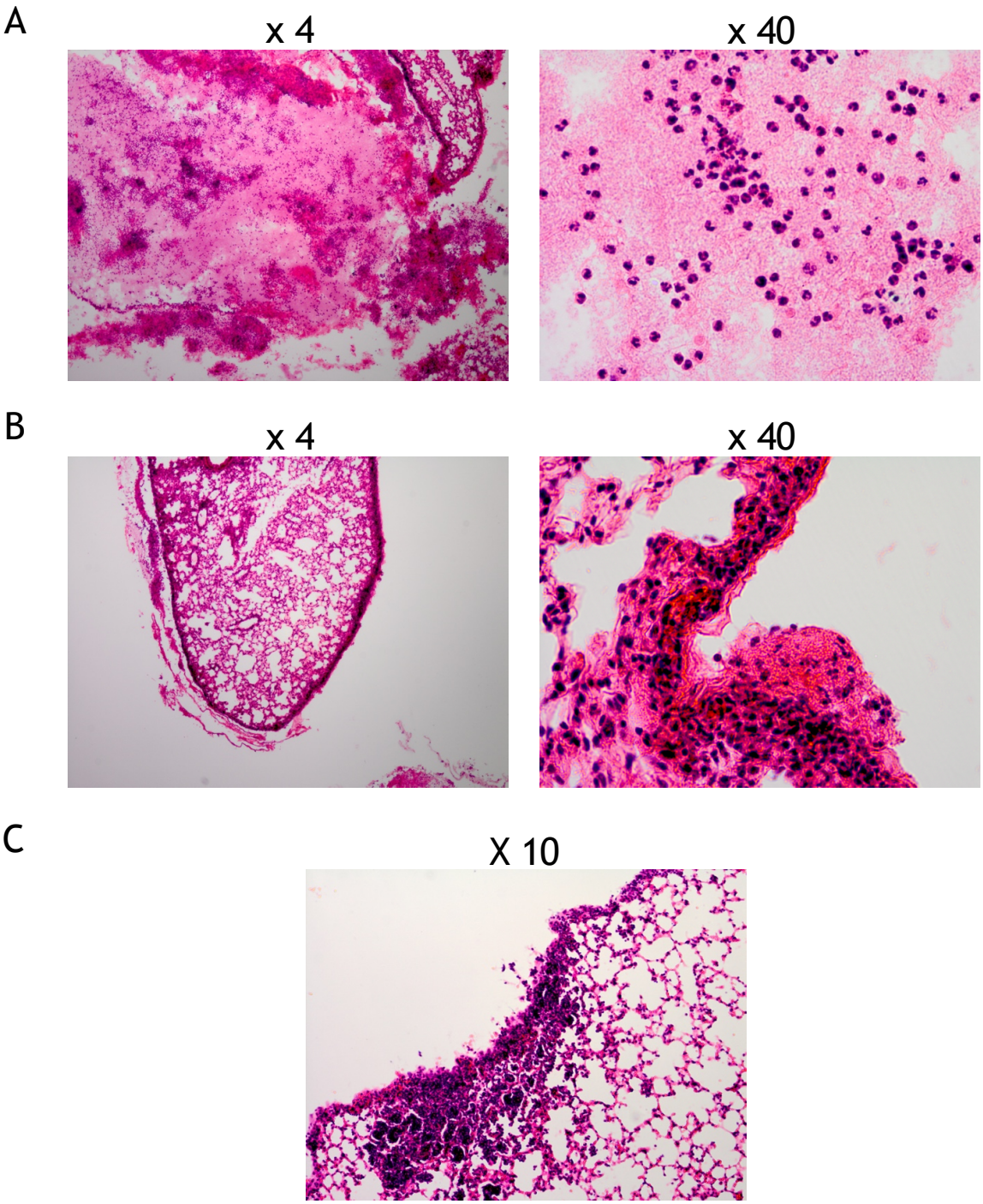

Figure 4-23. Course of infection with SRL1: histopathology of pleura.
H&E staining of lung from animals infected 48 previously with 10^6 cfu/mouse SRL1. Representative sections of (A) pleural contents, (B) pleural surface and (C) subpleural inflammation.

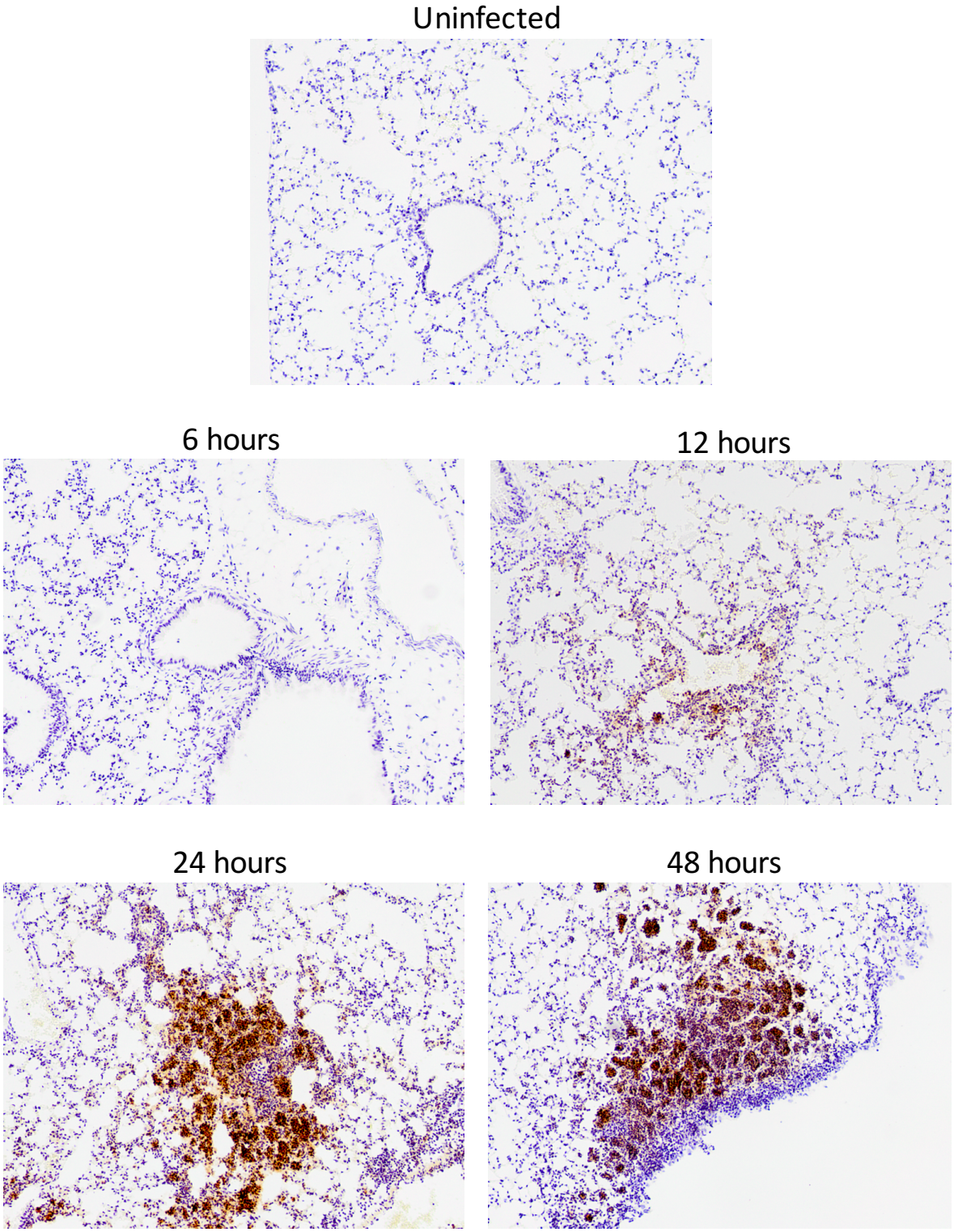

Figure 4-24. Course of infection with SRL1: immunohistochemistry.
Immunohistochemical staining of lungs from mice infected with 10^6 cfu/mouse SRL1. Lungs were incubated overnight at 4˚C with 500 ng/ml anti-Ly6G antibody before further incubation with goat anti-rat secondary, avidin biotin complex with HRP and DAB.

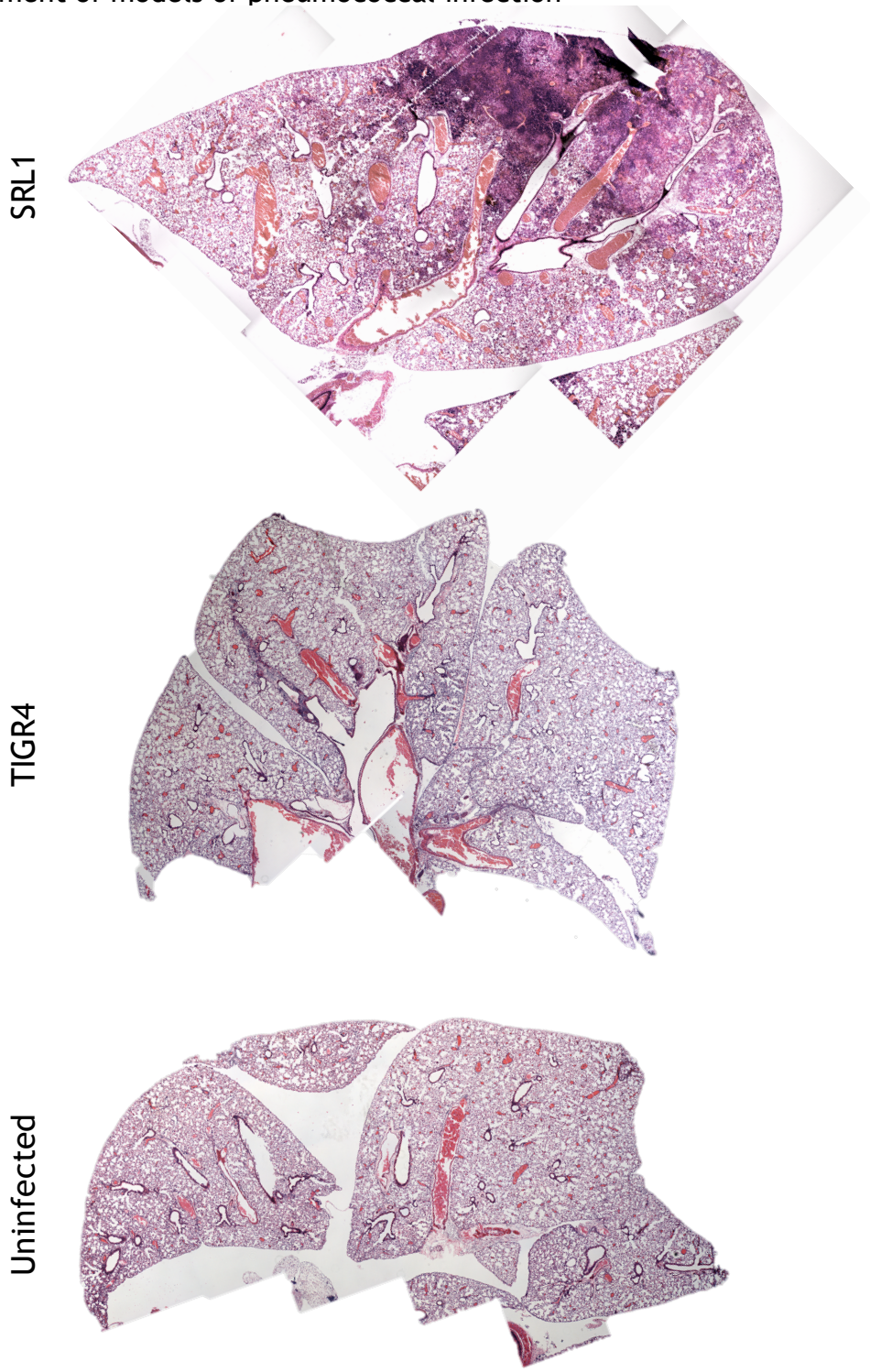

Figure 4-25. Comparison of TIGR4 and SRL1.

Whole lung sections reconstructed by stitching together multiple micrographs to produce an image of the whole lung. The mice infected with TIGR4 and SRL1 were infected with 5 x 10^6 cfu/mouse and 10^6 cfu/mouse respectively 48 hours before culling. Both animals were severely unwell at the time of the cull.

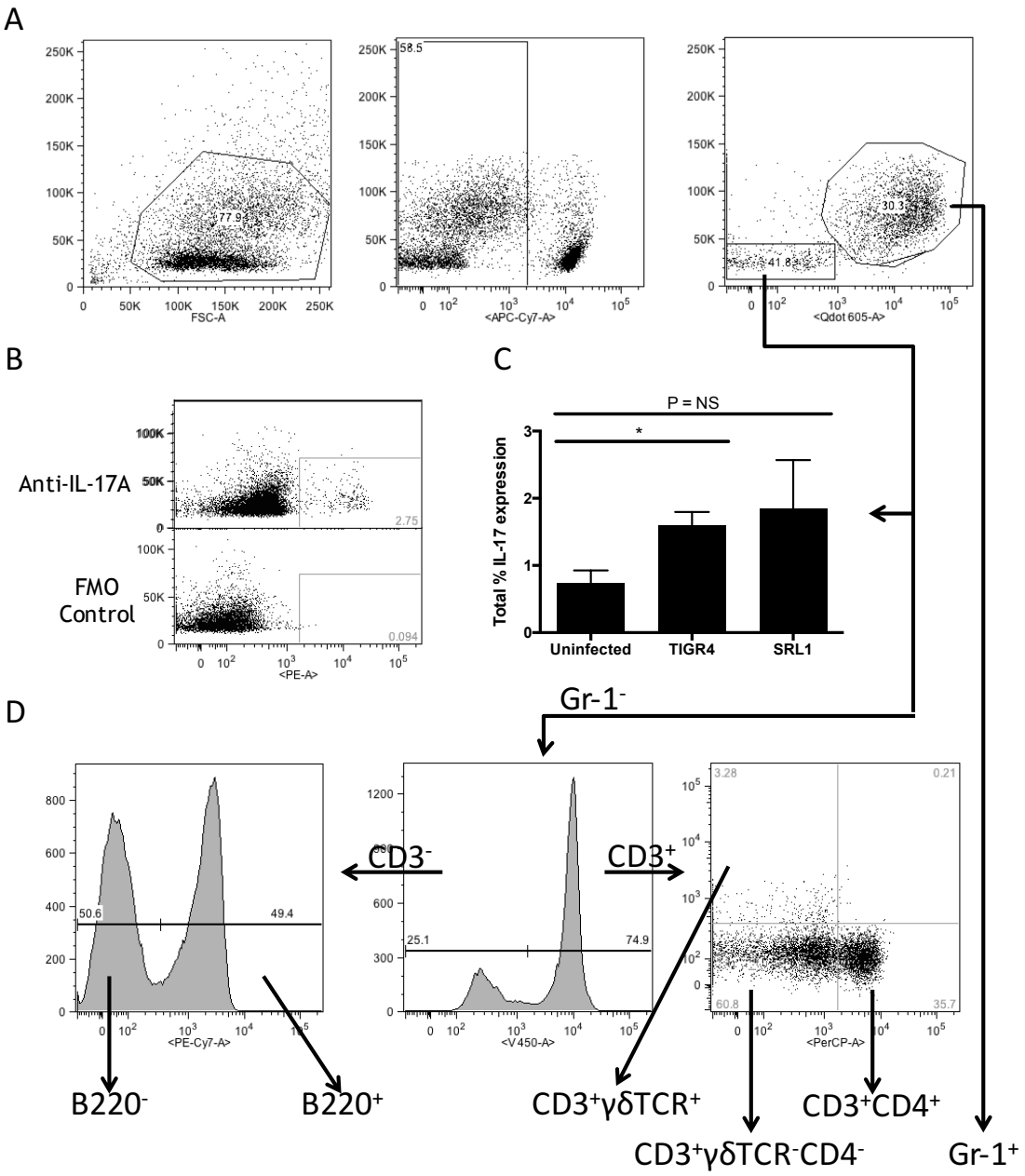

Figure 4-26. Cellular sources: gating strategy.

Gating strategy used in experiments involving the clonal stimulation of lung homogenates from animals infected with S. pneumoniae and IL-17^{+} cells found in whole Gr-$^{1-}$ subset. A. Exclusion of dead cells and Gr-1^{+} cells (neutrophils). B. Fluorescence of cells in Gr-1^{-} population with anti-IL-17A antibody or fluorescence minus one isotype control. C. IL-17A^{+} cells in Gr-1^{-} population in lung homogenates infected with SRL1, TIGR4 or PBS control. Data presented as mean ± SEM (n = 6). D. Further identification of populations of cells within Gr-1^{-} population for assessment of IL-17A expression (see next figure). * implies Student's T test $P < 0.05$.

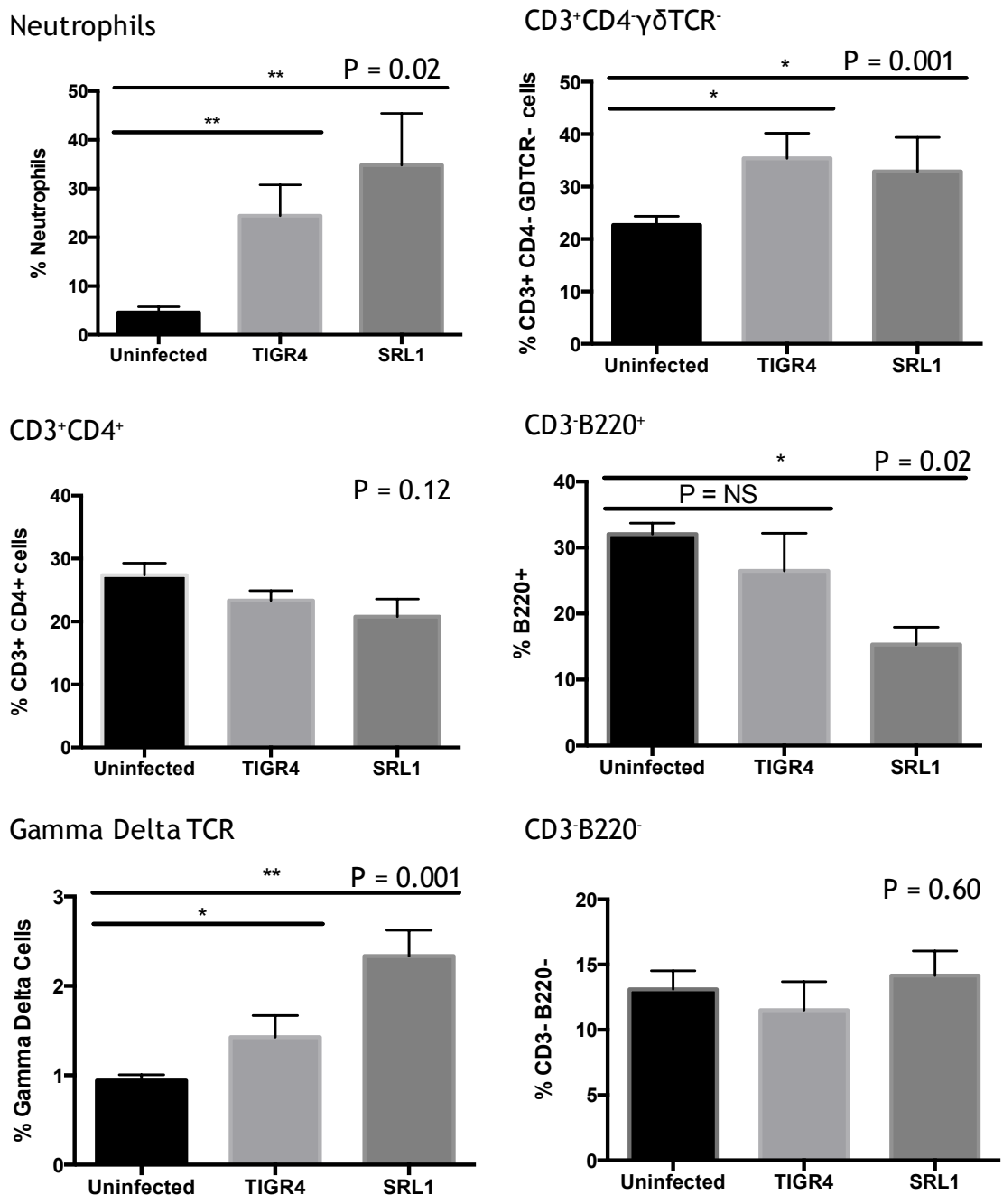

Figure 4-27. Cellular sources: cell populations.

Relative frequency of cells identified in the lung homogenate of animals infected with SRL1, TIGR4 or PBS control 48 hours before. Neutrophils are presented as a percentage of the total live cells while others are presented as the percentage of total live cells after the subtraction of the neutrophil fraction. P value represents one-way ANOVA, where the P value is < 0.05 there was subsequent significance testing of each infection condition with the uninfected mice. Data are presented as mean ± SEM (n = 6 females per group).

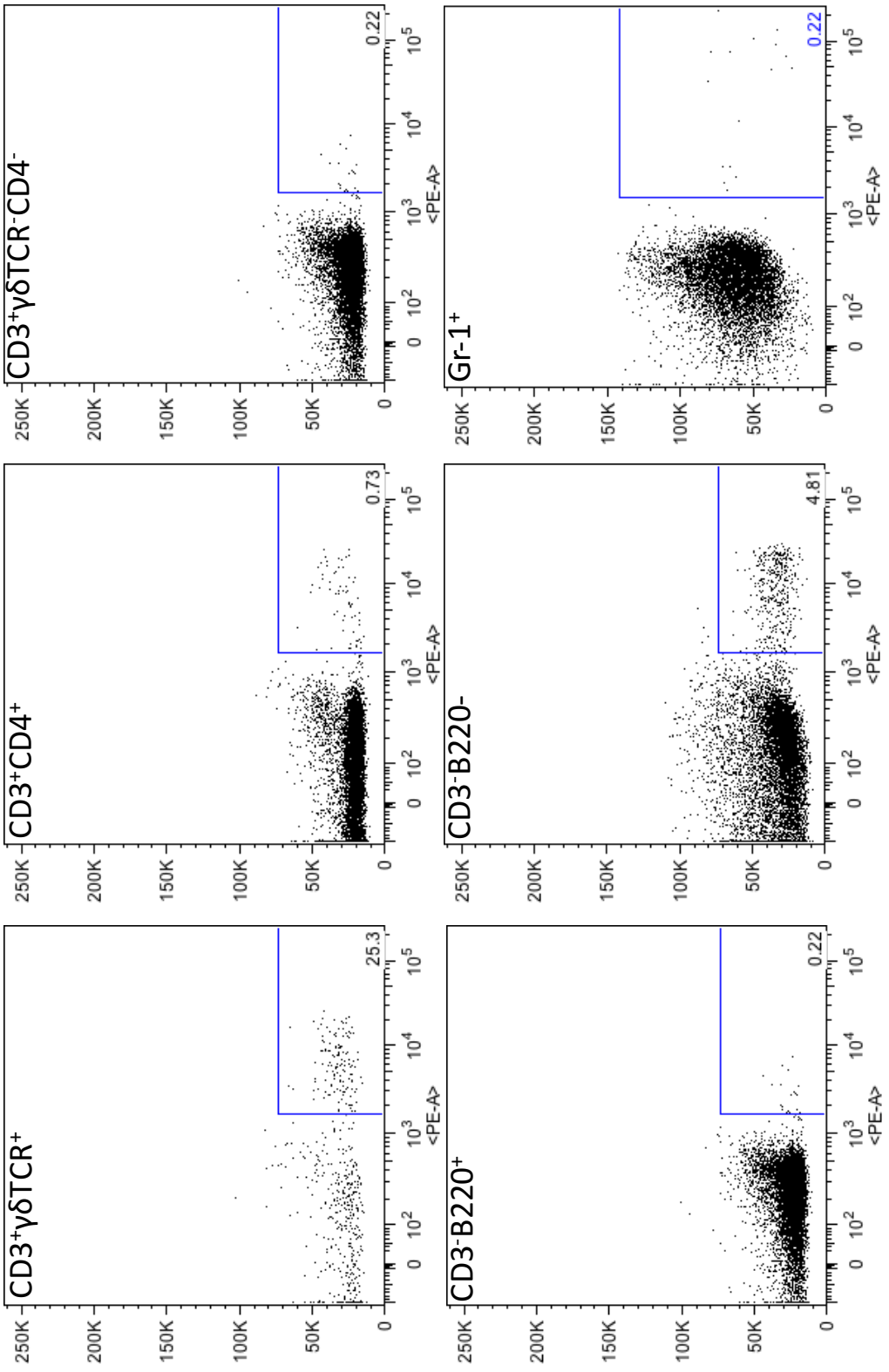

Figure 4-28. Cellular sources: intracellular staining.

Representative plots showing intracellular staining for IL-17 in lung homogenates following stimulation with PMA and ionomycin in the presence of Brefeldin A. Cells are gated as shown in figure 4-26 and IL-17 staining is identified using fluorescence minus one controls.

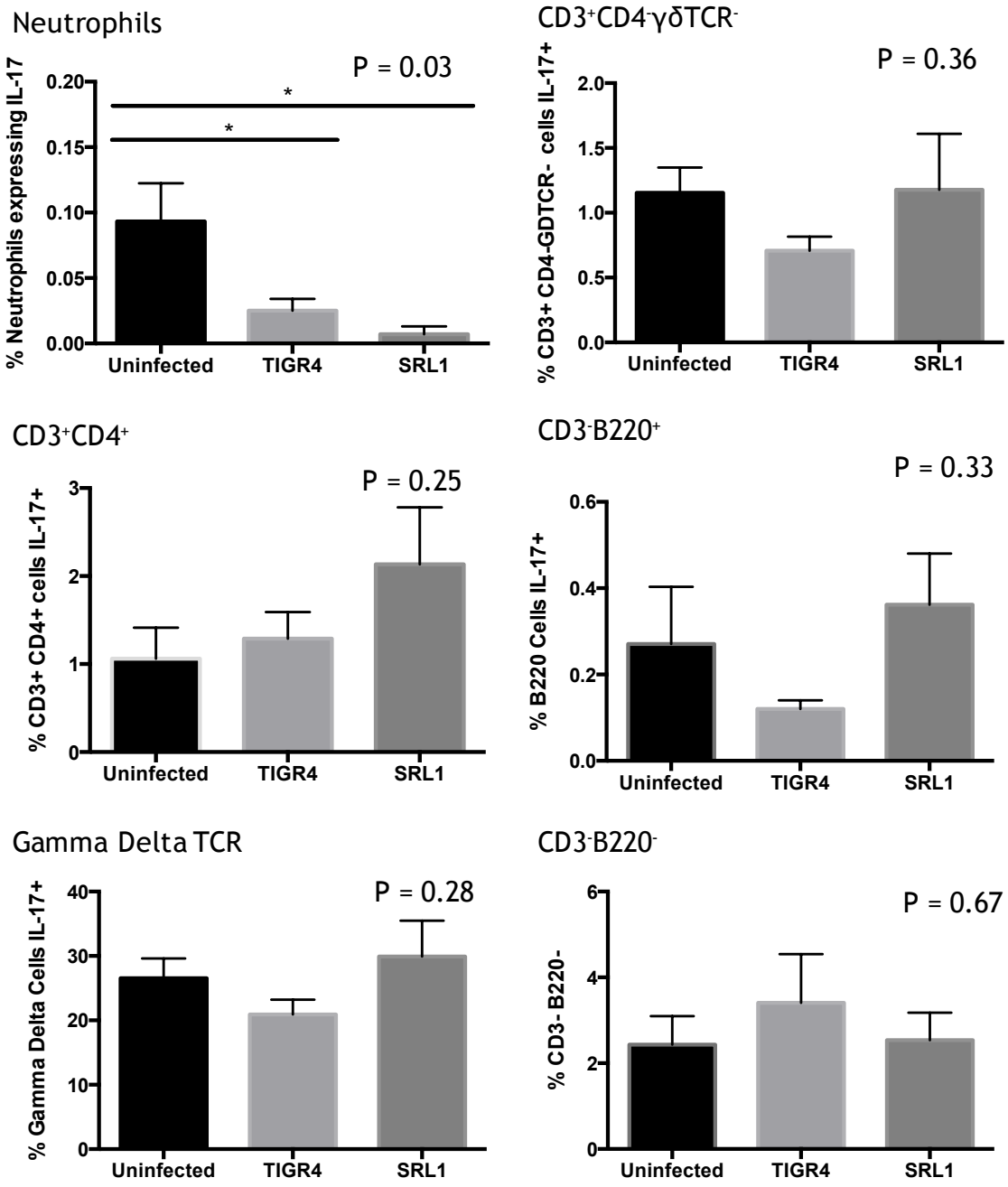

Figure 4-29. Cellular sources: summary of intracellular staining.
Lung homogenates were stimulated with PMA and ionomycin in the presence of Brefeldin A and analysed according to the strategy shown in figure 4-26. The percentage of cells staining positive for IL-17 in each group is shown (n = 6 females per group). P value represents one-way ANOVA with further testing performed only where the P value was < 0.05. * denotes P < 0.05.

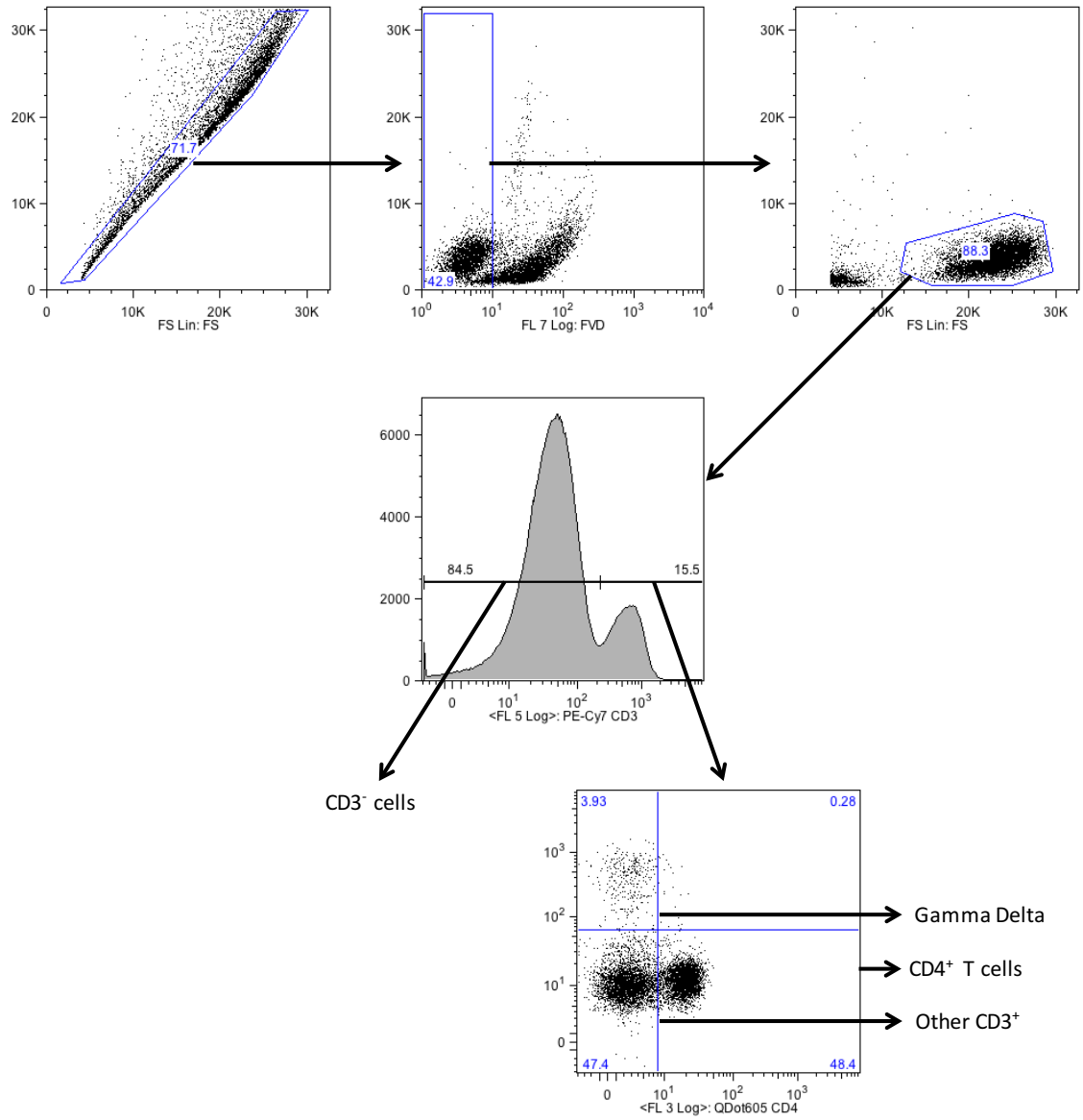

Figure 4-30. In-vivo Brefeldin A assay: gating strategy.

Identification of candidate IL-17 and IL-22 producing cells in mouse lung during *in vivo* brefeldin A study. Animals were infected with 10^6 cfu/mouse TIGR4 and simultaneously administered 250 ηg brefeldin A by intra-peritoneal injection. Doublets and dead cells were excluded and then gated on the basis of CD3 expression. $CD3^+$ cells were then further gated based on the presence of CD4 and the γδ T cell receptor and examined for evidence of IL-17 expression (see **figure 4-31**).

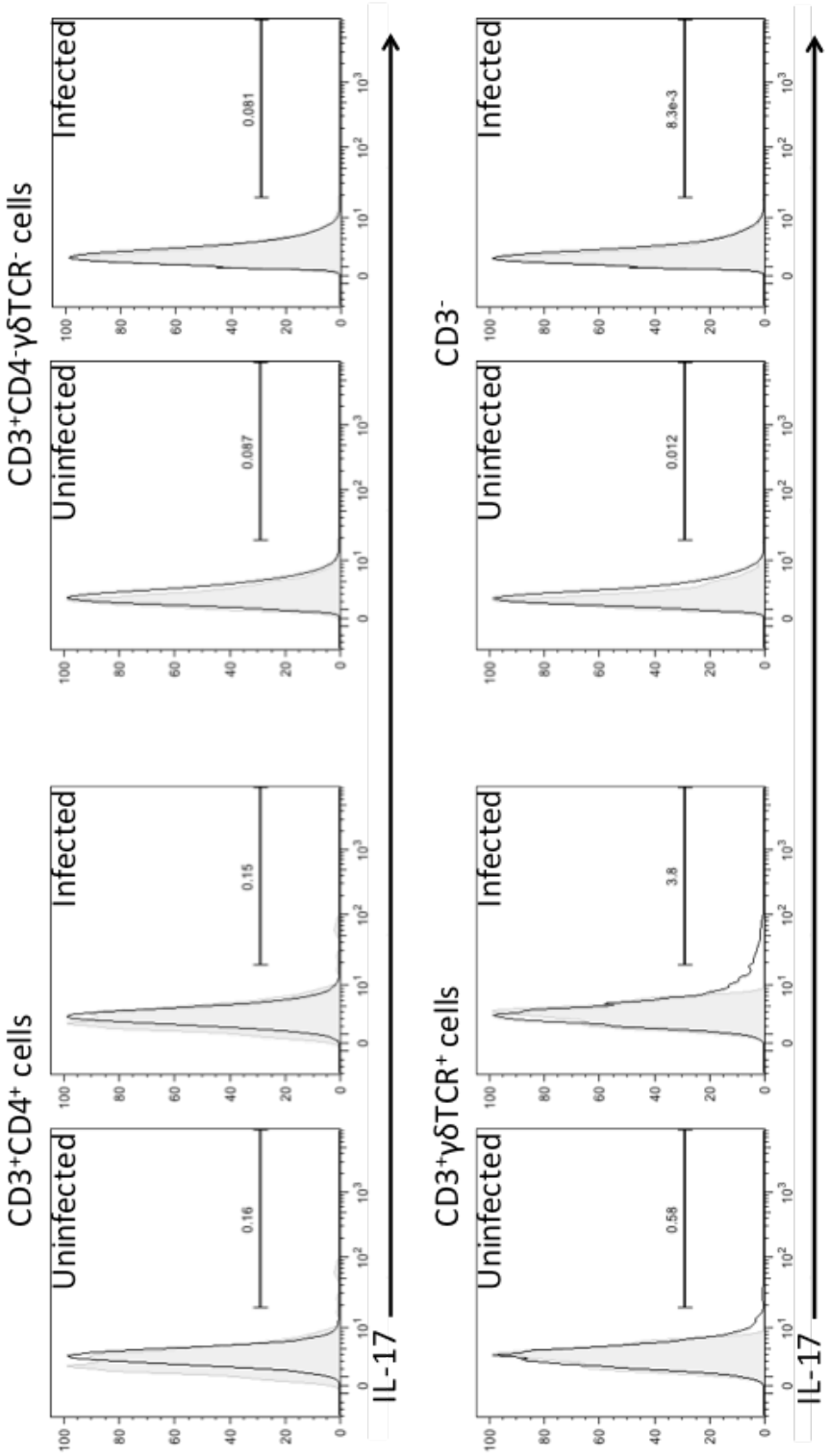

Figure 4-31. In-vivo Brefeldin A assay: intracellular staining.
Intracellular IL-17A expression in lung cells after *in vivo* administration of brefeldin A. IL-17 expression in groups of cells is shown in black with fluorescence minus one isotype control in grey. Results representative of two independent experiments which demonstrated similar results. One further experiment did not demonstrate any IL-17 expression in infected lungs.

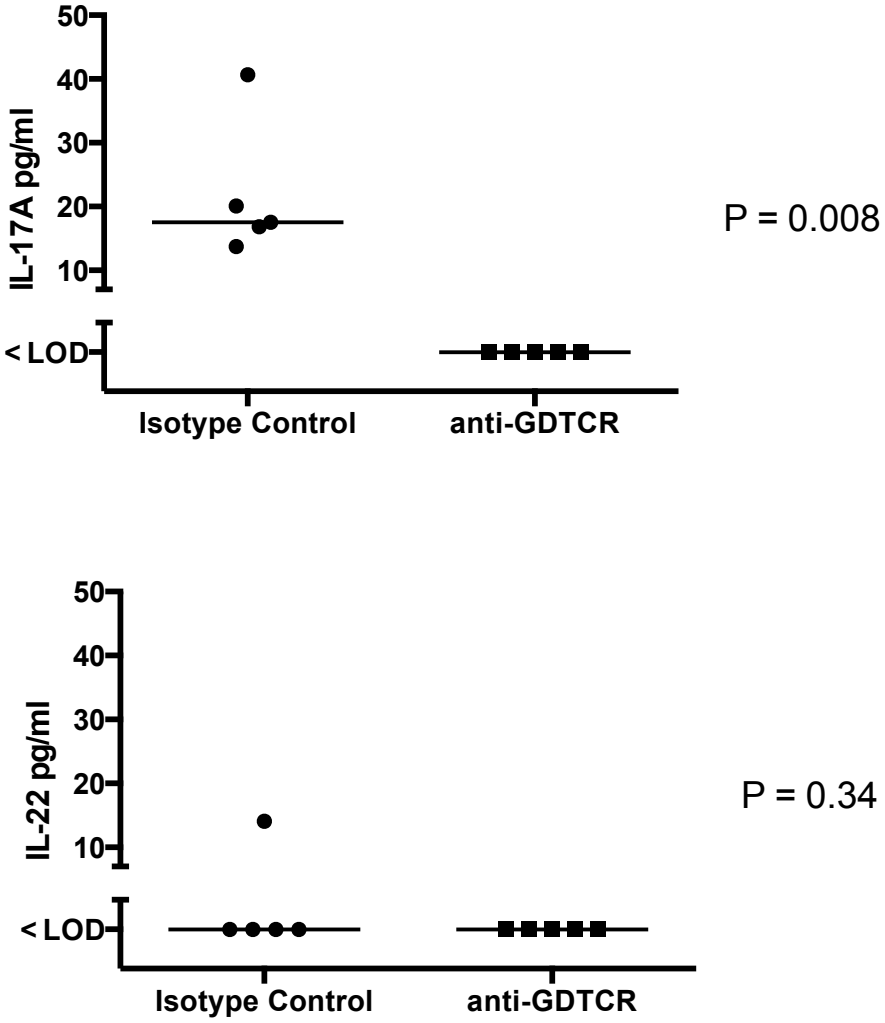

Figure 4-32. Gamma-delta depletion.

Mice were treated with an i.p injection of 100 µg of the monoclonal antibody UC7-13D5 or a matched isotype control. 24 hours later, mice were infected with 10^6 cfu/mouse of TIGR4 and culled 6 hours later (n = 5 females per group). BALF supernatant was analysed by ELISA for the presence of IL-17 and IL-22. The assay limit of detection (LOD) was 7 pg/ml. P value represents Mann Whitney test.

5. THE ROLE OF IL-17 AND IL-22 IN INVASIVE PNEUMOCOCCAL DISEASE

5-1 Introduction

IL-17 has been implicated in the acquired immune response to pneumococcal nasal colonisation through experiments involving active nasal immunisation with live bacteria, killed bacteria and bacterial components. However, as has been discussed, the role of IL-17 in innate immunity and invasive disease remains largely unexplored. IL-17 is involved in the anti-bacterial and anti-fungal defences of mucosal surfaces through stimulation of anti-bacterial products, recruitment of neutrophils and activation of phagocytes. However, pneumococcal disease is characterised by a fine balance between protective bactericidal immunity and harmful inflammatory tissue destruction.

In the previous chapter, I presented data establishing murine models of invasive pneumococcal disease that, despite being models of aspiration pneumonia induced under anaesthesia by pneumococci, were distinct in the phenotype of infection produced. Whereas TIGR4 caused a predominantly bacteraemic illness characterised by moribund animals with overwhelming sepsis and relatively few organisms in the lungs, SRL1 caused necrotising pneumonia with relatively late bacteraemia occurring when the animal was already extremely unwell. IL-17 was detected in both infections. TIGR4 was characterised by relatively patchy infiltration of neutrophils into the lungs whereas SRL1 infection was characterised by dense accumulation of neutrophils filling the alveolar spaces resulting lobar consolidation with sparse aeration of the affected lung.

I therefore set out to explore the role of IL-17 and the associated cytokine IL-22 in these very different infections. IL-17RA$^{-/-}$ mice were a gift from Jay Kolls, University of Pittsburgh[435] and IL-22$^{-/-}$ mice were a gift from Wenjun Ouyang, Genentech[319].

5-2 Confirmation of status of knockout animals

Splenocytes were obtained from wild type C57Bl/6 mice and IL-17RA$^{-/-}$ mice and stained for IL-17RA (figure 5-1A). An absence of staining confirmed that IL-17RA$^{-/-}$ mice did not express IL-17RA.

Ear lobe sampling was undertaken from wild type C57Bl/6 mice and IL-22$^{-/-}$ mice and DNA extracted. PCR analysis of the IL-22 gene was undertaken to confirm the presence of the insertion fragment (figure 5-1B) that caused premature termination of IL-22 gene transcription.

Throughout this chapter, male and female mice were used in experiments. Whenever this was done, mice were sex matched and the mice used in each experiment are shown in table 5-1. There was no evidence of a significant difference between the susceptibility of wild type male and female mice to pneumococcal disease in end point studies although there was insufficient statistical power to detect even a relatively large difference in this heterogeneous group of experiments (Random effects model: ΔRR Male vs Female 1.12 (0.54 - 1.84), P = 0.63).

5-3 High dose TIGR4 infection in knockout animals

Initial experiments using TIGR4 in knockout animals were conducted to investigate whether there was a difference in mortality between strains. As outlined in the methods, all ‘mortality’ studies were actually continued only to moribundity with animals monitored carefully and culled prior to death. I used the same dose (5×10^6 cfu per mouse) for this experiment to that used in the previous chapter to induce infection in the mice. The experiment was continued for 100 hours at which point all remaining animals were showing no signs of disease, no weight loss and had sterile blood.

There was no difference in survival or survival time among mice infected with high dose TIGR4 with 70-80% mortality in all three groups (figure 5-2A). There was also no difference in bacteraemia at 24 or 48 hours between the three groups (figure 5-2B). In all three groups, most animals that would go on to experience severe illness and be culled had detectable bacteraemia (LOD = 10^3 cfu/ml) by 24 hours post infection (WT: 7/8, 88%; IL-17RA$^{-/-}$: 7/8, 88%; IL-22$^{-/-}$: 7/7, 100%) and all animals that would reach the end-point were bacteraemic by 48 hours post-infection. Weight change and clinical score is shown in figure 5-3. There was no significant difference in these observations although there was a trend towards decreased weight loss among IL-17RA$^{-/-}$ mice which did not reach statistical significance (2 way ANOVA adjusted for multiple time point comparisons: P value for interaction between group (WT or IL-17RA$^{-/-}$) and time = 0.14).

5-4 Low dose TIGR4 infection in knockout animals

While performing another experiment to investigate outcome in knockout animals with a similar protocol to the first high dose TIGR4 challenge (5 animals per group) I inadvertently delivered a lower than anticipated dose of TIGR4 in the intra-nasal challenge (10^6 cfu/animal). Unexpectedly, this resulted in a markedly different result to the experiment outlined above. This result was subsequently confirmed by repeating with the same dose (9-11 animals per group).

The mortality in WT mice challenged with 10^6 cfu/animal of TIGR4 was much lower than that arising from high dose infection (pooled mortality 1/16, 6%). However, time to cull in the one animal which became severely ill was in line with the high dose infection (low dose animal: 76 hours; median time to cull in high dose group 72 hours). In view of the higher statistical power, I will present the results for the second experiment in full here but the results of the initial smaller experiment are similar.

Survival curves are shown in figure 5-4A. Mortality was highest among IL-17RA$^{-/-}$ mice and, while the P value for comparison across the three groups was 0.14, there was a statistically significant difference between WT and IL-17RA$^{-/-}$ on

the log rank test (P = 0.04). There was no evidence of a difference between IL-22$^{-/-}$ and WT in low dose infection although more IL-22$^{-/-}$ animals succumbed to infection than WT (IL-22$^{-/-}$ 3/10 and WT 1/10, P = 0.26). Therefore, the IL-22$^{-/-}$ phenotype appeared to be intermediate to that of IL-17RA$^{-/-}$.

Bacteriology data is shown in figure 5-4B and C. There was a trend towards increased bacteraemia in IL-17RA$^{-/-}$ mice but this did not reach statistical significance (P = 0.06). There was no difference in weight loss between groups overall (figure 5-5A). If analysis was limited only to animals requiring cull then the tendency for IL-17RA$^{-/-}$ mice to lose less weight than IL-22$^{-/-}$ and WT mice became statistically significant (P = 0.02). IL-17RA$^{-/-}$ mice had higher mean clinical scores than wild type with IL-22$^{-/-}$ intermediate (figure 5-5B, P = 0.01).

A pooled analysis of the two low dose TIGR4 experiments is presented in figure 5-6. Pooled analysis reinforces the difference between IL-17RA$^{-/-}$ (P < 0.001) and WT with IL-22$^{-/-}$ falling far short of statistical significance (P = 0.26). Pooled analysis also demonstrates the increased bacteraemia in IL-17RA$^{-/-}$ mice at 48 hours (P = 0.02).

5-5 Validation of flow cytometric method for quantifying neutrophils

Before moving on to characterise the responses of IL-17RA$^{-/-}$ mice following TIGR4 infection I developed a method of assessing peripheral neutrophil counts by flow cytometry. The rat monoclonal antibody RB6-8C5 can be used to stain mouse neutrophils for flow cytometry although it is also reported to stain monocytes and some macrophages. However, neutrophils can usually easily be distinguished by the combination of RB6-8C5 staining and their granular structure that causes them to be side scatter high compared to mononuclear cells. The validation of this technique is shown in figure 5-7. Peripheral blood neutrophil percentages measured by light microscopic analysis of blood smears and flow cytometry were highly correlated (figure 5-7C). A Bland-Altman plot shows a relatively modest degree of bias (approx 2% after the exclusion of a single outlier) that was not thought to be significant (figure 5-7D). Therefore, although using microscopy would permit analysis of neutrophil appearance, the

flow cytometric method was adopted to permit the high throughput required during animal models. In survival experiments, where assessment of peripheral blood neutrophils was used to monitor experimental progress, neutrophil percentage only was assessed. In time point experiments, where a primary outcome was neutrophil enumeration and high throughput was not required, absolute neutrophil number was calculated.

5-6 TIGR4 infection in knockout animals (time point)

To further investigate the increased mortality of IL-17RA$^{-/-}$ mice after infection I initiated TIGR4 infection and culled the animals 24 hours after infection. 24 hours was chosen as a time point because bacteraemia was usually detected in animals that would go on to develop disseminated TIGR4 infection at this point and therefore I decided that the effect of IL-17 signalling deficit was likely to be apparent by this time. Because of the lack of a significant difference between IL-22$^{-/-}$ mice and WT in the mortality studies it was decided not to investigate these animals further in TIGR4 infection. The experiment was conducted twice although the number of bacteria actually delivered in the experiment differed between the two experiments – in one it was 9 x 10^5 whereas in the other it was 4 x 10^6. Both experiments yielded similar results although histological analysis of lung tissue was performed only in the second of these experiments.

24 hours after inoculation with TIGR4, there was a marked difference in the recruitment of neutrophils to the peripheral blood and alveolar space but not the pleural space (figure 5-8). There was a trend towards increased bacterial numbers in the blood but not in the BAL in both experiments (figure 5-9). In the first experiment, there were no bacteria detected in the pleura but in the second there were more bacteria detected in IL-17RA$^{-/-}$ animals than in WT. Taken together, there was definite evidence of impaired recruitment of neutrophils into blood and relevant mucosal surfaces in IL-17RA$^{-/-}$ but only weak evidence of increased bacterial numbers invading into blood and pleura after 24 hours. It was not possible to pool the experimental data because of the heterogeneity in infecting dose.

Several other non-specific measures of inflammation were assessed in infected animals (figure 5-10). As was observed by trend in the mortality studies, IL-17RA$^{-/-}$ mice lost less weight after 24 hours than wild type mice although the absolute difference was small (% weight change: WT –2.2%; IL-17RA$^{-/-}$ +0.7%; P = 0.007). Lung wet/dry ratio is a surrogate for inflammatory interstitial oedema and while there was a trend towards decreased wet/dry ratio in IL-17RA$^{-/-}$ mice the difference was not statistically significant and the difference between the groups was small (wet/dry ratio: WT 9.8; IL-17RA$^{-/-}$ 8.3, P = 0.12) which was in keeping with the relatively modest pulmonary inflammation in TIGR4 infection. MPO assay of infected lung revealed a trend towards increased myeloperoxidase activity in WT lungs but this was not statistically significant (MPO activity: WT 0.97 OD/lobe/min; IL-17RA$^{-/-}$ 0.60 OD/lobe/min, P = 0.27).

H&E stained tissue sections from lungs of infected animals is shown in figure 5-11A. Blinded inflammation scoring in IL-17RA$^{-/-}$ was lower than that of WT animals (figure 5-11B, P = 0.02). While both groups had peribronchial infiltrate and, to a more limited extent, alveolar infiltrate this tended to be less pronounced in IL-17RA$^{-/-}$ animals. Lung immunohistochemistry using anti-Ly6G antibody supported these findings. Representative images are shown in figure 5-12.

RNA was extracted from a single lobe of lung and RT-PCR conducted for genes known to be targets of IL-17. Using this method, there was a trend towards decreased expression of IL-17 target genes but the variation in expression was high and they did not reach statistical significance (data not shown). Since it was felt to be important to confirm that expression of IL-17 target genes was inhibited in IL-17RA$^{-/-}$ mice, the experiment was repeated using an earlier time point (12 hours) and using RNA extracted from the whole lung rather than a single lobe since it was hypothesised that the patchy nature of the inflammatory change seen in TIGR4 infection might introduce suboptimal variation in the gene expression. Three target genes were chosen: the anti-microbial protein β-defensin 4, calprotectin subunit S100A8 and neutrophil chemokine MIP-1α (CCL3). These genes are all known to be upregulated by IL-17 stimulation. The

results of this further experiment are shown in figure 5-13; TIGR4 induced upregulation of all three genes was greatly inhibited in IL-17RA$^{-/-}$ mice.

5-7 SRL1 infection in knockout animals

We then investigated the role of IL-17 and IL-22 in SRL1 infection. The dose of SRL1 selected for these experiments was 10^6 cfu/mouse because this had caused moderate illness in WT animals at 48 hours in the dose titration study and I hypothesised that IL-17RA$^{-/-}$ mice would have impaired survival. Mortality studies with SRL1 were performed twice with very similar results. The first experiment is presented in detail here.

Mortality in WT mice was high with 10/11 (91%) requiring cull before the end of the experiment. In contrast, survival in IL-17RA$^{-/-}$ mice was significantly lower (4/9, 44%; figure 5-14A). Mirroring the findings with TIGR4, IL-22$^{-/-}$ mice displayed an intermediate phenotype which did not reach statistical significance. Bacteraemia data is shown in figure 5-14B and C. As with the time course experiment, invasion occurred late with SRL1 and animals were usually severely unwell before bacteraemia was detected. It was unusual to survive longer than 24 hours after the appearance of measurable bacteraemia (LOD >10^3). WT mice were significantly more likely to be bacteraemic at 48 hours than IL-17RA$^{-/-}$ mice ($P = 0.02$). Weight change and clinical score is shown in figure 5-15. IL-17RA$^{-/-}$ mice had less weight loss and lower clinical scores than WT controls ($P < 0.001$ in both cases)

Peripheral blood neutrophil percentages are shown in figure 5-16. Neutrophil percentages were measured at baseline and at 24 hour intervals thereafter. Since a large number of mice were culled between 48 and 72 hours post infection, sampling was not undertaken beyond 48 hours. At baseline there was no significant difference in percentage neutrophils between groups but at 24 hours there was a marked difference in neutrophil counts with reduced recruitment of neutrophils to the blood in the IL17RA$^{-/-}$ mice. At 48 hours the neutrophil percentages had come back together with a continued rise in IL-17RA$^{-/-}$ and falls in WT and IL-22$^{-/-}$. The fall in peripheral neutrophil percentage was seen inconsistently in experiments in which neutrophils were

monitored sequentially – see later in this chapter. Since peripheral blood neutrophil percentage rather than absolute count was assessed in this experiment, it not possible to exclude the possibility that the differences observed in neutrophil percentage are influenced by changes in other blood leukocyte populations. However, absolute neutrophil numbers were calculated in the subsequent time point experiment involving SRL1.

5-8 SRL1 infection in knockout animals (time point)

I then investigated the decreased mortality associated with IL-17RA$^{-/-}$ by infecting WT and IL-17RA$^{-/-}$ mice with SRL1 and culling at 24 hours post-infection. The results of these experiments gave similar findings to the TIGR4 24 hour experiments in that neutrophil recruitment to blood, BAL and pleura was significantly lower in IL-17RA$^{-/-}$ mice (figure 5-17). It was notable that pleural neutrophils were significantly elevated compared to uninfected animals in both WT and IL-17RA$^{-/-}$ despite the absence of detectable bacteria in the pleural aspirate (figure 5-18). As would be anticipated from existing experience with SRL1, there was also no detectable bacteraemia at this time point in any of the animals. There was no significant difference in BAL bacteria, although there was a trend towards decreased numbers of bacteria in IL-17RA$^{-/-}$ mice (P = 0.08).

There were also statistically significant differences in non-specific measures of inflammation between groups (figure 5-19). IL-17RA$^{-/-}$ mice lost less weight that WT (WT −3.8%, IL-17RA$^{-/-}$ +1.7%; P = 0.03), had a lower lung wet/dry ratio than WT (WT 14.9, IL-17RA$^{-/-}$ 10.6; P = 0.02) and had lower lung MPO activity than WT (WT 0.83, IL-17RA$^{-/-}$ 0.37; P = 0.01). Histological analysis of lung from infected animals revealed higher histological scores (indicating greater inflammation) in WT mice than IL-17RA$^{-/-}$. While IL-17RA$^{-/-}$ mice had focal areas of inflammation, they had only very infrequent areas of the dense consolidation typical of disease in wild type animals (figure 5-20). This impression was also confirmed on immunohistochemical staining of lung tissue. While both groups had focal areas of dense neutrophilic infiltrate, the IL-17RA$^{-/-}$ mice tended to have smaller areas which only rarely involved whole lobules. This was in contrast to WT mice in which large areas of dense consolidation were visible on most sections (figure 5-21).

RT-PCR of RNA extracted from whole lung of animals infected 12 hours before with SRL1 demonstrated similar findings to that of TIGR4 with decreased expression of the genes ß-defensin 4, S100A8 and MIP-1α in IL-17RA$^{-/-}$ mice compared to WT (figure 5-22).

5-9 Bacteriology of SRL1 survivors

Mice culled during and at the conclusion of mortality experiments involving SRL1 had BAL fluid sampled and cultured for pneumococci (figure 5-23). Mice culled during experiments were culled at the point of moribundity and this occurred at various times post infection. However all mice culled at the conclusion of the experiments were all culled at one week post infection. No wild type or IL-22$^{-/-}$ mouse culled at one week had any detectable SRL1 in BALF. In contrast, 7/10 (70%) of surviving IL-17RA$^{-/-}$ mice had detectable SRL1 present (P value compared to WT: 0.02). There was no difference in the bacterial density of BALF among animals culled with severe illness (P = 0.28).

5-10 Summary of TIGR4 and SRL1 in knockout animals

As I have demonstrated above, IL-17RA$^{-/-}$ animals had a consistent phenotype of reduced neutrophil recruitment to blood and lung. There was also a consistent decrease in several non-specific measures of systemic and local inflammation. However, the impact of the phenotype of IL-17RA$^{-/-}$ animals on survival was divergent in the two infections caused by TIGR4 and SRL1. IL-17RA$^{-/-}$ mice infected with TIGR4 tended to have increased early invasion of bacteria and greater mortality than WT. In contrast, IL-17RA$^{-/-}$ mice infected with SRL1 had decrease mortality although surviving animals often failed to clear SRL1 from the lower airways. IL-22$^{-/-}$ mice had an intermediate phenotype in each infection which failed to achieve statistical significance.

Given the central role of neutrophils in the phenotype of IL-17RA$^{-/-}$ mice, I decided to investigate the role of neutrophils further using both *in vitro* and *in vivo* methods.

5-11 Neutrophil mediated pneumococcal phagocytosis and killing

It has been previously reported that capsular serotype affects the phagocytosis of pneumococci by neutrophils and I sought to confirm these differences in neutrophil mediated phagocytosis and killing were present for TIGR4 and SRL1. To quantify neutrophil phagocytosis and killing I used the method of Hampton[436]. This method uses a two-compartment model (supernatant and cell associated bacteria) and also uses a neutrophil free control. The difference between the bacterial count in the neutrophil containing and neutrophil free cultures is assumed to represent the bacteria killed by neutrophils. In these experiments, mouse serum was not inactivated to preserve complement function.

A representative plot from these experiments is shown in figure 5-24A. Both TIGR4 and SRL1 were phagocytosed and killed by neutrophils. However, the rate of phagocytosis and killing was substantially lower in cultures containing SRL1 than TIGR4 (figure 5-24B, P = 0.01). Phagocytosis was also measured using fluorescent bacteria (figure 5-25A). When measured by flow cytometry at time points over 80 minutes following infection of neutrophils, there was only a relatively minor increase in staining intensity over time with SRL1 but a marked increase in staining with TIGR4 (figure 5-25B). In separate experiments, neutrophils were removed from culture and subjected to cytocentrifugation before nuclear staining (figure 5-26). This experiment also demonstrated increased association of TIGR4 bacteria with neutrophils than SRL1.

5-12 Neutrophil extracellular traps[†]

The formation of neutrophil extracellular traps (NETs) is an important mechanism by which neutrophils trap and inactivate bacteria *in vivo*. To investigate whether there were differences in the formation of NETs between TIGR4 and SRL1 I used a model of *in vitro* NET formation using human neutrophils. NETs are characterised by the formation of extracellular complexes

[†] The experiments reported in this section were conducted jointly with Dr Ihsan Ullah.

of neutrophil granular proteins with DNA. Bacteria can then become trapped in the NET facilitating phagocytosis or directly killing the organisms.

I sought to detect NETs by carefully fixing neutrophils lightly adhered to a chamber slide and staining both DNA and neutrophil elastase. Unstimulated neutrophils and the characteristic appearance of a NET after stimulation with TIGR4 are shown in figure 5-27A. Heat inactivated serum was used because the use of competent serum was associated with large numbers of NETs in unstimulated neutrophils (data not shown, courtesy of Dr Ihsan Ullah). Wide-field views of NET formation after infection with TIGR4 and SRL1 are shown in figure 5-27B along with uninfected neutrophils and neutrophils stimulated with PMA (which is a potent inducer of NETosis). In order to assess the capture of bacteria in NETs, fluorescent pneumococci were generated using proliferation dye and bacteria were imaged directly within NETs (figure 5-28). NETs were quantified by counting the neutrophils involved in NET formation and through image analysis of NET size and the mean percentage of pixels above a consistent threshold per NET (figure 5-29).

Unstimulated neutrophils produced very few NETs and neutrophils stimulated with PMA produced extensive NET. SRL1 was a more potent inducer of NET formation than TIGR4 as measured by neutrophils included in NETs and average size of NET. However, despite the more extensive NETosis in SRL1 cultures, the fluorescent staining of NETs associated with the presence of bacteria was lower in SRL1 cultures.

5-13 Neutrophil depletion

In view of the differences observed in neutrophil mediated phagocytosis, killing and NET formation, I decided to explore the role of neutrophils *in vivo* using a depleting antibody. The rat monoclonal antibody 1A8 is reported to effectively deplete neutrophils following intra-peritoneal injection. Since the neutrophil deficiency in IL-17RA$^{-/-}$ mice was most apparent within the first 24 hours after infection, I decided to give just one dose of the monoclonal antibody at 24 hours prior to infection.

The antibody 1A8 binds to the same surface receptor (Ly6G) as the monoclonal RB6-8C5 used in flow cytometric staining although it binds to a different epitope. Therefore, 1A8 was an effective inhibitor of RB6-1A8 binding of neutrophils complicating the identification of neutrophils by flow cytometry (figure 5-30A). A group of side-scatter high cells stained with RB6-8C5 could still be identified following i.p. injection of 1A8 but the intensity of staining was significantly reduced binding (figure 5-30B). However, CD-11b staining was unaffected by 1A8 (figure 5-30C).

A dose finding study was undertaken with intra peritoneal injection of 250 μg or 500 μg of antibody 1A8 or a matched isotype control (figure 5-31A). There was no evidence of a difference in peripheral neutrophil percentage between the two isotype control doses (250 μg: 9.6%, 500 μg: 9.3%; P = 0.91) and these were therefore combined for statistical purposes. Both the 250 μg and 500 μg doses of 1A8 significantly reduced peripheral neutrophil percentages compared to isotype control (P value for each compared with isotype control < 0.001). There was a trend towards a reduced peripheral neutrophil percentage in mice treated with the higher dose of antibody (250 μg: 3.9%, 500 μg: 2.6%; P = 0.12). While this difference did not reach statistical significance, it was decided to conduct further experiments using 500 μg of antibody. In order to further confirm the depletion of neutrophils, neutrophil counts were also obtained using counting beads and these correlated highly with the peripheral neutrophil percentages previously obtained (figure 5-31B). Therefore, peripheral blood neutrophil percentages were used in these experiments since this is a less complex assay.

5-14 Neutrophil depletion in TIGR4 infected mice

This experiment was performed twice and the results pooled. Both experiments showed the same trend which did not individually reach statistical significance. One mouse from the anti-Ly6G antibody group was excluded from the results as it was culled shortly after the start of the experiment with evidence at post-mortem of an iatrogenic caecal puncture associated with the intra-peritoneal injection. The overall difference in the survival curves was small and did not reach statistical significance in the log rank test (figure 5-32A, P = 0.09). However, there was a shortening in the median time to moribundity of mice

treated with the antibody 1A8 (anti-Ly6G antibody: 52 hours, isotype control: 66 hours; figure 5-32B, P = 0.01). 1A8 treated mice also had a increased weight loss (P = 0.03, figure 5-33A) and a strong trend towards increased clinical scores compared to isotype control treated animals (P = 0.07, figure 5-33B) which was particularly apparent at 60 hours (P = 0.04 at this timepoint).

Assessment of peripheral blood neutrophil percentage (figure 5-34) confirmed effective baseline depletion of neutrophils in 1A8 treated animals (anti-Ly6G antibody: 2.5%, isotype control: 7.0%; P < 0.001) and there was a particularly marked depletion of neutrophils at 24 hours (anti-Ly6G antibody: 8.3%, isotype control: 28.6%; P < 0.001) although this difference had largely disappeared by 48 hours (anti-Ly6G antibody: 8.3%, isotype control: 14.3%; P = 0.20). This fall in peripheral neutrophil counts after 48 hours was previously seen earlier in this chapter in the context of SRL1 infection (figure 5-16) although it is not seen consistently.

5-15 Neutrophil depletion in SRL1 infected mice

Like in TIGR4 infected mice, two experiments were performed in SRL1 infected mice and the results pooled to give 20 mice per group. Both experiments showed the same trend. Depletion of neutrophils in SRL1 infection was associated with a modest but statistically significant improvement in survival (anti-Ly6G antibody: 6/20 (30%), isotype control: 2/20 (10%), figure 5-35A, P = 0.02). There was also decreased clinical score (P = 0.01) and a trend towards decreased weight loss among 1A8 treated animals (P = 0.12).

Peripheral blood neutrophil testing confirmed effective depletion of neutrophils at baseline (anti-Ly6G antibody: 2.5%, isotype control: 7.0%; figure 34A, P < 0.001) that persisted throughout the first 48 hours of the experiment.

5-16 Summary of neutrophil studies

Following the finding that infection with SRL1 and TIGR4 produces divergent mortality in IL-17RA$^{-/-}$ mice compared to wild type animals I hypothesised that differences in neutrophil recruitment and consequent differences in bacterial killing and tissue damage might explain this difference.

TIGR4 was effectively killed *in vitro* by mouse neutrophils but SRL1 was very poorly killed in the same experimental system. Similarly, using our model of neutrophil NETosis, there was evidence of increased NET formation but decreased bacterial capture in NETs among SRL1 infected neutrophils. When mice were depleted of neutrophils *in vivo* there was a modest effect on survival but the same pattern was seen with evidence of earlier severe illness in TIGR4 infected neutrophil depleted mice but improved survival in SRL1 infected neutrophil depleted mice. This suggests that neutrophils may mediate some of the phenotype encountered in IL-17RA$^{-/-}$ mice.

5-17 Characterisation of other pneumococcal strains

In order to further explore the role of pneumococcal capsular type in defining the role of IL-17 in pneumococcal disease I attempted to generate capsular switch mutants. I attempted to use the method developed by Sung *et al* [437] to generate an organism expressing serotype 3 capsular polysaccharide on a TIGR4 background and an organism expressing serotype 4 capsular polysaccharide on a SRL1 background. However, despite repeated attempts to use this method, I was not successful in generating the mutants.

After the failure to generate capsular switch mutants, I decided to assess the role of serotype using existing strains of different capsular type. I selected additional strains from the collection of the local reference laboratory with the aim of selecting two strains expressing capsular polysaccharides associated with a high invasive potential and two strains with low invasive potential based on the findings of Sleeman *et al*[438] previously summarised in figure 1-5. I therefore selected serotypes 7F and 5 (high invasive potential) and 6B and 19F (low invasive potential). However, SHLMPRL did not have a serotype 5 pneumococcus in its collection (personal correspondence from Dr Giles Edwards) and so I selected serotype 14 as an alternative. The basic *in vitro* characterisation of these strains (designated SRL2-5 respectively in ascending order of serotype) has already been reported in the last chapter.

Standard innocula were generated by culturing blood (serotypes 7F and 14) and BALF (6B and 19F). Each bacteria was then given to wild type mice at a range of

doses between 10^5 and 10^7 cfu/mouse and monitored for 48 hours. At this point, animals were culled and infections were characterised by bacteriology and histology.

The clinical course of infection is shown in figure 5-38. All groups demonstrated a dose dependent effect on body weight. However, in the case of SRL3 and 4 the loss of weight was minor and resolved by the conclusion of the experiment. Mice in the highest dose group of SRL4 lost more than 10% of body weight but had begun to recover by the conclusion of the experiment. No animals infected with SRL3, 4 or 5 became clinically unwell during the experiment. Mice infected with the highest dose of SRL2 lost weight during the second day of the experiment and developed clinical evidence of severe disease.

Bacteriology studies from blood, BAL and pleura are shown in figure 5-39. Only a single mouse infected with SRL3 had a detectable bacteraemia at 48 hours and no mouse had any detectable bacteria in pleura. All mice had cleared bacteria from the alveolar space at 48 hours except mice in the highest dose SRL2 group which had pneumococci readily detectable in BALF.

Histology from animals infected with 10^7 cfu/mouse at 48 hours is shown in figure 5-40. Mice from groups infected with lower numbers of bacteria had either no detectable or mild inflammatory infiltrate. Mice infected with SRL3, 4 and 5 had mild peribronchial infiltrate seen. Only mice infected with SRL2 had evidence of alveolar inflammation with areas of consolidated lung. The areas of inflammatory change were less dense that those seen with SRL1.

5-18 SRL2 in knockout animals

In the last section, several other pneumococcal isolates were screened for their ability to cause disease in wild type mice. Of these, SRL2 was selected to be used in a further assessment of disease in IL-17RA$^{-/-}$ mice since it shared certain characteristics with SRL1: it was a serotype 6B, which is associated with high mortality but a low odds ratio of invasiveness in epidemiological studies; it caused severe illness in WT mice after around 48 hours despite only modest numbers of bacteria being detected in the peripheral blood; and it caused

persistent pulmonary infection. The experiment was conducted without IL-22$^{-/-}$ mice since these did not display a clear phenotype with SRL1.

Mice were infected with 10^7 cfu since this was the dose which produced clinical disease in wild type animals. The survival curve for this experiment is shown in figure 5-40A. No animals in the IL-17RAKO group reached the clinical end-point prior to the end of the experiment (1 week post-infection). In contrast, four wild type mice developed severe infection and needed to be culled during the third day of the experiment. This difference was statistically significant (P = 0.03). One mouse in the IL-17RA$^{-/-}$ group developed significant weight loss (>10%) which had not resolved by the end of the experiment. This mouse was clinically unwell (clinical score at 1 week was 2) although the illness did not appear to progress.

Levels of bacteraemia are shown in figure 5-41B. Only two mice (both culled shortly after blood was taken) were bacteraemic at 48 hours with all other blood sterile. Weight loss and clinical score are shown in figure 5-42. There was a strong trend towards decreased weight loss in IL-17RA$^{-/-}$ mice that fell just short of statistical significance (P = 0.06). Clinical scores were significantly higher in WT mice (P < 0.001). Unfortunately, peripheral blood neutrophil percentages at baseline were not available due to an error in specimen handling. Peripheral neutrophil percentages were available at 24 hours and are shown in figure 5-43. As previously demonstrated in the context of other pneumococcal infection, IL-17RA$^{-/-}$ had a markedly attenuated neutrophilia compared to WT (WT: 50.3%, IL-17RA$^{-/-}$: 20.5%; P = 0.03). Interestingly, three of the four mice that would require to be culled due to severe illness had low peripheral blood neutrophil counts at 24 hours although this narrowly missed statistical significance (P = 0.07).

Bacterial burden in the BAL of animals surviving to the conclusion of the experiment is shown in figure 5-44. No surviving wild type mice had detectable pneumococci in BAL at this time point. However, 6/10 (60%) of surviving IL-17RA$^{-/-}$ mice had detectable pneumococci (P = 0.03). The mouse with significant weight loss and non-progressing clinical illness had large numbers of bacteria present in the BAL (8×10^5 cfu/ml) and therefore should be regarded as having persistent infection rather than lower airways colonisation. However, if

this mouse is excluded from the analysis then the difference remains statistically significant (P = 0.044).

5-19 Discussion

In the last chapter of this thesis I used two strains of pneumococci to produce a model of invasive pneumococcal disease with a pulmonary source and a model of pneumococcal pneumonia. In this chapter I used IL-17RA$^{-/-}$ and IL-22$^{-/-}$ mice to explore the role of these cytokines in this model. Because IL-17RA is required for signalling from all IL-17 family cytokines, the phenotype of IL-17RA$^{-/-}$ is characterised by ablation of all IL-17 signalling. One practical difficulty with the use of IL-17RA$^{-/-}$ mice was the relatively poor breeding associated with the strain. This generated early difficulties in obtaining sufficient mice for planned work. Once sufficient breeding pairs were established, sufficient mice were available but it was necessary to use male and female mice in experiments. All experiments were carefully controlled by age and sex matching. This is important since gender related differences in susceptibility to pneumococcal infection have been observed before[439].

IL-17RA$^{-/-}$ mice had consistently reduced early recruitment of neutrophils to blood and lung in infection with both TIGR4 and SRL1. This was confirmed by flow cytometric counting of neutrophils and histopathology. This is consistent with the many other studies that have examined the effects of IL-17. MPO activity, as a biochemical assay of neutrophil activity, was significantly lower in IL-17RA$^{-/-}$ in SRL1 infection and a trend was observed in TIGR4. There was wide variation in MPO activity in TIGR4 infected mice and the failure to reach statistical significance may be due to the sampling of a single lobe only given the patchy nature of pulmonary changes in TIGR4 infection. I had hypothesised that the loss of IL-17 dependent neutrophil recruitment would impair the pneumococcal immune response. In infection caused by TIGR4 this hypothesis was confirmed in that IL-17RA$^{-/-}$ mice had increased mortality following infection with a dose of TIGR4 associated with low mortality in wild type mice (10^6 cfu/mouse). The course of infection in animals succumbing to TIGR4 infection was similar with bacteraemia detectable at 24 hours and progressing until severe illness and moribundity. As mentioned in the last chapter, only one mouse (a

wild type mouse) survived TIGR4 bacteraemia and development of bacteraemia was unusual after 24 hours post infection. Therefore, TIGR4 infection was marked by an early critical decision point with the bacteria either entering the blood in sufficient numbers to initiate a persistent systemic infection within the first hours of the infection or failing to do so and being eradicated by the immune response. It seems that IL-17 has an impact on this process but not on the subsequent bacteraemic phase of infection. This conclusion is supported by the finding that when a five-fold higher dose associated with high mortality in wild type mice was used the difference in mortality between wild type and knockout was not apparent.

When SRL1 was used to infect IL-17RA$^{-/-}$ mice there was a divergent effect of loss of IL-17 signalling on mortality compared to TIGR4. IL-17RA$^{-/-}$ mice infected with SRL1 had significantly decreased mortality compared to wild type. This was a surprising result given my hypothesis that IL-17 is important in host defence against pneumococcal disease. However, there is evidence in the published literature of IL-17 mediated harm associated with mucosal infection. The infections in which harm has been documented include chronic infections such as *H. pylori* gastritis[336], peritoneal abscess formation[335] and two models of influenza pulmonary infection[337], [338]. These heterogeneous infections are united by the common feature that neutrophil infiltration into infected tissues are unlikely to contribute to clearing of the infection but are likely to contribute to tissue damage through inflammation. I found SRL1 to have a very thick capsular polysaccharide and this is well attested in the literature. It is reported that pneumococcal capsular thickness correlates with protection against neutrophil phagocytosis[139] and serotype 3 is reported to be highly resistant to phagocytosis[440], a finding that I replicated in this study. Pneumococcal resistance to phagocytosis has also been reported to correlate with resistance to surface complement deposition[73] and factor H binding[441]. While capsular serotype plays a role, there is also evidence of significant strain to strain variation[442]. It is already known that TIGR4 is resistant to complement deposition[443] and establishing If SRL1 displays high level resistance would be an important future direction.

Lung homogenate cfu counts were not used in these experiments as I wished to study a variety of other lung tissue parameters such as MPO activity, wet/dry ratio and RNA expression. In early experiments, lung cfu counts correlated with BALF measurements but this was demonstrated only in TIGR4 infection. Measurement of lung cfu counts in the time point experiments might have provided additional insight into the dynamics of infection in IL-17RA$^{-/-}$ mice.

I hypothesised that the marked difference in phenotype observed with the IL-17RA$^{-/-}$ mice in these experiments was due to the effectiveness of neutrophil mediated clearance of bacteria. To test this hypothesis I performed *in vitro* experiments demonstrating that while TIGR4 was effectively phagocytosed and killed by mouse neutrophils SRL1 was poorly phagocytosed and killed. Indeed, in these experiments the number of bacteria present in the supernatants of the neutrophil containing and control cultures was similar. It should be noted that these experiments were conducted using serum from naïve mice and so do not reflect phagocytosis efficiency in the presence of anti-pneumococcal antibody. However, there is evidence from elsewhere that serotype 3 is also highly resistant to phagocytosis in the presence of anti-capsular antibody.

I then used a neutrophil depleting antibody to induce neutrophil deficiency early in the course of infection. The monoclonal antibody 1A8 was used which has been shown to selectively deplete neutrophils from peripheral blood and impede the migration of neutrophils into sites of inflammation. The other available monoclonal antibody (RB6-8C5) also depletes monocytes and was therefore avoided. The neutrophil depletion experiments produced a similar result following infection with the two pneumococcal strains to that obtained with IL-17RA$^{-/-}$ mice. However, there were a number of important differences. The effect size was smaller and required larger groups of animals to demonstrate a significant difference (20 mice per group). It was also notable that the difference demonstrated in infection with TIGR4 was in length of time to moribundity whereas in IL-17RA$^{-/-}$ mice it was survival that was impaired with similar time to moribundity. This suggests that, while neutrophils are important in host defence against TIGR4 pulmonary infection, there are other factors mediating the immunoparesis in IL-17RA$^{-/-}$ mice.

The finding that the balance between neutrophil mediated control of infection and tissue damage may be weighted differently between pneumococcal strains is not entirely new. As discussed in the introduction, several studies have demonstrated the importance of neutrophils in defence against pneumococcal disease. However, one study by Marks *et al*[195] demonstrated a marked improvement in survival in a model of pneumococcal pulmonary infection following depletion of neutrophils by antibody treatment (RB6-8C5 in this case). This study used a serotype 8 strain which expressed a non-haemolytic pneumolysin. It is notable that serotype 8 is one of a small number of pneumococcal strains reported to produce mucoid colony morphology[444] although the authors do not state if the strain used in their work was mucoid in appearance. A recent study found depletion of neutrophils using 1A8 was detrimental in a model of serotype 2 *S. pneumoniae* pulmonary infection but that partial inhibition of neutrophil recruitment and activation by pharmacological inhibition of proteinase activated receptor-1 reduced neutrophil mediated lung damage without compromising host defence[445]. These studies reinforce the fine balance that exists in the inflammatory response between control of infection and tissue damage.

Further experiments could seek to provide further evidence of a link between reduced neutrophil recruitment in IL-17RA$^{-/-}$ mice and the infection outcomes observed. If neutrophil recruitment is responsible for the phenotype observed then depletion of neutrophils in IL-17RA$^{-/-}$ mice might be expected to have limited impact on outcome. This experiment would require large numbers of knockout mice and would therefore be resource intensive. Other observations that could specifically link neutrophil recruitment to lung damage in SRL1 infection could involve the use of labelled dextrans to assess leakage of serum proteins through damaged endothelium.

In order to further characterise the factors contributing to the improved outcome of IL-17RA$^{-/-}$ mice, I sought to identify other strains that share similar characteristics to the serotype 3 SRL1. SRL2 and SRL5 are from serotypes (6B and 19F respectively) that like serotype 3 are associated with relatively low invasiveness compared to other common serotypes. SRL5 was not sufficiently virulent in wild type animals to take forward into knockout models but SRL2

caused a pneumonic illness characterised by significant weight loss and lung bacterial burden but did not cause invasive disease. Therefore SRL2 was used in subsequent studies with knockout animals. This model also showed reduced illness and improved outcome in IL-17RA$^{-/-}$ mice. The dose required to replicate the phenotype was 10 times higher than SRL1 but despite this mortality among wild type mice was only 40%. Since serotype 6B is also associated with a thick capsular polysaccharide and resistance to phagocytosis, this supports the hypothesis that these are characteristics associated with a maladaptive role for IL-17 in pneumococcal pneumonia.

IL-22$^{-/-}$ mice had no consistent phenotype in the model of pneumococcal disease used in this study. In experiments involving both strains, IL-22$^{-/-}$ mice had a change in mortality in the same direction as the IL-17RA$^{-/-}$ mice but the effect was smaller and did not reach statistical significance. There are very little data on the role IL-22 in pneumococcal disease. One study found that ILCs could be stimulated to produce IL-22 by administration of a TLR-5 agonist and that this was associated with decreased mortality although IL-22 secretion was not causally linked to the action of the TLR-5 agonist[225]. Since in this study no clear mortality difference emerged between wild type and IL-22$^{-/-}$ mice, no detailed exploration of the differences in phenotype was conducted using IL-22$^{-/-}$ mice.

This study raises a number of questions for future research. The role of adaptive immunity in nasal colonisation has been intensively studied and Th17 responses implicated in the clearance of pneumococci. Several approaches for the vaccination of humans with the aim of eliciting Th17 responses are currently under development. If IL-17 can have a detrimental effect on the course of pneumococcal infection then this would have clear implications for these vaccine strategies. Future work is needed to define if the increased susceptibility of mice to mucosal pneumococcal infection in the presence of effective IL-17 signalling is also relevant to adaptive IL-17 responses as well as naïve responses. Further work will also define whether this effect is generalizable to other sites of infection. One example would be bacterial meningitis in which there is already considerable evidence of over-exuberant inflammatory responses causing tissue damage and the presence of IL-17 might have an adverse effect on outcome particularly of treated meningitis.

Unfortunately, since severe disease confirmed to be caused by serotypes with characteristics like serotype 3 is relatively unusual on an individual level it is unlikely that vaccine trials of any prospective new vaccines would provide evidence to support or refute a similar effect in vaccinated humans and given the difficulties and biases inherent in observational trials of infection in humans it may be difficult to assess under any practical circumstances. However, consideration of the possibility of adverse outcomes when disease occurs should be considered in the design of trials of vaccines exploiting IL-17 mediated immunity for the prevention of pneumococcal disease.

In conclusion, this chapter provides evidence of a divergent role for IL-17 and associated neutrophil mediated inflammation in pneumococcal disease depending on the nature of the strain involved with a role for IL-17 in preventing early invasion of a highly invasive strain but also a role for the same cytokine in maladaptive pulmonary inflammation in infection caused by a pneumonia causing strain with low invasive potential but a high level of resistance to phagocytosis. This finding may have implications for vaccine developers.

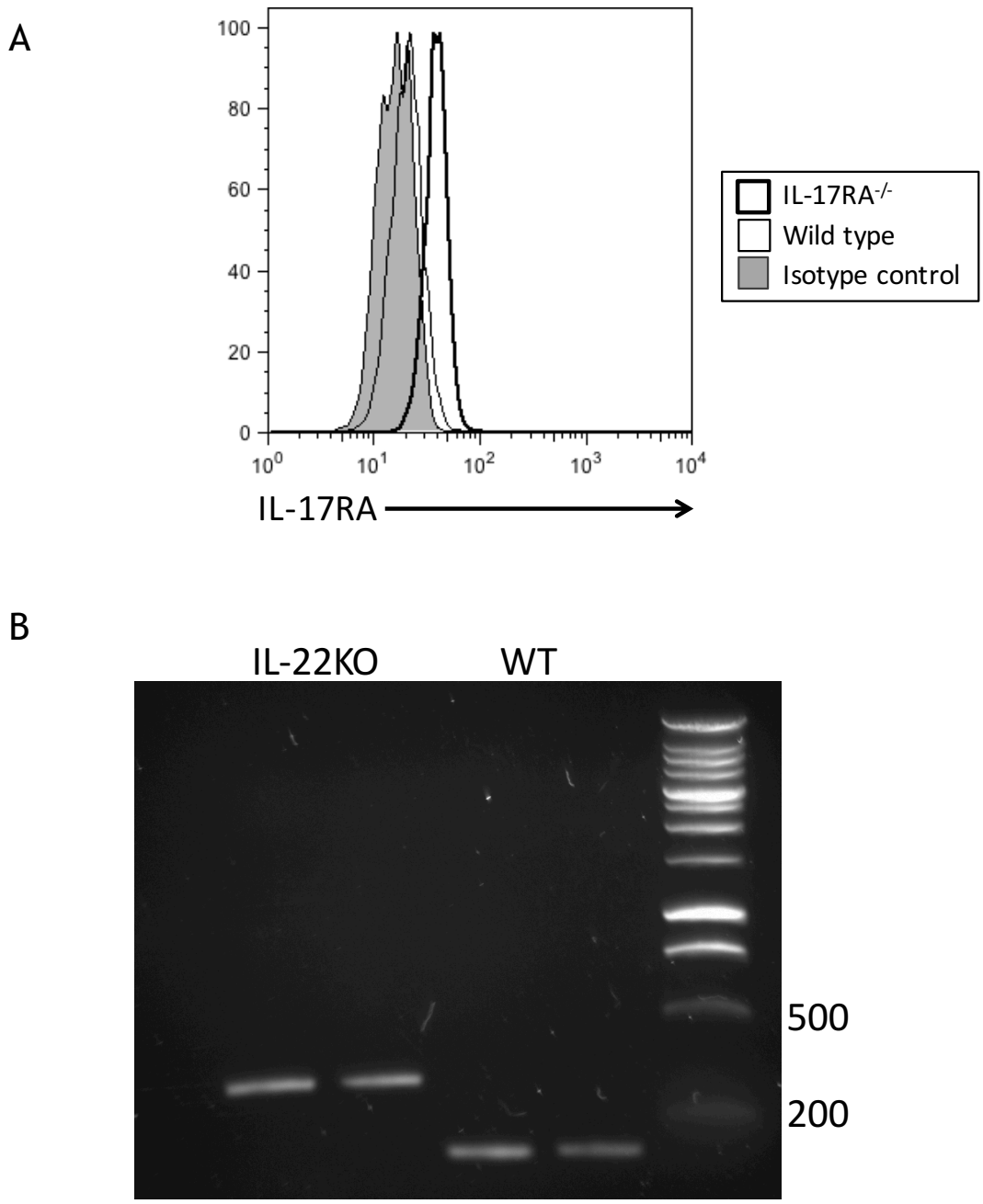

Figure 5-1. Confirmation of knockout animals.

A. Splenocytes from wild type or IL-17RA-/- mice were stained with anti-IL17RA antibody conjugated to PE. Dead cells were excluded with SYTOX Green. B. DNA was extracted from ear biopsies taken from WT or IL-22-/- mice. Primers p-1 (5'- CTC AGA CCT CTA CAG ACA ATC ATC-3') and p-2 (5'- CAG CTG GCG GCC AAA GTC CC-3') were used to amplify the wild type gene product (194bp) while p-1 and p-3 (5'- GAT ACA GGT GCA GCT AAG CGA G-3') were used to amplify IL-22-/- gene product (374bp). All three primers were added to each reaction to ensure detection of heterozygotes.

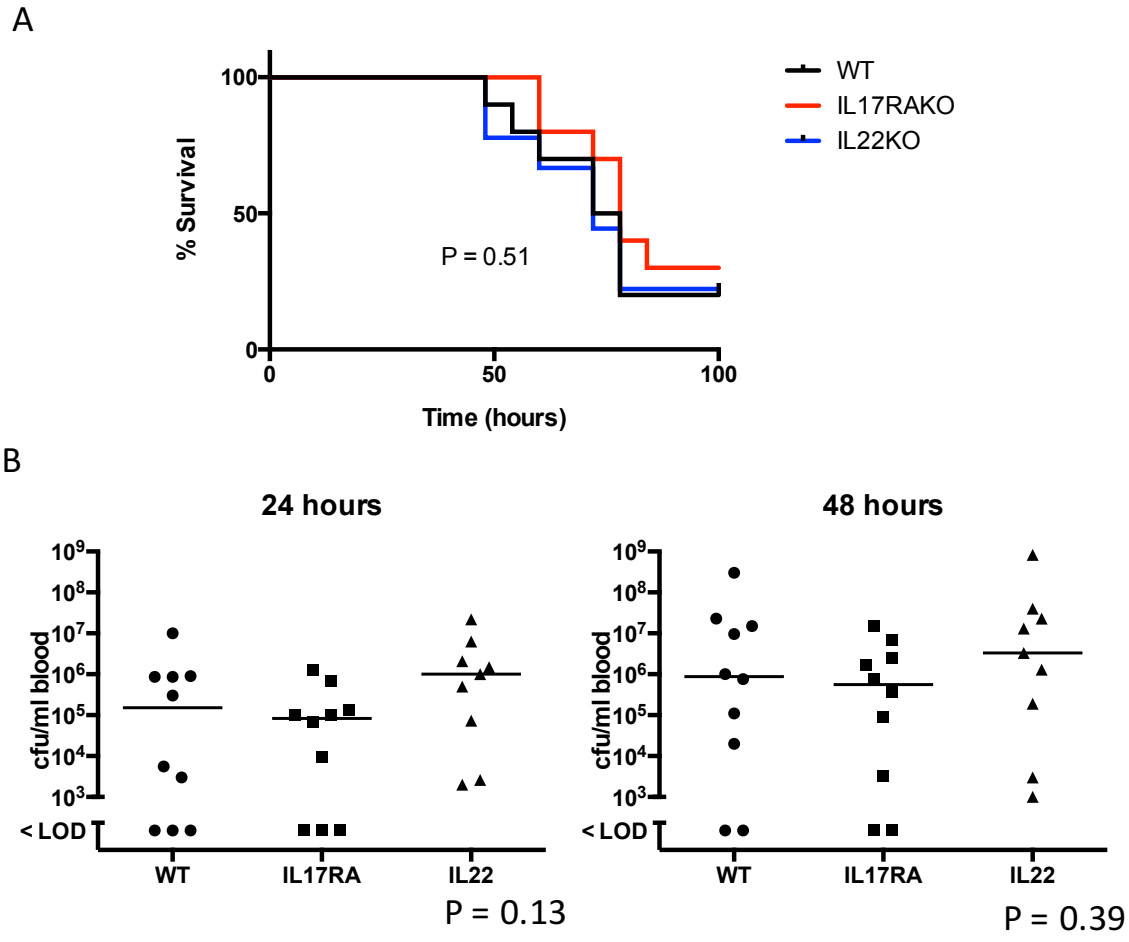

Figure 5-2. Administration of high dose TIGR4 in knockout animals.
Mice (10/group) were given 5 x 10^6 cfu TIGR4 via intranasal innoculation and monitored for 100 hours. A. Kaplan-Meier Plot of survival (log rank test) B. Bacteraemia at 24 and 48 hours showing individual data points (Kruskal-Wallis test).

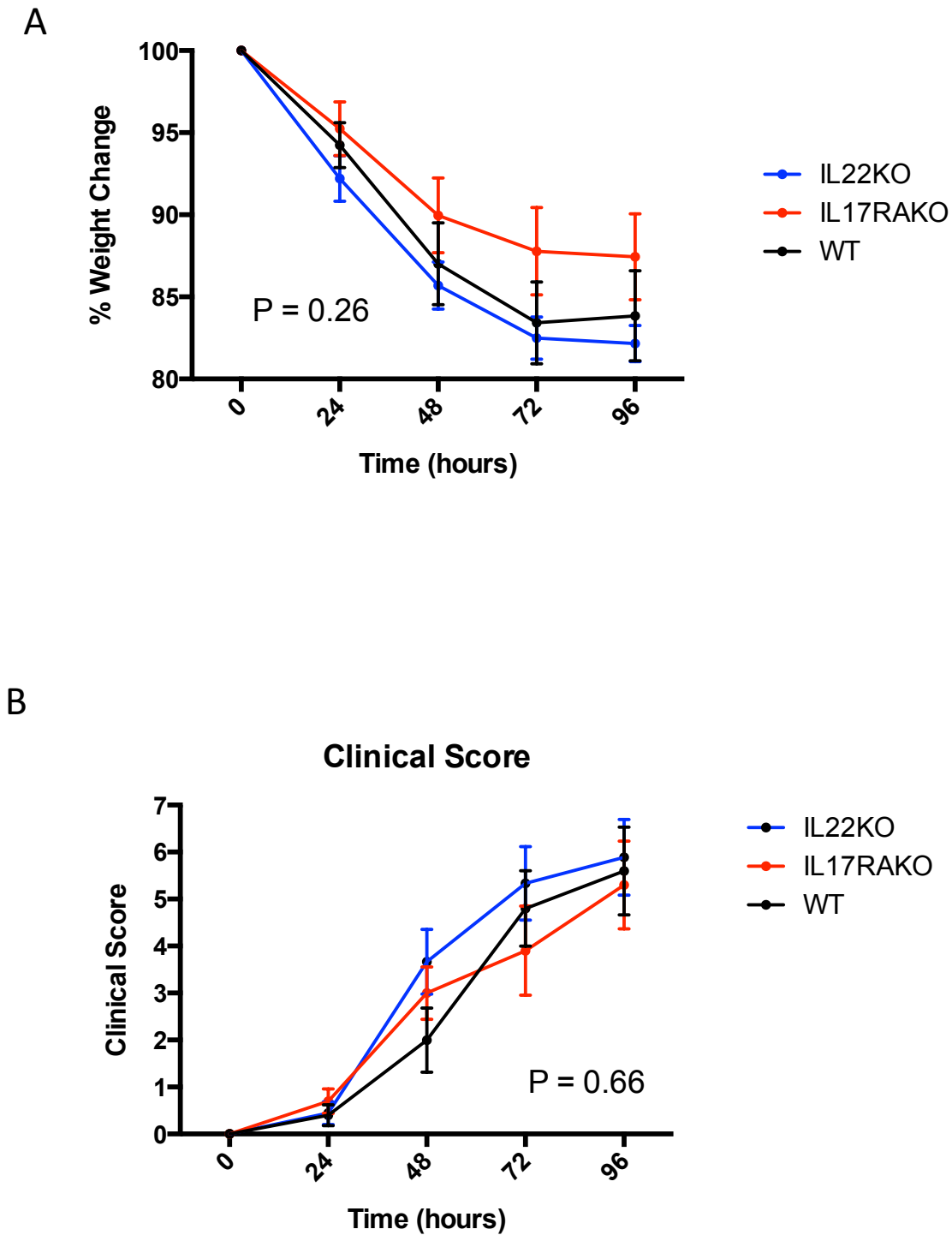

Figure 5-3. Administration of high dose TIGR4 in knockout animals.
Mice (10/group) were given 5 x 10^6 cfu TIGR4 via intranasal innoculation and monitored for 100 hours. A. Mean weight change expressed as percentage of initial body weight ± SEM. B. Mean clinical scores ± SEM. Both P values are two-way ANOVA.

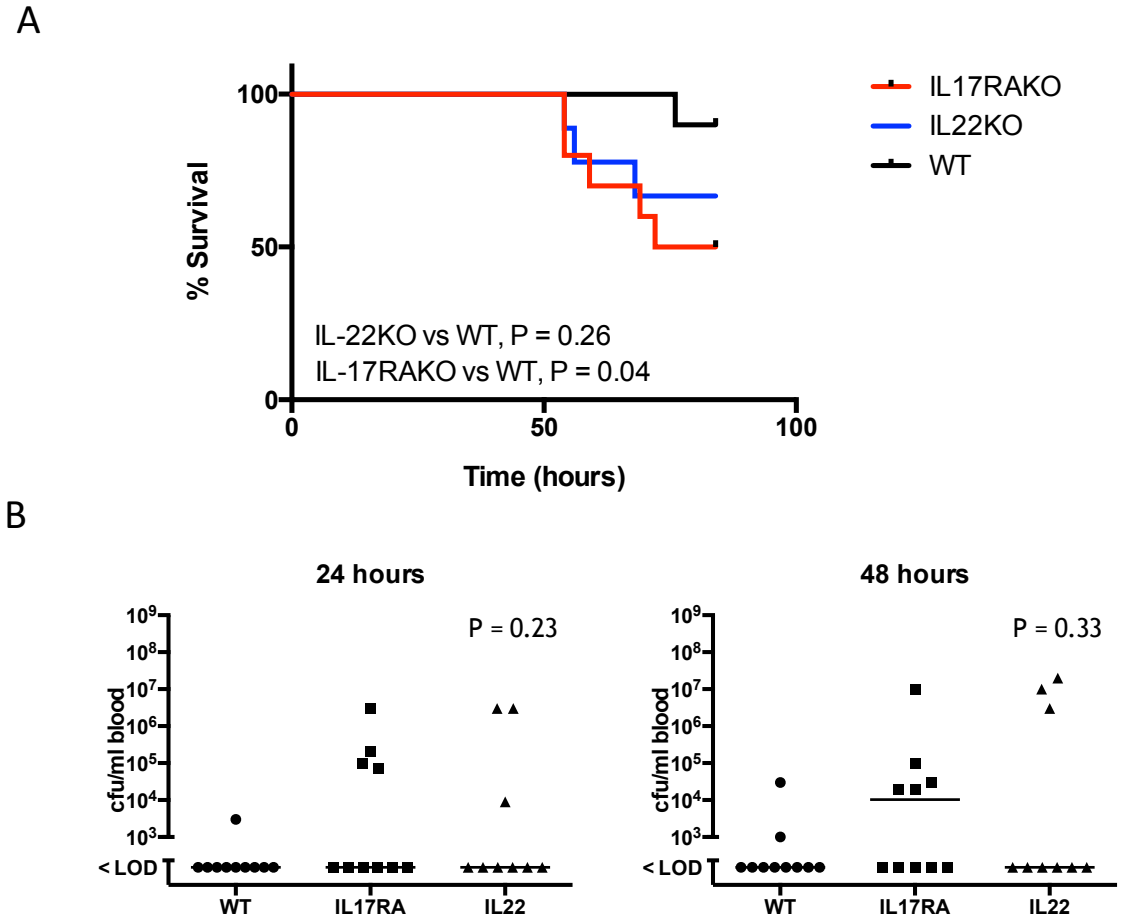

Figure 5-4. Administration of low-dose TIGR4 in knockout animals.

Mice (9-11/group) were given 1 x 10^6 cfu TIGR4 via intranasal innoculation and monitored for 100 hours. A. Kaplan-Meier Plot of survival (log rank test) B. Bacteraemia at 24 and 48 hours showing individual data points. Two-way ANOVA corrected for repeated measures of these data, P =0.06.

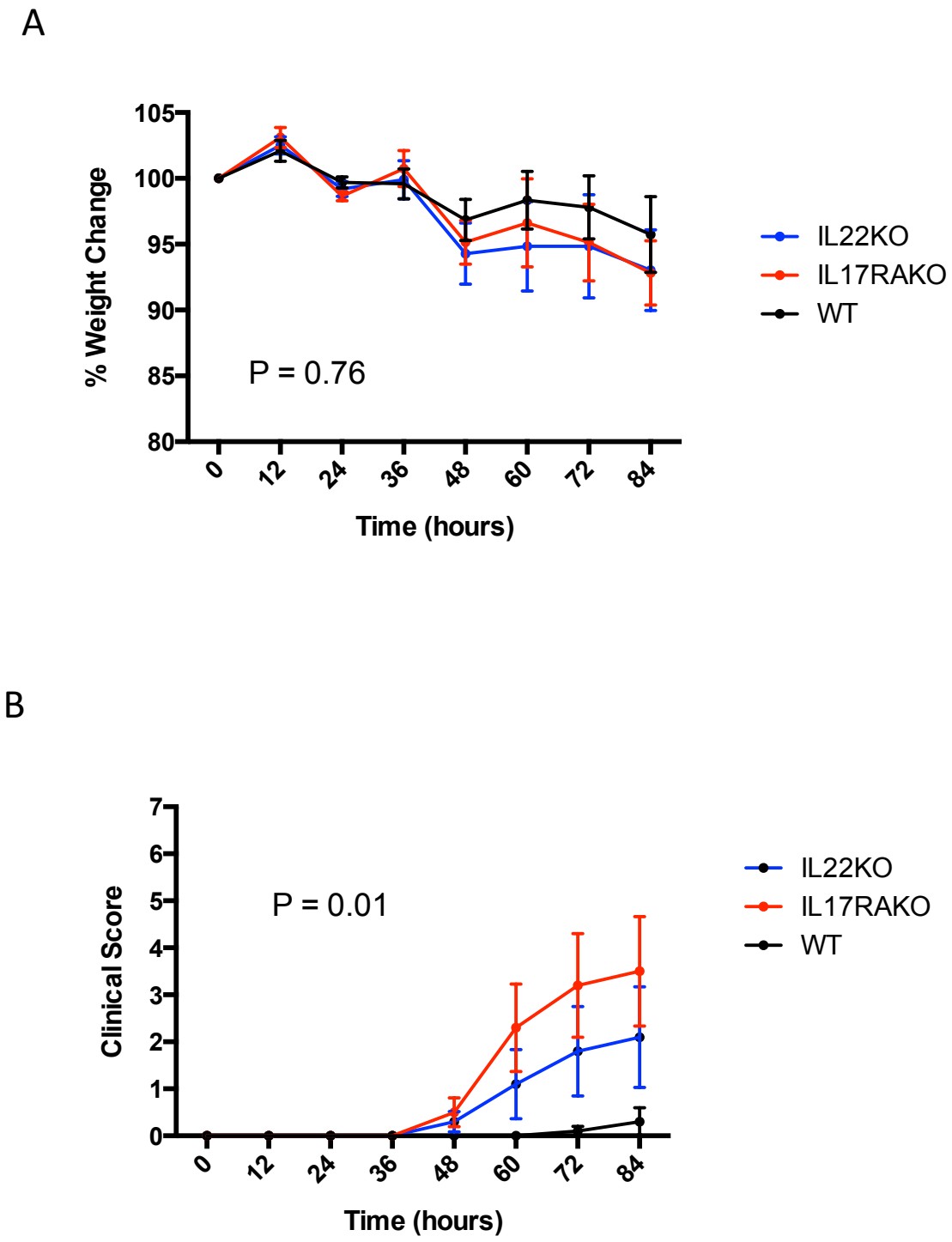

Figure 5-5. Administration of low-dose TIGR4 in knockout animals.
Mice (9-11/group) were given 10^6 cfu TIGR4 via intranasal innoculation and monitored for 100 hours. A. Weight change expressed as percentage of initial body weight ± SEM. B. Clinical scores ± SEM. Both P values are two-way ANOVA.

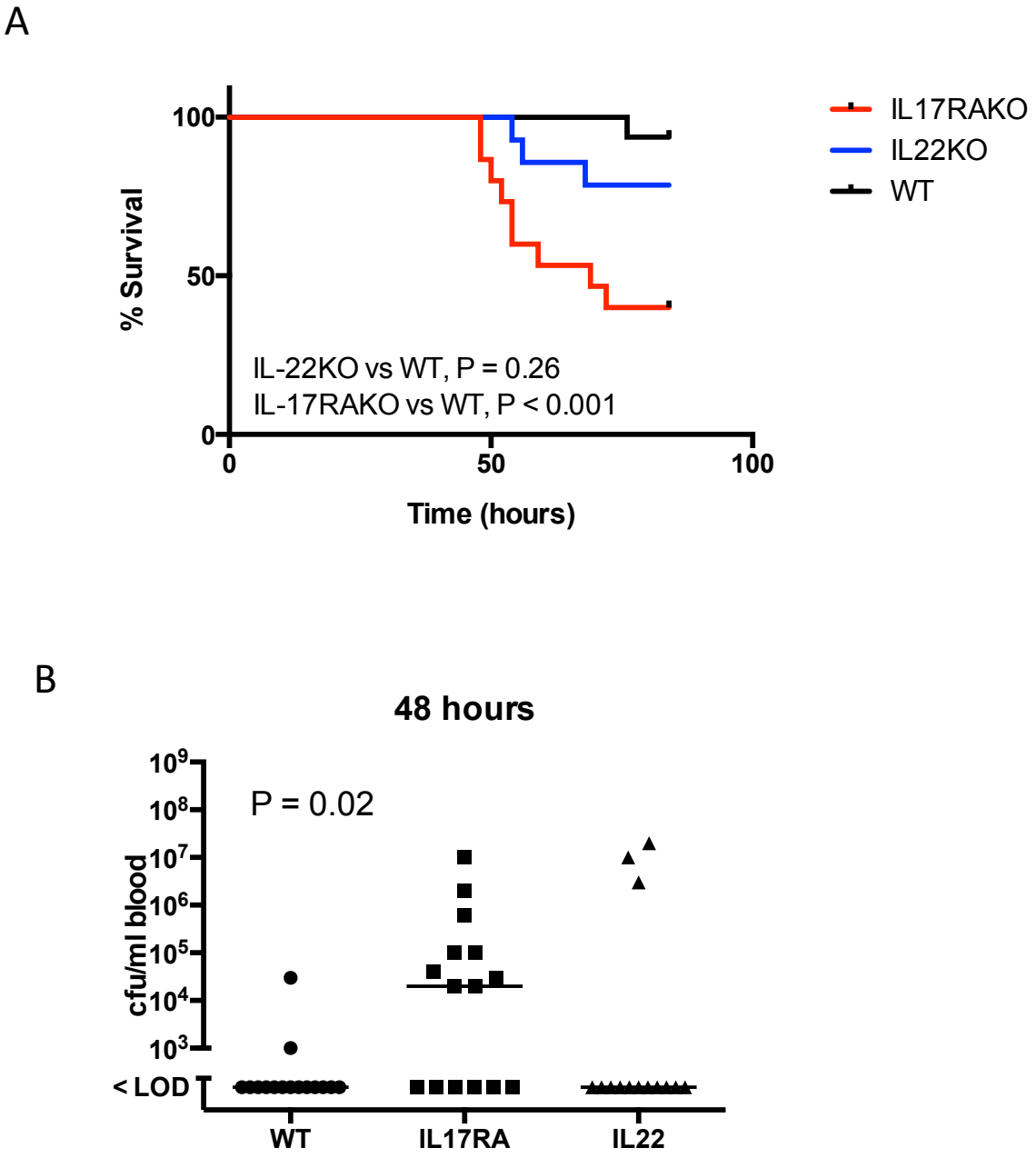

Figure 5-6. Pooled analysis from two experiments involving low dose TIGR4 infection in knock-out animals.

When results are pooled there are a total of 15 animals per group. A. Kaplan-Meier plot (Log rank test). B. Bacteraemia at 48 hours. 24 hour bacteraemia data were not collected in one of the experiments.

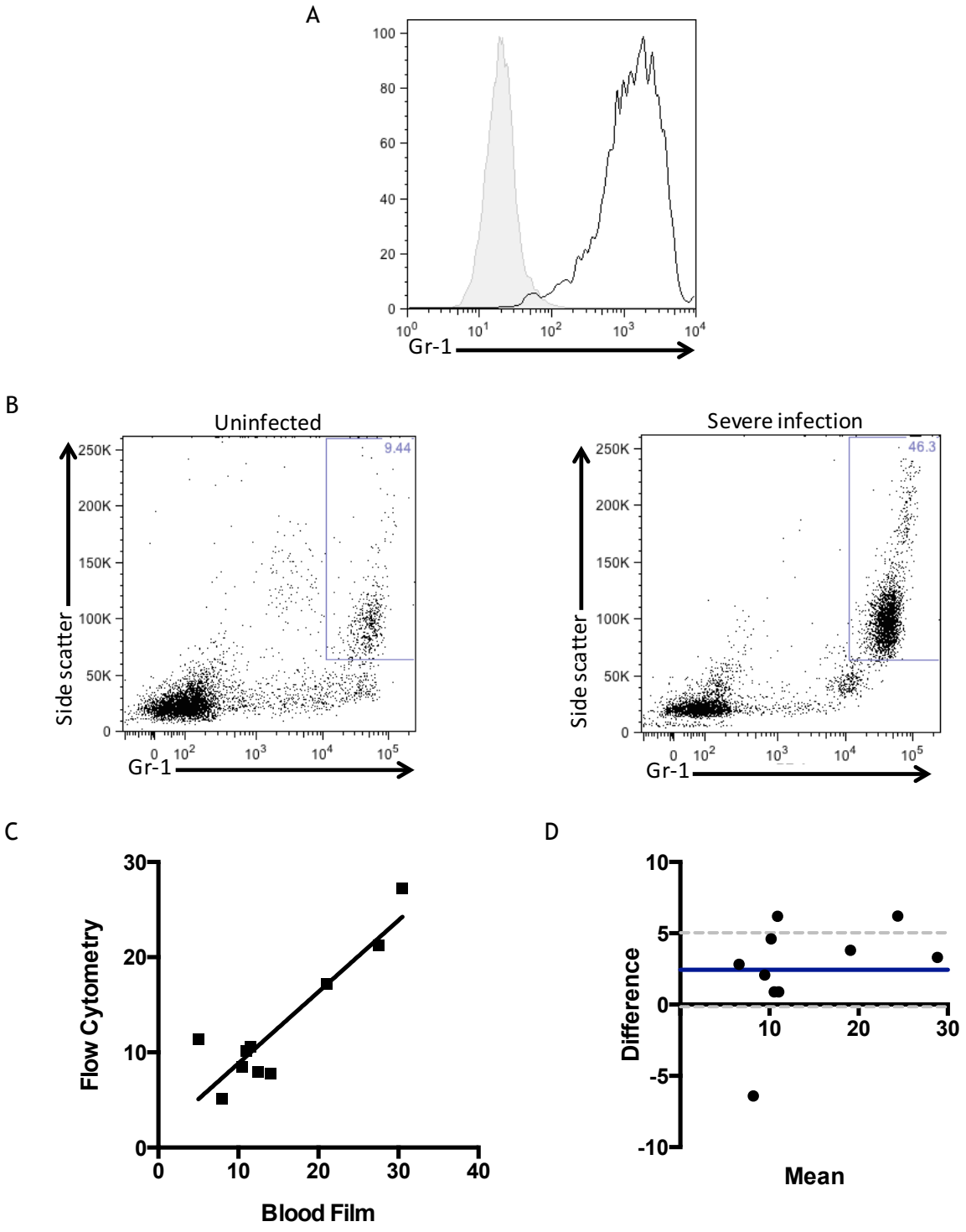

Figure 5-7. Neutrophil identification by flow cytometry.

A. Gr-1 staining of neutrophils purified from peritoneal fluid after injection of 7% casein. Specific antibody staining shown in black with isotype control shaded grey. B. Representative plots from lysed peripheral blood of an uninfected and severely infected mouse. Peripheral blood neutrophil percentages were calculated using blood film manual counting and flow cytometry and plotted as (C) a scatter plot and (D) Bland-Altman plot.

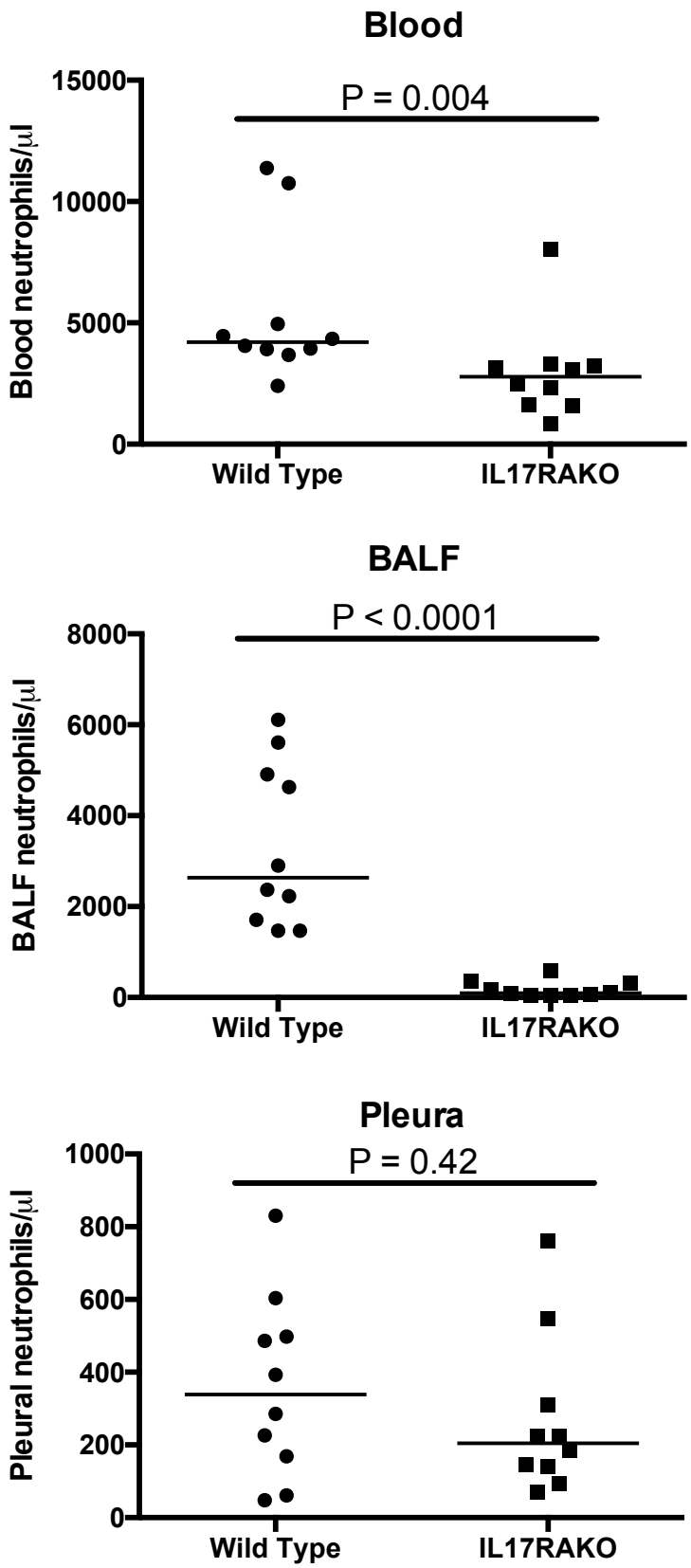

Figure 5-8. Neutrophils in TIGR4 infection.

Wild type or IL-17RA$^{-/-}$ mice were infected with 4 x 10^6 cfu TIGR4 by i.n. route. Absolute neutrophil numbers were quantified by flow cytometry. P values represent results of Mann-Whitney tests.

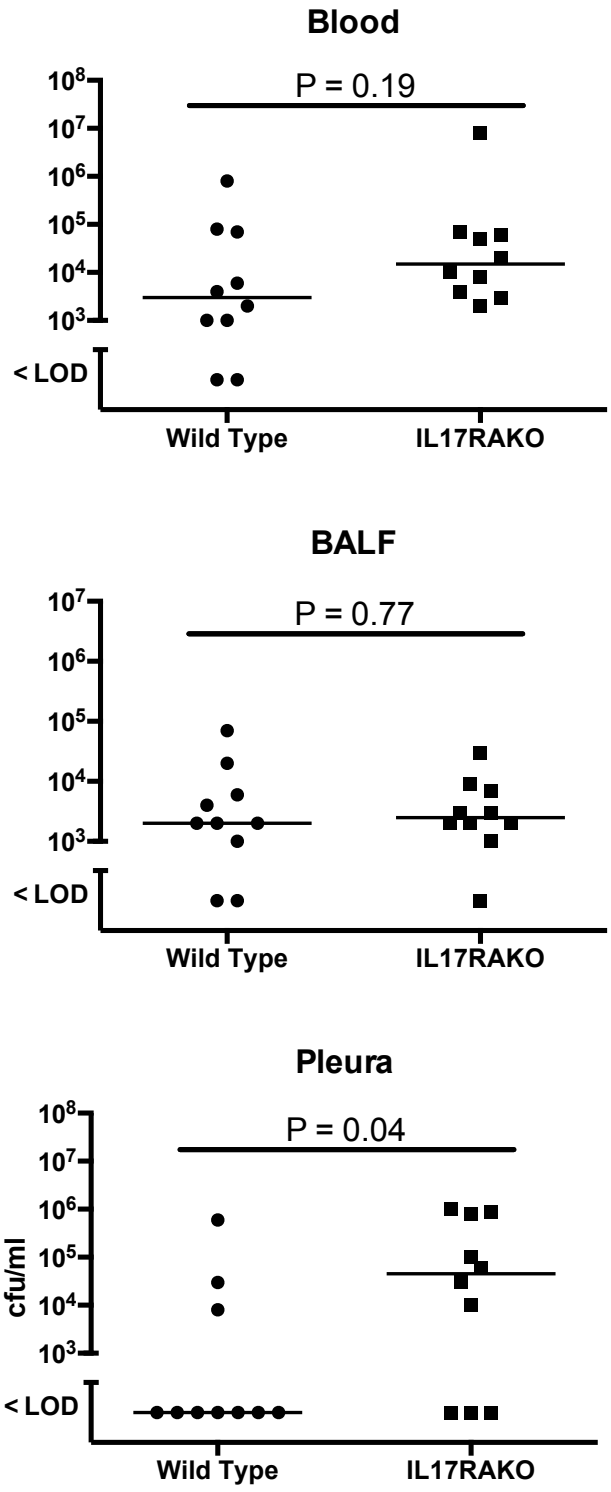

Figure 5-9. Bacterial density in TIGR4 infection.

Wild type or IL-17RA-/- mice were infected with 4 x 10^6 cfu TIGR4 by i.n. route. Bacteria from each site were enumerated by serial dilution. LOD: Limit of detection (10^3 cfu).

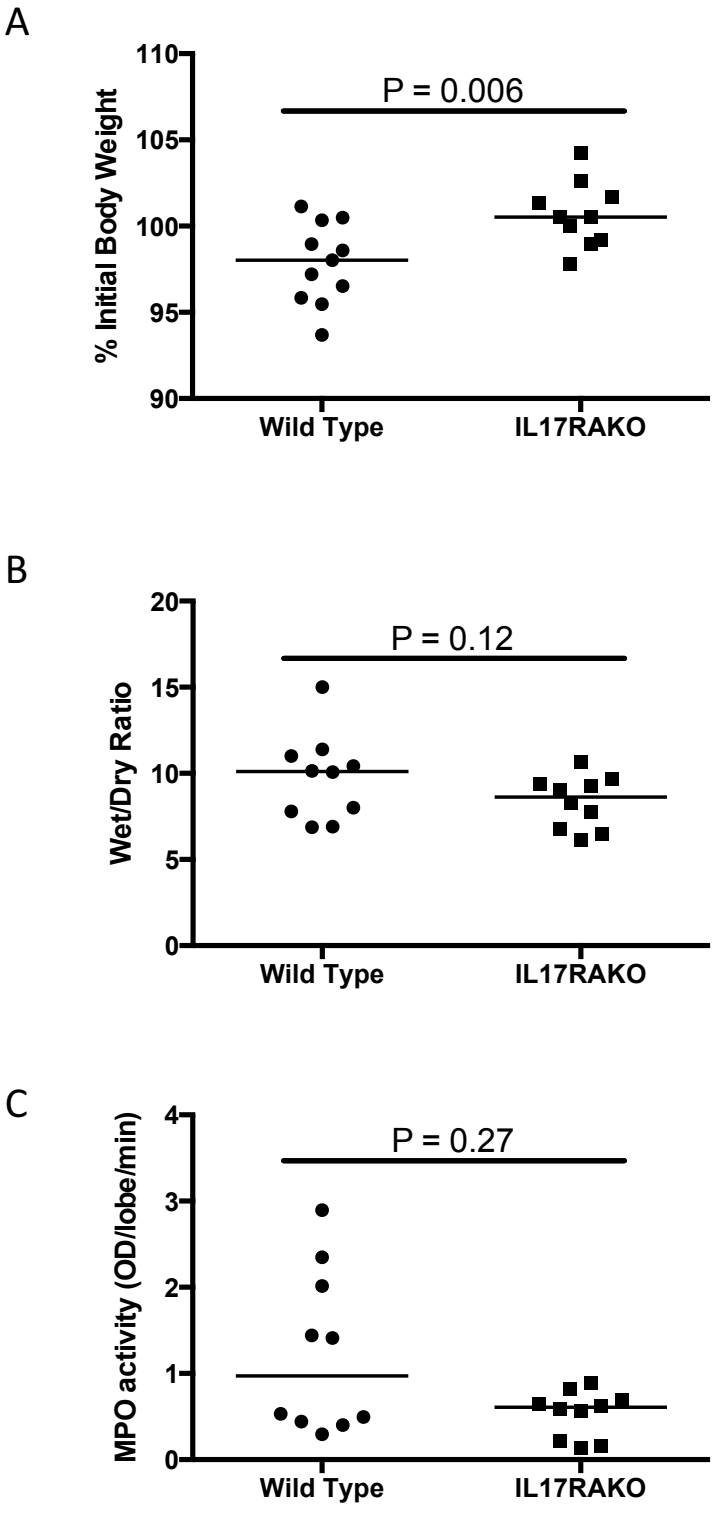

Figure 5-10. Other measures of inflammation during TIGR4 infection.
Wild type or IL-17RA$^{-/-}$ mice were infected with 4 x 10^6 cfu TIGR4 by i.n. route and culled after 24 hours. A. % of initial body weight. B. Lung wet/dry ratio. C. Lung MPO assay.

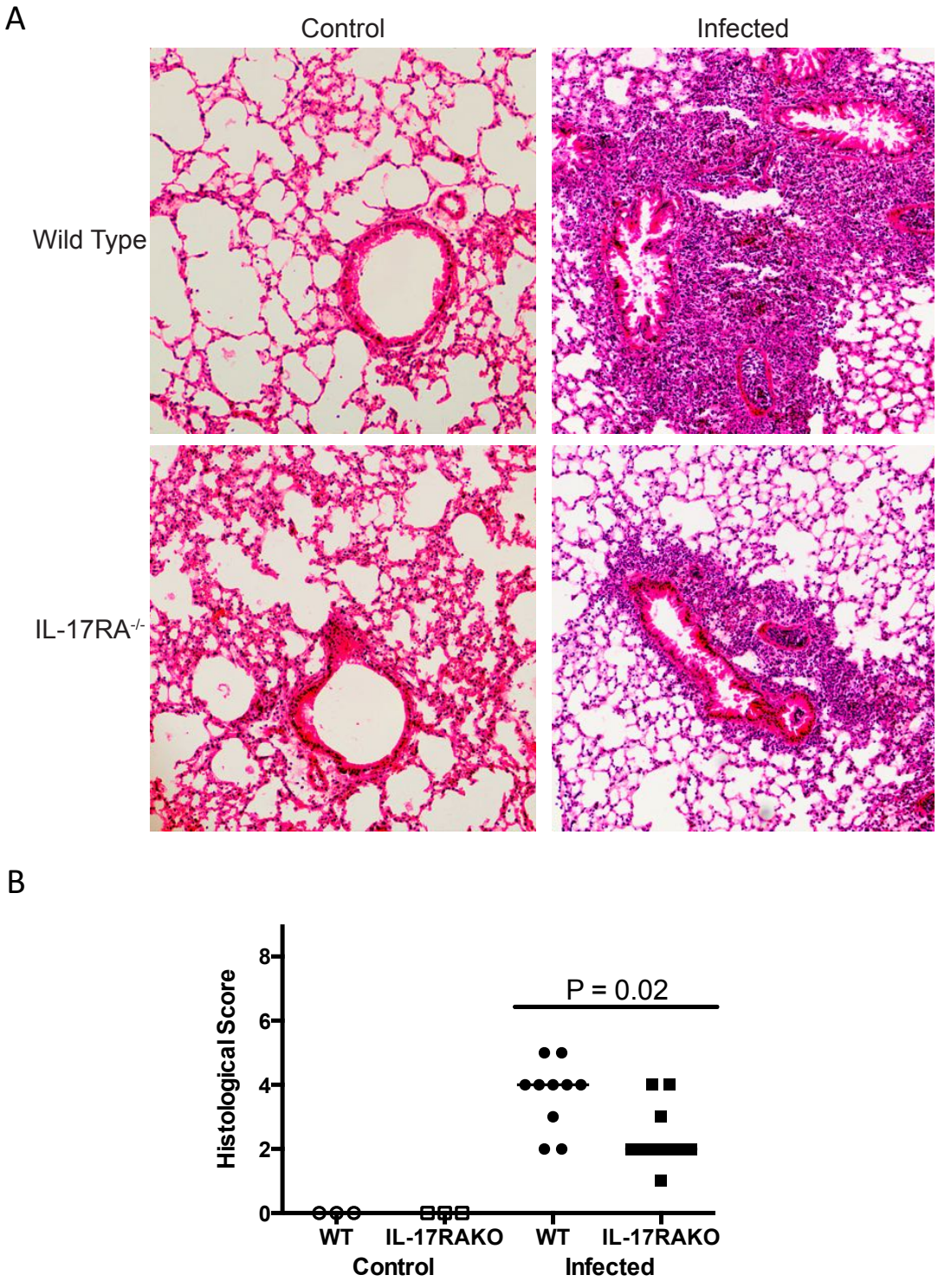

Figure 5-11. Comparison of IL17RA$^{-/-}$ and wild type mice in TIGR4 infection. Mice were infected with 4 x 10^6 cfu TIGR4 and culled 24 hours later. A. H&E stained tissue sections from infected and control mice. Control mice were not included in experiment so control sections are taken from banked uninfected animals. Among infected mice, images show the most significant area of inflammation from the mouse in each group with the median histological score (B). P value represents Mann Whitney test.

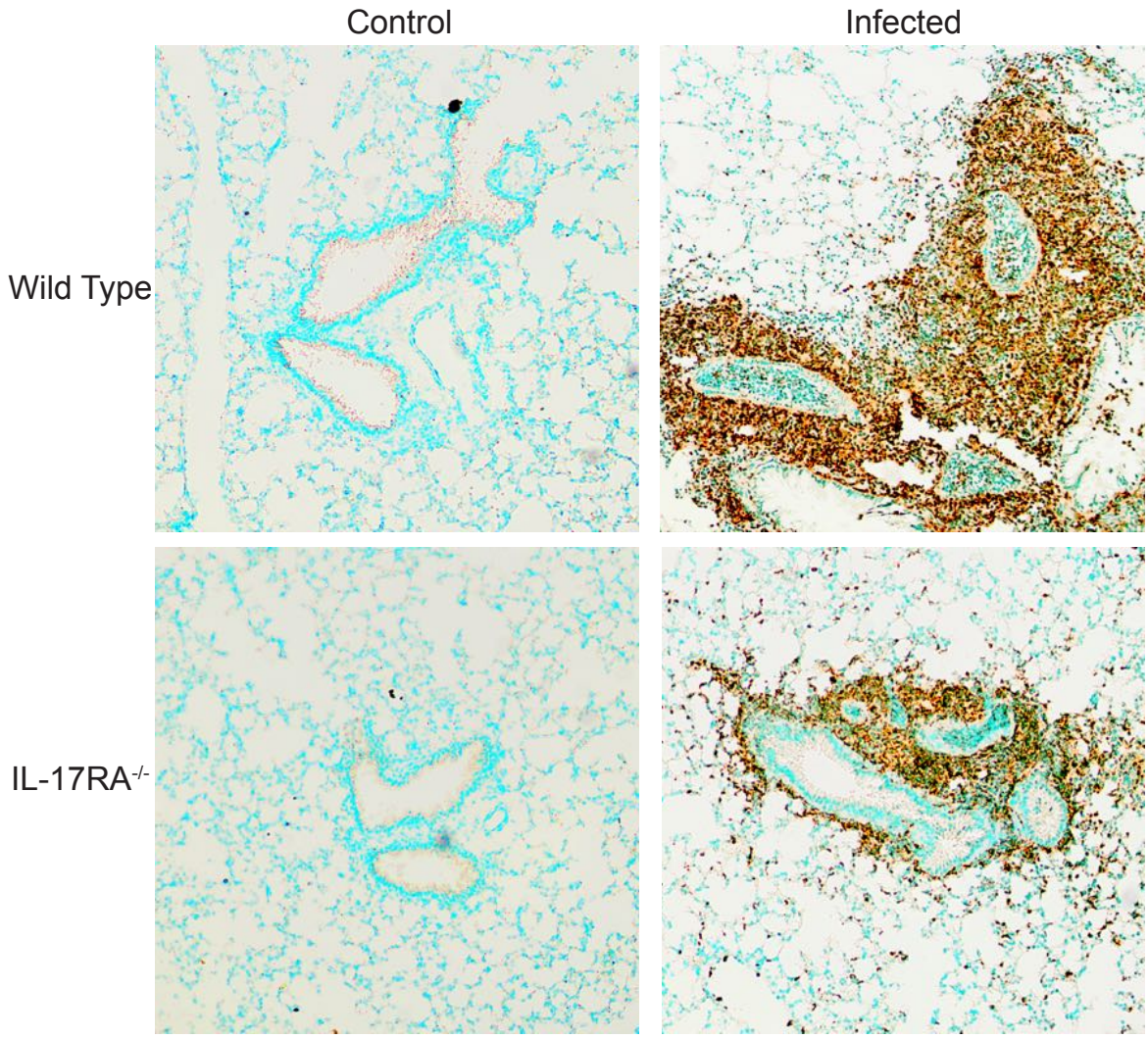

Figure 5-12. Comparison of IL17RA-/- and wild type mice in TIGR4 infection. Mice were infected with 4 x 10^6 cfu TIGR4 and culled 24 hours later. Zinc fixed sections were incubated with anti-Ly6G antibody (1A8) before goat anti-rat secondary before developing with 3,3'-diaminobenzidine and counterstaining with methyl green.

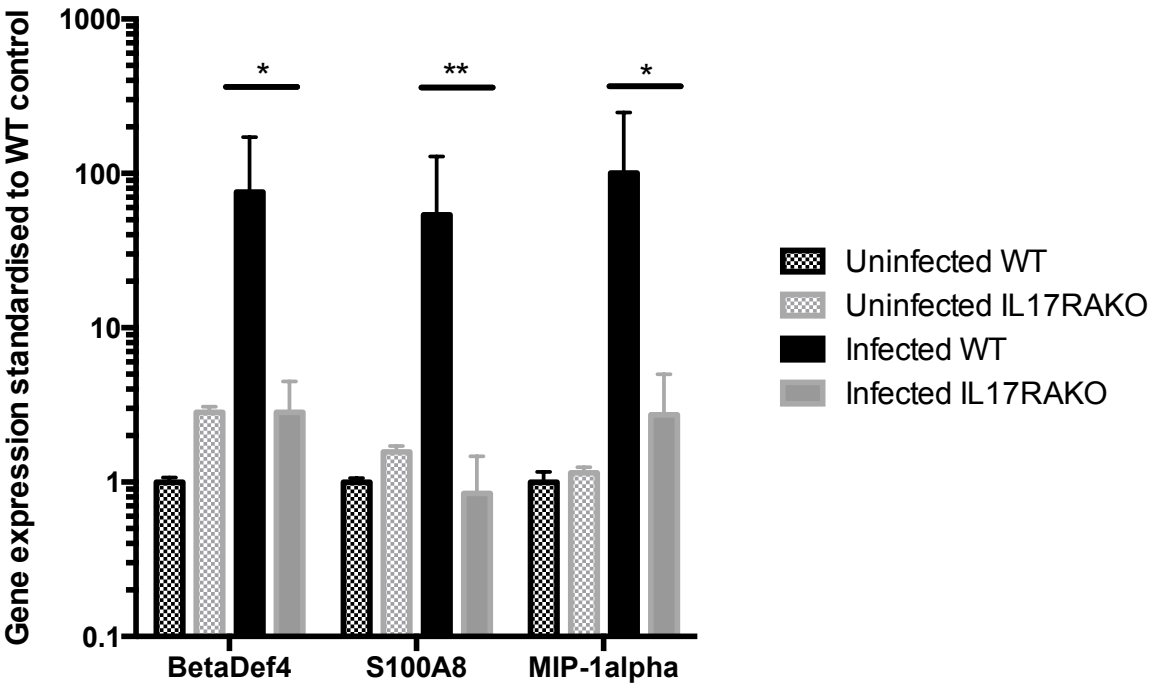

Figure 5-13. Gene expression of IL-17 target genes in TIGR4 infection.
Gene expression was quantified by RT-PCR in wild type and IL17RA$^{-/-}$ animals 12 hours after infection with 10^6 cfu of TIGR4 (n=3/group). Gene expression is normalised to expression of TATA-binding protein (TBP) and expressed as a ratio of expression in uninfected wild-type animals ± SEM. P values calculated by Student's t-test : * <0.05, ** <0.01.

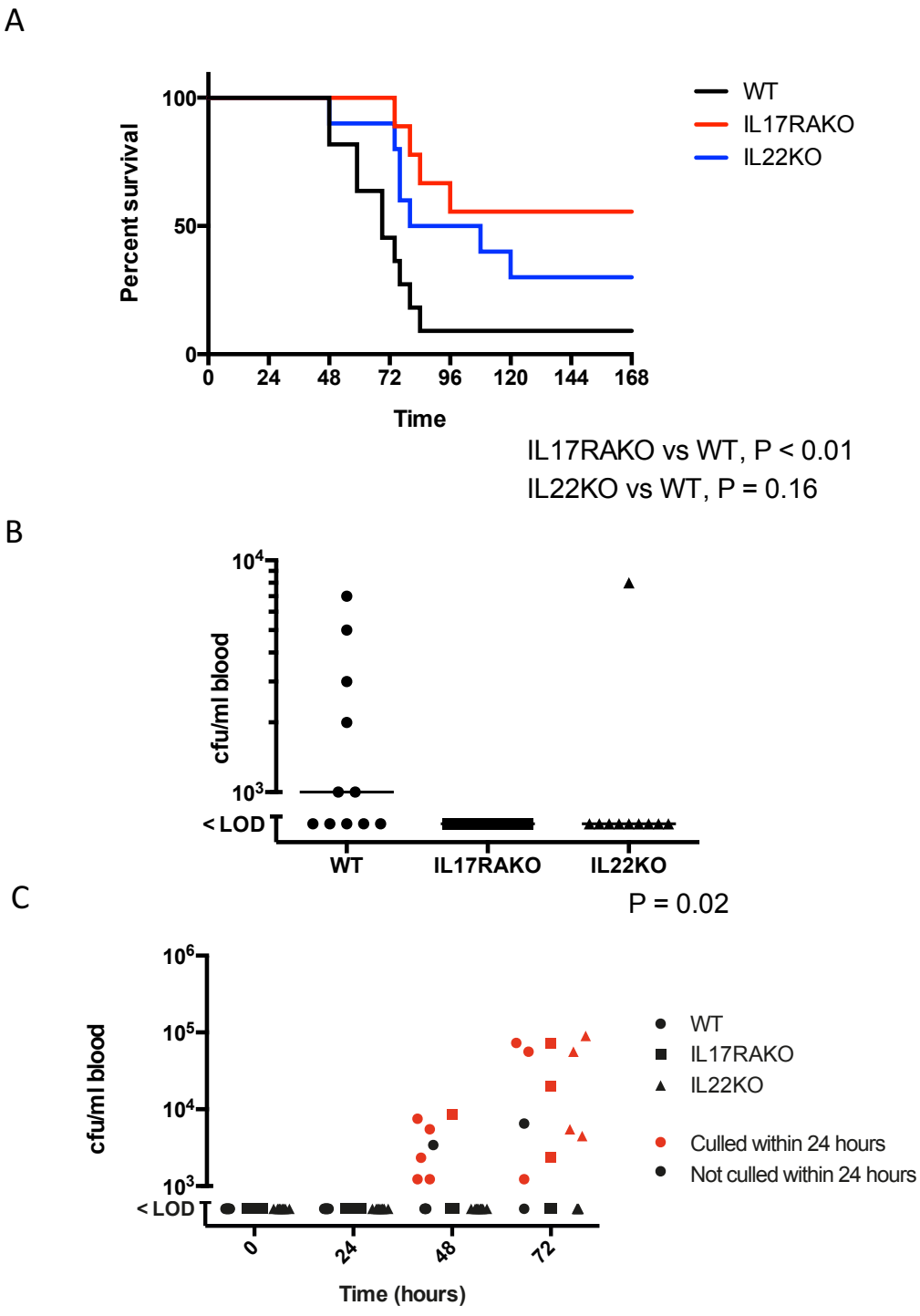

Figure 5-14. Comparison of IL17RA$^{-/-}$, IL22$^{-/-}$ and WT mice in SRL1 infection. Mice (9-11/group) were infected with 10^6 cfu SRL1 and monitored for 7 days. A. Kaplan-Meier survival plot (Log rank test). Level of bacteraemia at (B) 48 hours post-infection (Kruskal-Wallis test) and (C) plotted over the first 72 hours of the infection. Mice culled within 24 hours of blood sampling are shown in red (and are not shown plotted for subsequent time-points).

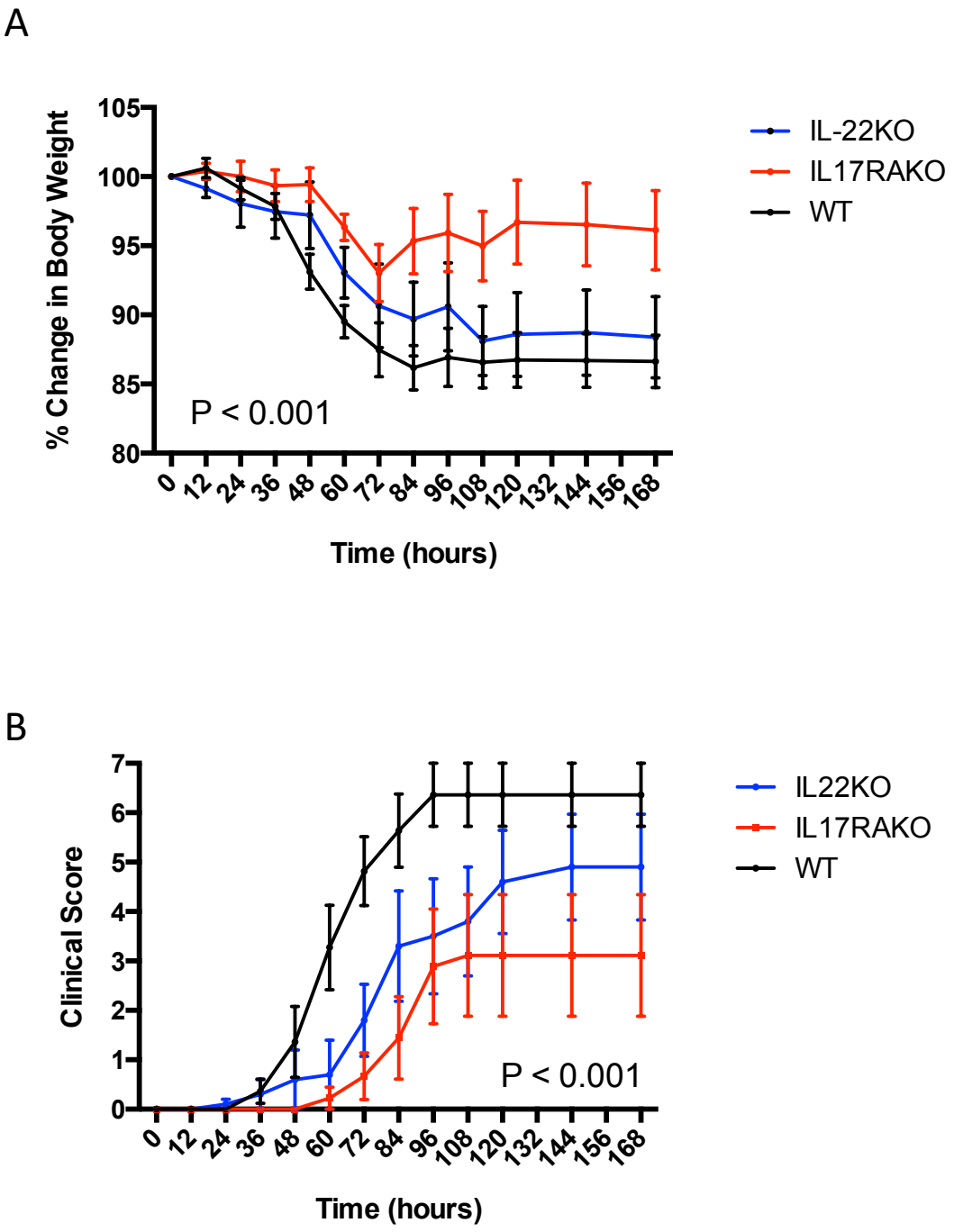

Figure 5-15. Comparison of IL17RA-/-, IL22-/- and WT mice in SRL1 infection. Mice (9-11/group) were infected with 10^6 cfu SRL1 and monitored for 7 days. A. % change in weight. B. Clinical score. Both are expressed as mean ± SEM (two-way ANOVA).

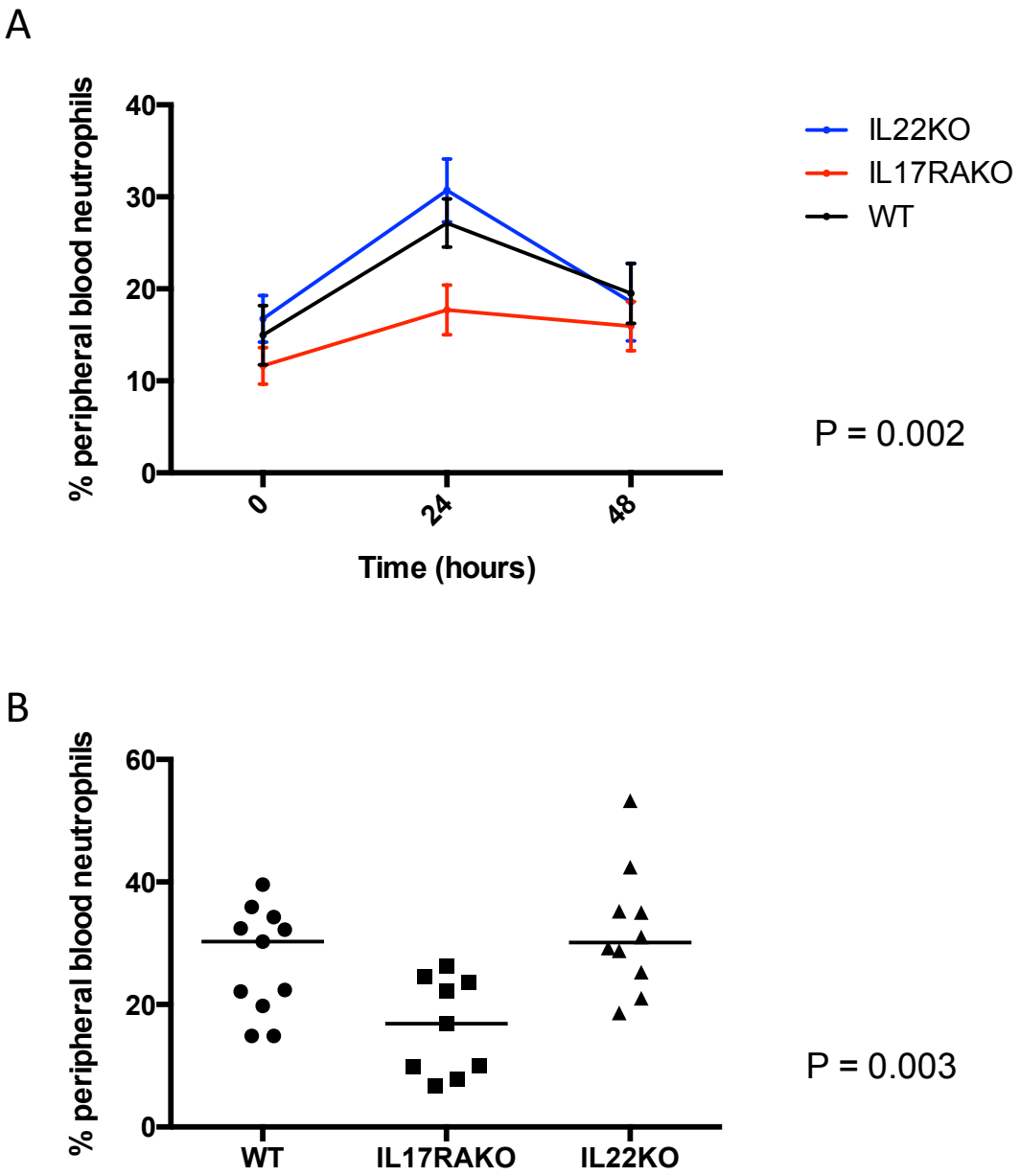

Figure 5-16. Comparison of IL17RA$^{-/-}$, IL22$^{-/-}$ and WT mice in SRL1 infection. Mice (9-11/group) were infected with 10^6 cfu SRL1 and monitored for 7 days. A. Peripheral blood neutrophil counts during initial 48 hours of experiment expressed as mean ± SEM (two-way ANOVA). B. Individual data points at 24 hours (one-way ANOVA).

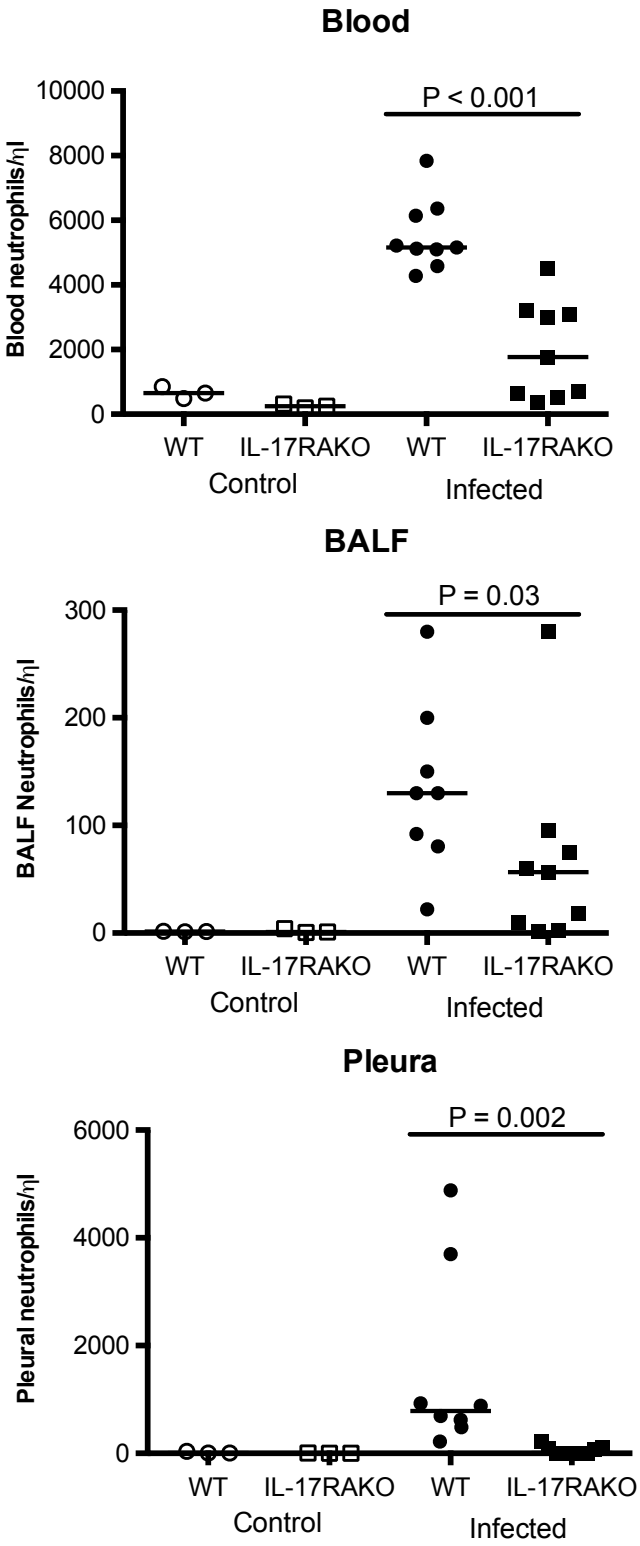

Figure 5-17. Comparison of IL17RA$^{-/-}$ and wild type mice in SRL1 infection. Mice were infected with 10^6 cfu SRL1 and culled 24 hours later. Neutrophils were quantified by flow cyotmetry. In peripheral blood, neutrophil percentage of total white blood cells was calculated while in BALF and pleura, absolute neutrophil numbers were calculated. P values represent results of Mann-Whitney tests.

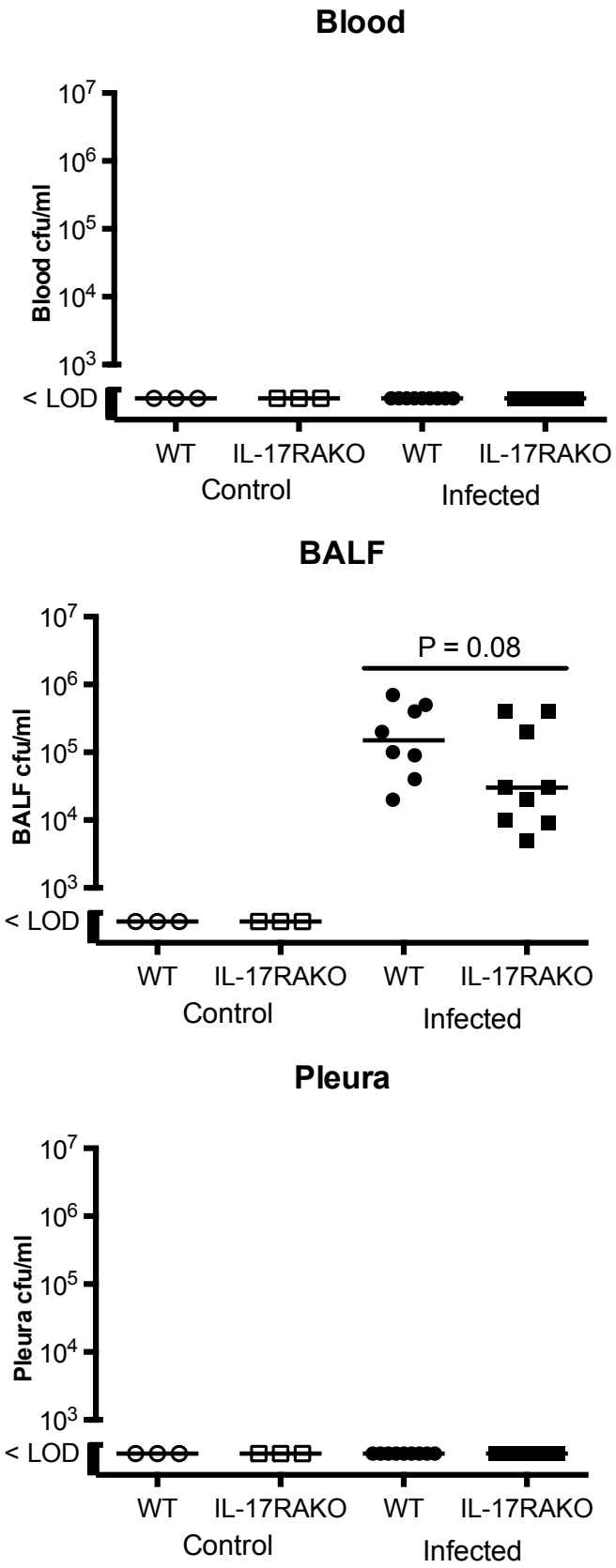

Figure 5-18. Comparison of IL17RA$^{-/-}$ and wild type mice in SRL1 infection. Mice were infected with 10^6 cfu SRL1 and culled 24 hours later. No bacteria were recovered from blood or pleural wash fluid. Bacterial counts in BALF are shown (Mann-Whitney test). Limit of detection (LOD) = 10^3 cfu/ml

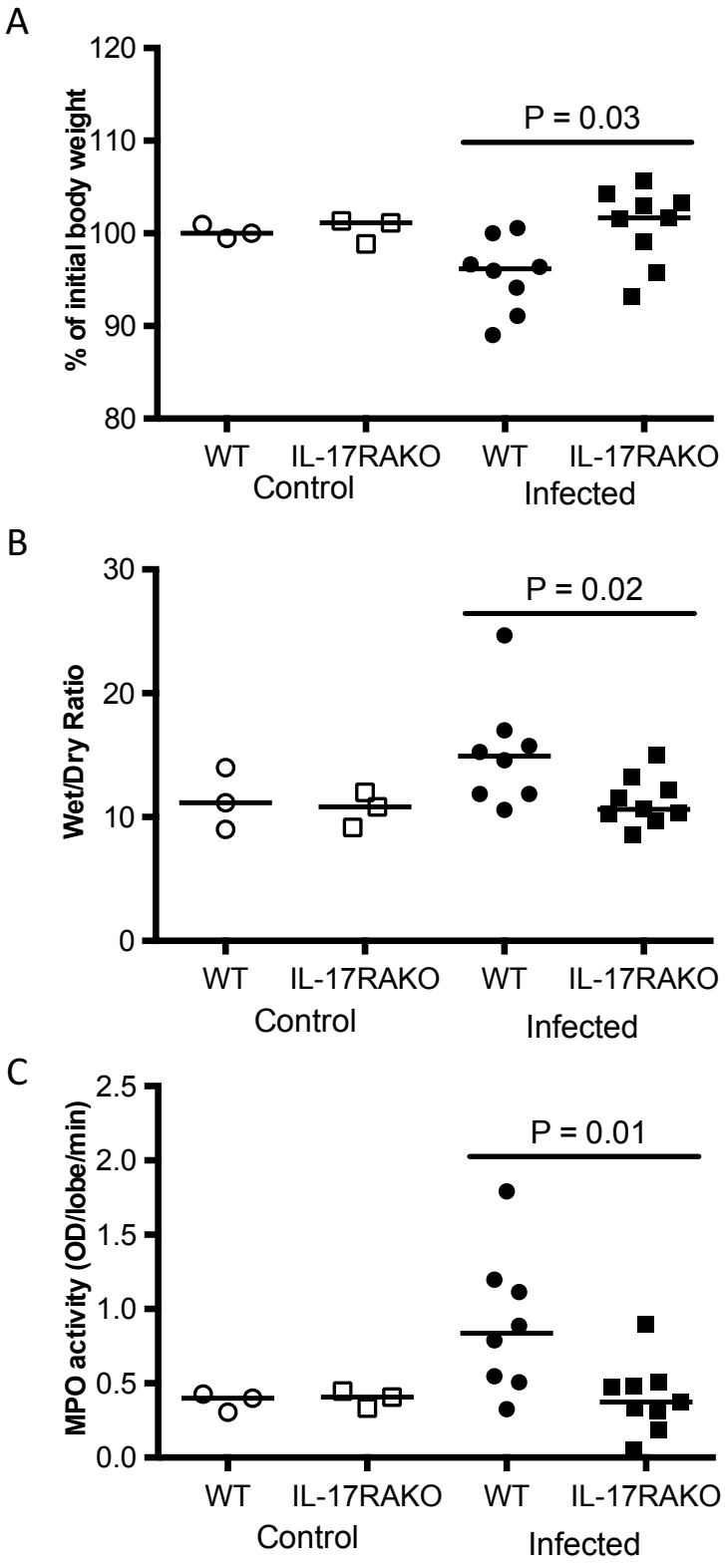

Figure 5-19. Comparison of IL17RA$^{-/-}$ and wild type mice in SRL1 infection. Mice were infected with 10^6 cfu SRL1 and culled 24 hours later. A. Percentage change in body weight. B. Ratio of the wet weight of a single lobe of lung to the weight after heating to 60˚C for 48 hours. C. MPO activity of a single lobe of lung expressed in arbitrary units.

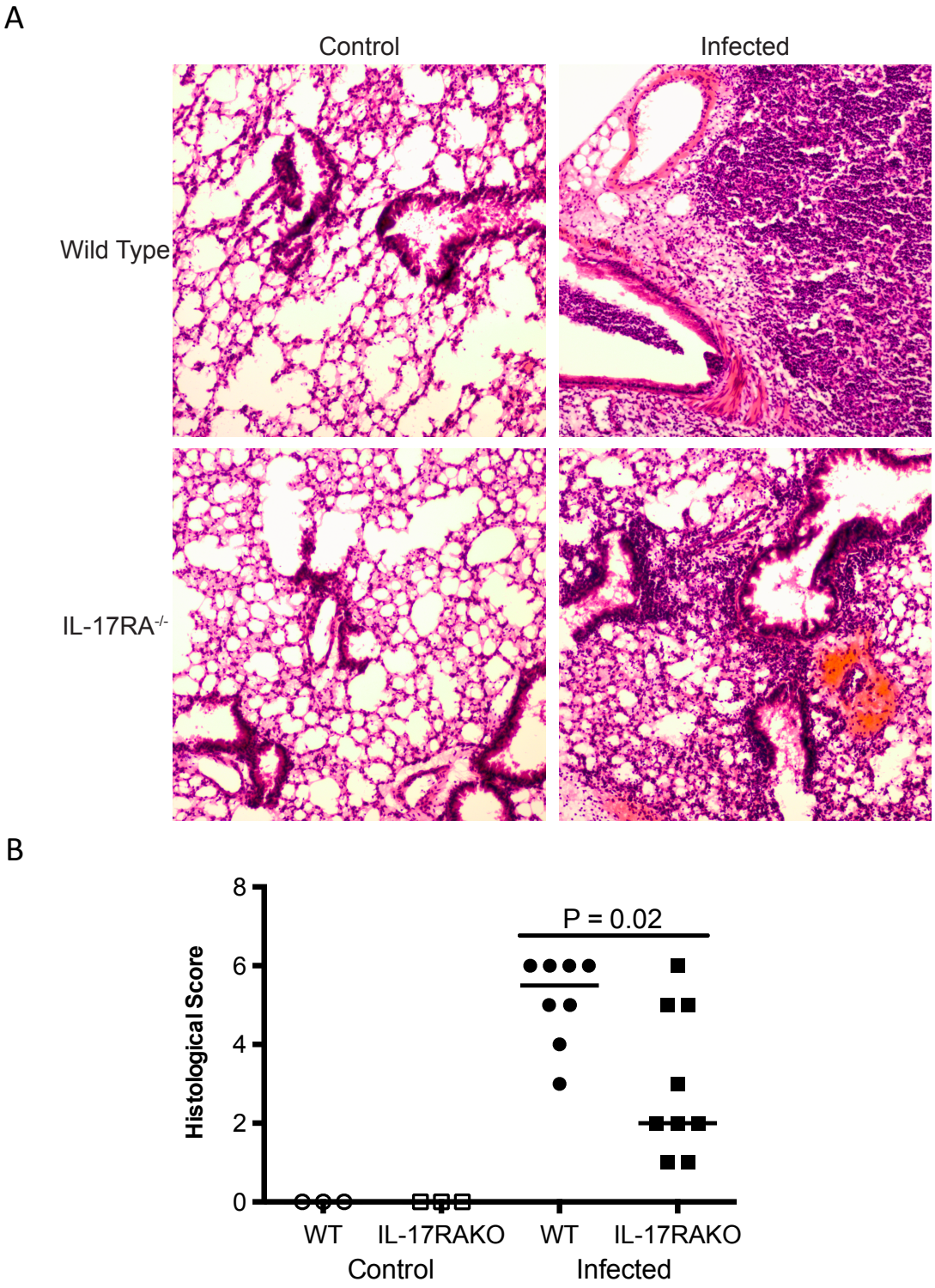

Figure 5-20. Comparison of IL17RA$^{-/-}$ and wild type mice in SRL1 infection. Mice were infected with 10^6 cfu SRL1 and culled 24 hours later. A. H&E stained tissue sections from infected and control mice. Among infected mice, images show the most significant area of inflammation from the mouse in each group with the median histological score (B). P value represents Mann Whitney test.

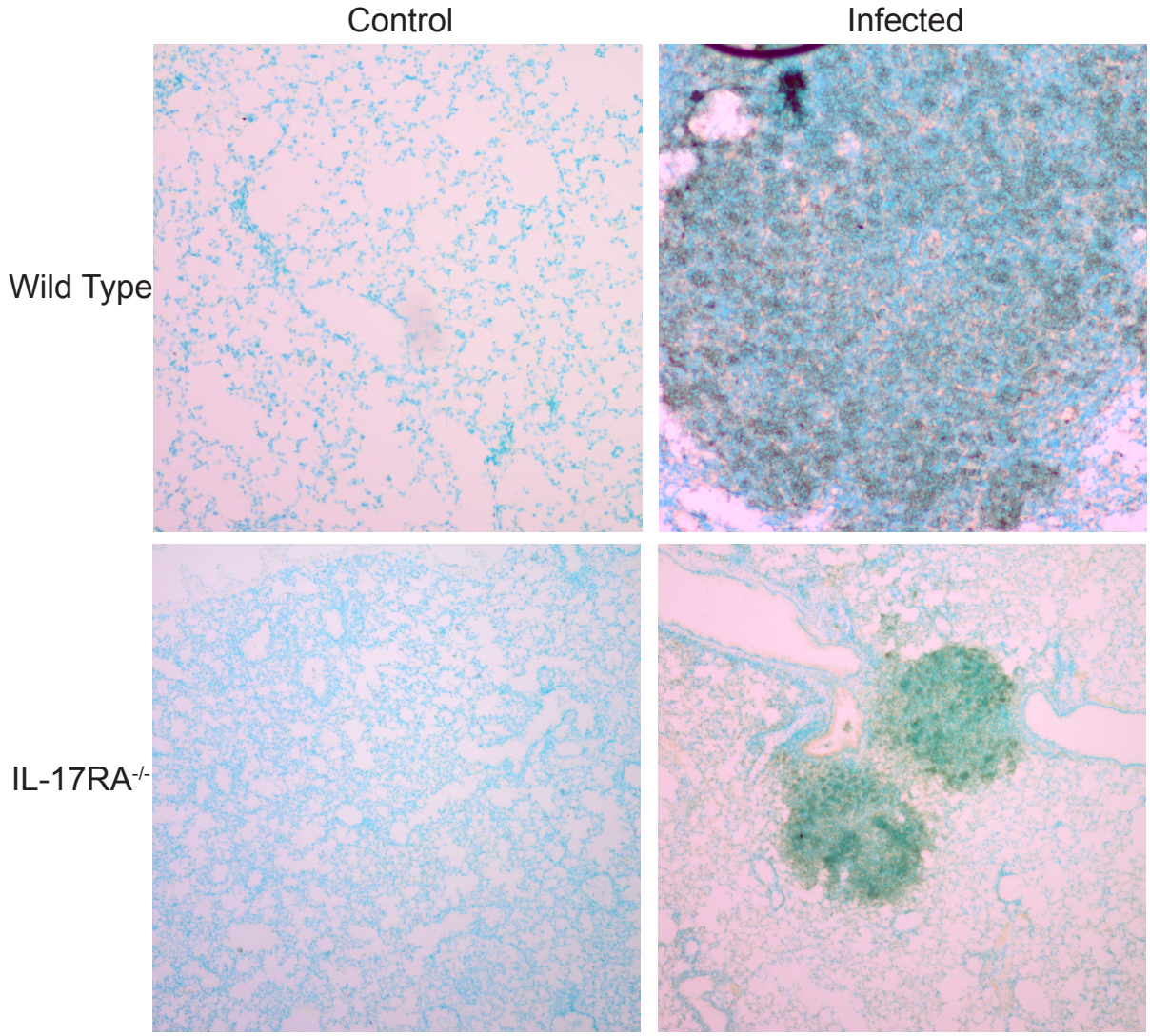

Figure 5-21. Comparison of IL17RA$^{-/-}$ and wild type mice in SRL1 infection. Mice were infected with 10^6 cfu SRL1 and culled 24 hours later. Lungs from infected and control animals were labeled with rat anti-Ly6G antibody and goat anti-rat secondary before developing with 3,3'-diaminobenzidine and counterstaining with methyl green.

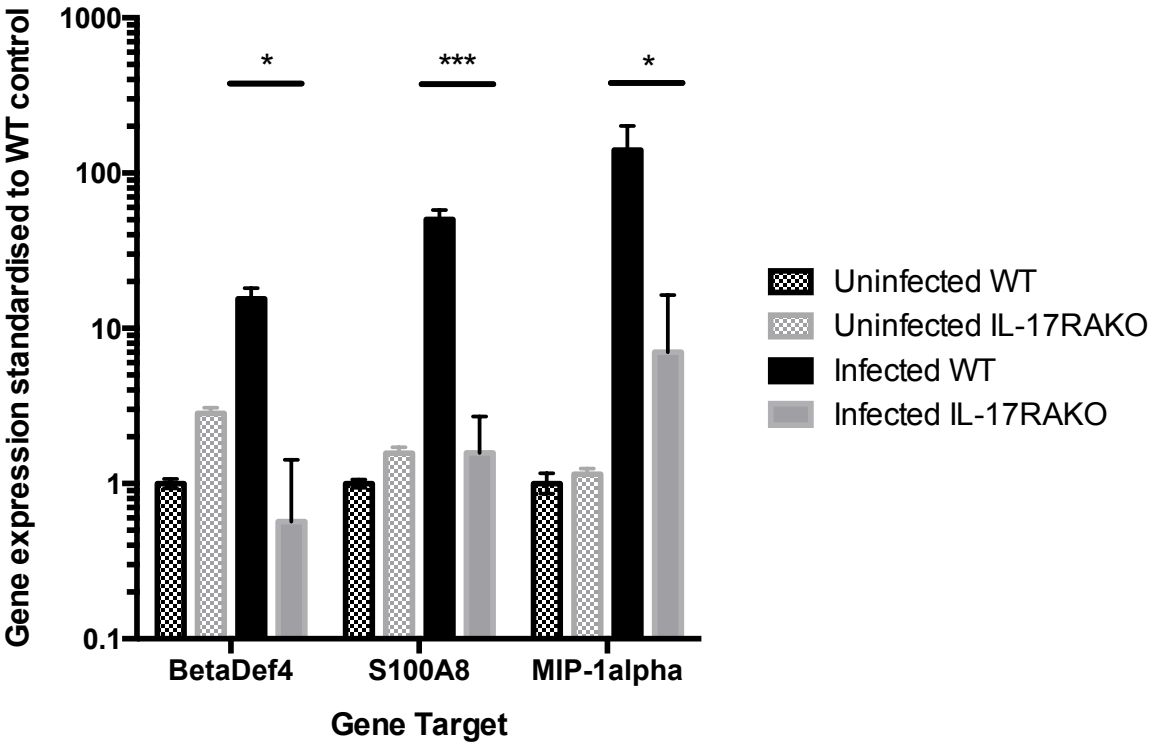

Figure 5-22. Gene expression of IL-17 target genes in SRL1 infection.
Gene expression was quantified by RT-PCR in wild type and IL17RA$^{-/-}$ animals 12 hours after infection with 10^6 cfu SRL1 **(n = 3/group)**. Gene expression is normalised to expression of TATA-binding protein (TBP) and expressed as a ratio of expression in uninfected wild-type animals ± SEM. P values calculated by Student's t-test : * <0.05, *** <0.001.

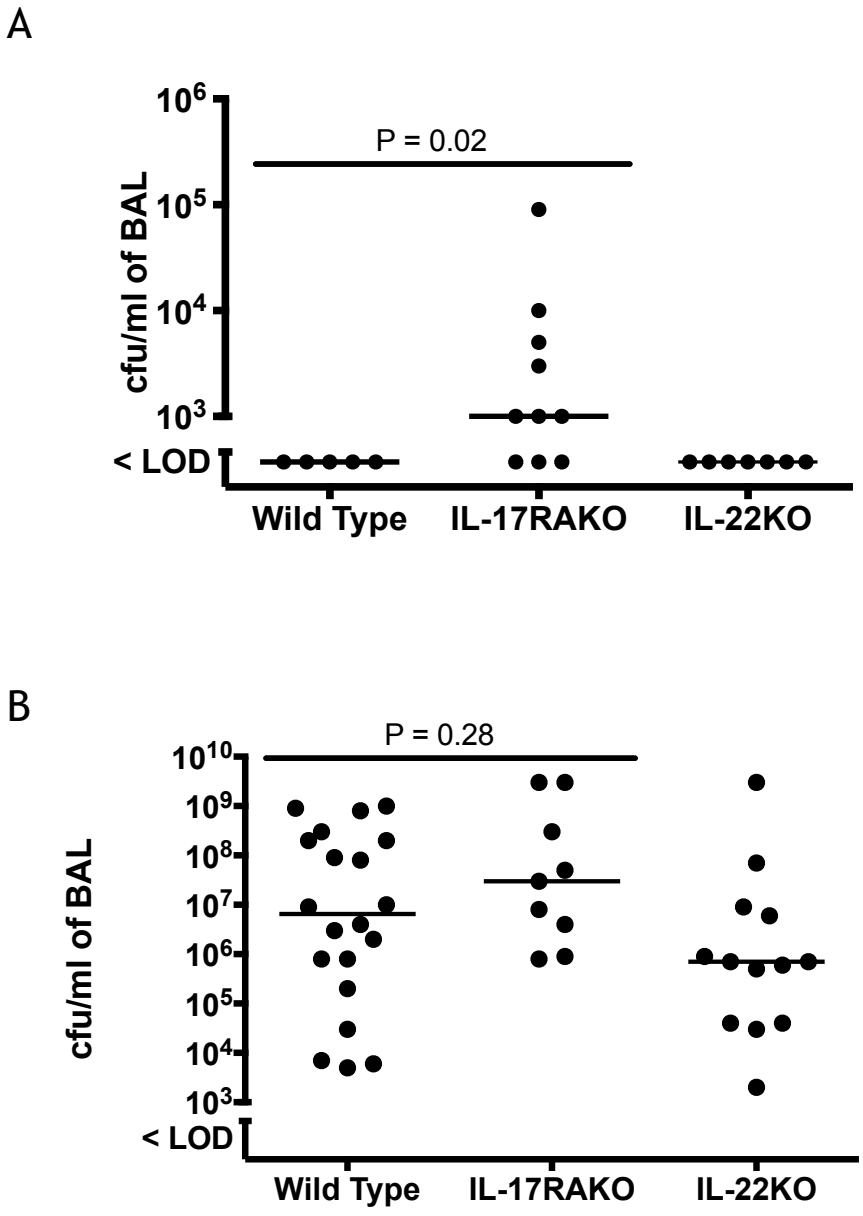

Figure 5-23. Persistent lower respiratory tract bacteria in IL17RA$^{-/-}$ mice following infection with 10^6 cfu SRL1.

A. Surviving mice were killed after 7 days and pneumococci in BAL fluid were quantified (Mann-Whitney test). Results from four experiments involving wild-type and/or IL17RA$^{-/-}$ animals infected with SRL1 and monitored for one week were pooled for this analysis. 3/5 (80%) of mice had received 500µg of the rat monoclonal antibody 2A3 (an isotype control), which is not believed to have significant biological effects. B. There was no difference in the bacterial counts among animals succumbing to infection with SRL1.

A

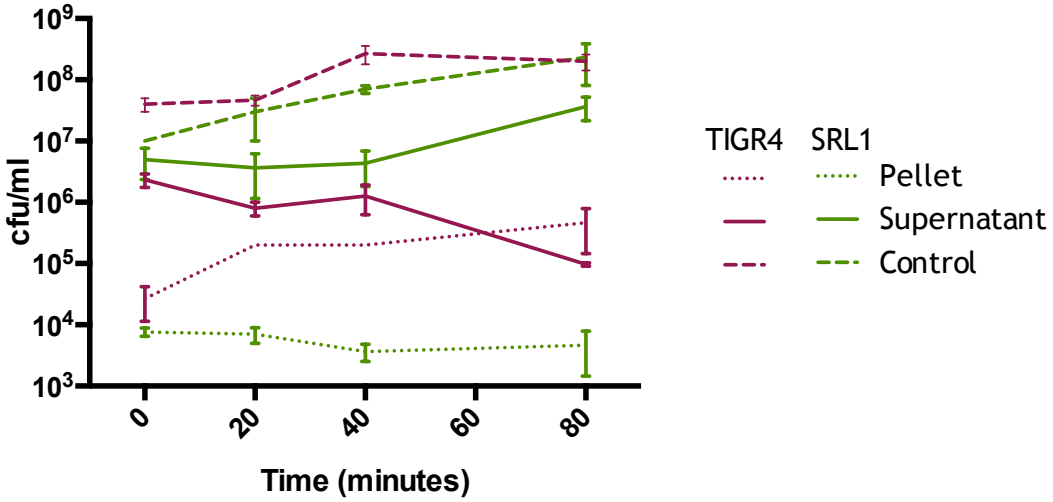

B

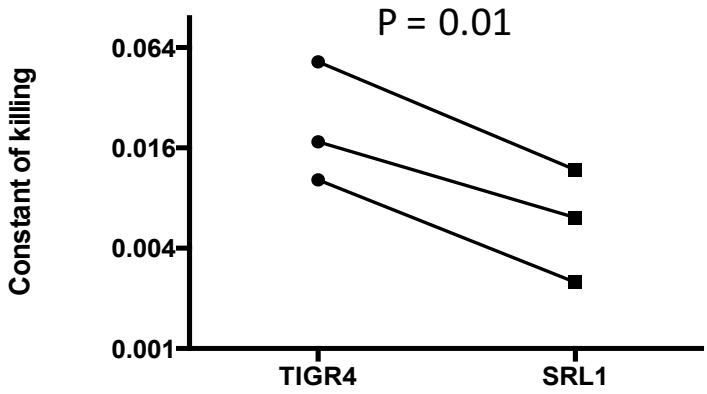

Figure 5-24. Comparison of TIGR4 and SRL1 in neutrophil phagocytosis and killing assay.

Neutrophils were suspended in naïve serum and either mixed with bacteria in a 1:1 ratio or sterile buffer (Control). To assess phagocytosis and killing, bacteria were enumerated within the control, supernatant and pellet to allow calculation of the rate of bacterial killing by neutrophils. A. Representative results from a single experiment. cfu were plated in triplicate and plotted as mean ± SEM. B. Constants of killing pooled from 3 experiments. P value represents paired Student's t-test.

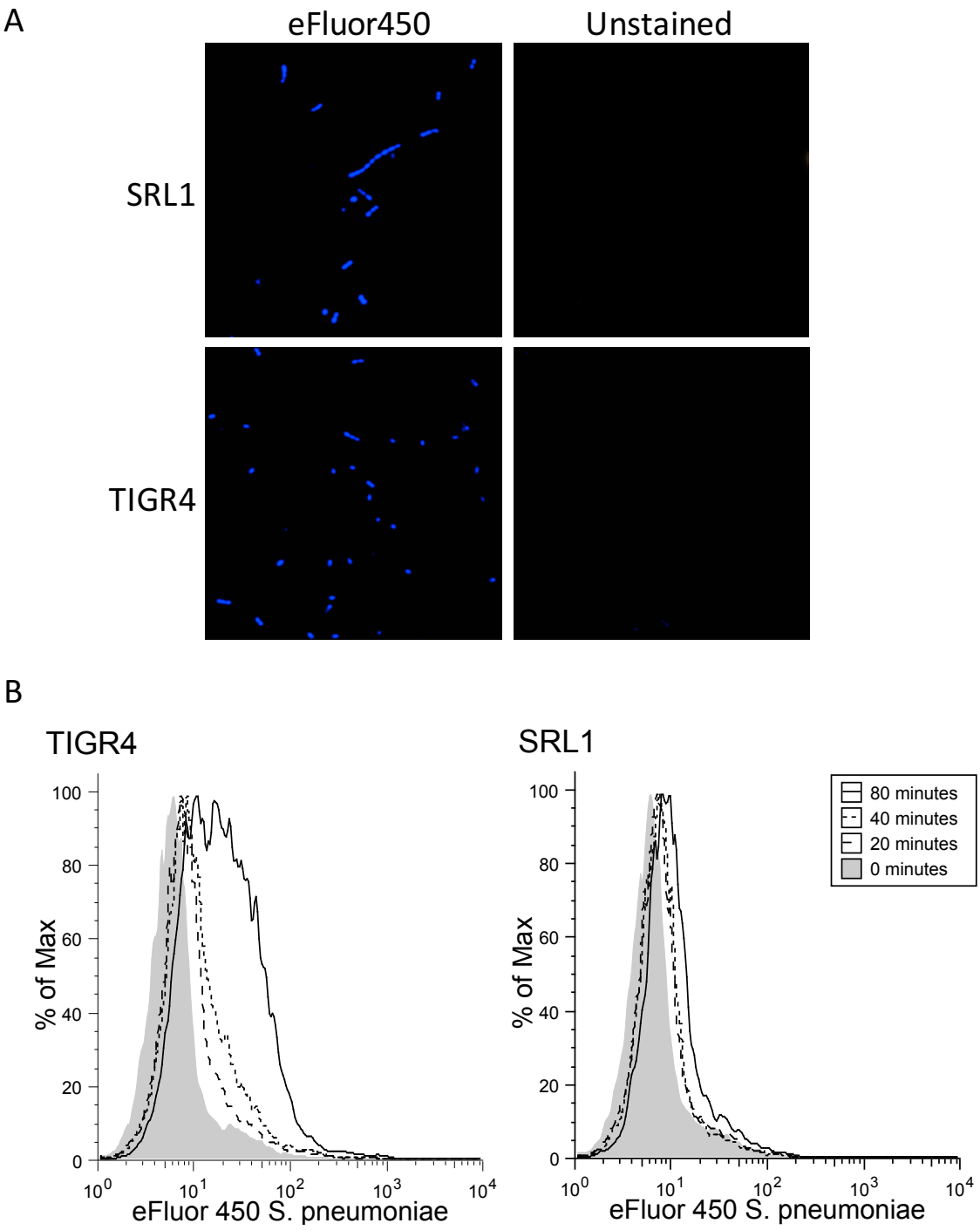

Figure 5-25. Comparison of TIGR4 and SRL1 phagocytosis using flow cytometry.

A. Pneumococci were stained with 20 μM eFluor450 Proliferation Dye and imaged with confocal microscopy. B: Pneumococci were mixed with neutrophils in a 10:1 ratio. Plots show histograms of eFluor450 fluorescence following incubation with TIGR4 or SRL1 at baseline and subsequent timepoints. Representative of 2 experiments.

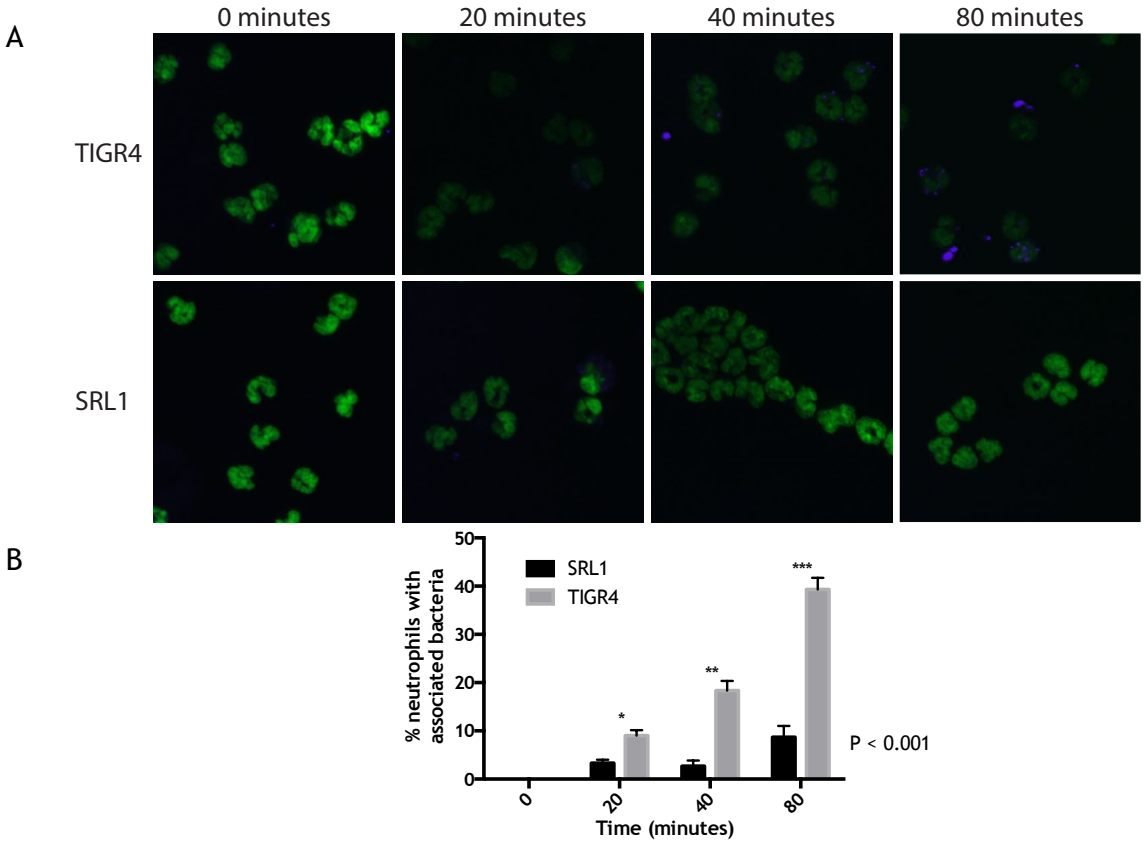

Figure 5-26. Comparison of TIGR4 and SRL1 phagocytosis using fluorescence microscopy.

eFluor450 stained pneumococci were mixed with neutrophils in a 10:1 ratio before cytocentrifugation onto microscope slides, fixation and staining with SYTOX Green. Images were captured using confocal microscopy. A. Representative confocal images of neutrophils. B. mean % of neutrophils associated with bacteria at each time point ± SEM. Representative of 2 experiments.

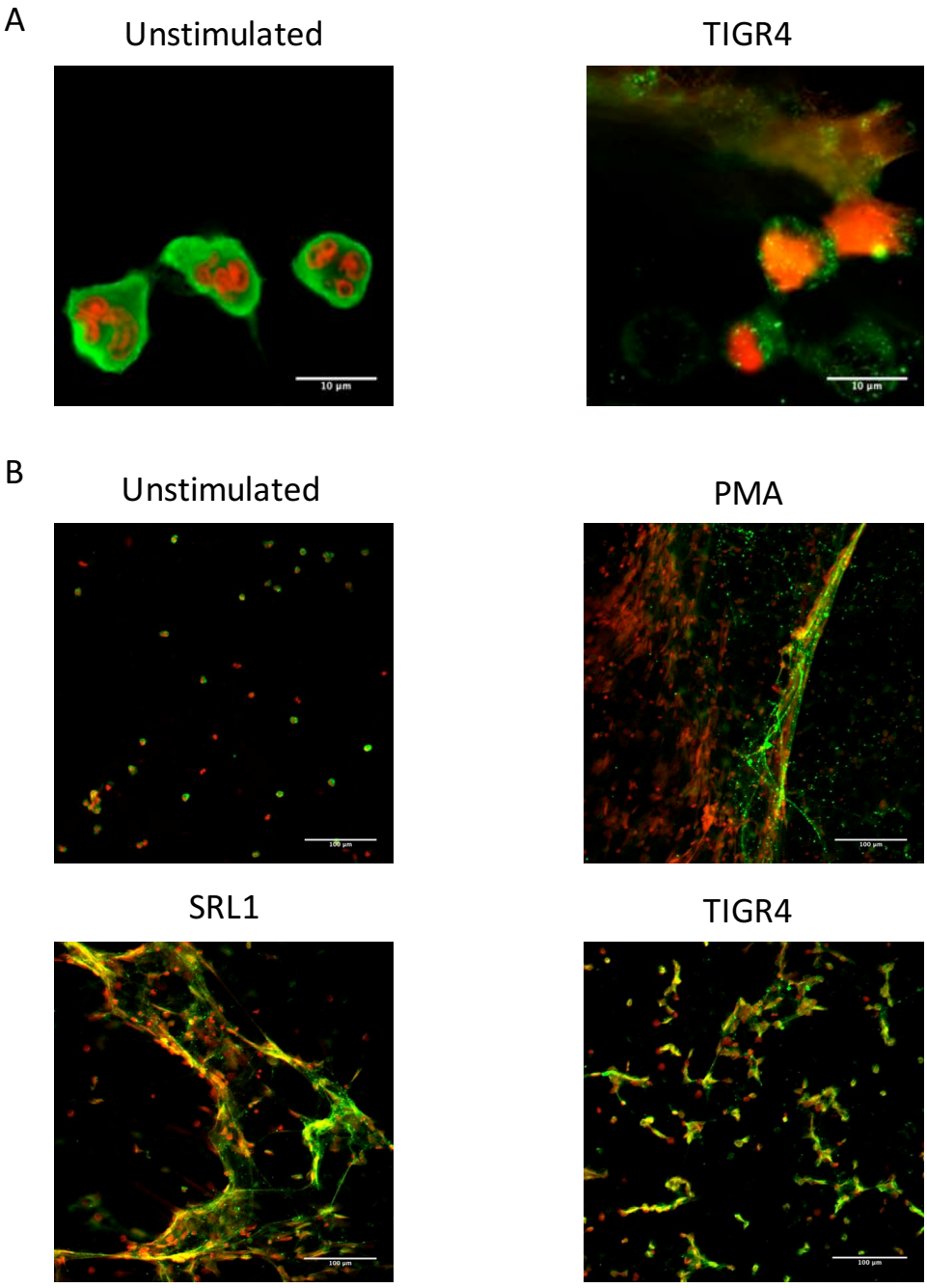

Figure 5-27. Detection of NET formation in neutrophils following stimulation with S. pneumoniae.

Neutrophils were stimulated for 2 hours and then incubated with rabbit anti-neutrophil elastase followed by Alexa Fluor 488 goat anti-rabbit secondary before staining DNA with SYTOX Orange. A. High power views of typical neutrophil morphology with and without infection with pneumococcus for 2 hours. B. Low power views of neutrophil NET formation in neutrophils after infection with pneumococcus or stimulation with phorbol 12-myristate 13-acetate (PMA) to induce NET formation or no stimulation. Representative of two independent experiments.

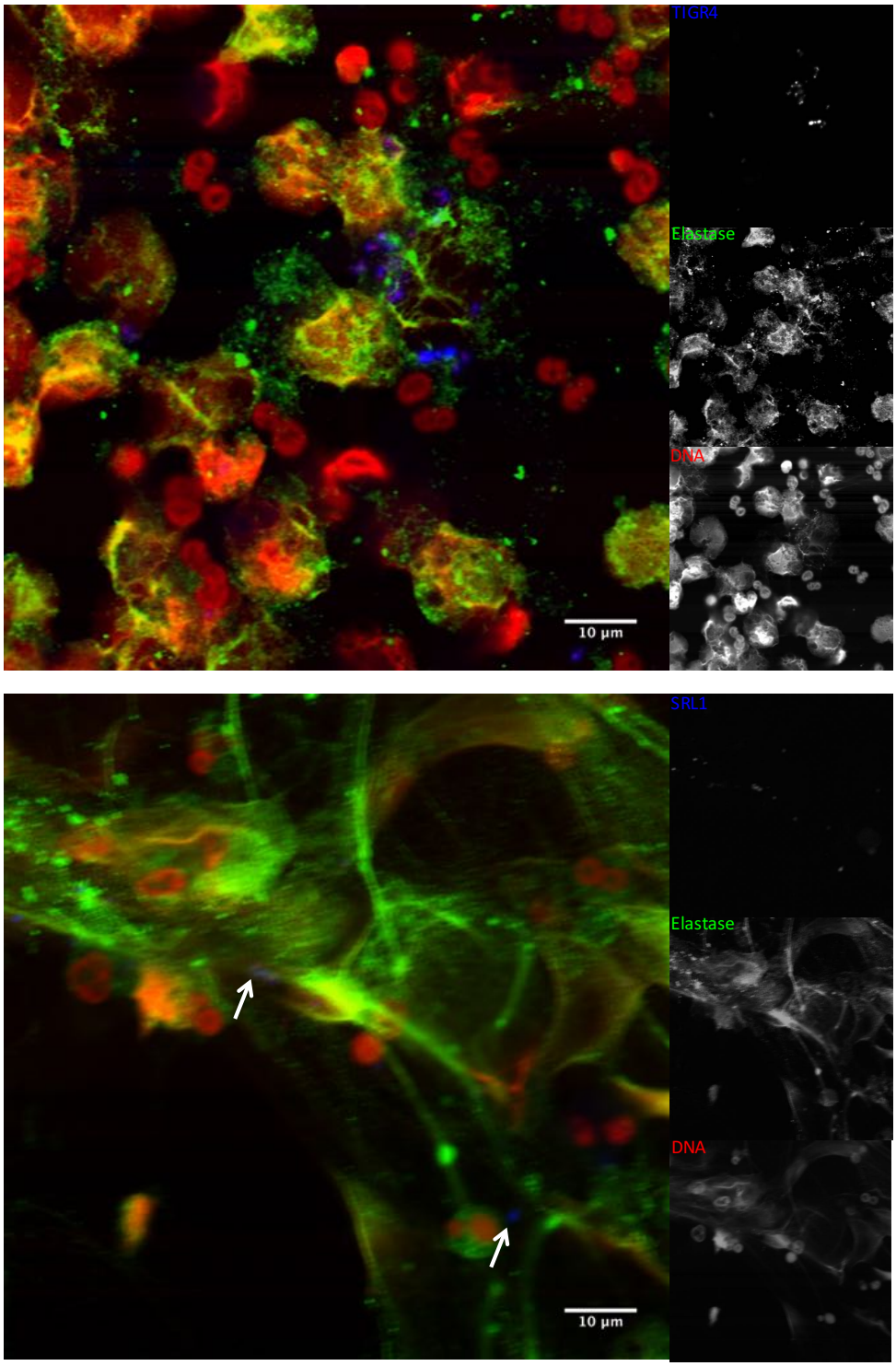

Figure 5-28. High resolution confocal images of S. pneumoniae caught in neutrophil extracellular traps (NET).

Pneumococci labeled with eFluor450 (blue) were added to neutrophils at a multiplicity of infection of 10 and incubated for 2 hours. After fixation, cells were staining with rabbit anti-neutrophil elastase (Alexa fluor 488, green) and SYTOX Orange DNA stain (Red). Both TIGR4 and SRL1 could be seen trapped within NETs on high power views.

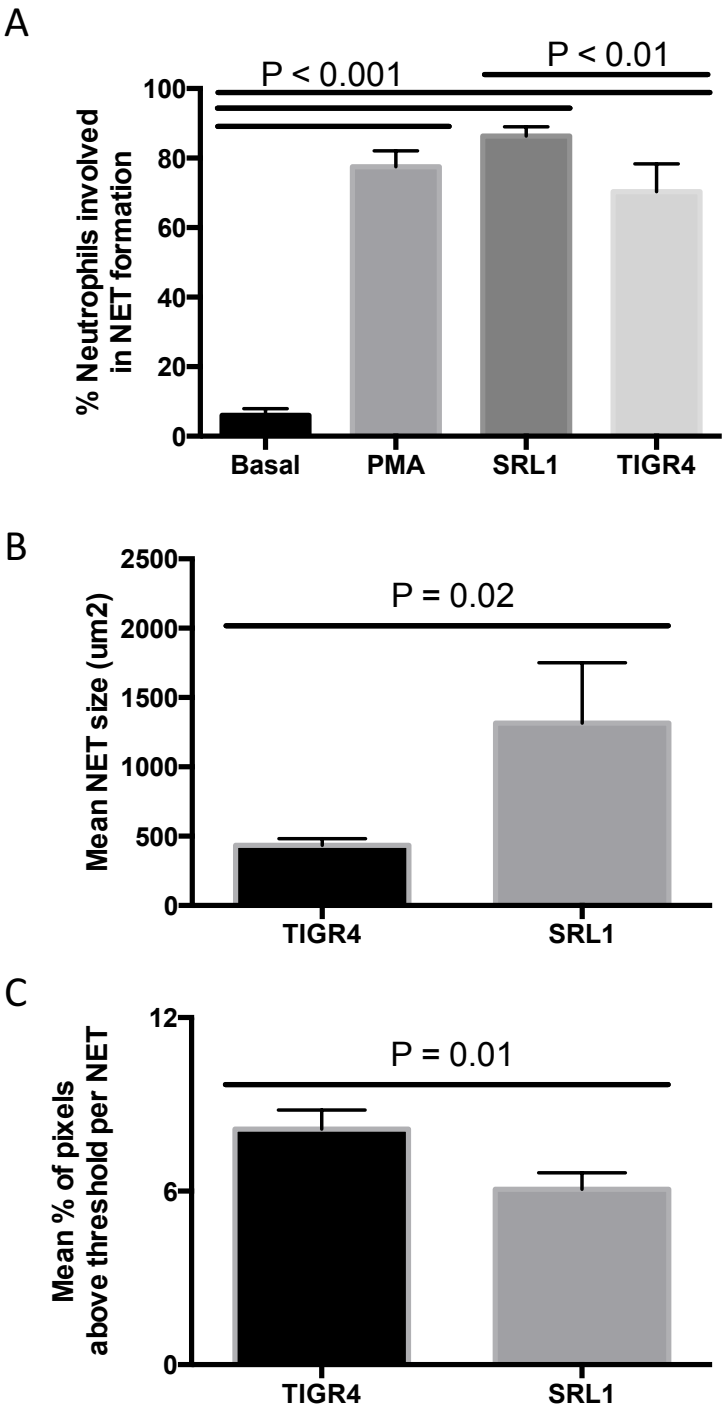

Figure 5-29. Summary statistics from comparison of NET formation after stimulation with SRL1 or TIGR4.

A. Percentage of neutrophils involved in NET formation. At least four low power microscope fields assessed B. Size of NET structures assessed by image analysis C. Percentage of pixels within NET structures above threshold for detection of pneumococcus (eFluor 450). In B and C, at least 90 individual NETs were analysed. All graphs show mean ± SEM. Representative of two independent experiments.

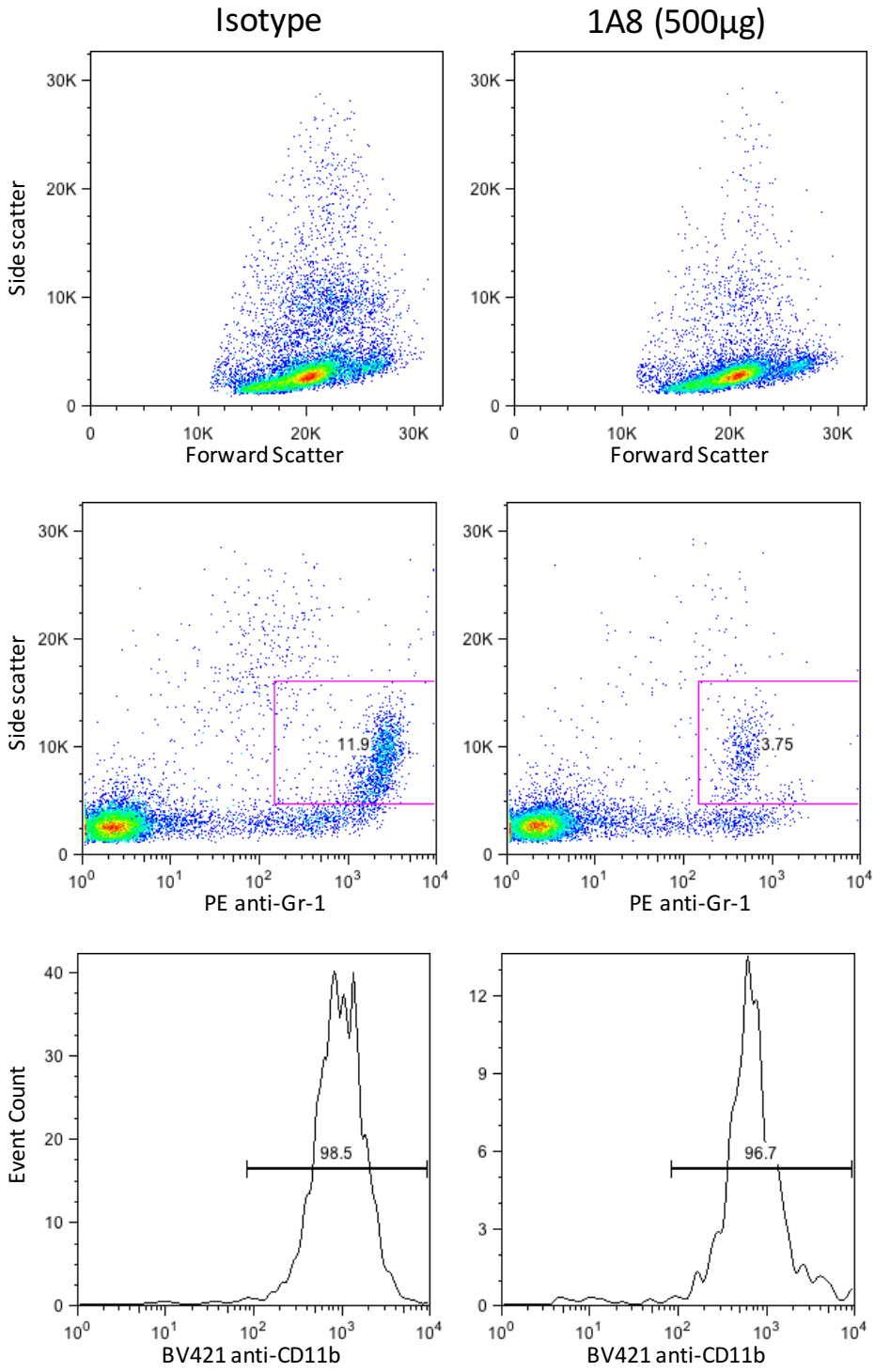

Figure 5-30. Depletion of neutrophils with antibody 1A8.

Animals were administered an intra-peritoneal injection of 500ug of monoclonal antibody 1A8 or matched isotype control 2A3 and blood was taken 24 hours later. A. Depletion of neutrophils was apparent by scatter characteristics alone. B. Neutrophils were identifiable as Gr-1^{+} SSc^{Int} cells but there was a reduction in Gr-1 staining in antibody treated animals. C. Cells identified as neutrophils in B were confirmed to be CD11b^{+}.

A

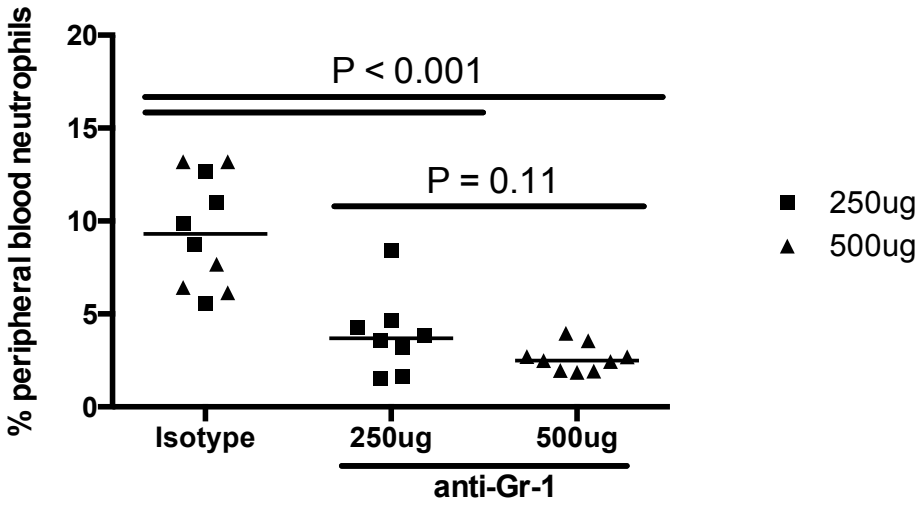

B

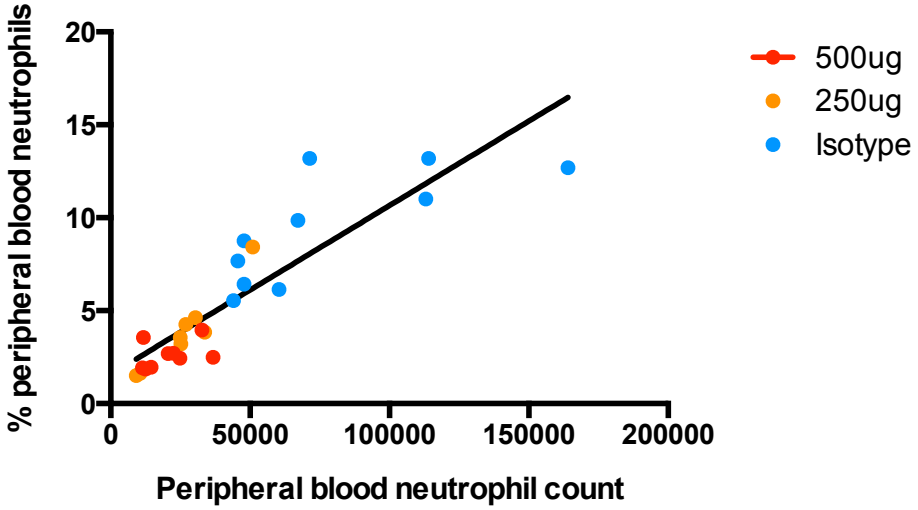

Figure 5-31. Peripheral blood neutrophils are effectively depleted by the monoclonal antibody 1A8 24 hours after intra-peritoneal injection.

A. Blood was obtained from mice 24 hours after injection of 1A8 or isotype control and neutrophils enumerated, either as a percentage of all cells (A) or as an absolute number using counting beads. (B) The correlation between neutrophil % and absolute neutrophil count is shown.

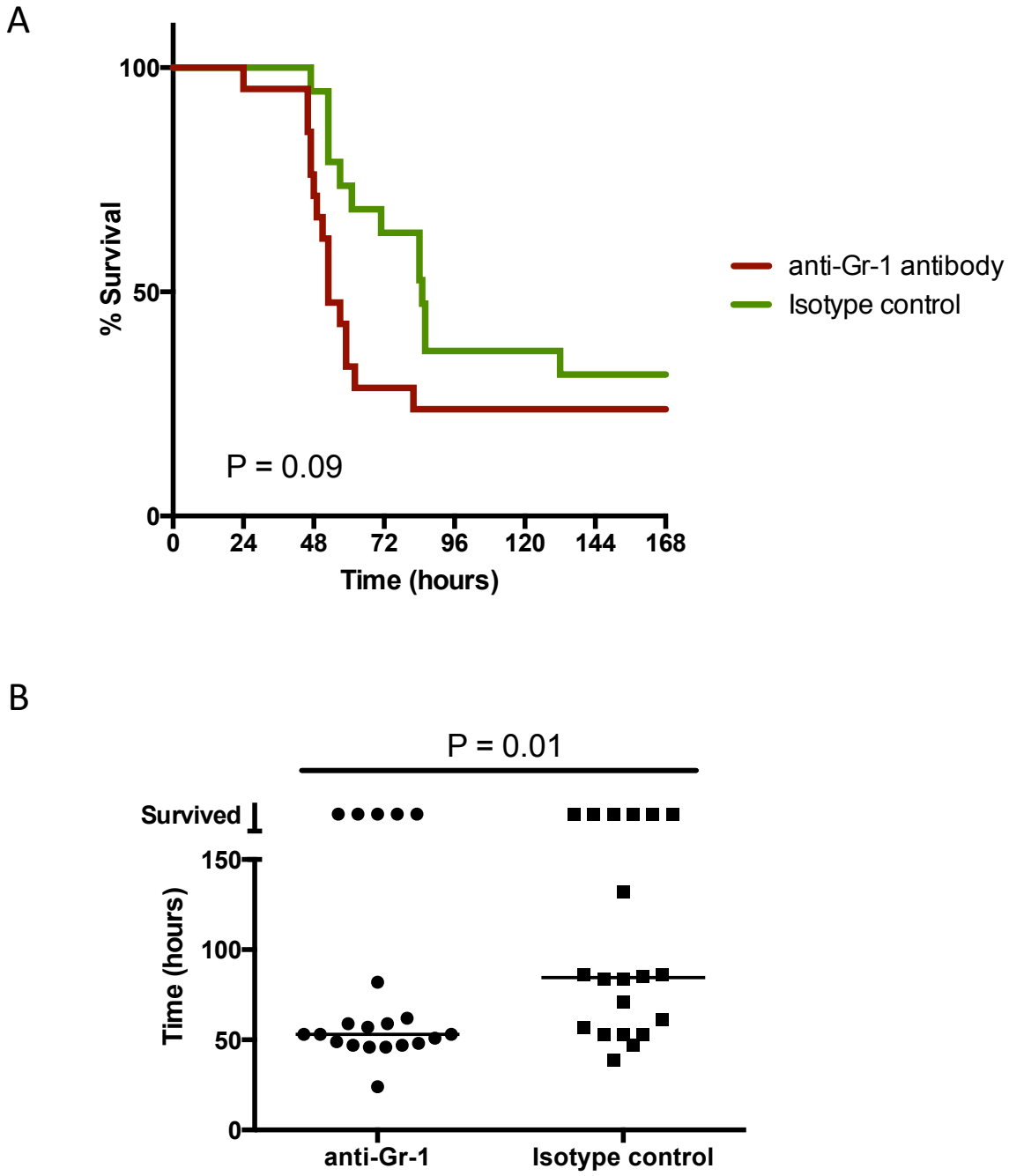

Figure 5-32. Neutrophil depletion in TIGR4 infection.

Depletion of neutrophils with monoclonal antibody 1A8 does not affect overall survival but does reduce the time to moribundity following intra-nasal infection with 10^6 cfu TIGR4 24 hours after i.p. injection of 500µg antibody or isotype control (n = 20-21/group). A. Kaplan-Meier survival curve (Log-rank test). B. Survival time (Mann-Whitney test). Results shown are pooled results of two independent experiments which both showed the same trend.

A

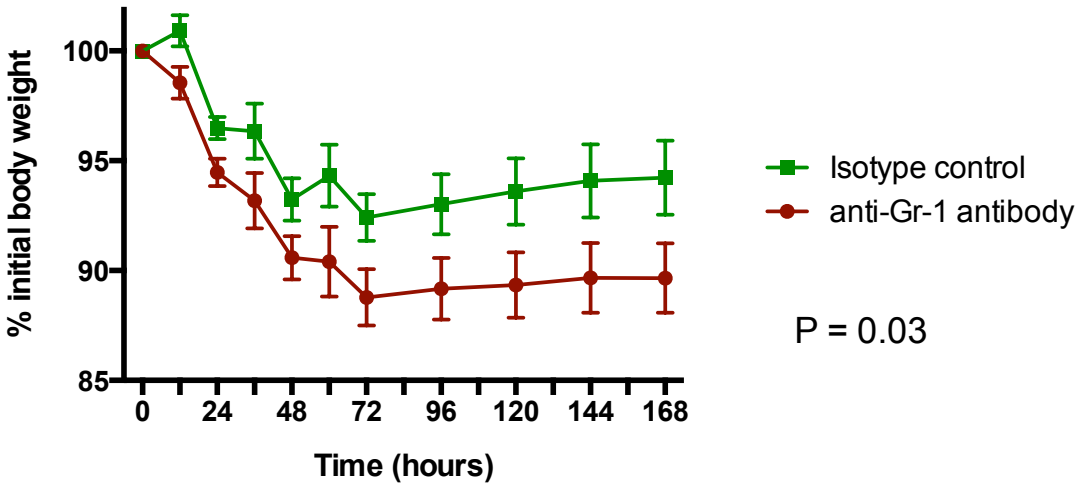

B

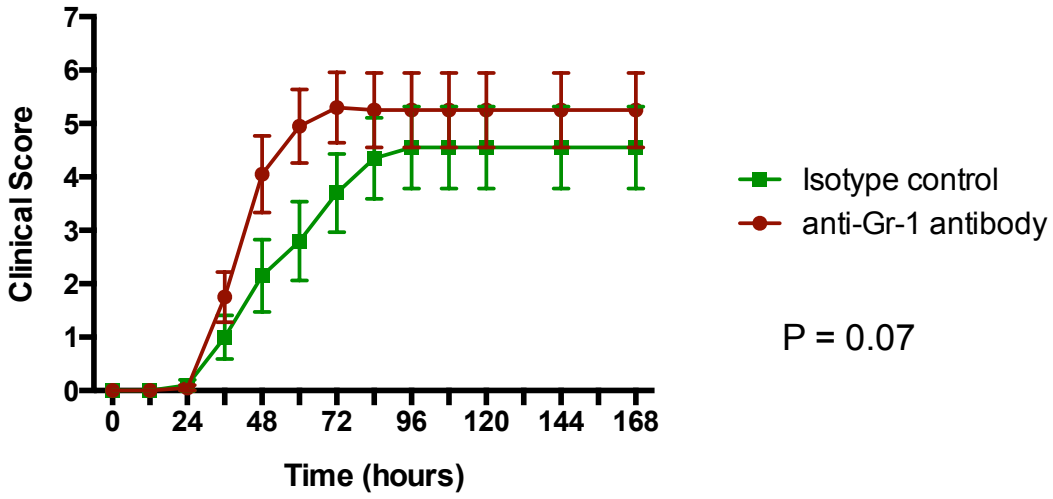

Figure 5-33. Weight loss and clinical score in animals infected with TIGR4 after depletion of neutrophils with anti-Ly6G antibody.

Animals were weighed (A) and scored clinically (B) regularly during the experiment **(n = 20-21/group)**. P value represents 2 way ANOVA corrected for repeated measures.

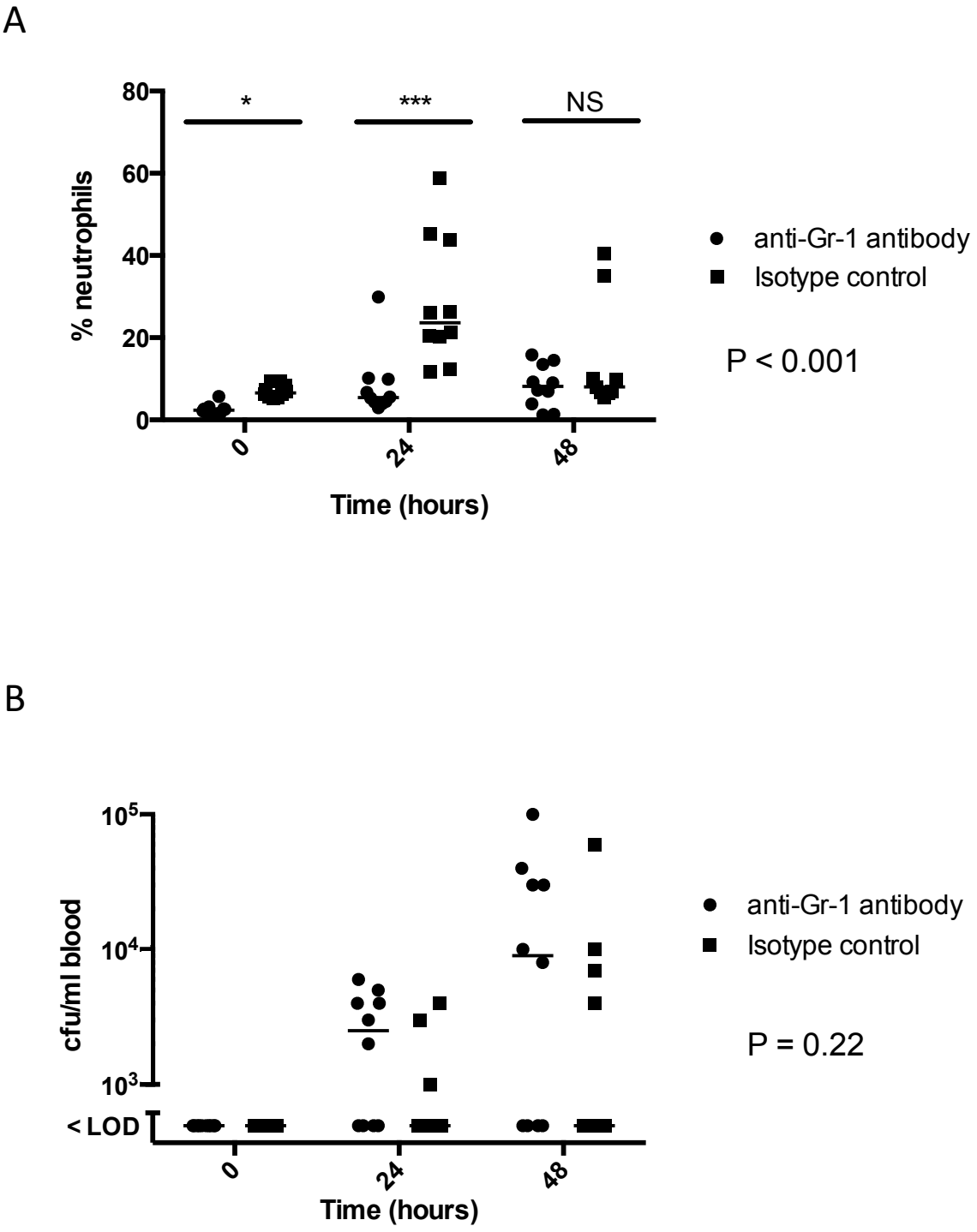

Figure 5-34. Peripheral blood neutrophil percentage and pneumococcal bacteraemia during the first 48 hours of TIGR4 infection following treatment with anti-Ly6G antibody or isotype control.

A. Peripheral blood neutrophil percentages in infected animals. B. Level of bacteraemia in infected animals (n = 20-21/group).

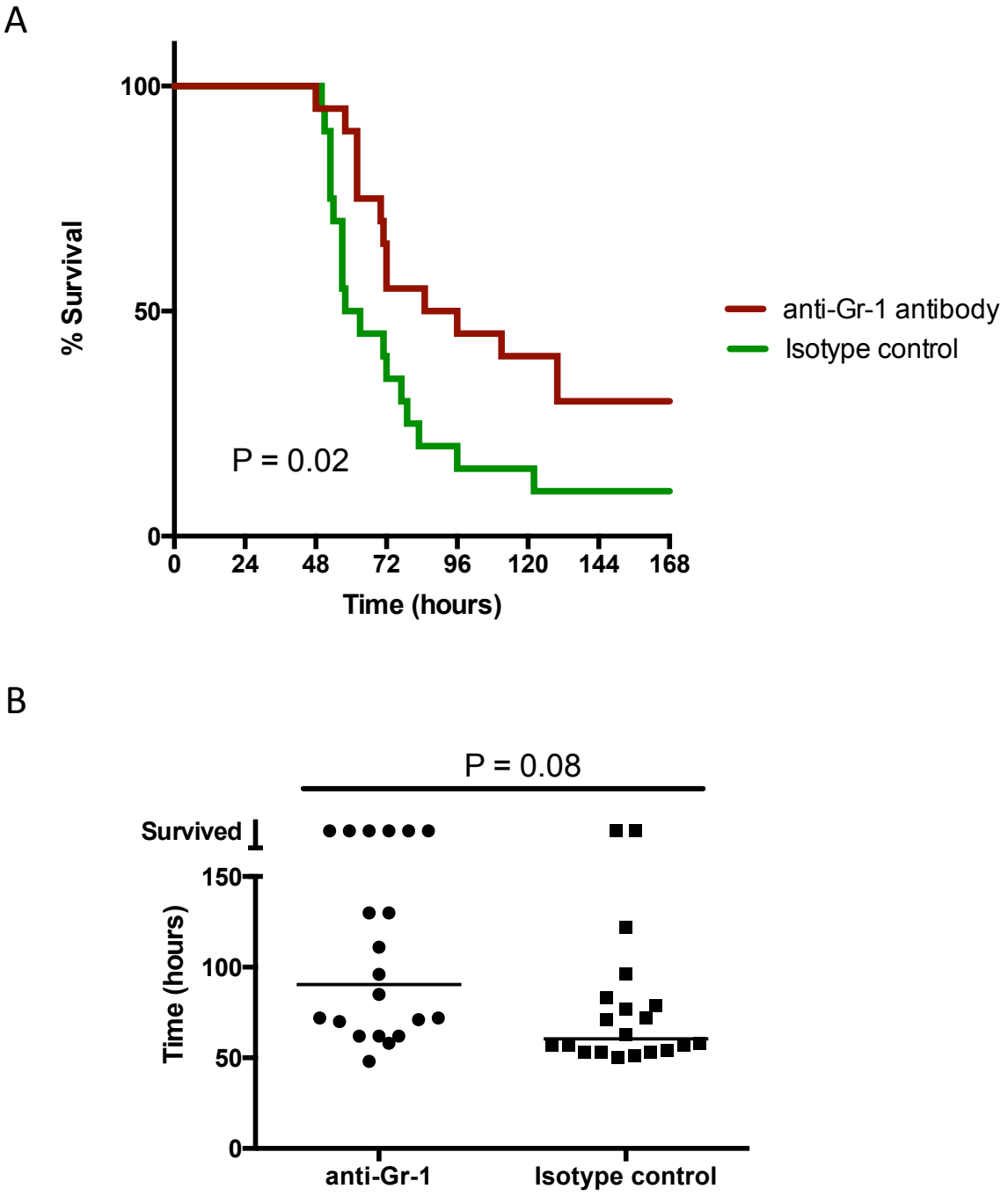

Figure 5-35. Depletion of neutrophils with monoclonal antibody 1A8 improves survival following infection with SRL1.

10^6 cfu were administered intranasally 24 hours after i.p. injection of 500µg antibody or isotype control (n = 20/group). A. Kaplan-Meier survival curve (Log-rank test). B. Survival time (Mann-Whitney test). Results shown are pooled results of two independent experiments which both showed the same trend.

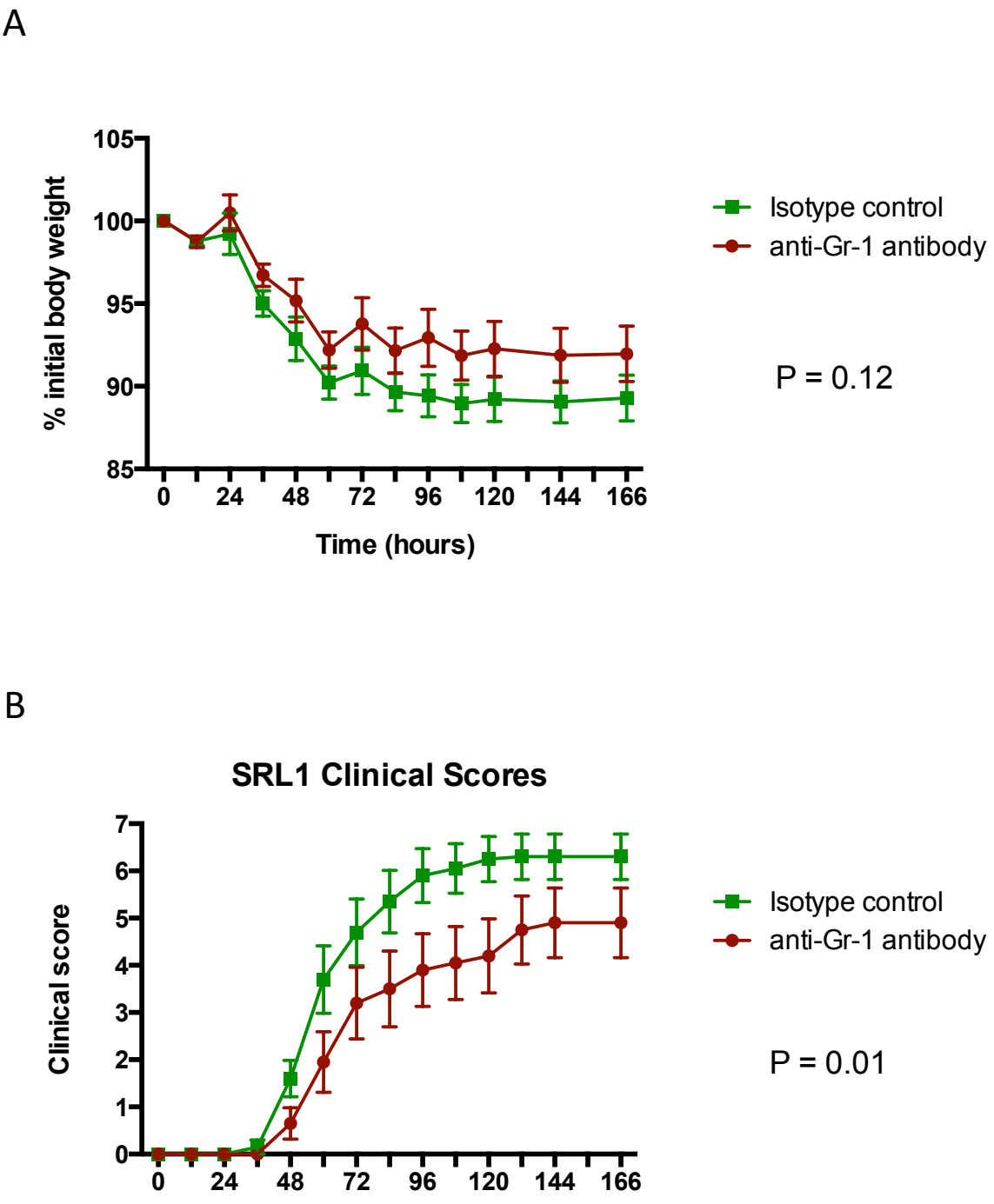

Figure 5-36. Weight loss and clinical score in animals infected with SRL1 after depletion of neutrophils with anti-Ly6G antibody.

Animals were weighed (A) and scored clinically (B) regularly during the experiment (n = 20/group). P value represents 2 way ANOVA corrected for repeated measures.

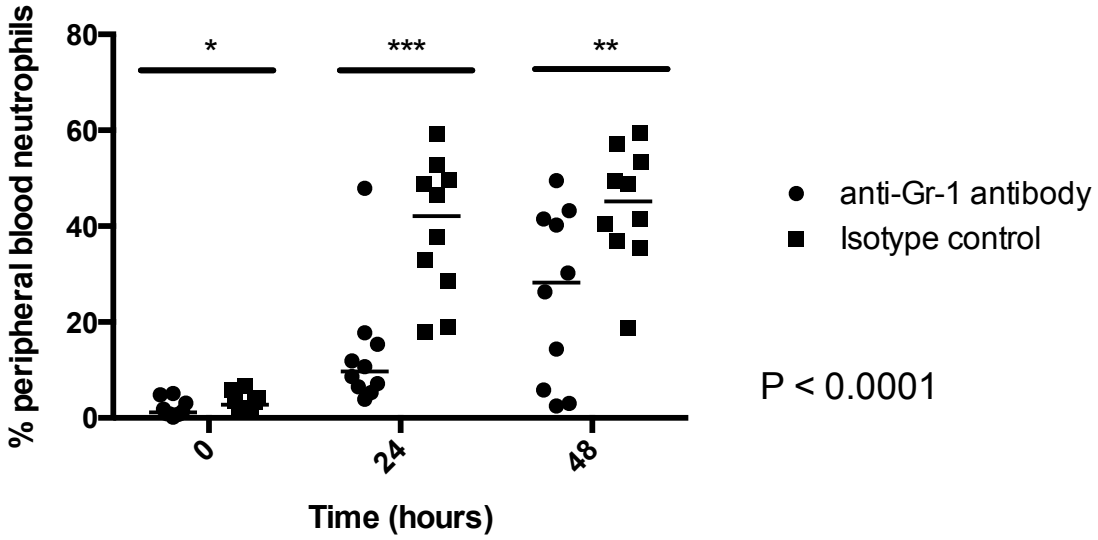

Figure 5-37. Depletion of neutrophils with monoclonal antibody 1A8 results in depletion of neutrophils for at least 48 hours after the induction of infection with 10^6 SRL1.

Blood was obtained from mice before and at intervals after infection and neutrophils were quantified by flow cytometry (n = 20/group). Mann-Whitney test * P < 0.05, ** P < 0.01, *** P < 0.001. P value shown is from two-way ANOVA.

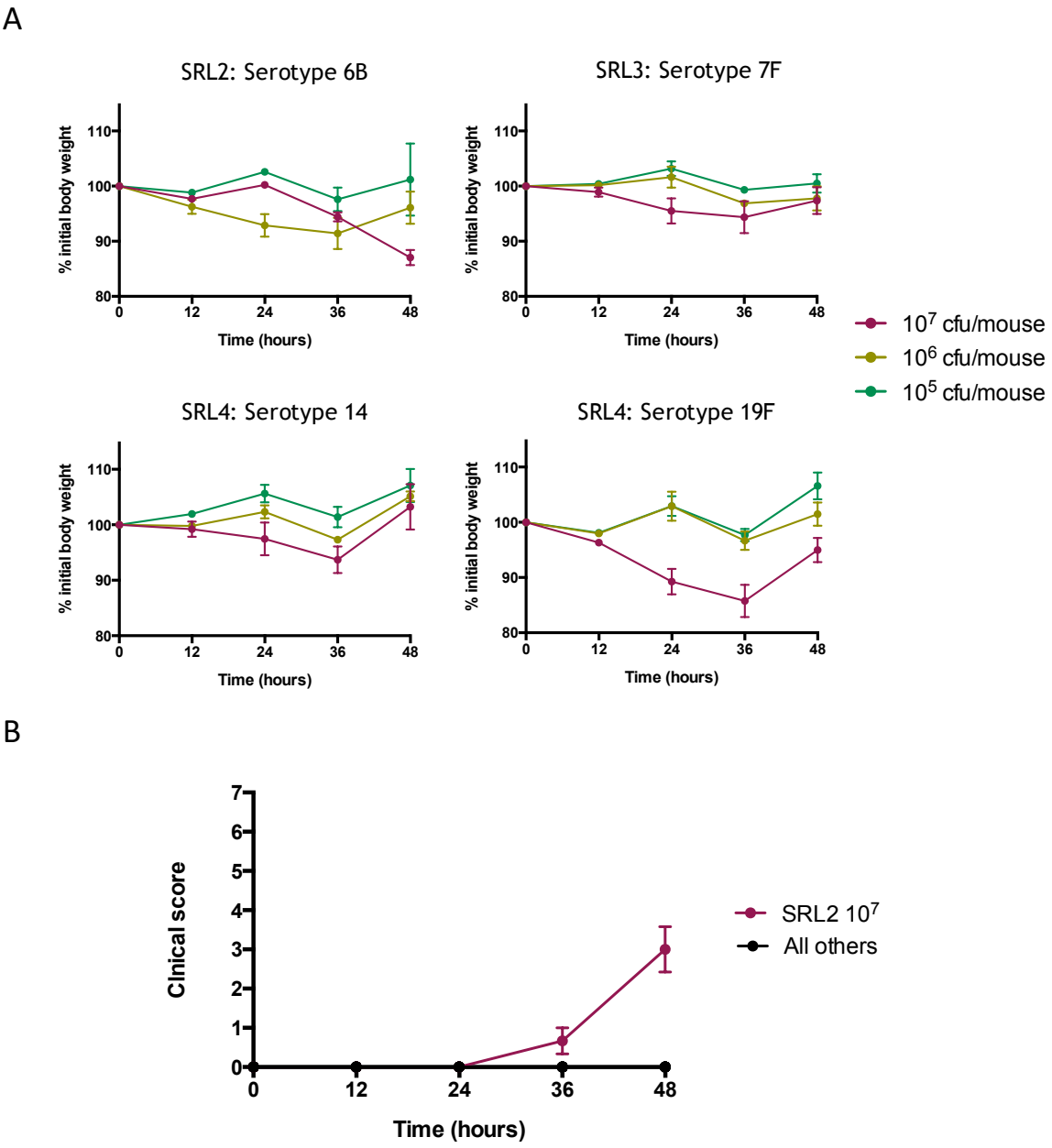

Figure 5-38. Course of infection caused by SRL2-5 in wild type mice. Animals were infected with a range of innocula via the intra-nasal route and monitored for 48 hours (n = 3 females/group). A. Change in body weight during experiment. B. Clinical scoring of mice during infection.

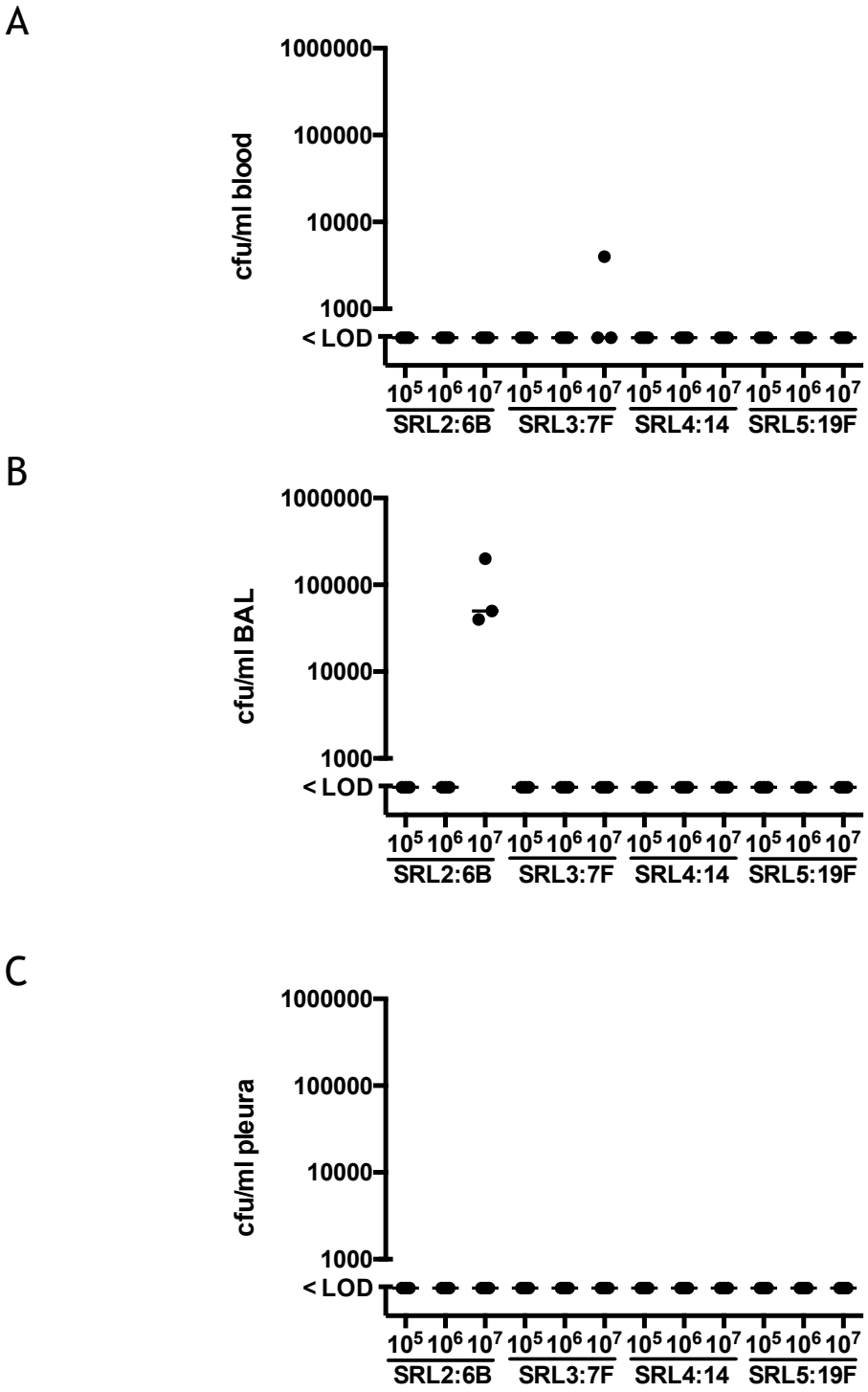

Figure 5-39. Bacteriology from mice infected 48 hours previously with various innocula of SRL2-5.

Samples were taken of (A) blood, (B) BALF, (C) pleural wash and cultured for pneumococci (n = 3 females/group). The power of 10 associated with each group represents the number of cfu/mouse.

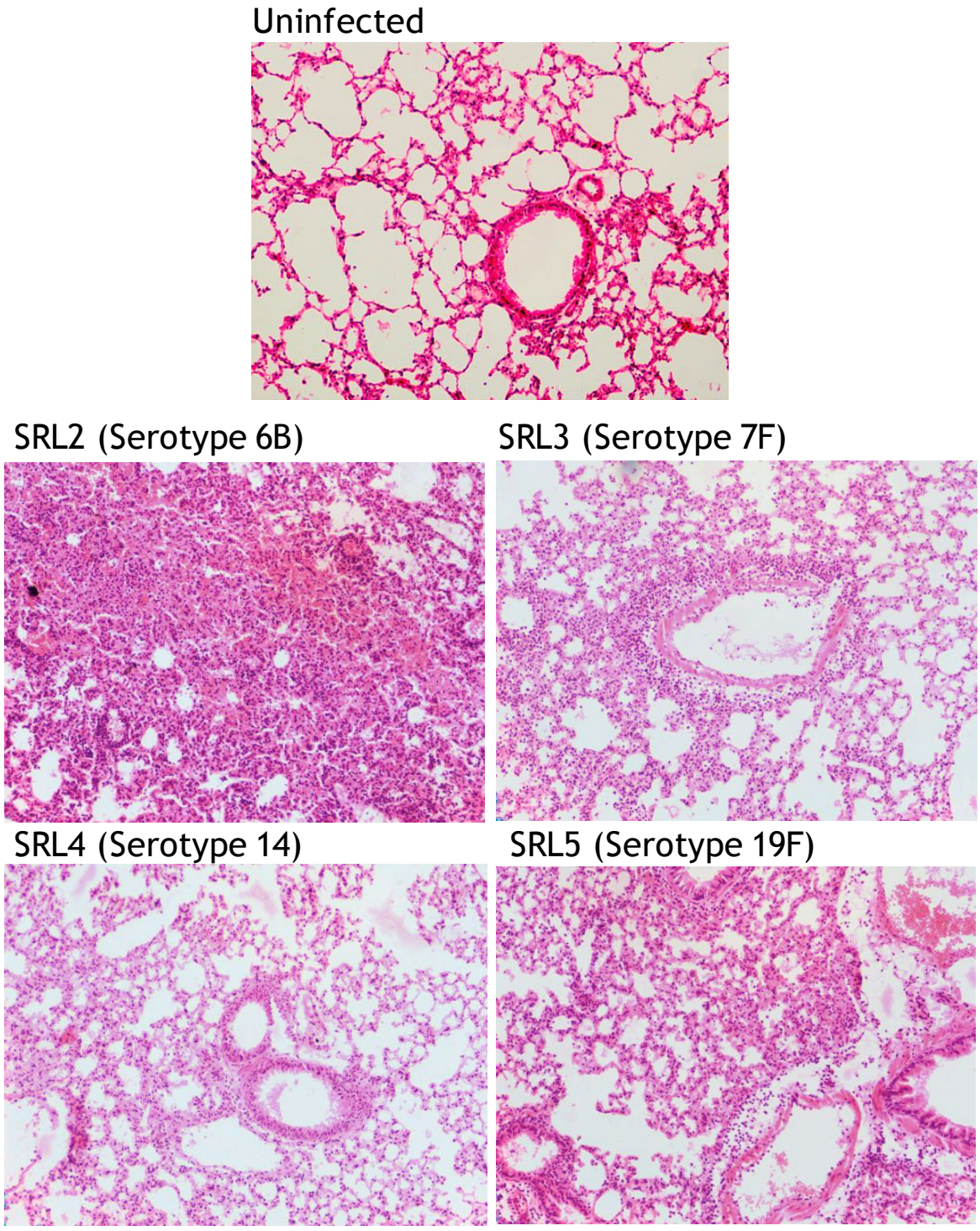

Figure 5-40. Representative histology from animals infected with 10^7 cfu/mouse SRL2-5 48 hours before.

No uninfected control was included in these experiments so a control was taken from banked tissue. Images were taken at x10 original magnification.

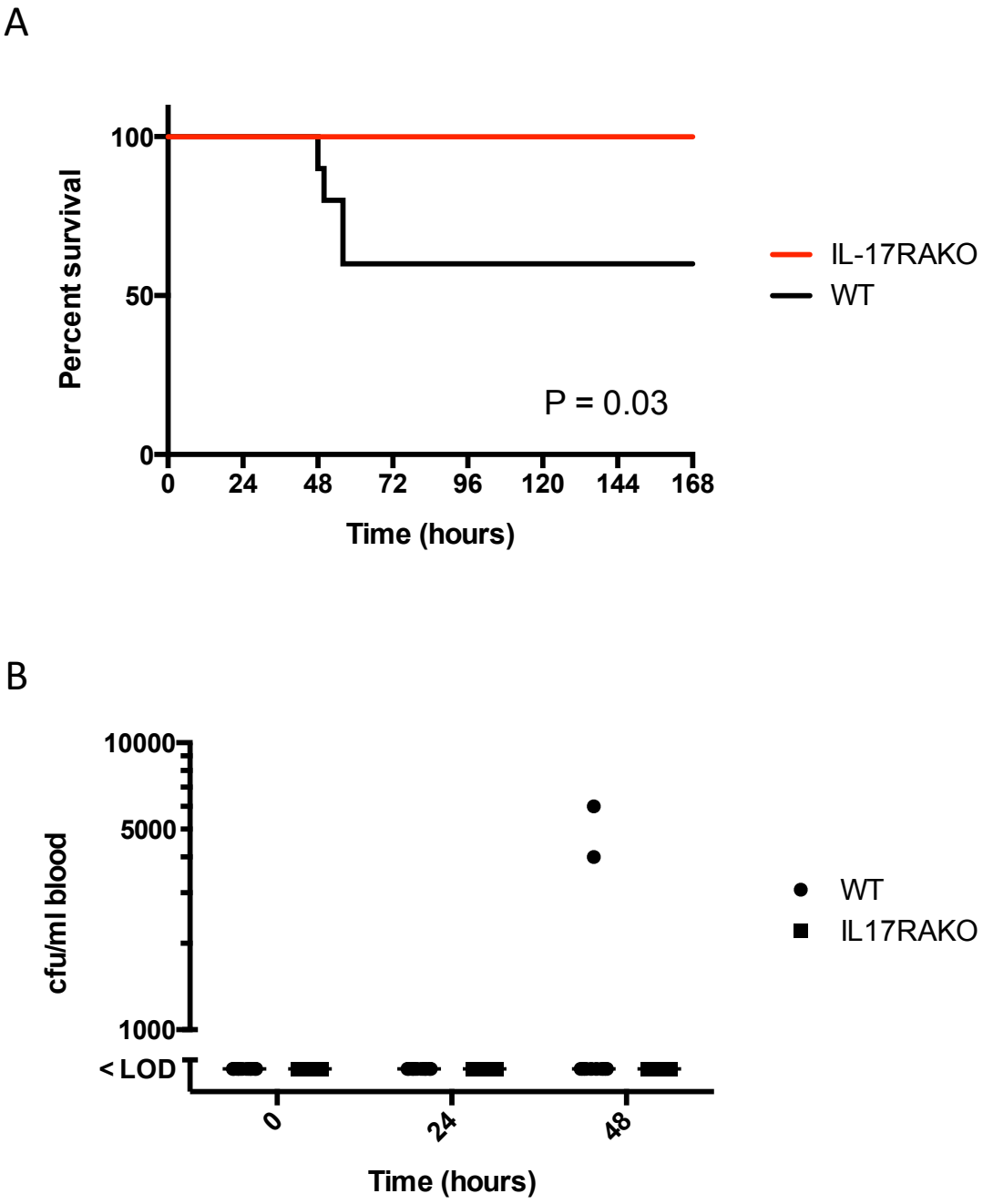

Figure 5-41. Outcome after intranasal infection with 10^7 cfu SRL4 in IL17RA$^{-/-}$ and wild type animals.

A. Kaplan-Meier survival plot (Log-rank test). B. Bacteraemia among infected animals (n = 10/group).

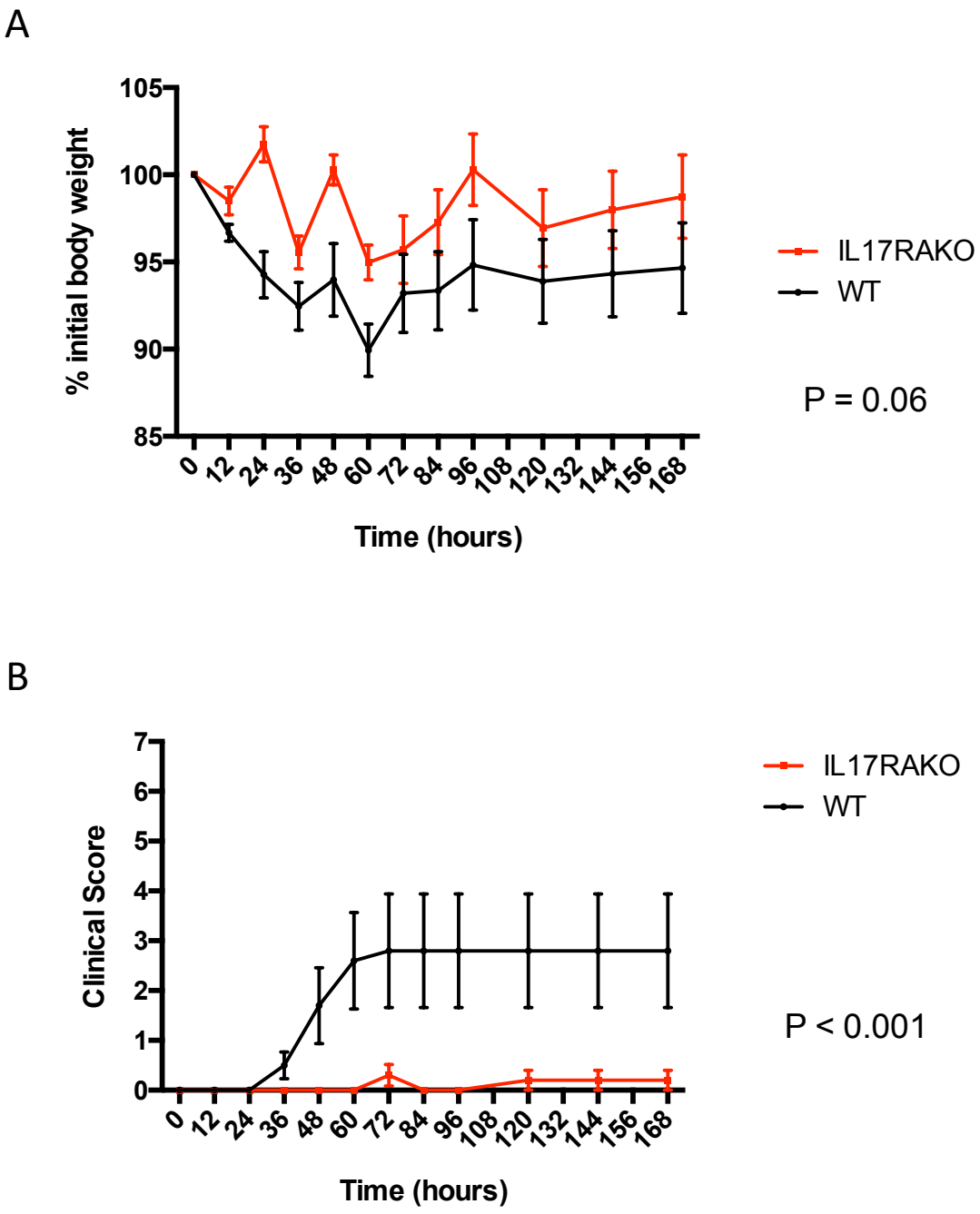

Figure 5-42. Outcome after intranasal infection with 10^7 cfu SRL4 in IL17RA$^{-/-}$ and wild type animals.

A. Weight change. B. Clinical scores. Data shown is mean ± SEM (n = 10/group). P values represent two-way ANOVA.

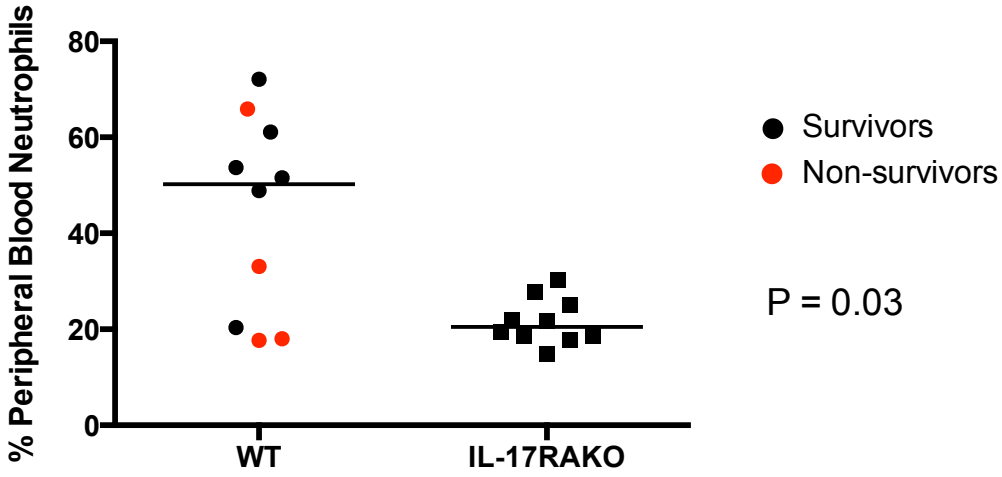

Figure 5-43. Peripheral blood neutrophil percentages in wild type and IL-17RA$^{-/-}$ mice 24 hours after infection with SRL2.

Animals surviving to the end of the experiment are shown in black while those reaching the clinical end-point prior to the conclusion of the experiment are shown in red. P value represents a Mann-Whitney test.

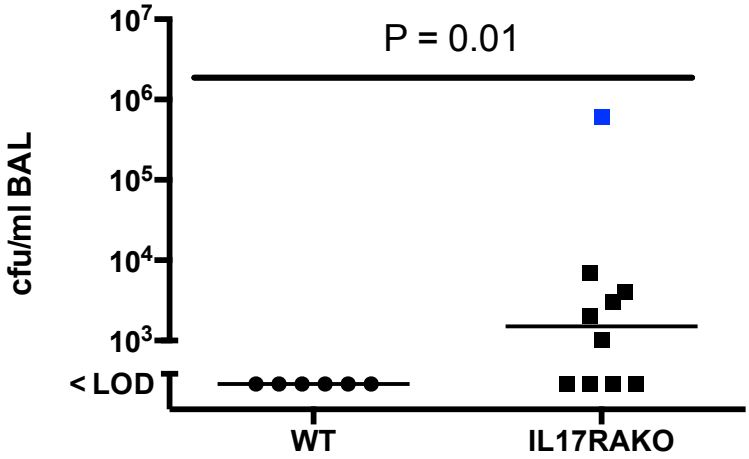

Figure 5-44. Persistent presence of SRL4 in the lower airways of survivors one week after infection occurs only in IL-17RA$^{-/-}$ animals.
Surviving mice were culled at the conclusion of the mortality study and BAL conducted. P value represents Fisher's exact test. Animal shown in blue experienced mild clinical illness and significant weight loss at the end of the experiment (see text). Exclusion of this mouse results in a P value of 0.044.

Experiment title	Figure	Wild Type/Iso		IL-17RA$^{-/-}$/1A8		IL-22$^{-/-}$	
		Male	Female	Male	Female	Male	Female
High dose TIGR4 survival	5-2	5 (4)	5 (4)	5 (4)	5 (3)	5 (4)	5 (4)
Low dose TIGR4 survival	5-4	3 (0)	7 (1)	3 (1)	7 (4)	3 (1)	6 (2)
TIGR4 24 hour time point	5-8	5	5	5	5	ND	ND
TIGR4 RNA extraction	5-13	2	1	2	1	ND	ND
SRL1 survival	5-14	5 (5)	6 (5)	5 (2)	5 (2)	5 (5)	5 (2)
SRL1 24 hour time point	5-17	7	3	7	3	ND	ND
SRL1 RNA extraction	5-22	2	1	2	1	ND	ND
TIGR4 neutrophil depletion*	5-32	13 (11)	7 (6)	13 (12)	7 (6)	ND	ND
SRL1 neutrophil depletion*	5-35	11 (10)	9 (7)	10 (7)	9 (6)	ND	ND
SRL2 survival	5-41	4 (3)	6 (1)	4 (0)	6 (0)	ND	ND

Table 5-1. Sex balancing of groups in experiments involving male and female mice.

Experiments reported in this chapter are outlined with mice in each group split according to gender. Where appropriate, number of mice per group culled before the conclusion of the experiment are shown in brackets. * experiments involving neutrophil depletion involve exclusively wild type mice. Groups shown are those receiving anti-Ly6G antibody (1A8) or isotype matched control (Iso).

6. THE ROLE OF IL-17 IN NASAL COLONISATION

6-1 Introduction

In the previous chapter I demonstrated the importance of IL-17 as a mediator of neutrophil recruitment in naïve mice with pulmonary infection with pneumococci. Surprisingly, there was a marked reduction in mortality associated with infection with the mucoid serotype 3 strain SRL1 and this reduction in mortality was also noted with infection with another strain selected for its capacity to cause pulmonary disease without invasion. However, it was also noted that most surviving IL-17RA$^{-/-}$ mice had failed to clear the pneumococci from the lower respiratory tract within one week.

As already discussed, a number of studies have investigated the role of IL-17 in mucosal clearance of pneumococci within the nasal cavity. Most of these studies have focused on acquired immunity to pneumococcal disease with studies on the role of prior nasal colonisation or vaccination in shortening subsequent nasal colonisation[265,352,382]. It is clear from these studies that IL-17 is a critical cytokine mediating the clearance of pneumococci from the nose in the context of acquired immunity. One study investigated the role of IL-17 in primary pneumococcal colonisation by using neutralising antibody[172]. In this study involving a serotype 23F strain derived from a human otitis media isolate there was a failure of pneumococcal clearance at 21 days when IL-17 neutralising antibody was administered. The clearance of pneumococci was also dependent on CD4 (again assessed by administration of depleting antibody).

IL-17 deficiency has also been associated with a failure to clear mucosal colonisation or infection with a number of other pathogens. These include *Candida albicans*[328], *Staphylococcus aureus*[332], uropathogenic *Escherichia coli*[446]

and *Neisseria gonorrhoea*[396]. IL-17 genotype was associated with bacterial airways colonisation with pneumococci during viral bronchiolitis[447].

In the light of the differences observed in models of infection, I decided to investigate the role of IL-17 in nasal colonisation by the bacterial strains used in the earlier experiments. This was achieved using a model of nasal colonisation with basic microbiology and then by investigating the respiratory tract microbiome of resting mice and following colonisation.

6-2 Nasal Colonisation studies

6-2.1 Establishment of nasal colonization model

Mice were colonised with pneumococci by inoculation of the nares of restrained, conscious mice with 5 x 10^5 cfu/mouse. Neither TIGR4 nor SRL1 were associated with clinical evidence of illness or weight loss over 1 week of monitoring (figure 6-1A). At the conclusion of the experiment, nasal wash from affected animals confirmed the presence of nasal colonisation with both pneumococcal strains (figure 6-1B).

6-2.2 Nasal colonization in IL-17RA$^{-/-}$ mice – TIGR4

IL-17RA$^{-/-}$ and wild type mice were colonised with 5 x 10^5 cfu/mouse of TIGR4. On this occasion, 1 mouse from each group developed clinical evidence of illness after 48 hours and was culled after 72 hours (figure 2A). Both mice had high level bacteraemia (>10^6 cfu/ml). There was a statistically significant difference between the body weight of the mice (P = 0.02, figure 6-2B). However, the absolute difference between the means of the two groups was only 3.6% of initial body weight and the significance of this finding is uncertain.

IL-17RA$^{-/-}$ mice had a 39 fold higher median density of TIGR4 in the nasal wash than wild type (WT: 600 cfu/ml; IL17RA$^{-/-}$ 23,300 cfu/ml; P = 0.031, figure 6-3A). Median abundance of neutrophils in nasal wash was similar between the two groups although there was a trend towards a higher neutrophil percentage in IL-17RA$^{-/-}$ mice (WT: 42.9%; IL17RA$^{-/-}$ 59.3%; P = 0.132, figure 6-3B).

6-2.3 Nasal colonization in IL-17RA$^{-/-}$ mice – SRL1

IL-17RA$^{-/-}$ and wild type mice were then colonised with 5 x 10^5 cfu/mouse of SRL1. No animals in this experiment developed any clinical illness. There was no significant difference in weight change between groups although there was a trend towards increased weight loss among IL-17RA$^{-/-}$ mice (P = 0.07, figure 6-4).

As with TIGR4, IL-17RA$^{-/-}$ mice had a higher median density of nasal *S. pneumoniae* than wild type controls although the density in knockout mice was only around 7 fold higher (WT 550 cfu/ml; IL-17RA$^{-/-}$ 4000 cfu/ml; P = 0.022, figure 6-5A). IL-17RA$^{-/-}$ mice had a lower density of neutrophils in the nasal wash than wild type controls (WT 36.4%; IL-17RA$^{-/-}$ 59.2%; P = 0.047, figure 6-5B).

6-2.4 Nasal colonisation in IL-17RA$^{-/-}$ mice – time course

To further investigate the dynamics of respiratory tract colonisation, mice colonised with SRL1 were culled at intervals and the density of *S. pneumoniae* in nasal wash and BALF assessed. In this experiment, nasal wash colony counts following inoculation with 5 x 10^5 cfu/ml of SRL1 were lower than in previous experiments but there was again a trend towards increased weight loss in IL-17RA$^{-/-}$ mice (P = 0.19, figure 6-6A). There was no clinical illness observed at any stage.

In both upper and lower respiratory tract samples there was clear evidence of a higher bacterial density in IL-17RA$^{-/-}$ mice following colonisation (Upper P < 0.001, figure 6B; Lower P = 0.003, figure 6-6C). In both the upper and lower airways, bacterial density peaked at three days and then declined throughout the remainder of the time course.

6-2.5 Presence of non-*S. pneumoniae* species in nasal wash

During the course of this project and others involving IL-17RA$^{-/-}$ mice, hundreds of samples of BAL were collected from both the resting and infected state. While data were not systematically collected, it was unusual to see other colonies other than those of *S. pneumoniae* visible after overnight incubation on blood agar. Plates were generally incubated at 37˚C in room air since these

conditions reduced the colony size of SRL1 and made colony counting easier. However, over the course of the experiments outlined in this chapter, it was noted that nasal wash usually yielded small colonies with a mixture of haemolysis types when incubated in similar conditions. Informal observation did not reveal an obvious difference between the numbers of these colonies and they were not formally quantified. However, IL-17RA$^{-/-}$ nasal wash frequently contained colonies of organisms growing with large colonies on blood agar. These organisms were generally gram negative and oxidase positive and were uncommon in the nasal wash of wild type animals. When the results of the two initial experiments involving IL-17RA$^{-/-}$ colonised with TIGR4 and SRL1 were pooled, such organisms were seen more frequently in IL-17RA$^{-/-}$ mice (WT: 1/20 [5%]; IL-17RA$^{-/-}$: 10/24 [42%]; Fisher's exact test P = 0.006).

6-3 Nasal Microbiome

In order to further characterise the differences between IL-17RA$^{-/-}$ mice and wild type controls in terms of nasal colonisation we sought to study the respiratory tract microbiome of resting and colonised animals.

6-3.1 16S RNA Sequencing

In order to reduce variation in microbiome occurring by segregation of mice by strain we mixed knock out and wild type mice together shortly after weaning and allowed them to mature for a further 6 weeks. By this stage the two strains of mice had been bred within the same animal facility for more than ten generations and handled exclusively by only three researchers. They were fed the same food and kept in the same room. Great care was taken to avoid contamination of nasal wash and BALF with extrinsic bacteria and the animals' skin and external nasal tissue was cleansed with alcohol and washed before taking samples.

Amplification of V_1-V_2 region of the 16S gene was successfully achieved in 94/96 (98%) samples with little evidence of non-specific amplification products observed on agarose gel electrophoresis (figure 6-7A). Following PCR cleanup, a single clear band matching the predicted size was obtained (figure 6-7B). After processing of sequences through the clean-up and clustering pipeline,

rarefaction curves indicate good sequencing depth with samples approaching their asymptote (figure 6-8A). Sample coverage estimated using the Abundance-based coverage estimator function (ACE) supported this conclusion with a median OTU coverage of 92.7% and no evidence of a difference in OTU coverage between sample groups (figure 6-8B). After clustering, 6,736,577 sequences were clustered into 2632 OTUs. Of these, seven OTUs were classified as Archaea and fourteen OTUs as chloroplasts (representing 0.7% and 1.6% of the total number of sequences respectively) and were excluded.

6-3.2 Wild Type Microbiome

The microbiome of the upper and lower respiratory tract was distinct. The upper respiratory tract of the wild type mouse had a higher number of OTUs (figure 6-9A, $P < 0.0001$) and higher alpha diversity (the Inverse Simpson diversity index is shown in figure 6-9B ($P = 0.004$) but this was confirmed on several indices of alpha diversity). The clustering of samples on non-metric multidimensional scaling analysis (NMDS) was highly divergent (figure 6-9C, $P < 0.0001$).

In keeping with the alpha diversity findings, lower respiratory tract samples tended to be dominated by a small number of OTUs. Whereas in lower respiratory tract samples the five most abundant OTUs accounted for more than 50% of sequences, in the upper respiratory tract the fifteen most abundant OTUs were needed to account for 50% of sequences (figure 6-10A). In the lower airways, the most abundant organisms were gram negatives with 16S sequences identified as belonging to the genera *Thermomonas*, *Cupriavidus*, *Bosea*, *Methylobacterium* and *Pasteurella* (all proteobacteria) the five most abundant OTUs. In contrast, the upper airways contained a much more varied range of bacteria including *Pasteurella* and *Thermomonas* (proteobacteria), *Streptococcus* and *Allobaculum* (firmicutes), and *Limibacter* (a bacteroidete) as the five most abundant genera. There was evidence of significant inter-individual variation in microbiome content among both upper and lower respiratory tract samples (both $P < 0.0001$, figure 6-10B).

Specific differences in the bacterial populations were examined using multiple Kruskal-Wallis tests corrected for multiple comparisons. The analysis was limited

to the fifty most abundant bacterial families in the data set. The analysis revealed the substantial differences between the upper and lower respiratory tract samples with 39/50 (78%) of tested bacterial families significant with an uncorrected p-value of < 0.05 and 36/50 (72%) significant with a q-value < 0.05 (figure 6-11A). Amongst the common bacterial families, the Streptococcaceae and Pasteurellaceae were more abundant in upper respiratory tract samples (figure 6-11B). When analysed at the phylum level there were also significant differences between upper and lower respiratory tract samples (figure 6-12A). Proteobacteria and fibrobacteres were more abundant in lower respiratory tract samples whereas other phyla were less common (figure 6-12B).

In summary, the difference between the microbiome of the upper and lower airways was readily apparent with lower diversity in the lower airways, clear separation in NMDS analysis and a high abundance of proteobacteria. Streptococci were more than twenty times as common in the upper respiratory tract as in the lower airways, where they were relatively uncommon.

6-3.3 IL-17RA$^{-/-}$ Microbiome – Upper Respiratory Tract

IL-17RA$^{-/-}$ mice had a lower number of OTUs detected in the upper respiratory tract than wild type controls (figure 6-13A, P = 0.018). The Inverse Simpson diversity index was lower in IL-17RA$^{-/-}$ mice (figure 6-13B, P < 0.001). NMDS analysis demonstrated clear separation of the mouse strains from each other with the IL-17RA$^{-/-}$ mice clustered tightly compared to the more widely distributed wild type mice (P < 0.0001).

At the phylum level, wild type mice had greater abundance of acidobacteria, bacteroidetes and acidobacteria than IL-17RA$^{-/-}$ while proteobacteria were overrepresented in the knockout animals (figure 6-14). Notably, there was no difference in the abundance of firmicutes (the phylum which includes *Streptococci*).

OTU level analysis is shown in figure 6-15. In keeping with the lower OTU count and alpha diversity observed in IL-17RA$^{-/-}$ mice, there were considerable differences between wild type and knockout with a relatively small number of

OTUs dominating the IL-17RA$^{-/-}$ nasal microbiome. Only three OTUs (4, 11 and 23) were required to make up almost half (49.4%) of the IL-17RA$^{-/-}$ microbiome, identified as Pasteurella, Streptococcus and Escherichia/Shigella, while fifteen OTUs would be required to make up the same proportion of the wild type microbiome. Despite this marked difference in OTU abundance, the two most abundant OTUs in wild type and IL-17RA$^{-/-}$ mice were the same (OTU 4 and OTU 11). OTU 4 was identified as a Pasteurella sp. and shared 99% homology to previously sequenced isolates of *Pasteurella pneumotropica*, an organism known to be commonly found colonising laboratory mice. OTU 11 was identified as a Streptococcus sp. and shared 99% sequence homology with *Streptococcus danielliae*, an organism only recently defined and known to be a member of the viridans group of Streptococci. Also notable in the OTU level analysis was the presence of OTU 23 at high abundance in IL-17RA$^{-/-}$ mice (median 4.4%, IQR 0.1% - 12.3%) while it was not found at an abundance greater than 0.03% in wild type animals (median 0.006%, IQR 0.0007% - 0.012%; $P < 0.001$). Family level analysis (figure 6-16) largely confirmed the impressions of the above analysis with pasteurellaceae relatively more abundant in IL-17RA$^{-/-}$ mice while other significant differences were the relatively reduced abundance of other families in the knock out animals (figure 6-16B).

In summary, the microbiome of the upper respiratory tract of IL-17RA$^{-/-}$ mice was substantially different from that of wild type mice in that it had significantly reduced diversity and clear separation of the clusters on NMDS analysis. The nasal microbiome of IL-17RA$^{-/-}$ mice was dominated by a relatively small number of OTUs and proteobacteria were significantly more abundant in these mice, a finding which is in keeping with the excess of gram negative bacilli noted on routine culture of the nasal washes.

6-3.4 IL-17RA$^{-/-}$ Microbiome – Lower Respiratory Tract

The lower respiratory tract microbiome of the wild type and knockout mice was also examined. As already discussed, the lower respiratory tract microbiome was less diverse than the upper respiratory tract with a greater preponderance of proteobacteria. The difference between the wild type and knockout mice was far less marked at this site with a small (but statistically significant) difference

in OTU count (median WT: 230 OTUs; IL-17RA$^{-/-}$: 249 OTUs; P = 0.019, figure 6-17A) and inverse Simpson diversity (median WT: 9.3; IL-17RA$^{-/-}$ 12.3; P = 0.011, figure 6-17B). The NMDS analysis plot is shown in figure 6-17C. Again there was a significant difference in the distribution of the clusters but, in contrast to the upper respiratory tract, there was considerable overlap in the distribution although it remained statistically significant (P = 0.030).

Bacterial phyla are shown in figure 6-18A. The distribution was similar between the two groups with no difference in the abundance of any of the principal phyla (figure 6-18B).

At the OTU level, the lower respiratory tract was also very similar, with the most common taxa present in similar distributions (figure 6-19) and the analysis of bacteria at the family distribution was also similar (figure 6-20). No bacterial families approached statistical significance with the q-value of the most dissimilar family being 0.27.

In summary, there were small differences between the measures of diversity in wild type and IL-17RA$^{-/-}$ mice and some difference in distribution on NMDS analysis. However, there was little difference identified at various taxonomic levels.

A further summary of the differences between wild type and IL-17RA$^{-/-}$ mice is shown in figure 6-21. A similarity tree of Bray distances shows the clustering of upper and lower respiratory tract samples with clear separation of airway samples by site and separation of upper airway samples between wild type and knockouts. The lower respiratory tract samples are mixed in the middle of the plot underlining the lack of a clear difference between lower respiratory tract microbiomes of the two groups.

6-3.5 Respiratory tract microbiome following colonisation with SRL1

The differences in the respiratory tract microbiome between wild type and knockout animals were further explored using the model of nasal colonisation. Mice were inoculated with 5 x 10^5 cfu of SRL1 or PBS and the respiratory tract microbiome sampled on days 3, 7 and 14. Since nasal wash cannot be completed

in live animals, sampling at each time point represents different mice. PBS inoculated mice were culled and sampled on day 14.

It was noted that following colonisation OTU 2 (which has the same sequence as that expected of SRL1) was detected in all samples at least low abundance, including those mice which had not been colonised with SRL1. OTU2 was found in low abundance among unexposed mice (<1% in all but one sample from the upper respiratory tract). Mice are not known to be naturally colonised with *S. pneumoniae* and no colonies of *S. pneumoniae* were ever identified from the respiratory tract samples of unexposed mice. Mice infected or colonised with *S. pneumoniae* were always kept in separate rooms in the animal facility from stock animals. The phylogeny tree for all OTUs is shown in figure 6-22A with the sequences identified as belonging to streptococci highlighted and expanded in figure 6-22B. OTU2 was closely related to a number of other streptococcal sequences, differing from OTU 100 and OTU 97 by the minimum distance possible given the clustering method used. Both of these sequences were identified as belonging to viridans (non-pneumococcal) streptococci. It was therefore concluded that the finding of small numbers of sequences belonging to OTU 2 among un-exposed animals does not present evidence of colonisation with *S. pneumoniae*. To reinforce this, pcr for *cpsa* was conducted on the respiratory tract lysates using the positive control primer used in the CDC sequencing multiplex reaction. A strong band was observed in most of the previously exposed mice and a weak band observed in most others. However, none of the unexposed mice had any evidence of the presence of the *cpsa* gene (figure 6-22C).

The impact of nasal colonisation on the upper and lower respiratory tract is shown in figure 6-23. OTU counts are shown in figure 6-23A and the inverse Simpson index in figure 6-23B. In the upper respiratory tract, the inoculation with SRL1 was associated with a significant change in both the OTU count and inverse Simpson index among wild type animals with a fall in both measures of bacterial diversity after exposure to SRL1. This fall in diversity remains out to day fourteen, although there is some evidence of an increase in the scores again on day 14 although they do not reach the pre-colonisation levels. IL-17RA$^{-/-}$ mice also had a reduction in the OTU count in upper respiratory tract samples

following colonisation, although the reduction was less marked. There is little evidence of a difference in inverse Simpson index among these mice. Overall, there was evidence of a significant group-wise difference in both measures of diversity on 2-way ANOVA ($P < 0.001$ and $P = 0.02$ respectively).

In the lower respiratory tract, there was less evidence of a difference in alpha diversity following nasal colonisation. There was evidence that OTU count was reduced in both groups of mice following colonisation but there was no evidence of a time-wise difference following colonisation in the inverse Simpson index. There was no evidence of a group-wise difference in either measure during the time-course.

NMDS analysis is shown in figure 6-23C. In the upper respiratory tract, colonisation induced a significant shift away from the uncolonised samples. Many of the samples clustered close together on the plot and the locations of samples on the plot was often similar among wild type and IL-17RA$^{-/-}$ mice despite the different location of the uncolonised samples. This is most notable among the samples in which OTU 2 was not present in high abundance. The difference in the distribution of samples within the upper respiratory tract following colonisation was highly significant ($P < 0.0001$ for both groups).

In the lower respiratory tract, the change in distribution of samples differed between groups of mice. Among wild type animals, there was no statistically significant difference in the distribution of exposed and unexposed mice ($P = 0.09$). In contrast, the difference in distribution among IL-17RA$^{-/-}$ mice was clear with exposed mice clearly separated from the unexposed group ($P < 0.0001$).

The effect of exposure to SRL1 on the upper respiratory tract at the OTU level is shown in figure 6-24. Although colonies of SRL1 could be detected in the nasal wash of most wild type animals at days 3 and 7 (figure 6-6B), most wild type animals did not have OTU 2 present in high abundance in the microbiome data. There was a clear difference between the abundance of OTU 2 in upper respiratory tract samples between wild type and IL-17RA$^{-/-}$ mice with the density of OTU 2 significantly higher among IL-17RA$^{-/-}$ mice than wild type ($P = 0.013$). In

some IL-17RA$^{-/-}$ mice there was an extremely high density of OTU 2 (up to 85% in one case). There was a striking difference between exposed and un-exposed animals in terms of the other taxa observed with the microbiome. Even in mice with low abundance of OTU 2, there was a dramatic change in the constitution of the microbiome with several OTUs common among unexposed animals becoming uncommon following exposure to SRL1. For example, OTU 4 (identified as a pasteurella) and OTU 11 (a streptococcus) are the two most common OTUs in both groups of mice before exposure to SRL1 but account for only 1.5% and 0.6% after colonisation even after exclusion of OTU 2. OTU 1 (an ochrobactrum) increases markedly in abundance following exposure to SRL1, but only in mice that do not have high abundance of OTU 2. Therefore, the upper airway microbiome is substantially altered by exposure to SRL1 whether or not the SRL1 is able to successfully colonise with high abundance.

In the lower respiratory tract, there was a less significant difference between exposed and unexposed samples. There was again, however, a significant difference between the wild type and IL-17RA$^{-/-}$ mice in terms of OTU 2 abundance with greater abundance of OTU 2 in the lower respiratory tract of IL-17RA$^{-/-}$ (figure 6-25A, P = 0.019). There was again an expansion of ochrobactrum within mice exposed to SRL1 but without high-level colonisation.

The association between OTU 1 and OTU 2 was explored using linear modelling (figure 6-26). This model revealed a dichotomous relationship between these OTUs (which were the 2nd and 3rd most common OTUs overall in the dataset). In the upper respiratory tract of un-exposed animals, there was a strong positive correlation between OTU1 and OTU2 ($P < 0.0001$) whereas among exposed animals the correlation was strongly negative ($P < 0.0001$). A similar pattern was repeated in the lower respiratory tract samples among exposed mice ($P < 0.0001$), although in this case there was no correlation among unexposed mice ($P=0.25$).

In summary, exposure of the upper respiratory tract to SRL1 induced a number of significant changes within the respiratory tract microbiome of wild type and IL-17RA$^{-/-}$ mice. It should be noted that the colonisation density in this experiment was lower than that achieved during the initial experiments

involving SRL1 in nasal colonisation and that colonisation was not achieved in all wild type animals at 7 days. However, despite this the difference that colonisation makes to the respiratory tract microbiome is marked with significant loss of diversity and distinct clustering in NMDS analysis even in animals that appear to have cleared SRL1 from the respiratory tract. In both the upper and lower airways, IL-17RA$^{-/-}$ mice had increased colonisation density with SRL1 and some mice had microbiomes dominated by SRL1.

6-4 Discussion

In the experiments outlined above I have explored the role of IL-17 in the nasal colonisation of mice with *S. pneumoniae* as well as the complex nasal microbiome of unexposed animals. To some extent this work confirms that of others who have demonstrated the increased susceptibility of mice lacking IL-17, either because of depletion or genetic manipulation, to colonisation with *S. pneumoniae*. In the last chapter, I described the difference in pulmonary infection with TIGR4 and SRL1 and the difference in the role of IL-17 in this model. In contrast, IL-17 had a similar role in nasal colonisation with these strains of *S. pneumoniae*: it was protective. IL-17RA$^{-/-}$ mice had higher colonisation density at seven days and consistently higher bacterial density over a time course involving SRL1. I evaluated the percentage of neutrophils in the nasal wash at the same time as sampling. Relative abundance was assessed and the other cellular content of the wash was not assessed. The experiments involving TIGR4 and SRL1 were divergent in terms of the impact of IL-17 on neutrophil percentage. In IL-17RA$^{-/-}$ mice, neutrophil percentage was lower than wild type in SRL1 colonisation but higher in TIGR4 colonisation. Furthermore, this observation suffers from the same problems discussed earlier with regards to lung homogenates, that changes in neutrophil percentages could be due to undetected fluctuations in other cell types. Previous data have suggested that IL-17 mediated clearance of nasal colonisation in naïve mice is dependent on macrophages rather than neutrophils[172]. Since I did not more extensively examine the role of neutrophils in this experiment, the data should be regarded with caution.

In view of the differences outlined above, I decided to investigate the respiratory tract microbiome of IL-17RA$^{-/-}$ mice. To the best of my knowledge, the resting upper respiratory tract microbiome in wild type mice has only been described once in the published literature[448]. This study investigated differences in the microbiota of young and old mice before and after colonisation with *S. pneumoniae*. It is inevitable that mice housed in geographically distinct facilities will have significant differences between their microbiota. However, there were many similarities demonstrated between the respiratory microbiota of the animal populations used in the two studies. Both studies found high levels of diversity in the upper respiratory tract of healthy laboratory mice with proteobacteria, firmicutes, bacteroidetes and actinobacteria most abundant. This is in contrast to the healthy human nasal microbiome, in which actinobacteria (particularly *Propionibacteria* and *Corynebacteria*) and firmicutes predominate with relatively sparse abundance of proteobacteria and bacteroidetes[449,450].

No previous study has directly compared the mouse upper and lower respiratory tract microbiome. However, the lower respiratory tract microbiome of laboratory mice has been described before [451,452]. In both studies, proteobacteria predominated with *Acinetobacter sp.* and *Pseudomonas sp.* found in each study respectively. Assessing the human lower respiratory tract microbiome is more challenging, since the only sampling method (BAL) inevitably involves transiting a bronchoscope through the upper respiratory tract. There is wide variation in the human lower respiratory tract but some studies have also demonstrated a high abundance of proteobacteria such as *Pseudomonas sp.* and *Ralstonia sp.* [453,454]. In the present study, diversity in the lower respiratory tract was much lower than in the nose and there was a high abundance of proteobacteria such as *Thermomonas and Cupriavidus*. This is similar to the situation in humans, where there is much lower bacterial diversity in the lower respiratory tract[455].

There was a substantial difference between the nasal microbiome of IL-17RA$^{-/-}$ and wild type mice with decreased microbial diversity among the IL-17RA$^{-/-}$ mice. While the leading constituents of the microbiome were similar – the majority of the top twenty OTUs were members of this set in both groups – the IL-17RA$^{-/-}$ nasal microbiome was dominated by a small number of bacterial

species which were expanded compared to wild type. Decreased bacterial diversity in the gut has frequently been associated with disease states such as inflammatory bowel disease[456,457], type 1 diabetes[458] or obesity[459]. The pattern in respiratory diseases is more mixed, with – for example – severity of obstructive disease found to correlate positively[460], negatively[453] or not at all[461] with bacterial diversity. It is attractive to speculate that decreased bacterial diversity representing failure to control overgrowth of dominant clones will correlate with failure to control the colonisation of pathogens but in the study by Krone *et al*[462], elderly mice were more susceptible to colonisation but had similar levels of bacterial diversity at baseline[448].

Great care was taken to attempt to minimize the effects of environment on the nasal microbiome. Since mouse colonies had been housed in the same animal facility in identical conditions for greater than 3 years, it was felt to be likely that sufficient time had elapsed for microbiomes to equalise. For these experiments, animals were mixed at the earliest time possible and for at least 6 weeks prior to microbiome sampling or artificial colonisation. However, since nasal microbiome is likely to be acquired early in life, the necessity of caging animals separately during the infant period could result in a persistent, effectively inherited, distinct microbiome between colonies. The mouse gut microbiome undergoes rapid change in relative abundance but not composition in the period following weaning until stabilising as the mouse matures[463]. There are no data on the development of the respiratory tract microbiome in mice but data in humans shows that microbiome is established early in life but undergoes significant changes as the infant grows[464]. This concern could be addressed by breeding IL-17RA$^{+/-}$ heterozygotes and sampling microbiome from the second generation. However, this was not possible with the time and resources available. The similarity of the lower respiratory tract microbiome between the two groups provides further reassurance that the differences noted in nasal microbiome are likely to be related to IL-17 signalling rather than confounded.

The effect of pneumococcal colonisation on the microbiome was striking. In contrast to the colonisation study outlined above, the present study used a tenfold lower inoculum of *S. pneumoniae* (5×10^5 rather than 5×10^6 pneumococci). This was sufficient to colonise wild type mice for one week but at

relatively low level. It is unfortunate that the experiment in which the microbiome was assessed resulted in lower levels of colonisation than other similar experiments. However, even mice which were colonised with *S. pneumoniae* at low level demonstrated marked loss of diversity and in particular there was increased abundance of *Ochrobactrum sp*. The study by Krone *et al* also demonstrated marked loss of diversity in the nasal microbiome associated with induction of colonisation[448]. However, experimental pneumococcal colonisation in humans was associated with little change or a small increase in diversity depending on the strain used[465] as was use of nasal influenza vaccine[466]. These differences may be due to the inoculating dose, which was significantly lower in absolute terms than even the relatively low dose used in my experiments. Given the difference in nasal cavity size between mice and humans, the relative dose is likely to be several orders of magnitude lower. Mice colonised with pneumococci in my experiments recruited neutrophils to the nasal mucosa and it is likely that this inflammation results in important changes in bacterial diversity. One study monitoring the human nasal microbiome during a transition to an inflammatory state involved experimental challenge with rhinovirus and involved the development of clinical illness, at least in some subjects[467]. Subjects successfully infected with rhinovirus had significantly lower bacterial diversity than uninfected controls. Since SRL1 is highly resistant to phagocytosis by neutrophils, it seems likely that commensal bacteria will be disrupted by the immune response as well as bacterial competition. Pneumococcal colonisation in children is known to be associated with viral URTI[21] and it may be that inflammation within the nasal cavity facilitates this by clearing other bacteria from the niche.

The role of the *Ochrobactrum sp*. is unclear. In many of the pneumococcal samples following colonisation there is a marked increase in abundance which is negatively correlated with SRL1 abundance. The interaction between different colonising bacteria and the immune response is complex[468]. It may be that the inflammatory milieu generated by pneumococcal challenge allows the Ochrobactrum to outcompete other organisms unless SRL1 becomes the dominant species. However, the finding that Ochrobactrum fails to outcompete SRL1 suggests that artificial inoculation of this organism would be unlikely to be useful in the prophylaxis against pneumococcal colonisation.

The observed differences in the neutrophil population noted in the nasal wash may be a causative factor in the difference in pneumococcal colonisation density and microbiome between wild type and knockout animals. However, there are other possible other explanations of the differences observed. Differences in endothelial cell function and secretion of antimicrobial peptides was not assessed and it is possible that these important. It is also possible that the microbiome differences directly contribute to the differences in pneumococcal colonisation. However, this is unlikely, since the previous study on pneumococcal nasal colonisation in naïve mice demonstrated similar effects on colonisation with IL-17A depleting antibody.

This study has several implications for pneumococcal vaccination. It adds further evidence that IL-17 is an important cytokine in the control of nasal colonisation with *S. pneumoniae* and demonstrates that this association is maintained among two pneumococcal strains already demonstrated to be very different in their infectious phenotype and to interact with IL-17 differently in the context of disease. It is impossible to exclude that the altered nasal microbiome of IL-17RA$^{-/-}$ at baseline could be responsible for the increased propensity to pneumococcal colonisation seen in this and other studies rather than a direct relationship. However, the finding that antibody neutralisation of IL-17 also increases susceptibility to colonisation makes this considerably less likely[352]. There is concern that vaccines targeted at eliminating one bacterial species from the nose might lead to replacement with other bacterial species, such as *Neisseria meningitidis* or *Staphylococcus aureus* and potentially important effects of PCV vaccination on infant nasal microbiomes has already been reported[469]. This study underlines how sensitive the nasal microbiome is to immune manipulation and emphasises the importance of surveillance if vaccines exploiting IL-17 immunity reach the market.

There has recently been increased attention on the role of contamination in low biomass microbial ecology samples[456]. My study used a no template control but this control had not been passed through the DNA extraction process – which is implicated as a common source of contamination in the study by Salter *et al*[456]. Furthermore, several of the abundant OTUs in the data are represented in the list of commonly contaminating bacteria, such as *Cupriavidus sp*. It is therefore

difficult to exclude the possibility of contamination in this study. However, if contamination were present, it would be unlikely to impact the conclusions reached, particularly in upper respiratory tract samples and colonised samples since differences between mouse groups are clear.

In conclusion, despite the important differences between SRL1 and TIGR4 in symptomatic disease, IL-17RA$^{-/-}$ mice were more vulnerable to nasal colonisation with both strains of pneumococcus. IL-17RA$^{-/-}$ mice also had significant differences in their resting microbiome compared to wild type controls reinforcing the important role of IL-17 in regulating mucosal immunity in the respiratory tract.

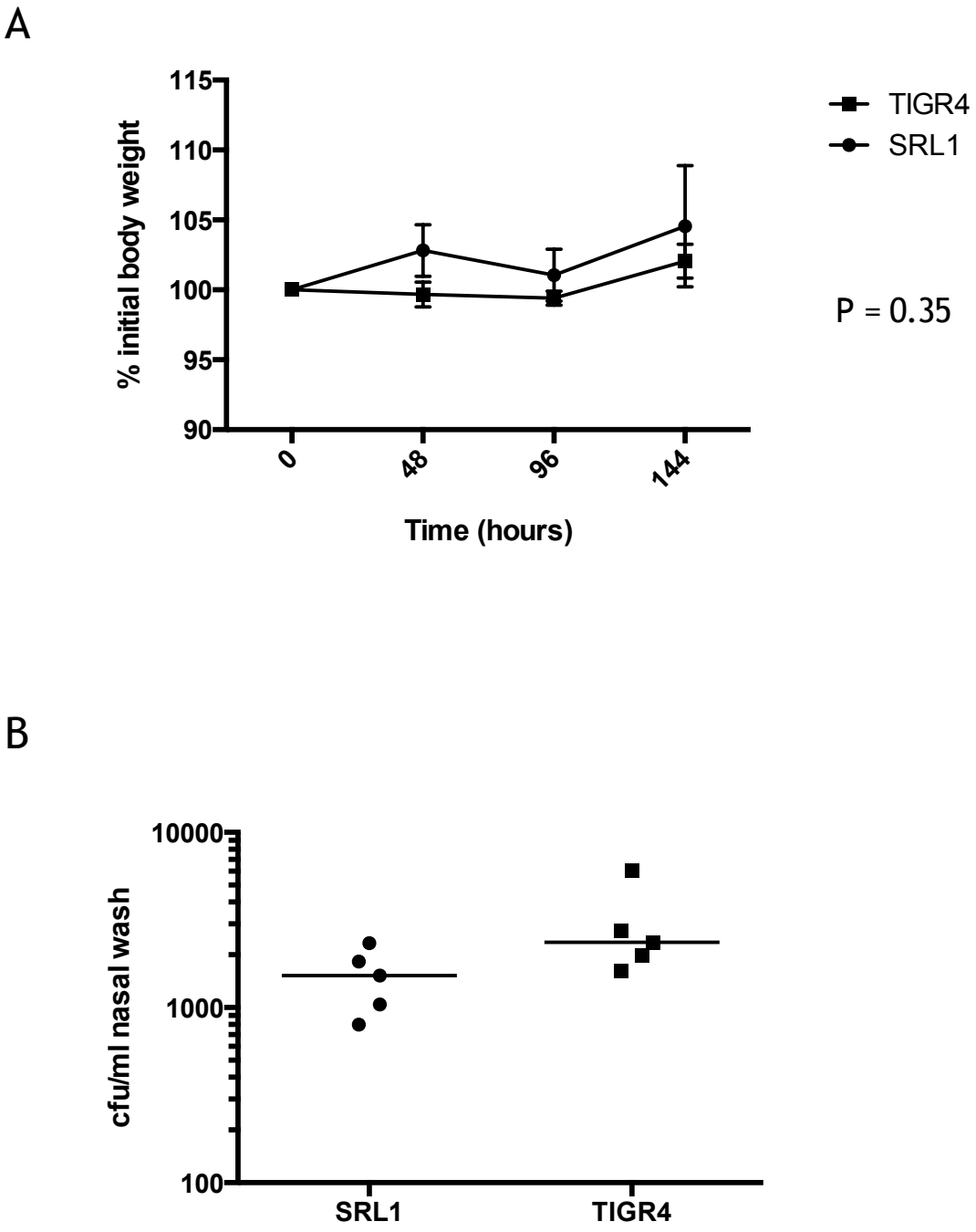

Figure 6-1. Establishment of nasal colonisation in wild type mice with SRL1 and TIGR4.

Mice were administered 5 x 10^5 cfu/mouse of bacteria onto their nostrils without anaesthesia. Mice were then monitored for 1 week before being culled and nasal washes performed. A. Change in body weight over the course of the experiment. B. Bacterial burden within the nasal cavity after seven days. Note that the limit of detection of bacteria was 100 cfu/ml in this experiment.

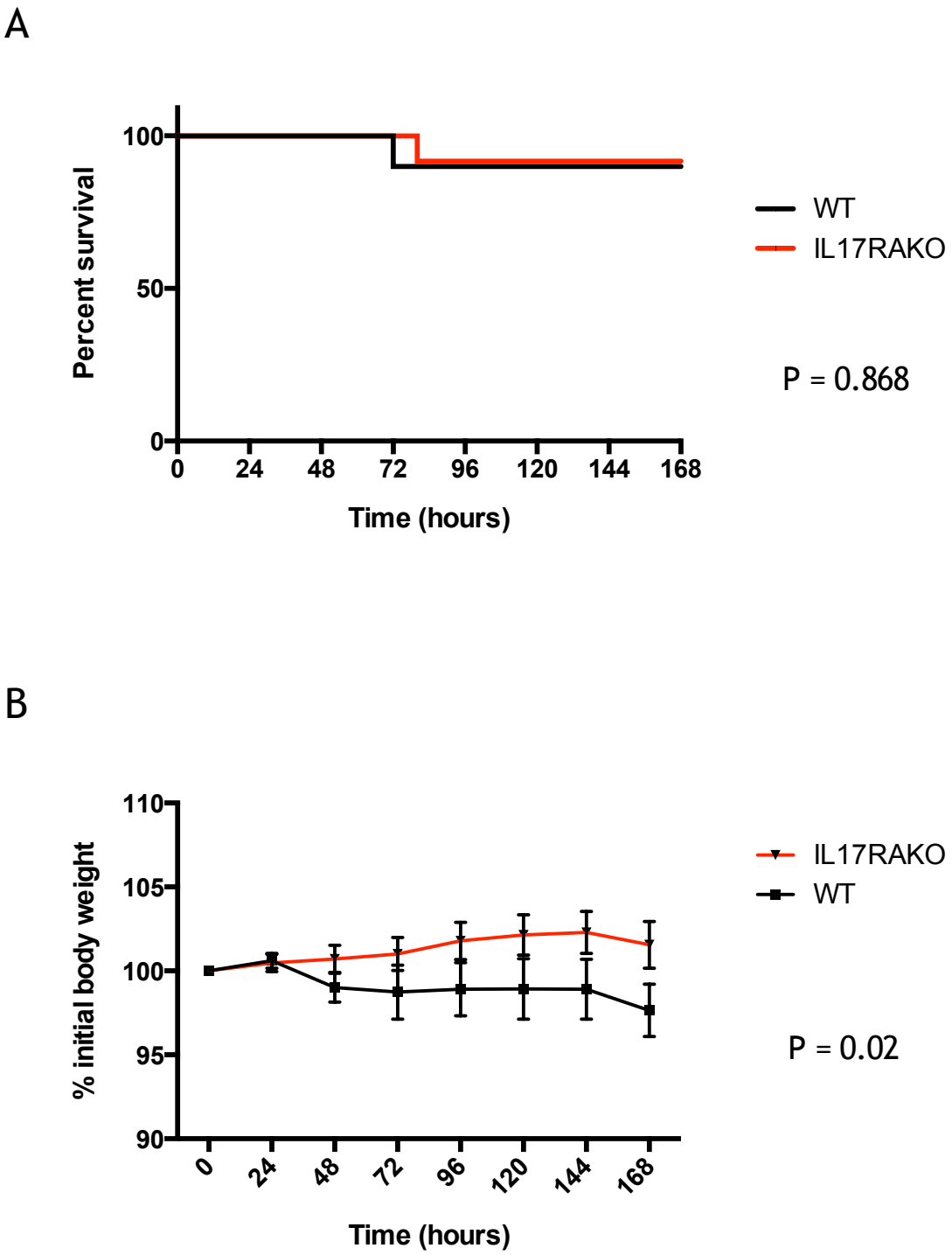

Figure 6-2. The role of IL-17 in TIGR4 nasal colonisation.

Survival and weight change. Wild type and IL-17RA$^{-/-}$ mice were inoculated via the intra-nasal route with 5 x 10^5 cfu of TIGR4 without anaesthesia. Animals were monitored for seven days. A. Survival curve. B. Change in body weight during experiment.

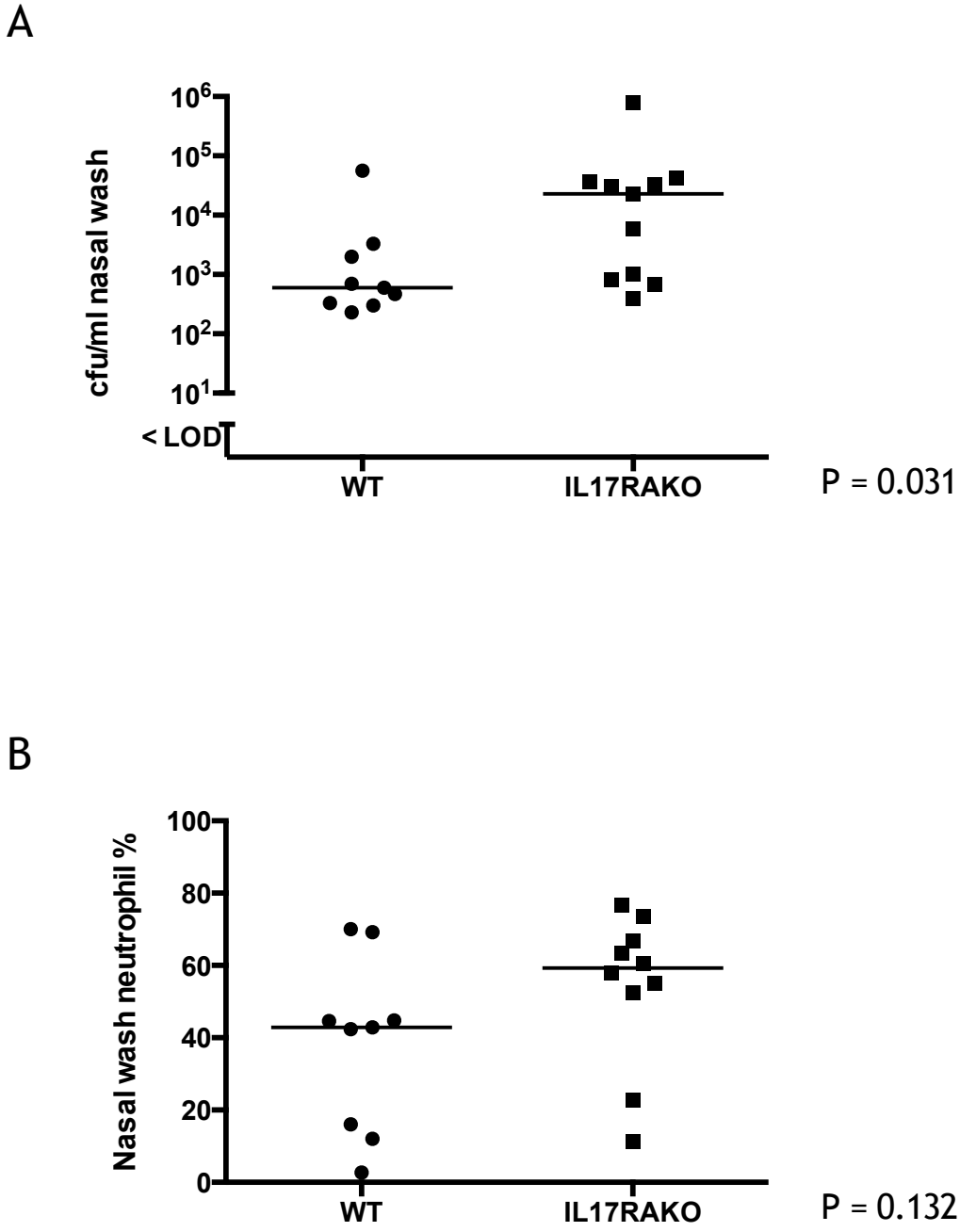

Figure 6-3. The role of IL-17 in TIGR4 nasal colonisation.
Survival and weight change. Wild type and IL-17RA$^{-/-}$ mice were inoculated via the intra-nasal route with 5 x 10^5 cfu of TIGR4 without anaesthesia. Animals were monitored for seven days. Bacterial burden (A) and neutrophil percentage ascertained with flow cytometry (B) of animals surviving to the end of the experiment.

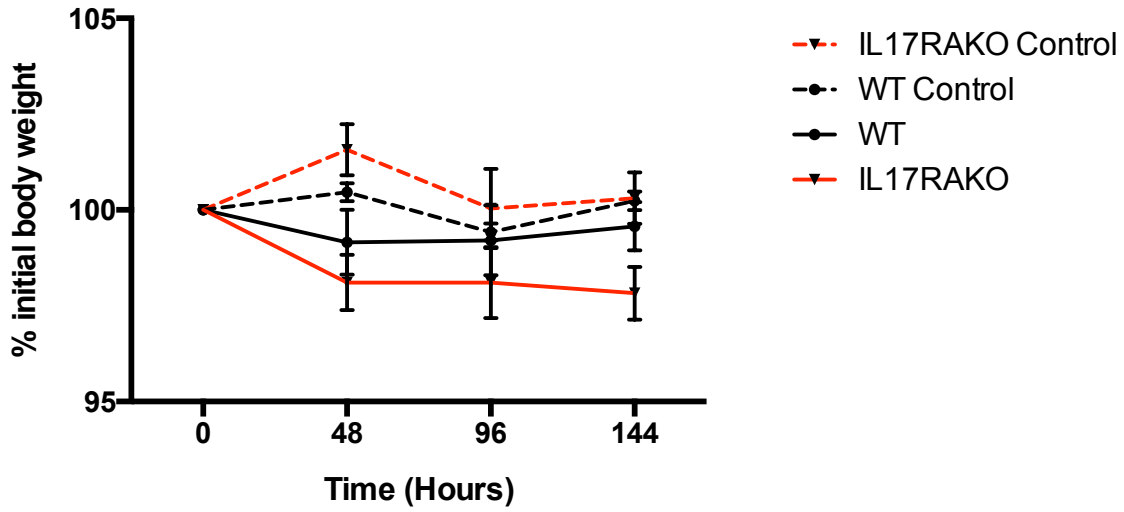

Figure 6-4. The role of IL-17 in SRL1 nasal colonisation: survival and weight change.

Wild type and IL-17RA$^{-/-}$mice were inoculated via the intra-nasal route with 5 x 10^5 cfu of SRL1 without anaesthesia. Change in body weight during experiment.

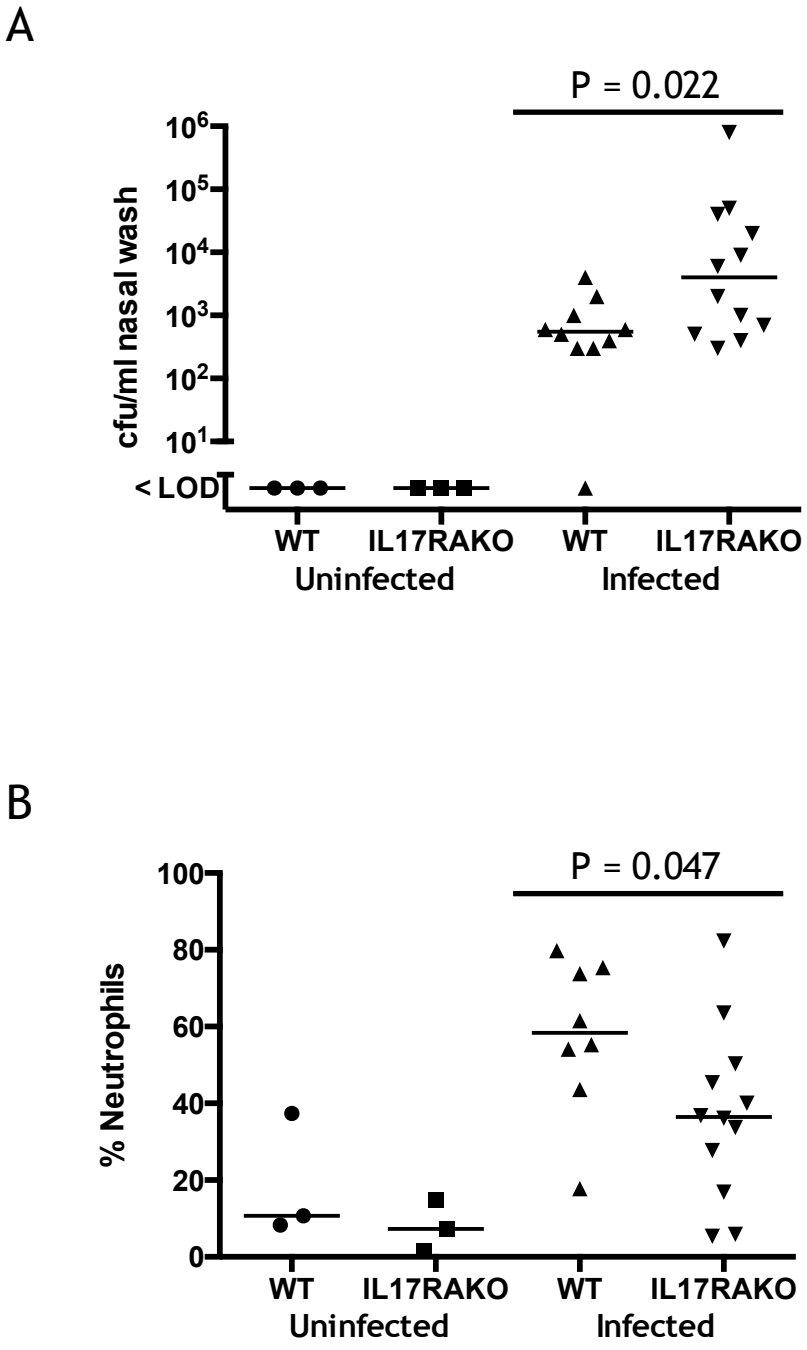

Figure 6-5. The role of IL-17 in SRL1 nasal colonisation: nasal wash.
Wild type and IL-17RA$^{-/-}$mice were inoculated via the intra-nasal route with 5 x 10^5 cfu of SRL1 without anaesthesia. Animals were monitored for seven days. Bacterial burden (A) and neutrophil percentage ascertained with flow cytometry (B) of animals surviving to the end of the experiment.

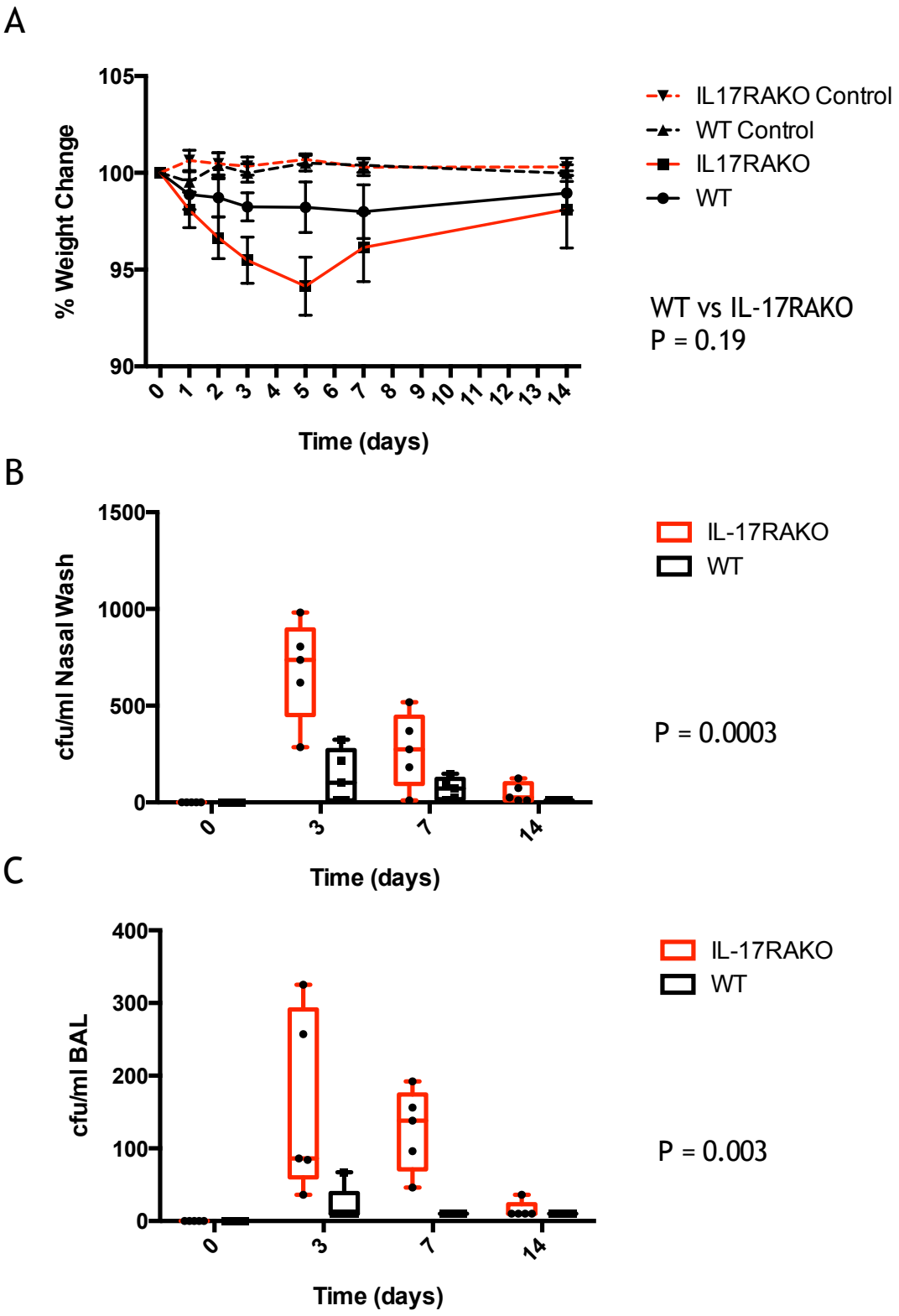

Figure 6-6. The role of IL-17 in SRL1 nasal colonisation: time series.
Wild type and IL-17RA$^{-/-}$ mice were inoculated via the intra-nasal route with 5 x 10^5 cfu of SRL1 without anaesthesia. Animals were monitored for up to 14 days. A. Change in body weight during experiment. B. Bacterial burden in nasal wash. C. Bacterial burden in BALF.

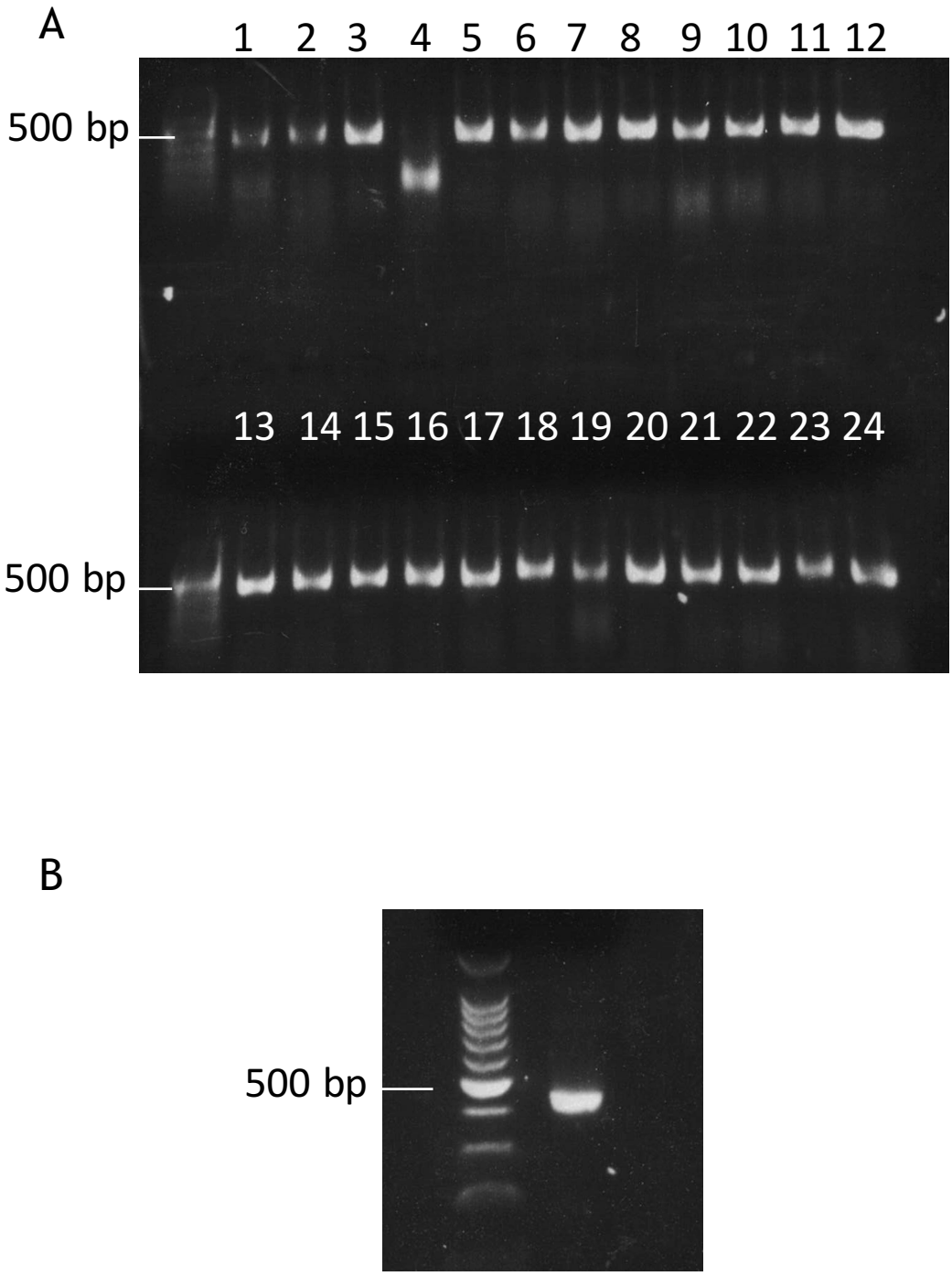

Figure 6-7. Amplification of V_1-V_2 region of bacterial 16S gene from respiratory tract samples.

Representative agarose gel electrophoresis showing (A) PCR products obtained from amplification of lavage lysate and (B) following cleanup and mixing of amplicons prior to sequencing. Note the failure of amplification in sample 4. The predicted band length of amplicon with barcode and adapters is 440bp.

A

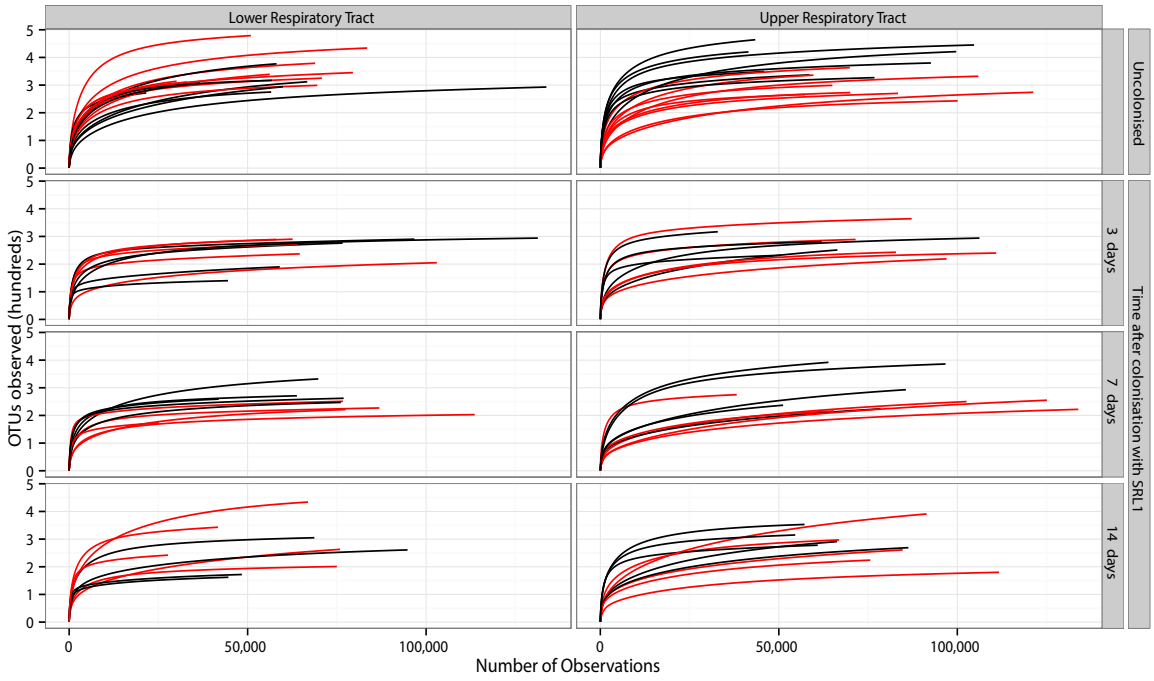

B

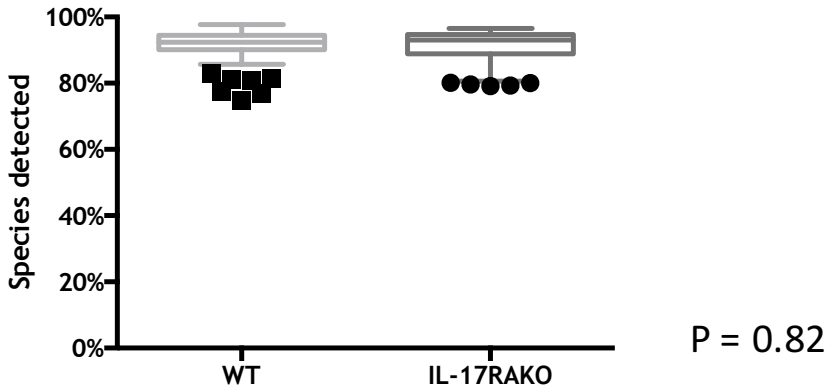

Figure 6-8. Assessment of sequencing depth.

A. Rarefaction curves for upper and lower respiratory tract samples by time of colonisation. Time in days represents time after colonisation. B. Percentage of OTUs detected per sample using the Abundance-based coverage estimator (ACE).

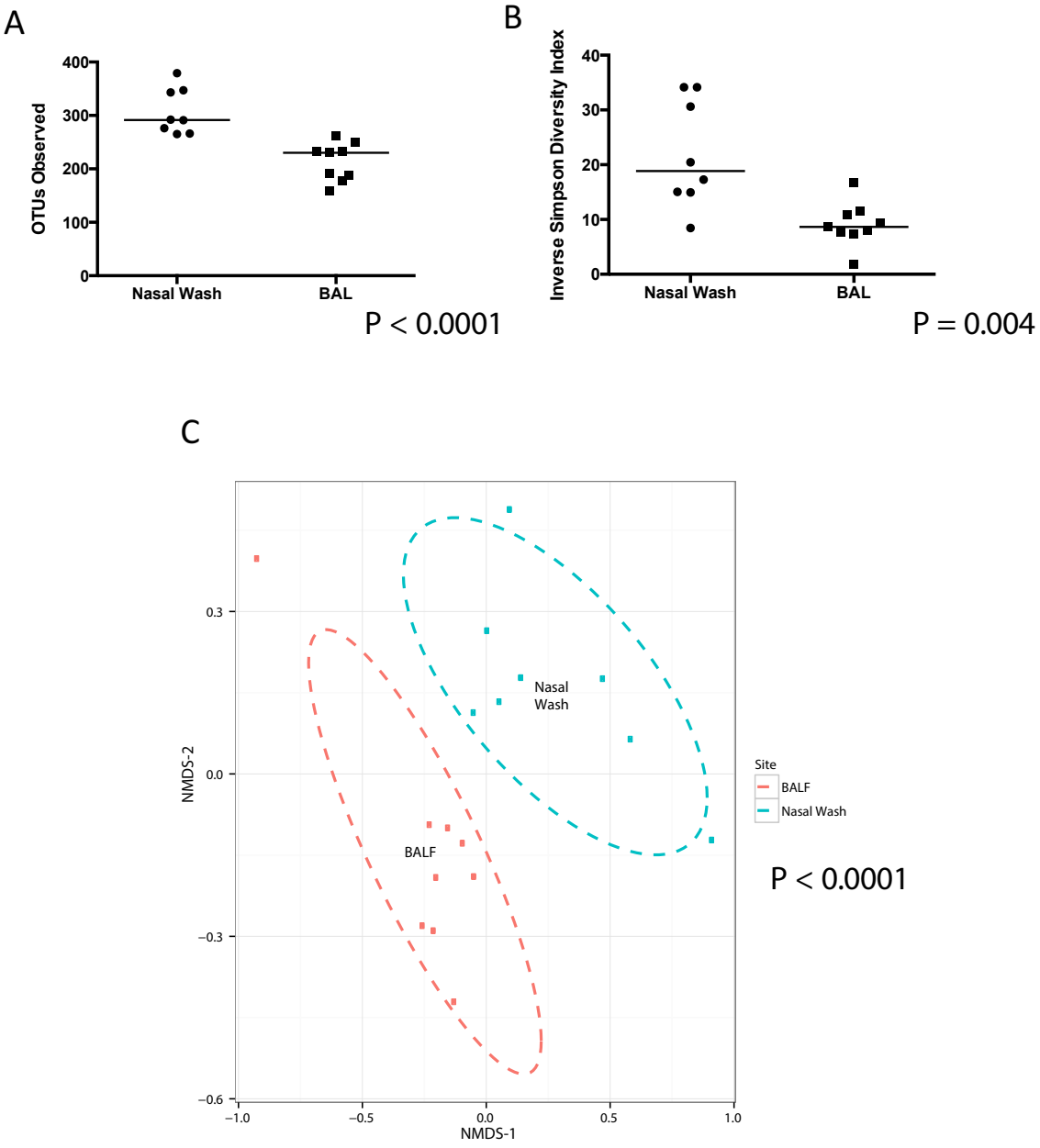

Figure 6-9. Comparison between nasal wash and BALF in untreated wild type animals.

A. OTU count and B. inverse Simpson index in samples rarefied to even sequencing depth. P value represents Mann-Whitney test. C. Multidimensional scaling analysis of samples with curves indicating 80% confidence of sample distribution. P value represents multivariate ANOVA.

A

	Upper Respiratory Tract			Lower Respiratory Tract		
	OTU	Genus	%	OTU	Genus	%
1	**OTU 4**	**Pasteurella**	**5.5**	**OTU 3**	**Thermomonas**	**18.6**
2	OTU 11	Streptococcus	4.9	**OTU 672**	**Cupriavidus**	**9.9**
3	OTU 28	Allobaculum	4.9	**OTU 7**	**Bosea**	**9.3**
4	**OTU 3**	**Thermomonas**	**4.3**	**OTU 5**	**Methylobacterium**	**7.9**
5	OTU 26	Limibacter	3.8	**OTU 4**	**Pasteurella**	**7.6**
6	OTU 25	Gemella	3.2	**OTU 6**	**Ralstonia**	**4.5**
7	**OTU 1**	**Ochrobactrum**	**3.1**	OTU 14	Sphingomonas	4.1
8	OTU 33	Aerococcus	3.1	OTU 13	Rhizobium	4.1
9	**OTU 18**	**Streptococcus**	**3.1**	**OTU 1**	**Ochrobactrum**	**2.3**
10	**OTU 672**	**Cupriavidus**	**2.8**	OTU 57	Enhydrobacter	2.2
11	**OTU 5**	**Methylobacterium**	**2.4**	OTU 9	Methylobacterium	1.9
12	**OTU 10**	**Propionibacterium**	**2.2**	**OTU 18**	**Streptococcus**	**1.8**
13	OTU 21	Dyella	2.0	OTU 27	Microbacterium	1.4
14	**OTU 6**	**Ralstonia**	**1.9**	**OTU 10**	**Propionibacterium**	**1.0**
15	OTU 52	Paludibacter	1.7	OTU 20	Staphylococcus	0.8
16	**OTU 7**	**Bosea**	**1.5**	OTU 221	Hymenobacter	0.6
17	OTU 22	Dermacoccus	1.4	OTU 114	Roseomonas	0.6
18	OTU 45	Campylobacter	1.3	OTU 8	Roseomonas	0.6
19	OTU 41	Allobaculum	1.3	OTU 44	Sphingomonas	0.6
20	OTU 37	Elizabethkingia	1.2	OTU 31	Acinetobacter	0.5
		Others	44.6		Others	19.7

B

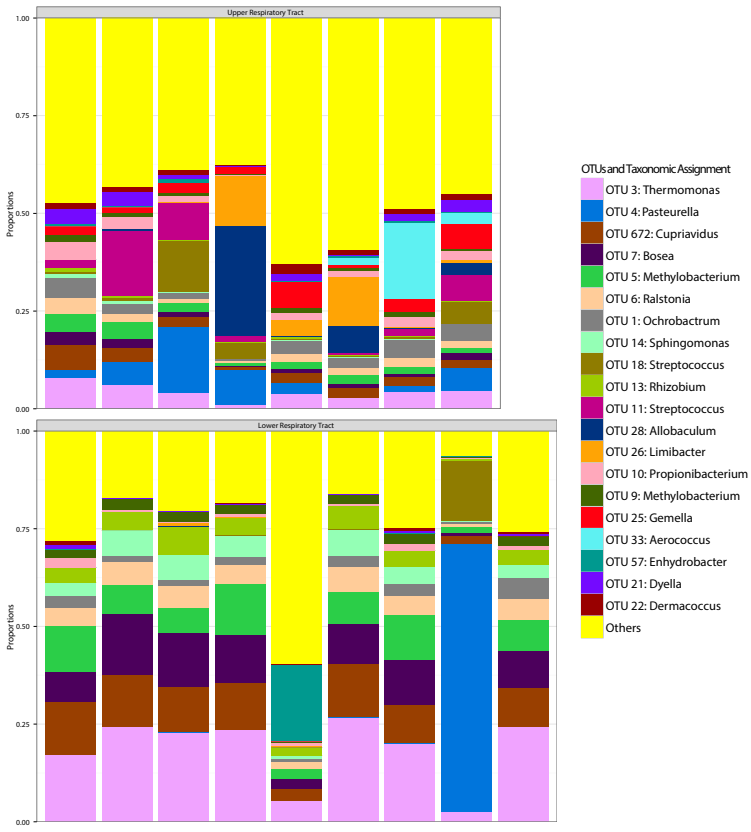

Figure 6-10. OTU level analysis of respiratory tract microbiome.
Taxa relative abundance in upper and lower respiratory tract samples among wild type animals. A. 20 most abundant OTUs in wild type microbiome at each site. OTUs occurring in both lists are shown in bold. B. Relative abundance 20 most abundant OTUs in individual samples. Other OTUs are shown in yellow.

A

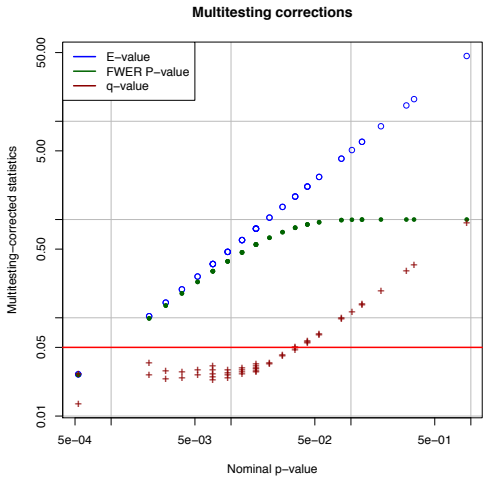

B

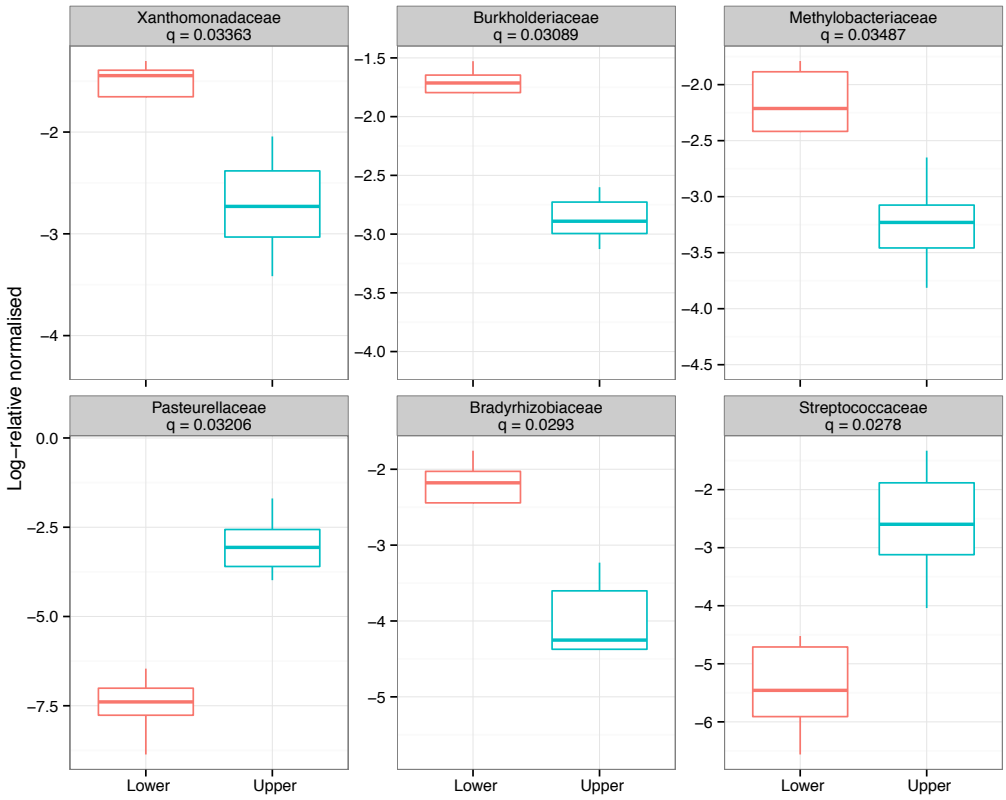

Figure 6-11. Differences among bacterial families in the respiratory tract. Multiple testing of differences between bacterial species at the genera level between upper and lower respiratory tract samples from wild type mice. Significance tests involve the 50 most abundant bacterial families. A. Results of multiple Kruskal-Wallis tests with uncorrected p-value plotted against E-value and q-value. Signifiicant results are regarded as those with a corrected significance level < 0.05. B. Plots showing log normalised relative adundance of selected individual bacterial families achieving statistical significance after correction.

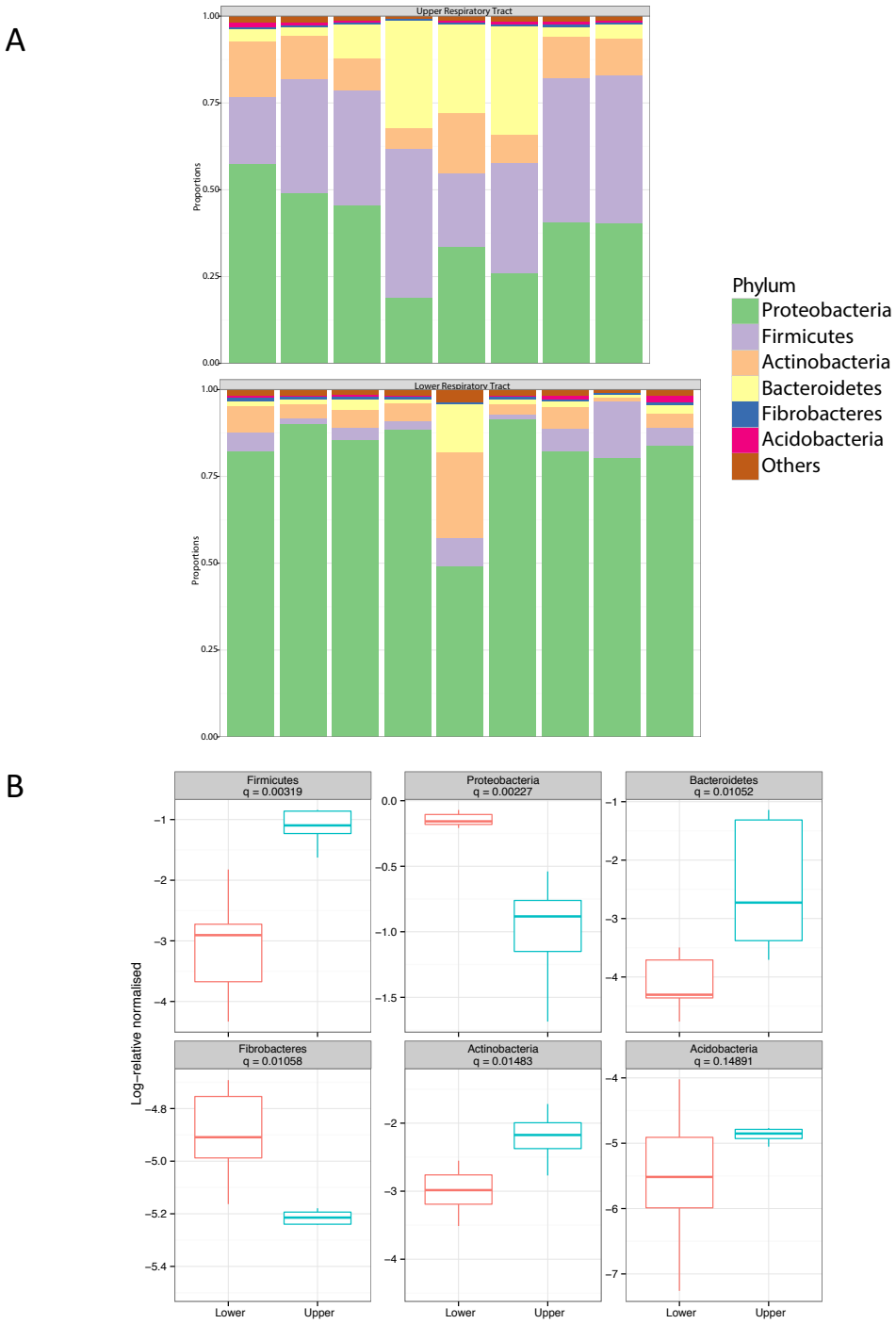

Figure 6-12. Multiple testing of differences between bacterial species at the phylum level between upper and lower respiratory tract samples from wild type mice.

Significance tests involve the 50 most abundant bacterial families. A. Results of multiple Kruskal-Wallis tests with uncorrected p-value plotted against E-value and q-value. Signifiicant results are regarded as those with a corrected significance level < 0.05. B. Plots showing log normalised relative adundance of selected individual bacterial families achieving statistical significance after correction.

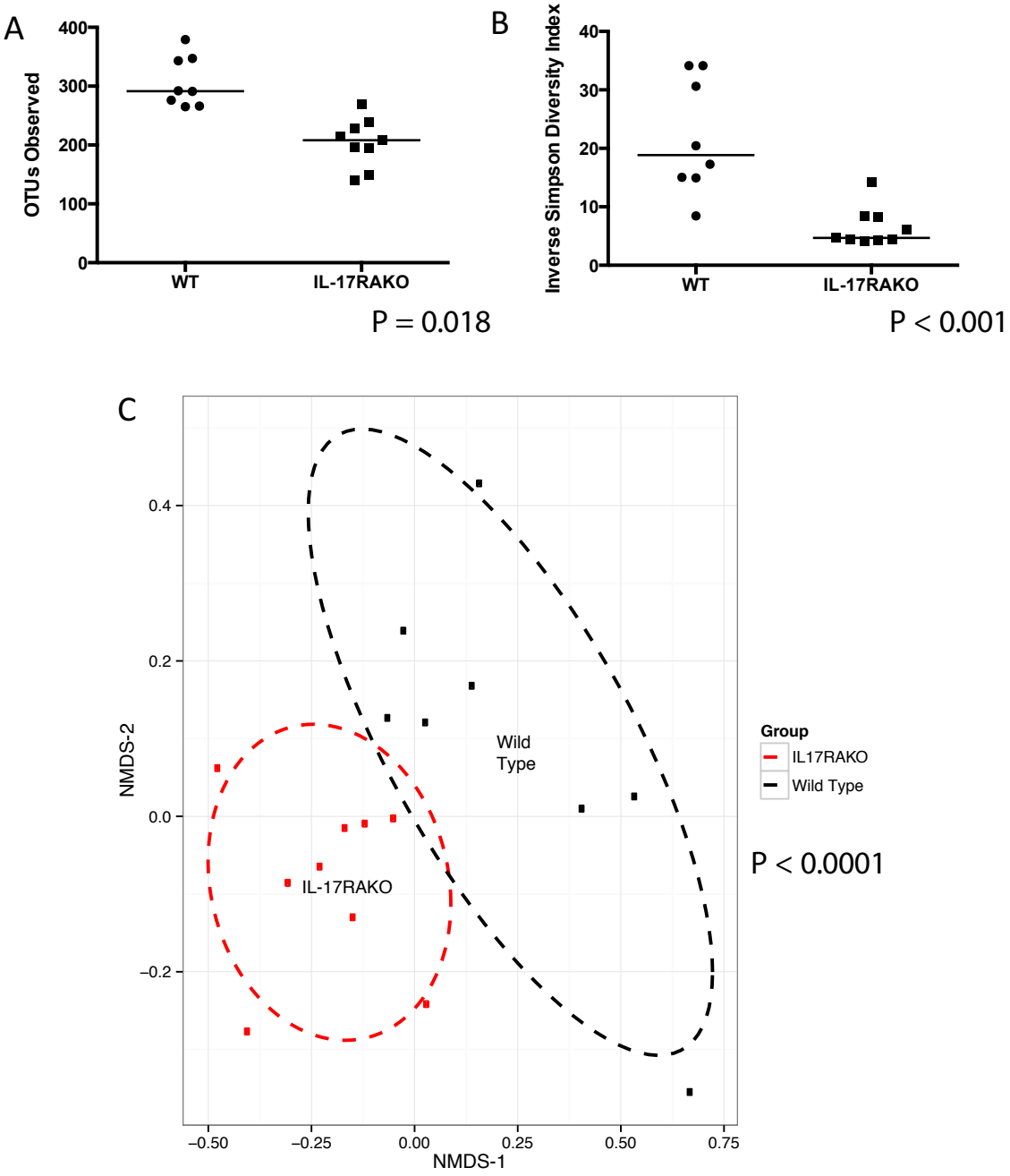

Figure 6-13. Comparison of diversity among upper respiratory tract samples of wild type and IL-17RA$^{-/-}$ mice.

A. OTU count and B. Inverse Simpson Index in samples rarefied to even sequencing depth. P value represents Mann-Whitney test. C. Multidimensional scaling analysis of samples with curves indicating 80% confidence of sample distribution. P value represents multivariate ANOVA.

A

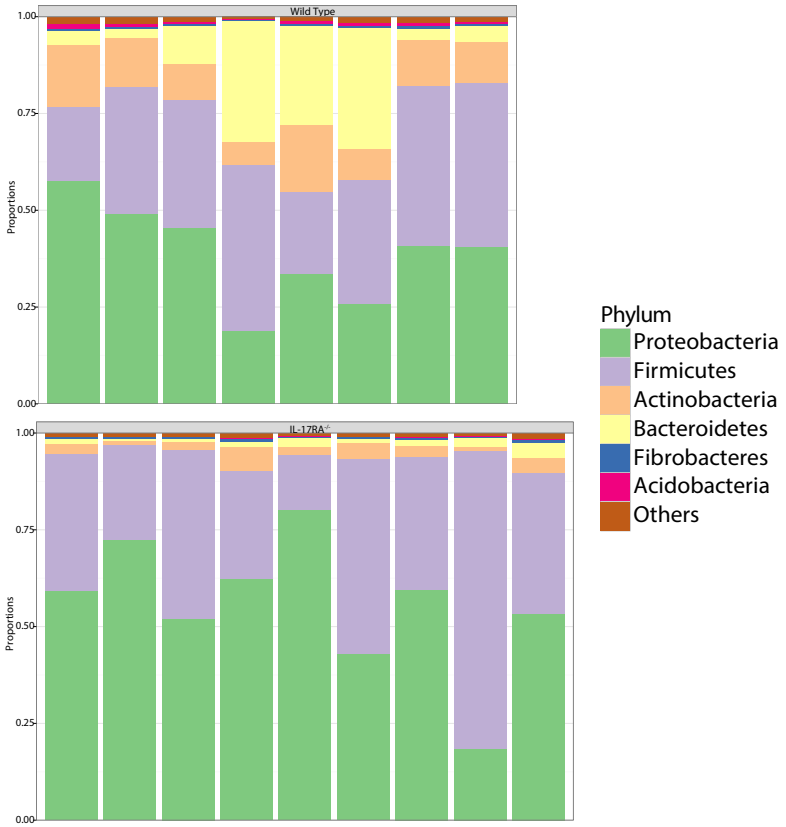

B

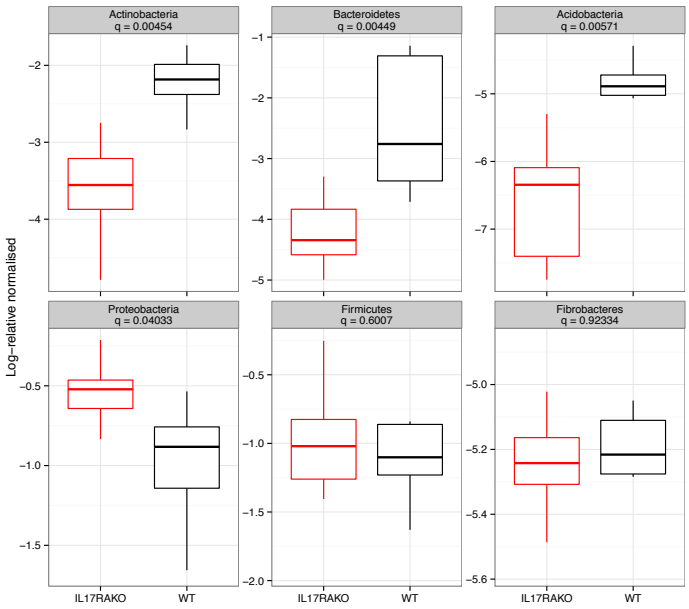

Figure 6-14. Role of IL-17 in determining phyla distribution in the upper airways.

Multiple testing of differences between bacterial species at the phylum level among wild type and IL-17RA$^{-/-}$ mice. Significance tests involve the 6 most abundant bacterial phyla. A. Results of multiple Kruskal-Wallis tests with uncorrected p-value plotted against E-value and q-value. Significant results are regarded as those with a corrected significance level < 0.05. B. Plots showing log normalised relative adundance of the most abundant bacterial phyla.

A

	Wild Type			IL-17RA$^{-/-}$		
	OTU	Genus	%	OTU	Genus	%
1	**OTU 4**	**Pasteurella**	**5.5**	**OTU 4**	**Pasteurella**	**27.9**
2	**OTU 11**	**Streptococcus**	**4.9**	**OTU 11**	**Streptococcus**	**11.1**
3	OTU 28	Allobaculum	4.9	OTU 23	Escherichia/Shigella	10.4
4	**OTU 3**	**Thermomonas**	**4.3**	OTU 12	Streptococcus	7.2
5	OTU 26	Limibacter	3.8	OTU 16	Staphylococcus	4.6
6	**OTU 25**	**Gemella**	**3.2**	OTU 24	Staphylococcus	3.8
7	**OTU 1**	**Ochrobactrum**	**3.1**	**OTU 25**	**Gemella**	**3.7**
8	OTU 33	Aerococcus	3.1	OTU 29	Lactobacillus	2.7
9	OTU 18	Streptococcus	3.1	**OTU 3**	**Thermomonas**	**2.4**
10	**OTU 672**	**Cupriavidus**	**2.8**	**OTU 672**	**Cupriavidus**	**1.5**
11	**OTU 5**	**Methylobacterium**	**2.4**	OTU 2286	Streptococcus	1.2
12	**OTU 10**	**Propionibacterium**	**2.2**	**OTU 1**	**Ochrobactrum**	**1.2**
13	**OTU 21**	**Dyella**	**2.0**	**OTU 5**	**Methylobacterium**	**1.0**
14	**OTU 6**	**Ralstonia**	**1.9**	**OTU 6**	**Ralstonia**	**1.0**
15	OTU 52	Paludibacter	1.7	OTU 71	Streptococcus	1.0
16	**OTU 7**	**Bosea**	**1.5**	**OTU 10**	**Propionibacterium**	**0.9**
17	OTU 22	Dermacoccus	1.4	OTU 930	Escherichia/Shigella	0.8
18	OTU 45	Campylobacter	1.3	OTU 49	Klebsiella	0.8
19	OTU 41	Allobaculum	1.3	**OTU 21**	**Dyella**	**0.6**
20	OTU 37	Elizabethkingia	1.2	**OTU 7**	**Bosea**	**0.6**
		Others	44.6		Others	15.4

B

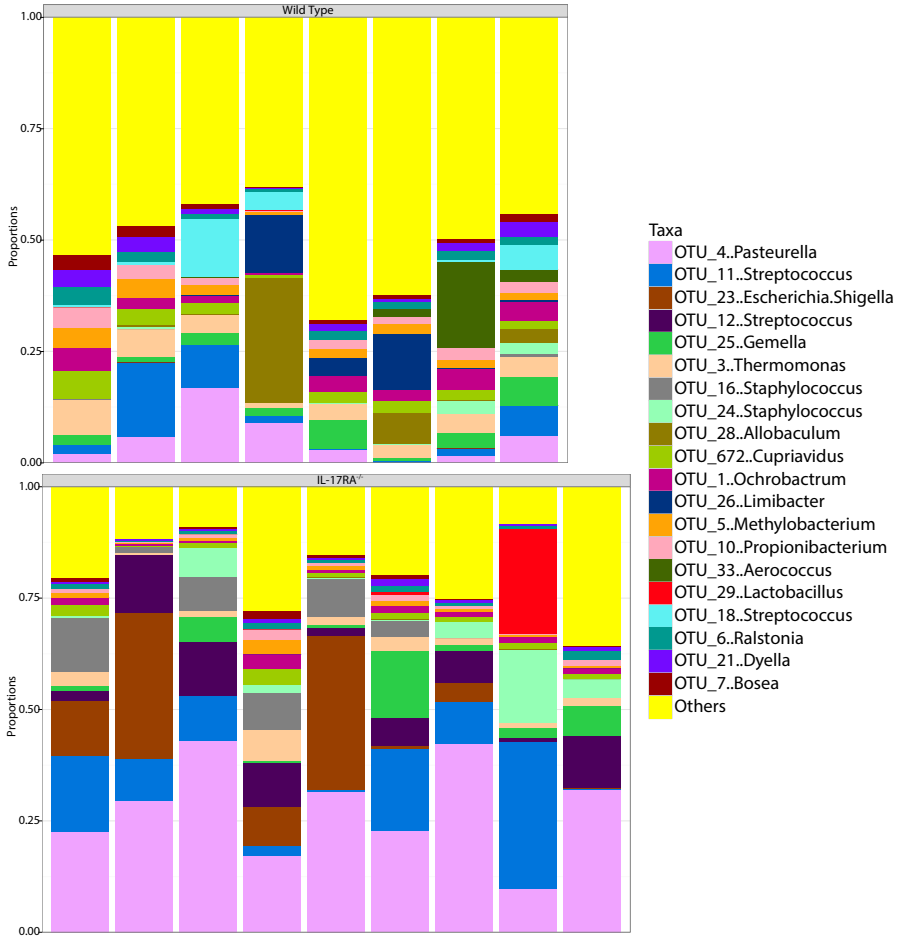

Figure 6-15. OTU level analysis of upper respiratory tract samples.
Taxa relative abundance among wild type and IL-17RA$^{-/-}$ mice. A. 20 most abundant OTUs in wild type microbiome at each site. OTUs occurring in both lists are shown in bold. B. Relative abundance 20 most abundant OTUs in individual samples. Other OTUs are shown in yellow.

A

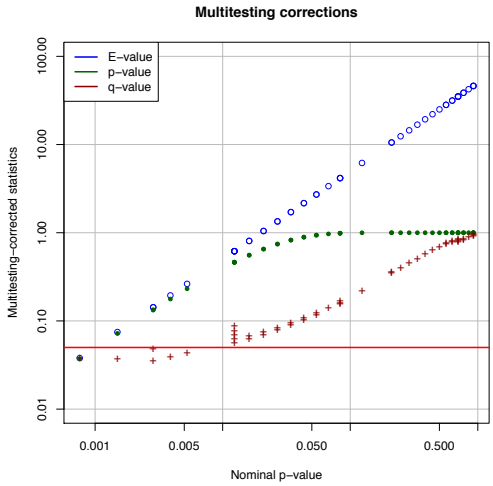

B

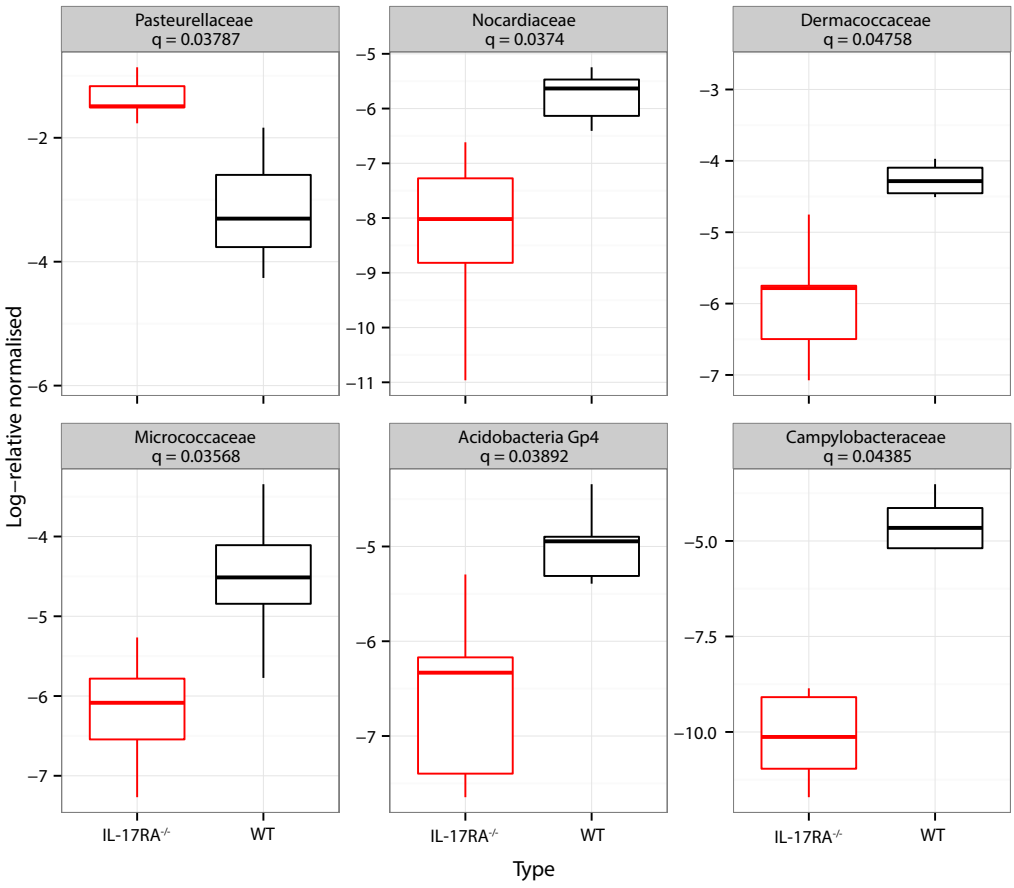

Figure 6-16. Multiple testing of differences between bacterial species at the family level between upper respiratory tract samples from wild type and IL-17RA$^{-/-}$ mice.

Significance tests involve the 50 most abundant bacterial families. A. Results of multiple Kruskal-Wallis tests with uncorrected p-value plotted against E-value and q-value. Signifiicant results are regarded as those with a significance level < 0.05. B. Plots showing log normalised relative adundance of individual bacterial families achieving statistical significance after correction.

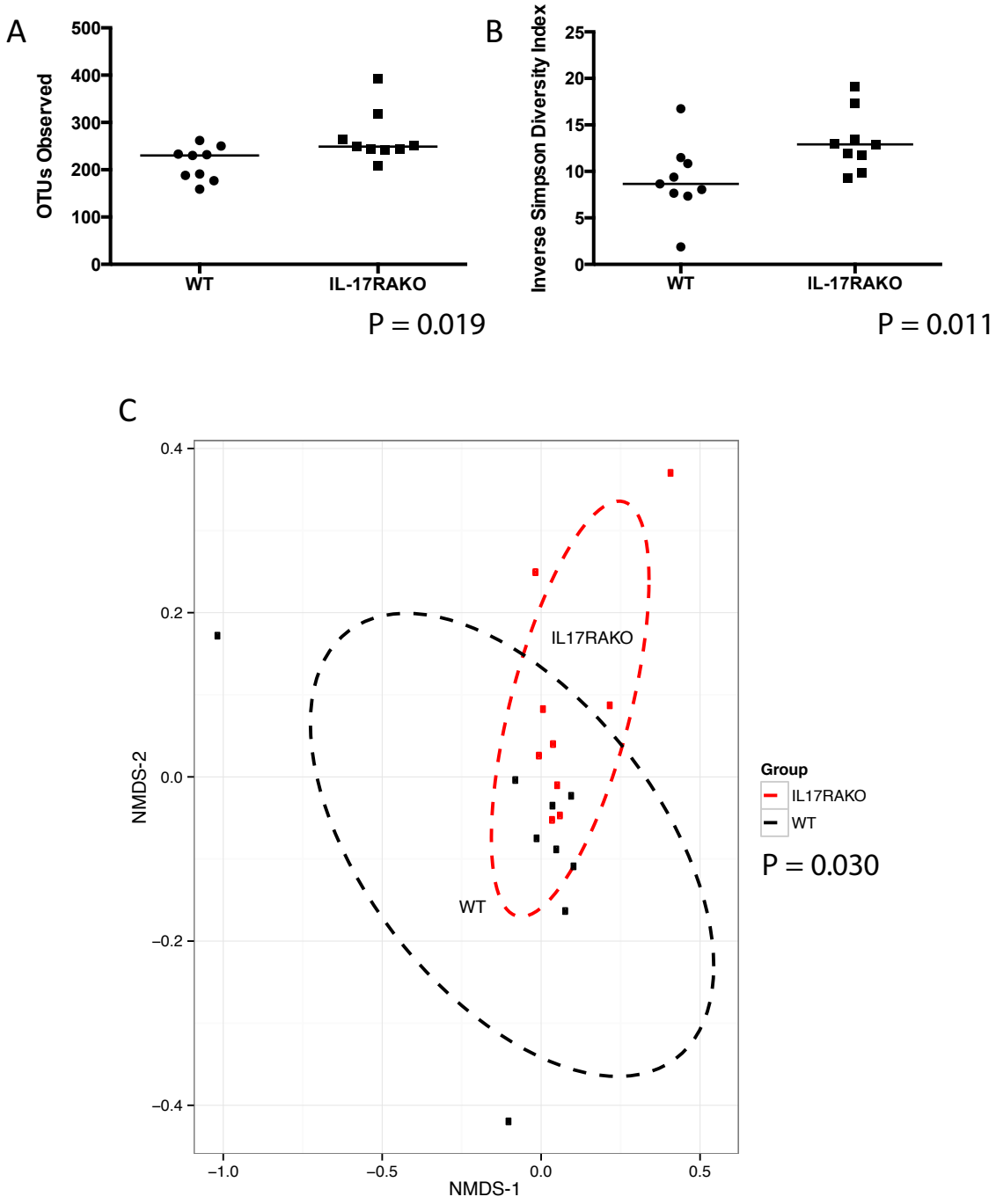

Figure 6-17. Comparison of diversity among lower respiratory tract samples of wild type and IL-17RA$^{-/-}$ mice.

A. OTU count and B. Inverse Simpson Index in samples rarefied to even sequencing depth. P value represents Mann-Whitney test. C. Multidimensional scaling analysis of samples with curves indicating 80% confidence of sample distribution. P value represents multivariate ANOVA.

A

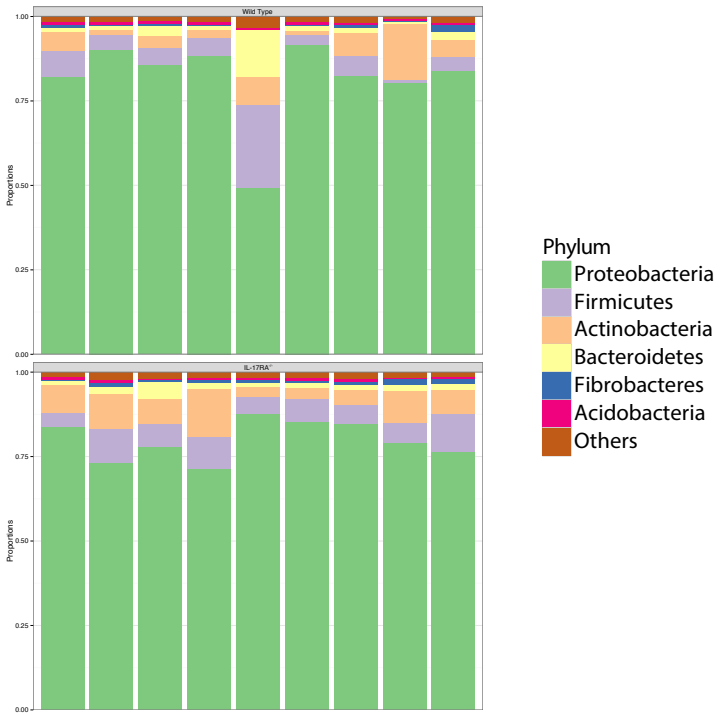

B

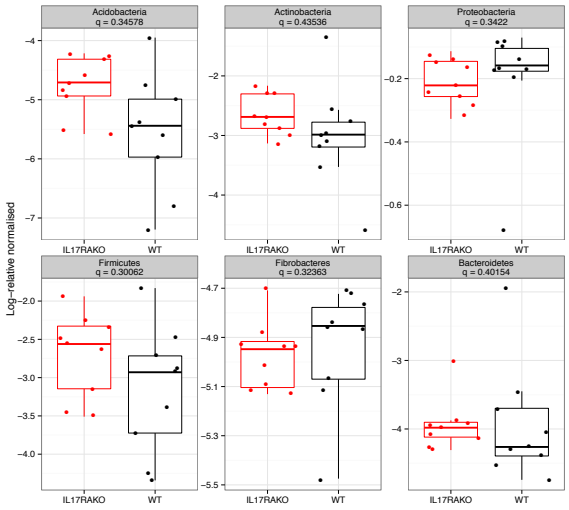

Figure 6-18. Multiple testing of differences between bacterial species at the phylum level between upper respiratory tract samples from wild type mice and IL-17RA$^{-/-}$ mice.

Significance tests involve the 50 most abundant bacterial families. A. Results of multiple Kruskal-Wallis tests with uncorrected p-value plotted against E-value and q-value. Signifiicant results are regarded as those with a corrected significance level < 0.05. B. Plots showing log normalised relative adundance of selected individual bacterial families achieving statistical significance after correction.

A

	Wild Type			IL-17RA$^{-/-}$		
Rank	WT	Genus	%	IL-17RA$^{-/-}$	Genus	%
1	**OTU 3**	**Thermomonas**	**18.4**	**OTU 3**	**Thermomonas**	**16.8**
2	**OTU 672**	**Cupriavidus**	**9.8**	**OTU 672**	**Cupriavidus**	**8.8**
3	**OTU 7**	**Bosea**	**9.2**	**OTU 5**	**Methylobacterium**	**8.1**
4	**OTU 5**	**Methylobacterium**	**7.7**	**OTU 7**	**Bosea**	**7.8**
5	OTU 4	Pasteurella	7.6	**OTU 1**	**Ochrobactrum**	**4.7**
6	**OTU 6**	**Ralstonia**	**4.4**	**OTU 6**	**Ralstonia**	**4.3**
7	**OTU 14**	**Sphingomonas**	**4.1**	**OTU 13**	**Rhizobium**	**3.7**
8	**OTU 13**	**Rhizobium**	**4.0**	**OTU 14**	**Sphingomonas**	**3.2**
9	**OTU 1**	**Ochrobactrum**	**2.3**	**OTU 10**	**Propionibacterium**	**2.8**
10	OTU 57	Enhydsrobacter	2.2	OTU 35	Rhizobium	2.4
11	**OTU 9**	**Methylobacterium**	**2.0**	**OTU 9**	**Methylobacterium**	**2.1**
12	OTU 18	Streptococcus	1.7	OTU 49	Klebsiella	1.7
13	**OTU 27**	**Microbacterium**	**1.4**	OTU 11	Streptococcus	1.4
14	**OTU 10**	**Propionibacterium**	**1.0**	**OTU 8**	**Roseomonas**	**1.3**
15	**OTU 20**	**Staphylococcus**	**0.8**	**OTU 20**	**Staphylococcus**	**1.3**
16	OTU 221	Hymenobacter	0.6	**OTU 27**	**Microbacterium**	**1.0**
17	**OTU 8**	**Roseomonas**	**0.6**	**OTU 1847**	**Cupriavidus**	**1.0**
18	OTU 114	Roseomonas	0.6	OTU 23	Escherichia/Shigella	1.0
19	OTU 44	Sphingomonas	0.6	OTU 61	Derxia	0.8
20	**OTU 1847**	**Cupriavidus**	**0.5**	OTU 19	Acidobacteria Gp 4	0.8
		Others	20.6		Others	24.8

B

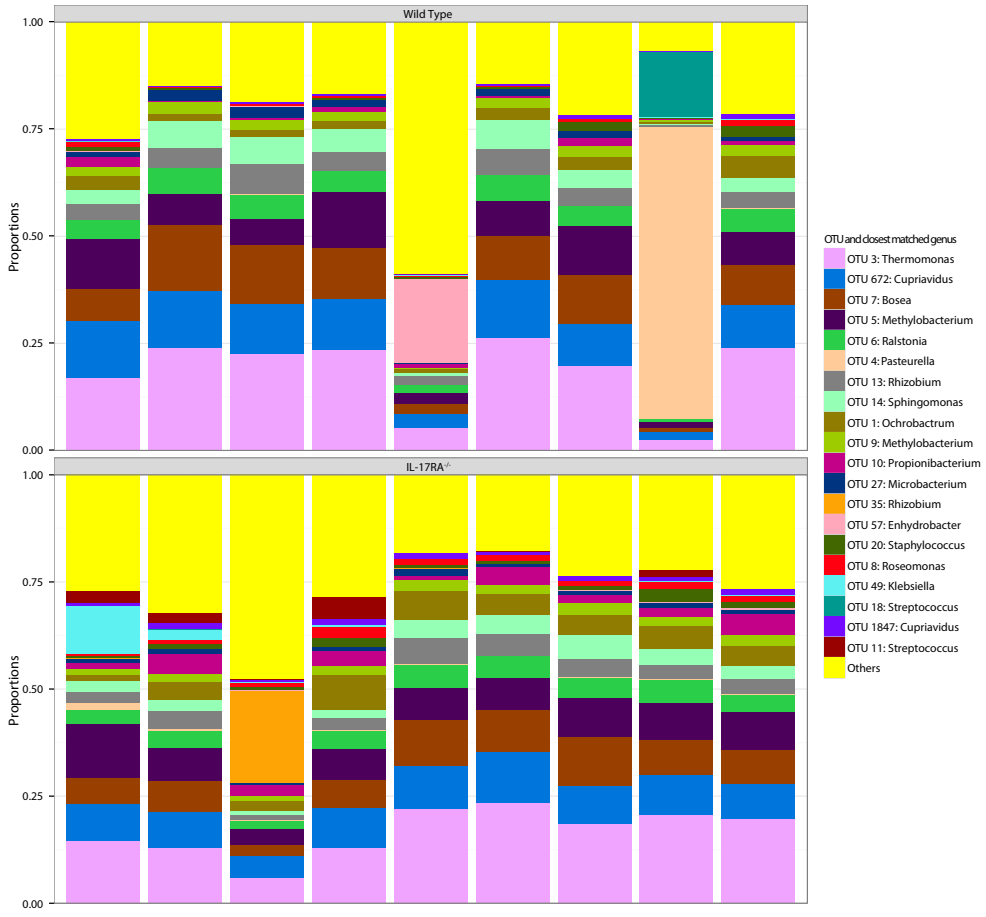

Figure 6-19. OTU level analysis of lower respiratory tract microbiome. Taxa relative abundance among wild type and IL-17RA$^{-/-}$ mice.

A. 20 most abundant OTUs in wild type microbiome at each site. OTUs occurring in both lists are shown in bold. B. Relative abundance 20 most abundant OTUs in individual samples. Other OTUs are shown in yellow.

A

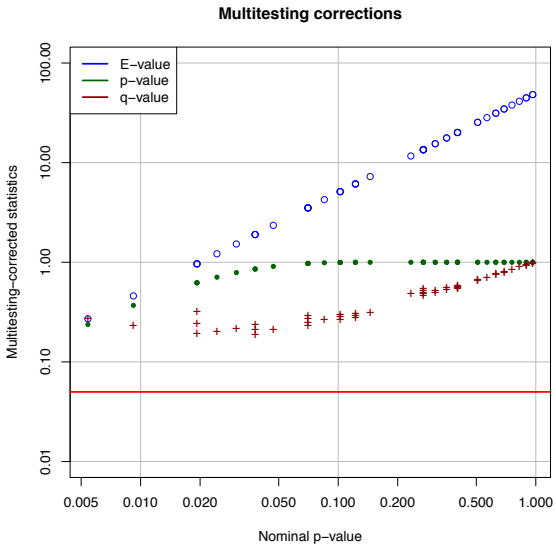

B

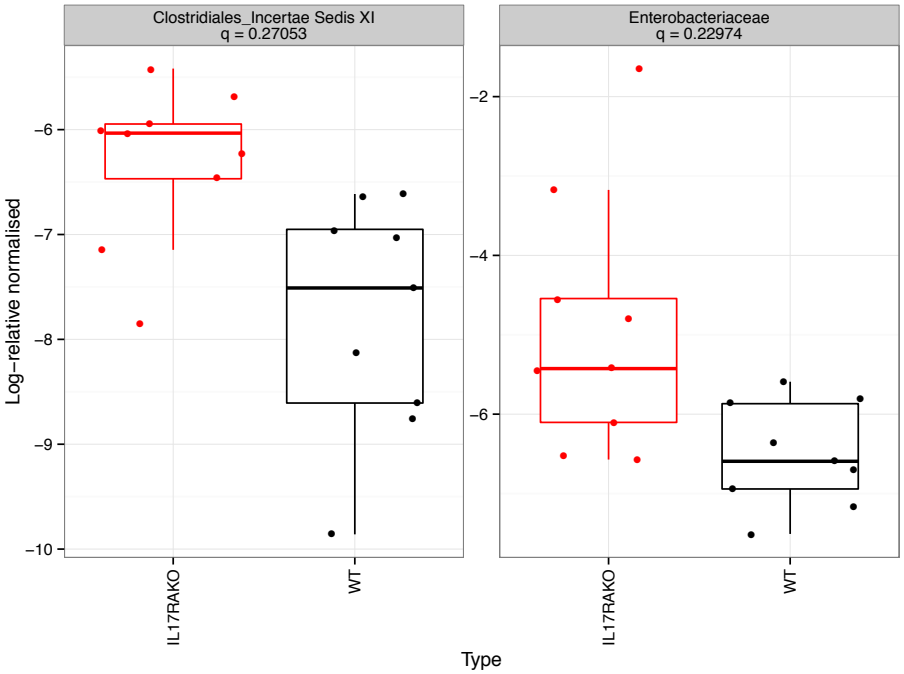

Figure 6-20. Multiple testing of differences between bacterial species at the family level between lower respiratory tract samples from wild type and IL-17RA$^{-/-}$ mice.

Significance tests involve the 50 most abundant bacterial families. A. Results of multiple Kruskal-Wallis tests with uncorrected p-value plotted against E-value and q-value. Signifiicant results are regarded as those with a significance level < 0.05. B. Plots showing log normalised relative adundance of individual bacterial families. No bacterial families approached the corrected significance level but the two plots shown are those with the lowest q-value.

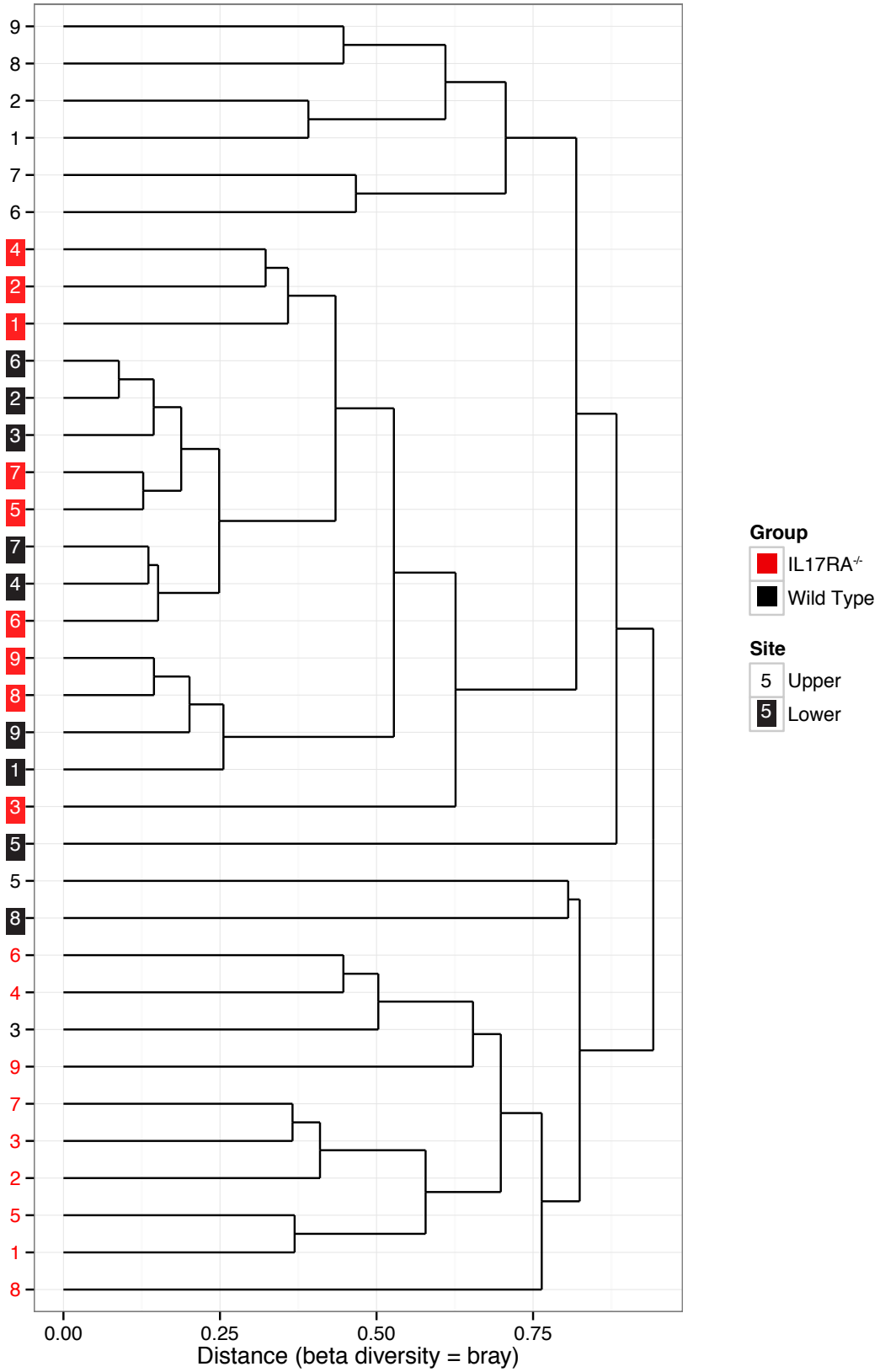

Figure 6-21. Dispersion of all respiratory tract samples by Bray distance. Similarity tree of samples using bray distance to demonstrate clustering of samples. Number represents identity of mouse while colour and background fill represent group and site respectively.

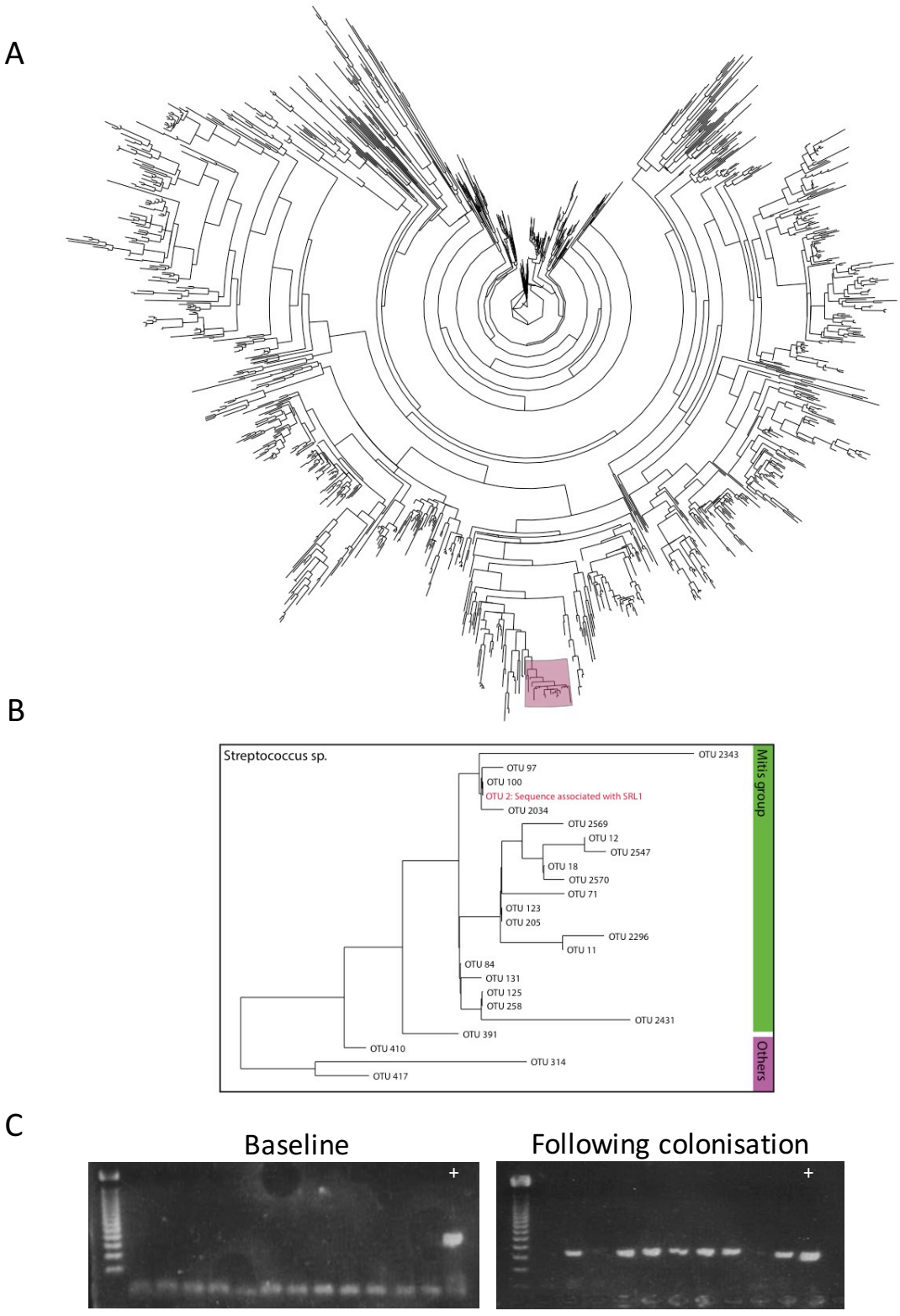

Figure 6-22. Identification of streptococci within respiratory tract microbiome.

Phylogenetic trees showing (A) all OTUs and (B) only OTUs identified as streptococcal occurring with a mean abundance greater than 10^{-4}. Streptococcal OTUs are shaded on the upper plot. C. Representative *cpsa* PCR on respiratory tract lysates. + denotes positive control reactions.

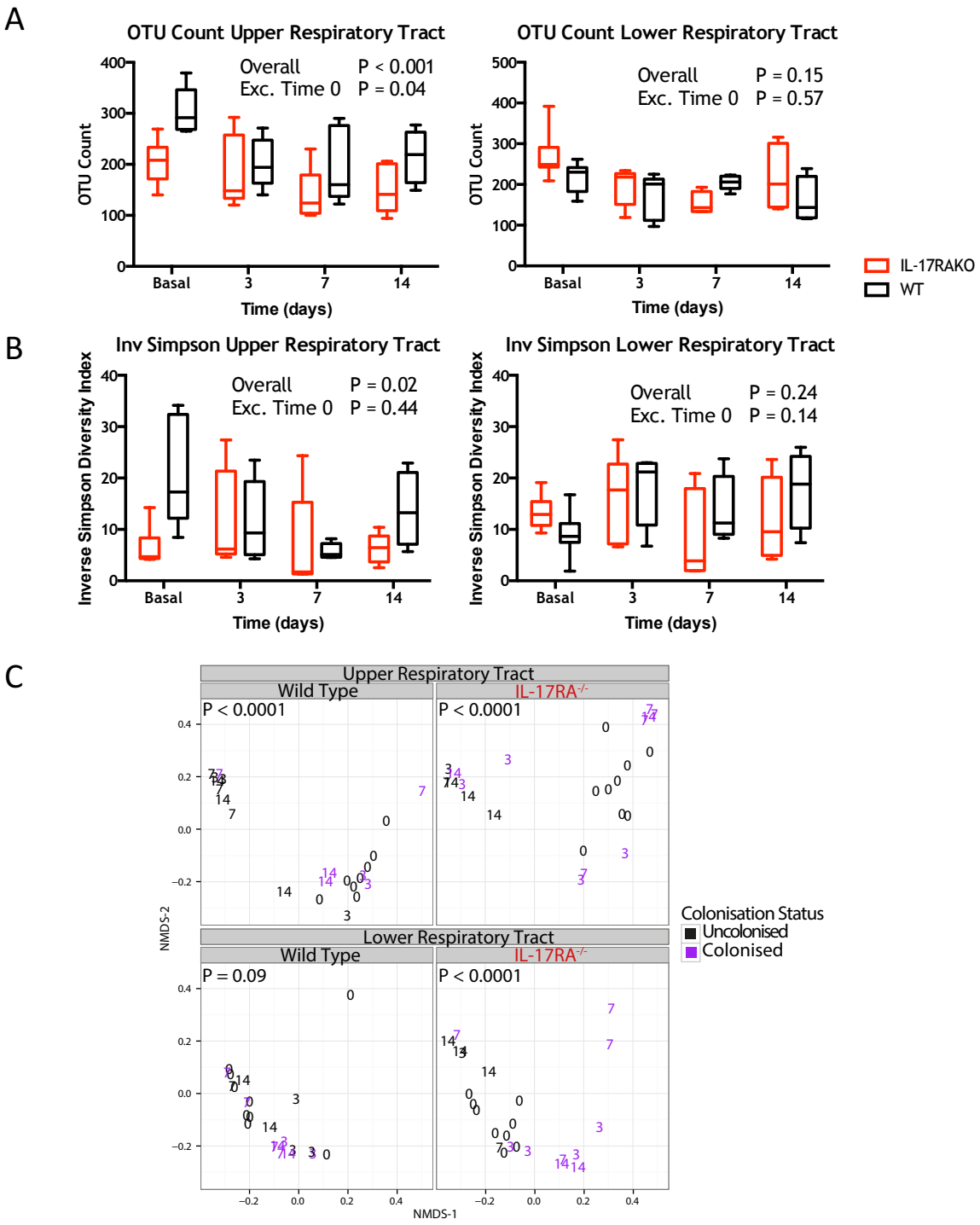

Figure 6-23. Change in alpha diversity over time.

Diversity measured in (A) observed OTUs per rarefied sample and (B) Inverse Simpson diversity index. P values represent 2-way ANOVA analysis. C. NMDS analysis. All samples were fitted to the NMDS model together but plotted on separate panels for clarity. Plotted numbers represent the time since intra-nasal inoculation with SRL1 with 0 implying unexposed animals. Colonised samples are those animals colonised with *S. pneumoniae* at the time of sampling (see main text for definition). P values represent analysis with PERMANOVA.

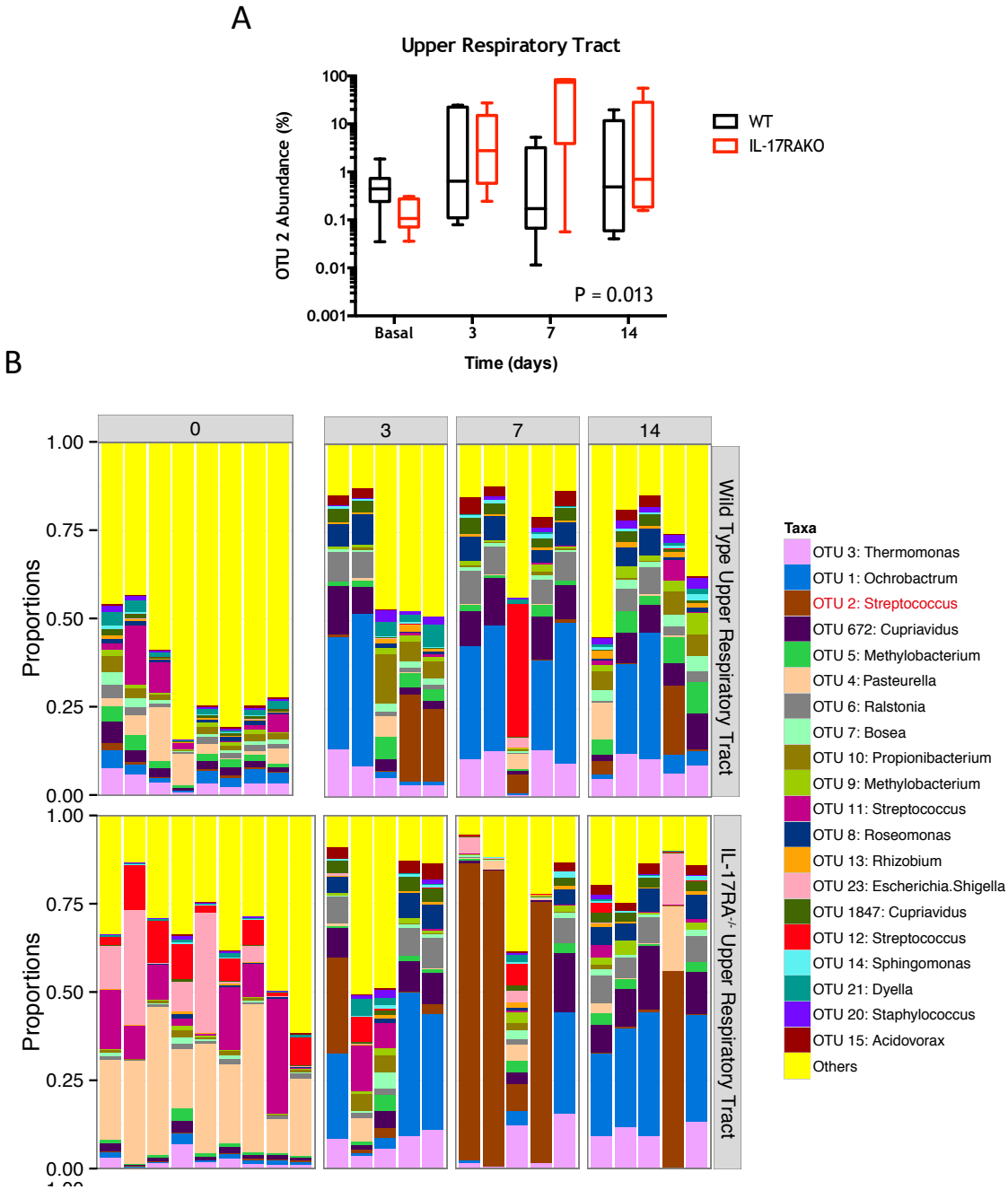

Figure 6-24. Distribution of individual OTUs in upper respiratory tract following SRL1 exposure.

A. Relative abundance of OTU 2 (the OTU corresponding to streptococci with the same sequence as SRL1). P value represents two-way ANOVA. B. Plots showing the twenty most abundant OTUs among samples. Legend shows OTUs with closest matched genus.

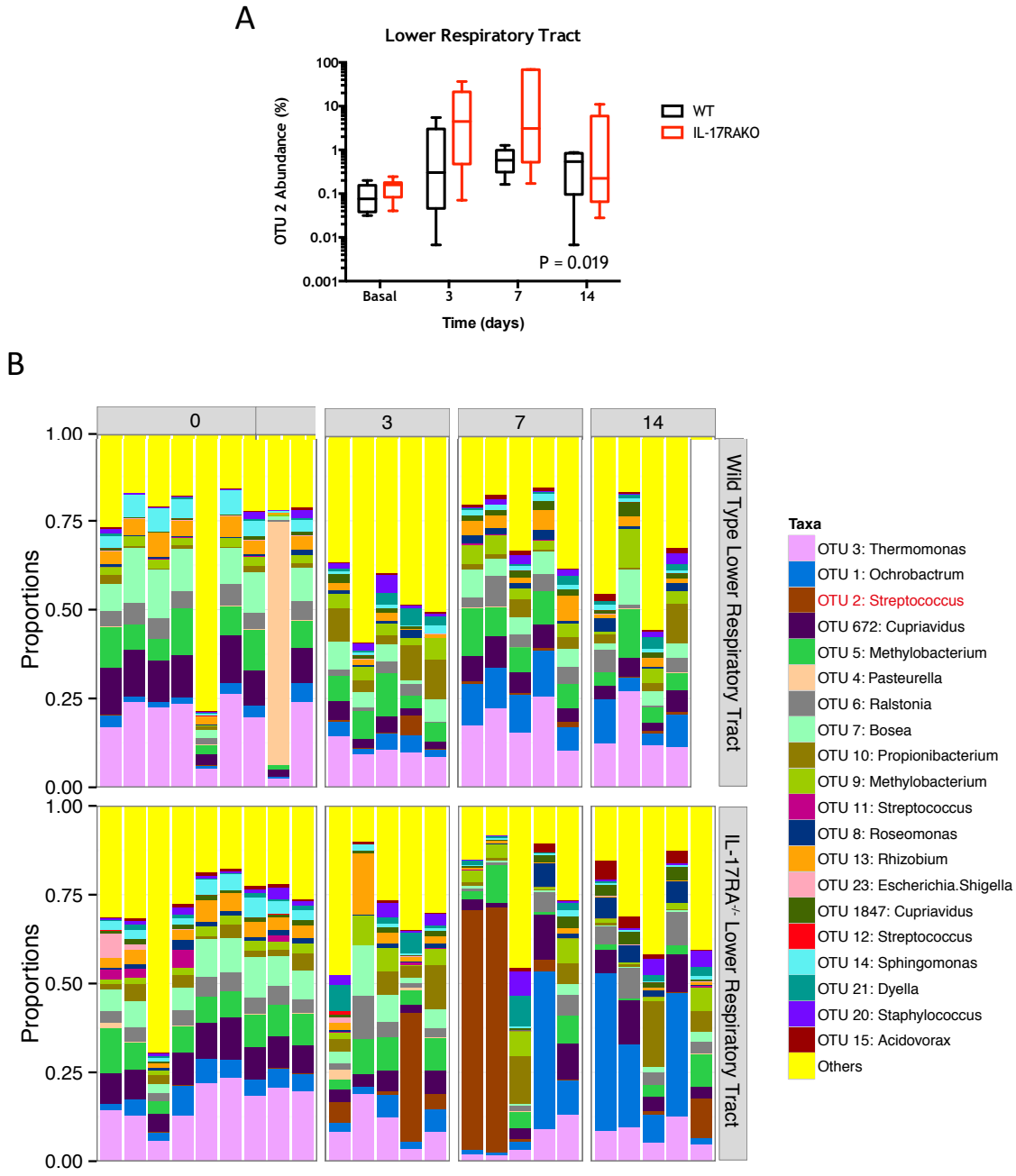

Figure 6-25. Distribution of individual OTUs in lower respiratory tract following exposure to SRL1.

A. Relative abundance of OTU 2 (the OTU corresponding to streptococci with the same sequence as SRL1). P value represents two-way ANOVA. B. Plots showing the twenty most abundant OTUs among samples. Legend shows OTUs with closest matched genus.

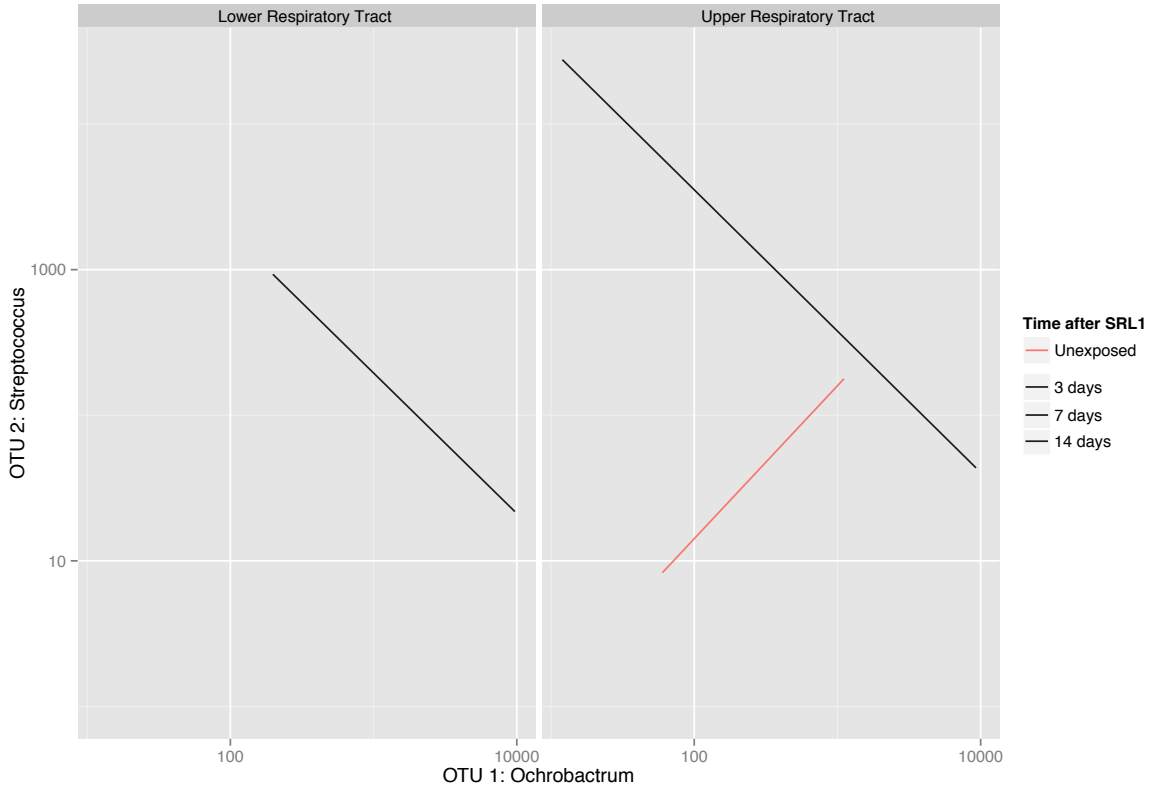

Site	Exposed	Slope (log/log)	P value	r^2
Upper	No	-0.55	$<1 \times 10^{-5}$	0.54
	Yes	0.66	$<1 \times 10^{-4}$	0.71
Lower	No	0.31	0.25	0.08
	Yes	-0.19	0.018	0.19

Figure 6-26. Association between OTU2 (Streptococcus including SRL1) and OTU1 (Ochrobactrum).

Rarefied abundance data is plotted with generalised linear modelled lines of best fit shown for exposed and non-exposed mice. No line of best fit is shown for the unexposed, lower respiratory tract samples because there was no evidence of a correllation. Statistics arising from the best-fit model are shown in the table below the plot.

7. RNA-SEQ TO QUANTIFY BACTERIAL GENE EXPRESSION DURING SRL1 INFECTION

7-1 Introduction

One of the challenges of describing bacterial pathogenesis is to understand the transcription of bacterial genes in the context of infection. qRT-PCR is a simple method for assessing bacterial gene transcription but the method is limited by the need to run individual assays for each gene product and therefore is limited in capacity. In contrast, DNA micro-arrays offer simultaneous assessment of each transcriptional product but must be manufactured for each organism studied. RNA-Seq uses shotgun sequencing to blindly sequence the entire transcriptome present in a sample. The large number of reads obtained using modern next generation sequencing platforms allow the comparison of gene expression with high power. However, when RNA-Seq is employed in the context of infection, the number of bacterial reads obtained will inevitably be heavily diluted by the transcriptome of the host organism lessening the power of the analysis [470]. Methods of enriching for bacterial DNA can be employed – such as culture enrichment or gradient centrifugation [471] – but these are likely to introduce bias into the assay, since transcription varies within minutes of the bacteria being removed from its host. RNA-Seq has been used extensively to study the transcriptome of bacteria including *S. pneumoniae* [472-474]. However, a far smaller number of studies have examined the prokaryotic transcriptome within the host [471] and this study used DNA micro-array technology.

The model of pulmonary and pleural infection with SRL1 described already in this thesis generates high bacterial densities within the infected tissue. This gave me the opportunity to attempt to use next generation sequencing (NGS) to sequence the transcriptome of SRL1 within these locations. I decided to compare the transcriptome in these locations with SRL1 grown to mid-log phase in BHI.

7-2 SRL1 genome sequencing

Reads from SRL1 sequencing were aligned against the reference strain (OXC141) [392] and *de novo* sequencing of the reads was also undertaken. The outcome of the alignment is shown in figure 7-1. In general, the SRL1 genome was very similar to that of OXC141 with significant differences noted in the figure. 92 non-synonymous oligonucleotide sequence variations were identified (approx. 1/20kb).

There were also five significant structural variations identified which are outlined in figure 7-1. The most prominent structural variation was the deletion of a 34kb section of the genome corresponding to a putative pro-phage sequence[475]. This pro-phage (ΦSpn_OXC) was not present in the DNA and therefore appeared to have been excised from the genome rather than relocated. A further 88bp deletion involved a non-coding region located between the SPNOXC_RS00835 gene (a putative DNA binding gene of unknown function) and SPNOXC_RS00840 gene (an ABC protein transporter with sequence homology to bacteriocin transporters). There was an area of low coverage in a highly repetitive region of the *PspA* gene (a known virulence factor with a role in the inhibition of complement binding) but the significance of this low coverage is not clear. SRL1 possesses a full copy of the glutamine ABC transporter gene (SPNOXC_RS_03950) whereas OXC141 is missing 250bp from the 3' end of the gene. The gene in SRL1 could be entirely reconstructed and was found to have 100% sequence homology with the sequence found in the widely used reference strain D39. Finally, there was a 93bp in frame deletion in SPNOXC_07855 (a putative transmembrane protein with sequence homology to peptide transporter permeases). The deletion occurred at the 3' end of the gene and is of uncertain functional significance.

Therefore, the SRL1 genome was very similar to the reference genome for ST180 serotype 3 S. pneumoniae strains. This is an expected finding, since ST180 is a stable genotype that is known to have persisted in the pneumococcal population for many decades and has limited evidence of recombination events[392]. Due to the close similarity of the genomes, it was decided to align RNA-Seq experiments against the reference genome.

7-3 SRL1 *In vivo* infection RNA-Seq

7-3.1 Infection with SRL1

3 C57Bl/6 mice were infected as described before with 10^6 cfu/ml SRL1 and were culled at 48 hours post infection. Mice lost weight and developed clinical illness as expected (figure 7-2A & B). Bacterial density is shown in figure 7-2C. One of the mice had lower bacterial density than the other two but still showed signs of infection at 48 hours and had >10^6 bacteria in BALF and pleura.

7-3.2 Extraction and sequencing of RNA from infection model

In extracting RNA from BALF and pleura, I followed the method of Robinson *et al*[393] which has been used in successfully in my laboratory to isolate bacterial RNA from sputum for NGS by Sharon Irvine (unpublished). RNA was successfully isolated from mouse samples although post-extraction cleanup was required prior to ribosomal RNA depletion and library generation (figure 7-3). It proved difficult to isolate RNA from broth culture of SRL1 with low yields of RNA generated (<1µg of total RNA extracted from 20ml of mid-log culture). Therefore following extraction, RNA from two mid-log cultures was combined to produce RNA suitable for further analysis.

Samples were multiplexed and sequenced using the Illumina Hi-Seq platform. After exclusion of low quality and adapter reads, for infection model samples 4.6 – 16.7 x 10^7 (median 5.9 x 10^7) reads per sample were obtained while broth samples generated 5.8 – 6.3 x 10^7 (median 6.2 x 10^7) reads per sample.

Sample alignment statistics are shown in figure 7-4A. Broth samples contained a high proportion of reads that could be mapped to the OXC141 genome (>60%). As

expected, the proportion of reads from *in vivo* samples that could be mapped to the OXC141 genome was much lower. BALF was particularly inefficient with only one of the three samples delivering sufficient numbers of reads to align but all three of the pleural samples generated sufficient numbers to include in the RNA-Seq analysis. Principal component analysis demonstrated separation of distribution of the broth samples from the BALF and pleura samples (figure 7-4B).

7-3.3 Gene expression analysis

RNA-Seq gene expression analysis was conducted to compare broth samples with pleura and with BALF. EDGE-R analysis on a negative binomial distribution was used to identify significantly upregulated genes (table 7-1). The overlap between genes upregulated in BALF and pleura was high, with 100% (10/10) of genes found to be upregulated in BALF also upregulated in pleura. A further 12 significantly upregulated genes were found in pleural samples. With one exception (RSOO805, arginosuccinate synthase), all upregulated genes came from four regions of the bacterial genome which will be outlined below. These four regions are shown in figure 7-5. With the exception of the OXC prophage (see next section) the gene upregulation within each region was highly correlated regardless of whether a gene reached statistical significance (figure 7-6).

89 genes were found to be significantly down-regulated in the pleural samples compared to broth with only 1 in the BALF sample (table 2). This gene was significantly downregulated in both sample groups: RS10140, a possible tRNA synthetase. Other genes, significantly downregulated in the pleural samples, encode a wide range of proteins with a variety of functions.

7-3.4 Upregulated region 1: ΦSpn_OXC prophage

The first region of the OXC141 genome from which genes upregulated in infected samples are found is the 34kb putative prophage ΦSpn_OXC. This prophage is notable by its absence from the SRL1 genome (see section 7-2 above). Consistent with this, broth samples are almost completely lacking in reads mapped to this region of the OXC141 genome – only 64 reads from a total of 9.4×10^7 were

mapped to this region constituting 1.7% of the genome. The proportion of reads mapped to this region of the genome among infected samples was much higher: 128 reads from a total of 4 x 10^6 – a 20 fold increase. However, this still constitutes a very low number of reads mapped to the regions in question. Reads mapped to this region are usually unpaired and often imperfectly matched the mapped sequence. It is therefore very likely that this region represents non-specific read mapping and shall not be considered further.

7-3.5 Upregulated region 2: purine metabolism and *VanZ*

The second significantly upregulated genomic region is a 10kb polycistronic transcript containing several genes involved in purine metabolism and the glycopeptide resistance determinant VanZ. While only 3 of 7 genes in the operon were significantly upregulated, all genes in the operon were found more frequently in the pleural samples with normalised fold increases of between 2.7 and 5.1. The purine metabolism genes found in this operon all have well defined functions in the synthesis of inosine monophosphate. VanZ in known to be associated with low level glycopeptide resistance in *Enterococcus faecalis* [476]. The mechanism was not linked to altered D-alanine residues in peptidoglycan biosynthesis and beyond this the function of the protein is not well understood.

The regulation of purine metabolism is known to be mediated by the *purR* gene, which functions as a repressor [477]. *purR* is represented in the OXC141 genome by SPNOXC_RS09520 and this gene is found less frequently in BALF and pleural samples although this did not reach statistical significance (fold change -1.94, FDR P = 0.22 and fold change -2.71, FDR P = 0.14 respectively).

7-3.6 Upregulated region 3: *Blp* bacteriocin locus

The bacteriocin-like peptide (*Blp)* bacteriocin locus[478] is found in the genome of most *S. pneumoniae* [479]. It is known to be involved in intra-strain competition in the context of nasal colonisation [480]. 9/15 genes in the Blp locus were significantly upregulated in the context of infection compared to broth with the other gene products also increased to a similar extent without reaching the threshold of statistical significance. The *Blp* locus contains the bacteriocin genes

as well as genes responsible for the regulation, excretion and tolerance of the bacteriocins.

7-3.7 Upregulated region 4: Pneumococcal surface adhesin A

The three genes making up the *psaBCA* locus are transcribed as a single polycistronic mRNA and encode for an adenosine triphosphate (ATP) binding protein, an integral membrane protein and a Mn^{2+} binding protein respectively [110]. These proteins complex to produce a functional manganese ATP binding cassette (ABC) transporter. *PsaA* is also reported to function in pneumococcal virulence independent of its action in Mn^{2+} transport with a role in adhesion [111]. All three genes in the *psaBCA* locus were significantly upregulated in pleural samples with normalised fold increases of between 5.5 and 9.9.

PsaA gene expression is known to be regulated by the two component signal transduction system (TCS)4 involving the response regulator protein *rr04* [481]. However, there was no evidence of any difference in the expression of *rr04* at either infection site.

7-4 Discussion

In this chapter I have reported an experiment to perform RNA-Seq on SRL1 to assess gene expression during infection. Gene expression was assessed in BALF and pleural fluid, which are characterised by high bacterial densities in the late stages of infection. Despite the high numbers of bacteria present in these fluids, the proportion of reads which could be mapped to the reference OXC141 genome was low – an expected finding given that eukaryotic RNA is likely to predominate in these samples. However, it also proved unexpectedly challenging to isolate RNA from SRL1 grown in broth. Furthermore, this RNA required cleanup steps prior to library preparation. While RNA preparation can be highly operator dependent, I obtained high yields of RNA when performing RNA isolation from other material (data not shown) suggesting that this was specific to SRL1. SRL1 is known to produce large amounts of capsule and has historically been referred to as the “outer slime layer” [440]. It could be hypothesised that this thick polysaccharide layer which is also shed into the broth by virtue of the non-covalent attachment of the serotype 3 capsule[68] saturates the column based

methods of RNA purification used in this study. Despite the low yields encountered, broth cultures of SRL1 still provided 98 million reads for further analysis while BALF and pleura generated 6.9 and 4.2 million reads respectively.

Upregulated genes were very stable between the BALF and pleural samples with the same genomic regions being identified as upregulated at both sites. The apparent low level expression of ΦOXC141 is unlikely to represent genuine gene expression but the other three genomic regions appeared to be robustly upregulated with many genes significantly upregulated and evidence that genes not reaching the threshold of statistical significance were also deteceted more frequently with evidence of a similar magnitude of upregulation. All three of the genomic regions identified have been previously described in gene expression studies and have been previously associated with pneumococcal virulence or stress response.

Several genes in the purine metabolism/*VanZ* locus were significantly upregulated with weaker evidence of downregulation of the *purR* repressor. This locus was previously described in a gene expression study investigating *in vitro* pneumococcal responses to bacteriostatic antibiotics involving the unencapsulated strain R6[482]. The R6 *purCLFMN-vanZ-purH* locus shares more than 99% sequence homology to SRL1. It is unclear what survival advantage within the host would be obtained by upregulating this gene locus given the central role of purine metabolism in DNA synthesis rather than virulence. The function of the *vanZ* gene is unknown although it is known to confer low level glycopeptide resistance in *E. faecalis*[476]. Whether increased expression of this gene might confer a survival advantage within the host is therefore unclear. Upregulation of genes within the *purCLFMN-vanZ-purH* locus was also identified in a study of gene expression using DNA microarray in pneumococcal infection[471]. Purine metabolism genes were upregulated in bloodstream infection but not in CSF. It maybe that upregulation of this gene locus represents a general stress response.

The next upregulated genomic region was the *Blp* bacteriocin domain. Bacteriocins are small proteins with anti-bacterial properties useful in inter- and intra-species competition[483]. The SRL1 *Blp* locus contains genes responsible for

regulation, secretion and immunity[478] along with three bacteriocin genes. *Blp* bacteriocins are widely distributed in *S. pneumoniae*[479]. However, it is believed that the majority of pneumococci are incapable of autonomously producing bacteriocins due to truncation of the *BlpA* gene[484]. The *BlpC* gene encodes a pheromone which is known to stimulate production of *Blp* bacteriocins and *BlpA* and *BlpB* are required for secrtion of this peptide[485]. However, *BlpA* deficient strains are often capable of producing bacteriocins when stimulated with exogenous *BlpC* pheromone[484]. SRL1 has two copies of the *BlpA* gene arranged in tandem (RS02660 and RS02665) with one truncated and the other apparently functional. Therefore, it is likely that SRL1 is capable of autonomously producing *Blp* bacteriocins and this is supported by the finding of *Blp* gene expression in broth samples.

The domain has been shown to contribute to competition within nasal colonisation and pneumococci with deletion of the *Blp* locus were unable to compete adequately in a murine model of nasal colonisation[483]. However, it is unclear what survival advantage would be associated with bacteriocin production in a monobacterial infection. The stimulus for *BlpC* production is not clear but it could be hypothesised that the upregulation of *Blp* represents a stress response. In the DNA microarray gene expression study described previously, there was either no significant difference in *Blp* gene expression (D39 bacteraemia) or downregulation (TIGR4 meningitis) [471]. However, both of these strains lack functional *BlpA* so the significance of this difference is uncertain.

The final genomic region upregulated was the polycistronic *psaBCA* operon. As discussed above, these genes complex into a Mn^{2+} ABC transporter. However, psaA is also known to be involved in pneumococcal virulence as an adhesin[111]. It is challenging to investigate the role of psaA independent of its role as a manganese transporter because mutants experience growth retardation and fitness deficiency related to manganese deficiency[486] as well as increased susceptibility to oxidative stress[487]. However, *psaA* blocking experiments demonstrate the role of *psaA* in adhesion independent of manganese transport[488]. *psaA* was also strongly upregulated in blood, CSF and endothelial cell infection in the DNA microarray study already described[471].

Only one gene outside of the three genomic regions described above was significantly upregulated in either BALF or pleura. This was the argininosuccinate synthase gene which was significantly upregulated in pleura. Argininosuccinate synthase is involved in the urea cycle and is not a known virulence factor. The significance of this upregulation is uncertain. It is a feature of this study that the number of genes significantly upregulated is relatively low. While the known virulence factor *psaA* was significantly upregulated, other well-known virulence factors did not feature in these data. This is surprising, since pneumococcal virulence factors are believed to be of critical importance to the organism in causing disease[489]. In the Orihuela study[471], the gene expression among virulence factors was variable but only two virulence factors were consistently upregulated – *prtA,* the pneumococcal C5a peptidase, and *pspA,* a complement binding inhibitor. Both tended to be downregulated in pleura and BALF, although only *prtA* achieved statistical significance in pleura. It may be that this experiment captured pneumococcal gene expression too late to detect virulence factor expression since many of the known virulence factors may be most important early in the course of infection – during initial immune system evasion. It would be difficult to obtain a pathogen gene expression profile early in infection since the number of organisms is much lower and a high bacterial density was required to achieve sufficient read depth in this experiment.

The method described in this chapter is one of the first to report a pneumococcal gene expression profile within the host. It therefore offers a valuable insight into the pneumococcal response within the host. However, it does not permit conclusions about the function of the gene products identified as upregulated. Further work would be required to define whether the genes identified in this study have a function in bacterial virulence. Future work could involve knocking out the gene products identified to assess their impact on virulence.

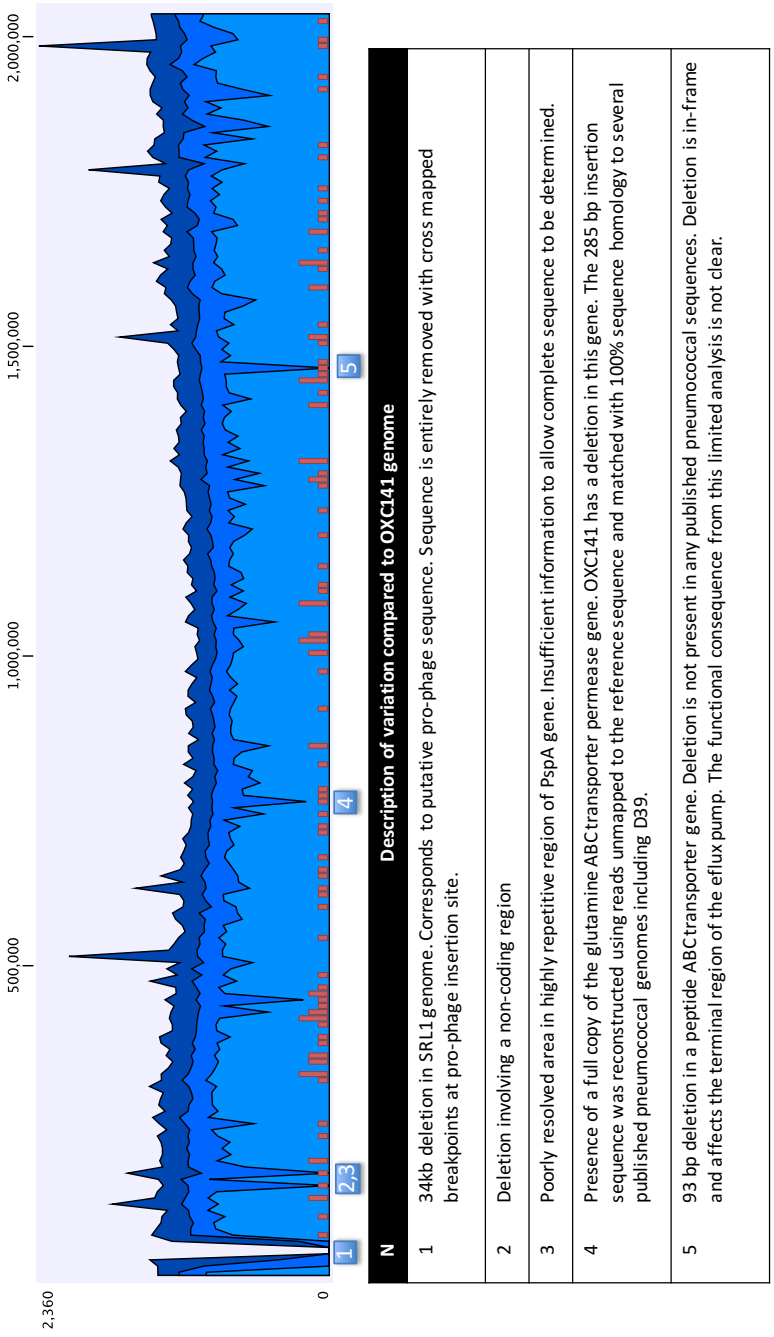

N	Description of variation compared to OXC141 genome
1	34kb deletion in SRL1 genome. Corresponds to putative pro-phage sequence. Sequence is entirely removed with cross mapped breakpoints at pro-phage insertion site.
2	Deletion involving a non-coding region
3	Poorly resolved area in highly repetitive region of PspA gene. Insufficient information to allow complete sequence to be determined.
4	Presence of a full copy of the glutamine ABCtransporter permease gene. OXC141 has a deletion in this gene. The 285 bp insertion sequence was reconstructed using reads unmapped to the reference sequence and matched with 100% sequence homology to several published pneumococcal genomes including D39.
5	93 bp deletion in a peptide ABCtransporter gene. Deletion is not present in any published pneumococcal sequences. Deletion is in-frame and affects the terminal region of the efflux pump. The functional consequence from this limited analysis is not clear.

Figure 7-1. Sequencing of the SRL1 genome aligned against the OXC141 reference genome.

The sequence mapping is shown at the top of the figure with oligonucleotide variants per 10 kb shown at the bottom of the plot. Significant variations are marked blow the plot and summarised in the table. Borders between shades of blue in the above figure represent the minimum, median and maximum read depth.

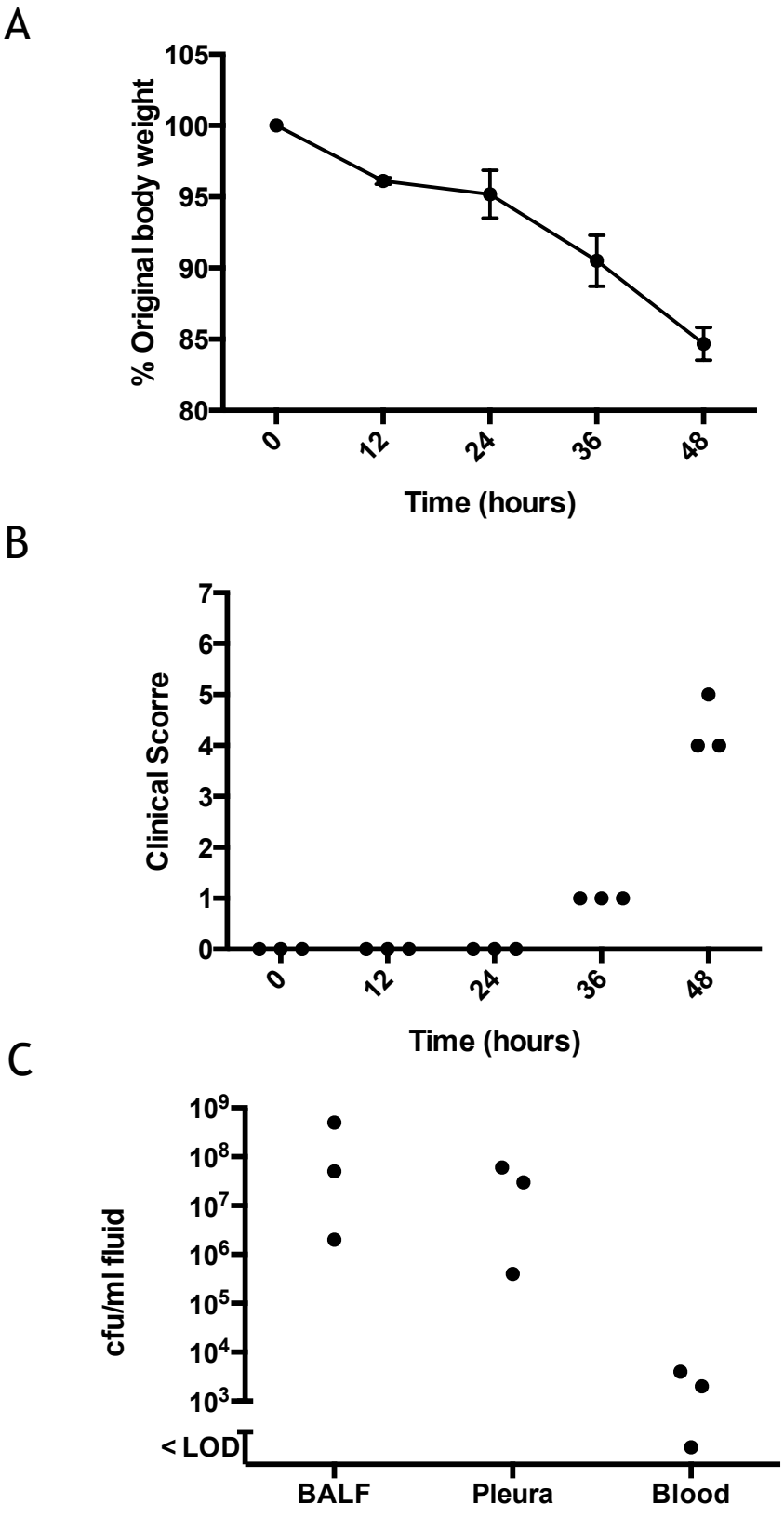

Figure 7-2. Course of SRL1 infection.

The course of SRL1 infection in RNA-Seq experiment. A. Change in body weight, B. clinical score and C. bacterial burden.

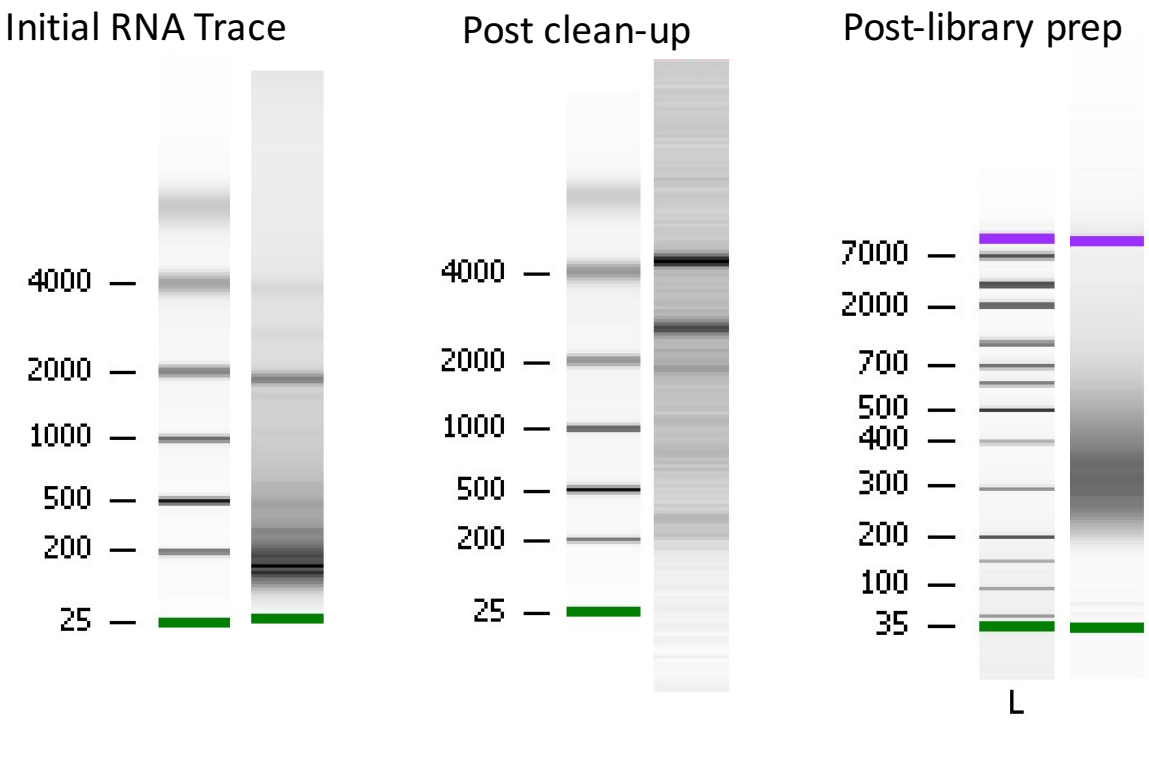

Figure 7-3. Isolation of RNA from in vivo samples.

Representative bioanalyser traces from RNA samples. Initial traces following RNA isolation by bead beating in Trizol and on-column extraction, following cleanup with bead based system and following ribosomal RNA depletion and library preparation.

A

Sample	Total reads	Paired reads aligned	Single reads aligned	Total Reads	% Reads aligned
Broth 1	61,987,154	44,551,264	5,247,430	49,798,694	80.4
Broth 2	57,882,676	31,983,782	4,008,135	35,991,917	62.0
Broth 3	15,145,016	10,084,854	2,137,236	12,222,090	80.3
BALF 1	46,267,280	7,098	4,798	11,896	<0.1
BALF 2	60,494,608	6,061,080	702,159	6,763,239	11.2
BALF 3	58,380,798	102,326	16,771	119,097	0.2
Pleura 1	57,787,368	252,434	36,239	288,673	0.5
Pleura 2	166,408,846	2,513,398	259,667	2,773,065	1.7
Pleura 3	19,445,100	875,970	228,254	1,104,224	5.7

Summary	Total reads	Paired reads aligned	Single reads aligned	Total Reads	% Reads aligned
Broth	135,014,846	86,619,900	11,392,801	98,012,701	72.6
BALF	165,142,686	6,170,504	723,728	6,894,232	4.2
Pleura	243,641,314	3,641,802	524,160	4,165,962	1.7

B

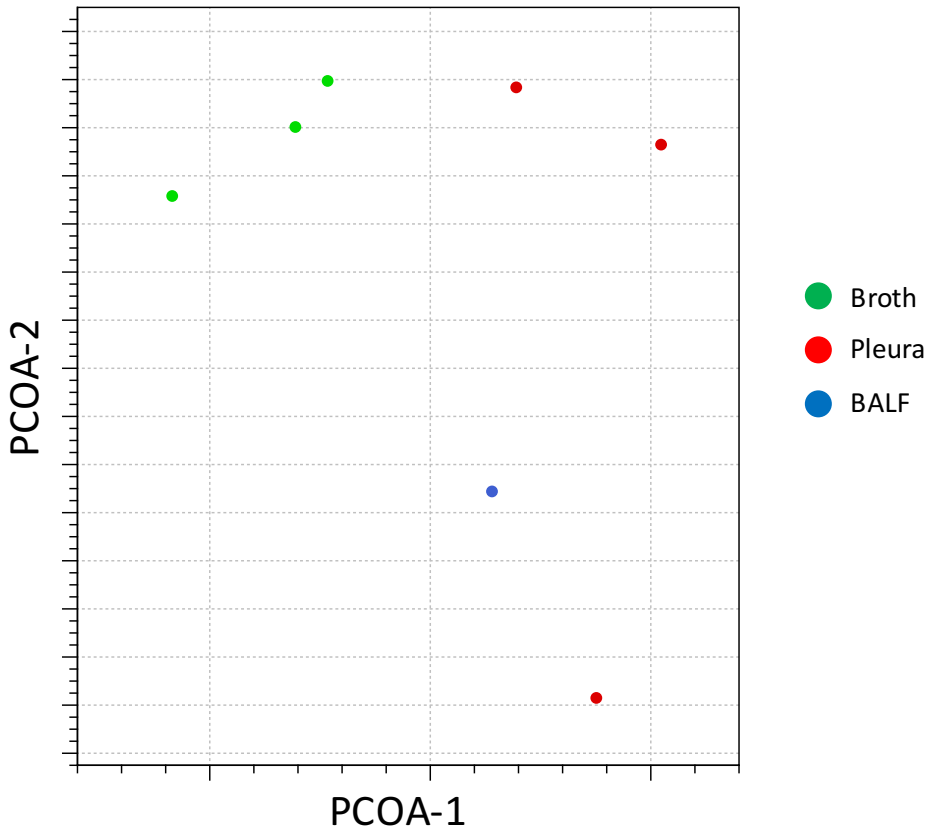

Figure 7-4. Outcome of read mapping against OXC141 reference genome. A. Table showing outcome of read mapping for each sample with summary statistics shown below. B. Principal component analysis of samples with >0.5% of reads successfully aligned.

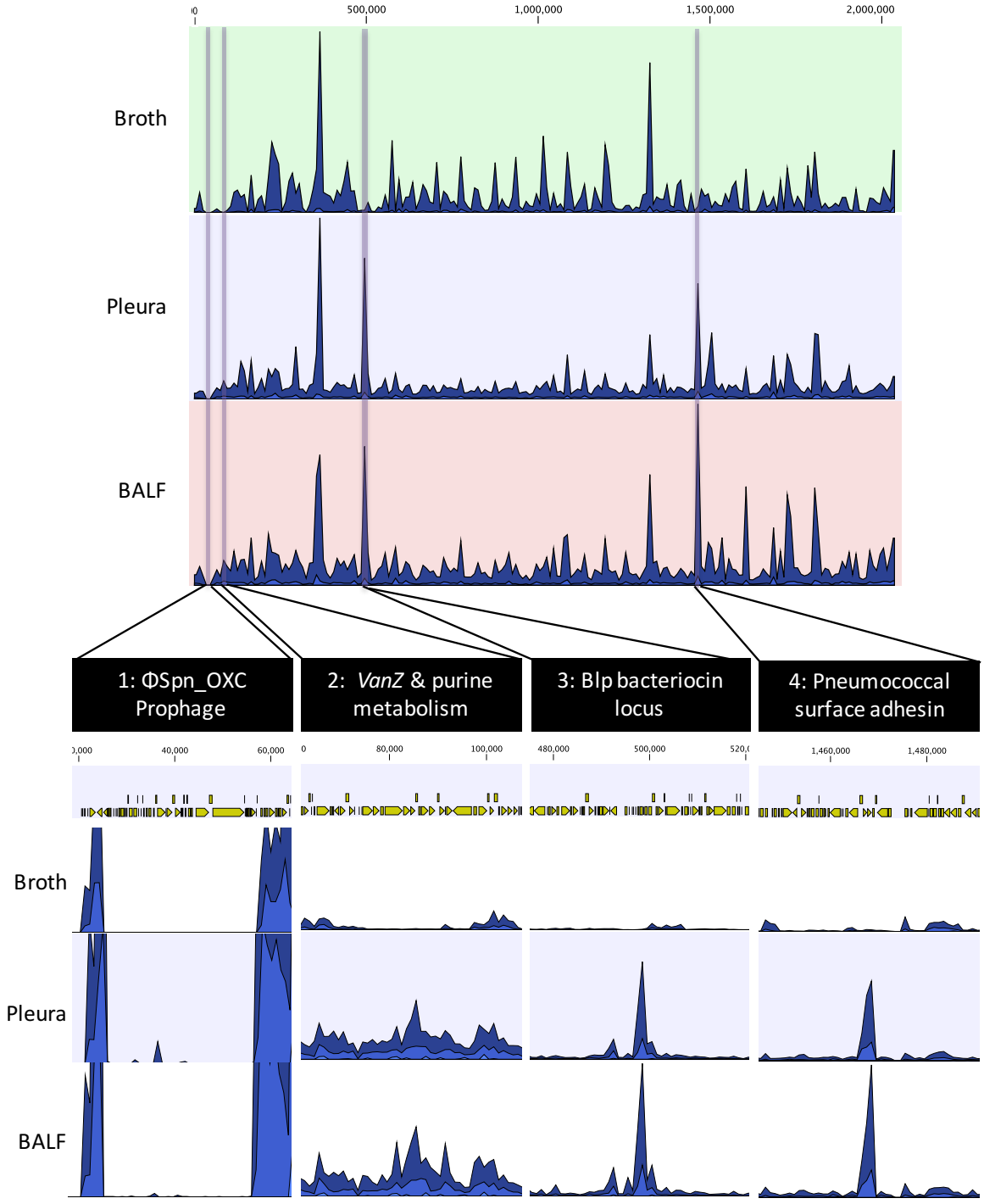

Figure 7-5. Mapping of reads against reference genome.

Reads were mapped to the OXC141 reference genome using CLC and gene expression between samples compared using the EDGE-R method. Data are shown from representative samples in each group. Genomic regions with significant upregulation of gene expression in both pleura and BALF compared to broth samples are shown below. Light blue represents median expression while dark blue represents maximum expression recorded at each location.

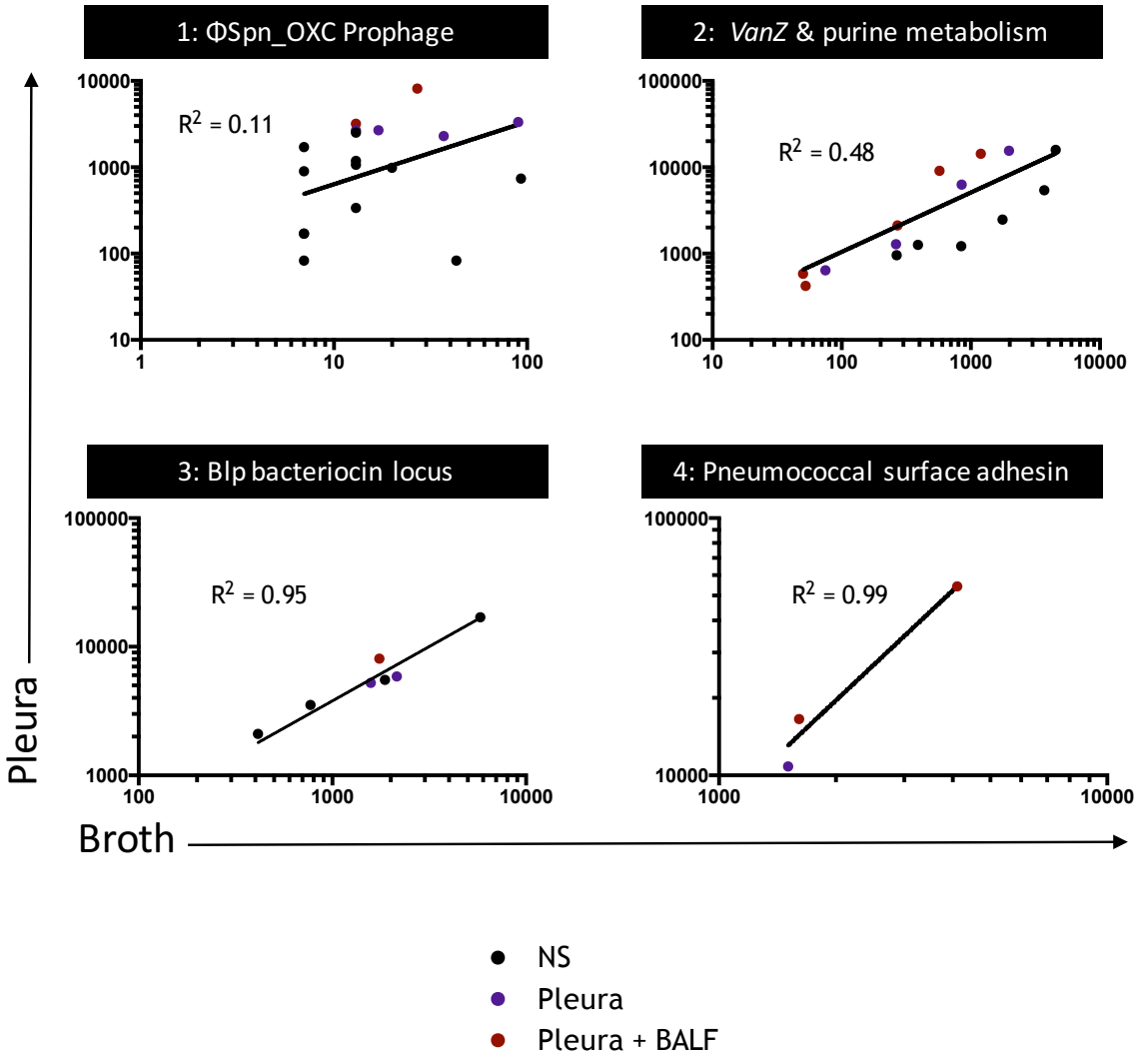

Figure 7-6. Correlation between normalised gene expression in broth and pleura.

Log normalised gene expression values are plotted and linear correlation calculated for each of the genomic regions found to be upregulated. R^2 values are shown on the plots. Statistical significance (FDR adjusted $P < 0.05$) of comparison between broth and pleura or BALF are shown in colour.

Pleura vs Broth

Region	Feature ID	Description	Fold change	P-value	FDR p-value	Broth	Pleura
Region 1	RS00135	Integrase	14.67	1.56E-04	8.49E-03	0.9	33.5
	RS00195	**Replisome organiser**	**86.18**	**8.02E-05**	**5.22E-03**	**0.1**	**32.0**
	RS00245	**Endonuclease**	**225.89**	**3.83E-07**	**2.78E-04**	**0.3**	**81.4**
	RS00275	Capsid protein	39.72	1.51E-03	0.03	0.2	26.9
	RS00315	TMP repeat protein	75.68	2.23E-05	2.56E-03	0.1	26.7
	RS00325	Phage protein	28.13	2.79E-04	0.01	0.4	23.0
Region 2	RS00515	purL	3.59	8.31E-04	0.02	771.1	3523.9
	RS00520	**VanZ**	**3.73**	**7.60E-04**	**0.02**	**413.1**	**2097.5**
	RS00525	purH	3.53	9.10E-04	0.03	1749.2	8069.9
Other	RS00805	Argininosuccinate synthase	2.98	1.43E-03	0.03	1477.5	6009.4
Region 3	RS02630	Bacteriocin transporter	3.73	2.20E-04	0.01	263.4	1283.9
	RS02670	**Bacteriocin**	**5.92**	**5.58E-07**	**2.78E-04**	**270.6**	**2115.8**
	RS02675	Bacteriocin	6.41	2.04E-06	4.22E-04	74.9	640.5
	RS02680	**Bacteriocin**	**8.45**	**8.26E-07**	**2.78E-04**	**50.3**	**583.6**
	RS02685	**PncM**	**6.18**	**2.96E-04**	**0.01**	**52.6**	**423.1**
	RS02690	**Immunity protein BlpX**	**12.43**	**1.79E-06**	**4.12E-04**	**573.1**	**9080.1**
	RS02695	CAAX protease	6.31	1.35E-03	0.03	1978.5	15490.9
	RS02700	**BlpZ**	**9.85**	**2.03E-04**	**0.01**	**1196.0**	**14334.9**
	RS02705	CAAX protease	5.81	1.11E-04	6.56E-03	850.8	6285.5
Region 4	**RS07830**	**PsaA B**	**7.82**	**1.38E-04**	**7.73E-03**	**1608.9**	**16540.9**
	RS07835	PsaA C	5.5	6.52E-04	0.02	1507.6	10826.1
	RS07840	**PsaA A**	**9.87**	**3.35E-04**	**0.01**	**4106.6**	**54244.0**

BALF vs Broth

Region	Feature ID	Description	Fold change	P-value	FDR p-value	Broth	BALF
Region 1	**RS00195**	**Replisome organiser**	**991**	**6.36E-05**	**0.02**	**0.1**	**242.6**
	RS00245	**Endonuclease**	**853.07**	**7.37E-08**	**7.63E-05**	**0.3**	**485.2**
Region 2	**RS00520**	**VanZ**	**7.59**	**2.17E-05**	**8.98E-03**	**413.1**	**1455.6**
Region 3	**RS02670**	**Bacteriocin**	**9.29**	**2.16E-06**	**1.49E-03**	**270.6**	**1576.9**
	RS02680	**Bacteriocin**	**10.95**	**4.19E-06**	**2.17E-03**	**50.3**	**303.2**
	RS02685	**PncM**	**9.66**	**1.58E-04**	**0.03**	**52.6**	**182.0**
	RS02690	**Immunity protein BlpX**	**18.62**	**4.13E-08**	**7.63E-05**	**573.1**	**5701.1**
	RS02700	**BlpZ**	**14.13**	**4.33E-05**	**0.01**	**1196.0**	**7945.2**
Region 4	**RS07830**	**PsaA B**	**8.35**	**2.22E-04**	**0.04**	**1608.9**	**6489.6**
	RS07840	**PsaA A**	**12.44**	**1.09E-04**	**0.03**	**4106.6**	**23289.7**

Table 7-1. Upregulation of coding regions during infection in SRL1.
Reads were mapped to the OXC141 genome using CLC and gene expression between samples compared using the EDGE-R method. Coding regions with higher expression during infection than growth in broth are shown if the FDR adjusted p-value is less than 0.05. Coding regions significantly upregulated in pleura and BALF are shown in bold.

Description	Feature ID	P-value	Fold change	Weighted difference	FDR p-value correction	Broth	Pleura
Pyruvate lyase	pflA	1.04E-03	-3.44	-7.74E-04	0.03	6,790.87	2,760.47
Phosphoglucose isomerase	pgi	1.88E-03	-4.33	-2.24E-03	0.04	17,412.60	5,804.27
30S ribosomal subunit protein S16	rpsP	1.12E-03	-12.01	-3.35E-03	0.03	20,154.97	2,521.80
SecE secretion complex component	secE	5.68E-05	-7.86	-2.39E-04	4.53E-03	1,526.87	303.83
Sulfurtransferase	RS00700	6.91E-04	-5.8	-2.36E-03	0.02	16,266.17	4,219.63
amino acid ABC transporter substrate-binding protein	RS01075	8.06E-05	-9.71	-2.07E-03	5.22E-03	12,903.50	2,078.40
Hypothetical protein: unknown function	RS01220	6.68E-05	-4.31	-2.45E-04	5.12E-03	1,844.93	636.53
Aminopeptidase C	RS01650	3.92E-05	-6.79	-3.12E-03	3.53E-03	22,336.67	4,590.47
Hypothetical protein: possible transcriptional regulator	RS01765	2.66E-03	-2.62	-1.52E-04	0.05	1,459.47	809.77
Transcriptional regulator	RS01845	1.24E-03	-3.66	-9.89E-04	0.03	8,603.00	3,207.27
Cell division protein GpsB	RS01995	3.00E-05	-4.22	-3.59E-04	2.96E-03	2,752.93	968.57
Hypothetical protein: unknown function	RS02000	8.09E-04	-7.21	-0.02	0.02	136,240.63	23,703.77
tRNA synthetase	RS02135	5.25E-04	-3.91	-1.88E-04	0.02	1,447.30	552.77
alkylhydroperoxidase	RS02155	7.59E-05	-5.08	-1.12E-03	5.22E-03	8,404.70	2,369.33
MarR family transcriptional regulator	RS02185	8.69E-04	-10.26	-2.74E-03	0.02	17,074.30	2,493.33
3-oxoacyl-ACP synthase	RS02190	1.03E-03	-9.69	-5.45E-03	0.03	34,241.27	5,279.40
acyl carrier protein	RS02195	7.60E-04	-11.58	-3.14E-03	0.02	19,325.43	2,583.33
Hypothetical protein: unknown function	RS02350	2.88E-03	-2.75	-3.26E-04	0.05	3,129.97	1,600.80
Formate acetyltransferase	RS02395	7.00E-06	-9.99	-0.02	1.12E-03	120,906.27	16,188.13
Likely membrane protein, unknown function	RS02470	9.66E-05	-4.05	-7.43E-04	5.90E-03	5,905.67	2,087.20
Possible membrane acyltransferase	RS02485	2.22E-05	-3.95	-3.24E-04	2.56E-03	2,572.53	952.57
Likely membrane protein, unknown function	RS02595	1.92E-04	-10.16	-5.61E-04	9.96E-03	4,596.33	534.53
Fructose bisphosphate aldolase	RS02975	5.17E-04	-6.48	-5.45E-03	0.02	40,403.00	8,251.47
50S ribosomal protein L1	RS03105	2.43E-03	-6.78	-1.25E-03	0.05	8,084.93	1,797.23
Possible membrane protein, unknown function	RS03350	5.15E-04	-7.53	-3.55E-04	0.02	2,237.43	461.57
L-lactate oxidase	RS03455	1.26E-03	-4.61	-1.54E-03	0.03	12,142.17	3,634.77
Chlorohydrolase	RS03465	9.78E-04	-5.51	-4.46E-05	0.03	304.03	78.77
phosphomethylpyrimidine kinase	RS03515	7.28E-05	-5.31	-1.15E-03	5.22E-03	9,105.63	2,261.90
uracil phosphoribosyltransferase	RS03605	1.87E-03	-5.28	-2.12E-03	0.04	14,828.83	4,215.63
ATP-dependent Clp protease proteolytic subunit	RS03610	4.69E-05	-8.03	-1.62E-03	4.05E-03	10,536.30	1,967.93
Superoxide dismutase	RS03695	1.05E-05	-8.18	-1.54E-03	1.56E-03	11,002.13	1,821.93
RNA-binding protein	RS03740	3.21E-04	-7.8	-3.38E-04	0.01	2,146.83	431
ribonucleoside-triphosphate reductase	RS03760	9.23E-04	-3.22	-1.46E-04	0.03	1,251.80	545.4
Hypothetical protein: unknown function	RS03945	9.93E-04	-4.59	-6.00E-04	0.03	4,357.30	1,459.33
Hypothetical protein: unknown function	RS04140	5.61E-05	-9.76	-1.05E-04	4.53E-03	650.67	106.53
Possoble stress response transcriptional regulator	RS04415	7.66E-04	-4.45	-5.66E-04	0.02	4,247.67	1,364.37
Ribosome recycling factor	RS04600	2.26E-04	-4.89	-6.40E-04	0.01	4,568.47	1,400.20
preprotein translocase subunit SecG	RS04750	2.10E-03	-4.09	-9.79E-05	0.04	727.1	270.27
Foldase prsA	RS04785	1.61E-03	-5.59	-1.24E-03	0.04	8,372.30	2,280.50
cytochrome C biogenesis protein	RS04870	5.48E-04	-3.42	-5.95E-04	0.02	5,100.47	2,113.20
Thioredoxin	RS04875	2.15E-05	-3.93	-3.34E-04	2.56E-03	2,748.93	988.83
large conductance mechanosensitive channel protein MscL	RS04930	7.25E-04	-4.82	-6.15E-04	0.02	4,325.50	1,397.73
queuosine transporter QueT	RS04940	2.51E-04	-4.51	-2.88E-04	0.01	2,092.33	716.43
Hypothetical protein: unknown function	RS05010	8.91E-04	-6.85	-5.57E-03	0.03	37,675.87	7,797.33
Iron compound ABC transporter	RS05030	1.14E-05	-7.04	-1.36E-03	1.57E-03	9,351.87	1,985.27
histone-lysine N-methyltransferase	RS05185	1.40E-03	-4.68	-3.87E-04	0.03	2,850.43	924.33
DNA binding protein	RS05435	3.46E-05	-5.28	-4.75E-04	3.25E-03	3,409.10	968.63
50S ribosomal protein L21	RS05445	3.31E-04	-13.51	-3.51E-03	0.01	20,963.47	2,306.57
Ribosomal protein	RS05450	1.34E-03	-10.04	-5.98E-03	0.03	36,804.47	5,427.40
50S ribosomal protein L27	RS05455	1.92E-03	-7.49	-2.25E-03	0.04	14,421.07	2,888.67
DeoR family transcriptional regulator	RS05725	2.43E-05	-6.08	-1.14E-03	2.65E-03	8,979.70	1,963.50
tagatose-bisphosphate aldolase	RS05755	7.91E-05	-14.23	-4.20E-03	5.22E-03	30,619.60	2,746.47
tagatose-6-phosphate kinase	RS05760	1.87E-04	-10.99	-2.73E-03	9.94E-03	20,157.90	2,344.60
galactose-6-phosphate isomerase	RS05770	2.52E-04	-9.56	-1.47E-03	0.01	10,912.47	1,458.93
chlorohydrolase	RS05800	9.37E-07	-7.06	-1.99E-04	2.78E-04	1,416.03	282.9
lactate dehydrogenase	RS05890	5.18E-04	-5.84	-2.01E-03	0.02	14,313.27	3,480.17
2-C-methyl-D-erythritol 4-phosphate cytidylyltransferase	RS06130	2.89E-03	-4.46	-7.47E-04	0.05	5,358.50	1,832.17
adapter protein MecA	RS06440	9.46E-04	-4.17	-8.55E-04	0.03	6,432.00	2,342.40
thioredoxin reductase	RS06900	2.33E-04	-6.47	-3.41E-03	0.01	27,243.07	5,291.60
2,5-diketo-D-gluconic acid reductase	RS06995	3.36E-04	-3.33	-5.10E-04	0.01	4,378.17	1,877.23
bacterocin transport accessory protein	RS07075	2.59E-05	-4.05	-1.38E-04	2.68E-03	1,133.63	384.73
F0F1 ATP synthase subunit C	RS07145	2.50E-03	-3.56	-2.49E-04	0.05	1,953.00	822.5
Csb-D like protein	RS07245	9.40E-07	-9.33	-9.92E-04	2.78E-04	6,610.90	989.37
30S ribosomal subunit protein S18	RS07285	9.77E-04	-9.83	-1.03E-03	0.03	6,334.43	956.17
30S ribosomal subunit protein S6	RS07295	1.34E-04	-12.18	-1.03E-03	7.70E-03	6,228.47	770
NADPH-dependent FMN reductase	RS07325	7.01E-06	-7.23	-1.24E-03	1.12E-03	8,953.70	1,768.03
Ferritin	RS07455	7.04E-09	-54.01	-5.49E-03	1.46E-05	31,738.30	897.03
adenine phosphoribosyltransferase	RS07480	2.84E-03	-3.06	-5.84E-04	0.05	5,077.33	2,394.87
pyridine nucleotide-disulfide oxidoreductase	RS07525	2.51E-03	-2.9	-6.53E-04	0.05	6,104.30	2,990.60
cadmium resistance protein CadD	RS07715	2.36E-03	-4.39	-1.74E-03	0.05	13,168.77	4,339.57
30S ribosomal subunit protein S15	RS07720	1.44E-03	-9.47	-1.52E-03	0.03	9,455.00	1,485.63
lipid hydroperoxide peroxidase	RS07845	2.28E-04	-4.11	-4.48E-04	0.01	4,064.77	1,227.73
Ribosomal protein	RS08365	5.50E-06	-37.81	-0.01	1.04E-03	77,068.17	2,268.67
Thioredoxin	RS08370	1.21E-06	-20.79	-3.44E-03	3.13E-04	25,934.03	1,497.93
Aquaporin	RS08385	1.29E-03	-4.84	-8.26E-04	0.03	5,796.13	1,840.50
Likely membrane protein, unknown function	RS08540	1.59E-03	-5.33	-3.83E-03	0.03	28,300.40	7,277.23
General stress protein	RS08550	2.71E-03	-5.05	-3.54E-03	0.05	27,634.87	7,168.93
polyketide cyclase	RS08865	4.50E-04	-4.25	-8.97E-04	0.02	6,955.17	2,401.77
MarR family transcriptional regulator	RS08870	6.74E-07	-6.26	-4.85E-04	2.78E-04	3,463.67	805.5
molecular chaperone GroES	RS09215	9.69E-05	-7.48	-4.73E-04	5.90E-03	3,862.90	641.77
Likely membrane protein, unknown function	RS09490	2.78E-03	-3.93	-1.09E-03	0.05	8,549.00	3,150.27
Transcriptional regulator	RS09635	1.69E-03	-4.04	-5.76E-04	0.04	4,287.43	1,648.37
50S ribosomal protein L33	RS09750	1.42E-03	-4.24	-6.02E-04	0.03	4,495.00	1,562.43
glyceraldehyde-3-phosphate dehydrogenase	RS09765	2.66E-03	-6.37	-0.02	0.05	171,171.37	35,256.63
Hypothetical protein: possible tRNA synthetase	**RS10140**	**3.18E-04**	**-4.22**	**-1.24E-04**	**0.01**	**927.4**	**338.6**
30S ribosomal subunit protein S2	RS10830	1.24E-03	-7.63	-3.25E-03	0.03	20,955.33	4,082.47
TetR family transcriptional regulator	RS10930	8.10E-04	-2.87	-3.76E-04	0.02	3,596.30	1,776.40
Serine protease	RS10970	2.45E-04	-7.67	-0.01	0.01	90,691.13	15,484.50
chromosome partitioning protein ParB	RS10975	5.63E-04	-7.18	-5.66E-03	0.02	40,266.60	7,478.13

Table 7-2. Downregulation of coding regions during infection in SRL1. Reads were mapped to the OXC141 genome using CLC and gene expression between samples compared using the EDGE-R method. Coding regions with lower expression during infection than growth in broth are shown if the FDR adjusted p-value is less than 0.05. Coding regions significantly upregulated in pleura and BALF are shown in bold.

8. THE ROLE OF IL-22 IN RECOVERY FOLLOWING PNEUMOCOCCAL PNEUMONIA

8-1 Introduction

It is a striking feature of pneumonic illnesses that recovery of the lungs from the dense consolidation that is a feature of the disease is usually rapid and complete. Chest radiography six weeks after admission to hospital with pneumonia is usually normal even where there has been very extensive consolidation. However, even despite this rapid resolution of consolidation, patients with severe pneumonia usually require only a few days of antibiotics but often take considerably longer to resolve their illness. There are relatively little published data on the resolution of pulmonary inflammation in infectious pneumonia. Neutrophil recruitment to affected areas in a self-limiting rabbit model ceased within 48 hours of induction of pneumonia suggesting that resolution begins promptly as bacterial infection improves. Removal of inflammatory cells is thought to be by the mechanism of apoptosis and phagocytosis by macrophages. Damage to alveolar membranes heals with organisation of the alveolar membranes and in some cases can result in interstitial fibrosis. Human lung collagen rises during acute lung injury of any cause and the presence of fibrosis is a poor prognostic factor.

IL-22 is known to be involved in the resolution of inflammatory processes. Inhibition of IL-22 accentuated lung fibrosis caused by *Bacillus subtilis* hypersensitivity[342] and bleomycin[322]. IL-22 also protected against chemically induced liver fibrosis[490]. There is evidence of an interaction with IL-17A, with

IL-22 apparently acting as a pro-inflammatory mediator in a presence of IL-17A but anti-inflammatory without it.

In order to explore the role of IL-22 in the recovery of the mouse lung from pneumococcal pneumonia, I decided to investigate the resolution of the inflammation associated with pulmonary infection by SRL1 following treatment with antibiotics. Because of the well-known efficacy, long elimination half-life and ease of administration I selected the 3rd generation cephalosporin antibiotic ceftriaxone, which is commonly used in the management of severe pneumococcal infection in humans. In order to maximise the probability of severe disease developing, a dose of 3 x 10^6 cfu/mouse of SRL1 was selected compared to most experiments involving SRL1 which used 10^6 cfu/mouse. Ceftriaxone was given once mice started showing clinical signs of illness and a further dose given the following day.

8-2 Recovery following pneumococcal pneumonia

Two experiments investigating recovery from infection with SRL1 were undertaken. Both demonstrated similar results although quantitative assessment of lung collagen content was conducted only once and this experiment is presented here.

IL-22$^{-/-}$ and wild type mice were infected with SRL1 and carefully monitored. After 36 hours, mice began to show clinical signs of infection and had lost around 8% of initial body weight and the animals with clinical signs of disease had lost between 10-15% of body weight (figure 8-1A). Weight loss stabilised after administration of antibiotics and animals then achieved a stable body weight by day 6 following infection. Clinical scores are shown in figure 8-1B. There was no evidence of any difference in weight change (P = 0.48) or clinical score (P = 0.67) between the two groups. There was a trend towards decreased body weight among WT mice compared to IL-22$^{-/-}$ at the end of the experiment but the absolute difference was small (WT 99.7% IBW, IL-22$^{-/-}$ 97.4% IBW, P = 0.07). All mice survived the experiment and all mice were free of clinical signs of disease by four days post infection.

8-3 Histopathology of recovering lung tissue

H&E staining compared mice used in this experiment with mice culled 36-48 hours after infection with SRL1 without treatment. The lungs of uninfected IL-22$^{-/-}$ mice were normal at baseline. As previously described, WT and IL-22$^{-/-}$ mice without treatment both demonstrated severe consolidation and there was no significant difference between the two groups.

5 animals were culled seven days after antibiotics and histological analysis of the lungs typically demonstrated moderate peribronchial inflammatory change with patchy alveolar infiltrates. There were some areas of focal haemorrhage and focal pleural thickening and subpleural inflammation. One wild type mouse had marked pleural thickening with evidence of mononuclear infiltration of the pleural surface presumably reflecting resolving pleural infection. There was no evidence of a difference in the histopathological changes in mice after seven days (median score: WT 3 and IL-22$^{-/-}$ 4, P = 0.52).

After fourteen days there was a significantly higher histological score among IL-22$^{-/-}$ mice compared to wild type two weeks after antibiotics (median score: WT 1 and IL-22$^{-/-}$ 2, P = 0.033). This difference was primarily due to an increase in alveolar changes among IL-22$^{-/-}$ mice. While 6/10 IL-22$^{-/-}$ mice had persistent alveolar abnormalities, principally patchy hyalinisation of alveoli with some clot and infiltrating polymorphs and mononuclear cells. In contrast none of the wild type mice showed similar changes (0/9, Fisher's exact test 0.011). One wild type mouse did demonstrate a single small patch of focal subpleural mononuclear infiltrate without hyaline membrane formation. Other aspects of the histological analysis were similar.

8-4 Collagen composition of recovering lung tissue

8-4.1 Histological assessment

Collagen distribution in recovering lungs was assessed using the picrosirius red stain, which stains collagen fibres with a dye that demonstrates birefringence that may be visualised under polarised light microscopy. Unfortunately, the

polarised light microscope available was not equipped with a facility for digital image acquisition and this limited the quality of images available for analysis.

Assessment of picrosirius red staining was subjective and difficult to score. Most of the lung in all animals appeared similar to control lung. However, there was some increase in collagen staining visible in both wild type and IL-22$^{-/-}$. Representative images are shown in Figure 8-4A. The overall impression was of a mild, patchy increase in collagen deposition in IL-22$^{-/-}$ mice involving a small proportion of the lung area.

8-4.2 Chemical assessment

In view of the subjectivity of the histological assessment of collagen within the lung, a chemical method of quantitative collagen assessment was undertaken. Total collagen composition of left lung of recovering animals was assessed. Resting wild type and IL-22$^{-/-}$ mice displayed very little variation in the abundance of collagen present in the lungs with no evidence of a difference between groups (mean: WT 6.9 µg/ml and IL-22$^{-/-}$ 6.7 µg/ml). Collagen composition of lungs was increased during the early recovery period before decreasing towards baseline over the next week although collagen composition remained above baseline at two weeks. There was a difference between groups, with collagen composition higher amongst IL-22$^{-/-}$ mice than WT (Figure 8-4B, two-way ANOVA P =0.011).

8-5 Discussion

In this chapter, I have outlined experiments assessing the recovery of mice following infection with SRL1. Both wild type and IL-22$^{-/-}$ mice recovered well from pneumococcal pneumonia and, considering the severe inflammatory changes known to be present in the lungs of animals with clinical signs of SRL1 pulmonary infection, the relatively mild histological changes in the lungs of treated animals is remarkable. The weight loss in infected animals stabilised within 24 hours of antibiotic administration and recovered back to baseline with resolution of clinical illness within five days. In two experiments involving 60 animals only one animal had to be culled due to failure to respond to antibiotic administration.

A small but statistically significant difference was observed between WT and IL-22$^{-/-}$ mice, with IL-22$^{-/-}$ mice being slower to resolve alveolar changes than WT mice and demonstrating increased collagen deposition within the lungs during recovery. This is despite a trend towards decreased severity of infection in IL-22$^{-/-}$ mice during mortality studies involving SRL1. The changes were relatively small and given that the areas of inflammation and collagen deposition were small there is unlikely to be any significant difference in lung function between the WT and IL-22$^{-/-}$ mice. This is also suggested by the lack of a difference between the groups in measures of global health such as weight and clinical score. Therefore, while this study underlines the role of IL-22 in resolution of pulmonary inflammation described by others, it is clear that in the context of pneumococcal pneumonia the role of IL-22 is secondary to other factors which are able to function to resolve the majority of inflammatory change effectively.

Most studies on resolution of lung inflammation use potent chemical or immunological stimulators of inflammation such as bleomycin or *Bacillus subtilis* hypersensitivity to model the development of fibrosis. As already discussed, a clear role for IL-22 has been established in these models. However, there has been relatively little published work on the resolution of bacterial pneumonia. Studies have reported several factors to be important in the complete resolution of inflammatory changes in bacterial pneumonia. Absence of gamma delta cells was implicated in delayed resolution of pneumococcal pneumonia in one study[222], possibly by inducing apoptosis in pulmonary phagocytes. Absence of CD44, a cell surface glycoprotein important in cell migration and homing, was associated with increased survival time in pneumococcal pneumonia compared to WT controls[491]. In contrast, CD44$^{-/-}$ mice were slow to resolve a sublethal challenge with pneumococci and had persistant inflammatory changes despite improved bacterial clearance. IL-10 has also been implicated in the resolution of bacterial pneumonia. Two studies involving bacterial pneumonia caused by the Gram negative bacteria *Pseudomonas aeruginosa*[492] and *Klebsiella pneumoniae*[493] have both demonstrated a role for IL-10 in accelerating resolution of the lung injury induced by sub-lethal pneumonic challenge. IL-10 was modulated by immunological priming or genetic manipulation respectively in the two studies. Both studies demonstrate early decreased inflammation in IL-10 deficient animals followed by marked failure to resolve inflammation during the recovery

period. These studies demonstrate the fine balance between adequate bacterial control during the acute phase followed by effective resolution once the infection is controlled. It is notable that there was a trend towards milder acute disease in IL-$22^{-/-}$ mice (see section 5-7) followed by delayed resolution in recovery. Therefore the pattern in relation to IL-22 is similar to that seen with IL-10 and CD44, albeit with less intensity. Given the importance of rapid transition from a inflammation to resolution in patients critically ill with pneumonia, for example in patients requiring assisted ventilation, who are highly vulnerable to complications such as secondary bacterial infection while lung function is improving sufficiently to wean this support, further work should focus on the transition between these states and how it is detected. It has been suggested that IL-17 may mediate the pro- and anti- inflammatory effects of IL-22[304]. Further work could address the interaction between IL-17 and IL-22 in recovery.

In conclusion, this chapter has demonstrated a small difference in the resolution of pulmonary inflammation associated with pneumococcal pneumonia in IL-$22^{-/-}$ mice although the functional consequences of this difference are unclear.

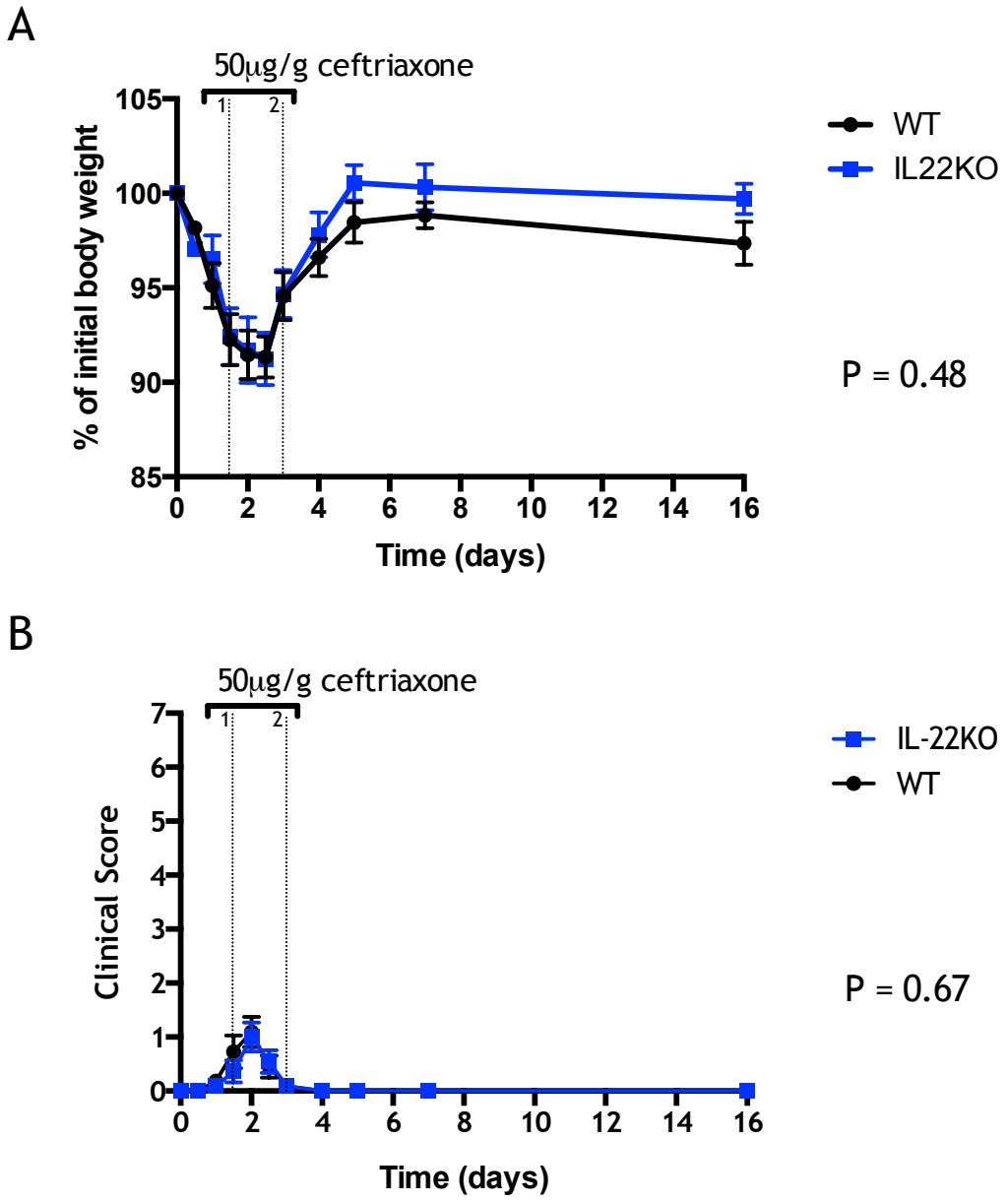

Figure 8-1. Course of SRL1 infection interrupted with antibiotic therapy. Mice were infected with 3 x 10^6 cfu/mouse of SRL1 and monitored for signs of infection. Mice were then treated with two doses of 50mg/kg ceftriaxone 36 hours apart and observed through the recovery period. A. Change in body weight. B. Clinical score. To preserve continuity of the data, mice culled after 7 days are excluded from the plots (n = 10/group). Data are presented as mean ± SEM. P value represents two way ANOVA.

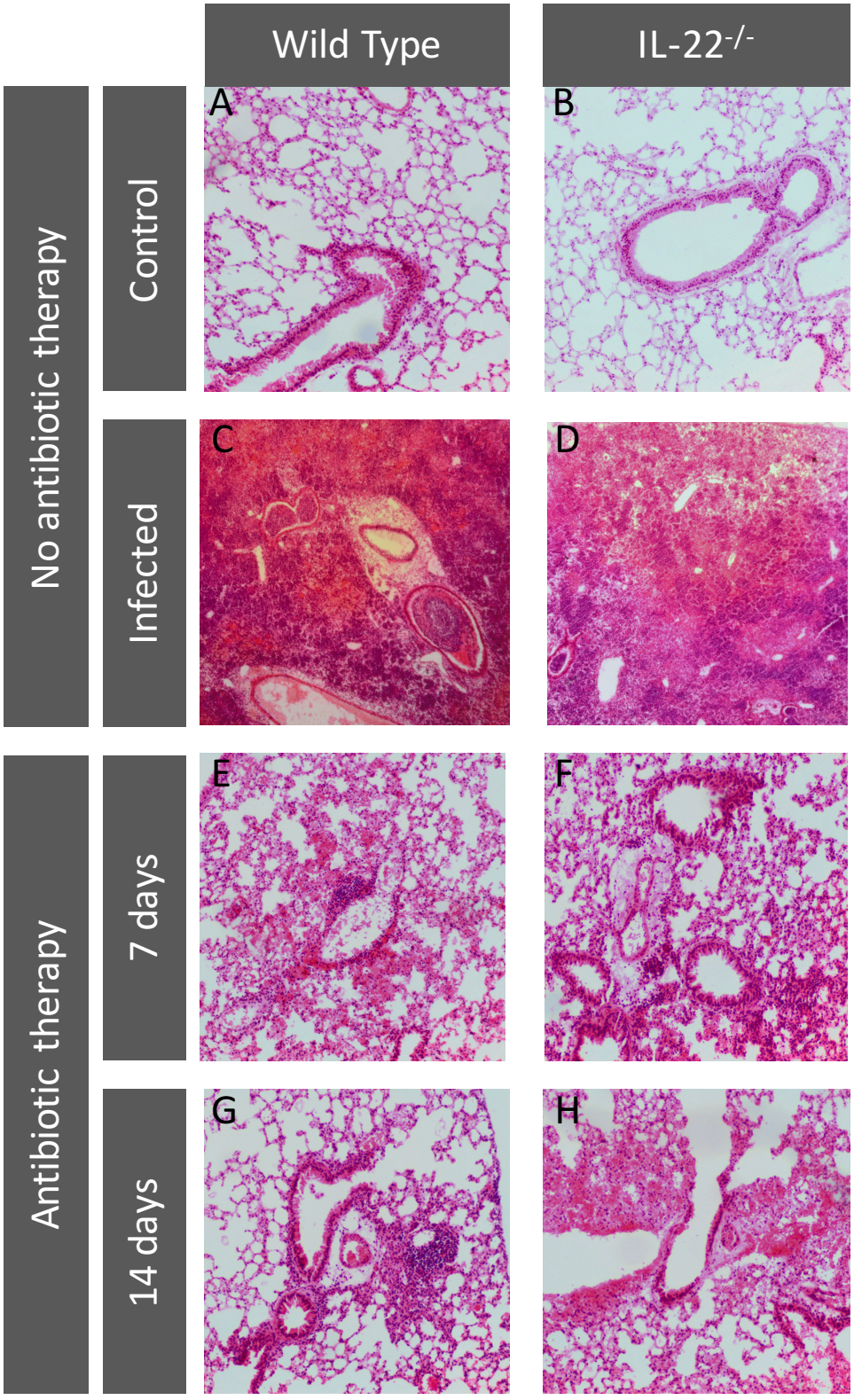

Figure 8-2. Histological changes in animals recovering from pneumococcal pneumonia.

Full legend is shown on the next page under figure 8-3.

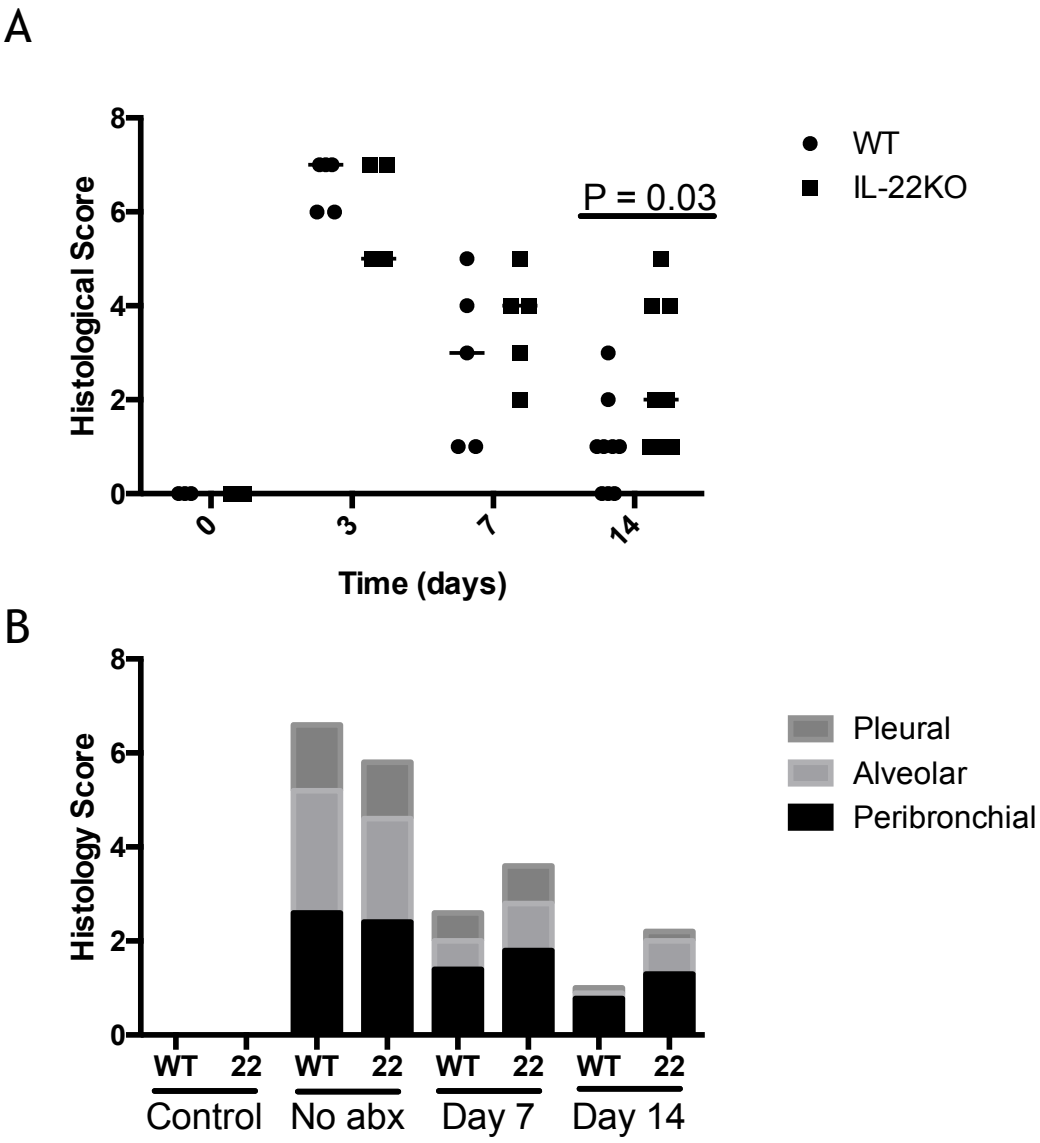

Figure 8-3. Summary of histological scoring in SRL1 infection treated with antibiotics.

A. Histological scores of individual animals in each group. B. Average histological scores displayed by score component. (n = 5-10/group)

Figure 8-2**. Histological changes in animals recovering from pneumococcal pneumonia.**

A-B. Control lungs from wild type and IL-22$^{-/-}$ mice demonstrating normal appearances. C-D. Lungs from animals infected with SRL1 without antibiotic treatment and culled at around 48 hours after infection. E-F. Alveolar and peribronchial infiltrate in mouse lungs 7 days after antibiotic therapy. G-H. Persistance of alveolar infiltrate in IL-22$^{-/-}$ mice at 14 days. No control mice were included in this experiment and so A-D are taken from banked samples used in other experiments.

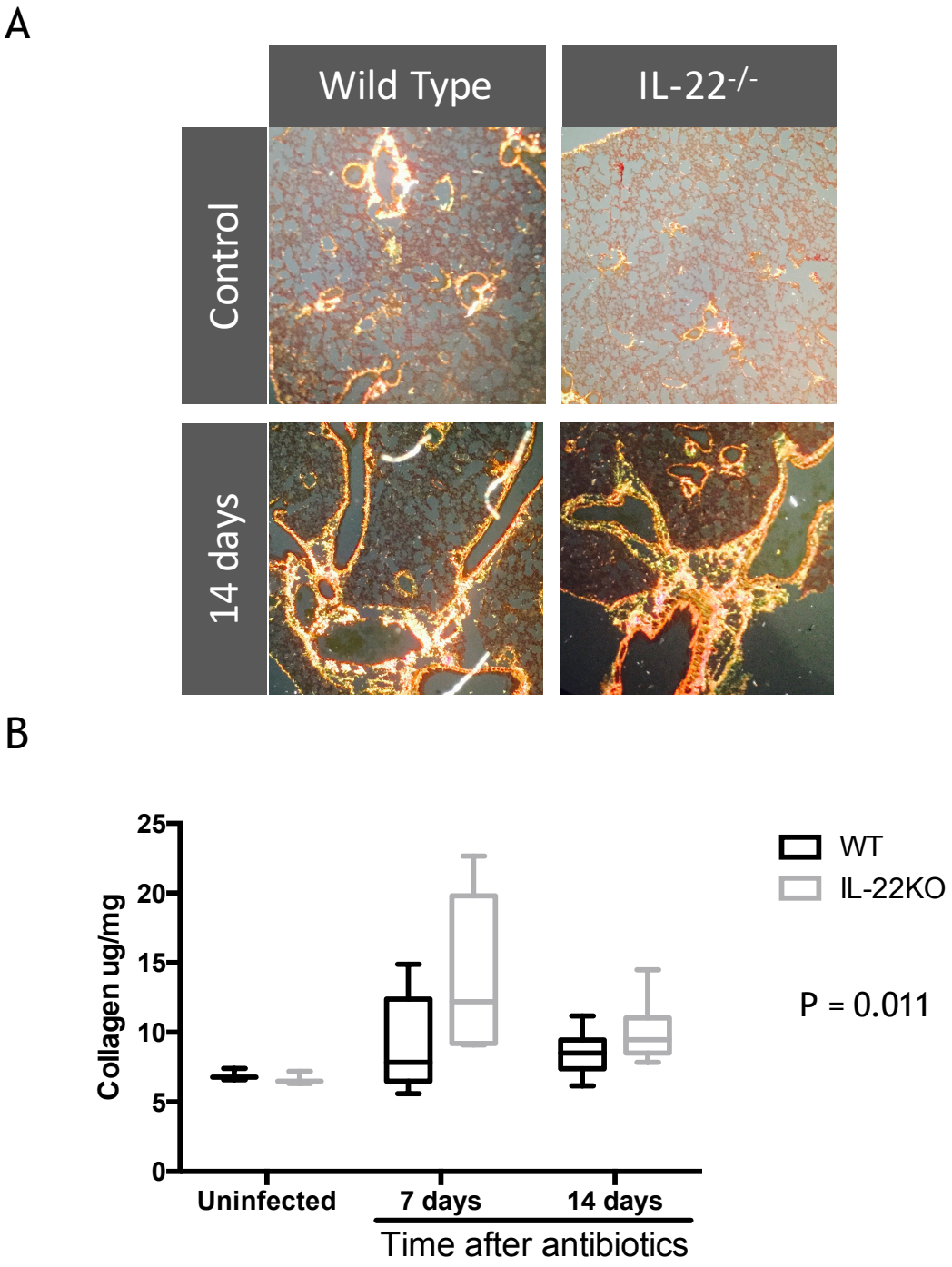

Figure 8-4. Collagen composition of lungs during recovery from pneumococcal pneumonia.

A. Representative images of polarised light microscopy following picrosirius red staining. Sections from animals 14 days after antibiotic therapy and uninfected mice are shown. B. Total lung collagen composition of lungs in recovering mice (n = 5/group at 7 days and 10/group at 14 days). P value represents two way ANOVA.

9. GENERAL DISCUSSION

9-1 Key findings

In this thesis I have described experiments exploring the role of IL-17 and IL-22 in pneumococcal colonisation and disease. I have described a number of different techniques to explore this aim. I had planned that the work on human lymphocytes described in chapter 3 and the subsequent work on an animal model of pneumococcal infection described in chapters 4-6 would be complementary but in fact they focused on different aspects of the immune response to *S. pneumoniae*. The human studies investigated acquired immunity in the form of memory T-cells responding to exposure to *S. pneumoniae;* in contrast, the experiments using the animal model focused on innate immunity to pneumococcal infection.

The key findings of the human work were to confirm the work of others who have demonstrated a memory $CD4^+$ response to pneumococci in healthy volunteers. The method used in this thesis allowed me to explore the cytokine expression profile of lymphocytes proliferating in co-culture. This demonstrated that a high proportion of IL-17 and IL-22 secreting lymphocytes are capable of co-expressing interferon γ rather than traditional Th17 cells which are usually reported not to express interferon γ -more than 50% of $IL\text{-}17^+$ lymphocytes proliferating in response to pneumococcal stimulation were also $IFN\gamma^+$, which was an unexpected finding. However, it was expected that $IL\text{-}17^+$ lymphocytes would come from the $CCR6^+$ population of lymphocytes.

In view of the increased risk of pneumococcal disease in older patients, I went on to compare the immune responses in young and old adults. There was evidence of reduced cytokine secretion and proliferation in the older group. While it is not possible to suggest a causative link between this finding and the increased risk of IPD in older adults, it suggests that augmenting cell mediated immunity is another possible avenue to explore when developing vaccination strategies in older adults.

When I went on to explore the roles of IL-17 in a mouse model of infection. I established two models of disease in mice distinguished by the clone of *S. pneumoniae used*. The first, using the serotype 4 organism TIGR4, caused highly invasive disease with the animals dying from overwhelming sepsis. In contrast, the serotype 3 pneumococcus SRL1 caused a disease characterised by limited invasion but overwhelming necrotic pulmonary infection. In both models of infection, IL-17 and IL-22 peaked in BAL early in the course of infection suggesting an innate source in naïve animals. This was supported by the finding in TIGR4 infected animals that γδ lymphocytes were the most likely source of early IL-17.

Subsequent experiments explored the role of IL-17 and IL-22 in pneumococcal infection using the mouse model. No clear phenotype was seen in IL-$22^{-/-}$ mice. A unifying feature of both models was the finding that IL-$17RA^{-/-}$ mice had reduced transcription of pro-inflammatory and anti-bacterial factors early in infection and delay in the recruitment of neutrophils to the inflammatory response to pneumococcal infection. However, the outcome of infection was markedly different between the two infection models with IL-$17RA^{-/-}$ mice demonstrating increased mortality in TIGR4 infection but improved mortality in SRL1 infection. The finding in TIGR4 demonstrated a threshold effect, with a high density inoculum having high mortality in both groups but a dose that only occasionally induced disease in wild type mice still causing significant mortality in IL-$17RA^{-/-}$ mice. Subsequent experiments demonstrated marked differences in the ability of neutrophils to phagocytose and kill the two pneumococcal strains and experiments involving neutrophil depletion in wild type mice demonstrated that the findings could be partly replicated using this method. This suggests that, while IL-17 is important in the recruitment of neutrophils in pneumococcal

infection, the role of neutrophil influx on the outcome of infection is finely balanced between neutrophil mediated bacterial clearance and tissue damage. I went on to investigate the role of IL-17 in nasal colonisation. In this context, IL-17 was found to have a role in bacterial control in models of TIGR4 and SRL1 colonisation. The resting nasal microbiome was also markedly different among IL-17RA$^{-/-}$ mice with decreased microbial diversity compared to WT mice.

In chapters 7 and 8, I explored other aspects of SRL1 infection. RNA-Seq was used to investigate the transcriptome of SRL1 during infection. Several genomic regions were upregulated including the known virulence factor PsaA. This could guide future work exploring the virulence of this clinically important pneumococcal clone. I also investigated the role of IL-22 in recovery following pneumococcal infection. In IL-22$^{-/-}$ mice there was some evidence of delayed resolution of pulmonary inflammation, although this may not have been functionally significant given that difference was relatively minor and there was no delay in clinical recovery.

9-2 Therapeutic implications and limitations

There are a number of important limitations to the work presented here. The clear focus of translational science should be on providing experimental results that ultimately lead to improvements in clinical care. In the context of infectious diseases, the most important outcomes are in the prevention, diagnosis and management of infection. Increased understanding of host pathogen interactions permit the rational design of vaccines and improved therapeutic targeting.

The limitations of existing pneumococcal vaccines have been discussed in the introduction to this thesis. A number of vaccination strategies are currently being actively investigated, including strategies seeking to promote cell-mediated immunity to serotype independent pneumococcal antigens. Some of these strategies seek to induce a Th17 immune response. My work adds to the body of evidence suggesting that CD4^{+} mediated immune responses are present in adults. Optimal vaccination strategies in the elderly remain unclear, in view of the relative lack of efficacy of PPV-23 and lack of serotype coverage in

elderly patients of, the otherwise highly efficacious, PCV-13[380] — at the time of writing less than 25% of isolates causing IPD in the over 65s in England and Wales are from serotypes included in PCV-13[494].

This thesis describes diminished pneumococcal responses among memory $CD4^+$ cells among older adults and this suggests a possible target for vaccination in the future. A significant limitation of these studies in humans is the lack of any demonstration of protective efficacy. The literature is replete with examples of immune responses which do not correlate with protection[495] and while $CD4^+$ cells may be protective in animal models of pneumococcal colonisation[266,352,434], the evidence for a role of $CD4^+$ cells in protection against pneumococcal disease in humans is limited and largely observational — for example the high incidence of IPD in HIV infection[42].

The co-cultures used in this study were stimulated with live pneumococci: this condition was selected to model infection as accurately as possible. However, this does not allow assessment of the relative contributions of pneumococcal components to the immune response. Therefore, while the study provides evidence for the presence of memory T-cell responses to pneumococci, significant further work would be needed to refine the antigens involved.

After the work on human immune responses I went on to study pneumococcal disease through the application of an animal model in mice. The limitations of such an approach are clear and significant. While an animal model can mimic some aspects of the disease process there are major differences between humans and mice. *S. pneumoniae* is not a primary mouse pathogen and infection is induced by the aspiration of a large number of bacteria placed in the nasopharynx of an anaesthetised animal. This is quite different from the presumed mechanism of infection in humans, in which bacteria enter the lower respiratory tract from the nose through micro-aspiration. Given that this work suggests the innate role of IL-17 in the lower respiratory tract is likely to be active in the first hours of infection, it is far from certain that the results obtained from this model will be relevant to human disease. Furthermore, mice are able to tolerate far higher levels of bacteraemia than humans (it was common for TIGR4 infected mice to have $>10^6$ organisms/ml of blood whereas

severely unwell humans usually have bacteraemias in the range of 10^0-10^3 organisms/ml of blood[496,497]. Such problems of applicability are an inevitable part of the process of animal modelling and it is clear that work on the early hours of infection would not be possible in humans. Larger mammals including non-human primates may be more similar to humans but do not necessarily overcome the limitations, are much more resource intensive to perform and are less amenable to genetic manipulation than mice. The finding that IL-17 can be beneficial or harmful depending on the context must be viewed through the lens of these limitations. It does, however, raise the concern that exploiting IL-17 immunity through vaccination could be associated with harm.

A further concern, which could significantly limit future studies, is the difficulty encountered in the transformation of SRL1. Both my experience and the lack of evidence of recombination in clinical isolates[392] suggest that SRL1 is unlikely to be amenable to genetic manipulation. Since hypotheses suggested by many of the experiments reported in this thesis, particularly transcriptomics, suggest experiments involving genetic manipulation of the bacteria, for example deletion of an upregulated genomic region, this would be a major limitation of future study.

9-3 Future directions

The data presented in this thesis suggests a number of possibilities for future work. While the experiments contribute to the literature on the role of IL-17 in pneumococcal disease, they also suggest a number of other important research questions with potential translational implications.

As discussed above, the memory T cells described in the results of the human study were stimulated by live pneumococci. Future work could use recombinant proteins and other pneumococcal components to seek to identify potential vaccine candidate molecules. Possible candidates include virulence factors, surface protein and cell wall polysaccharides although a previous screen of pneumococcal factors involved in cellular immunity in mice did not identify known virulence factors[357]. Experiments using the co-culture methodology developed in this thesis to examine cellular responses to candidate molecules

could rapidly provide data on lymphoproliferative responses to pneumococcal molecules.

The finding that older adults have reduced pneumococcal memory T cell responses compared to younger adults and that this finding is not demonstrated in memory T cell responses to HKCA is novel. Further work could focus on patients with known risk factors for pneumococcal disease and investigate their memory T cells responses. Such groups are potential candidates for novel pneumococcal vaccination.

The focus of the experiments in the animal modelling of invasive disease described in this thesis became the role of innately produced IL-17 in disease caused by two virulent strains of pneumococcus, one highly invasive and the other minimally invasive. In the final part of chapter 5, I demonstrated that a 6B strain also demonstrated less severe disease in IL-17RA$^{-/-}$ but the factors which define this relationship between invasiveness and immune response are as yet unexplored. I have suggested that the balance between neutrophil mediated bacterial clearance and tissue damage is the underlying cause, but the biological mechanism by which this is defined is not clear. As explained in the introduction to this thesis, there is a well recognized association between serotype and invasiveness. Therefore, screening a larger collection of strains for invasiveness in a mouse model would provide further information on the role of serotype. The generation of isogenic capsular mutants and assessing the degree of invasiveness of these strains would further characterise the role of the *cps* locus in capsular behavior. The non-capsular genetic background of the pneumococcus is also likely to be important although recent work on natural capsular switch events has suggested that the situation is likely to be much more complex than clones evolved to be highly invasive or not. Croucher *et al* recently demonstrated that, while capsular switch events occurring between two organisms of the same serogroup are relatively common, between serogroup events are much less common. However, analysis of these events suggests no correlation between the invasiveness of the donor and recipient serotype (figure 9-1). Isogenic capsular switch mutants are often of greatly reduced virulence compared to the parent strain[498]. Therefore, the factors that determine the suitability of strain genetic background for capsular switch events are likely to be complex and it is likely

that further detailed work with large scale sequencing projects and artificial genetic manipulation will be needed to define them.

At the start of my project, I intended to explore the role of acquired immunity to pneumococcal disease using the IL-17RA$^{-/-}$ and IL-22$^{-/-}$ mice. However, the data led me to explore innate immunity given the finding that the principal source of IL-17A in the model were γδ lymphocytes. However, acquired immunity is clearly very important, particularly to the vital translational goal of improved vaccination strategies. Therefore, working with the strains outlined in this thesis following vaccination is an important future goal. The balance between bacterial clearance and tissue damage in pneumococcal disease is fine and therefore the impact of mucosal vaccination, particularly on the course of SRL1 infection, is not clear. Use of immunizing events, such as experimental carriage or whole cell vaccination, to elicit a Th17 response prior to SRL1 infection in wild type mice is a natural next step in investigating the role of IL-17 in disease caused by this strain. It is known that whole cell vaccination protects against invasive disease by an antibody mediated process so it may be that this is sufficient to overcome any adverse effect of IL-17 mediated excess tissue damage if invasive disease occurs but this would need to be established experimentally.

A further model to assess the impact of vaccination on would be to investigate the changes in the microbiome associated with whole cell pneumococcal vaccine. A striking feature of the data presented in chapter 6 was the marked loss of diversity in wild type animals despite the modest abundance of pneumococci in the nose. In chapter 6, I hypothesised that this loss of diversity was likely to be due to inflammation stimulated by the arrival of pneumococci in the nose and possibly also due to the direct action of pneumococci on nasal commensals – possibly through the action of bacteriocins. Chapter 7 demonstrates that SRL1 is capable of transcribing bacteriocins from the *Blp* locus *in vivo*. Investigating the microbiome of mice following inoculation of inactivated pneumococci would provide useful initial data. While RNA-Seq is likely to be challenging with the much lower bacterial density encountered in the nose, qRT-PCR could be used to assess transcription of bacteriocins in the nose. The likely lack of transformability of SRL1 may limit further assessment of

the role of bacteriocins in nasal colonization, for example through generation of knockout strains, and it may be that other pneumococcal strains capable of colonizing the nasopharynx of mice would be better suited to this work.

Finally, the genes identified in the RNA–Seq analysis of pneumococcal infection could be further investigated. It might be hypothesised that upregulation of genes involved in purine metabolism represent a general stress response but the function of the *VanZ* gene remains poorly understood. That this gene is highly conserved within the purine metabolism operon of pneumococci suggests it confers a significant survival advantage and this could be tested experimentally. In addition to investigating the role of *Blp* bacteriocins in the nose, further work could investigate novel roles for this locus in virulence. While the upregulation of *Blp* in disease could be a response to high bacterial density even in the absence of polymicrobial infection, the strong upregulation of this locus in disease suggests a possible alternative role, although again the difficulty in making SRL1 knockouts may limit investigation of this. The last gene product identified by RNA-Seq is PsaA. While this is a recognized virulence factor its role remains controversial. That it is the only established pneumococcal surface accessible virulence factor identified in this model suggests a role in high density pneumococcal infection, especially empyema. Further work could assess the role of this surface protein in similar conditions.

In conclusion, this thesis suggests further important work in pneumococcal pathogenesis and host-pathogen interactions as well as complex interactions between host, pathogen and microbiome. This work could provide important data to address important research questions in pneumococcal biology.

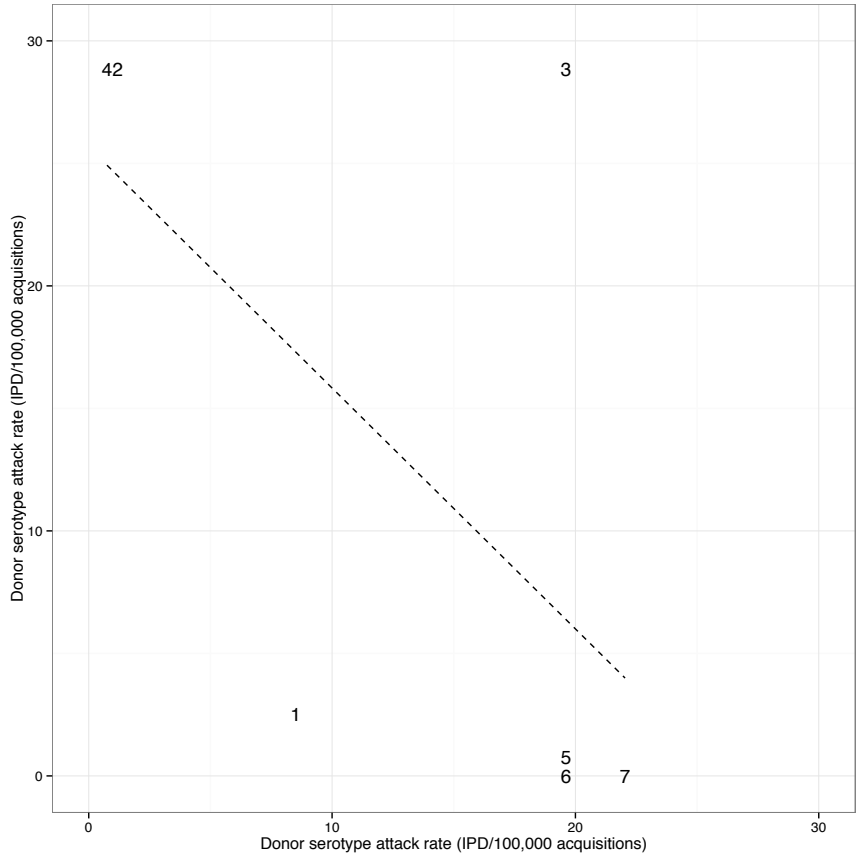

	Donor		Recipient	
	Serotype	Attack Rate	Serotype	Attack Rate
1	10A	2.52	6A	8.51
2	9V	28.85	11A	0.862
3	9V	28.85	19A	19.62
4	9V	28.85	15B.C	0.75
5	15B/C	0.75	19A	19.62
6	15A	0	19A	19.62
7	23A	0	18C	22.04

Figure 9-1. Absence of positive correlation between attack rates of donor and recipient serotypes in naturally occurring serotype switches.

A. Serotype switches occurring outside serogroup identified by Croucher et al (2015) plotted by attack rate of serotypes identified by Sleeman et al (2006). If serotype switches occur preferentially between serotypes with invasiveness then a positive correlation would be expected. Line represents linear correlation with R^2 and P value for correlation shown.

References

1 Sternberg G. Virulence of normal human saliva. *Phila Med Times* 1882; **12**: 836–9.

2 Pasteur L. Note sur la maladie nouvelle provoquee par la salive d'un enfant mort de la rage. *Bull Acad Ntl Med (Paris)* 1881; **10**: 94–103.

3 Buchanan RE, Gibbons NE. Bergey's Manual of Determinative Bacteriology, 8 edn. 1974.

4 Mandell GL, Bennett JE, Dolin R. Mandell, Douglas, and Bennett's principles and practice of infectious diseases. Churchill Livingstone, 2010.

5 Henrichsen J. Six newly recognized types of *Streptococcus pneumoniae*. *J Clin Microbiol* 1995; **33**: 2759–62.

6 Lefevre JC, Faucon G, Sicard AM, Gasc AM. DNA fingerprinting of *Streptococcus pneumoniae* strains by pulsed-field gel electrophoresis. *J Clin Microbiol* 1993; **31**: 2724–8.

7 Nesin M, Ramirez M, Tomasz A. Capsular transformation of a multidrug-resistant *Streptococcus pneumoniae* in vivo. *J Infect Dis* 1998; **177**: 707–13.

8 Enright MC, Spratt BG. A multilocus sequence typing scheme for *Streptococcus pneumoniae*: identification of clones associated with serious invasive disease. *Microbiology* 1998; **144 (Pt II)**: 3049–60.

9 Obert C, Sublett J, Kaushal D, *et al*. Identification of a Candidate *Streptococcus pneumoniae* core genome and regions of diversity correlated with invasive pneumococcal disease. *Infect Immun* 2006; **74**: 4766–77.

10 Blomberg C, Dagerhamn J, Dahlberg S, *et al*. Pattern of accessory regions and invasive disease potential in *Streptococcus pneumoniae*. *J Infect Dis* 2009; **199**: 1032–42.

11 Croucher NJ, Harris SR, Fraser C, *et al*. Rapid pneumococcal evolution in response to clinical interventions. *Science* 2011; **331**: 430–4.

12 Hansman DJ, Bullen MM. A resistant pneumococcus. *Lancet* 1967; **290**: 264–5.

13 Hackel M, Lascols C, Bouchillon S, Hilton B, Morgenstern D, Purdy J. Serotype prevalence and antibiotic resistance in *Streptococcus pneumoniae* clinical isolates among global populations. *Vaccine* 2013; **31**: 4881–7.

14 Pelton SI, Huot H, Finkelstein JA, *et al*. Emergence of 19A as virulent and multidrug resistant Pneumococcus in Massachusetts following universal immunization of infants with pneumococcal conjugate vaccine. *Pediatr Infect Dis J* 2007; **26**: 468–72.

15 Gray BM, Converse GM, Dillon HC. Epidemiologic studies of *Streptococcus pneumoniae* in infants: acquisition, carriage, and infection during the first 24 months of life. *J Infect Dis* 1980; **142**: 923–33.

16 Regev-Yochay G, Raz M, Dagan R, *et al*. Nasopharyngeal carriage of *Streptococcus pneumoniae* by adults and children in community and family settings. *Clin Infect Dis* 2004; **38**: 632–9.

17 Ekdahl K, Ahlinder I, Hansson HB, *et al*. Duration of nasopharyngeal carriage of penicillin-resistant *Streptococcus pneumoniae*: experiences from the South Swedish Pneumococcal Intervention Project. *Clin Infect Dis* 1997; **25**: 1113–7.

18 Mackenzie FM, Leach AJ, Carapetis JR, Fisher J, Morris PS. Epidemiology of nasopharyngeal carriage of respiratory bacterial pathogens in children and adults: cross-sectional surveys in a population with high rates of pneumococcal disease. *BMC Infect Dis* 2010; **10**: 304.

19 Ridda I, MacIntyre CR, Lindley R, *et al*. Lack of pneumococcal carriage in the hospitalised elderly. *Vaccine* 2010; **28**: 3902–4.

20 Gray BM, Turner ME, Dillon HC. Epidemiologic studies of *Streptococcus pneumoniae* in infants. The effects of season and age on pneumococcal acquisition and carriage in the first 24 months of life. *Am J Epidemiol* 1982; **116**: 692–703.

21 Rodrigues F, Foster D, Nicoli E, *et al*. Relationships between rhinitis symptoms, respiratory viral infections and nasopharyngeal colonization with *Streptococcus pneumoniae*, *Haemophilus influenzae* and *Staphylococcus aureus* in children attending daycare. *Pediatr Infect Dis J* 2013; **32**: 227–32.

22 Weiser J, Austrian R, Sreenivasan PK, Masure HR. Phase variation in pneumococcal opacity: relationship between colonial morphology and nasopharyngeal colonization. *Infect Immun* 1994; **62**: 2582–9.

23 Briles DE, Nahm M, Schroer K, *et al*. Antiphosphocholine antibodies found in normal mouse serum are protective against intravenous infection with type 3 *Streptococcus pneumoniae*. *J Exp Med* 1981; **153**: 694–705.

24 Kim JO, Weiser J. Association of intrastrain phase variation in quantity of capsular polysaccharide and teichoic acid with the virulence of *Streptococcus pneumoniae*. *J Infect Dis* 1998; **177**: 368–77.

25 Briles DE, Novak L, Hotomi M, van Ginkel FW, King J. Nasal colonization with *Streptococcus pneumoniae* includes subpopulations of surface and invasive pneumococci. *Infect Immun* 2005; **73**: 6945–51.

26 Burman LA, Norrby R, Trollfors B. Invasive pneumococcal infections: incidence, predisposing factors, and prognosis. *Rev Infect Dis* 1985; **7**: 133–42.

27 Paradise JL, Rockette HE, Colborn DK, *et al*. Otitis media in 2253 Pittsburgh-area infants: prevalence and risk factors during the first two years of life. *Pediatrics* 1997; **99**: 318–33.

28 Chonmaitree T, Revai K, Grady JJ, *et al*. Viral upper respiratory tract infection and otitis media complication in young children. *Clin Infect Dis* 2008; **46**: 815–23.

29 Park K, Bakaletz LO, Coticchia JM, Lim DJ. Effect of influenza A virus on ciliary activity and dye transport function in the chinchilla eustachian tube. *Ann Otol Rhinol Laryngol* 1993; **102**: 551–8.

30 Revai K, Mamidi D, Chonmaitree T. Association of nasopharyngeal bacterial colonization during upper respiratory tract infection and the development of acute otitis media. *Clin Infect Dis* 2008; **46**: e34–7.

31 Smith-Vaughan H, Byun R, Nadkarni M, *et al*. Measuring nasal bacterial load and its association with otitis media. *BMC Ear Nose Throat Disord* 2006; **6**: 10.

32 Huxley EJ, Viroslav J, Gray WR, Pierce AK. Pharyngeal aspiration in normal adults and patients with depressed consciousness. *Am J Med* 1978; **64**: 564–8.

33 Corrin B, Nicholson AG. Pathology of the Lungs. Elsevier Health Sciences, 2011.

34 2008/426/EC. *Official Journal of the European Union*: L159–46–90.

35 Health Protection Agency. Invasive pneumococcal disease incidence rate per 100,000 population by age grouping England and Wales, 1996-2005. http://www.hpa.org.uk/Topics/InfectiousDiseases/InfectionsAZ/Pneumococcal/EpidemiologicalDataPneumococcal/BackgroundEpidemiologyPneumococcal/IPDGraphs/pneumoIPDIncidenceRate/ (accessed Feb 16, 2014).

36 Talbot TR, Hartert TV, Mitchel E, *et al*. Asthma as a risk factor for invasive pneumococcal disease. *N Engl J Med* 2005; **352**: 2082–90.

37 Seminog OO, Goldacre MJ. Risk of pneumonia and pneumococcal disease in people hospitalized with diabetes mellitus: English record-linkage studies. *Diabetic Medicine* 2013; **30**: 1412–9.

38 Kyaw MH, Rose CE, Fry AM, *et al*. The influence of chronic illnesses on the incidence of invasive pneumococcal disease in adults. *J Infect Dis* 2005; **192**: 377–86.

39 Nuorti JP, Butler JC, Farley MM, *et al*. Cigarette smoking and invasive pneumococcal disease. Active Bacterial Core Surveillance Team. *N Engl J Med* 2000; **342**: 681–9.

40 Gopal V, Bisno AL. Fulminant Pneumococcal Infections in 'Normal' Asplenic Hosts. *Arch Intern Med* 1977; **137**: 1526–30.

41 Heffernan RT, Barrett NL, Gallagher KM, *et al*. Declining incidence of invasive *Streptococcus pneumoniae* infections among persons with AIDS in an era of highly active antiretroviral therapy, 1995-2000. *J Infect Dis* 2005; **191**: 2038–45.

42 Dworkin MS, Ward JW, Hanson DL, Jones JL, Kaplan JE, Adult and Adolescent Spectrum of HIV Disease Project. Pneumococcal disease among human immunodeficiency virus-infected persons: incidence, risk factors, and impact of vaccination. *Clin Infect Dis* 2001; **32**: 794–800.

43 Yin Z, Rice BD, Waight P, *et al*. Invasive pneumococcal disease among HIV-positive individuals, 2000–2009. *AIDS* 2012; **26**: 87–94.

44 Shapiro ED, Aaron NH, Wald ER, Chiponis D. Risk factors for development of bacterial meningitis among children with occult bacteremia. *J Pediatr* 1986; **109**: 15–9.

45 Wilkinson M, Bulloch B, Smith M. Prevalence of occult bacteremia in children aged 3 to 36 months presenting to the emergency department with fever in the post pneumococcal conjugate vaccine era. *Acad Emerg Med* 2009; **16**: 220–5.

46 Lee GM, Fleisher GR, Harper MB. Management of febrile children in the age of the conjugate pneumococcal vaccine: a cost-effectiveness analysis. *Pediatrics* 2001; **108**: 835–44.

47 Epstein D, Raveh D, Schlesinger Y, Rudensky B, Gottehrer NP, Yinnon AM. Adult patients with occult bacteremia discharged from the emergency department: epidemiological and clinical characteristics. *Clin Infect Dis* 2001; **32**: 559–65.

48 Austrian R, Gold J. Pneumococcal bacteremia with especial reference to bacteremic pneumococcal pneumonia. *Ann Intern Med* 1964; **60**: 759–76.

49 Inverarity D, Lamb K, Diggle M, *et al*. Death or survival from invasive pneumococcal disease in Scotland: associations with serogroups and multilocus sequence types. *J Med Microbiol* 2011; **60**: 793–802.

50 Okike IO, Ribeiro S, Ramsay ME, Heath PT, Sharland M, Ladhani SN. Trends in bacterial, mycobacterial, and fungal meningitis in England and Wales 2004-11: an observational study. *Lancet Infect Dis* 2014; **14**: 301–7.

51 Thigpen MC, Whitney CG, Messonnier NE, *et al*. Bacterial meningitis in the United States, 1998–2007. *N Engl J Med* 2011; **364**: 2016–25.

52 Austrian R. The syndrome of pneumococcal endocarditis, meningitis and rupture of the aortic valve. *Trans Am Clin Climatol Assoc* 1956; **68**: 40–50.

53 Lefort A, Mainardi JL, Selton-Suty C, Casassus P, Guillevin L, Lortholary O. *Streptococcus pneumoniae* endocarditis in adults. A multicenter study in France in the era of penicillin resistance (1991-1998). The Pneumococcal Endocarditis Study Group. *Medicine* 2000; **79**: 327–37.

54 van Ginkel FW, McGhee JR, Watt JM, Campos-Torres A, Parish LA, Briles DE. Pneumococcal carriage results in ganglioside-mediated olfactory tissue infection. *Proc Natl Acad Sci USA* 2003; **100**: 14363–7.

55 Winter AJ, Cornis SD, Osborne MP, *et al*. A role for pneumolysin but not neuraminidase in the hearing loss and cochlear damage induced by experimental pneumococcal meningitis in guinea pigs. *Infect Immun* 1997; **65**: 4411–8.

56 Nau R, Brück W. Neuronal injury in bacterial meningitis: mechanisms and implications for therapy. *Trends Neurosci* 2002; **25**: 38–45.

57 Saukkonen K, Sande S, Cioffe C, *et al*. The role of cytokines in the generation of inflammation and tissue damage in experimental gram-positive meningitis. *J Exp Med* 1990; **171**: 439–48.

58 de Gans J, van de Beek D, European dexamethasone in adulthood bacterial meningitis study investigators. Dexamethasone in adults with bacterial meningitis. *N Engl J Med* 2002; **347**: 1549–56.

59 Light RW, Girard WM, Jenkinson SG, George RB. Parapneumonic effusions. *Am J Med* 1980; **69**: 507–12.

60 Chalmers JD, Singanayagam A, Murray MP, Scally C, Fawzi A, Hill AT. Risk factors for complicated parapneumonic effusion and empyema on presentation to hospital with community-acquired pneumonia. *Thorax* 2009; **64**: 592–7.

61 Honkinen M, Lahti E, Svedström E, *et al*. Long-term recovery after parapneumonic empyema in children. *Pediatr Pulmonol* 2014; **49**: 1020–7.

62 Marimon JM, Ercibengoa M, García-Arenzana JM, Alonso M, Pérez-Trallero E. *Streptococcus pneumoniae* ocular infections, prominent role of unencapsulated isolates in conjunctivitis. *Clin Microbiol Infect* 2013; **19**: E298–305.

63 Aronin SI, Mukherjee SK, West JC, Cooney EL. Review of pneumococcal endocarditis in adults in the penicillin era. *Clin Infect Dis* 1998; **26**: 165–71.

64 Hemsley C, Eykyn SJ. Pneumococcal peritonitis in previously healthy adults: case report and review. *Clin Infect Dis* 1998; 27: 376–9.

65 Raad J, Peacock JE Jr. Septic arthritis in the adult caused by *Streptococcus pneumoniae*: A report of 4 cases and review of the literature. *Semin Arthritis Rheum* 2004; 34: 559–69.

66 Aanensen DM, Mavroidi A, Bentley SD, Reeves PR, Spratt BG. Predicted functions and linkage specificities of the products of the *Streptococcus pneumoniae* capsular biosynthetic loci. *J Bacteriol* 2007; **189**: 7856–76.

67 Bentley SD, Aanensen DM, Mavroidi A, *et al*. Genetic analysis of the capsular biosynthetic locus from all 90 pneumococcal serotypes. *PLoS Genet* 2006; **2**: e31.

68 Cartee RT, Forsee WT, Schutzbach JS, Yother J. Mechanism of type 3 capsular polysaccharide synthesis in *Streptococcus pneumoniae*. *J Biol Chem* 2000; **275**: 3907–14.

69 Mavroidi A, Aanensen DM, Godoy D, *et al*. Genetic relatedness of the *Streptococcus pneumoniae* capsular biosynthetic loci. *J Bacteriol* 2007; **189**: 7841–55.

70 Wyres KL, Lambertsen LM, Croucher NJ, *et al*. Pneumococcal capsular switching: a historical perspective. *J Infect Dis* 2013; **207**: 439–49.

71 Brueggemann AB, Pai R, Crook DW, Beall B. Vaccine escape recombinants emerge after pneumococcal vaccination in the United States. *PLoS Pathog* 2007; **3**: e168.

72 Abeyta M, Hardy GG, Yother J. Genetic alteration of capsule type but not PspA type affects accessibility of surface-bound complement and surface antigens of *Streptococcus pneumoniae*. *Infect Immun* 2003; **71**: 218–25.

73 Hyams C, Camberlein E, Cohen JM, Bax K, Brown JS. The *Streptococcus pneumoniae* capsule inhibits complement activity and neutrophil phagocytosis by multiple mechanisms. *Infect Immun* 2010; **78**: 704–15.

74 Musher DM. Infections caused by *Streptococcus pneumoniae*: clinical spectrum, pathogenesis, immunity, and treatment. *Clin Infect Dis* 1992; **14**: 801–9.

75 Winkelstein JA, Abramovitz AS, Tomasz A. Activation of C3 via the alternative complement pathway results in fixation of C3b to the pneumococcal cell wall. *J Immunol* 1980; **124**: 2502–6.

76 Nelson AL, Roche AM, Gould JM, Chim K, Ratner AJ, Weiser J. Capsule enhances pneumococcal colonization by limiting mucus-mediated clearance. *Infect Immun* 2007; **75**: 83–90.

77 Wartha F, Beiter K, Albiger B, *et al*. Capsule and D-alanylated lipoteichoic acids protect *Streptococcus pneumoniae* against neutrophil extracellular traps. *Cell Microbiol* 2007; **9**: 1162–71.

78 Austrian R. Morphologic variation in pneumococcus. II. Control of pneumococcal morphology through transformation reactions. *J Exp Med* 1953; **98**: 35–40.

79 Weiser J, Markiewicz Z, Tuomanen EI, Wani JH. Relationship between phase variation in colony morphology, intrastrain variation in cell wall physiology, and nasopharyngeal colonization by *Streptococcus pneumoniae*. *Infect Immun* 1996; **64**: 2240–5.

80 Saluja SK, Weiser J. The genetic basis of colony opacity in *Streptococcus pneumoniae*: evidence for the effect of box elements on the frequency of phenotypic variation. *Mol Microbiol* 1994; **16**: 215–27.

81 Hammerschmidt S, Wolff S, Hocke A, Rosseau S, Müller E, Rohde M. Illustration of pneumococcal polysaccharide capsule during adherence and invasion of epithelial cells. *Infect Immun* 2005; **73**: 4653–67.

82 Weiser J, Bae D, Epino H, *et al*. Changes in availability of oxygen accentuate differences in capsular polysaccharide expression by phenotypic variants and clinical isolates of *Streptococcus pneumoniae*. *Infect Immun* 2001; **69**: 5430–9.

83 Shainheit MG, Mulé M, Camilli A. The core promoter of the capsule operon of *Streptococcus pneumoniae* is necessary for colonization and invasive disease. *Infect Immun* 2014; **82**: 694–705.

84 Tweten RK. Cholesterol-dependent cytolysins, a family of versatile pore-forming toxins. *Infect Immun* 2005; **73**: 6199–209.

85 Hotze EM, Tweten RK. Membrane assembly of the cholesterol-dependent cytolysin pore complex. *Biochim Biophys Acta* 2012; **1818**: 1028–38.

86 Srivastava A, Henneke P, Visintin A, *et al*. The apoptotic response to pneumolysin is Toll-like receptor 4 dependent and protects against pneumococcal disease. *Infect Immun* 2005; **73**: 6479–87.

87 Mitchell TJ, Andrew PW, Saunders FK, Smith AN, Boulnois GJ. Complement activation and antibody binding by pneumolysin via a region of the toxin homologous to a human acute-phase protein. *Mol Microbiol* 1991; **5**: 1883–8.

88 Malley R, Henneke P, Morse SC, *et al*. Recognition of pneumolysin by Toll-like receptor 4 confers resistance to pneumococcal infection. *Proc Natl Acad Sci USA* 2003; **100**: 1966–71.

89 McNeela EA, Burke A, Neill DR, *et al*. Pneumolysin activates the NLRP3 inflammasome and promotes proinflammatory cytokines independently of TLR4. *PLoS Pathog* 2010; **6**: e1001191.

90 Witzenrath M, Pache F, Lorenz D, *et al*. The NLRP3 inflammasome is differentially activated by pneumolysin variants and contributes to host defense in pneumococcal pneumonia. *J Immunol* 2011; **187**: 434–40.

91 Feldman C, Munro NC, Jeffery PK, *et al*. Pneumolysin induces the salient histologic features of pneumococcal infection in the rat lung in vitro. *Am J Resp Cell Mol Biol* 1991; **5**: 416–23.

92 Walker JA, Allen RL, Falmagne P, Johnson MK, Boulnois GJ. Molecular cloning, characterization, and complete nucleotide sequence of the gene for pneumolysin, the sulfhydryl-activated toxin of *Streptococcus pneumoniae*. *Infect Immun* 1987; **55**: 1184–9.

93 Johnson M. Cellular location of pneumolysin. *FEMS Microbiol Lett* 1977; **2**: 243–5.

94 Price KE, Greene NG, Camilli A. Export requirements of pneumolysin in *Streptococcus pneumoniae*. *J Bacteriol* 2012; **194**: 3651–60.

95 Berry AM, Yother J, Briles DE, Hansman DJ, Paton JC. Reduced virulence of a defined pneumolysin-negative mutant of *Streptococcus pneumoniae*. *Infect Immun* 1989; **57**: 2037–42.

96 Benton KA, Everson MP, Briles DE. A pneumolysin-negative mutant of *Streptococcus pneumoniae* causes chronic bacteremia rather than acute sepsis in mice. *Infect Immun* 1995; **63**: 448–55.

97 Alexander JE, Berry AM, Paton JC, Rubins JB, Andrew PW, Mitchell TJ. Amino acid changes affecting the activity of pneumolysin alter the behaviour of pneumococci in pneumonia. *Microb Pathog* 1998; **24**: 167–74.

98 Jounblat R, Kadioglu A, Mitchell TJ, Andrew PW. Pneumococcal behavior and host responses during bronchopneumonia are affected differently by the cytolytic and complement-activating activities of pneumolysin. *Infect Immun* 2003; **71**: 1813–9.

99 Kirkham L-AS, Jefferies JMC, Kerr AR, *et al*. Identification of invasive serotype 1 pneumococcal isolates that express nonhemolytic pneumolysin. *J Clin Microbiol* 2006; **44**: 151–9.

100 Jefferies JMC, Johnston CHG, Kirkham L-AS, *et al*. Presence of nonhemolytic pneumolysin in serotypes of *Streptococcus pneumoniae* associated with disease outbreaks. *J Infect Dis* 2007; **196**: 936–44.

101 Jefferies JMC, Tocheva AS, Rubery H, *et al*. Identification of novel pneumolysin alleles from paediatric carriage isolates of *Streptococcus pneumoniae*. *J Med Microbiol* 2010; **59**: 808–14.

102 Rubins JB, Paddock AH, Charboneau D, Berry AM, Paton JC, Janoff EN. Pneumolysin in pneumococcal adherence and colonization. *Microb Pathog* 1998; **25**: 337–42.

103 van Rossum AMC, Lysenko ES, Weiser J. Host and bacterial factors contributing to the clearance of colonization by *Streptococcus pneumoniae* in a murine model. *Infect Immun* 2005; **73**: 7718–26.

104 Matthias KA, Roche AM, Standish AJ, Shchepetov M, Weiser J. Neutrophil-toxin interactions promote antigen delivery and mucosal clearance of *Streptococcus pneumoniae*. *J Immunol* 2008; **180**: 6246–54.

105 Orihuela CJ, Gao G, Francis KP, Yu J, Tuomanen EI. Tissue-specific contributions of pneumococcal virulence factors to pathogenesis. *J Infect Dis* 2004; **190**: 1661–9.

106 Kadioglu A, Taylor S, Iannelli F, Pozzi G, Mitchell TJ, Andrew PW. Upper and lower respiratory tract infection by *Streptococcus pneumoniae* is affected by pneumolysin deficiency and differences in capsule type. *Infect Immun* 2002; **70**: 2886–90.

107 Tu AH, Fulgham RL, McCrory MA, Briles DE, Szalai AJ. Pneumococcal surface protein A inhibits complement activation by *Streptococcus pneumoniae*. *Infect Immun* 1999; **67**: 4720–4.

108 Duthy TG, Ormsby RJ, Giannakis E, *et al*. The human complement regulator factor H binds pneumococcal surface protein PspC via short consensus repeats 13 to 15. *Infect Immun* 2002; **70**: 5604–11.

109 Zhang JR, Mostov KE, Lamm ME, *et al*. The polymeric immunoglobulin receptor translocates pneumococci across human nasopharyngeal epithelial cells. *Cell* 2000; **102**: 827–37.

110 Novak R, Braun JS, Charpentier E, Tuomanen E. Penicillin tolerance genes of *Streptococcus pneumoniae*: the ABC-type manganese permease complex Psa. *Mol Microbiol* 1998; **29**: 1285–96.

111 Berry AM, Paton JC. Sequence heterogeneity of PsaA, a 37-kilodalton putative adhesin essential for virulence of *Streptococcus pneumoniae*. *Infect Immun* 1996; **64**: 5255–62.

112 Proctor M, Manning PJ. Production of immunoglobulin A protease by *Streptococcus pneumoniae* from animals. *Infect Immun* 1990; **58**: 2733–7.

113 Fasching CE, Grossman T, Corthésy B, Plaut AG, Weiser J, Janoff EN. Impact of the molecular form of immunoglobulin A on functional activity in defense against *Streptococcus pneumoniae*. *Infect Immun* 2007; **75**: 1801–10.

114 Weiser J, Bae D, Fasching C, Scamurra RW, Ratner AJ, Janoff EN. Antibody-enhanced pneumococcal adherence requires IgA1 protease. *Proc Natl Acad Sci USA* 2003; **100**: 4215–20.

115 Janoff EN, Rubins JB, Fasching C, *et al*. Pneumococcal IgA1 protease subverts specific protection by human IgA1. *Mucosal Immunol* 2013; **7**: 249–56.

116 Tomasz A, Moreillon P, Pozzi G. Insertional inactivation of the major autolysin gene of *Streptococcus pneumoniae*. *J Bacteriol* 1988; **170**: 5931–4.

117 Berry AM, Lock RA, Hansman DJ, Paton JC. Contribution of autolysin to virulence of *Streptococcus pneumoniae*. *Infect Immun* 1989; **57**: 2324–30.

118 Sato K, Quartey MK, Liebeler CL, Le CT, Giebink GS. Roles of autolysin and pneumolysin in middle ear inflammation caused by a type 3 *Streptococcus pneumoniae* strain in the chinchilla otitis media model. *Infect Immun* 1996; **64**: 1140–5.

119 Heffron R. Pneumonia, with special reference to pneumococcus lobar pneumonia. New York: Commonwealth Fund Press, 1939.

120 Austrian R, Gold J. Pneumococcal Bacteremia with Especial Reference to Bacteremic Pneumococcal Pneumonia. *Ann Intern Med* 1964; **60**: 759–76.

121 Harboe ZB, Thomsen RW, Riis A, *et al*. Pneumococcal serotypes and mortality following invasive pneumococcal disease: a population-based cohort study. *PLoS Med* 2009; **6**: e1000081.

122 Weinberger DM, Harboe ZB, Sanders EAM, *et al*. Association of serotype with risk of death due to pneumococcal pneumonia: a meta-analysis. *Clin Infect Dis* 2010; **51**: 692–9.

123 Garcia-Vidal C, Ardanuy C, Tubau F, *et al*. Pneumococcal pneumonia presenting with septic shock: host- and pathogen-related factors and outcomes. *Thorax* 2010; **65**: 77–81.

124 Ahl J, Littorin N, Forsgren A, Odenholt I, Resman F, Riesbeck K. High incidence of septic shock caused by *Streptococcus pneumoniae* serotype 3 - a retrospective epidemiological study. *BMC Infect Dis* 2013; **13**: 492.

125 Pande A, Nasir S, Rueda AM, *et al*. The incidence of necrotizing changes in adults with pneumococcal pneumonia. *Clin Infect Dis* 2012; **54**: 10–6.

126 Benfield T, Skovgaard M, Schønheyder HC, *et al*. Serotype distribution in non-bacteremic pneumococcal pneumonia: association with disease severity and implications for pneumococcal conjugate vaccines. *PLoS ONE* 2013; **8**: e72743.

127 Hsieh YC, Wang C-W, Lai S-H, *et al*. Necrotizing Pneumococcal Pneumonia With Bronchopleural Fistula Among Children in Taiwan. *Pediatr Infect Dis J* 2011; **30**: 740–4.

128 McKee AJ, Ives A, Balfour Lynn IM. Increased incidence of bronchopulmonary fistulas complicating pediatric pneumonia. *Pediatr Pulmonol* 2011; **46**: 717–21.

129 Jourdain S, Drèze P-A, Verhaegen J, Van Melderen L, Smeesters PR. Carriage-associated *Streptocccus pneumoniae* serotype 1 in Brussels, Belgium. *Pediatr Infect Dis J* 2013; **32**: 86–7.

130 Trotter CL, Waight P, Andrews NJ, *et al*. Epidemiology of invasive pneumococcal disease in the pre-conjugate vaccine era: England and Wales, 1996-2006. *J Infect* 2010; **60**: 200–8.

131 Sá-Leão R, Pinto F, Aguiar S, *et al*. Analysis of invasiveness of pneumococcal serotypes and clones circulating in Portugal before widespread use of conjugate vaccines reveals heterogeneous behavior of clones expressing the same serotype. *J Clin Microbiol* 2011; **49**: 1369–75.

132 Sá-Leão R, Simões AS, Nunes S, Sousa NG, Frazão N, de Lencastre H. Identification, prevalence and population structure of non-typable *Streptococcus pneumoniae* in carriage samples isolated from preschoolers attending day-care centres. *Microbiology* 2006; **152**: 367–76.

133 Chewapreecha C, Harris SR, Croucher NJ, *et al*. Dense genomic sampling identifies highways of pneumococcal recombination. *Nature Genetics* 2014; **46**: 305–9.

134 Bewick T, Sheppard C, Greenwood S, *et al*. Serotype prevalence in adults hospitalised with pneumococcal non-invasive community-acquired pneumonia. *Thorax* 2012; **67**: 540–5.

135 Inverarity D, Diggle MA. Observations regarding historical accounts of pneumococcal diseases due to serotypes 1 and 3. *J R Coll Physicians Edinb* 2010; **40**: 354–61.

136 Harboe ZB, Benfield TL, Valentiner-Branth P, *et al*. Temporal trends in invasive pneumococcal disease and pneumococcal serotypes over 7 decades. *Clin Infect Dis* 2010; **50**: 329–37.

137 Wessels MR, Kasper DL. Antibody recognition of the type 14 pneumococcal capsule. Evidence for a conformational epitope in a neutral polysaccharide. *J Exp Med* 1989; **169**: 2121–31.

138 Roy S, Knox K, Segal S, *et al*. MBL genotype and risk of invasive pneumococcal disease: a case-control study. *Lancet* 2002; **359**: 1569–73.

139 Weinberger DM, Trzciński K, Lu Y-J, *et al*. Pneumococcal capsular polysaccharide structure predicts serotype prevalence. *PLoS Pathog* 2009; **5**: e1000476.

140 Li Y, Weinberger DM, Thompson CM. Surface Charge of *Streptococcus pneumoniae* Predicts Serotype Distribution. *Infect immun* 2013; **81**: 4519–24.

141 Yuste J, Khandavilli S, Ansari N, *et al*. The effects of PspC on complement-mediated immunity to *Streptococcus pneumoniae* vary with strain background and capsular serotype. *Infect Immun* 2010; **78**: 283–92.

142 Hirst RA, Mohammed BJ, Mitchell TJ, Andrew PW, O'Callaghan C. *Streptococcus pneumoniae*-induced inhibition of rat ependymal cilia is attenuated by antipneumolysin antibody. *Infect Immun* 2004; **72**: 6694–8.

143 Rayner CF, Jackson AD, Rutman A, *et al*. Interaction of pneumolysin-sufficient and -deficient isogenic variants of *Streptococcus pneumoniae* with human respiratory mucosa. *Infect Immun* 1995; **63**: 442–7.

144 Pittet LA, Hall-Stoodley L, Rutkowski MR, Harmsen AG. Influenza virus infection decreases tracheal mucociliary velocity and clearance of *Streptococcus pneumoniae*. *Am J Resp Cell Mol Biol* 2010; **42**: 450–60.

145 McKenzie CW, Klonoski JM, Maier T, *et al*. Enhanced response to pulmonary *Streptococcus pneumoniae* infection is associated with primary ciliary dyskinesia in mice lacking Pcdp1 and Spef2. *Cilia* 2013; **2**: 18.

146 Scharf S, Zahlten J, Szymanski K, Hippenstiel S, Suttorp N, N'Guessan PD. *Streptococcus pneumoniae* induces human ß-defensin-2 and -3 in human lung epithelium. *Exp Lung Res* 2012; **38**: 100–10.

147 Kim Y-J, Shin H-S, Lee J-H, Jung YW, Kim H-B, Ha U-H. Pneumolysin-mediated expression of ß-defensin 2 is coordinated by p38 MAP kinase-MKP1 in human airway cells. *J Microbiol* 2013; **51**: 194–9.

148 Lee H-Y, Andalibi A, Webster P, *et al*. Antimicrobial activity of innate immune molecules against *Streptococcus pneumoniae*, *Moraxella catarrhalis* and nontypeable *Haemophilus influenzae*. *BMC Infect Dis* 2004; **4**: 12.

149 Moser C, Weiner DJ, Lysenko E, Bals R, Weiser J, Wilson JM. beta-Defensin 1 contributes to pulmonary innate immunity in mice. *Infect Immun* 2002; **70**: 3068–72.

150 Ward HK, Enders JF. An analysis of the opsonic and tropic action of normal and immune sera based on experiments with the pneumococcus. *J Exp Med* 1933; **57**: 527–47.

151 Ram S, Lewis LA, Rice PA. Infections of People with Complement Deficiencies and Patients Who Have Undergone Splenectomy. *Clin Microbiol Rev* 2010; **23**: 740–80.

152 Brown JS, Hussell T, Gilliland SM, *et al*. The classical pathway is the dominant complement pathway required for innate immunity to *Streptococcus pneumoniae* infection in mice. *Proc Natl Acad Sci USA* 2002; **99**: 16969–74.

153 Melin M, Di Paolo E, Tikkanen L, *et al*. Interaction of Pneumococcal Histidine Triad Proteins with Human Complement. *Infect Immun* 2010; **78**: 2089–98.

154 Knapp S, Leemans JC, Florquin S, *et al*. Alveolar macrophages have a protective antiinflammatory role during murine pneumococcal pneumonia. *Am J Resp Crit Care Med* 2003; **167**: 171–9.

155 Hashimoto M, Tawaratsumida K, Kariya H, *et al*. Not lipoteichoic acid but lipoproteins appear to be the dominant immunobiologically active compounds in *Staphylococcus aureus*. *J Immunol* 2006; **177**: 3162–9.

156 Tomlinson G, Chimalapati S, Pollard T, *et al*. TLR-mediated inflammatory responses to *Streptococcus pneumoniae* are highly dependent on surface expression of bacterial lipoproteins. *J Immunol* 2014; **193**: 3736–45.

157 Chuang T-H, Lee J, Kline L, Mathison JC, Ulevitch RJ. Toll-like receptor 9 mediates CpG-DNA signaling. *J Leukocyte Biol* 2002; **71**: 538–44.

158 Kawai T, Adachi O, Ogawa T, Takeda K, Akira S. Unresponsiveness of MyD88-deficient mice to endotoxin. *Immunity* 1999; **11**: 115–22.

159 Hemmi H, Takeuchi O, Kawai T, *et al*. A Toll-like receptor recognizes bacterial DNA. *Nature* 2000; **408**: 740–5.

160 Bauernfeind FG, Horvath G, Stutz A, *et al*. Cutting edge: NF-kappaB activating pattern recognition and cytokine receptors license NLRP3 inflammasome activation by regulating NLRP3 expression. *J Immunol* 2009; **183**: 787–91.

161 Davis KM, Nakamura S, Weiser J. Nod2 sensing of lysozyme-digested peptidoglycan promotes macrophage recruitment and clearance of S. pneumoniae colonization in mice. *J Clin Invest* 2011; **121**: 3666–76.

162 Inohara N, Ogura Y, Fontalba A, *et al*. Host recognition of bacterial muramyl dipeptide mediated through NOD2. Implications for Crohn's disease. *J Biol Chem* 2003; **278**: 5509–12.

163 Pan Q, Mathison J, Fearns C, *et al*. MDP-induced interleukin-1beta processing requires Nod2 and CIAS1/NALP3. *J Leukocyte Biol* 2007; **82**: 177–83.

164 Schröder NWJ, Morath S, Alexander C, *et al*. Lipoteichoic acid (LTA) of *Streptococcus pneumoniae* and Staphylococcus aureus activates immune cells via Toll-like receptor (TLR)-2, lipopolysaccharide-binding protein (LBP), and CD14, whereas TLR-4 and MD-2 are not involved. *J Biol Chem* 2003; **278**: 15587–94.

165 Dessing MC, Florquin S, Paton JC, Van Der Poll T. Toll-like receptor 2 contributes to antibacterial defence against pneumolysin-deficient pneumococci. *Cell Microbiol* 2007; **10**: 237–46.

166 Albiger B, Dahlberg S, Sandgren A, *et al*. Toll-like receptor 9 acts at an early stage in host defence against pneumococcal infection. Cell Microbiol. 2007; **9**: 633–44.

167 Lee KS, Scanga CA, Bachelder EM, Chen Q, Snapper CM. TLR2 synergizes with both TLR4 and TLR9 for induction of the MyD88-dependent splenic cytokine and chemokine response to *Streptococcus pneumoniae*. *Cellular Immunology* 2007; **245**: 103–10.

168 Albiger B, Sandgren A, Katsuragi H, *et al*. Myeloid differentiation factor 88-dependent signalling controls bacterial growth during colonization and systemic pneumococcal disease in mice. *Cell Microbiol* 2005; **7**: 1603–15.

169 Bernuth von H, Picard C, Jin Z, *et al*. Pyogenic bacterial infections in humans with MyD88 deficiency. *Science* 2008; **321**: 691–6.

170 Latz E, Xiao TS, Stutz A. Activation and regulation of the inflammasomes. *Nat Rev Immunol* 2013; **13**: 397–411.

171 Pétrilli V, Papin S, Dostert C, Mayor A, Martinon F, Tschopp J. Activation of the NALP3 inflammasome is triggered by low intracellular potassium concentration. *Cell Death Differ* 2007; **14**: 1583–9.

172 Zhang Z, Clarke TB, Weiser J. Cellular effectors mediating Th17-dependent clearance of pneumococcal colonization in mice. *J Clin Invest* 2009; **119**: 1899–909.

173 Dockrell DH, Marriott HM, Prince LR, *et al*. Alveolar macrophage apoptosis contributes to pneumococcal clearance in a resolving model of pulmonary infection. *J Immunol* 2003; **171**: 5380–8.

174 Camberlein E, Cohen JM, José R, *et al*. Importance of bacterial replication and alveolar macrophage-independent clearance mechanisms during early lung infection with *Streptococcus pneumoniae*. *Infect Immun* 2015; **83**: 1181–9.

175 Shimada J, Moon SK, Lee H-Y, *et al*. Lysozyme M deficiency leads to an increased susceptibility to *Streptococcus pneumoniae*-induced otitis media. *BMC Infect Dis* 2008; **8**: 134.

176 Biggar WD, Buron S, Holmes B. Bactericidal mechanisms in rabbit alveolar macrophages: evidence against peroxidase and hydrogen peroxide bactericidal mechanisms. *Infect Immun* 1976; **14**: 6–10.

177 Dockrell DH, Marriott HM, Hellewell PG, Whyte MKB. Contrasting roles for reactive oxygen species and nitric oxide in the innate response to pulmonary infection with *Streptococcus pneumoniae*. *Vaccine* 2007; **25**: 2485–90.

178 Pericone CD, Park S, Imlay JA, Weiser J. Factors contributing to hydrogen peroxide resistance in *Streptococcus pneumoniae* include pyruvate oxidase (SpxB) and avoidance of the toxic effects of the fenton reaction. *J Bacteriol* 2003; **185**: 6815–25.

179 Kerr AR, Wei X-Q, Andrew PW, Mitchell TJ. Nitric oxide exerts distinct effects in local and systemic infections with *Streptococcus pneumoniae*. *Microb Pathog* 2004; **36**: 303–10.

180 Abraham E, Carmody A, Shenkar R, Arcaroli J. Neutrophils as early immunologic effectors in hemorrhage- or endotoxemia-induced acute lung injury. *Am J Physiol Lung Cell Mol Physiol* 2000; **279**: L1137–45.

181 Lieschke GJ, Grail D, Hodgson G, *et al*. Mice lacking granulocyte colony-stimulating factor have chronic neutropenia, granulocyte and macrophage progenitor cell deficiency, and impaired neutrophil mobilization. *Blood* 1994; **84**: 1737–46.

182 Liu F, Wu HY, Wesselschmidt R, Kornaga T, Link DC. Impaired production and increased apoptosis of neutrophils in granulocyte colony-stimulating factor receptor-deficient mice. *Immunity* 1996; **5**: 491–501.

183 Walker F, Zhang H-H, Matthews V, *et al*. IL6/sIL6R complex contributes to emergency granulopoietic responses in G-CSF- and GM-CSF-deficient mice. *Blood* 2008; **111**: 3978–85.

184 Wengner AM, Pitchford SC, Furze RC, Rankin SM. The coordinated action of G-CSF and ELR + CXC chemokines in neutrophil mobilization during acute inflammation. *Blood* 2008; **111**: 42–9.

185 Sadik CD, Kim ND, Luster AD. Neutrophils cascading their way to inflammation. *Trends Immunol* 2011; **32**: 452–60.

186 Brinkmann V. Neutrophil extracellular traps kill bacteria. *Science* 2004; **303**: 1532–5.

187 Grommes J, Soehnlein O. Contribution of neutrophils to acute lung injury. *Mol Med* 2011; **17**: 293–307.

188 Maus UA, Srivastava M, Paton JC, *et al*. Pneumolysin-induced lung injury is independent of leukocyte trafficking into the alveolar space. *J Immunol* 2004; **173**: 1307–12.

189 Hagio T, Kishikawa K, Kawabata K, *et al*. Inhibition of neutrophil elastase reduces lung injury and bacterial count in hamsters. *Pulm Pharmacol Ther* 2008; **21**: 884–91.

190 Yanagihara K, Fukuda Y, Seki M, *et al*. Effects of specific neutrophil elastase inhibitor, sivelestat sodium hydrate, in murine model of severe pneumococcal pneumonia. *Exp Lung Res* 2007; **33**: 71–80.

191 Yamada K, Yanagihara K, Araki N, *et al*. In vivo efficacy of KRP-109, a novel elastase inhibitor, in a murine model of severe pneumococcal pneumonia. *Pulm Pharmacol Ther* 2011; **24**: 660–5.

192 Hahn I, Klaus A, Janze A-K, *et al*. Cathepsin G and neutrophil elastase play critical and nonredundant roles in lung-protective immunity against *Streptococcus pneumoniae* in mice. *Infect Immun* 2011; **79**: 4893–901.

193 Stegemann S, Dahlberg S, Kröger A, *et al*. Increased susceptibility for superinfection with *streptococcus pneumoniae* during influenza virus infection is not caused by TLR7-mediated lymphopenia. *PLoS ONE* 2009; **4**: e4840.

194 Matthias KA, Roche AM, Standish AJ, Shchepetov M, Weiser J. Neutrophil-toxin interactions promote antigen delivery and mucosal clearance of *Streptococcus pneumoniae*. J Immunol. 2008; **180**: 6246–54.

195 Marks M, Burns T, Abadi M, *et al*. Influence of neutropenia on the course of serotype 8 pneumococcal pneumonia in mice. *Infect Immun* 2007; **75**: 1586–97.

196 Garvy BA, Harmsen AG. The importance of neutrophils in resistance to pneumococcal pneumonia in adult and neonatal mice. *Inflammation* 1996; **20**: 499–512.

197 Lysenko ES, Lijek RS, Brown SP, Weiser J. Within-Host Competition Drives Selection for the Capsule Virulence Determinant of *Streptococcus pneumoniae*. *Current Biology* 2010; **20**: 1222–6.

198 Holtmeier W, Chowers Y, Lumeng A, Morzycka-Wroblewska E, Kagnoff MF. The delta T cell receptor repertoire in human colon and peripheral blood is oligoclonal irrespective of V region usage. *J Clin Invest* 1995; **96**: 1108–17.

199 Morita CT, Beckman EM, Bukowski JF, *et al*. Direct presentation of nonpeptide prenyl pyrophosphate antigens to human γδ T cells. *Immunity* 1995; **3**: 495–507.

200 Augustin A, Kubo RT, Sim GK. Resident pulmonary lymphocytes expressing the gamma/delta T-cell receptor. *Nature* 1989; **340**: 239–41.

201 Lalor SJ, Dungan LS, Sutton CE, Basdeo SA, Fletcher JM, Mills KHG. Caspase-1-processed cytokines IL-1beta and IL-18 promote IL-17 production by gammadelta and CD4 T cells that mediate autoimmunity. *J Immunol* 2011; **186**: 5738–48.

202 Jensen KDC, Su X, Shin S, *et al*. Thymic Selection Determines γδ T Cell Effector Fate: Antigen-Naive Cells Make Interleukin-17 and Antigen-Experienced Cells Make Interferon γ. *Immunity* 2008; **29**: 90–100.

203 Caccamo N, La Mendola C, Orlando V, *et al*. Differentiation, phenotype, and function of interleukin-17-producing human Vγ9Vδ2 T cells. *Blood* 2011; **118**: 129–38.

204 Blink SE, Miller SD. The contribution of gammadelta T cells to the pathogenesis of EAE and MS. *Curr Mol Med* 2009; **9**: 15–22.

205 Lockhart E, Green AM, Flynn JL. IL-17 production is dominated by gammadelta T cells rather than CD4 T cells during *Mycobacterium tuberculosis* infection. *J Immunol* 2006; **177**: 4662–9.

206 Cheng P, Liu T, Zhou W-Y, *et al*. Role of gamma-delta T cells in host response against *Staphylococcus aureus*-induced pneumonia. *BMC Immunol* 2012; **13**: 38.

207 Hiromatsu K, Yoshikai Y, Matsuzaki G, *et al*. A protective role of gamma/delta T cells in primary infection with *Listeria monocytogenes* in mice. *J Exp Med* 1992; **175**: 49–56.

208 Moore TA, Moore BB, Newstead MW, Standiford TJ. Gamma delta-T cells are critical for survival and early proinflammatory cytokine gene expression during murine *Klebsiella pneumonia*. *J Immunol* 2000; **165**: 2643–50.

209 Exley M, Garcia J, Balk SP, Porcelli S. Requirements for CD1d recognition by human invariant Vα24+ CD4-CD8- T cells. *J Exp Med* 1997; **186**: 109–20.

210 Arora P, Baena A, Yu KOA, *et al*. A single subset of dendritic cells controls the cytokine bias of natural killer T cell responses to diverse glycolipid antigens. *Immunity* 2014; **40**: 105–16.

211 Kinjo Y, Illarionov P, Vela JL, *et al*. Invariant natural killer T cells recognize glycolipids from pathogenic Gram-positive bacteria. *Nat Immunol* 2011; **12**: 966–74.

212 Joyee AG, Qiu H, Wang S, Fan Y, Bilenki L, Yang X. Distinct NKT cell subsets are induced by different Chlamydia species leading to differential adaptive immunity and host resistance to the infections. *J Immunol*. 2007; **178**: 1048–58.

213 Nieuwenhuis EES, Matsumoto T, Exley M, *et al*. CD1d-dependent macrophage-mediated clearance of *Pseudomonas aeruginosa* from lung. *Nat Med* 2002; **8**: 588–93.

214 Rothchild AC, Jayaraman P, Nunes-Alves C, Behar SM. iNKT cell production of GM-CSF controls *Mycobacterium tuberculosis*. PLoS Pathog. 2014; **10**: e1003805.

215 Imai Y, Yasuda K, Sakaguchi Y, *et al*. Skin-specific expression of IL-33 activates group 2 innate lymphoid cells and elicits atopic dermatitis-like inflammation in mice. *Proc Natl Acad Sci USA* 2013; **110**: 13921–6.

216 Spits H, Artis D, Colonna M, *et al*. Innate lymphoid cells—a proposal for uniform nomenclature. *Nat Rev Immunol* 2013; **13**: 145–9.

217 Mear JB, Gosset P, Kipnis E, *et al*. Candida albicans airway exposure primes the lung innate immune response against *Pseudomonas aeruginosa* infection through innate lymphoid cell recruitment and interleukin-22-associated mucosal response. *Infect Immun* 2014; **82**: 306–15.

218 Xu X, Weiss ID, Zhang HH, *et al*. Conventional NK cells can produce IL-22 and promote host defense in *Klebsiella pneumoniae* pneumonia. *J Immunol* 2014; **192**: 1778–86.

219 Kirby AC, Newton DJ, Carding SR, Kaye PM. Evidence for the involvement of lung-specific gammadelta T cell subsets in local responses to *Streptococcus pneumoniae* infection. *Eur J Immunol* 2007; **37**: 3404–13.

220 Nakasone C, Yamamoto N, Nakamatsu M, *et al*. Accumulation of gamma/delta T cells in the lungs and their roles in neutrophil-mediated host defense against pneumococcal infection. *Microbes Infect* 2007; **9**: 251–8.

221 Li W, Moltedo B, Moran TM. Type I interferon induction during influenza virus infection increases susceptibility to secondary *Streptococcus pneumoniae* infection by negative regulation of γδ T cells. *J Virol* 2012; **86**: 12304–12.

222 Kirby AC, Newton DJ, Carding SR, Kaye PM. Pulmonary dendritic cells and alveolar macrophages are regulated by gammadelta T cells during the resolution of *S. pneumoniae*-induced inflammation. *J Pathol* 2007; **212**: 29–37.

223 Kawakami K, Yamamoto N, Kinjo Y, *et al*. Critical role of Vα14+ natural killer T cells in the innate phase of host protection against *Streptococcus pneumoniae* infection. *Eur J Immunol* 2003; **33**: 3322–30.

224 Ivanov S, Fontaine J, Paget C, *et al*. Key role for respiratory CD103+ dendritic cells, IFN-γ and IL-17 in protection against *Streptococcus pneumoniae* infection in response to α-galactosylceramide. *J Infect Dis* 2012; **206**: 723–34.

225 Van Maele L, Carnoy C, Cayet D, *et al*. Activation of type 3 innate lymphoid cells and interleukin 22 secretion in the lungs during *Streptococcus pneumoniae* infection. *J Infect Dis* 2014; **210**: 493–503.

226 Jameson JM, Cauvi G, Witherden DA, Havran WL. A keratinocyte-responsive gamma delta TCR is necessary for dendritic epidermal T cell activation by damaged keratinocytes and maintenance in the epidermis. *J Immunol* 2004; **172**: 3573–9.

227 Avery OT, Morgan HJ. Immunological reactions of the isolated carbohydrate and protein of pneumococcus. *J Exp Med* 1925; **42**: 347–53.

228 Shapiro ED, Austrian R, Berg AT, *et al*. The protective efficacy of polyvalent pneumococcal polysaccharide vaccine. *N Engl J Med* 1991; **325**: 1453–60.

229 Quiambao B, Nohynek H, Käyhty H, *et al*. Maternal immunization with pneumococcal polysaccharide vaccine in the Philippines. *Vaccine* 2003; **21**: 3451–4.

230 Mond JJ, Lees A, Snapper CM. T cell-independent antigens type 2. *Annu Rev Immunol* 1995; **13**: 655–92.

231 Barrett DJ, Ayoub EM. IgG2 subclass restriction of antibody to pneumococcal polysaccharides. *Clin Exp Immunol* 1986; **63**: 127–34.

232 ZHANG J, Liu YJ, MacLennan IC, Gray D, Lane PJ. B cell memory to thymus-independent antigens type 1 and type 2: the role of lipopolysaccharide in B memory induction. *Eur J Immunol* 1988; **18**: 1417–24.

233 Koskela M, Leinonen M, Häivä VM, Timonen M, Mäkelä PH. First and second dose antibody responses to pneumococcal polysaccharide vaccine in infants. *Pediatr Infect Dis* 1986; **5**: 45–50.

234 Simell B, Lahdenkari M, Reunanen A, Käyhty H, Väkeväinen M. Effects of ageing and gender on naturally acquired antibodies to pneumococcal capsular polysaccharides and virulence-associated proteins. *Clin Vaccine Immunol* 2008; **15**: 1391–7.

235 Kobrynski LJ, Sousa AO, Nahmias AJ, Lee FK. Cutting edge: antibody production to pneumococcal polysaccharides requires CD1 molecules and CD8+ T cells. *J Immunol* 2005; **174**: 1787–90.

236 Moens L, Jeurissen A, Nierkens S, *et al*. Generation of antibody responses to pneumococcal capsular polysaccharides is independent of CD1 expression in mice. *Infect Immun* 2009; **77**: 1976–80.

237 Mongini PK, Stein KE, Paul WE. T cell regulation of IgG subclass antibody production in response to T-independent antigens. *J Exp Med* 1981; **153**: 1–12.

238 Rodriguez-Barradas MC, Musher DM, Lahart C, *et al*. Antibody to capsular polysaccharides of *Streptococcus pneumoniae* after vaccination of human immunodeficiency virus-infected subjects with 23-valent pneumococcal vaccine. *J Infect Dis* 1992; **165**: 553–6.

239 Kalka-Moll WM, Tzianabos AO, Bryant PW, Niemeyer M, Ploegh HL, Kasper DL. Zwitterionic polysaccharides stimulate T cells by MHC class II-dependent interactions. *J Immunol* 2002; **169**: 6149–53.

240 Ritchie ND, Mitchell TJ, Evans TJ. What is different about serotype 1 pneumococci? *Future Microbiol* 2012; **7**: 33–46.

241 Balmer P, Borrow R, Findlow J, *et al*. Age-stratified prevalences of pneumococcal-serotype-specific immunoglobulin G in England and their relationship to the serotype-specific incidence of invasive pneumococcal disease prior to the introduction of the pneumococcal 7-valent conjugate vaccine. *Clin Vaccine Immunol* 2007; **14**: 1442–50.

242 Malley R, Stack AM, Ferretti ML, Thompson CM, Saladino RA. Anticapsular polysaccharide antibodies and nasopharyngeal colonization with *Streptococcus pneumoniae* in infant rats. *J Infect Dis* 1998; **178**: 878–82.

243 Lipsitch M, Whitney CG, Zell E, Kaijalainen T, Dagan R, Malley R. Are anticapsular antibodies the primary mechanism of protection against invasive pneumococcal disease? *PLoS Med* 2005; **2**: e15.

244 Granat SM, Ollgren J, Herva E, Mia Z, Auranen K, Mäkelä PH. Epidemiological evidence for serotype – independent acquired immunity to pneumococcal carriage. *J Infect Dis* 2009; **200**: 99–106.

245 Black S, Shinefield H, Fireman B, *et al*. Efficacy, safety and immunogenicity of heptavalent pneumococcal conjugate vaccine in children. Northern California Kaiser Permanente Vaccine Study Center Group. *Pediatr Infect Dis J* 2000; **19**: 187–95.

246 Malley R, Trzciński K, Srivastava A, Thompson CM, Anderson PW, Lipsitch M. CD4+ T cells mediate antibody-independent acquired immunity to pneumococcal colonization. *Proc Natl Acad Sci USA* 2005; **102**: 4848–53.

247 Ogunniyi AD, Folland RL, Briles DE, Hollingshead SK, Paton JC. Immunization of mice with combinations of pneumococcal virulence proteins elicits enhanced protection against challenge with *Streptococcus pneumoniae*. *Infect Immun* 2000; **68**: 3028–33.

248 Hollingshead SK, Baril L, Ferro S, *et al*. Pneumococcal surface protein A (PspA) family distribution among clinical isolates from adults over 50 years of age collected in seven countries. *J Med Microbiol* 2006; **55**: 215–21.

249 McCool TL, Cate TR, Moy G, Weiser J. The immune response to pneumococcal proteins during experimental human carriage. *J Exp Med* 2002; **195**: 359–65.

250 McCool TL, Weiser J. Limited role of antibody in clearance of *Streptococcus pneumoniae* in a murine model of colonization. Infect Immun. 2004; **72**: 5807–13.

251 Trzcinski K, Thompson C, Malley R, Lipsitch M. Antibodies to conserved pneumococcal antigens correlate with, but are not required for, protection against pneumococcal colonization induced by prior exposure in a mouse model. *Infect Immun* 2005; **73**: 7043–6.

252 Lebon A, Verkaik NJ, Labout JAM, *et al*. Natural antibodies against several pneumococcal virulence proteins in children during the pre-pneumococcal-vaccine era: the generation R study. *Infect Immun* 2011; **79**: 1680–7.

253 Prevaes SMPJ, van Wamel WJB, de Vogel CP, *et al*. Nasopharyngeal colonization elicits antibody responses to staphylococcal and pneumococcal proteins that are not associated with a reduced risk of subsequent carriage. *Infect Immun* 2012; **80**: 2186–93.

254 Pichichero ME, Kaur R, Casey JR, Xu Q, Almudevar A, Ochs M. Antibody response to *Streptococcus pneumoniae* proteins PhtD, LytB, PcpA, PhtE and Ply after nasopharyngeal colonization and acute otitis media in children. *Hum Vaccin Immunother* 2012; **8**: 799–805.

255 Paton JC, Lock RA, Hansman DJ. Effect of immunization with pneumolysin on survival time of mice challenged with *Streptococcus pneumoniae*. *Infect Immun* 1983; **40**: 548–52.

256 Briles DE, Hollingshead SK, Paton JC, *et al*. Immunizations with pneumococcal surface protein A and pneumolysin are protective against pneumonia in a murine model of pulmonary infection with *Streptococcus pneumoniae*. *J Infect Dis* 2003; **188**: 339–48.

257 Salha D, Szeto J, Myers L, *et al*. Neutralizing antibodies elicited by a novel detoxified pneumolysin derivative, PlyD1, provide protection against both pneumococcal infection and lung injury. *Infect Immun* 2012; **80**: 2212–20.

258 Holmlund E, Quiambao B, Ollgren J, Nohynek H, Käyhty H. Development of natural antibodies to pneumococcal surface protein A, pneumococcal surface adhesin A and pneumolysin in Filipino pregnant women and their infants in relation to pneumococcal carriage. *Vaccine* 2006; **24**: 57–65.

259 Francis JP, Richmond PC, Pomat WS, *et al*. Maternal antibodies to pneumolysin but not to pneumococcal surface protein A delay early pneumococcal carriage in high-risk Papua New Guinean infants. *Clin Vaccine Immunol* 2009; **16**: 1633–8.

260 Zhang Q, Bernatoniene J, Bagrade L, *et al*. Serum and mucosal antibody responses to pneumococcal protein antigens in children: relationships with carriage status. *Eur J Immunol* 2006; **36**: 46–57.

261 Zhou Z-H, Zhang Y, Hu Y-F, Wahl LM, Cisar JO, Notkins AL. The broad antibacterial activity of the natural antibody repertoire is due to polyreactive antibodies. *Cell Host Microbe* 2007; **1**: 51–61.

262 Jones HE, Taylor PR, McGreal E, Zamze S, Wong SYC. The contribution of naturally occurring IgM antibodies, IgM cross-reactivity and complement dependency in murine humoral responses to pneumococcal capsular polysaccharides. *Vaccine* 2009; **27**: 5806–15.

263 Haas KM, Poe JC, Steeber DA, Tedder TF. B-1a and B-1b cells exhibit distinct developmental requirements and have unique functional roles in innate and adaptive immunity to S. pneumoniae. *Immunity* 2005; **23**: 7–18.

264 Rothstein TL, Griffin DO, Holodick NE, Quach TD, Kaku H. Human B-1 cells take the stage. *Ann N Y Acad Sci* 2013; **1285**: 97–114.

265 Lu Y-J, Gross J, Bogaert D, *et al*. Interleukin-17A mediates acquired immunity to pneumococcal colonization. *PLoS Pathog* 2008; **4**: e1000159.

266 Basset A, Thompson CM, Hollingshead SK, *et al*. Antibody-independent, CD4+ T-cell-dependent protection against pneumococcal colonization elicited by intranasal immunization with purified pneumococcal proteins. *Infect Immun* 2007; **75**: 5460–4.

267 Roche AM, King SJ, Weiser J. Live attenuated *Streptococcus pneumoniae* strains induce serotype-independent mucosal and systemic protection in mice. *Infect Immun* 2007; **75**: 2469–75.

268 Lu Y-J, Forte S, Thompson CM, Anderson PW, Malley R. Protection against pneumococcal colonization and fatal pneumonia by a trivalent conjugate of a fusion protein with the cell wall polysaccharide. *Infect Immun* 2009; **77**: 2076–83.

269 Rouvier E, Luciani MF, Mattéi MG, Denizot F, Golstein P. CTLA-8, cloned from an activated T cell, bearing AU-rich messenger RNA instability sequences, and homologous to a herpesvirus saimiri gene. *J Immunol* 1993; **150**: 5445–56.

270 Hymowitz SG, Filvaroff EH, Yin JP, *et al*. IL-17s adopt a cystine knot fold: structure and activity of a novel cytokine, IL-17F, and implications for receptor binding. *EMBO J* 2001; **20**: 5332–41.

271 Yao Z, Painter SL, Fanslow WC, *et al*. Human IL-17: a novel cytokine derived from T cells. *J Immunol* 1995; **155**: 5483–6.

272 Harrington LE, Hatton RD, Mangan PR, *et al*. Interleukin 17-producing CD4+ effector T cells develop via a lineage distinct from the T helper type 1 and 2 lineages. *Nat Immunol* 2005; **6**: 1123–32.

273 Park H, Li Z, Yang XO, *et al*. A distinct lineage of CD4 T cells regulates tissue inflammation by producing interleukin 17. *Nat Immunol* 2005; **6**: 1133–41.

274 Xie MH, Aggarwal S, Ho WH, *et al*. Interleukin (IL)-22, a novel human cytokine that signals through the interferon receptor-related proteins CRF2-4 and IL-22R. *J Biol Chem* 2000; **275**: 31335–9.

275 Wolk K, Kunz S, Asadullah K, Sabat R. Cutting edge: immune cells as sources and targets of the IL-10 family members? *J Immunol* 2002; **168**: 5397–402.

276 Wolk K, Kunz S, Witte E, Friedrich M, Asadullah K, Sabat R. IL-22 increases the innate immunity of tissues. *Immunity* 2004; **21**: 241–54.

277 Chang SH, Dong C. A novel heterodimeric cytokine consisting of IL-17 and IL-17F regulates inflammatory responses. *Cell Res* 2007; **17**: 435–40.

278 Toy D, Kugler D, Wolfson M, *et al*. Cutting edge: interleukin 17 signals through a heteromeric receptor complex. *J Immunol* 2006; **177**: 36–9.

279 Chang SH, Park H, Dong C. Act1 adaptor protein is an immediate and essential signaling component of interleukin-17 receptor. *J Biol Chem* 2006; **281**: 35603–7.

280 Schwandner R, Yamaguchi K, Cao Z. Requirement of tumor necrosis factor receptor-associated factor (TRAF)6 in interleukin 17 signal transduction. *J Exp Med* 2000; **191**: 1233–40.

281 Ge D, You Z. Expression of interleukin-17RC protein in normal human tissues. *Int Arch Med* 2008; **1**: 19.

282 Laan M, Cui ZH, Hoshino H, *et al*. Neutrophil recruitment by human IL-17 via C-X-C chemokine release in the airways. *J Immunol* 1999; **162**: 2347–52.

283 Jovanovic DV, Di Battista JA, Martel-Pelletier J, *et al*. IL-17 stimulates the production and expression of proinflammatory cytokines, IL-beta and TNF-alpha, by human macrophages. *J Immunol* 1998; **160**: 3513–21.

284 Jones CE, Chan K. Interleukin-17 stimulates the expression of interleukin-8, growth-related oncogene-alpha, and granulocyte-colony-stimulating factor by human airway epithelial cells. *Am J Resp Cell Mol Biol* 2002; **26**: 748–53.

285 Kao C-Y, Chen Y, Thai P, Wachi S. IL-17 markedly up-regulates β-defensin-2 expression in human airway epithelium via JAK and NF-κB signaling pathways. 2004; **173**: 3482–91.

286 Chabaud M, Garnero P, Dayer JM, Guerne PA, Fossiez F, Miossec P. Contribution of interleukin 17 to synovium matrix destruction in rheumatoid arthritis. *Cytokine* 2000; **12**: 1092–9.

287 Miyamoto M, Prause O, Sjöstrand M, Laan M, Lötvall J, Lindén A. Endogenous IL-17 as a mediator of neutrophil recruitment caused by endotoxin exposure in mouse airways. *J Immunol* 2003; **170**: 4665–72.

288 Ivanov II, McKenzie BS, Zhou L, *et al*. The orphan nuclear receptor RORgammat directs the differentiation program of proinflammatory IL-17+ T helper cells. *Cell* 2006; **126**: 1121–33.

289 Langrish CL, Chen Y, Blumenschein WM, *et al*. IL-23 drives a pathogenic T cell population that induces autoimmune inflammation. *J Exp Med* 2005; **201**: 233–40.

290 Mangan PR, Harrington LE, O'Quinn DB, *et al*. Transforming growth factor-beta induces development of the T(H)17 lineage. *Nature* 2006; **441**: 231–4.

291 Annunziato F, Cosmi L, Santarlasci V, *et al*. Phenotypic and functional features of human Th17 cells. *J Exp Med* 2007; **204**: 1849–61.

292 Starner TD, Barker CK, Jia HP, Kang Y, Paul B McCray J. CCL20 Is an inducible product of human airway epithelia with innate immune properties. *Am J Resp Cell Mol Biol* 2012; **29**: 627–33.

293 Reibman J, Hsu Y, Chen LC, Bleck B, Gordon T. Airway epithelial cells release MIP-3α/CCL20 in response to cytokines and ambient particulate matter. *Am J Resp Cell Mol Biol* 2003; **28**: 648–54.

294 Yamazaki T, Yang XO, Chung Y, *et al*. CCR6 regulates the migration of inflammatory and regulatory T cells. *J Immunol* 2008; **181**: 8391–401.

295 Buonocore S, Ahern PP, Uhlig HH, *et al*. Innate lymphoid cells drive interleukin-23-dependent innate intestinal pathology. *Nature* 2010; **464**: 1371–5.

296 Ferretti S, Bonneau O, Dubois GR, Jones CE, Trifilieff A. IL-17, produced by lymphocytes and neutrophils, is necessary for lipopolysaccharide-induced airway neutrophilia: IL-15 as a possible trigger. *J Immunol* 2003; **170**: 2106–12.

297 Song C, Luo L, Lei Z, *et al*. IL-17-producing alveolar macrophages mediate allergic lung inflammation related to asthma. *J Immunol* 2008; **181**: 6117–24.

298 Martin B, Hirota K, Cua DJ, Stockinger B, Veldhoen M. Interleukin-17-producing gammadelta T cells selectively expand in response to pathogen products and environmental signals. *Immunity* 2009; **31**: 321–30.

299 Tachiiri A, Imamura R, Wang Y, Fukui M, Umemura M, Suda T. Genomic structure and inducible expression of the IL-22 receptor alpha chain in mice. *Genes Immun* 2003; **4**: 153–9.

300 Lejeune D, Dumoutier L, Constantinescu S, Kruijer W, Schuringa JJ, Renauld J-C. Interleukin-22 (IL-22) activates the JAK/STAT, ERK, JNK, and p38 MAP kinase pathways in a rat hepatoma cell line. Pathways that are shared with and distinct from IL-10. *J Biol Chem* 2002; **277**: 33676–82.

301 Dhiman R, Indramohan M, Barnes PF, *et al*. IL-22 produced by human NK cells inhibits growth of Mycobacterium tuberculosis by enhancing phagolysosomal fusion. *J Immunol* 2009; **183**: 6639–45.

302 Wolk K, Witte E, Wallace E, *et al*. IL-22 regulates the expression of genes responsible for antimicrobial defense, cellular differentiation, and mobility in keratinocytes: a potential role in psoriasis. *Eur J Immunol* 2006; **36**: 1309–23.

303 Guilloteau K, Paris I, Pedretti N, *et al*. Skin Inflammation Induced by the Synergistic Action of IL-17A, IL-22, Oncostatin M, IL-1{alpha}, and TNF-{alpha} Recapitulates Some Features of Psoriasis. *J Immunol* 2010; **184**: 5263–70.

304 Sonnenberg GF, Nair MG, Kirn TJ, Zaph C, Fouser LA, Artis D. Pathological versus protective functions of IL-22 in airway inflammation are regulated by IL-17A. *J Exp Med* 2010; **207**: 1293–305.

305 Pickert G, Neufert C, Leppkes M, *et al*. STAT3 links IL-22 signaling in intestinal epithelial cells to mucosal wound healing. *J Exp Med* 2009; **206**: 1465–72.

306 Zindl CL, Lai J-F, Lee YK, *et al*. IL-22-producing neutrophils contribute to antimicrobial defense and restitution of colonic epithelial integrity during colitis. *Proc Natl Acad Sci USA* 2013; **110**: 12768–73.

307 Eyerich S, Eyerich K, Pennino D, *et al*. Th22 cells represent a distinct human T cell subset involved in epidermal immunity and remodeling. *J Clin Invest* 2009; **119**: 3573–85.

308 Rutz S, Eidenschenk C, Ouyang W. IL-22, not simply a Th17 cytokine. *Immunol Rev* 2013; **252**: 116–32.

309 Liang SC, Tan X-Y, Luxenberg DP, *et al*. Interleukin (IL)-22 and IL-17 are coexpressed by Th17 cells and cooperatively enhance expression of antimicrobial peptides. *J Exp Med* 2006; **203**: 2271–9.

310 Volpe E, Touzot M, Servant N, *et al*. Multiparametric analysis of cytokine-driven human Th17 differentiation reveals a differential regulation of IL-17 and IL-22 production. *Blood* 2009; **114**: 3610–4.

311 Ness-Schwickerath KJ, Jin C, Morita CT. Cytokine requirements for the differentiation and expansion of IL-17A- and IL-22-producing human Vγ2Vδ2 T cells. *J Immunol* 2010; **184**: 7268–80.

312 Goto M, Murakawa M, Kadoshima-Yamaoka K, *et al*. Murine NKT cells produce Th17 cytokine interleukin-22. *Cellular Immunology* 2009; **254**: 81–4.

313 Satoh Takayama N, Lesjean Pottier S, Sawa S, Vosshenrich CAJ, Eberl G, Di Santo JP. Lymphotoxin-ß receptor-independent development of intestinal IL-22-producing NKp46+ innate lymphoid cells. *Eur J Immunol* 2011; **41**: 780–6.

314 Hansson M, Silverpil E, Lindén A, Glader P. Interleukin-22 produced by alveolar macrophages during activation of the innate immune response. *Inflamm Res* 2013; **62**: 561–9.

315 Ramirez JM, Brembilla NC, Sorg O, *et al*. Activation of the aryl hydrocarbon receptor reveals distinct requirements for IL-22 and IL-17 production by human T helper cells. *Eur J Immunol* 2010; **40**: 2450–9.

316 Komiyama Y, Nakae S, Matsuki T, *et al*. IL-17 plays an important role in the development of experimental autoimmune encephalomyelitis. *J Immunol* 2006; **177**: 566–73.

317 Lubberts E, Joosten LA, Oppers B, *et al*. IL-1-independent role of IL-17 in synovial inflammation and joint destruction during collagen-induced arthritis. *J Immunol* 2001; **167**: 1004–13.

318 Kobayashi T, Okamoto S, Hisamatsu T, *et al*. IL23 differentially regulates the Th1/Th17 balance in ulcerative colitis and Crohn's disease. *Gut* 2008; **57**: 1682–9.

319 Zheng Y, Danilenko DM, Valdez P, *et al*. Interleukin-22, a T(H)17 cytokine, mediates IL-23-induced dermal inflammation and acanthosis. *Nature* 2007; **445**: 648–51.

320 Tse MT. IL-17 antibodies gain momentum. Nat Rev Drug Discov. 2013; **12**: 815–6.

321 Wang Y-H, Wills-Karp M. The potential role of interleukin-17 in severe asthma. *Curr Allergy Asthma Rep* 2011; **11**: 388–94.

322 Liang M, Wang J, Chu H, *et al*. Interleukin-22 inhibits bleomycin-induced pulmonary fibrosis. *Mediators Inflamm* 2013; **2013**: 209179–11.

323 Ye P, Garvey PB, Zhang P, *et al*. Interleukin-17 and lung host defense against Klebsiella pneumoniae infection. *Am J Resp Cell Mol Biol* 2001; **25**: 335–40.

324 Liu J, Feng Y, Yang K, *et al*. Early production of IL-17 protects against acute pulmonary *Pseudomonas aeruginosa* infection in mice. *FEMS Immunol Med Microbiol* 2011; **61**: 179–88.

325 Umemura M, Yahagi A, Hamada S, *et al*. IL-17-mediated regulation of innate and acquired immune response against pulmonary *Mycobacterium bovis* bacille Calmette-Guérin infection. *J Immunol* 2007; **178**: 3786–96.

326 Garraud K, Cleret A, Mathieu J, *et al*. Differential role of the interleukin-17 axis and neutrophils in resolution of inhalational anthrax. *Infect Immun* 2012; **80**: 131–42.

327 Wu Q, Martin RJ, Rino JG, Breed R, Torres RM, Chu HW. IL-23-dependent IL-17 production is essential in neutrophil recruitment and activity in mouse lung defense against respiratory *Mycoplasma pneumoniae* infection. *Microbes Infect* 2007; **9**: 78–86.

328 Conti HR, Shen F, Nayyar N, *et al*. Th17 cells and IL-17 receptor signaling are essential for mucosal host defense against oral candidiasis. *J Exp Med* 2009; **206**: 299–311.

329 Yu JJ, Ruddy MJ, Wong GC, *et al*. An essential role for IL-17 in preventing pathogen-initiated bone destruction: recruitment of neutrophils to inflamed bone requires IL-17 receptor-dependent signals. *Blood* 2007; **109**: 3794–802.

330 Symonds EL, Riedel CU, O'Mahony D, Lapthorne S, O'Mahony L, Shanahan F. Involvement of T helper type 17 and regulatory T cell activity in *Citrobacter rodentium* invasion and inflammatory damage. *Clin Exp Immunol* 2009; **157**: 148–54.

331 Mayuzumi H, Inagaki-Ohara K, Uyttenhove C, Okamoto Y, Matsuzaki G. Interleukin-17A is required to suppress invasion of *Salmonella enterica* serovar Typhimurium to enteric mucosa. *Immunology* 2010; **131**: 377–85.

332 Ishigame H, Kakuta S, Nagai T, *et al*. Differential roles of interleukin-17A and -17F in host defense against mucoepithelial bacterial infection and allergic responses. *Immunity* 2009; **30**: 108–19.

333 Cho JS, Pietras EM, Garcia NC, *et al*. IL-17 is essential for host defense against cutaneous *Staphylococcus aureus* infection in mice. *J Clin Invest* 2010; **120**: 1762–73.

334 Chung DR, Kasper DL, Panzo RJ, *et al*. CD4+ T cells mediate abscess formation in intra-abdominal sepsis by an IL-17-dependent mechanism. *J Immunol* 2003; **170**: 1958–63.

335 Flierl MA, Rittirsch D, Gao H, *et al*. Adverse functions of IL-17A in experimental sepsis. *FASEB J* 2008; **22**: 2198–205.

336 Shiomi S, Toriie A, Imamura S, *et al*. IL-17 is involved in *Helicobacter pylori*-induced gastric inflammatory responses in a mouse model. *Helicobacter* 2008; **13**: 518–24.

337 Crowe CR, Chen K, Pociask DA, *et al*. Critical role of IL-17RA in immunopathology of influenza infection. *J Immunol* 2009; **183**: 5301–10.

338 Maroof A, Yorgensen YM, Li Y, Evans JT. Intranasal vaccination promotes detrimental Th17-mediated immunity against influenza infection. *PLoS Pathog* 2014; **10**: e1003875.

339 Aujla SJ, Chan YR, Zheng M, *et al*. IL-22 mediates mucosal host defense against Gram-negative bacterial pneumonia. *Nat Med* 2008; **14**: 275–81.

340 Schulz SM, Köhler G, Schütze N, *et al*. Protective immunity to systemic infection with attenuated *Salmonella enterica* serovar enteritidis in the absence of IL-12 is associated with IL-23-dependent IL-22, but not IL-17. *J Immunol* 2008; **181**: 7891–901.

341 Zheng Y, Valdez PA, Danilenko DM, *et al*. Interleukin-22 mediates early host defense against attaching and effacing bacterial pathogens. *Nat Med* 2008; **14**: 282–9.

342 Simonian PL, Wehrmann F, Roark CL, Born WK, O'Brien RL, Fontenot AP. γδ T cells protect against lung fibrosis via IL-22. *J Exp Med* 2010; **207**: 2239–53.

343 Sugimoto K, Ogawa A, Mizoguchi E, *et al*. IL-22 ameliorates intestinal inflammation in a mouse model of ulcerative colitis. *J Clin Invest* 2008; **118**: 534–44.

344 Brunialti MKC, Santos MC, Rigato O, Machado FR, Silva E, Salomao R. Increased percentages of T helper cells producing IL-17 and monocytes expressing markers of alternative activation in patients with sepsis. *PLoS ONE* 2012; **7**: e37393.

345 Ma CS, Chew GYJ, Simpson N, *et al*. Deficiency of Th17 cells in hyper IgE syndrome due to mutations in STAT3. *J Exp Med* 2008; **205**: 1551–7.

346 Puel A, Döffinger R, Natividad A, *et al*. Autoantibodies against IL-17A, IL-17F, and IL-22 in patients with chronic mucocutaneous candidiasis and autoimmune polyendocrine syndrome type I. *J Exp Med* 2010; **207**: 291–7.

347 Nakada T-A, Russell JA, Boyd JH, Walley KR. IL17A genetic variation is associated with altered susceptibility to Gram-positive infection and mortality of severe sepsis. *Crit Care* 2011; **15**: R254.

348 Ocejo-Vinyals JG, de Mateo EP, Hoz MÁ, *et al*. The IL-17 G-152A single nucleotide polymorphism is associated with pulmonary tuberculosis in northern Spain. *Cytokine* 2013; **64**: 58–61.

349 Hennig BJ, Frodsham AJ, Hellier S, *et al*. Influence of IL-10RA and IL-22 polymorphisms on outcome of hepatitis C virus infection. *Liver Int* 2007; **27**: 1134–43.

350 Kim B-J, Lee S, Berg RE, Simecka JW, Jones HP. Interleukin-23 (IL-23) deficiency disrupts Th17 and Th1-related defenses against *Streptococcus pneumoniae* infection. *Cytokine* 2013; **64**: 375–81.

351 Ma J, Wang J, Wan J, *et al*. Morphine disrupts interleukin-23 (IL-23)/IL-17-mediated pulmonary mucosal host defense against *Streptococcus pneumoniae* infection. *Infect Immun* 2010; **78**: 830–7.

352 Malley R, Srivastava A, Lipsitch M, *et al*. Antibody-independent, interleukin-17A-mediated, cross-serotype immunity to pneumococci in mice immunized intranasally with the cell wall polysaccharide. *Infect Immun* 2006; **74**: 2187–95.

353 Roche AM, King SJ, Weiser J. Live attenuated *Streptococcus pneumoniae* strains induce serotype-independent mucosal and systemic protection in mice. Infect Immun. 2007; **75**: 2469–75.

354 Richards L, Ferreira D, Miyaji EN, Andrew PW, Kadioglu A. The immunising effect of pneumococcal nasopharyngeal colonisation; protection against future colonisation and fatal invasive disease. *Immunobiology* 2010; **215**: 251–63.

355 Wright AKA, Bangert M, Gritzfeld JF, *et al*. Experimental Human Pneumococcal Carriage Augments IL-17A-dependent T-cell Defence of the Lung. *PLoS Pathog* 2013; **9**: e1003274.

356 Lundgren A, Bhuiyan TR, Novak D, *et al*. Characterization of Th17 responses to *Streptococcus pneumoniae* in humans: Comparisons between adults and children in a developed and a developing country. *Vaccine* 2012; **30**: 3897–907.

357 Moffitt KL, Gierahn TM, Lu Y-J, *et al*. T(H)17-based vaccine design for prevention of *Streptococcus pneumoniae* colonization. *Cell Host Microbe* 2011; **9**: 158–65.

358 Liu Y, Wang H, Zhang S, *et al*. Mucosal immunization with recombinant fusion protein DnaJ-ΔA146Ply enhances cross-protective immunity against *Streptococcus pneumoniae* infection in mice via interleukin 17A. *Infect Immun* 2014; **82**: 1666–75.

359 Cohen JM, Khandavilli S, Camberlein E, Hyams C, Baxendale HE, Brown JS. Protective contributions against invasive *Streptococcus pneumoniae* pneumonia of antibody and Th17-Cell responses to nasopharyngeal colonisation. *PLoS ONE* 2011; **6**: e25558.

360 Wilson R, Cohen JM, Jose RJ, de Vogel C, Baxendale H, Brown JS. Protection against *Streptococcus pneumoniae* lung infection after nasopharyngeal colonization requires both humoral and cellular immune responses. *Mucosal Immunol* 2015; **8**: 627–39.

361 Austrian R. The Jeremiah Metzger Lecture: Of gold and pneumococci: a history of pneumococcal vaccines in South Africa. *Trans Am Clin Climatol Assoc* 1978; **89**: 141–61.

362 Macleod CM, Hodges RG, Heidelberger M, Bernhard WG. Prevention of pneumococcal pneumonia by immunization with specific capsular polysaccharides. *J Exp Med* 1945; **82**: 445–65.

363 Austrian R, Douglas RM, Schiffman G, *et al*. Prevention of pneumococcal pneumonia by vaccination. *Trans Assoc Am Physicians* 1976; **89**: 184–94.

364 Pneumococcal. In: Immunisation against infectious disease. Department of Health, 2006.

365 Moberley S, Holden J, Tatham DP, Andrews RM. Vaccines for preventing pneumococcal infection in adults. *Cochrane Database Syst Rev* 2013; **1**: CD000422.

366 Musher DM, Manoff SB, McFetridge RD, *et al*. Antibody persistence ten years after first and second doses of 23-valent pneumococcal polysaccharide vaccine, and immunogenicity and safety of second and third doses in older adults. *Hum Vaccin* 2011; **7**: 919–28.

367 Andrews NJ, Waight PA, George RC, Slack MPE, Miller E. Impact and effectiveness of 23-valent pneumococcal polysaccharide vaccine against invasive pneumococcal disease in the elderly in England and Wales. *Vaccine* 2012; **30**: 6802–8.

368 Törling J, Hedlund J, Konradsen HB, Ortqvist A. Revaccination with the 23-valent pneumococcal polysaccharide vaccine in middle-aged and elderly persons previously treated for pneumonia. *Vaccine* 2003; **22**: 96–103.

369 de Roux A, Schmöle-Thoma B, Schmöele-Thoma B, *et al*. Comparison of pneumococcal conjugate polysaccharide and free polysaccharide vaccines in elderly adults: conjugate vaccine elicits improved antibacterial immune responses and immunological memory. *Clin Infect Dis* 2008; **46**: 1015–23.

370 French N, Nakiyingi J, Carpenter LM, *et al*. 23-valent pneumococcal polysaccharide vaccine in HIV-1-infected Ugandan adults: double-blind, randomised and placebo controlled trial. *Lancet* 2000; **355**: 2106–11.

371 Plosker GL. 13-Valent Pneumococcal Conjugate Vaccine: A Review of Its Use in Infants, Children, and Adolescents. *Pediatr Drugs* 2013; **15**: 403–23.

372 Yeh SH, Gurtman A, Hurley DC, *et al*. Immunogenicity and safety of 13-valent pneumococcal conjugate vaccine in infants and toddlers. *Pediatrics* 2010; **126**: e493–505.

373 Centers for Disease Control and Prevention (CDC). Progress in introduction of pneumococcal conjugate vaccine - worldwide, 2000-2012. *MMWR Morb Mortal Wkly Rep* 2013; **62**: 308–11.

374 Flasche S, Van Hoek AJ, Sheasby E, *et al*. Effect of pneumococcal conjugate vaccination on serotype-specific carriage and invasive disease in England: a cross-sectional study. *PLoS Med* 2011; **8**: e1001017.

375 Ghaffar F, Barton T, Lozano J, *et al*. Effect of the 7-valent pneumococcal conjugate vaccine on nasopharyngeal colonization by *Streptococcus pneumoniae* in the first 2 years of life. *Clin Infect Dis* 2004; **39**: 930–8.

376 Jacobs MR, Good CE, Bajaksouzian S, Windau AR. Emergence of *Streptococcus pneumoniae* serotypes 19A, 6C, and 22F and serogroup 15 in Cleveland, Ohio, in relation to introduction of the protein-conjugated pneumococcal vaccine. *Clin Infect Dis* 2008; **47**: 1388–95.

377 Kaplan SL, Barson WJ, Lin PL, *et al*. Serotype 19A Is the most common serotype causing invasive pneumococcal infections in children. *Pediatrics* 2010; **125**: 429–36.

378 Moore CE, Paul J, Foster D, *et al*. Reduction of Invasive Pneumococcal Disease 3 Years After the Introduction of the 13-Valent Conjugate Vaccine in the Oxfordshire Region of England. *J Infect Dis* 2014; : jiu213.

379 Health Protection Agency. Cumulative weekly number of reports of Invasive Pneumococcal Disease due to any of the serotypes NOT IN Prevenar13™ : Children aged 2 to 4 years in England and Wales by Epidemiological Year: July-June (2005- To Date). http://www.hpa.org.uk/Topics/InfectiousDiseases/InfectionsAZ/Pneumoccoccal/EpidemiologicalDataPneumococcal/CurrentEpidemiologyPneumococcal/NotInPrevenar13/pneumo05Cummulativeweekly24NOTINPrevenar13vacc/ (accessed June 26, 2014).

380 Bonten MJM, Huijts SM, Bolkenbaas M, *et al*. Polysaccharide Conjugate Vaccine against Pneumococcal Pneumonia in Adults. *N Engl J Med* 2015; **372**: 1114–25.

381 Fukuyama Y, King JD, Kataoka K, *et al*. A combination of Flt3 ligand cDNA and CpG oligodeoxynucleotide as nasal adjuvant elicits protective secretory-IgA immunity to *Streptococcus pneumoniae* in aged mice. *J Immunol* 2011; **186**: 2454–61.

382 Richards L, Ferreira D, Miyaji EN, Andrew PW, Kadioglu A. The immunising effect of pneumococcal nasopharyngeal colonisation; protection against future colonisation and fatal invasive disease. *Immunobiology* 2010; **215**: 251–63.

383 Veldhoen M, Hirota K, Christensen J, O'Garra A, Stockinger B. Natural agonists for aryl hydrocarbon receptor in culture medium are essential for optimal differentiation of Th17 T cells. *J Exp Med* 2009; **206**: 43–9.

384 Ijaz UZ. **AMPLICONprocessing**: Pipeline for 16S rRNA datasets analysis. userweb.eng.gla.ac.uk. http://userweb.eng.gla.ac.uk/umer.ijaz/bioinformatics/AMPLICONprocessing.pdf (accessed Jan 5, 2015).

385 Masella AP, Bartram AK, Truszkowski JM, Brown DG, Neufeld JD. PANDAseq: paired-end assembler for illumina sequences. *BMC Bioinformatics* 2012; **13**: 31.

386 Edgar RC, Haas BJ, Clemente JC, Quince C, Knight R. UCHIME improves sensitivity and speed of chimera detection. *Bioinformatics* 2011; **27**: 2194–200.

387 Edgar RC. UPARSE: highly accurate OTU sequences from microbial amplicon reads. *Nat Methods* 2013; **10**: 996-98.

388 Wang Q, Garrity GM, Tiedje JM, Cole JR. Naïve Bayesian Classifier for Rapid Assignment of rRNA Sequences into the New Bacterial Taxonomy. *Applied and Environmental Microbiology* 2007; **73**: 5261–7.

389 Dixon P. VEGAN, a package of R functions for community ecology. *J Veg Sci* 2003; **14**: 927–30.

390 McMurdie PJ, Holmes S. phyloseq: an R package for reproducible interactive analysis and graphics of microbiome census data. *PLoS ONE* 2013; **8**: e61217.

391 Wickham H. ggplot2: elegant graphics for data analysis. Springer New York, 2009 http://had.co.nz/ggplot2/book.

392 Croucher NJ, Mitchell AM, Gould KA, *et al*. Dominant role of nucleotide substitution in the diversification of serotype 3 pneumococci over decades and during a single infection. *PLoS Genet* 2013; **9**: e1003868.

393 Robinson MD, McCarthy DJ, Smyth GK. edgeR: a Bioconductor package for differential expression analysis of digital gene expression data. *Bioinformatics* 2010; **26**: 139–40.

394 Mureithi MW, Finn A, Ota MO, *et al*. T cell memory response to pneumococcal protein antigens in an area of high pneumococcal carriage and disease. *J Infect Dis* 2009; **200**: 783–93.

395 Pido-Lopez J, Kwok WW, Mitchell TJ, Heyderman RS, Williams NA. Acquisition of pneumococci specific effector and regulatory CD4+ T cells localising within human upper respiratory-tract mucosal lymphoid tissue. *PLoS Pathog* 2011; **7**: e1002396.

396 Bayes HK, Bicknell S, MacGregor G, Evans TJ. T helper cell subsets specific for Pseudomonas aeruginosa in healthy individuals and patients with cystic fibrosis. *PLoS ONE* 2014; **9**: e90263.

397 Sallusto F, Lenig D, Förster R, Lipp M, Lanzavecchia A. Two subsets of memory T lymphocytes with distinct homing potentials and effector functions. *Nature* 1999; **402**: 34–8.

398 Campbell JJ, O'Connell DJ, Wurbel M-A. Cutting Edge: Chemokine receptor CCR4 is necessary for antigen-driven cutaneous accumulation of CD4 T cells under physiological conditions. *J Immunol* 2007; **178**: 3358–62.

399 Mikhak Z, Strassner JP, Luster AD. Lung dendritic cells imprint T cell lung homing and promote lung immunity through the chemokine receptor CCR4. *J Exp Med* 2013; **210**: 1855–69.

400 Duhen T, Geiger R, Jarrossay D, Lanzavecchia A, Sallusto F. Production of interleukin 22 but not interleukin 17 by a subset of human skin-homing memory T cells. *Nat Immunol* 2009; **10**: 857–63.

401 Bengsch B, Seigel B, Flecken T, Wolanski J, Blum HE, Thimme R. Human Th17 cells express high levels of enzymatically active dipeptidylpeptidase IV (CD26). *J Immunol* 2012; **188**: 5438–47.

402 Maggi L, Santarlasci V, Capone M, *et al*. CD161 is a marker of all human IL-17-producing T-cell subsets and is induced by RORC. *Eur J Immunol* 2010; **40**: 2174–81.

403 Duhen T, Campbell DJ. IL-1β Promotes the Differentiation of Polyfunctional Human CCR6+CXCR3+ Th1/17 Cells That Are Specific for Pathogenic and Commensal Microbes. *J Immunol* 2014; **193**: 120–9.

404 Morrison PJ, Bending D, Fouser LA, *et al*. Th17-cell plasticity in *Helicobacter hepaticus*-induced intestinal inflammation. *Mucosal Immunol* 2013; **6**: 1143–56.

405 Domingues HS, Mues M, Lassmann H, Wekerle H, Krishnamoorthy G. Functional and pathogenic differences of Th1 and Th17 cells in experimental autoimmune encephalomyelitis. *PLoS ONE* 2010; **5**: e15531.

406 Kunkel EJ, Boisvert J, Murphy K, *et al*. Expression of the chemokine receptors CCR4, CCR5, and CXCR3 by human tissue-infiltrating lymphocytes. *Am J Pathol* 2002; **160**: 347–55.

407 Etuwewe OM, Swann N, Hollingshead S, *et al*. Effect of recurrent invasive pneumococcal disease on serum anti-pneumolysin IgG titres in HIV infected adults. *Vaccine* 2009; **27**: 3881–4.

408 Fernandez-Botran R, Sanders VM, Mosmann TR, Vitetta ES. Lymphokine-mediated regulation of the proliferative response of clones of T helper 1 and T helper 2 cells. *J Exp Med* 1988; **168**: 543–58.

409 Sidman CL, Luther EA, Marshall JD, Nguyen KA, Roopenian DC, Worthen SM. Increased expression of major histocompatibility complex antigens on lymphocytes from aged mice. *Proc Natl Acad Sci USA* 1987; **84**: 7624–8.

410 Ordemann R, Hutchinson R, Friedman J, *et al*. Enhanced allostimulatory activity of host antigen-presenting cells in old mice intensifies acute graft-versus-host disease. *J Clin Invest* 2002; **109**: 1249–56.

411 Castle SC, Uyemura K, Crawford W, Wong W, Makinodan T. Antigen presenting cell function is enhanced in healthy elderly. *Mechanisms of Ageing and Development* 1999; **107**: 137–45.

412 Xiong J, Kang K, Liu L, Yoshida Y, Cooper KD, Ghannoum MA. Candida albicans and Candida krusei differentially induce human blood mononuclear cell interleukin-12 and gamma interferon production. *Infect Immun* 2000; **68**: 2464–9.

413 van de Veerdonk FL, Marijnissen RJ, Kullberg BJ, *et al*. The macrophage mannose receptor induces IL-17 in response to Candida albicans. *Cell Host Microbe* 2009; **5**: 329–40.

414 Smeekens SP, van de Veerdonk FL, Joosten LAB, *et al*. The classical $CD14^{++}$ $CD16^{-}$ monocytes, but not the patrolling $CD14^{+}$ $CD16^{+}$ monocytes, promote Th17 responses to Candida albicans. *Eur J Immunol* 2011; **41**: 2915–24.

415 Fermin Lee A, Chen H-Y, Wan L, *et al*. Galectin-3 modulates Th17 responses by regulating dendritic cell cytokines. *Am J Pathol* 2013; **183**: 1209–22.

416 Whatmore AM, King SJ, Doherty NC, Sturgeon D, Chanter N, Dowson CG. Molecular Characterization of equine isolates of *Streptococcus pneumoniae*: natural disruption of genes encoding the virulence factors pneumolysin and autolysin. *Infect Immun* 1999; **67**: 2776–82.

417 Daley JM, Thomay AA, Connolly MD, Reichner JS, Albina JE. Use of Ly6G-specific monoclonal antibody to deplete neutrophils in mice. *J Leukocyte Biol* 2007; **83**: 64–70.

418 Beckstead JH. A simple technique for preservation of fixation-sensitive antigens in paraffin-embedded tissues. *Journal of Histochemistry and Cytochemistry* 1994; **42**: 1127–34.

419 Tettelin H, Nelson KE, Paulsen IT, *et al*. Complete genome sequence of a virulent isolate of *Streptococcus pneumoniae*. *Science* 2001; **293**: 498–506.

420 Aaberge IS, Eng J, Lermark G, Løvik M. Virulence of *Streptococcus pneumoniae* in mice: a standardized method for preparation and frozen storage of the experimental bacterial inoculum. *Microb Pathog* 1995; **18**: 141–52.

421 Kerr AR, Paterson GK, McCluskey J, *et al*. The contribution of PspC to pneumococcal virulence varies between strains and is accomplished by both complement evasion and complement-independent mechanisms. *Infect Immun* 2006; **74**: 5319–24.

422 Orihuela CJ, Gao G, McGee M, Yu J, Francis KP, Tuomanen E. Organ-specific models of *Streptococcus pneumoniae* disease. *Scand J Infect Dis* 2003; **35**: 647–52.

423 Gingles NA, Alexander JE, Kadioglu A, *et al*. Role of genetic resistance in invasive pneumococcal infection: identification and study of susceptibility and resistance in inbred mouse strains. *Infect Immun* 2001; **69**: 426–34.

424 Hahn C, Harrison EM, Parkhill J, Holmes MA, Paterson GK. Draft Genome sequence of the *Streptococcus pneumoniae* Avery strain A66. *Genome Announc* 2015; **3**: e00697–15.

425 McAllister LJ, Ogunniyi AD, Stroeher UH, Leach AJ, Paton JC. Contribution of serotype and genetic background to virulence of serotype 3 and serogroup 11 pneumococcal isolates. *Infect Immun* 2011; **79**: 4839–49.

426 Trappetti C, van der Maten E, Amin Z, *et al*. Site of isolation determines biofilm formation and virulence phenotypes of *Streptococcus pneumoniae* serotype 3 clinical isolates. *Infect Immun* 2013; **81**: 505–13.

427 Wilkosz S, Edwards LA, Bielsa S, *et al*. Characterization of a new mouse model of empyema and the mechanisms of pleural invasion by *Streptococcus pneumoniae*. *Am J Resp Cell Mol Biol* 2011; **46**: 2011–0182OCv1–187.

428 Liu F, Whitton JL. Cutting edge: re-evaluating the in vivo cytokine responses of CD8+ T cells during primary and secondary viral infections. *J Immunol* 2005; **174**: 5936–40.

429 Shibata K, Yamada H, Hara H, Kishihara K, Yoshikai Y. Resident Vδ1+ gammadelta T cells control early infiltration of neutrophils after *Escherichia coli* infection via IL-17 production. *J Immunol* 2007; **178**: 4466–72.

430 Takatori H, Kanno Y, Watford WT, *et al*. Lymphoid tissue inducer-like cells are an innate source of IL-17 and IL-22. *J Exp Med* 2009; **206**: 35–41.

431 Lykens JE, Terrell CE, Zoller EE, Risma K, Jordan MB. Perforin is a critical physiologic regulator of T-cell activation. *Blood* 2011; **118**: 618–26.

432 Barletta KE, Cagnina RE, Wallace KL, Ramos SI, Mehrad B, Linden J. Leukocyte compartments in the mouse lung: distinguishing between marginated, interstitial, and alveolar cells in response to injury. *J Immunol Methods* 2012; **375**: 100–10.

433 Marqués JM, Rial A, Muñoz N, *et al*. Protection against *Streptococcus pneumoniae* serotype 1 acute infection shows a signature of Th17- and IFN-γ-mediated immunity. *Immunobiology* 2012; **217**: 420–9.

434 Lu Y-J, Gross J, Bogaert D, *et al*. Interleukin-17A mediates acquired immunity to pneumococcal colonization. *PLoS Pathog* 2008; **4**: e1000159.

435 Ye P, Rodriguez FH, Kanaly S, *et al*. Requirement of Interleukin 17 Receptor Signaling for Lung Cxc Chemokine and Granulocyte Colony-Stimulating Factor Expression, Neutrophil Recruitment, and Host Defense. *J Exp Med* 2001; **194**: 519–28.

436 Hampton MB, Vissers MC, Winterbourn CC. A single assay for measuring the rates of phagocytosis and bacterial killing by neutrophils. *J Leukocyte Biol* 1994; **55**: 147–52.

437 Sung CK, Li H, Claverys JP, Morrison DA. An rpsL Cassette, Janus, for Gene Replacement through Negative Selection in *Streptococcus pneumoniae*. *Applied and Environmental Microbiology* 2001; **67**: 5190–6.

438 Sleeman K, Griffiths D, Shackley F, *et al*. Capsular serotype-specific attack rates and duration of carriage of *Streptococcus pneumoniae* in a population of children. *J Infect Dis* 2006; **194**: 682–8.

439 Kadioglu A, Cuppone AM, Trappetti C, *et al*. Sex-based differences in susceptibility to respiratory and systemic pneumococcal disease in mice. *J Infect Dis* 2011; **204**: 1971–9.

440 Wood WB, Smith MR. The inhibition of surface phagocytosis by the capsular slime layer of pneumococcus type III. *J Exp Med* 1949; **90**: 85–96.

441 Hyams C, Trzcinski K, Camberlein E, *et al*. Streptococcus *pneumoniae* capsular serotype invasiveness correlates with the degree of factor H binding and opsonization with C3b/iC3b. *Infect Immun* 2013; **81**: 354–63.

442 Hyams C, Opel S, Hanage W, *et al*. Effects of *Streptococcus pneumoniae* strain background on complement resistance. *PLoS ONE* 2011; **6**: e24581.

443 Hyams C, Yuste J, Bax K, Camberlein E, Weiser J, Brown JS. *Streptococcus pneumoniae* resistance to complement-mediated immunity is dependent on the capsular serotype. *Infect Immun* 2010; **78**: 716–25.

444 Waite RD, Penfold DW, Struthers JK. Spontaneous sequence duplications within capsule genes *cap8E* and *tts* control phase variation in *Streptococcus pneumoniae* serotypes 8 and 37. *Microbiology* 2003. DOI:10.1099/mic.0.26011-0.

445 José RJ, Williams AE, Mercer PF, Sulikowski MG, Brown JS, Chambers RC. Regulation of neutrophilic inflammation by proteinase-activated receptor 1 during bacterial pulmonary infection. *J Immunol* 2015; **194**: 6024–34.

446 The innate immune response to uropathogenic *Escherichia coli* involves IL-17A in a murine model of urinary tract infection. *J Immunol* 2010; **184**: 2065–75.

447 Chen J, Deng Y, Zhao J, *et al*. The polymorphism of IL-17 G-152A was associated with childhood asthma and bacterial colonization of the hypopharynx in bronchiolitis. *J Clin Immunol* 2010; **30**: 539–45.

448 Krone CL, Biesbroek G, Trzciński K, Sanders EAM, Bogaert D. Respiratory microbiota dynamics following *Streptococcus pneumoniae* acquisition in young and elderly mice. *Infect Immun* 2014; **82**: 1725–31.

449 Bassis CM, Tang AL, Young VB, Pynnonen MA. The nasal cavity microbiota of healthy adults. *Microbiome* 2014; **2**: 27.

450 Frank DN, Feazel LM, Bessesen MT, Price CS, Janoff EN, Pace NR. The human nasal microbiota and *Staphylococcus aureus* carriage. *PLoS ONE* 2010; **5**: e10598.

451 Shen MC, Preston AM, Gillilland MG III, *et al*. Characterization of the lung microbiome of specific pathogen-free mice with and without exposure to cigarette smoke *in vivo*. American Thoracic Society, 2011: A6210–0.

452 Barfod KK, Roggenbuck M, Hansen LH, *et al*. The murine lung microbiome in relation to the intestinal and vaginal bacterial communities. *BMC Microbiol* 2013; **13**: 303.

453 Erb-Downward JR, Thompson DL, Han MK, *et al*. Analysis of the lung microbiome in the 'healthy' smoker and in COPD. *PLoS ONE* 2011; **6**: e16384.

454 Morris A, Beck JM, Schloss PD, *et al*. Comparison of the respiratory microbiome in healthy nonsmokers and smokers. *Am J Resp Crit Care Med* 2013; **187**: 1067–75.

455 Charlson ES, Bittinger K, Haas AR, *et al*. Topographical continuity of bacterial populations in the healthy human respiratory tract. *Am J Resp Crit Care Med* 2011; **184**: 957–63.

456 Salter SJ, Cox MJ, Turek EM, *et al*. Reagent and laboratory contamination can critically impact sequence-based microbiome analyses. *BMC Biol* 2014; **12**: 87.

457 Willing BP, Dicksved J, Halfvarson J, *et al*. A pyrosequencing study in twins shows that gastrointestinal microbial profiles vary with inflammatory bowel disease phenotypes. *Gastroenterology* 2010; **139**: 1844–1854.e1.

458 Giongo A, Gano KA, Crabb DB, *et al*. Toward defining the autoimmune microbiome for type 1 diabetes. *The ISME Journal* 2011; **5**: 82–91.

459 Turnbaugh PJ, Hamady M, Yatsunenko T, *et al*. A core gut microbiome in obese and lean twins. *Nature* 2009; **457**: 480–4.

460 Pragman AA, Kim HB, Reilly CS, Wendt C, Isaacson RE. The lung microbiome in moderate and severe chronic obstructive pulmonary disease. *PLoS ONE* 2012; **7**: e47305.

461 Sze MA, Dimitriu PA, Hayashi S, *et al*. The lung tissue microbiome in chronic obstructive pulmonary disease. *Am J Resp Crit Care Med* 2012; **185**: 1073–80.

462 Krone CL, Trzciński K, Zborowski T, Sanders EAM, Bogaert D. Impaired innate mucosal immunity in aged mice permits prolonged *Streptococcus pneumoniae* colonization. *Infect Immun* 2013; **81**: 4615–25.

463 Schloss PD, Schubert AM, Zackular JP, Iverson KD, Young VB, Petrosino JF. Stabilization of the murine gut microbiome following weaning. *Gut Microbes* 2012; **3**: 383–93.

464 Biesbroek G, Tsivtsivadze E, Sanders EAM, *et al*. Early respiratory microbiota composition determines bacterial succession patterns and respiratory health in children. *Am J Resp Crit Care Med* 2014; **190**: 1283–92.

465 Cremers AJ, Zomer AL, Gritzfeld JF, *et al*. The adult nasopharyngeal microbiome as a determinant of pneumococcal acquisition. *Microbiome* 2014; **2**: 44.

466 Lambert N, Salk H, Kennedy R, *et al*. Intranasal vaccination with live attenuated influenza vaccine increases diversity of the human nasal microbiome (VAC8P.1001). *J Immunol* 2014; **192**: 142.7–142.7.

467 Allen EK, Koeppel AF, Hendley JO, Turner SD, Winther B, Sale MM. Characterization of the nasopharyngeal microbiota in health and during rhinovirus challenge. *Microbiome* 2014; **2**: 22.

468 Margolis E, Yates A, Levin BR. The ecology of nasal colonization of *Streptococcus pneumoniae*, *Haemophilus influenzae* and *Staphylococcus aureus*: the role of competition and interactions with host's immune response. *BMC Microbiol* 2010; **10**: 59.

469 Kwambana BA. Infant nasopharyngeal microbial ecology and the pneumococcal conjugate vaccine (Thesis). 2011; published online Dec 1. http://hdl.handle.net/2381/10049.

470 Westermann AJ, Gorski SA, Vogel J. Dual RNA-seq of pathogen and host. *Nat Rev Micro* 2012; **10**: 618–30.

471 Orihuela CJ, Radin JN, Sublett JE, Gao G, Kaushal D, Tuomanen EI. Microarray analysis of pneumococcal gene expression during invasive disease. *Infect Immun* 2004; **72**: 5582–96.

472 Chancey ST, Bai X, Kumar N, *et al*. Transcriptional attenuation controls macrolide inducible efflux and resistance in *Streptococcus pneumoniae* and in other Gram-positive bacteria containing mef/mel(msr(D)) elements. *PLoS ONE* 2015; **10**: e0116254.

473 Pettigrew MM, Marks LR, Kong Y, Gent JF, Roche-Hakansson H, Hakansson AP. Dynamic changes in the *Streptococcus pneumoniae* transcriptome during transition from biofilm formation to invasive disease upon influenza A virus infection. *Infect Immun* 2014; **82**: 4607–19.

474 Lupien A, Gingras H, Bergeron MG, Leprohon P, Ouellette M. Multiple mutations and increased RNA expression in tetracycline-resistant *Streptococcus pneumoniae* as determined by genome-wide DNA and mRNA sequencing. *J Antimicrob Chemother* 2015; published online April 9. DOI:10.1093/jac/dkv060.

475 Romero P, Croucher NJ, Hiller NL, *et al*. Comparative genomic analysis of ten *Streptococcus pneumoniae* temperate bacteriophages. *J Bacteriol* 2009; **191**: 4854–62.

476 Arthur M, Depardieu F, Molinas C, Reynolds P, Courvalin P. The vanZ gene of Tn1546 from enterococcus faecium BM4147 confers resistance to teicoplanin. *Gene* 1995; **154**: 87–92.

477 Weng M, Nagy PL, Zalkin H. Identification of the Bacillus subtilis pur operon repressor. *Proc Natl Acad Sci USA* 1995; **92**: 7455–9.

478 de Saizieu A, Gardès C, Flint N, *et al*. Microarray-based identification of a novel *Streptococcus pneumoniae* regulon controlled by an autoinduced peptide. *J Bacteriol* 2000; **182**: 4696–703.

479 Lux T, Nuhn M, Hakenbeck R, Reichmann P. Diversity of bacteriocins and activity spectrum in *Streptococcus pneumoniae*. *J Bacteriol* 2007; **189**: 7741–51.

480 Dawid S, Roche AM, Weiser J. The *blp* bacteriocins of *Streptococcus pneumoniae* mediate intraspecies competition both *in vitro* and *in vivo*. *Infect Immun* 2007; **75**: 443–51.

481 McCluskey J, Hinds J, Husain S, Witney A, Mitchell TJ. A two-component system that controls the expression of pneumococcal surface antigen A (PsaA) and regulates virulence and resistance to oxidative stress in *Streptococcus pneumoniae*. *Mol Microbiol* 2004; **51**: 1661–75.

482 Ng W-L, Kazmierczak KM, Robertson GT, Gilmour R, Winkler ME. Transcriptional regulation and signature patterns revealed by microarray analyses of *Streptococcus pneumoniae* R6 challenged with sublethal concentrations of translation inhibitors. *J Bacteriol* 2003; **185**: 359–70.

483 Riley MA, Wertz JE. Bacteriocins: evolution, ecology, and application. *Annu Rev Microbiol* 2002; **56**: 117–37.

484 Son MR, Shchepetov M, Adrian PV, *et al*. Conserved mutations in the pneumococcal bacteriocin transporter gene, blpA, result in a complex population consisting of producers and cheaters. *MBio* 2011; **2**: e00179–11.

485 Pinchas MD, LaCross NC, Dawid S. An Electrostatic interaction between BlpC and BlpH dictates pheromone specificity in the control of bacteriocin production and immunity in *Streptococcus pneumoniae*. *J Bacteriol* 2015; **197**: 1236–48.

486 Dintilhac A, Alloing G, Granadel C, Claverys JP. Competence and virulence of *Streptococcus pneumoniae*: Adc and PsaA mutants exhibit a requirement for Zn and Mn resulting from inactivation of putative ABC metal permeases. *Mol Microbiol* 1997; **25**: 727–39.

487 Tseng H-J, McEwan AG, Paton JC, Jennings MP. Virulence of *Streptococcus pneumoniae*: PsaA mutants are hypersensitive to oxidative stress. *Infect Immun* 2002; **70**: 1635–9.

488 Romero-Steiner S, Caba J, Rajam G, *et al*. Adherence of recombinant pneumococcal surface adhesin A (rPsaA)-coated particles to human nasopharyngeal epithelial cells for the evaluation of anti-PsaA functional antibodies. *Vaccine* 2006; **24**: 3224–31.

489 Kadioglu A, Weiser J, Paton JC, Andrew PW. The role of *Streptococcus pneumoniae* virulence factors in host respiratory colonization and disease. *Nat Rev Micro* 2008; **6**: 288–301.

490 Kong X, Feng D, Wang H, *et al*. Interleukin-22 induces hepatic stellate cell senescence and restricts liver fibrosis. *Hepatology (Baltimore, Md)* 2012; **56**: 1150–9.

491 van der Windt GJW, Hoogendijk AJ, de Vos AF, Kerver ME, Florquin S, Van Der Poll T. The role of CD44 in the acute and resolution phase of the host response during pneumococcal pneumonia. *Lab Invest* 2011; **91**: 588–97.

492 Aggarwal NR, Tsushima K, Eto Y, *et al*. Immunological priming requires regulatory T cells and IL-10-producing macrophages to accelerate resolution from severe lung inflammation. *J Immunol* 2014; **192**: 4453–64.

493 Poe SL, Arora M, Oriss TB, *et al*. STAT1-regulated lung MDSC-like cells produce IL-10 and efferocytose apoptotic neutrophils with relevance in resolution of bacterial pneumonia. *Mucosal Immunol* 2012; **6**: 189–99.

494 Pneumococcal disease: guidance, data and analysis. gov.uk. https://www.gov.uk/government/collections/pneumococcal-disease-guidance-data-and-analysis#epidemiology (accessed June 18, 2015).

495 Plotkin SA. Correlates of protection induced by vaccination. *Clin Vaccine Immunol* 2010; **17**: 1055–65.

496 Dorn GL, Burson GG, Haynes JR. Blood culture technique based on centrifugation: clinical evaluation. *J Clin Microbiol* 1976; **3**: 258–63.

497 Brannon P, Kiehn TE. Large-scale clinical comparison of the lysis-centrifugation and radiometric systems for blood culture. *J Clin Microbiol* 1985; **22**: 951–4.

498 Kelly T, Dillard JP, Yother J. Effect of genetic switching of capsular type on virulence of *Streptococcus pneumoniae*. *Infect Immun* 1994; **62**: 1813–9.